International Symposium on

Standards, Applications and Quality Assurance in Medical Radiation Dosimetry (IDOS 2019)

18–21 June 2019
Vienna, Austria

Book of Extended Synopses

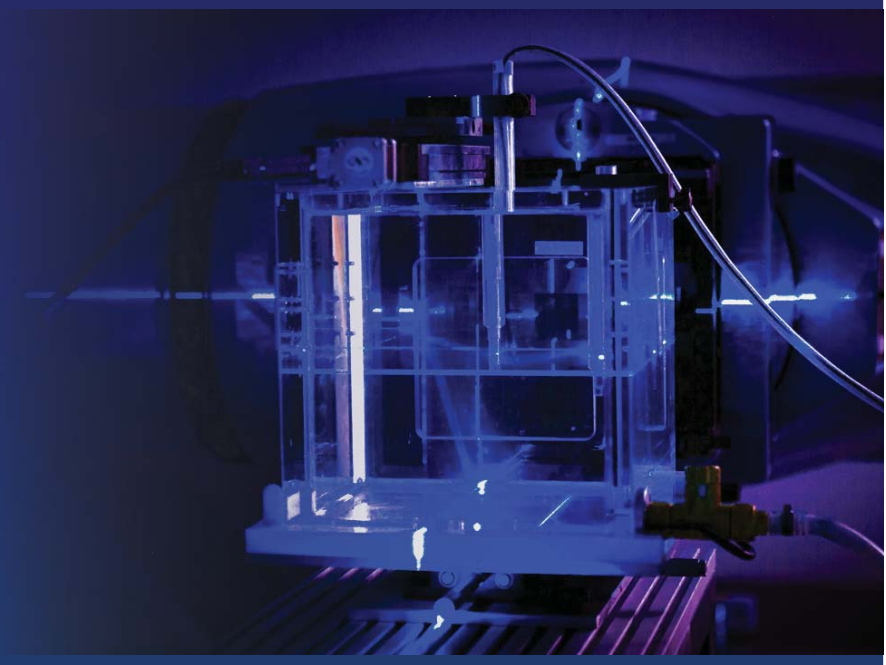

IDOS 2019

Organized by the

IAEA
International Atomic Energy Agency

CN-273

TABLE OF CONTENTS

ORAL PRESENTATIONS

Small Field Dosimetry

Implementation of the International Code of Practice on Dosimetry of Small Static Fields used in External Beam Radiotherapy (TRS-483)

M Saiful Huq[a]
R. Alfonso-Laguardia[b], M. Arib[c], K. Christaki[d], A. Ismail[e], R. Kinhikar[f], J. Larraga-Gutierrez[g], W. Lechner[h], K. Mani[i], N. Maphumule[j], O. Sauer[k], S. Shoeir[l], S. Suriyapee[m]

[a]Department of Radiation Oncology, Division of Medical Physics, University of Pittsburgh School of Medicine and UPMC Hillman Cancer Center, Pittsburgh, Pennsylvania, USA
[b]Faculty of Nuclear Sciences and Technologies, University of Havana, 10400 Havana, Cuba
[c]King Faisal Specialist Hospital and Research Centre, Riyadh 11211, Saudi Arabia
[d]IAEA, Vienna, Austria.
[e]Atomic Energy Commission of Syria, Department of Protection and Safety, Damascus, P. O. Box 6091, Syria.
[f]Tata Memorial Hospital, Mumbai 400012, India.
[g]Instituto Nacional de Neurologia y Neurocrurgia "Manuel Velasco suarez", 14269 Ciudad de Mexico, Mexico.
[h]Department of Radiation Oncology, AKH Wien, 1090 Vienna, Austria.
[i]United Hospital Limited, Dhaka 1212, Bangladesh.
[j]Charlotte Maxeke Johannesburg Academic Hospital, 2000 Johannesburg, South Africa
[k]Universitätsklinikum Wurzburg, 97080 Wurzburg, Germany.
[l]Children's Cancer Hospital Egypt, 11617 Cario, Egypt.
[m]Chulalongkorn University, Faculty of Medicine, 10330 Bangkok, Thailand.

Email address of Corresponding Author: huqs@upmc.edu

BACKGROUND

In 2017, the International Atomic Energy Agency (IAEA) and the American Association of Physicists in Medicine (AAPM) jointly published a Code of Practice (CoP) on the dosimetry of small static fields used in external beam radiotherapy (TRS-483) [1]. A summary of this CoP was published separately in Medical Physics by Palman's et al. [2]. This CoP provided formalisms and recommendations for performing reference dosimetry in non-standard machine specific reference fields as well as relative dosimetry in small clinical fields. In 2015, the IAEA initiated a coordinated research project (CRP E2.40.21: Testing of the Code of Practice for Small Field Dosimetry) to test the recommendations given in TRS-483 for both reference dosimetry as well as relative dosimetry. Twelve investigators from different countries were invited to participate in this initiative. The goal of this presentation is to present the results of the work of this group.

METHODS

The main goal of the coordinated research project was to investigate the clinical implementation of the following tasks recommended in TRS-483 using various combinations of ionization chamber, solid state and other detector types, and linear accelerators, CyberKnife, Gamma Knife, Tomotherapy and Co-60 machines:

1. Investigate the validity of the equation given in TRS-483 for the determination of beam quality index $TPR_{20,10}(10,10)$ and $\%(10,10)_X$ from measurements made in clinical fields that are smaller than the conventional 10cm x 10cm reference field size for 6 and 10 MV photon beams with and without flattening filter

2. Performing reference dosimetry measurements in machine specific reference fields using Co-60, 6 and 10 MV beams with and without flattening filters
3. Determination of field output factors from measurements made with various combinations of detectors, field sizes and machine types
4. Determination of uncertainties for all measurements performed for both reference and relative dosimetry

Assignments were given to all participants such that the above tests can be investigated and results compared for measurements made for various combinations of machine and detector types used. Participants performed measurements in Co-60 machines, linear accelerators (linacs) manufactured by Varian Medical Systems, Elekta, Accuray (Tomotherapy) and Siemens Medical and in specialized radiosurgery machines such as CyberKnife and Gamma Knife. Linac based measurements involved beam shaping devices such as multileaf collimators (MLC) as well as add-on MLCs and cones. Measurements were done both in liquid water as well as in solid water phantoms.

RESULTS

Members of the CRP have performed an extensive set of measurements for all the three tasks listed above. Analysis of all the data is still ongoing. Presented below are initial analysis of some of the data that were gathered and results from the literature published some members of the CRP. It should be noted that the final results may turn out to be slightly different from what is presented below:

1. Data from thirteen machines using $TPR_{20,10}(S)$ and seven machines using $\%dd(10,S)$ were collected for 6MV beam. The $TPR_{20,10}(S)$ values ranged between 0.667 and 0.685 while the $\%dd(10,S)$ values ranged between 66.4% and 67.6%. The mean value of the differences between calculated $TPR_{20,10}(10)$ and experimentally determined $TPR_{20,10}(10)$ in the 10 x 10 cm² field was -0.02% with a standard deviation of the mean of 0.1%. The mean value of the differences between calculated $\%dd(10,10)_X$ and experimentally determined $\%dd(10,10)_X$ in the 10 x 10 cm² field was -0.05% with a standard deviation of 0.2%. The differences of the individual centres did not exceed 1.1% and 1.2% for $TPR_{20,10}(10)$ and $\%dd(10,10)_X$, respectively.
   Data were also collected for 6MV FFF, 10MV WFF and 10MV FFF beams where WFF denotes beam without flattening filter and FFF denotes flattening filter free beams. These results show similar behaviour which will be presented at the meeting.
2. TRS-483 recommended both $TPR_{20,10}(10)$ and as $\%(10,10)_X$ as indices for beam quality specification. Results of Huq et al [3] show that for 6MV (WFF and FFF) beams absorbed dose to water per monitor unit determined at the depth of maximum dose using both approaches agree to within 0.1% [3]. This agreement changed to 0.2% when 10 MV (both WFF and FFF) beams were used [3]. Additional analysis by Huq et al [3] show excellent agreement (to within 0.05% with IAEA TRS 398 CoP [4] and to within 0.3% with AAPM TG51 [5] and TG51 Addendum protocols [6]) in the mean values of the ratios TRS398/TRS483, TG51/TRS483, and TG51 addendum/TRS483 absorbed doses to of water per monitor unit between determined using both approaches for both 6 and 10 MV beams (WFF and FFF).
   Results of the consistencies of absorbed doses to water determined at the reference depth using different detectors for all thirteen machines will be presented for both 6 and 10 MV (WFF and FFF) beams.
3. Perhaps the most important results are those of the field output factors determined by all participants using a variety of detectors in different machines using different

combinations of beam collimation system. Described below are examples of data for 6MV WFF and 10 MV FFF beams. Thirteen institutions provided field output factor measurements for 6 MVWFF beams five institutions provided data for 10MV FFF beams. Measurements were done using different detectors for the following field sizes ranging from and using either two or three detectors per field the field sizes: 10 x 10 cm², 6 x 6 cm², 4 x 4 cm², 3 x 3 cm², 2 x 2 cm², 1 x 1 cm² and 0.5 x 0.5 cm². Figure 1 depicts the relative spread (sprd) of the field output factors for the 6MVWFF beam, which was used as measure for the consistency of the field output correction factors. The spread increased with decreasing field size, reaching a maximum of little over 3% for the 0.5 x 0.5 cm² field. For the 10MV FFF beam, the spread reached to about 8% for the 1cm x 1cm field size (Figure 2). Further analysis of this large deviation is being investigated with respect to experimental setup and detector design.
Results from all centers for field output factor measurements will be presented at the meeting.

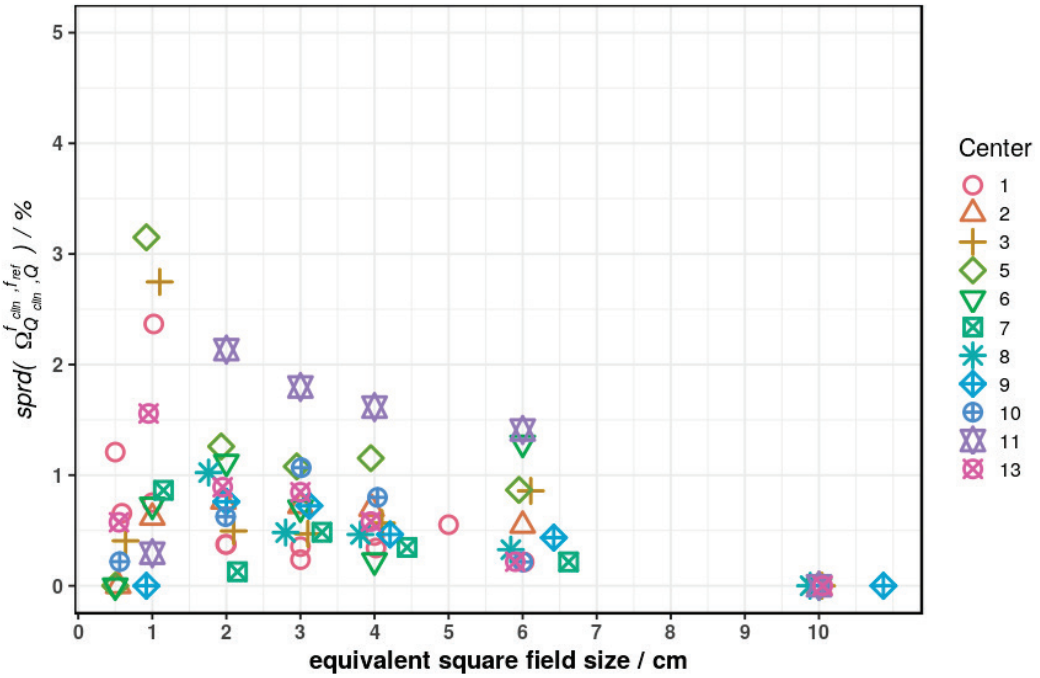

Figure 1. Data for standard deviation of the mean for field output factor for 6MV WFF beams

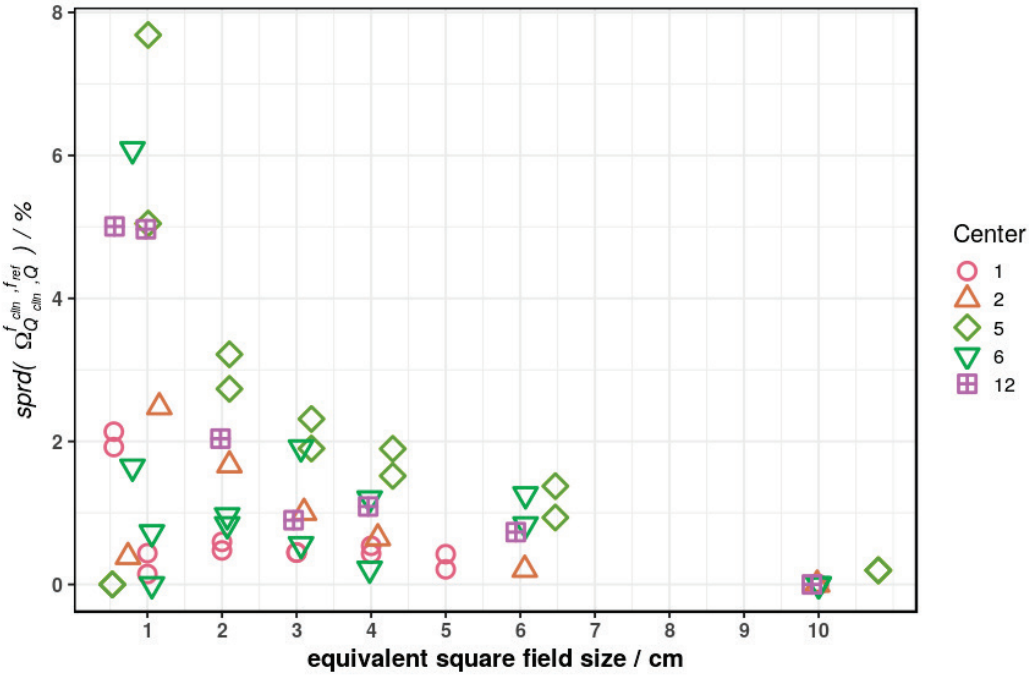

Figure 2. Data for standard deviation of the mean for field output factor for 10MV FFF beams

CONCLUSIONS

TRS-483 is the first international guidance given by the IAEA and AAPM for performing reference and relative dosimetry in machine specific reference field and small clinical fields. Strict adherence to the recommendations given in TRS-483 significantly improves the dosimetry in small fields and brings harmonization in the results obtained in different clinics.

REFERENCES

[1] INTERNATIONAL ATOMIC ENERGY AGENCY, Technical Report Series No, 483, IAEA, Vienna (2017).

[2] PALMANS, H., ANDREO, P., HUQ, M.SAIFUL., SEUNTJENS, J., CHRISTAKI, K.E., MEGHZIFENE, A., Dosimetry of small static fields used in external photon beam radiotherapy: Summary of TRS483, the IAEA-AAPM international Code of Practice for reference and relative dose determination, Medical Physics **45** (2018) e1123.

[3] HUQ, M.SAIFUL, HWANG, M., TEO, T.P., JANG, S., HERON, D.E., LALONDE, R.J., A dosimetric evaluation of the IAEA-AAPM TRS483 code of practice for dosimetry of small static fields in conventional linac beams and comparison with IAEA TRS-398, AAPM TG51 and TG51 addendum protocols, Medical Physics **45** (2018) 4257.

[4] INTERNATIONAL ATOMIC ENERGY AGENCY, Technical Report Series No, 398, IAEA, Vienna (2017).

[5] ALMOND, P.R., BIGGS, P.J., COURSEY, B.M., HANSON, W.F., HUQ, M. SAIFUL, NATH, R., ROGERS, D.W.O., AAPM'S TG51 protocol for clinical reference dosimetry of high-energy photon and electron beams, Medical Physics **26** (1999) 1847.

[6] McEWEN, M., DeWARD, L., IBBOTT, G., FOLLOWILL, D., ROGERS, D.W.O., SELTZER, S., SEUNTJENS, J., Addendum to the AAPM's TG-51 protocol for clinical reference dosimetry of high-energy photon beams, Medical Physics **41** (2014) 041501.

Detector Choice for Depth Dose Curves Including the Build-Up Region of Small MV Photon Fields

S. Wegener[a]
B. Herzog[a,b], **O.A. Sauer**[a]

[a]University of Wuerzburg, Radiation Oncology, Josef-Schneider-Str. 11, 97080 Wuerzburg, Germany
[b]Martin-Luther-Universität Halle Wittenberg, Institute of Physics, Von-Danckelmann-Platz 3, 06120 Halle (Saale), Germany

Email address of Corresponding Author: Wegener_S1@ukw.de

BACKGROUND

The right detector choice is an issue in all situations without charged-particle equilibrium, such as in the build-up region of photon fields. As the field size decreases, typically chosen plate-parallel ionization chambers are no longer feasible due to volume averaging effects. Alternatively, one of the numerously available small field detectors is recommended. Here, it is necessary to know how the different detectors respond as a function of field size and depth and which factors influence the signal.

METHODS

We compared depth dose curves measured with different detectors and with a special emphasis on the build-up region against the results obtained with EBT3 film. All measurements were carried out in a water phantom at a source-to-surface distance of 100 cm using a Primus accelerator at 6 MV. Each curve was normalized to the signal at 10 cm depth. Five field sizes between nominal 0.6×0.6 cm² and 10×10 cm² were chosen. Studied detectors were plane-parallel, Farmer, cylindrical and micro-ionization chambers, a microDiamond and different shielded and unshielded diodes - in total 14 detectors.

Volume averaging due to divergence, and thus larger field sizes at increasing depth, was calculated from the beam profiles recorded on film in different planes. The contribution of electron contamination to the detector signal was studied by filtering it out with a lead foil near the collimator opening. The position of the detectors at the water surface heavily influences the results. Therefore, for different ionization chambers, the effective point of measurement was determined on an individual basis. Measurements for the ionization chambers at both polarities were taken and compared.

RESULTS

EBT3 film, the Farmer chamber and the Roos type chamber yielded very similar results in the 4x4 cm² field and larger. For most detectors and at smaller field sizes, detector response deviated from the film (example see Figure 1). For small fields, Si-diodes over responded at small depths, agreeing with the trends observed in Monte Carlo simulations [1]. The details of the response heavily depended on the detector type. Shielded diodes typically required the largest corrections. The microDiamond and the smallest studied ionization chambers required the smallest corrections. Volume averaging effects for depth dose curves played a negligible role for diodes.

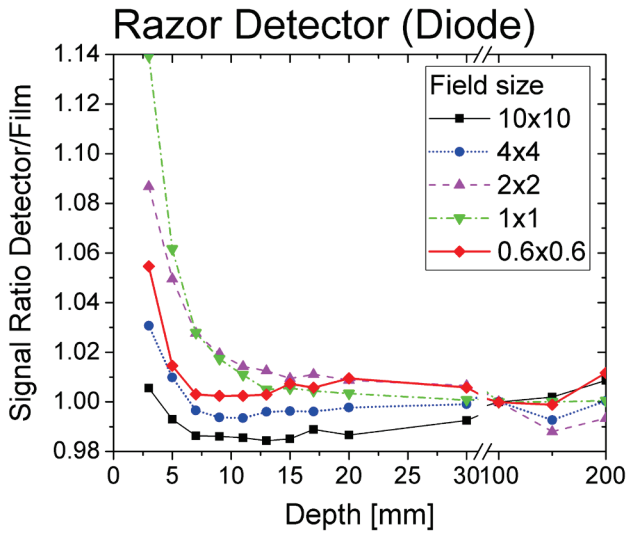

Figure 1. Ratio of the depth dose curves obtained with a diode (iba Razor Detector) and EBT3 film for different fields sizes (given in cm²).

By introducing a lead foil, the relative depth dose decreased by approximately 2% to 3% for unshielded and shielded diodes in the build-up region. This cannot account for the much larger differences observed between the curves measured with those detector types.

Small ionization chambers typically needed effective points of measurement to be shifted from the central chamber axes by less than the 0.5 or 0.6-times the radius of the active volume currently recommended in dosimetry protocols, which agrees with other conducted studies [2]. Curves obtained with small ionization chambers at different polarities deviate in the build-up region, for example by difference of 12% for the CC003 (3 mm³ volume) and 6% for the CC01 (10 mm² volume) at 3 mm depth.

CONCLUSIONS

No ideal detector for measurements in the build-up region of small photon fields was identified. Down to a field size of 4x4 cm², the Roos type chamber is suitable. At smaller sizes, the microDiamond and small ionization chambers require the smallest corrections at large depth as well as near the surface. For the diodes, the response depends heavily on the individual type of detector. For small ionization chambers, data obtained near the surface should be averaged between both polarities.

REFERENCES

[1] FRANCESCON, P. et al., “Variation of kQclin , Qmsr (fclin , f msr) for the small-field dosimetric parameters percentage depth dose, tissue-maximum ratio, and off-axis ratio”. Med Phys, 2014. **41**(10): p. 101708.

[2] TESSIER, F., KAWRAKOW, I.”Effective point of measurement of thimble ion chambers in megavoltage photon beams”. Med Phys, 2010. **37**(1): p. 96-107.

Output Correction Factors for Eight Ionization Chambers in Small Static Photon Fields

B. Casar[a]
E. Gershkevitsh[b], **I. Mendez**[a]

[a]Institute of Oncology, Zaloska 2, Ljubljana, Slovenia
[b]North Estonia Medical Centre, J. Sütiste tee 19, Tallinn, Estonia

Email address of Corresponding Author: bcasar@onko-i.si

BACKGROUND

Recently published International Code of Practice TRS-483 provides a formalism and guidance for dosimetry in small photon fields [1]. Also, it includes data for detector specific output correction factors (OCF) for a large number of detector types, among them for several ionization chambers (IC). However, TRS-483 does not provide OCFs for several ICs currently in clinical use. Therefore, the primary goal of our experimental study was to determine OCFs for eight ICs to compare them with the data from TRS-483, including OCFs for five ICs for which the data are not presented in the TRS-483 protocol. In addition, we investigated the behavior of ICs at very small field sizes below 1.0 cm, thus compiling a valuable supplement to the data set given in TRS-483.

METHODS

All measurements for the determination of field output factors (FOF) and OCFs were performed on two different linear accelerators, Elekta Versa HD™ and Varian TrueBeam™, using 6 and 10 MV photon beams with and without flattening filters (WFF and FFF). The measurement geometry consisted of an isocentric set-up with SSD = 90 cm, a depth of 10 cm and gantry at 0°. For each point measurement, 100 MU were delivered for nine square small fields with nominal side lengths of 0.5, 0.8, 1.0, 1.5, 2.0, 3.0, 4.0, 5.0 and 10.0 cm. On the Elekta linac, fields were shaped with MLC (cross-line direction) and jaws (in-line direction), while on the Varian linac they were shaped with jaws in both directions. The 10 cm field size was used as the reference for the calculation of field output factors (FOFs). Measurements using ICs and W1 plastic scintillator detector (PSD) were performed in a water phantom, while for film measurements RW3 and Virtual Water slabs were used instead.

Determination of Output Correction Factor (OCFs) was based on the FOFs obtained experimentally with two reference detectors, EBT3 radiochromic films and W1 (PSD), following a novel method published recently by our group [2]. Both sets of measured FOFs were corrected for volume averaging effect [2] and fitted by the analytical function:

$$FOF(S_{clin}) = P_{\infty}\frac{S_{clin}^{n}}{l^{n}+S_{clin}^{n}} + S_{\infty}(1 - e^{-b\cdot S_{clin}}) \qquad (1)$$

proposed by Sauer and Wilbert [3]. S_{clin} denotes equivalent square small field size (clinical field size), calculated as $S_{clin} = \sqrt{A \cdot B}$ [4]; A and B correspond to the radiation field widths (FWHM) in in-line and cross-line direction, in our case measured with EBT3 films [2].

OCFs were experimentally determined on two different types of linac for eight small (active volume V < 0.1 cm^3) ionization chambers: IBA CC04, IBA Razor IC, IBA Razor Nano Chamber (Varian linac only), PTW 31016 3D PinPoint, PTW 31021 3D Semiflex, PTW 31022

3D PinPoint, PTW 31023 PinPoint and SI Exradin A16. Calculated values for FOFs (S_{clin}) from Eq. (1) were used for the determination of detector specific OCFs as shown in Eq. (2)

$$OCF(S_{clin}) = \frac{FOF(S_{clin})}{\frac{M(S_{clin})}{M(S_{ref})}} \qquad (2)$$

$M(S_{clin})$ and $M(S_{ref})$ denote measured signals in a particular clinical and reference field, respectively. The orientation of each IC was kept with its stem perpendicular to the central beam axis, following the recommendation from TRS-483.

RESULTS

OCFs were determined on Elekta Versa HD and Varian TrueBeam linacs for seven ICs and four energies. OCFs for the Elekta linac are shown in Figure 1 as discrete values, as well as curves of the analytical function from Eq. (1). For all ICs, most significant under-response was observed for field sizes below 1.0 cm, attributed mainly to the volume averaging effect; the highest OCF values were observed for PTW 31021 3D Semiflex IC (V = 0.07 cm^3), while for IBA Razor IC (V = 0.01 cm^3) those values were the lowest for all investigated beams.

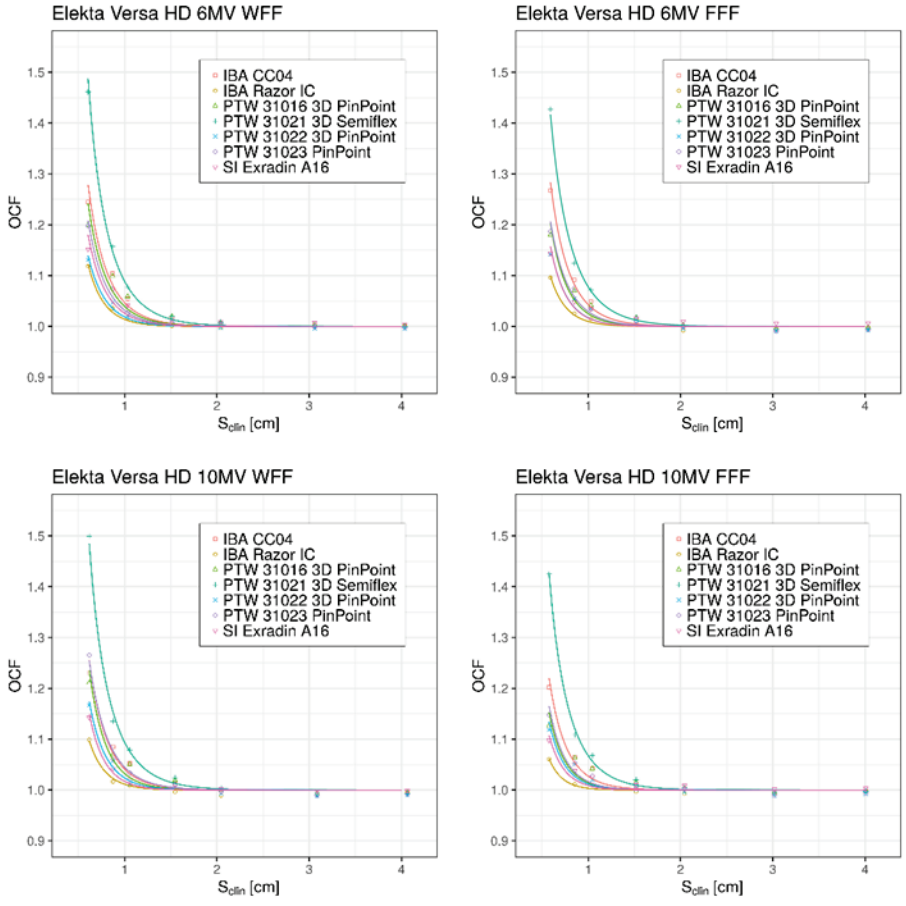

Figure 1. Detector specific output correction factors OCFs for seven ICs for four beam energies on Elekta Versa HD linac, presented as individual values/points and as curves of the analytical function proposed in the TRS-483. Measured data represent "total" OCFs and include contributions from both, volume averaging effect as well as perturbation correction factors.

CONCLUSIONS

A large set of detector specific OCFs for eight types of ICs in four beam energies was determined on two linacs. Furthermore, data for OCFs were determined also for small fields below 1.0 cm. All these data are a valuable supplement to the literature and the TRS-483 dataset.

REFERENCES

[1] PALMANS, H., ANDREO, P., HUQ, S., SEUNTJENS, J. Dosimetry of small static fields used in external beam radiotherapy: An IAEA-AAPM International Code of Practice for reference and relative dose determination. Technical Report Series No. 483. IAEA Trs483. 2017

[2] CASAR, B., GERSHKEVITSH, E., MENDEZ, I., JURKOVIĆ, S., HUQ, S. A novel method for the determination of field output factors and output correction factors for small static fields for six diodes and a microdiamond detector in megavoltage photon beams, *Med Phys*. 2018, doi: 10.1002/mp.13318

[3] SAUER, O.A., WILBERT, J. Measurement of output factors for small photon beams. *Med Phys*. 2007;34(6):1983-1988. doi:10.1118/1.2734383

[4] CRANMER-Sargison, G., Charles, P.H., Trapp, J. V., Thwaites, D.I. A methodological approach to reporting corrected small field relative outputs. *Radiother Oncol*. 2013;109(3):350-355. doi:10.1016/j.radonc.2013.10.002.

Reference Dosimetry of a New Biology-Guided Radiotherapy (BgRT) System Following the IAEA TRS-483 CoP

L. Mirzakhanian[a]
R. Bassalow[b], D. Zaks[b], C. Huntzinger[b], J. Seuntjens[a]

[a]McGill University, Medical Physics Unit, Montreal, QC H4A 3J1
[b]RefleXion Medical, 25821 Industrial Blvd, Hayward, CA, 94545

Email address of Corresponding Author: lalageh.mirzakhanian@mail.mcgill.ca

BACKGROUND

The design of the RefleXion biology-guided radiotherapy (BgRT) system limits the maximum field size to 2 cm or 3 cm in the IEC 61217 Y dimension at the source-to-axis distance (SAD) of 85 cm. The beam is nominally 6 MV and flattening filter free (FFF). The closest clinically used field size to the conventional reference field in this system is 10 x 2 cm^2 at the isocenter. The 10 x 2 cm^2 field size does not meet the lateral charged particle equilibrium (LCPE) condition of the machine-specific reference (*msr*) field introduced in the IAEA TRS-483 Code of Practice (CoP) [1]. Therefore, the TRS-483 cannot be directly used for the calibration of this system. In this study, two approaches are proposed for reference dosimetry of the BgRT system and the results of two methods are compared.

METHODS

First approach: This is the most common approach suggested in the TRS-483[1]. The dose to water in the *msr* field ($D_{w,Qmsr}^{fmsr}$) is determined according to the equation:

$$D_{w,Qmsr}^{fmsr} = M_{Qmsr}^{fmsr} N_{D,w,Q0}^{fref} k_{Qmsr,Q0}^{fmsr,fref}.$$

Since the 10 x 2 cm^2 field size of the BgRT is not a *msr*, we have generalized this methodology and referred to this field as "A" instead of "*msr"*. In this study, the mean absorbed dose to water over a small volume and to the sensitive volume of two chambers (Exradin A1SL and A26) are calculated for both setups: the BgRT and reference Co^{60} ($D_{cav,QA}^{fA}$ and $D_{cav,Q0}^{fref}$ respectively). The generic correction factors ($k_{QA,Q0}^{fA,fref}$) are determined using the following equation:

$$k_{QA,Q0}^{fA,fref} = \left(D_{w,QA}^{fA}/D_{cav,QA}^{fA}\right)/\left(D_{w,Q0}^{fref}/D_{cav,Q0}^{fref}\right)$$

where the absorbed doses are calculated using Monte Carlo (MC) techniques based on detailed chamber and accelerator source models.

Second approach: This approach is recommended in the TRS-483 when the MC correction factors are not available. The $D_{w,Qmsr}^{fmsr}$ is determined using this equation:

$$D_{w,Qmsr}^{fmsr} = M_{Qmsr}^{fmsr} N_{D,w,Q0}^{fref} k_{Q,Q0}^{fref} k_{Qmsr,Q}^{fmsr,fref}.$$

The $k_{Qmsr,Q}^{fmsr,fref}$ corrects for the difference between the response of chamber in a 10 x 10 cm^2 field with beam quality Q using the same machine as *msr* field and the response of chamber in the *msr* field with beam quality Q_{msr} [1]. $k_{Q,Q0}^{fref}$ is the beam quality correction factor for which

the beam quality Q of the hypothetical 10 x 10 cm^2 field and ultimately the square equivalent field need to be determined. Knowing the Q, the $k_{Q,Q0}^{fref}$ can be looked up in standard reference dosimetry protocols. However, this methodology cannot be directly used for the calibration of the BgRT system, since the data provided in the TRS-483 for determining equivalent field size and the equation for deriving the beam quality specifier (equations 28-29 of the TRS-483) are limited to 3 and 4 cm fields respectively. Additionally, the tabulated $k_{Q,Q0}^{fref}$ values are provided only for larger reference chambers not suitable for small fields. In this study, we extended the IAEA-AAPM methodology to 2 cm field size by providing the data for the equivalent square field and deriving the beam quality specifier following the same methodology described in the TRS-483. We calculate the $k_{Q,Q0}^{fref}$ values analytically for our beam quality specifier and chambers used, using the data in TRS-398[2]. As per TRS-483, the volume averaging and water to air stopping power ratio corrections are also applied to the $k_{Q,Q0}^{fref}$ values to correct for the differences between the WFF (with flattening filter) and FFF beams.

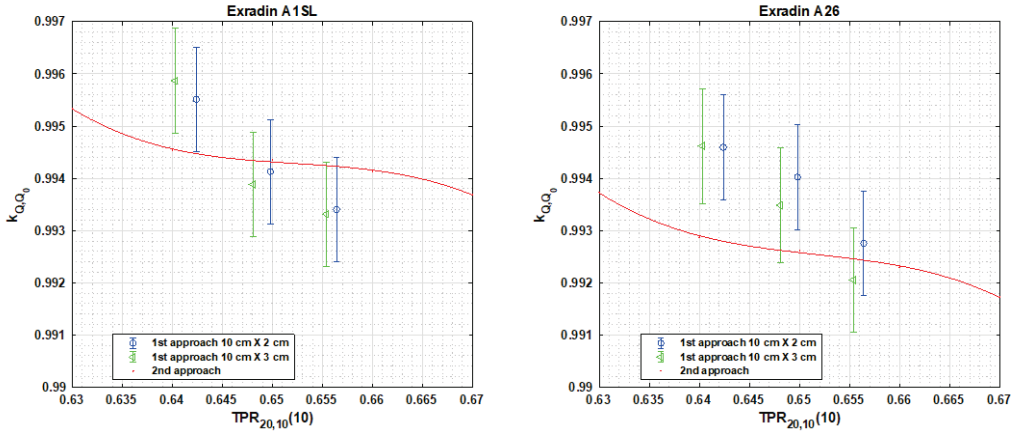

Figure 1. The corrections for A1SL and A26 as a function of $TPR_{20,10}(10)$

RESULTS

The equivalent square fields size for the BgRT system is found to be 3.6 cm and 4.8 cm for the 10 x 2 cm^2 and 10 x 3 cm^2 fields respectively. It is verified that equation 28 of TRS-483 can be used to derive the $TPR_{20,10}(10)$ from $TPR_{20,10}(S)$ with a maximum difference of 1.3% for the 2 cm field size. The 1.3% difference in the $TPR_{20,10}(10)$ has a negligible impact (0.02% on the correction for Exradin-A1SL). The correction factors for two chambers as a function of $TPR_{20,10}(10)$ calculated using both approaches are shown in figure 1 and summarized in Table 1 for the nominal beam qualities.

Table 1. The corrections for two chambers as a function of $TPR_{20,10}(10)$

Chamber type	Field size (cm^2)	$TPR_{20,10}(10)$	$k_{QA,Q0}^{fA,fref}$ (1st approach)	$k_{Q,Q0}^{fref}$ (2nd approach)	Difference app 2-1 (%)
Exradin-A1SL	10 x 2	0.6498	0.9941	0.9944	0.03%
Exradin-A1SL	10 x 3	0.6481	0.9939	0.9944	0.05%
Exradin-A26	10 x 2	0.6498	0.9940	0.9926	0.14%
Exradin-A26	10 x 3	0.6481	0.9935	0.9927	0.08%

CONCLUSIONS

Even with the condition of LCPE not met in the fields clinically available on the BgRT system, depending on the detector used, MC-based correction factors can be applied for the purpose of clinical reference dosimetry. We found that these factors are in excellent agreement (to within 0.14%) with values following the *msr*-field based calibration procedure suggested in TRS-483.

REFERENCES

[1] H. Palmans, P. Andreo, K. Christaki, M. Huq, and J. Seuntjens, IAEA TRS 483, (2017).
[2] P. Andreo, D. T. Burns, K. Hohlfeld, M. S. Huq, T. Kanai, F. Laitano, V. Smyth, and S. Vynckier, IAEA TRS 398 (2000).

Uncertainty Contributors in the Dosimetry of Small Static Fields

Z. Msimang[a]
D. van der Merwe[b], **N. Maphumulo**[c]

[a]National Metrology Institute of South Africa, Scientia 627-Jr, Pretoria, Meiring Naude Rd, Pretoria, 0184
[b]Wits University, 1 Jan Smuts Ave, Johannesburg, 2000
[c]Charlotte Maxeke Johannesburg Academic Hospital, Jubilee Rd, Parktown, Johannesburg, 2196

Email address of Corresponding Author: zmsimang@nmisa.org

BACKGROUND

Estimating measurement uncertainties for measurement capabilities is something that is standard practice for primary and secondary standard laboratories who have a quality management system following ISO/IEC 17025 [1] standard. This is not usually the case for measurements performed at hospitals. Estimating and publishing of uncertainties is unfortunately not a common practice for routine measurements in hospitals. This is also evident in the data published by several authors for small static fields in which there is a lack of estimation of uncertainties for several steps in the determination of correction factors [2].

The ICRU 83 [3] report recommends that for reporting purposes, as part of clinical trials, publications, etc., the uncertainties associated with the relevant quantities and parameters should be estimated and presented [3, 4]. There is still some confusion as to how uncertainties are estimated and misunderstanding of the difference between uncertainties and accuracy.

METHODS

The estimation of measurement uncertainties involves establishing an uncertainty budget and evaluating type A and type B uncertainties [5, 6, 7, 8]. Type A standard uncertainties are those evaluated by statistical means of a measured quantity for defined conditions [6, 7, 8]. Type B standard uncertainties are those defined by means other than statistical evaluation of a series of observations [6, 7, 8]. The basis of an uncertainty budget is the measurement model used for the calculation of the measurand. The formalism for the determination of absorbed dose to water for small static fields, using an ionization chamber that has been calibrated for absorbed dose to water in a 10 cm x 10 cm field size under reference conditions, using generic beam qualities published, is defined by Alfonso et al and IAEA TRS 483 as [2, 9]:

$$D_{w,Q_{msr}}^{f_{msr}} = M_{Q_{msr}}^{f_{msr}} N_{D,w,Q_0}^{f_{ref}} k_{Q_{msr}Q_0}^{f_{msr}f_{ref}} \quad (1)$$

The field output factor is given by [2]:

$$\Omega_{Q_{clin}Q_{msr}}^{f_{clin}f_{msr}} = \frac{M_{Q_{clin}}^{f_{clin}}}{M_{Q_{msr}}^{f_{msr}}} k_{Q_{clin},Q_{msr}}^{f_{clin},f_{msr}} \quad (2)$$

Each quantity in equations (1) and (2) contributes to the measurement uncertainty together with the associated covariances, applied probability distribution and degrees of freedom [6, 7, 8].

Positional uncertainties associated with the setting of the collimator, the determination of the beam central axis, and the accuracy of the scanning system were evaluated through

measurements using several detectors for various field sizes. Their contribution to the $M_{Q_{msr}}^{f_{msr}}$, $k_{Q_{msr}Q_0}^{f_{msr}f_{ref}}$ and $\Omega_{Q_{clin}Q_{msr}}^{f_{clin}f_{msr}}$ were evaluated. Uncertainty contributions from cross calibrations performed using the daisy chain methodology were also evaluated. The multileaf collimators were recalibrated at specified intervals, and the uncertainty contribution caused by this calibration was evaluated. Measurements were performed using an automated beam scanning system and the machine used was a Siemens Primus linear accelerator operated at 6 MV.

RESULTS

For reference measurements, the most significant standard uncertainty arose from the traceability, including the calibration of the reference instrument and the process of daisy chaining to the required small field. For the relative measurements, the standard uncertainty associated with the determination of field output factors contribute a significant uncertainty and this is dependent on the leaf calibration, detector type and its orientation. They each range from 0.5 % to 1 % depending on the detector used.

CONCLUSIONS

It is critical to identify uncertainty contributors and the risks they contribute to the measurement chain. This gives confidence in a measurement and the dosimetric accuracy at which dose can be delivered. All contributors to the uncertainty of measurements need to be identified so that measures can be taken to minimize the risk they may impose in dose delivery.

REFERENCES

[1] INTERNATIONAL ORGANISATION FOR STANDARDISATION, General requirements for the competence of testing and calibration laboratories, ISO/IEC 17025, Geneva (2017).

[2] INTERNATIONAL ATOMIC ENERGY AGENCY, Dosimetry of small static fields used in external beam radiotherapy: an IAEA-AAPM International Code of Practice for reference and relative dose determination, TRS 483, Vienna (2017).

[3] INTERNATIONAL COMMISSION ON RADIATION UNITS AND MEASUREMENTS, Prescribing, Recording, and Reporting Intensity-Modulated Photon-Beam Therapy (IMRT ICRU Report 83). Bethesda, MD; 2010.

[4] Debbie van der Merwe, Jacob Van Dyk, Brendan Healy, Eduardo Zubizarreta, Joanna Izewska, Ben Mijnheer & Ahmed Meghzifene (2017) Accuracy requirements and uncertainties in radiotherapy: a report of the International Atomic Energy Agency, Acta Oncologica, 56:1, 1-6, DOI: 10.1080/0284186X.2016.1246801.

[5] INTERNATIONAL ATOMIC ENERGY AGENCY, Accuracy requirements and uncertainties in radiation therapy, Vienna (2016).

[6] JOINT COMMITTEE FOR GUIDES IN METROLOGY, Evaluation of Measurement Data — Guide to the Expression of Uncertainty in Measurement, JCGM 100:2008, Paris (2008).

[7] JOINT COMMITTEE FOR GUIDES IN METROLOGY, Evaluation of Measurement Data —– An introduction to the "Guide to the expression of uncertainty in measurement", JCGM 104, Paris (2009).

[8] JOINT COMMITTEE FOR GUIDES IN METROLOGY, International Vocabulary of Metrology – Basic and General Concepts and Associated Terms (VIM 3rd edition) JCGM 200:2012.

[9] ALFONSO, R., et al., A new formalism for reference dosimetry of small and nonstandard fields, Med. Phys. 35 (2008) 5179–5186.

Small Field Photon Beams Audit Pilot Study: Preliminary Results

K. Repnin[a]
P. Wesolowska, K. Christaki, A. Baumgartner, P. Kazantsev, J. Izewska

[a]International Atomic Energy Agency, Dosimetry and Medical Radiation Physics Section, Vienna, Austria.

Email address of Corresponding Author: p.wesolowska@iaea.org

BACKGROUND

Various radiotherapy techniques such as intensity modulated radiation therapy (IMRT), stereotactic radiotherapy (SRT) and radiosurgery (SRS) utilize small photon fields and require the highest level of accuracy in the dose delivery. At the same time, dose measurements in small photon fields have higher uncertainty therefore special dosimetry procedures are required. An IAEA/AAPM code of practice for small static fields (IAEA TRS483) was recently published [2] and tested within an IAEA co-ordinated research project. Taking this into account, an audit methodology for small photon beams was developed by the IAEA and tested in a pilot study. The results are presented here.

METHODS

This pilot audit was organized in three rounds (the third one is still ongoing), in total participants from 14 countries took part. The audit was performed with two detectors; radiophotoluminescent dosimeters (RPLDs) - model GD302M (AGC Techno Glass Co., Japan) used in the high dose mode (active area from 0.6 mm diameter), which were commissioned for measurements in small fields and EBT-3 Gafchromic films (Ashland, USA). A set of dosimeters sent to participants consisted of 13 RPLDs (3 dosimeters per field, 1 background dosimeter) for the dose measurements and 12 pieces of Gafchromic films for profile measurements as well as for positioning checks. Measured doses and profiles were compared with the Treatment Planning System (TPS). Irradiations of dosimeters were performed in the 100 cm SSD geometry for linacs and 80 cm SAD for CyberKnife at 10 cm depth in water using specially designed holders. The position of the holder was set to the center of the beam using film and this was checked before and after the irradiation session. RPLDs were irradiated with the dose of 4 Gy using four field sizes ranging from the machine specific reference field size to 1×1 cm^2 (or 1 cm diameter for circular fields) but the profiles were only measured for 1×1 cm^2 and 2×2 cm^2 fields (1 cm and 2 cm diameter) using film. RPLDs and films were analyzed at the IAEA Dosimetry Laboratory. The beam profiles were evaluated at 20%, 50%, 80 % of the maximum dose. Field sizes measured with the film were compared to dose calculation from TPS for in-plane and cross-plane beam profiles.

RESULTS

Dosimeters irradiated with 20 beam energies at 8 countries were analyzed so far. Three different linacs types with the following energies were used: 6 MV WFF (7), 6 MV FFF (3), 10 MV WFF (2) and 10 MV FFF (4). In addition, four CyberKnife units were audited; two equipped with cones, one with Iris collimation system and one with MLC. The analysis of films used for dosimeter positioning verification showed that the irradiation set up in approximately 80% of cases was accurate to within 1 mm.

The ratios of the IAEA measured dose (D_{meas}) and the TPS (D_{TPS}) calculated dose are given in Figure 1. As can be seen, the results for fields 2×2 cm^2 and larger are within 3%, whereas for

1×1 cm^2 field the results show greater scatter. The standard deviation of the results for 1×1 cm^2 field is 2.4% while for the larger field sizes it is 1.1%. No differences related to beam energy, flattening filter or collimation system were observed.

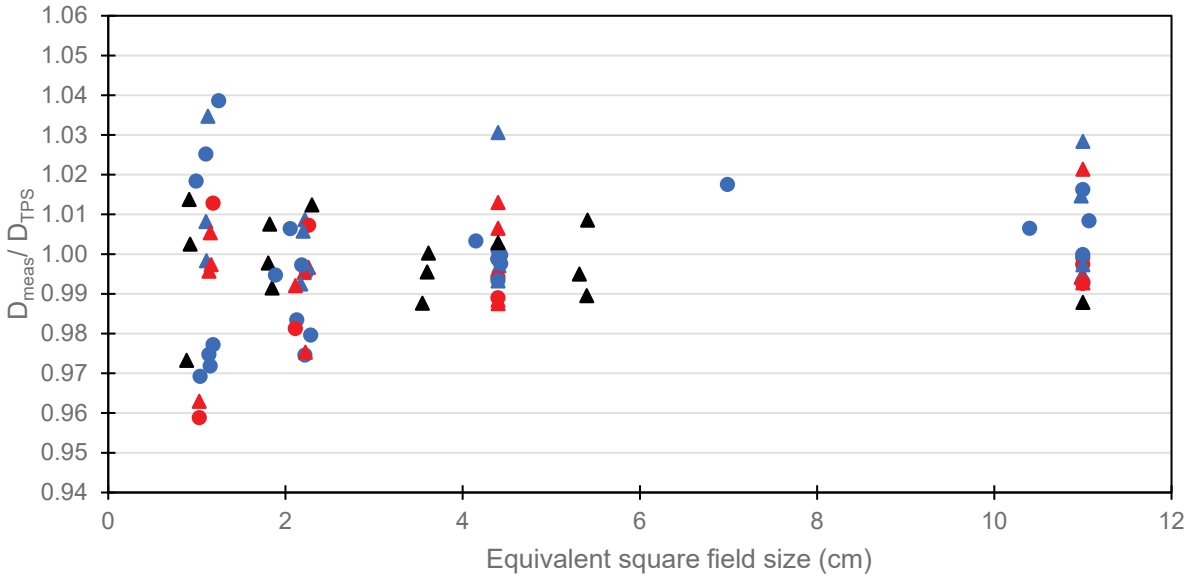

Figure 1. D_{meas}/D_{TPS} against field size for 20 audited beams energies. Circles represent beams with flattening filter (WFF), triangles – flattening filter free (FFF); blue symbols represent 6 MV beams, red – 10 MV beams, black symbols are CyberKnife beams.

The comparison of the calculated and measured dose profiles showed the field size differences lay within 3 mm acceptance limit as suggested in a previous study for 2×2 cm^2 and larger fields [1] for all except one institution. Moreover, only 15% deviations were in 1-3 mm range, with 2.4% deviations higher than 3 mm, mainly for 80% and 20% dose levels for 1×1 cm^2 and 2×2 cm^2 field sizes. Almost all deviations were found for standard linacs in the cross-plane direction, suggesting suboptimal MLC modeling.

It is worth mentioning that three participants (total of seven beams) only partially followed the audit instructions and their results were excluded from this analysis.

CONCLUSIONS

The pilot study results showed that the audit methodology developed by the IAEA is a suitable tool for detecting dosimetric errors in small photon fields. It also proves that clinical commissioning of small photon beams is a demanding procedure.

ACKNOWLEDGMENT

I would like to thank all pilot study participants for their contribution.

REFERENCES

[1] IZEWSKA, J., et al., Testing the methodology for dosimetry audit of heterogeneity corrections and small MLC-shaped fields: Results of IAEA multi-center studies, Acta Oncologica 55 (2016) 909-916.

[2] IAEA, Technical Reports Series 483. Dosimetry of Small Static Fields Used in External Beam Radiotherapy, IAEA, Vienna (2017).

On the Implementation of the Plan Class-Specific Reference Field Concept Using Multidimensional Clustering of Plan Features

V. Desai[a]
Z. Labby[b], L. DeWerd[a], W. Culberson[a]

[a]Department of Medical Physics, School of Medicine and Public Health, University of Wisconsin-Madison, Madison, WI 53705
[b]Department of Human Oncology, School of Medicine and Public Health, University of Wisconsin-Madison, Madison, WI 53705

Email address of Corresponding Author(s): vkdesai@wisc.edu

BACKGROUND

In 2008, the IAEA in cooperation with the AAPM released a formalism for dosimetry in nonstandard fields [1]. This formalism introduced the concept of the intermediate plan class-specific reference (pcsr) field where similarly modulated plans could theoretically be corrected using a single correction factor derived from a representative field. The implementation of the pcsr-field concept as described in the 2008 formalism has proven difficult due to a lack of quantitative guidelines. The recent IAEA Technical Report Series (TRS) number 483 further concedes that the large quantities of data required to investigate potentially representative fields have not yet been determined [2]. To help bridge this gap in knowledge, this work utilizes a multidimensional feature analysis and clustering analysis of numerous modulated treatments to determine if distinct plan clusters may help guide the creation of representative plans.

METHODS

A total of 627 modulated clinical plans originally delivered on a TrueBeam™ STx linear accelerator were investigated. These plans were comprised of 2180 beams and 193161 control points. 22 complexity metrics [3-10] were analyzed for each beam and stored in a database. Because the various features investigated involved different scales and units, all features were standardized prior to any clustering analysis. To reduce the dimensionality of the data, a number of principal components (PC) [11] explaining 95% of the total variance of the dataset were also determined. The optimal number of clusters was not known *a priori* so a series of k clusters ranging from 2 to 20 was evaluated using Caliński-Harabasz criterion values [12]. Silhouettes [13] were then used to evaluate inter- and intra- cluster variance to assess their distinction from one another.

RESULTS

The optimal number of clusters for the dataset investigated according to the Caliński-Harabasz criterion values was three with rapid falloff for successively higher numbers of clusters. Across 22 features evaluated in this work for 2180 modulated beams, 10 principal components were required to explain 95% of the total variance. A k-means objective algorithm seeking three clusters was then used on the first 10 principal components of the multidimensional data. For the ease of visualization, Figure 1 illustrates the results of the k-means clustering projected to only the first two of ten total principal components. The silhouettes of these three determined clusters demonstrated a high degree of overlap and provided little confidence that the clusters were in fact distinct.

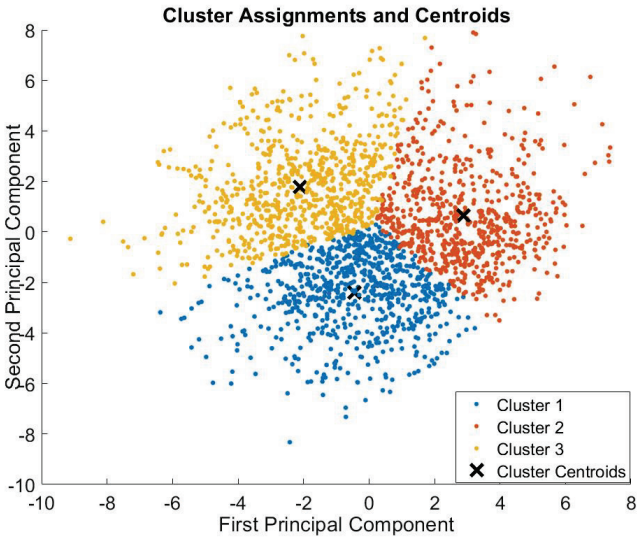

Figure 1. A 2D plot of the first 2 principal components (explaining 58.8% of the total variance) of the 2180 datapoints evaluated in this work along with classifications indicating which cluster each data point was assigned to.

CONCLUSIONS

The pcsr concept relies on an underlying distinction between modulated beams. The cluster analysis demonstrated that no intuitive plan clusters existed in the multidimensional space evaluated, indicating the difficulty in creating a truly representative plan. Stratification among the features investigated does exist likely due to the overwhelming variability within modulated beams but the correlation of detector-specific corrections with the complexity metrics remains unknown. This work indicates that it may be more useful to consider corrections on a case-by-case basis rather than attempting to use representative fields for the determination of absolute dose in nonstandard fields.

REFERENCES

[1] ALMOND PR, BIGGS PJ, COURSEY BM, et al. AAPM's TG-51 protocol for clinical reference dosimetry of high-energy photon and electron beams. *Medical physics.* 1999;26(9):1847-1870.

[2] IAEA T. *483. Dosimetry of small static fields used in external beam radiotherapy: an IAEA-AAPM International Code of Practice for reference and relative dose determination.* Technical Report Series.

[3] DU W, CHO SH, ZHANG X, HOFFMAN KE, KUDCHADKER RJ. Quantification of beam complexity in intensity-modulated radiation therapy treatment plans. *Medical physics.* 2014;41(2).

[4] MASI L, DORO R, FAVUZZA V, CIPRESSI S, LIVI L. Impact of plan parameters on the dosimetric accuracy of volumetric modulated arc therapy. *Medical physics.* 2013;40(7).

[5] McNIVEN AL, SHARPE MB, PURDIE TG. A new metric for assessing IMRT modulation complexity and plan deliverability. *Medical physics.* 2010;37(2):505-515.

[6] PARK JM, PARK S-Y, KIM H, KIM JH, CARLSON J, YE S-J. Modulation indices for volumetric modulated arc therapy. *Physics in medicine and biology.* 2014;59(23):7315.

[7] PARK JM, PARK S-Y, KIM H. Modulation index for VMAT considering both mechanical and dose calculation uncertainties. *Physics in medicine and biology.* 2015;60(18):7101.
[8] PARK SY, KIM IH, YE SJ, CARLSON J, PARK JM. Texture analysis on the fluence map to evaluate the degree of modulation for volumetric modulated arc therapy. *Medical physics.* 2014;41(11).
[9] WEBB S. Use of a quantitative index of beam modulation to characterize dose conformality: illustration by a comparison of full beamlet IMRT, few-segment IMRT (fsIMRT) and conformal unmodulated radiotherapy. *Physics in medicine and biology.* 2003;48(14):2051.
[10] ZYGMANSKI P, KUNG J. Method of identifying dynamic multileaf collimator irradiation that is highly sensitive to a systematic MLC calibration error. *Medical physics.* 2001;28(11):2220-2226.
[11] PEARSON KJTL, Edinburgh,, Magazine DP, Science Jo. LIII. On lines and planes of closest fit to systems of points in space. 1901;2(11):559-572.
[12] CALIŃSKI T, HARABASZ JJCiS-t, Methods. A dendrite method for cluster analysis. 1974;3(1):1-27.
[13] ROUSSEEUW PJ. Silhouettes: a graphical aid to the interpretation and validation of cluster analysis. *Journal of computational and applied mathematics.* 1987;20:53-65.

Computational Dosimetry

Determination of W_{air} in High-Energy Clinical Electron Beams Using Aluminium Detectors.

A. Bourgouin[a,b]
M. McEwen[b]

[a]Carleton University, 1125 Colonel By Dr, Ottawa, ON K1S 5B6
[b]National Reasearch council of Canada, 1200 Montreal Rd, Ottawa, ON K1A 0R6

Email address of Corresponding Author: alexandrabourgouin@cmail.carleton.ca

BACKGROUND

The recent report on dosimetric key value (ICRU 90) reaffirmed the accepted value of Wair, to be a constant, above 10 keV, with a value of 33.97 ± 0.12 eV. A recent publication [1] has showed a possible energy dependence and to investigate this further, an experiment was carried out [2] reproducing the Domen and Lamperti investigation [3]. Although the experiment yielded a value consistent with the ICRU90 value, it highlighted the problems of using graphite detectors [2], particularly related to density variations. The goal of this project is to obtain additional experimental data in high-energy electron beams to determine Wair using pure aluminium.

METHODS

To measured W_{air}, which is the quotient of charge released in dry air, Q_{air}, and energy deposited in this mass, $D_{air} \cdot m_{air}$, an ion chamber and a calorimeter have been designed and constructed using pure aluminum. The ionometric (Q_{air}), and calorimetric (D_{al}) measurements are combined with a Monte Carlo dose calculation (effectively a stopping power ratio, SPR) to obtain W_{air}:

$$W_{air} = \frac{D_{air} \cdot m_{air}}{Q_{air}} = \frac{D_{al}}{Q_{air}/m_{air}} \left(\frac{D_{air}}{D_{al}}\right) = \frac{D_{al}}{Q_{air}/m_{air}} SPR_{al}^{air} \quad (1)$$

The quantity m_{air} in equation (1) means that the volume of the ion chamber must be determined as for a cavity standard, and both mechanical and capacitive measurements were used. The calorimeter used was an open-to-atmosphere design using calibrated NTC thermistors in an AC Wheatstone Bridge to determine the radiation-induced temperature rise, and thus the dose to aluminium. Measurements were made in electron beams produced by the Elekta Precise linear accelerator at the NRC facility. The primary electron beam energy were 8, 12, 18 and 22 MeV with a range of aluminum buildup thickness between 0.0 to 1.0 cm to provide a range of electron energies at the point of measurement. The irradiation time was also varied as was the source-detector distance, to further investigate geometrical and thermal influence quantities.

RESULTS

Prior to the measurements described above, the ion chamber was extensively tested to demonstrate it met the requirements of a reference-class detector. Results for ion recombination, polarity and leakage current were as expected. The type A uncertainty for a series of calorimeter runs at a dose-rate of 3 Gy min^{-1} was consistent with literature values and analysis of temperature-time plots indicates that thermal isolation of the core was superior to the previous graphite calorimeter design. At this time, it has not been possible to carry out the necessary Monte-Carlo simulations to derive the theoretical dose ratio (D_{air}/D_{al}), so mono-

energetic mass stopping powers have been substituted in equation 1. This is a significant simplification but is useful as a first step in analyzing the data (Table 1).

Table 1. Radiation and buildup set-up for all different configurations with associated mass stopping power ratios and W_{air} values calculated. Uncertainties shown are only type A.

Nominal Energy (MeV)	Total Al. thickness (cm)	Energy at cavity (MeV)	SPR	W_{air} value (eV)	diff. with ICRU(%)
8	0.194	6.59	1.1300	31.1 ± 0.02	8%
	0.392	5.62	1.1300	31.5 ± 0.02	7%
	0.591	4.65	1.1300	31.9 ± 0.05	6%
12	0.194	10.16	1.1246	30.2 ± 0.02	11%
	0.392	9.10	1.1271	30.3 ± 0.02	11%
	0.693	7.50	1.1299	30.8 ± 0.03	9%
18	0.194	14.99	1.1065	28.9 ± 0.07	15%
	0.392	13.82	1.1109	29.2 ± 0.04	14%
	0.591	12.05	1.1175	29.4 ± 0.06	13%
	0.693	9.11	1.1271	30.1 ± 0.07	11%
22	0.194	19.11	1.0900	28.1 ± 0.05	17%
	0.392	17.85	1.0947	28.4 ± 0.11	16%
	0.591	15.95	1.1027	28.7 ± 0.02	15%
	0.693	12.76	1.1159	29.3 ± 0.09	14%

There is a significant energy dependence of the results and all the values are significantly lower than the current recommended value. Using aluminium is advantageous since it is an elemental material with no significant crystalline structure but the higher atomic number means that the fluence perturbation in electron beams could be significant and explain the deviations seen in the final column. Monte Carlo calculations, reproducing the entire geometry of the experiment will show the magnitude of this effect.

CONCLUSIONS

Although initial measurements with the aluminium ionization chamber and calorimeter indicate expected performance, preliminary analysis of the data yield a value for W_{air} different from recommended data. Further Monte Carlo and thermal simulations are required to investigate this further and additional measurements at higher electron beam energies are planned.

REFERENCES

[1] TESSIER F, COJOCARU CD, ROSS CK. Extracting W air from the electron beam measurements of Domen and Lamperti. Med Phys 2018;45(1):370–81.

[2] BOURGOUIN A, COJOCARU C, ROSS C, MCEWEN M. Investigation of the energy dependence of W air in high energy electron beams. 2018.

[3] DOMEN SR, LAMPERTI PJ. Comparisons of calorimetric and ionometric measurements in graphite irradiated with electrons from 15 to 50 MeV. Med Phys 1976;3(5):294–301.

Impact of Different Theoretical Models in the Calculation of Compton Mass Energy-Transfer Coefficients

X. J. Wang[a]
B. Miguel[b], J. Seuntjens[a], J. M. Fernández-Varea[c]

[a]McGill University, 3600 University, H3A 2T8, Montréal, Québec, Canada
[b]Universidad Politécnica de Cartagena, Paseo Alfonso XIII 44, E-30203 Cartagena, Spain
[c]Universitat de Barcelona, Diagonal 645, E-08028 Barcelona, Catalonia, Spain

Email address of Corresponding Author: xiaoya.wang@mail.mcgill.ca

BACKGROUND

Basic photon interaction data such as mass energy-transfer and mass energy-absorption coefficients for dosimetric purposes require as a main component the incoherent scattering energy-transfer fractions [1]. The simplest approach for calculating incoherent scattering cross sections is the Klein-Nishina (KN) model, in which the photon is scattered by a free electron initially at rest. As an improvement on KN, a well-known and frequently-used approximation is the Waller-Hartree (WH) model which accounts for binding effects approximately through the incoherent scattering function, but which neglects the spread in energy of photons scattered at a given angle. The relativistic impulse approximation (RIA) incorporates both binding effects and Doppler broadening and yields an expression for the DDCS differential in outgoing photon angle and energy. The key ingredient to the calculation of the RIA cross sections is the Compton profile (CP) of each atomic or molecular orbital, which is computed from the corresponding linear momentum distribution. The atomic CPs typically used are from the tabulation of Biggs et al [2].

Seltzer [3] derived mass energy-absorption coefficients for elements and compounds which used the WH model for Compton binding effects. In addition, interaction coefficients for compounds used in dosimetry were modeled using an independent-atom approach.

In this work we investigated for three materials of dosimetric interest (air, water, and carbon) the impact of the use of a molecular CP on the Compton energy-transfer cross section derived using the RIA. We also studied the difference between the RIA and the WH approach to modelling binding effects. The new energy-transfer cross sections are relevant for μ_{tr}^{C}/ρ values in the tens of keV range, where for these materials Compton becomes dominant.

METHODS

We calculated Compton cross sections within the RIA [4], which includes relativistic effects. The CPs were integrated from momentum densities obtained through self-consistent Hartree-Fock calculations, with wave functions expanded in a cc-pVTZ Gaussian basis set [5]. We performed the RIA calculations employing both molecular and atomic CPs in order to quantify the effect of using more accurate CPs to describe molecules. The atomic and molecular binding energies were taken from tabulated experimental data.

It should be noted that in our calculations of mass energy-transfer coefficients, we neglected for now the emission of characteristic x-rays in the relaxation process after the Compton interaction, as the magnitude of this effect is very small for low-*Z* atoms.

RESULTS

Figure 1 shows the Compton component of the mass energy-transfer coefficients for air and water calculated in the different formalisms discussed above, with insets showing eachμ_{tr}^{C}/ρnormalized by the$\mu_{tr}^{C}/\rho$for KN. Both RIA curves (molecular and atomic) are significantly closer to the KN mass energy-transfer coefficients than the WH model. The latter can differ by a large amount from the other models in the tens of keV range (e.g. ~6-10% at 20 keV).

We find that there is very little difference between the RIA with atomic and molecular CPs, thus the RIA does not seem to be particularly sensitive to the specific shape of the CPs. However, it can be slightly more sensitive to the choice of binding energies. Nevertheless, by far the biggest impact comes from the type of formalism which is employed.

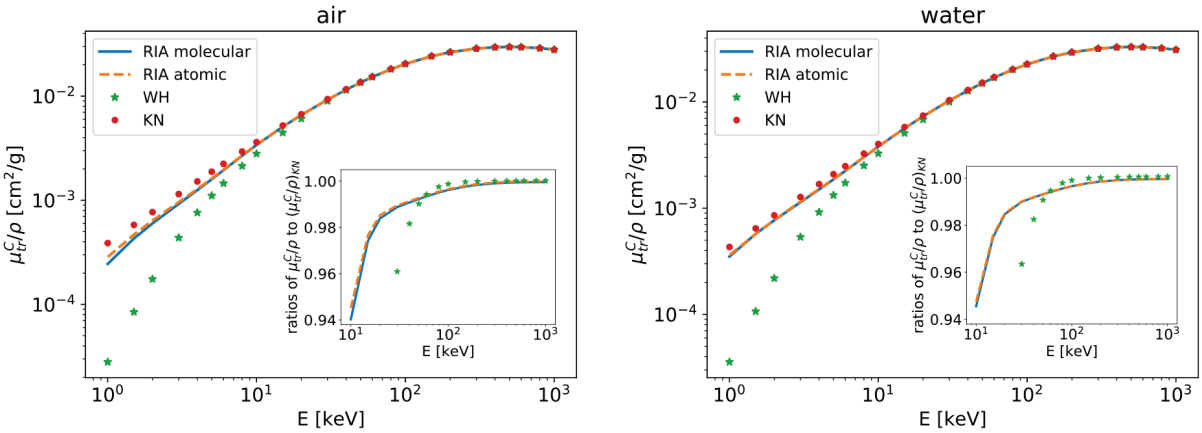

Figure 1. Mass energy-transfer coefficients for air (left) and water (right) calculated within KN, WH, and RIA (atomic & molecular CPs). The insets show data normalized to KN μ_{tr}^{C}/ρ.

CONCLUSIONS

The RIA using a variety of different CPs is always much closer to KN than to WH. In the immediate future we will continue with the main goal of this project, which is to determine the differences in the mass energy-absorption coefficient$\mu_{en}/\rho$from using the various Compton cross sections. We will incorporate fluorescence emissions and radiative losses, and include all other relevant photon interactions, to fully quantify the dosimetric impact.

REFERENCES

[1] ICRU Report 90: Key Data for Ionizing-Radiation Dosimetry: Measurement Standards and Applications, Oxford University Press, London, UK (2016).
[2] BIGGS, F., MENDELSOHN, L.B., and MANN, J.B., Hartree-Fock Compton profiles for the elements, At. Data Nucl. Data Tables 16, 201-309 (1975).
[3] SELTZER, S.M., Calculation of photon mass energy-transfer and mass energy-absorption coefficients, Rad. Res. 136, 147-170 (1993).
[4] RIBBERFORS, R. and BERGGREN, K.-F., Phys. Rev. A 26, 3325-3333 (1982).
[5] MIGUEL, B. and GARCÍA DE LA Vega, J.M., Influence of electronic correlation in monoelectronic density in p-space, Theor. Chem. Account 118, 723-732 (2007).

Ionization Quenching in Organic Plastic Scintillators for Particle Dosimetry

J. B. Christensen
C. E. Andersen

Center for Nuclear Technologies, Technical University of Denmark, Roskilde, Denmark

Email address of Corresponding Author: jepb@dtu.dk

BACKGROUND

Organic plastic scintillators are attractive for particle dosimetry due to a sub-mm size, prompt response, and a good water equivalence. However, the beam response curve measured with a scintillator deviates from that of an ideal detector. The scintillator measured response exhibits a non-linear signal reduction–termed ionization quenching–as the linear energy transfer (LET) increases. Ionization quenching is a common phenomenon in solid state dosimetry and is traditionally corrected with a semi-empirical model [1] relying on experimentally determined quenching parameters depending on the scintillator itself as well as the beam quality. The model has recently been shown to break down even in low-energy photon beams [2], whereas a shortcoming for heavy ions has been known for decades.

METHODS

We present a new approach to correct the ionization quenching in proton and heavier ion beams using an open-source software [3]. The software is based on the decay time and light yield of the scintillator as well as the ion track structure. Amorphous track structure theory is applied to account for the radial energy deposition by secondary electrons in an ion track, which consequently gives rise to different quenching correction between two ions with different atomic number but the same LET, as the track structures differ. A kinematic quenching model [4] is subsequently applied to evolve the initial energy distribution in time and space to calculate the quenching in the given ion track. The software is applied to investigate the temporal aspects of ionization quenching in plastic scintillators.

RESULTS

The fluorescence emission for three proton tracks in a plastic scintillator with light yield 8000 photons/MeV and decay time $\tau = 3.2$ ns is shown in figure 1(a). The quenching-free exponential scintillator signal with time constant τ is shown for reference. The luminescence emission from the proton track with 100 MeV/cm rapidly decreases but converges to a rate corresponding to that of the expected exponential decay after few ns. The ratios of the luminescence signals to the exponential function with time constant τ are shown in (b). The proton with a LET of 4 MeV/cm, corresponding to an energy of 240 MeV, is seen to follow the exponential emission which indicates the ionization quenching is negligible. On the other hand, the light emission from the LET = 100 MeV/cm proton track (4 MeV) is reduced around a factor 2. The arrows in (b) indicate the time it takes for half the quenching to occur in the proton tracks, i.e. the order of a few percent of the characteristic scintillator decay time for the two protons with LET > 4 MeV/cm in agreement with [5].

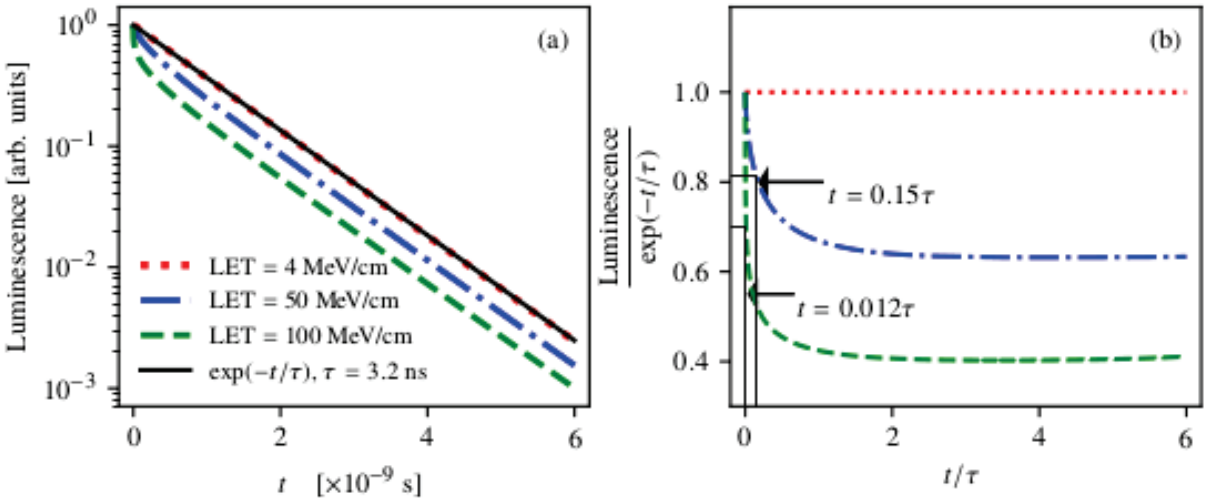

Figure 1. (a) The luminescence from 3 protons with different LET in a plastic scintillator. (b) The ratios of the luminescence to the quenching-free exponentially decaying scintillator signal.

CONCLUSIONS

The open-source software for quenching corrections in scintillator dosimetry enables an investigation of the temporal structure of ionization quenching. The inclusion of the temporal structure is in contrast to other quenching correction models which rely on fit to the experimental data without considering the temporal component. The results show that the quenching is negligible for a 240 MeV proton track as expected but decreases the light emission significantly for protons with higher LET. The ionization quenching in proton tracks thus occurs at a time scale faster than the characteristic decay time of the scintillator and may fade out as fast as 1 % of the decay time for high-LET cases.

REFERENCES

[1] BIRKS, J.B., Scintillations from organic crystals: specific fluorescence and relative response to different radiations. Proceedings of the Physical Society. Section A **64** (1951) 874.

[2] BOIVIN, J., BEDDAR, S., BONDE, C., SCHMIDT, D., CULBERSON, W., GUILLEMETTE, M., & BEAULIEU, L. A systematic characterization of the low-energy photon response of plastic scintillation detectors. Physics in Medicine & Biology **61** (2016) 5569.

[3] CHRISTENSEN, J.B, ANDERSEN, C.E, Relating ionization quenching in organic plastic scintillators to basic material properties by modelling excitation density transport and amorphous track structure during proton irradiation. Physics in Medicine & Biology **63** (2018) 195010.

[4] BLANC D., CAMBOU F., DeLAFOND Y.G., Kinetics of the fast component of scintillation in a pure organic medium. Application to anthracene. Comptes rendus l'Académie des Sci Paris **18** (1962) 3187.

[5] BIRKS, J.B, The Theory and Practice of Scintillation Counting: International Series of Monographs in Electronics and Instrumentation, Elsevier **27** (1964)

Comparing Measured and Simulated Prompt Gamma Cross-Section Data for Carbon Target Using AFRODITE Clover Detector System

R. Vijitha[a]
S. W. Peterson[b]

[a]Department of Radiography & Radiotherapy, Faculty of Allied Sciences, General Sir John Kotelawala Defence University, Sri Lanka
[b]Department of Physics, University of Cape Town, Rondebosch, 7701, Cape Town, South Africa

Email address of Corresponding Author: vijitha.r@kdu.ac.lk, viji07ra@ymail.com

BACKGROUND

Proton therapy has become a most popular in radiation oncology due the superior dose distribution of proton beam. However, the advantage of proton therapy cannot be fully utilized without proper measurement of in-patient proton dose. Currently, no clinically applicable method is available [1-3]. Detecting secondary gammas has been proposed as a potential method to measure in-patient proton dose since treatment protons stop within the patient as they deliver the dose [4]. One possibility is the development of an imaging device to measure the scattered gamma-rays produced during a proton therapy treatment [5-6]. During the design of this imaging device, Monte Carlo simulations have been performed to understand the production of these secondary (prompt) gamma-rays, particularly from tissue. Discrepancies have been reported in the Geant4 prompt gamma production specifically in the most prominent elements (^{12}C and ^{16}O) of tissue [3,7]. The goal of this study is to compare the measured and simulated prompt gamma cross section of 4.438 MeV of ^{12}C over the proton energy range of 80 – 125 MeV using Geant4 AFRODITE model.

METHODS

The measurement was carried at iThemba LABS using the AFRODITE clover detector system. A proton beam over the range of 80 -125 MeV were used to hit a natural carbon target of thickness 8.40±0.07 mg/cm^3. In the simulation study, the geometry of the AFRODITE detection system was carefully modelled to mimic the actual geometry by importing CAD models into the Geant4 code. The physics of the AFRODITE model was tested by comparison to the three standard gamma emitting sources, by testing the Compton suppression system and evaluating various hadronic physics processes. Once the model was validated, the experimental runs were simulated and the same procedures were followed in order to obtain absolute detector efficiency curves for the germanium crystals, as well as, differential cross-section data and total cross-section data for the 4.438 gamma peaks.

RESULTS

Figure 1 shows the total cross-section comparison of simulated and experimental total cross-section data with available experimental cross-section data for the 4.438 MeV photo peak from the carbon target.

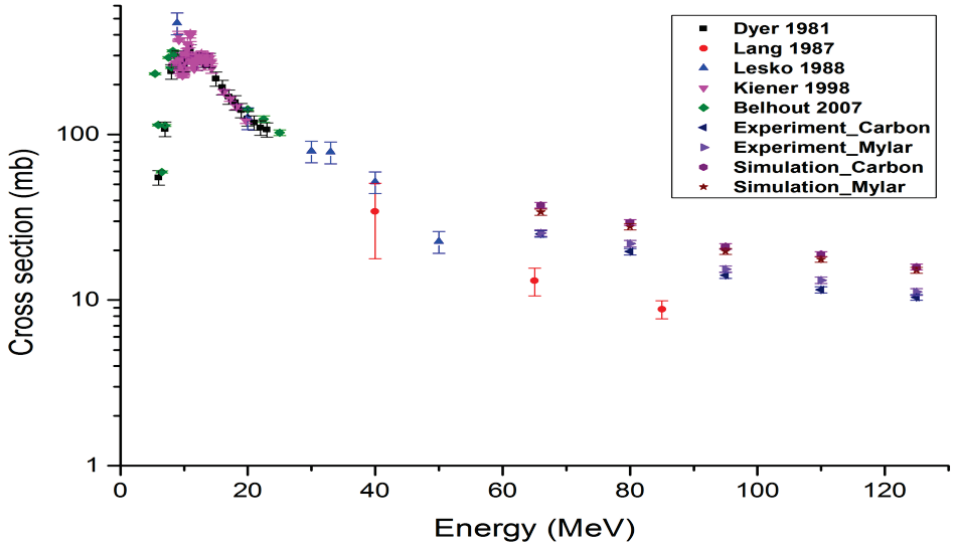

Figure 1. Comparison of measured and simulated total cross-section values for the 4.438 MeV photo peak with available experimental cross-section data.

CONCLUSIONS

As with the experimental 4.438 MeV cross-section data, Geant4 simulated cross section results appear to be higher than the expected values, but due to the scarcity of data, it is hard to determine if these data points are indeed too high.

REFERENCES

[1] SMEETS, J., ROELLINGHOFF, F., JANSSENS, G., PERALI, I., CELANI, A., FIORINI, C., FREUD, N., TESTA, E., PRIEELS, D., Experimental comparison of knife-edge and multi-parallel slit for prompt gamma imaging of proton pencil beams. Frontiers in Oncology 6, 156 (2016).

[2] PETERSON, S. W., ROBERTSON, D., POLF, J., Optimizing a three-stage Compton camera for measuring prompt gamma rays emitted during proton radiotherapy. Physics in Medicine and Biology 55 (22), 6841(2010).

[3] POLF, J.C., PETERSON, S., McCLESKEY, M., ROEDER, B.T., SPIRIDON, A., BEDDAR, S., TRACHE, L., Measurement and calculation of characteristic prompt gamma ray spectra emitted during proton irradiation. Physics in Medicine and Biology 54 (22), N519 (2009).

[4] JONGEN, Y., STICHELBAUT, F., Verification of the proton beam position in the patient by the detection of prompt gamma-rays emission. In: 42nd Meet. Particle Therapy Co- Operative Group (PTCOG) (2003).

[5] MIN, C., KIM, C.H., YOUN, M., KIM, J., Prompt gamma measurements for locating the dose falloff region in the proton therapy. Applied Physics Letters. 89, 183517 (2006).

[6] POLF, J.C., PETERSON, S., CIANGARU, G., GILLIN, M., BEDDAR, S., Prompt gamma-ray emission from biological tissues during proton irradiation: a preliminary study. Physics in Medicine and Biology 54, 731 (2009a).

[7] VERBURG, J.M., SHIH, H.A., SECO, J., Simulation of prompt gamma-ray emission during proton radiotherapy. Physics in Medicine and Biology, 57 (17), 5459 (201

Monte Carlo Calculated Conversion and Correction Factors for NPL's HDR ^{192}Ir Brachytherapy Absorbed Dose Standard and Measured Dose Rate Constant for the HDR ^{192}Ir Flexisource

T. Sander
A. Subiel, S. E. Galer

Medical Radiation Science, National Physical Laboratory, Hampton Road, Teddington, TW11 0LW, United Kingdom

Email address of Corresponding Author: thorsten.sander@npl.co.uk

BACKGROUND

The absorbed dose standard for high dose rate (HDR) ^{192}Ir brachytherapy sources at the UK National Physical Laboratory (NPL) is a graphite calorimeter [1]. Calorimetry offers a more direct method to measure absorbed dose compared to ionometry and usually results in lower overall measurement uncertainties. Radiation energy imparted in the annular calorimeter core with a mean radius of 2.5 cm is converted to the quantity of interest, absorbed dose rate to water at 1 cm distance from the centre of the source, $\dot{D}_{w,\,1\,cm}$. The required graphite-to-water conversion and perturbation correction factors for absorbed dose measurements of the HDR ^{192}Ir Isodose Control Flexisource have been calculated with Monte Carlo (MC) techniques. $\dot{D}_{w,\,1\,cm}$ of the HDR ^{192}Ir Flexisource was measured with the calorimeter and the reference air kerma rate (RAKR) was measured with NPL's HDR ^{192}Ir air kerma primary standard [2]. The dose rate constant of the Flexisource was measured by taking the ratio of the two quantities and was compared against the published consensus value [3].

METHODS

Conversion and perturbation correction factors for the final design of the HDR brachytherapy calorimeter [1] were determined using Monte Carlo simulations employing the cavity user code [4] that forms part of the EGSnrc system [5]. The MC calculated correction factor, F_{MC}, was factorized into six different components. F_{MC} transforms the dose rate to the graphite core of the real calorimeter to the quantity of interest, i.e. dose rate to a point in water at the reference distance of 1 cm under full scatter conditions, $\dot{D}_{w,\,1\,cm}$. The MC models were validated against previously published data [1] for the Nucletron microSelectron-v1 classic HDR ^{192}Ir source and a measured calorimeter response curve. Finally, the calorimeter was used to measure the dose rate constant of the HDR ^{192}Ir Flexisource.

RESULTS

The MC calculated factor for the calorimeter, F_{MC}, was factorized into six different components. The graphite-to-water conversion factor (6.9083 ± 0.12%) includes the inverse square correction from 2.5 cm depth in graphite to 1 cm depth in water. The five other components are correction factors for impurity (0.9995 ± 0.05%), volume averaging (1.0031 ± 0.12%), vacuum gaps (0.9989 ± 0.04%), inhomogeneities (1.0006 ± 0.04%) and full scatter conditions (1.0061 ± 0.04%). The fully characterized calorimeter was then used to measure $\dot{D}_{w,\,1\,cm}$ for six different HDR ^{192}Ir Flexisources. The RAKRs of these sources were measured with NPL's air kerma primary standard. Both measurements were combined which resulted in a measured dose rate constant of Λ = (1.124 ± 0.007) cGy h^{-1} U^{-1} (k = 1) for the Flexisource. The measured Λ was found to be 1% higher than the currently accepted consensus value

$_{CON}\Lambda$ = (1.113 ± 0.011) cGy h^{-1} U^{-1} (k = 1) which is solely based on MC calculations. The measured and published consensus values agree well within the expanded uncertainties (k = 2).

CONCLUSIONS

Correction factors have been calculated for NPL's HDR ^{192}Ir absorbed dose graphite calorimeter for use with the HDR ^{192}Ir Isodose Control Flexisource. The analysis method for the calorimetric measurements was changed from a spreadsheet-based method to a Matlab® code which considers heat transfer between different calorimeter components. This allows a direct measurement of $\dot{D}_{w,\,1\,cm}$ in quasi-adiabatic and isothermal modes of operation with reduced relative standard uncertainties of 0.67% and 0.44%, respectively. The absorbed dose measurements were also combined with RAKR measurements to yield a measured dose rate constant for the Flexisource with overall uncertainties lower than those quoted for the published consensus value.

NPL's HDR ^{192}Ir provides a primary standard method for HDR brachytherapy dosimetry and could enable more accurate measurements of $\dot{D}_{w,\,1\,cm}$ in clinics.

REFERENCES

[1] SANDER, T., DUANE, S., LEE, N.D., THOMAS, C.G., OWEN, P.J., BAILEY, M., PALMANS, H., NPL's new absorbed dose standard for the calibration of HDR ^{192}Ir brachytherapy sources, Metrologia **49** (2012) S184-S188.

[2] SANDER, T., NUTBROWN, R.F., The NPL Air Kerma Primary Standard TH100C for High Dose Rate ^{192}Ir Brachytherapy Sources, NPL Report RD004, Teddington, UK (2006).

[3] PEREZ-CALATAYUD, J., BALLESTER, F., DAS, R.K., DEWERD, L.A., IBBOTT, G.S., MEIGOONI, A.S., OUHIB, Z., RIVARD, M.J., SLOBODA, R.S., WILLIAMSON, J.F., Dose calculation for photon-emitting brachytherapy sources with average energy higher than 50 keV: Full Report of the AAPM and ESTRO, American Association of Physicists in Medicine, AAPM report 229 (2012).

[4] KAWRAKOW, I., MAINEGRA-HING, E., TESSIER, F., WALTERS, B.R.B., The EGSnrc C++ class library, NRCC Report, Ottawa, Canada (2009).

[5] KAWRAKOW, I., ROGERS, D.W.O., The EGSnrc code system: Monte Carlo simulation of electron and photon transport, NRCC Report, Ottawa, Canada (2006).

Towards Traceable Low-Energy X-ray Dosimetry with Alanine: Modelling the Spectral Distribution of a 50 kV X-ray Tube

J. G. Hjørringgaard
L. R. Lindvold, C. Ankjærgaard, A. Miller, M. Bailey, C. E. Anderson

Center for Nuclear Technologies, Technical University of Denmark, Roskilde, Denmark

Email address of Corresponding Author: jakg@dtu.dk

BACKGROUND

The more widespread use of low energy x-rays in the health sector, e.g. for blood irradiation and sterilization of medical equipment, requires support from improved dosimetry. The development of accurate and reliable dosimetry systems for low energy x-rays is difficult and the responses to dose of commonly used dosimetry systems, particularly solid-state dosimeters, are strongly energy dependent in the low energy range. The overall objective of this work is to establish reference conditions for traceable solid-state dosimetry using e.g. alanine pellets. Here, we specifically investigated a small 50 kV x-ray irradiator, using ion chamber measurements and Monte Carlo (MC) calculations.

METHODS

A 50 kV 1 mA VF-50J tube (Varian Medical Systems) with tungsten target was characterized. The x-ray tube utilizes a reflective geometry, where the filament is located close to the tube window, and the accelerated electrons hit the tungsten target at a 90 degree angle [2]. The advantage of such geometry is a small distance from focal spot to window which enables high dose rate to the irradiated object for a given power level. The beam quality, characterized by the beam attenuation in aluminium, was measured for different tube potentials using a plane-parallel ionization chamber (PTW 23344). MC modelling was carried out using the egs++ usercode of the EGSnrc code system [1].

RESULTS

Depth-dose profiles were calculated using the egs++ code. Initial computations were obtained using a spectrum provided by the manufacturer based on direct measurements at 40 kV tube potential with a LiF crystal and an XRF spectrometer. Since the full details of the measurements were not available, correction for spectrometer response could not be applied, and this spectrum resulted in a depth-dose profile that deviated significantly from the measured profile. We therefore choose to compute the spectrum of the x-ray tube using a simple electron beam model (monoenergetic beam of 0.1 cm radius) impinging on the tungsten target material with full account for other known details in the tube head such as window, collimator system, and external filtration.

MC calculations performed with these photon energy spectra for 30, 40, and 50 kV tube potential resulted in depth-dose profiles in good agreement with the measurements (relative standard deviation of residual = 2.6% for all three spectra shown in Fig. 1 and no significant structure in the deviations except perhaps at the very surface).

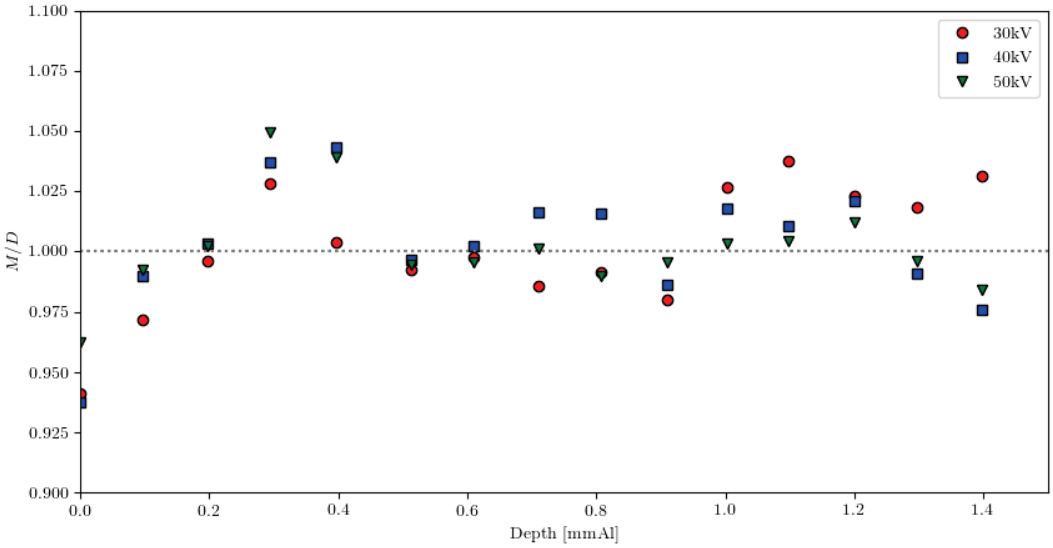

Figure 1: Ratio of MC calculated dose to measured ion chamber response for three beam qualities.

CONCLUSIONS

MC calculated spectra have been verified to reproduce observed beam attenuation in aluminium, allowing for greater flexibility in the usage as a reference beam for studies of alanine response. The calculated spectra will be used onward to establish correction factors for characterization of alanine dosimeter response to irradiations in the low energy x-rays beam.

REFERENCES

[1] KAWRAKOW, I., MAINEGRA-HING, E., ROGERS, D.W.O., TESSIER, F., WALTERS, B.R.B., The EGSnrc Code System: Monte Carlo simulation of electron and photon transport. Technical Report PIRS-701, National Research Council Canada (2017).

[2] ANDERSEN, C.E., BØTTER-JENSEN, L., MURRAY, A.S., A mini X-ray generator as an alternative to a 90Sr/90Y beta source in luminescence dating. Radiation Measurements 37 (2003) 557 – 561.

Traceability

The International Measurement System for Ionizing Radiation

S. Judge
D. Burns, R. Coulon, C. Kessler and C. Michotte

Bureau International des Poids et Mesures, 92312 Sèvres Cedex, France

Email address of Corresponding Author: steven.judge@bipm.org

BACKGROUND

Accurate measurement of radiation dose and radioactivity is key to the safe and effective use of ionizing radiation for cancer therapy and medical imaging. All such measurements rely on the international measurement system – the technical and administrative infrastructure that has been developed over many years to ensure measurements can be carried out at an accuracy that is fit for purpose.

National metrology institutes (NMIs) are at the heart of the international system. NMIs that develop and maintain primary measurement standards offer calibration services based on these standards to secondary laboratories and other users. However, there is a challenge to overcome: by definition, a primary measurement standard has no calibration to rely on, so how can a primary standard be checked? The solution for ionizing radiation is found in the work of the Bureau International des Poids et Mesures (BIPM) and the Consultative Committee on Ionizing Radiation (CCRI).

The origin of the BIPM was an international treaty called the Metre Convention [1]. The treaty was signed in Paris on 20th May 1875 and it established the BIPM as an intergovernmental organization under the authority of the General Conference on Weights and Measures. The Metre Convention established a permanent structure for member governments to act together on matters related to measurement science and measurement standards and included setting up the International Committee for Weights and Measures (CIPM) to promote world-wide uniformity of measurements and to oversee the work of the BIPM. The CIPM is advised by the CCRI on matters relating to ionizing radiation metrology. The IAEA is an important stakeholder in the CCRI, linking the work of the IAEA Laboratories and the SSDL network to the international measurement system.

The influence of the Metre Convention has grown from the original 17 countries to 59 member states (‘States Parties to the Metre Convention’, to use the correct terminology) plus 42 associated states and economies. The work was strengthened in 1999 with the publication of the CIPM Mutual Recognition Arrangement (CIPM MRA), which sets out in more detail how the international measurement system functions including a requirement for NMIs to demonstrate that national standards are equivalent through participation in comparison exercises.

The scope of the technical work has also grown; a department dedicated to ionizing radiation measurement standards was founded in 1960. As well as providing the scientific secretariat for the CCRI, the department offers on-demand comparison and calibration services for radiation dosimetry and radioactivity. These services are free of charge to signatories of the Metre Convention.

SUMMARY

The international measurement system works in the following way. NMIs that hold primary standards participate in comparison exercises to demonstrate the equivalence of the standards. The CCRI decides how often NMIs should participate in order to demonstrate continued competence. The comparisons can be large-scale exercises, organized by the CCRI with one NMI taking the lead as the pilot laboratory, or NMIs can decide to use the comparison services offered by the BIPM.

For radiation dosimetry, the BIPM has developed very stable primary standards for a limited number of qualities using well-characterized beams (see Table 1). The low measurement uncertainties and stability achieved for these instruments led to the CCRI deciding (in 1999) that the BIPM primary standards would be accepted as setting the world reference value for these qualities (the Key Comparison Reference Value (KCRV)).

Table 1. Radiation dosimetry comparison services at the BIPM.

Comparison	Description
BIPM.RI(I)-K1	Measurement of air kerma for ^{60}Co
BIPM.RI(I)-K2	Measurement of air kerma for low-energy x-rays
BIPM.RI(I)-K3	Measurement of air kerma for medium-energy x-rays
BIPM.RI(I)-K4	Measurement of absorbed dose to water for ^{60}Co
BIPM.RI(I)-K5	Measurement of air kerma for ^{137}Cs
BIPM.RI(I)-K6	Measurement of absorbed dose to water for high-energy photon beams
BIPM.RI(I)-K7	Measurement of air kerma in mammography beams
BIPM.RI(I)-K8	Measurement of reference air kerma rate for ^{192}Ir brachytherapy
BIPM.RI(I)-K9	Measurement of absorbed dose to water for medium-energy x-rays

The approach is different for radionuclide metrology. The BIPM has established very stable, reproducible, instrumentation for comparing primary radioactivity standards (see Table 2). In this field, the world reference value (KCRV) is determined from a weighted mean of measurements of national standards.

Table 2. Radionuclide standards comparison services at the BIPM.

Comparison	Description
BIPM.RI(II)-K1	Measurement of gamma-emitting radionuclides (SIR)
BIPM.RI(II)-K4	Measurement of short-lived gamma emitting radionuclides (SIRTI)
BIPM.RI(II)-K5	Measurement of beta-emitting radionuclides (ESIR) (in development)

Following approval by the CCRI, the results from all of the comparison exercises (large-scale and BIPM comparisons) are published in a database maintained by the BIPM – the Key Comparison Database (KCDB).

The next step in the international measurement system is for the NMIs to submit Calibration and Measurement Capabilities (CMCs) for publication. One requirement for publishing CMCs is that the laboratory must operate an ISO17025 quality assurance management system. Applications are also subject to peer-review; successful participation in a comparison exercise is an important part of the evidence used to demonstrate competency. With a multitude of different radiation qualities and radionuclides, it is unrealistic to arrange comparison exercises for every possibility; the CCRI oversees a system whereby successful participation in one comparison exercise is accepted as demonstrating competency for several radiation qualities or radionuclides.

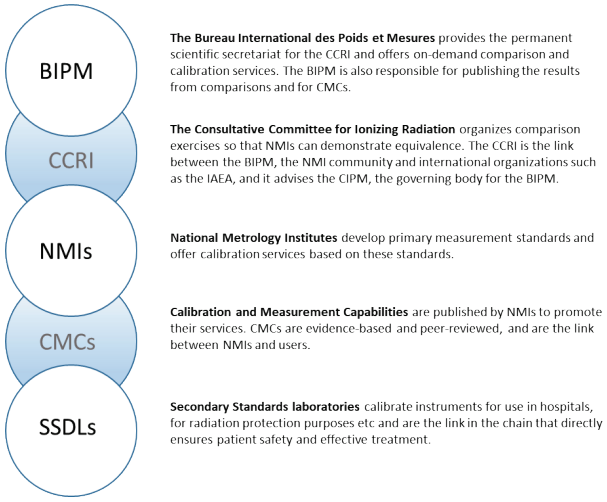

Figure 1. An overview of the international measurement system.

CMCs are also published on the KCDB, and a laboratory looking for a calibration service for an instrument or a radioactive reference material can search the database for NMIs that offer the service, confident in the knowledge that the entries in the KCDB have been subject to expert peer-review and practical demonstration of their capability.

A schematic overview of the international measurement system is shown in Figure 1; comprehensive reviews of ionizing radiation metrology can be found in three special issues of *Metrologia* [2-4].

CONCLUSIONS

Ionizing radiation metrology is a success story for the international measurement system. Over the past few decades, scientists from metrology institutes worldwide have worked together to establish a very robust framework to enable ionizing radiation to be used for cancer therapy and medical imaging, based on a system of comparisons and effective peer review. The system helps ensure that all measurements of ionizing radiation are fit for purpose, defendable and traceable to a single reference value – the key comparison reference value.

REFERENCES

[1] Available from the BIPM website: www.bipm.org.
[2] SHARPE, P, ed. Special issue on radiation dosimetry, Metrologia 46 (2009).
[3] SIMPSON, B. and JUDGE, S., eds. Special issue on radionuclide metrology, Metrologia 44 (2007).
[4] THOMAS, D., NOLTE, R. and GRESSIER, V., eds. Special issue on neutron metrology, Metrologia 48 (2011).

The Role of the CIPM Consultative Committee on Ionising Radiation (CCRI)

M. McEwen

National Research Council Canada, Ottawa, ON Canada

Email address of Corresponding Author: malcolm.mcewen@nrc-cnrc.gc.ca

BACKGROUND

Beginning in 1927, consultative committees of the International Committee of Weights and Measures (CIPM) have been formed for various measurement quantities of interest within the International System of Units (SI). Each CC provides a forum where National Measurement Institutes and Designated Institutes can meet to discuss common measurement challenges, identify strategic research goals and approve degrees of equivalence in calibration capabilities. CCRI was established in 1958, as new applications of ionizing radiation requiring measurement standards (e.g., Co-60 and linear accelerators for radiation therapy, personnel monitoring for nuclear power plant workers) became established in society. Sixty years later, the CCRI's role continues to be vital in ensuring international equivalence of dosimetric standards and identifying new radiation metrology issues that need to be addressed collectively.

This presentation will describe the function and operation of the CCRI and how it fits within the international radiation metrology framework. It complements the sister presentation on the role of the BIPM [1].

DISCUSSION

CCRI [2] brings together representatives from every continent, so it is a truly global collective. The committee is formed into three sections covering: I) x- and gamma-rays, charged particles; II) radionuclide measurements, and III) neutron measurements. This sub-specialisation recognizes that the expertise and requirements for the different fields are related but separate. The biennial section meetings, therefore, can focus on technical questions specific to each area. The CCRI itself acts as a type of Executive Committee that considers trends and commonalities and develops an overall strategy for ionizing radiation metrology.

One of the primary activities of the CCRI is to identify measurement quantities of international relevance and organize/oversee comparison programs to ensure equivalence between the primary standards of different countries. The concepts of degrees of equivalence and the CIPM Mutual Recognition Arrangement are dealt with elsewhere in this symposium, the role of the CCRI is to ensure that current comparison programs meet nations' needs and that comparisons for new measurement quantities or radiation modalities are developed in a timely manner.

The CCRI extends beyond national laboratories to key liaison organizations and stakeholders to ensure that the relevant subject matter experts are at the table and that activities in ionizing radiation metrology are in line with end-user needs. For example, the recently published ICRU Report 90 [3] was a result of a request from CCRI for a review and update of key dosimetric data. International medical physics organizations such as IOMP, AAPM and the IAEA provide essential input to the discussions on radiation metrology developments.

The CCRI also has an advocacy role, to provide a stronger voice on ionizing radiation metrology to governments and international organizations than any single laboratory. A particular issue that has arisen in recent years is the reliable shipment of radioactive sources,

both for comparison purposes (e.g. the BIPM SIR) and for re-sourcing calibrated radiation fields (e.g. Co-60).

CONCLUSION

The CCRI is a forum and enabler for the accurate use of ionizing radiation in industrial, medical and radiation protection applications.

REFERENCES

[1] JUDGE et al, The international measurement system for ionizing radiation, IDOS 2019
[2] Available from the BIPM website: https://www.bipm.org/en/committees/cc/ccri/
[3] INTERNATIONAL COMMISSION ON RADIATION UNITS, Report 90: Key Data for Ionizing-Radiation Dosimetry: Measurement Standards and Applications, Oxford: ICRU, 2016

The IAEA/WHO Network of Secondary Standards Dosimetry Laboratories

P. Toroi[a]

[a]International Atomic Energy Agency, PO Box 100, 1400 Vienna, Austria

Email address of Corresponding Author: p.toroi@iaea.org

BACKGROUND

In every country in which ionizing radiation is used, there is a need for accurate dosimetry. Appropriate calibration of the dose measurement equipment is part of this task. Therefore, each country should either maintain a national measurement standard for relevant quantities or make arrangements for access to such standards maintained in another country. National measurement standards should be nationally recognized and traceable to the International System of Units (SI). They may be either primary or secondary standards maintained at a primary standards dosimetry laboratory (PSDL) or at a secondary standards dosimetry laboratory (SSDL).

The International Atomic Energy Agency (IAEA) in collaboration with the World Health Organization (WHO) established the IAEA/WHO SSDL Network in 1976. The members of the Network are designated by the competent national authorities and they undertake the duties of providing a link in the traceability of radiation dosimetry for users within that country. The SSDL Charter explains the rights and duties of members in the Network [1].

IAEA SUPPORT TO SSDLs

An SSDL can be traceable to the SI and international measurement system in different ways (Figure 1). Some SSDLs are traceable to a PSDL or directly to the Bureau International des Poids et Mesures (BIPM), if there is no national primary standard and the country is a member of the Metre Convention. More than 50% of the SSDL Network Members are traceable to primary standards through the IAEA, at least for one dosimetric quantity used for their calibration services.

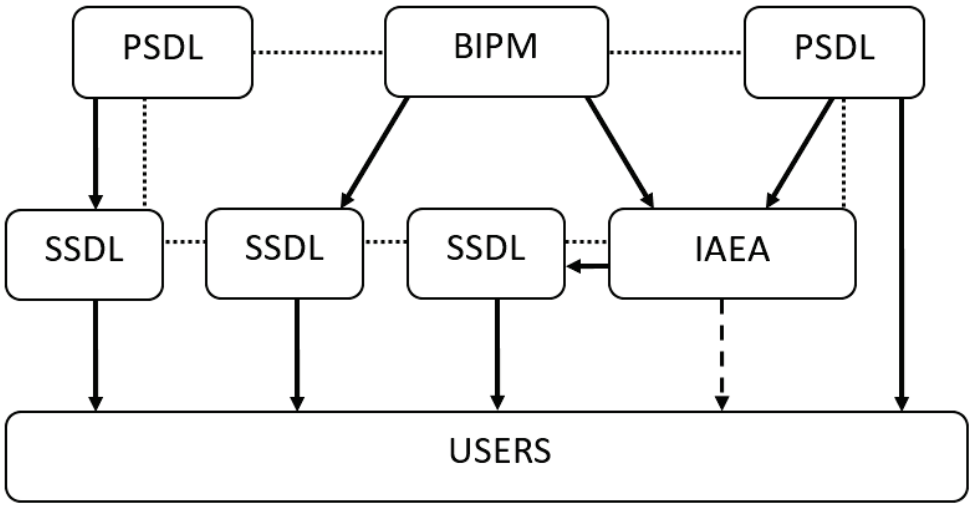

FIG. 1. A simplified representation of the international measurement system for radiation dosimetry. The arrows represent the calibrations which ensure the traceability chain to the international measurement standards and the dotted lines indicate comparisons of primary and secondary standards. Modified from [1]

The IAEA's Dosimetry laboratory (DOL) works as a central laboratory in the SSDL Network and provides calibrations, reference irradiations, comparison programmes and dosimetry audit services for the Member States. In average DOL provides yearly around 600 calibrations, 24 comparisons and 60 audits to SSDLs.

CALIBRATION SERVICES PROVIDED BY THE SSDL NETWORK MEMBERS

In May 2019, the IAEA/WHO Network of SSDLs included 86 members, 16 PSDLs and 5 international organizations as affiliated members. The up-to-date list of the Network members is included in every issue of the SSDL Newsletter and it is also available on the SSDL Network website [2]. One of the requirements of a full SSDL Network member is to submit an annual report. In 2017, 84 SSDL Network members submitted their annual report and a short summary of their calibration services is given in Table 1. Most of the calibrations provided by SSDL members are in the field of radiation protection.

Table 1. Calibration services provided by the SSDL Network members according to their annual report 2017 (n = 84).

Service scope	Number of SSDLs providing the service	Number of SSDLs traceable through IAEA	Number of calibrations provided by SSDLs in 2017
Radiation therapy including brachytherapy	50	24	9671
Radiation protection	71	37	116 963
Diagnostic radiology and mammography	43	15	4851

CONCLUSIONS

The IAEA/WHO SSDL Network has an important role in disseminating and supporting the correct use of the dosimetry quantities and units through the proper calibration of field instruments by the SSDLs. The challenge is that usually, there is only one SSDL in a country and there is a limited number of persons working in this field. Therefore, international cooperation between the SSDLs is very important; and this is also one of the main aims of the IAEA/WHO SSDL Network.

REFERENCES

[1] INTERNATIONAL ATOMIC ENERY AGENCY, SSDL Network Charter 2nd edition, IAEA, Austria (2018). https://ssdl.iaea.org/Home/SSDLNetworkCharter

[2] SSDL Network website: https://ssdl.iaea.org/

Calibration of Survey Meters by using a Newly Developed Quasi-Monoenergetic of ~190 keV Photon Field: A Preliminary Result

S. M. Tajudin[a]
Y. Namito[b], T. Sanami[b], H. Hirayama[b]

[a]Faculty of Health Sciences, Universiti Sultan Zainal Abidin (UniSZA), 21300 Kuala Nerus, Terengganu, Malaysia.
[b]High Energy Accelerator Research Organization (KEK), 1-1 Oho, Tsukuba, Ibaraki 305-0801, Japan.

Email address of Corresponding Author: suffian@unisza.edu.my

BACKGROUND

Radiation survey meters, or dosimeters, are important tools for the evaluation and examination of workplace safety when ionizing radiation is used in the workplace [1,2]. The sensitivities and detection efficiencies of the detectors are extremely important in these measurements. Efficiency of some detectors, such as the NaI(Tl) scintillation detector, may have a very strong photon energy dependence in diagnostic radiology photon field and care must be taken in using such instruments for dose-related measurements. To ensure the sensitivity and detection efficiency, it is desirable to calibrate each instrument for its energy response. Measurements of detector responses at both high and low energies are required to ensure the accuracy of photon dose measurements. Thus, monoenergetic photon fields are necessary.

As a reference calibration field, several radioisotopes have been used frequently, such as Am-241, Cs-137 and Co-60, providing photons with energies of 60, 662, 1173 and 1333 keV, respectively. However, there is no suitable radioactive source emitting photons with energies of a few hundred keV. This is an important energy region for radiation detector and dosimeter calibrations particularly in diagnostic radiology field because the dominant photon interaction changes from the photoelectric effect to Compton scattering. Only short-lived radioactive sources, such as Ce-139 (166 keV, T1/2=138 days) and Cr-51 (320 keV, T1/2=28 days), are available for a mono-energetic photon source in this energy range.

In our previous work, a backscatter layout provided photons with an energy of 190 keV by using a Cs-137 gamma source [3]. It could be possible to utilize the same layout with different radioactive sources to produce photon fields with various energies. In the present work, we present the preliminary results for calibration of CsI(Tl) survey meters for Horiba PA-1000 and Mr.Gamma A2700 under the proposed backscatter layout and using a 208-MBq Cs-137 source.

METHODS

Under the proposed layout with a 208-MBq Cs-137 source, a mono-energetic photon field with 190 ± 9.6 keV (FWHM) and a dose rate of 3.18 ± 0.18 μSv/h was obtained within the established volume which is adequate for various sizes of survey meters for calibration purposes. The approach presented here offers a way to provide low and high energy radiation from a single source that can allow the survey meters to be specifically tested for low energy applications as in diagnostic radiology.

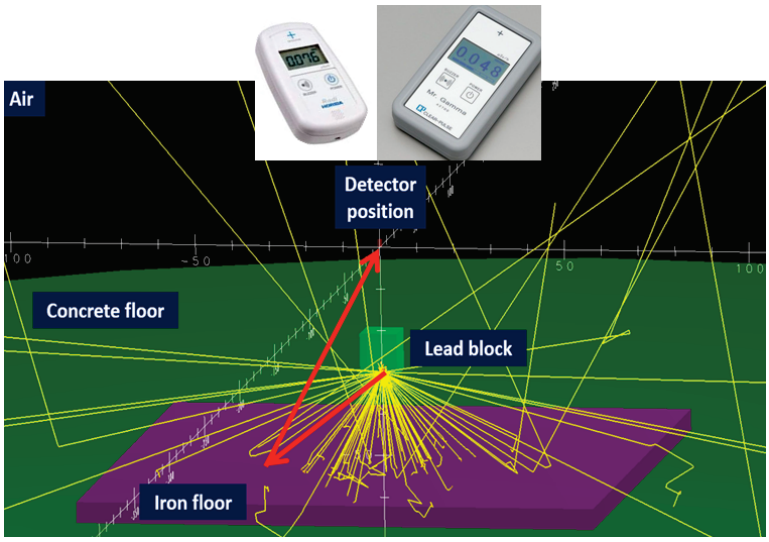

Figure 1. The backscatter layout for calibration field of ~ 190 keV mono-energetic photon field [3]. The survey meter was positioned at the established 'detector position volume'.

RESULTS

For the backscatter field energy, the responses of survey meters were normalized to the NaI(Tl) TCS-171 survey meter. NaI(Tl) was used as a reference survey meter due to it has energy compensation to display a more accurate dose value. For other energies of radioactive sources, the measured dose rate by the survey meters were divided to the theory dose rate by using Dose rate Conversion Factor ($mSv.m^2.MBq^{-1}.h^{-1}$). The Horiba survey meter (model:PA-1000) show a strong energy dependence for ~200 keV photon field.

CONCLUSIONS

Our approach enables us to obtain a "two-energy calibration" using the same source at both energies of 190 and 662 keV, which can be preferable to dosimeter calibration applications. As the users of radiation dosimeter should have a mechanism to ensure the instrument's performance, the approach presented offers a way to provide low and high energy radiation from a single source that can allow the detectors to be specifically tested for low energy applications. The proposed method to produce two-energy radiation could simplify the calibration process for small laboratories that do not have access to an X-ray generator facility. We are also looking for collaboration to setup in adjustable design so the variables can be changed if necessary but also held to perform the calibration repeatably and reliably.

REFERENCES

[1] D. THORELLI, Development of Constancy Control and Calibration Protocols for Radiation Monitor Devices and Estimations of Surface Dose Rates from Radioactive Waste Containers Used at University of Gothenburg, M.S. thesis (Univ. of Gothenburg, Sweden (2008).

[2] American National Standard Radiation Protection Instrumentation Test and Calibration, Portable Survey Instruments, ANSI N323 (1997).

[3] TAJUDIN S.M., NAMITO Y., SANAMI T., HIRAYAMA H., Quasi-monoenergetic 200 keV Photon Field Using a Radioactive Source with Backscatter Layout, Jpn. J. Appl. Phys. 53 116401 (2014).

Well Chamber Calibration Experience of the Polish SSDL

P. Ulkowski[a]
W. Bulski[a], K. Chelminski[a], W. Slusarczyk-Kacprzyk[a], A. Kowalczyk[a], E.Gruszczynska[a]

[a]Department of Medical Physics, The Maria Skłodowska-Curie Memorial Cancer Centre and Institute of Oncology, Roentgen Str. 5, 02-781 Warsaw, Poland.

Email address of Corresponding Author: w.bulski@zfm.coi.pl

BACKGROUND

In Poland, there are 35 centres which carry out brachytherapy. They treat about 12000 patients per year. In total, all these centres make use of about 50 HDR machines with Ir-192 sources. Each source has to be replaced every three months, and the new sources have to be calibrated. In every centre this is done by measuring the source output with a well ionization chamber. Each centre has at least one such chamber which in turn has to be calibrated against the secondary standard. The Polish Secondary Standard Dosimetry Laboratory [1] offers such calibrations for which it is accredited by the Polish Centre for Accreditation. The SSDL in Warsaw is the only laboratory in Poland and in central and eastern Europe which performs calibration of this type of chambers. The service began in 2012, and since then, 87 calibrations have been performed. In this presentation, the calibration results are analyzed.

METHODS

The calibration procedure for well chambers was established at the SSDL in 2012. As a secondary standard, a PTW well chamber type TW33004 has been used. The present secondary standard of the SSDL, a PTW well chamber type TW33004 with the Standard Imaging electrometer SUPERMAX 90018, was calibrated at the Primary Standard Laboratory PTB-Braunschweig, Germany in 2016. At the Polish SSDL, the extended uncertainty of the calibration coefficient for user's chambers is 3% (k=2). The calibrations are performed using the Ir-192 source of the MicroSelectron HDR unit. Until December 2018, the SSDL calibrated 41 well chambers from the following manufacturers: Standard Imaging – 19 chambers, Nucletron Holland – 10 chambers, and PTW Freiberg – 12 chambers. Most of the chambers are returned to the SSDL for recalibration approximately every two years.

RESULTS

Mean values and SD of calibration coefficients for each chamber type were calculated. For Standard Imaging HDR1000 Plus well chambers, the mean calibration coefficient was 0.4672±0.0022. For Nucletron Holland well chambers (type 77091, 77092 and 77094), the mean calibration coefficient was 0.9489±0.0144 and for PTW33004 well chambers, the mean calibration coefficient was 0.9656±0.0152. Some chambers were calibrated twice, which enabled the evaluation of their stability.

CONCLUSIONS

The smallest standard deviation of the calibration factors was observed for the Standard Imaging chambers (19 chambers). It indicates high manufacturing reproducibility. Furthermore, these chambers have higher sensitivity than the other types.

18 chambers of all types were calibrated three times over a period of six years. Their long-term stability is comparable, and it is within 0.5% over the period of 6 years for all the chamber

types. Another 25 chambers were calibrated twice over the period from 2012 to 2018 and it is expected that these chambers will shortly be sent to the SSDL for their third calibration. In 2018, within the procedures of the SSDL accreditation, one of the reference chambers was calibrated three times during a period of 6 months, each time by a different person. The calibration coefficients were as follows: Nk=0.9645 (May), Nk=0.9644 (October), Nk=0.9639 (December) mGy/(h·nA). The differences are within the range of 0.06%. This indicates a very high reproducibility of the measurements. This chamber was initially calibrated at the Primary Standard Laboratory PTB-Braunschweig, Germany in August 2012. The calibration coefficient was Nk=0.962 Gy/(h·nA). The difference over a period of six years was 0.3% which indicates a good long-term stability of the reference chamber.

REFERENCES

[1] BULSKI, W., ROSTKOWSKA, J., KANIA, M., GWIAZDOWSKA, B., External quality audits in radiotherapy in Poland (IAEA-CN--96). IAEA, (2002)

Development of Standards

Development of a New Primary Standard of Absorbed Dose to Water for Radiopharmaceutical Therapy

V. Smyth[a]
I. Billas[a], **D. Shipley**[a], **G. Bass**[a], **T. Sander**[a]

[a]National Physical Laboratory, Teddington TW11 0LW, UK

Email address of Corresponding Author: vere.smyth@npl.co.uk

BACKGROUND

Radiotherapy treatments using modalities such as external photon, electron, proton and carbon ion beams and brachytherapy are prescribed and delivered to the patient on the basis of absorbed doses measured in a way that is traceable to either a primary standard of absorbed dose to water or air kerma. Traceability to a measurement standard is universally accepted as a fundamental requirement to ensure uniformity of dose delivery across the radiotherapy community. In each of the modalities named above, the patient dose can be determined through a measurement of dose-rate using a dosimeter that has a calibration traceable to a primary standard. By contrast, the dose to the patient from radiopharmaceutical therapy (RPT) cannot be measured directly, but must be calculated from cumulated activity within the tissue of interest, derived from measurements of the radiopharmaceutical uptake and retention over time. The calculations employed rely completely on published nuclear data (radiation energy spectra and emission probabilities) and usually on calculations using the Monte Carlo method. Both have been thoroughly researched and benchmarked, so there is justified confidence in their accuracy.

Nevertheless, there is a natural feeling of discomfort among metrologists about placing total reliance on consensus/theoretical data and calculations for a quantity as critical as radiotherapy dose. This is particularly true when attempting to achieve comparability with the doses delivered by the other radiotherapy modalities, e.g. for the sake of combined therapies, or to transfer data on tumour response or normal tissue tolerance. The situation is similar to that when external beam therapy dosimetry was entirely based on measurements of ionisation in air traceable to primary standards of air kerma (coulombs per kilogram of dry air multiplied by the average amount of energy required to create an ion pair in air, W_{air}/e) [1]. Successive estimates of W_{air}/e did not give good agreement, so an average value was proposed by BIPM [2] and adopted by the radiotherapy community so that at least everyone would agree. As the technology became available, new standards that obtained absorbed dose to water directly were developed using the method of calorimetry, measuring the temperature rise from the absorption of radiation into a water or graphite phantom. Dosimetry protocols based on calorimetry have now been developed to avoid the reliance on W_{air}/e, [3].

Accordingly, we make the case here that dose measurement for RPT should be based on direct measurements traceable to a primary absorbed dose standard rather than nuclear data-based calculations, and describe the development and testing of a primary standard instrument for this purpose.

METHODS

The standard is based on a conventional extrapolation ionization chamber (Figure 1). The instrument is placed in close proximity to the surface of a volume of radioactive liquid in a PMMA phantom, so that as much as possible of the radiation emitted from the surface is measured. In this way the dose rate to water in the surface layer of the liquid is measured.

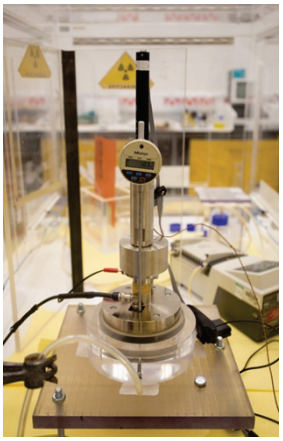

Figure 1. The primary standard.

A detailed Monte Carlo simulation of the phantom and chamber was performed in order to calculate factors to correct for attenuation and backscatter, and to determine the stopping-power ratio between air and water for the spectrum of particles entering the chamber. The simulation reproduced the relative response of the chamber within the estimated uncertainty at each of the 10 plate separation distances used. Therefore, instead of using the conventional extrapolation method and Bragg-Gray theory (which may not have been valid in the presence of very low-energy beta particles), we treated each plate separation setting as a separate independent measurement, and averaged the results. Full details of the method and first trial measurements are given in [4].

Careful consideration was given to the role of Monte Carlo simulation in the determination of the required corrections to the measured data, since the code itself uses the same nuclear data that the measurements are compared with. However, since every calculated correction factor is a ratio of Monte Carlo values, there is no dependence (to first order) on the absolute individual values. The calculated values were insensitive to the choice of nuclear data set.

RESULTS

Two sets of measurements were made using a solution of ^{90}YCl. The measurements were made in terms of mean absorbed dose to water per radionuclide disintegration. In order for the results to be compared with the dose calculated from published nuclear decay data, the dose at the surface of the solution was converted, using Monte Carlo simulation, to dose within a phantom large enough to establish equilibrium between the energy emitted per mass and the absorbed dose. This resulting comparison is with the nuclear data only, independent of radiation transport calculation methods. The source data were taken from RADAR [5] and MIRD [6]. The results for the two measurement runs are shown in Table 1.

Table 1. Measurement results. Units are Gy × 10^{-12}

	Run 1			Run 2		
	Measured	RADAR	MIRD	Measured	RADAR	MIRD
Absorbed dose per disintegration	2.204	2.172	2.171	2.223	2.203	2.202
Expanded uncertainty (k=2)	± 0.041	±0.005	±0.005	± 0.041	±0.005	±0.005

CONCLUSIONS

The measured results for ^{90}Y agree with calculated values from 2 separate published sources within the estimated uncertainties. This both demonstrates the feasibility of using an extrapolation chamber as a primary standard of absorbed dose (in the case of ^{90}Y), and provides reassurance that dosimetry based on the published data will be consistent with doses delivered using other modalities where the dosimetry is traceable to absorbed dose standards.

The radionuclide used in the initial demonstration was chosen because it is used clinically, and also because the emissions are predominantly high-energy betas (maximum energy 2.28 MeV, mean energy 0.93 MeV), rendering it particularly suitable for measurement with an extrapolation chamber. The entrance window of the chamber is only 5 microns thick, admitting a high proportion of the emitted betas. However, the dependence on the calculated correction for attenuation will increase in the case of radionuclides with lower-energy spectra (e.g. ^{177}Lu). Furthermore, calculated corrections to account for the low interaction probability in the chamber and backscatter from the surrounding material from gamma emissions (e.g. ^{131}I and ^{177}Lu) will test the practicality of the instrument further. Further investigations and trials are underway.

As a final note, the irony has not escaped the authors that the standard proposed uses the method of ionometry, and therefore is still dependent on the BIPM value of W_{air}/e.

REFERENCES

[1] INTERNATIONAL ATOMIC ENERGY AGENCY, Absorbed Dose Determination in Photon and Electron Beams, Technical Reports Series No. 277, 2nd edn, IAEA, Vienna (1997)

[2] BOUTILLON M, PERROCHE-ROUX A-M. Re-evaluation of the W value for electrons in dry air, 1987, Phys. Med. Biol. 32, 213-219.

[3] INTERNATIONAL ATOMIC ENERGY AGENCY, Absorbed Dose Determination in External Beam Radiotherapy, Technical Reports Series No. 398, IAEA, Vienna (2000).

[4] BILLAS, I., SHIPLEY, D., GALER, S., BASS, G., SANDER, T., FENWICK, A., SMYTH, V. Development of a primary standard for absorbed dose from unsealed radionuclide solutions. Metrologia, Volume 53, Number 6 (2016)

[5] STABIN, M. G., and DA LUZ, L. C., (2002) Decay data for internal and external dose assessment Health Physics. 83 471–75

[6] ECKERMAN, K. F., and ENDO, A., (2008) MIRD: Radionuclide Data and Decay Schemes 2nd edn (Reston, VA: Society of Nuclear Medicine) p 671

Aerrow-Mini: A Probe-Format Graphite Calorimeter for Absolute Dosimetry of Small High-Energy Photon Fields

B. Côté[a]
J. Seuntjens[a], **A. Sarfehnia**[b], **J. Renaud**[a]

[a]McGill University, Medical Physics Unit, McGill University, Montreal, QC, Canada
[b]Department of Radiation Oncology, University of Toronto, Toronto, ON, Canada

Email address of Corresponding Author: benjamin.cote@mail.mcgill.ca

BACKGROUND

Absorbed dose calorimetry is an absolute and direct method of measuring radiation doses. Calorimeters, used in various designs, are applied in radiation dosimetry and driven primarily by national metrology institutes with a principle aim of achieving the minimum uncertainty on the dose measurement. [1-2] With the newest specialized and nonconformal radiation modalities (MR-linacs, RelfeXion, Gamma Knife, Cyberknife, etc.), that cannot produce a standard reference field (10 × 10 cm^2), dosimetry has to be adapted for smaller fields. Small calorimeters have been developed [3-4] and rely on vacuum pump systems to achieve pressures of typically less than 10^{-3} Pa thereby limiting heat transfer between the absorbing bodies. Although, effective at thermal isolation, the challenges and time required to establish a partial vacuum and maintaining it within a volume of porous graphite, make these an impractical solution for routine clinical use. The aim of the Aerrow project was to develop a probe-format graphite calorimetry system specifically designed for routine use in the clinical environment. Originally constructed at McGill University by Renaud *et al*., the calorimeter, referred to herein as the Aerrow, has to-date been used to determine the absorbed dose to a small sensitive volume in high-energy clinical accelerator-based photon beams under reference conditions. [5] The aim of this work is to complete the prototyping of a miniature version of the Aerrow. The mini-version is designed especially for a small-field use. Because of the reduced size of the sensitive volume, the feasibility of absorbed dose measurement down to a field size of 0.5 × 0.5 cm^2 will be investigated in this study.

METHODS

The incorporation of a machinable aerogel has provided sufficient thermal insulator and mechanical support to the nested graphite components. The Aerrow-mini is a half-scale version of the original Aerrow prototype and has a sensitive volume (the core) that is 8 times smaller. The 3.1 mm diameter, 5.0 mm long graphite core was separated from the surrounding environment by two isotropic layers of aerogel insulation (Airloy X103, Aerogel Technologies) and graphite. Each of the core, jacket and shield were fitted with negative temperature coefficient thermistors, which serve as either temperature sensors or Joule heaters. Both the jacket and the shield graphite pieces were connected to wires to control their temperatures through ohmic heating. The Aerrow-mini was used in the isothermal mode which measures absorbed dose by taking the ratio of the integrated drop in electrical power to the core mass.

Because the aim of the project is to use the Aerrow-mini in small fields, TRS-483 is used as a reference for notation and correction factor calculation. In order to quantify small fields effects, $k_{Q_{clin},Q_{msr}}^{f_{clin},f_{msr}}$ for various commercially available densities of aerogel were calculated using MonteCarlo down to a field size of 0.5 × 0.5 cm^2. Monte Carlo simulations were done with ESGnrc with egs_chamber module, and a 6 MV Varian Novalis linac beam model and field

sizes were specified as nominal fields at the phantom surface and not as FWHM in-plane and cross-plane.

The read-out electronics include three Keithley Nanovoltmeter Model 2182A and three National Instrument source measure units (PXIe-4138). Measurements were performed in a water equivalent phantom with a clinical Varian TrueBeam Linac. A 6 MV 10 × 10 cm^2 field, SSD of 100 cm with a dose rate of 600 MU min^{-1} was used for primary testing of the probe.

RESULTS

The figure below shows the simulated results obtained for the detector in a vertical orientation with the sensitive volume positioned at a depth of 10 cm in water. PTW microDiamond $k_{Q_{clin},Q_{msr}}^{f_{clin},f_{msr}}$ is added to the figure for comparison with field size shown in an equivalent way to the measurements [6].

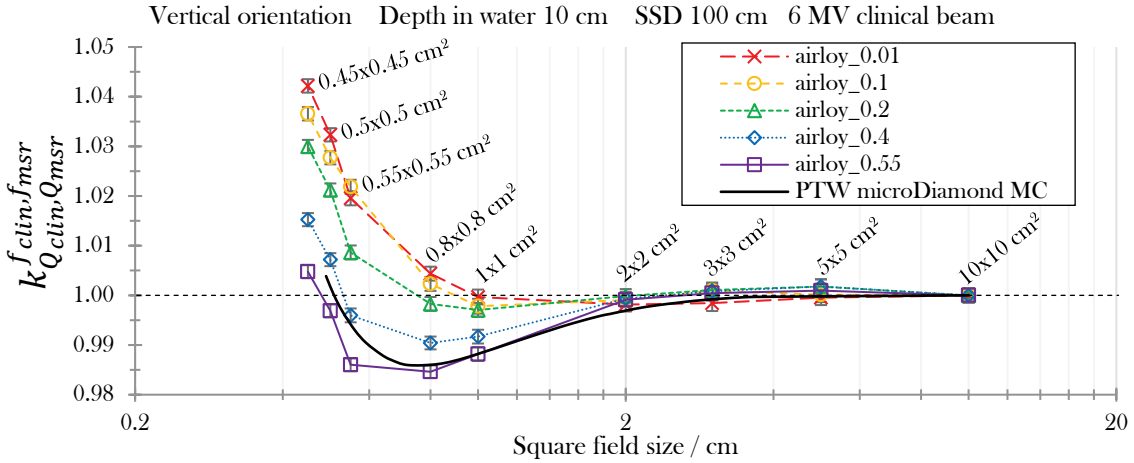

Figure 1. $k_{Q_{clin},Q_{msr}}^{f_{clin},f_{msr}}$ *for the Aerrow-mini as a function of the field size*

A prototype of the Aerrow-mini was successfully built and was used for absorbed dose measurements. A total of 9 runs of 60 seconds were done and an average signal of 6.016 µW with a relative standard deviation of 0.9 % was obtained. A minimum of 60 seconds of pre and post drift was acquired.

CONCLUSIONS

The Aerrow was successfully built and a repeatable signal was obtained. The simulation shows great potential for a small field use. The future work will be to validate the Monte Carlo simulations and fully characterize the probe in fields down to 0.5 × 0.5 cm^2.

REFERENCES

[1] SEUNTJENS, J., DUANE, S., Photon absorbed dose standards, Metrologia (2009) 46:39–58.

[2] SEUNTJENS, J., DUSAUTOY, AR., Review of calorimeter-based absorbed dose to water standards, IAEA-CN- 96-3, Vienna, Austria, IAEA (2003)

[3] DUANE, S., ALDEHAYBES, M., BAILEY, M., LEE, N.D., THOMAS, C.G., PALMANS, H., An absorbed dose calorimeter for IMRT dosimetry, Metrologia, (2012) 49:168–173.

[4] DAURES, J., OSTROWSK, Y.A., RAPP, B., Small section graphite calorimeter (GR-10) at LNE-LNHB for measurements in small beams for IMRT, Metrologia, (2012) 49:174–178.

[5] RENAUD, J., SARFEHNIA, A., BANCHERI, J., SEUNTJENS, J., Aerrow: A Probe-Format Graphite Calorimeter for Absolute Dosimetry of High-Energy Photon Beams in the Clinical Environment., Medical Physics (2017) 45:414–428.

[6] COSTE, V.D., FRANCESCON, P., Is the PTW 60019 MicroDiamond a Suitable Candidate for Small Field Reference Dosimetry?. Physics in Medicine & Biology (2017) 62:7036–7055

Design of a brass wall spherical ionization chamber for realizing air kerma in megavoltage photon beams

R. Minniti[a]
P. Bergstrom[a], **F. Bateman**[a]

[a]National Institute of Standards and Technology, Gaithersburg Maryand 20899-8460, U.S.A.

Email address of Corresponding Author: rminniti@nist.gov

BACKGROUND

The Dosimetry Group of the National Institute of Standards (NIST) maintains measurement standards for air kerma from reference kilovoltage x-ray, ^{137}Cs and ^{60}Co gamma-ray beams. These standards are disseminated through users of radiation instruments for medical dosimetry and radiation protection applications. Ionization chambers that need to be calibrated in photon fields with photon energies ranging from a few tens of keV up to 1.25 MeV benefit from the availability of these standards. More recently however a need in radiation protection has emerged for calibrating radiation detectors in terms of air kerma for use in megavoltage x-ray-based inspection systems with energies ranging between 1 MeV and 6 MeV, for which no measurement standards are available. Motivated by this need, we built a thick brass wall chamber to directly realize air kerma in photon fields with energies up to 6 MeV.

METHODS

Fig. 1 shows a picture of the new brass wall spherical chamber placed in a 6 MV x-ray beam from the NIST Clinical Linear Accelerator (Clinac).

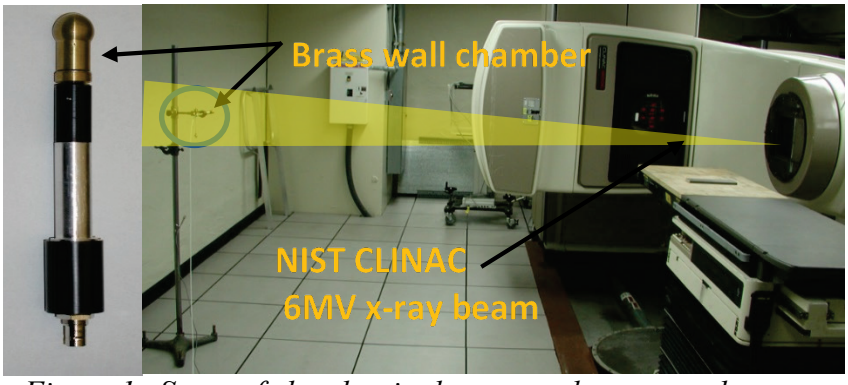

Figure 1. Setup of chamber in the megavoltage x-ray beam

The air kerma rate is realized directly using this brass wall chamber by evaluating the equation below

$$\dot{K} = \frac{I}{m}\frac{W}{e}\,(\bar{u}_{en})_b^a\,\bar{s}_a^b\,\prod k_i \qquad (1)$$

where I/m is the measured ionization current per unit mass of air in the chamber, W/e is the mean energy expended in air to produce an ion pair, $(\bar{u}_{en})_b^a$ is the ratio of the mean mass energy-absorption coefficients of air and brass, $\bar{s}_a^b$ is the ratio of the mean stopping powers of brass and air and $\prod k_i$ is the product of correction factors. Previously published [1,2] methods have been used here to evaluate the various factors of the above equation.

RESULTS

All factors in Equation 1 were evaluated for the newly designed brass wall chamber shown in Fig. 1 for realizing both the air kerma rate $\dot{K}_{Q_0}$ in the NIST ^{60}Co beam and the air kerma rate $\dot{K}_Q$, in the NIST Clinac 6 MV x-ray beam. A reasonable agreement was obtained between the air kerma rate $\dot{K}_{Q_0}$ realized with the brass chamber and the well-established ^{60}Co reference field value determined previously [1] with the NIST primary standard graphite wall chambers. This agreement serves as a measure of the confidence of the methods utilized for calculating the corrections and ratios from Eq. 1 for the brass chamber. However, not surprisingly, some of these corrections are significantly larger than those obtained previously [2] for the graphite standard chambers. Taking these findings into account, the air kerma rate $\dot{K}_Q$, was then realized with the brass wall chamber in the NIST Clinac 6 MV x-ray beam for two reference conditions and the values obtained were 1 mGy/s and 3 mGy/s.

The ability to realize the air kerma rate directly in a megavoltage x-ray reference beam with quality Q allows determining for any commercial chamber what is defined here as the *air kerma beam quality conversion factor,* k_{air,Q,Q_0} where Q_0 denotes the ^{60}Co reference beam quality. This is the air equivalent of the factor k_{Q,Q_0} derived for commercial chambers for absorbed dose to water measurements [3]. Experimental values of k_{air,Q,Q_0} were obtained for a commercial farmer type chamber using a suitable build up cap to ensure charge particle equilibrium conditions by evaluating the equation below:

$$k_{air,Q,Q_0} = \frac{\dot{K}_Q}{\dot{K}_{Q_0}} \frac{I_Q^{cc}}{I_{Q_0}^{cc}} \tag{2}$$

Where $\dot{K}_Q$ and $\dot{K}_{Q_0}$ are the air kerma rates realized in the reference beams with beam qualities Q and Q_0 respectively, and I_Q^{cc} and $I_{Q_0}^{cc}$ are the measured ionization currents produced by the commercial chamber (cc) in these beams.

CONCLUSIONS

The ability to realize the air kerma in photon fields with megavoltage energies using the brass wall chamber presented in this work will allow determining experimentally *air beam quality correction factors* k_{air,Q,Q_0} for various commercial chambers intended for use in megavoltage photon fields for radiation protection applications and thus enabling the determination of a suitable calibration coefficient for use of such chambers in megavoltage photon beams.

REFERENCES

[1] MINNITI, R., et al, The US radiation dosimetry standards for ^{60}Co therapy level beams, and the transfer to the AAPM accredited dosimetry calibration laboratories, Med. Phys. **33** (4), 1074-1077 (2006).

[2] SELTZER, S.M., BERGSTROM, P.M.: Changes in the U.S. primary standards for the air kerma from gamma-ray beams, J. Res. Natl. Inst. Stand. Technol. **108**, 359-381 (2003).

[3] ALMOND P. R., et al, AAPM's TG-51 protocol for clinical reference dosimetry of high-energy photon and electron beams, Med. Phys. **26**, (1997).

Absorbed Dose to Water Standard Using Fricke Dosimetry for 192Ir Brachytherapy Sources

C. Salata[a,b]
A. Mantuano[b], M. G. David[b], C. L. Mota[b], L. A. G. Magalhães[b], C. E. de Almeida[b]

[a]Brazilian National Nuclear Energy Authority (CNEN) – CGMI/DRS, Rio de Janeiro – RJ, Brazil.
[b]Laboratory of Radiological Sciences, Rio de Janeiro State University (LCR/UERJ). Rio de Janeiro – RJ, Brazil

Email address of Corresponding Author: camilas.salata@cnen.gov.br

BACKGROUND

The Fricke dosimeter is a water-based (95% by mass) chemical dosimetry system that offers the potential of measuring absorbed dose to water in an arbitrary geometry with minimal perturbation of the radiation field. The Laboratory of Radiological Sciences (LCR), in Rio de Janeiro State University has obtained good results using the Fricke dosimeter as a standard of absorbed dose for the high dose rate (HDR) brachytherapy 192Ir sources. In clinical practice the measurement of the absorbed dose to water is strictly necessary. However, a dosimetry primary standard for the direct measurement of the absorbed dose to water for this particular source type is currently not available [1-3]. One of the problems associated with the use of 192Ir sources is related to its calibration. The complex original emission spectrum of sources, associated to the additional contribution of the source walls, make the modeling of its dosimetry very difficult [4-5]. The main goal of work is to demonstrate the potential usefulness of the Fricke dosimetry technique for the standardization of the quantity absorbed dose in water for 192Ir HDR clinical sources, using a special vessel developed by the LCR.

METHODS

The Fricke solution was prepared using a 1L volumetric flask. First, 22ml of sulfuric acid 98% was diluted with 250ml of Mili-Q water. The PMMA Fricke vessel was constructed to ensure that the source of 192Ir is positioned exactly in the center of the circumference.

Measurements were conducted using a Gamma Med Plus HDR Ir-192 source. The Treatment Planning System was used to determine that the dose to water delivered at the center of the Fricke solution in the vessel was of 20 Gy. For the readings, it was used a Varian Cary 50 Bio spectrophotometer at 304nm UV light. Absorbed dose to Fricke solution was calculated using the equation (1), where the used G-value (radiation chemical yield of the ferric ions) of 192Ir was previously calculated by our group [5]:

$$D_W = f \cdot p_{wall} \cdot D_F \cdot F_h \cdot k_{dd} = f \cdot p_{wall} \cdot \frac{\Delta OD}{G(Fe^{3+}) \cdot L \cdot \rho \cdot \varepsilon} \cdot F_h \cdot k_{dd} \quad (1)$$

Where, ΔOD is the difference between the optical density of irradiated and control solutions; L is the optical path length of the cuvette, ρ is the density of the Fricke solution; ε is the molar linear absorption coefficient for ferric ions; *f* is the volume correction factor; *pwall* is the vessel PMMA walls correction factor; *Fh* and *kdd* are correction factors to the non-uniformity of the dose along X and Z axes.

RESULTS

One disadvantage of the developed vessel is that the dose is measured at 2,6 cm from the source, so a factor is required to convert to the standard reference position of 1 cm in water from the source. We determined this factor using PENELOPE simulations, and it we obtained a value of 7.1932. The first measurements were done in an international comparison to the National Research Council (NCR), Canada, and the results were published at C. Salata et al [5]. In Brazil more measurements were done, and results are showed in table 1.

Table 1. Dose Rate Calculated at 1cm

Manufacturer value of the dose rate	254,6 Gy/h
Obtained Dose Rate	250,5 Gy/h

The difference among the manufacturer and the calculated dose rate obtained with the Fricke dosimeter is 1,6%. More measurements need to be done in order to obtain lower uncertainties.

CONCLUSIONS

The obtained results are promising, and the Fricke dosimetry showed a good potential to be a primary standard for HDR Ir-192 sources. The developed vessel is feasible, and easier to be used when compared to previous vessels tested at the LCR. An improved vessel is been tested at LCR, the standard reference position of 1 cm in water from the source. We believe that this will help us to get better results, as the MC factor used to convert the dose from 2.7 to 1 cm is the of great influence at the measurements.

REFERENCES

[1] NATH, R., et al., “Dosimetry of interstitial brachytherapy sources: recommendations of the AAPM Radiation Therapy Committee Task Group No. 43 American Association of Physicists in Medicine”, Medical Physics, 22:209-234, 1995.

[2] RIVARD, M. J., et al., “Update of AAPM Task Group No. 43 Report: A revised AAPM protocol for brachytherapy dose calculations”, Medical Physics, 31:633-674, 2004.

[3] DI PRINZIO, R. and DEALMEIDA, C.E., “Air kerma standard for calibration of well-type chambers in Brazil using 192Ir HDR sources and its traceability”. Med Phys, 36(3):953-60, 2009.

[4] STUMP, K. E., et al., “Calibration of new high dose rate 192Ir sources”, Medical Physics, 29:1483-1482, 2002.

[5] SALATA, C., et al., “Validating Fricke dosimetry for the measurement of absorbed dose to water for HDR 192 Ir brachytherapy: a comparison between primary standards of the LCR, Brazil, and the NRC, Canada,” Phys. Med. Biol., 63(8):085004, 2018.

Can we use Monte Carlo Calculated Free-Air Chamber Attenuation Corrections?

E. Mainegra-Hing

National Research Council Canada, 1200 Montreal Rd, Ottawa K1A 0R6, Canada

Email address of Corresponding Author: ernesto.mainegra-hing@nrc.ca

BACKGROUND

Although most free-air chamber corrections are obtained using Monte Carlo (MC) simulation, the air attenuation correction, A_{att}, is still obtained from measurements due to the large uncertainties historically associated with photon cross sections and the estimation of the x-ray spectrum. ICRU report 90 suggests using Scofield's renormalized photoelectric (PE) cross-sections, $\sigma_{PE,re}$, may improve the agreement of MC calculations with measurements for low-energy x-ray beams [1]. This report also points out that from the experimental data in the literature, the two most recent high-precision data sets seemingly contradict each other regarding the choice of PE photon cross sections for air. Further experimental data for other materials are so widely spread that no conclusion can be drawn. From theoretical considerations, and the fact that $(\mu_{en}/\rho)_{air}$ is the relevant quantity for air-kerma calculation, the choice should be $\sigma_{PE,re}$ as recommended in CCRI(I) report 17-07 [2]. In light of the existing conundrum, national metrology institutes (NMI) maintaining air-kerma primary standards can provide further experimental evidence from their measured half-value layer (HVL) and air attenuation data for a large range of beam qualities. This high-quality experimental attenuation data is readily available for comparison with MC calculations for air, aluminum, and copper. An answer to the above question opens the possibility for MC-based FAC attenuation corrections, A_{att}, provided the existing models for bremsstrahlung and electron impact ionization (EII) required for modeling the production of x-ray spectra are accurate enough.

METHODS

The experimental setups used at NRC for HVL and A_{att} measurements are simulated using the EGSnrc [3] application egs_fac. A BEAMnrc simulation of an x-ray tube is used as an x-ray beam source for tube potentials between 10 kV and 80 kV and all filter thicknesses covering the whole range of beam qualities offered by NRC's low-energy x-ray calibration service. The most accurate physics parameters in this energy range are used except that calculations are carried out with the default XCOM unrenormalized photoelectric cross-sections, $\sigma_{PE,un}$, and the newly added compilation of $\sigma_{PE,re}$ from Sabbatucci and Salvat [4] based on a multi-configuration Dirac-Fock approach (MCDF). The effect on the HVL and A_{att} of using either default EGSnrc EII cross-sections (IK) or the compilation by Bote and Salvat [5] is also studied (Salvat).

RESULTS

MC-calculated A_{att} values using EGSnrc defaults (XCOM+IK) are larger than measured values by up to a 0.75% maximum difference at 80 kV for a 0.25 mm Al filter. This difference corresponds to a 25% difference in the air attenuation coefficient. If MCDF is used, the calculations are in significantly better agreement. A direct comparison between measured and calculated air attenuation values for all 80 kV beam qualities is shown in Figure 1, left panel. For filtrations above 0.2 mm Al the agreement is better than 0.2% while for very light filtration, where characteristic L-shell lines are present, the agreement with experiment worsens to about

0.3%. Consistently, Al HVL values obtained using XCOM+IK differ from measured values by as much as 35% at 80 kV (right panel). This maximum difference is reduced to about 20% if EII Salvat is used. Using MCDF with either EII cross-section compilation reduces these differences drastically to about 5% for EII IK and between -5% and -8% for EII Salvat.

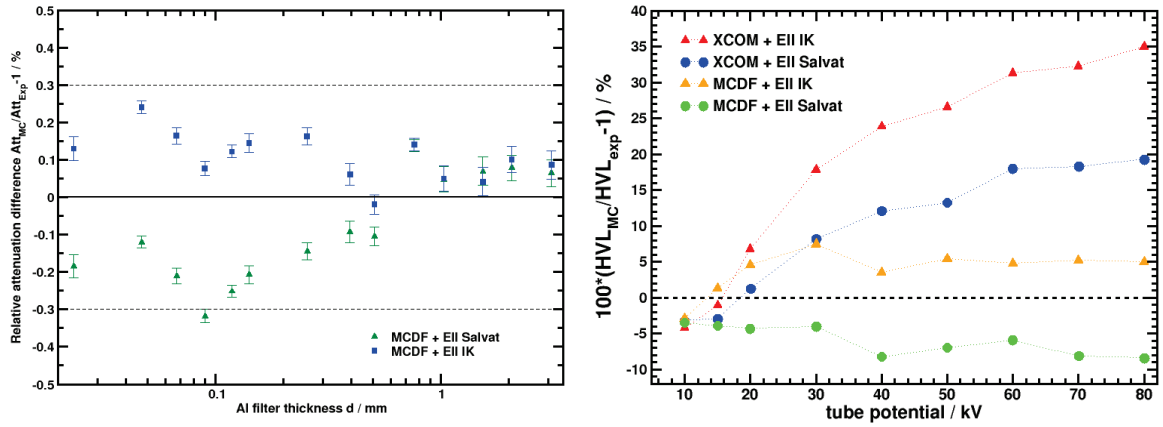

Figure 1. Comparison of MC-calculations with measurements for low-energy beams using different cross-sections options. ***Left:*** *Evacuated tube air attenuation experiment for an 80 kV beam.* ***Right:*** *Ratio of MC-calculated to measured HVL values for a 0.25 mm Al filter.*

CONCLUSIONS

Renormalized photoelectric cross sections reproduce experimental Al HVL and A_{att} data significantly better than unrenormalized cross sections. It is not clear which one of the considered EII options in EGSnrc gives the best answer since EII IK overestimates and EII Salvat underestimates the measured values by about the same amount. These observed differences can help establish confidence limits for MC-calculated FAC air attenuation corrections.

REFERENCES

[1] SELTZER, S., FERNÁNDEZ-VAREA, J., ANDREO, P., ET AL., Key data for ionizing-radiation dosimetry: measurement standards and applications. ICRU Report 90, J ICRU. 2016;14:1–110.

[2] MCEWEN, M., BURNS, D., DARIENZO, M., DE POOTER, J., PINTO, M., RAPP, B., Report to CCRI(I) on the recommendations of ICRU Report 90 CCRI(I)/17-07 (2017).

[3] KAWRAKOW, I., MAINEGRA-HING, E., ROGERS, D.W.O., TESSIER, F., WALTERS, B.R.B., "The EGSnrc Code System: Monte Carlo simulation of electron and photon transport", Technical Report PIRS-701, National Research Council Canada (2017).

[4] SABBATUCCI, L., SALVAT, F., Theory and calculation of the atomic photoeffect, Radiat. Phys. Chem. 121, 122–140 (2016).

[5] BOTE, D., SALVAT, F., Calculations of inner-shell ionization by electron impact with the distorted-wave and plane-wave Born approximations, Phys. Rev. A 77, (2008).

Design, Development and Operation of a Primary Standard Graphite Calorimeter for Proton Beam Dosimetry

R. Thomas[a]
A. Lourenco[a,b], **H. Palmans**[a,c], **N. Lee**[a]

[a]Medical Radiation Science, National Physical Laboratory, Teddington TW11 0LW, UK
[b]Department of Medical Physics and Biomedical Engineering, University College London, London WC1E 6BT, UK
[c]MedAustron Ion Therapy Center, Marie Curie-Strasse 5, 2700 Wiener, Neustadt, Austria

Email address of Corresponding Author: Russell.Thomas@npl.co.uk

BACKGROUND

The preferred method of calibration for any radiotherapy treatment facility is to calibrate the user's chamber in the beam that is to be used clinically or at least a beam similar in nature and beam structure. For photon treatments, a number of primary standards laboratories have linear accelerators which are very similar to those used for treatment thus offer calibrations for chambers across a range of beam qualities. This has shown to give a better uncertainty on the calibration coefficients of chambers, and hence improved reference dosimetry, than converting from a cobalt-60 calibration to linac MV photon energies.

Proton beam characteristics are even further removed from those of a cobalt-60 beam and yet it is common practice in proton reference dosimetry that an ionization chamber is calibrated in a cobalt-60 beam and then converted using a protocol such as described in IAEA TRS-398 [1]. Consequently, the uncertainties in proton reference dosimetry are larger in comparison with photon beams.

In the past few years, the number of proton centres worldwide has increased dramatically. It is no longer the case that ensuring consistency of dose in a single department is the priority but ensure consistency and accuracy of dose across all facilities in order to optimize our learning from clinical outcomes and maximize the benefits to patients.

METHODS

NPL has developed a dedicated primary standard graphite calorimeter for proton beams which may be taken into the clinic in order to calibrate user chambers directly. Thereby reducing the uncertainty in reference dosimetry of an individual calibration coefficient and ultimately reducing the variance in dose delivered between facilities.

With the introduction of a number of new proton therapy centres in the UK, this primary standard will be used as the basis for traceability in the UK. An Institute of Physics and Engineering in Medicine (IPEM) working Party are developing a code of practice for the dosimetry of proton beams which will utilise the NPL proton calorimeter and it will be implemented in all UK departments. Ionisation chamber calibrations will be made in a standard test volume which is similar to the actual dose volumes delivered to the tumour.

RESULTS

The NPL proton primary standard graphite calorimeter has been developed and tested over a number of years. The design is of a nested construction with a core of similar dimensions to

that of the sensitive volume of a PTW Roos ionization chamber with four thermistors embedded. Surrounding the core are two jackets each containing eight thermistors (figure 1).

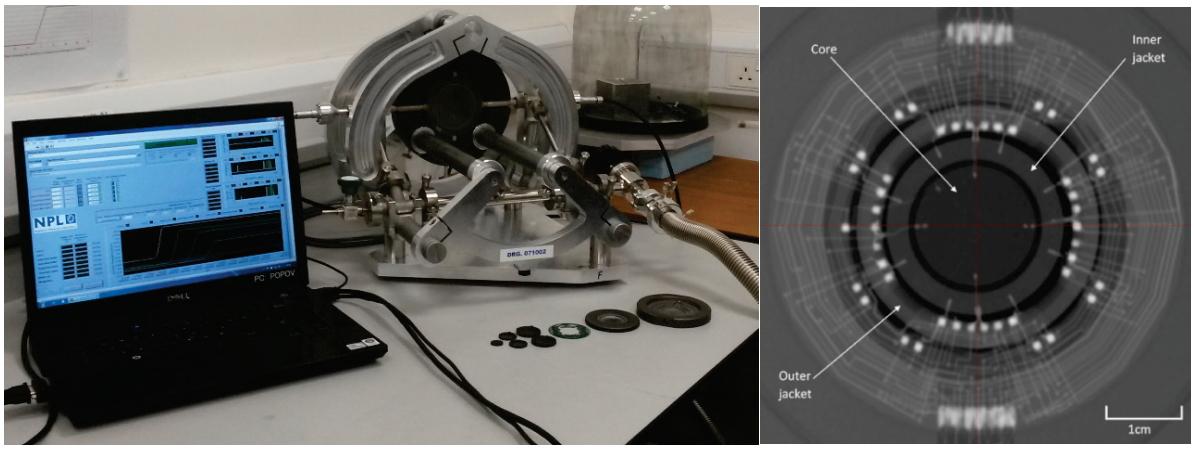

Figure 1. (a) NPL proton calorimeter with respective LabVIEW program running. In front of the calorimeter, a representation of the different graphite components (left-right: core, front and back inner jackets, front and back outer jackets, PCB, mantle lid and mantle base). (b) Radiograph of the NPL proton calorimeter which clearly shows the thermistors embedded in the core and inner jackets and the connections to the radial PCB.

The thermistors can be used to measure temperature or used as heaters. This allows the calorimeter to be operated in two different modes. Quasi-adiabatic - where the temperature of the core is allowed to increase when radiation is switched on. Isothermal - where the temperature of the calorimeter is maintained through control of the heater powers. In this mode when radiation is switched on the heater powers are reduced to maintain a constant temperature in the core. The energy deposited in the calorimeter is then calculated from the reduction in the heater power. Both methods have been successfully used in clinical proton beams.

CONCLUSIONS

NPL have built a robust and rugged primary standard calorimeter which is designed for use in clinical proton beams. Measurements have shown that the dose derived using this method is consistent and within the uncertainty of measurements when compared to the dose derived using the IAEA TRS 398 [1] protocol but with improved uncertainty on reference dosimetry. The implementation of this new primary standard will be through the implementation of the forthcoming IPEM UK code of practice for proton dosimetry.

REFERENCES

[1] ANDREO P, BURNS D T, HOHLFELD K, HUQ M S, KANAI T, LAITANO F, SMYTH V G, VYNCKIER S 2000 Absorbed dose determination in external beam radiotherapy: an international code of practice for dosimetry based on standards of absorbed dose to water IAEA *Technical Report Series 398* (Vienna: IAEA)

Status of the Update of TRS-398

Status of the Update of the IAEA TRS-398 Code of Practice

P. Andreo[a]
D. T. Burns[b], R.-P. Kapsch[c], M. McEwen[d], S. Vatnitsky[e]

[a]Karolinska University Hospital, Stockholm, Sweden
[b]International Bureau of Weights and Measures (BIPM), Paris, France
[c]Physikalisch-Technische Bundesanstal (PTB), Braunschweig, Germany
[d]National Research Council of Canada (NRCC), Ottawa, Canada
[e]MedAustron, Wiener Neustadt, Austria

Email address of Corresponding Author: pedro.andreo@ki.se

BACKGROUND

The writing of the first edition of the IAEA TRS-398 Code of Practice [1] was completed in the mid-1990s. A number of developments have taken place since that date, or will be implemented in the near future, that justify the need for updating the Code of Practice. This work presents the current status and the most important aspects of the update.

METHODS

A core group was formed in 2016 with the authors of this presentation, having the task of re-writing relevant pieces of text, coordinating the calculations and measurements of data by four international working groups, and analysing their results to produce a consensus set of data for the different radiation modalities.

The more relevant aspects considered in the update were:

i. The feedback received from users after years of application of TRS 398 in clinical practice is taken into account.

ii. The availability of new ionization chambers, requiring data for their clinical application.

iii. The implementation of new radiotherapy technologies, mostly related to megavoltage photon beams, protons and heavier ions, whose reference dosimetry requires guidance and data for end users.

iv. The ICRU Report 90 on key data for radiation dosimetry [2] recommending new values for the most relevant fundamental quantities and corrections. The impact of the new data on ionization chamber calibrations by standards laboratories and on beam quality correction factors for the different radiation modalities needs to be taken into account.

v. The Monte Carlo (MC) simulation of radiation transport has become a widely used technique for the accurate calculation of dosimetric quantities for all beam types, superseding many of the approximations used to determine the data in TRS-398.

vi. In the dosimetry of kV x rays, not only the previsions of TRS-398 for the availability of $N_{D,w}$ calibrations for these beams have not become a reality, but also there were no specific data recommended to users.

RELEVANT ASPECTS AND STATUS OF THE UPDATE

After almost 20 years of practical use of TRS-398, no major objections have been raised by feedback from users. Items of apparent difficulty have been the cross-calibration of ionization chambers and the concept of an intermediate beam quality Q_{int}, which have been re-written in an attempt to simplify further their understanding.

A number of new ionization chambers have become commercially available that require k_Q data for their use according to the recommendations of TRS-398. This requires an update of the list of chamber characteristics, some of them being already relatively old or even no longer available. Additionally, an exhaustive recent experimental study by McEwen [3] has revealed that not all chambers originally listed can be considered "reference class chambers". These aspects have motivated a number of small but significant changes in the implementation chapter with regard to the cylindrical, plane-parallel and low-energy x-ray chamber specification, calibrations, etc.

ICRU-90 key data

The ICRU Report 90 on key data for measurement standards in radiation dosimetry [2] has reviewed the quantities and correction factors that play a fundamental role in dosimetry, estimated the uncertainties of key data and analysed the implications of the new recommended data on measurements and calculations. The new data has been endorsed by the CCRI [4] and will successively be implemented in standards laboratories for the calibration of ionization chambers.

ICRU-90 includes values of fundamental quantities entering into the determination of stopping powers for light and heavy charged particles. It provides recommendations for the mean excitation energy, the *I*-value, of air (85.7 eV), graphite (81 eV) and water (78 eV), and for the graphite mass density to use when evaluating the density effect (2.265 g cm^{-3}) in the mass electronic stopping power. These quantities yield new stopping power values for electrons and positrons, protons and light ions (alpha particles and carbon ions) and, indirectly, also change the average energy required to produce an ion pair for protons and carbon ions. The recommended values for W_{air} are 33.97 eV for electrons (which is constant above about 10 keV) and 34.44 eV for protons; for carbon ions the value is subject to the same increase as for protons (0.6 %, assuming negligible perturbation correction factors for the chambers used in its determination), i.e. the resulting W_{air} is estimated to be 34.71 eV.

The state of the art and current trends regarding photon cross sections and mass energy-absorption values and ratios are analysed in detail, but no specific data were recommended in ICRU-90 due to specific issues related to the photoelectric and Compton effects, where various options were available. Other key data, such as the heat defect of liquid water and the radiation chemical yield for the Fricke dosimeter, and the correction to account for the charge of the initial electrons set in motion by low-energy photons, have also been reviewed.

The impact of the new data on measurement standards, and therefore on ionization chamber calibrations by standards laboratories, varies depending on the radiation modality and type of standard used. The changes are up to about 0.8 % for air-kerma standards for kV x-ray and ^{60}Co beams (also for some brachytherapy sources, e.g. ^{192}Ir). A similar change could have been expected for the ionometric absorbed dose to water standard for ^{60}Co at the BIPM, but the implementation of the new data is assessed in the context of known changes to other correction factors resulting in a change of only 0.1 %. For graphite-calorimetry standards there are only small changes, mostly associated with the transfer methods used for converting dose in graphite

to dose in water, which depends on the particular standard at each laboratory. No changes occur for water calorimetry.

The updated TRS-398 dosimetric data (e.g. k_Q values) are still under development. They are based on the ICRU-90 stopping power values for graphite, water and air, whereas data from previous ICRU Reports are used for other materials. For photons, the adopted values are those based on photoelectric renormalized cross sections for all materials.

Megavoltage photon beams

There have been significant linac-technology developments since the first edition of TRS-398 and among them flattening-filter free (FFF) photon beams have become widely used. Their reference dosimetry (for 10 cm × 10 cm fields) has therefore been included in the update, keeping consistency with the recommendations in TRS-483. Special linacs such as CyberKnife, MR-linacs etc, are however not included because either their use is rather limited or those delivering small fields are treated in detail in TRS-483.

The highest energy limit has been limited to 25 MeV and $TPR_{20,10}$ values between 0.6 and 0.8, these being considered to be the most widely used range in the clinic.

For the reference dosimetry of FFF beams an additional chamber-reading correction k_{vol} has been introduced to account for the volume averaging effect whenever the beam profile across the detector is not homogeneous. The correction is discussed in detail in the update along with the correction recommended in TRS-483. Note that the correction to the chamber reading has been preferred to the alternative of providing different k_Q values for FFF and conventional (with flattening filter, WFF) photon beams.

The first edition of TRS-398 included recommendations for the dosimetry of radiotherapy beams in non-standard conditions, i.e. for beam dimensions different from 10 cm × 10 cm. Recent developments, particularly for the dosimetry of small MV fields (see IAEA TRS-483 [5]), are linked to the present update to provide a consistent framework for these conditions.

High-energy electron beams

No substantial changes other than new k_Q data are foreseen for electron beams, whose upper energy limit is taken to be 25 MeV.

It is recognised that the effort required to implement reference electron dosimetry is significant and therefore the procedures will be rationalised, where consistent with the desired overall accuracy.

Despite the perceived simplicity of solid phantoms, the potential errors that can be introduced mean that there is an increased emphasis on the recommendation for not using plastic phantoms in the reference dosimetry of electron beams.

Proton and heavier ion beams

A significant technology change has taken place for proton and light ion beams in which the use of monoenergetic scanning beams using different techniques has become of common use. This is in contrast with the technology existing 20 years ago, when passively scattered beams were practically the only option available for protons; except for a minor footnote, the first edition of TRS-398 did not consider the dosimetry of monoenergetic proton beams.

The updated edition of the Code of Practice provides guidance and data for the determination of absorbed dose to water for both types of proton and light-ion beam delivery systems available in the clinic: broad-beam delivery systems using scattered or uniformly scanned beams and for pencil beam scanning systems using intensity-modulated scanned beams.

Additionally, it has been observed that the two-voltage technique for the recombination correction in ionization chambers can lead to significant errors and alternative methods have been proposed. The recommended correction procedures account for the beam behavior with respect to recombination, either as a continuous or as a pulsed beam.

These two major aspects, together with improved k_Q values, form the basis of the changes made for these radiation modalities.

Kilovoltage x-ray beams

For the dosimetry of low- and medium-energy kV x rays, not only the previsions of TRS-398 for the ready availability of $N_{D,w}$ calibrations for these beams have not become a reality, but also there were no specific data recommended.

For the metrology standards, it has been realized that $N_{D,w}$ calibrations for low-energy x rays are based on air-kerma standards and N_K is converted into $N_{D,w}$. In the case of medium-energies, some laboratories have developed absorbed dose to water standards, but it will take time to achieve their widespread clinical implementation. Hence, air kerma still is the most frequently used calibration modality and the present update incorporates its use as well as $N_{D,w}$ calibrations. It should be emphasized that this is not a step backwards, as for example most of the brachytherapy source calibrations worldwide are also based on air-kerma standards, and so are all the dosimetry procedures for radiation protection and radiodiagnostic and interventional radiology applications. The continued role and importance of air-kerma calibrations should therefore not be underestimated.

Considering that a major change in the new ICRU-90 data is due to cross sections and coefficients for the photoelectric effect, a revision of the dosimetric data available for x-ray beams in previous dosimetry protocols was deemed necessary. New values of backscatter coefficients and ratios of mass energy-absorption coefficients water/air (free-in-air and at 2 cm depth in water) have been calculated [6] that emphasize the importance of specifying x-ray beam qualities in terms of both kV and HVL. The use of old or new key data, or of old and modern MC codes, does not play an important role in the sometimes major changes that have been observed in dosimetric data for different field sizes and distances when both kV and HVL are taken into account. A large database of the relevant dosimetric data has been developed that will be accessible through an IAEA web page.

A modified formalism is included for kV x rays that considers N_K and $N_{D,w}$ calibration routes for low and medium energies. It emphasizes the role, particularly for low energies, of the field sizes and SSDs used for chamber calibration and the subsequent use under different ‘geometry’ conditions, accounting for the large dependence on field size of backscatter factors and, to a lesser extent, of ratios of mass energy-absorption coefficients water/air at 2 cm depth in water.

Determination of k_Q factors

The first edition of TRS-398 included a robust recommendation for using experimental values of beam quality correction factors. When such data were not available, k_Q values were derived using Bragg-Gray theory, where stopping-power ratios were calculated using MC simulations based on data from previous ICRU reports and chamber perturbation correction factors derived

from experiment, from MC or other calculations, or in some cases taken to be unity. In the last two decades, advanced MC techniques have been developed that enable the detailed simulation of ionization chambers and radiation sources with great efficiency. MC has become a widely used technique for the accurate calculation of dosimetric quantities for all beam types, superseding many of the approximations previously made. The cross sections and coefficients in the most commonly used MC systems have been updated following ICRU Report~90.

Using the ratio of MC-calculated absorbed doses in the chamber cavity and the dose to a point in water, values of k_Q for a large number of ionization chambers irradiated by ^{60}Co, high-energy photon, electron, proton and heavier ion beams are being calculated. For some chamber types, values of k_Q for photon and electron beams have also been obtained experimentally in standards laboratories, generally by water or graphite calorimetry. The resulting MC and experimental sets of beam quality factors for each chamber will be combined statistically to obtain consensus mean values and estimates of their relative standard uncertainty.

The MC calculations have been carried out by different groups worldwide using different MC systems. Detailed ionization chamber geometries were provided by the respective manufacturers to these groups, which using different radiation sources (published spectra or detailed phase-space files calculated for the various generators) have in all cases obtained values with type–A uncertainties of the order of 0.1 % or lower. Details on the calculations by the different groups will be given in an IAEA publication. To verify the homogeneity of the different calculations, all the MC groups were requested to carry out the specific simulation of a NE-2571 ionization chamber in megavoltage photon beams. The goal was to establish the degree of variation of the k_Q values due to the implementation of the chamber geometry and the MC transport parameters used by each group. The results of this exercise are shown in Figure 1 which also includes experimental data measured at PSDLs for this chamber type.

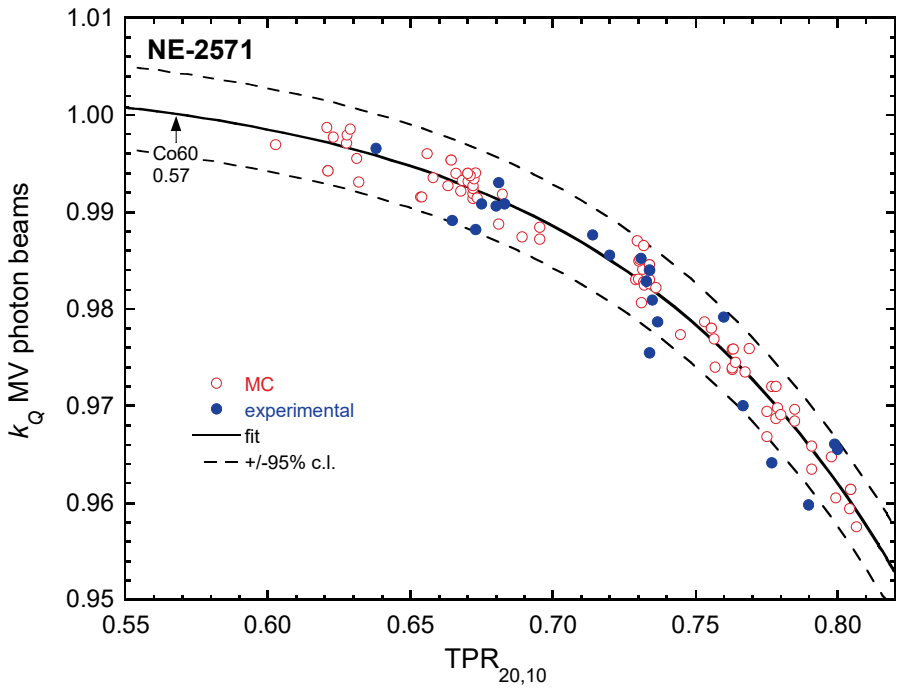

Figure 1. Values of k_Q for megavoltage photon beams obtained from Monte Carlo calculations by different groups (open circles) and measured at PSDLs (filled circles) for the NE-2571 ionization chamber type. The solid line is a fit to the data and the dashed lines are the 95 % confidence limits of the fit.

So far, the resulting k_Q data do not differ substantially from those given for chambers in the first edition of TRS-398, being generally within the uncertainties stated in that report, but the present data update is justified because of the increased confidence in the new data, to maintain consistency with the data used for measurement standards and to incorporate data for the new ionization chambers made available since the publication of the first edition.

CONCLUSIONS

Based on developments during the last two decades, the IAEA TRS-398 Code of Practice is being updated to incorporate changes in data, technology and numerical procedures. It is expected that the updated version will contribute to the harmonization and accuracy of radiotherapy beam calibrations based on a systematic and internationally unified approach.

REFERENCES

[1] INTERNATIONAL ATOMIC ENERGY AGENCY, Absorbed Dose Determination in External Beam Radiotherapy: An International Code of Practice for Dosimetry based on Standards of Absorbed Dose to Water, Technical Report Series No. 398, IAEA, Vienna (2000).

[2] INTERNATIONAL COMMISSION ON RADIATION UNITS AND MEASUREMENTS, Key Data for Ionizing Radiation Dosimetry: Measurement Standards and Applications, ICRU Report 90, Bethesda, MD (2016).

[3] McEWEN M R, Measurement of ionization chamber absorbed dose k_Q factors in megavoltage photon beams, Med. Phys. **37** (2010) 2179-2193.

[4] McEWEN M R, BURNS D T, DARIENZO M, DE POOTER J, PINTO M, RAPP B, Report to CCRI(I) on the recommendations of ICRU Report 90, Report CCRI(I)/17-07, BIPM, Sèvres (2017)

[5] INTERNATIONAL ATOMIC ENERGY AGENCY, Dosimetry of small static fields used in external beam radiotherapy: An IAEA-AAPM international Code of Practice for reference and relative dose determination, Technical Report Series No. 483, IAEA, Vienna (2017).

[6] ANDREO P, Data for the dosimetry of low- and medium-energy kV x rays (2018), available at https://ki.box.com/s/dp28y7yq46qi7uhbaau03br2i6mngxbx

Dosimetry in Nuclear Medicine

Cell-Level Dosimetry

I. Gardin[a]

[a]CHB et LITIS (EA4108), Rouen, France

Email address of Corresponding Author: isabelle.gardin@chb.unicancer.fr

BACKGROUND

The evaluation of biological risks, associated to the internal administration of diagnostic radiopharmaceutical, lies in the calculation of the mean absorbed dose to target organs [1]. This conventional dosimetric method assumes an uniform distribution of radioactivity and absorbed dose within organs. Following this approach, dosimetry assessment is a prerequisite for any clinical use of a radiopharmaceutical. The absorbed dose remains within very low values, because of the short residence time of radiotracers in biological tissues, the injected activity (less than 740 MBq), and the energy emitted per nuclear transition, which makes them suitable for human use. No adverse radiation effect on target organs has been described, provided that safety limits are not trespassed and that elementary precautions are taken.

Most radionuclides used for diagnostic imaging emit also Auger electrons (^{99m}Tc, ^{123}I, ^{111}In, ^{67}Ga, and ^{201}Tl). Their very short range in biological tissues may be responsible for dose heterogeneity at the cellular level and may have radiobiological consequences.

This paper describes the dosimetry models to calculate the mean dose absorbed by the cell nucleus from Auger radionuclides and outlines the biological implications of subcellular localization of such electron emitters.

PHYSICAL ASPECTS

Radionuclides used in nuclear medicine emit diagnostically useful photons (^{99m}Tc, ^{123}I, ^{111}In, ^{67}Ga, and ^{201}Tl). These emissions have a very wide area of action in relation to the size of human cells. As a result, conventional dosimetry is suitable for these radiations. These radionuclides emit not only photons but also mono-energetic electrons (internal conversion and Auger). Some of them (mainly Auger electrons) have very low energy from about ten keVs to less than one keV. The significance of these electrons in the dosimetry is generally neglected, largely because the energy deposited in tissue is usually small compared to the total energy emitted. In case of ^{99m}Tc, the total energy released per decay is 142.6 keV with only 0.63% coming from Auger electrons. The very low energy, and then, short range in biological material (several micrometers and below) may lead to dose heterogeneity at the cellular level and the local energy deposited may become very important when calculating the dose delivered to small volumes, as cell components (i. e. cell-level dosimetry).

The MIRD schema is the current manner to compute dosimetric data [1]. The utility of this formalism lies in its simplicity and generality. No assumption is made regarding the composition, geometry and dimensions of the source and the target. This model has been mainly used for organs and tumor, but it may also be used for smallest objects, as subcellular components.

In the aim to make dosimetry calculations for electron emissions at the cell-level and for the radionuclides used in diagnostic imaging, several authors have provided S-values, corresponding to the mean dose per unit of cumulated activity, according to the MIRD

formalism, with cells or subcellular compartments as target and source volumes. These values have been published by the MIRD committee [2]. In these models, the absorbed dose to a given cell or cell nucleus was considered as the contribution of two terms: the self-dose, which results from the radionuclide localized in the cell itself, and the cross-dose, which comes from radiations emanating from all the other cells of the tissue. The self-dose occurs alone when considering an isolated cell, as the cross-dose is needed for a multicellular model. Several subcellular distribution of radioactivity were simulated (cell nucleus, cytoplasm, cell membrane or throughout the entire cell). The cells were supposed to be concentric spheres or ellipsoids of unit-density matter. In case of cross-dose contribution, closed packed cubic or hexagonal compact cells arrangements were simulated [3]. Models assumed the same amount of radioactivity on every cell or heterogeneous uptake.

Several results may be expressed from computed simulations. As an example, cellular-to-conventional electron dose ratio delivered to the cell nucleus are given in Table 1 for five diagnostic radionuclides. In case of a same amount of radioactivity per cell, conventional electron dosimetry slightly overestimates the dose absorbed by the target cell nucleus, in case of cytoplasmic or cell membrane distribution of radioactivity. As a first approach, conventional dosimetry gives a good estimate of the mean dose delivered to the cell nucleus. In contrast, conventional electron dosimetry may strongly underestimate the mean absorbed dose to the target cell nucleus when the radioactivity is located in the nucleus. Then, dosimetric evaluation must be performed at the cellular level. This result extends to heterogeneous uptake between cells.

Table 1. Cellular-to-conventional electron dose ratio at the cell nucleus for several subcellular distributions of radioactivity, a nuclear radius of 4 µm and a cell radius of 12 µm (from Faraggi et al. [3]).

Radionuclide	Cell nucleus	Cytoplasm	Cell membrane
^{99m}Tc	6.77	0.85	0.82
^{123}I	7.40	0.86	0.74
^{111}In	5.79	0.89	0.80
^{67}Ga	7.28	0.86	0.81
^{201}Tl	11.7	0.73	0.61

BIOLOGICAL ASPECTS

Several techniques exist to determine the biodistribution of a radiopharmaceutical, such as secondary ion mass spectrometry, autoradiography and subcellular fractionation. The autoradiographic methods need a sufficient spatial resolution to determine the location of radioactivity at the subcellular level. The principle of subcellular fractionation is to separate homogenized cell fragments by centrifugation. Then, the location of the tracer is determined by assaying the different fractions for radioactivity. This technique provides only an average global repartition of the radioactivity between subcellular compartments, but not individual values for the different cells.

It is common for a radiopharmaceutical to have an intracellular uptake, preferably in one cell compartment, with a very heterogeneous amount of radioactivity per cell. For example, during hepatic scintigraphy with ^{99m}Tc macroaggregated albumin (MAA), the tracer uptake takes

place in Kupffer cells at the detriment of hepatocytes [4]. During the process of in-vitro labelling of lymphocytes with ^{99m}Tc-HMPAO, it was shown very different amount of radioactivity from one lymphocyte to another, with a mean dose to lymphocytes of 8 Gy in clinical conditions for infectious foci diagnosis (i. e. 320 MBq for 60 ml of blood) [5]. Lymphocytes viability was reduced as compared with unlabeled cells, but some lymphocytes were not dead according to the radiobiological definition. Three groups of cells may be defined: Group 1, cells receiving a high dose and are then prone to dying; Group 3, cells that have a low probability of developing cancer transformation; Group 2, cells with an intermediate dose that may have a high probability to survive and a certain probability of malignant transformation. This group might at least in theory be at risk of future cancer.

Biological effects of Auger emitters have been extensively investigated with both in-vitro and in-vivo experimental models. Most of them were performed with iodine 125, and several reviews were published on this topic (e. g. [6]). This Auger emitter has been widely studied by virtue of the high number of Auger electrons emitted per nuclear transition (25), and its half-life. Most of the results found with this radionuclide may be applied to others Auger emitters as radionuclides used in diagnostic imaging. Radiobiological studies have shown that when Auger emitters are localized outside the cell nucleus, the biological effects are characteristic of low linear energy transfer (LET) radiations. Cell survival curves have an initial shoulder. The relative biological effectiveness (RBE) is close to one in comparison to external X-ray. In contrast, Auger emitters directly incorporated into the DNA of mammalian cells give survival curves similar to those of high-LET radiations. These curves are characterized by the lack of a shoulder and a high RBE in comparison to X-rays of 7.9 for ^{125}I [7], while an upper limit of 1.5 of the RBE value was estimated for ^{99m}Tc, when all the nuclide is bound to DNA [8]. Due to the high value of RBE when the radionuclide has an intra-nucleus location, these Auger electron emitters have been proposed for targeted radiotherapy [9].

CONCLUSIONS

For radionuclides used in diagnostic nuclear medicine, conventional dosimetry is generally used to estimate the associated radiation risk in an organ. Only an average dose is obtained. This method is widely available and the results are generally acceptable. However, these radionuclides also emit very low-energy Auger electrons that can have a very different radiobiological effect from that expected by conventional dosimetry, with very large absorbed dose heterogeneities at the cellular level. This occurs when the radiopharmaceutical is internalized in the cell nucleus or when the radioactive concentration is very different from one cell to another. In these cases, cell-level dosimetry is necessary.

REFERENCES

[1] LOEVINGER, R.L., BUDINGER, T.F., WATSON, E.E. MIRD primer for absorbed dose calculations. The Society of Nuclear Medicine New York: 1988.

[2] GODDU, S.M., HOWELL, R.W., BOUCHET, L.G., BOLCH, W.E., RAO, D.V. MIRD cellular S values. The Society of Nuclear Medicine Reston: 1997.

[3] FARAGGI, M., GARDIN, I., STIEVENART, J-L., BOK, B.D., LE GULUDEC, D. Comparison of cellular and conventional dosimetry in assessing self-dose and cross-dose delivered to the cell nucleus by electron emissions of ^{99m}Tc, ^{123}I, ^{111}In, ^{67}Ga and ^{201}Tl. Eur J Nucl Med (1998) 25:205-14.

[4] GARDIN, I, COLAS-LINHART, N., PETIET, A., BOK, B.D. Dosimetry at the cellular level of Kupffer cells after technetium-99m-sulphur colloid injection. J Nucl Med (1992); 33:380-4.

[5] DE LABRIOLLE-VAYLET, C., PETIET, A., SALA-TREPAT, M., GARDIN, I., BOK, B.D., COLAS-LINHART, N. Biological consequences of the lymphocytes irradiation induced by ^{99m}Tc-HMPAO white blood cells labeling. *Sixth International Radiopharmaceutical Dosimetry Symposium*, May 7-10, 1996, Gatlinberg, Tenn., USA. ORISE 99-0164 (DE-AC05-76OR00033).

[6] YASUI, L.S. Molecular and cellular effects of Auger emitters: 2008-2011. Int J Radiat Biol. (2012) 88:864-70.

[7] NARRA, V.R., HOWELL, R.W., HARAPANHALLI, R.S., SASTRY, K.S.R., RAO, D.V. Radiotoxicity of some iodine-123, iodine-125 and iodine-131-labeled compounds in mouse testes: implications for radiopharmaceutical design. J Nucl Med (1992) 33:2196-201.

[8] NARRA, V.R., SASTRY, K.S.R, GODDU, S.M., HOWELL, R.W., STRAND, S.E., RAO, D.V. Relative biological effectiveness of ^{99m}Tc radiopharmaceuticals. Med Phys (1994) 21:1921-6.

[9] MARTIN, R.F., FEINENDEGEN, L.E. The quest to exploit the Auger effect in cancer radiotherapy - a reflective review. Int J Radiat Biol. (2016) 92:617-32.

Outcomes of the MRTDosimetry Project: Metrology for Clinical Implementation of Dosimetry in Molecular Radiotherapy

A. P. Robinson[a]
C. Bobin[b], M. Lassmann[c], V. Smyth[a], L. Struelens[d], J. Tipping[e] and the MRTDosimetry Collaboration

[a]National Physical Laboratory, Hampton Road, Teddington, Middlesex, TW11 0LW, UK
[b]CEA, LIST, Laboratoire National Henri Becquerel, (LNE-LNHB), 91191 Gif-sur-Yvette Cedex, France
[c]Department of Nuclear Medicine, University of Würzburg, Würzburg, Germany
[d]Belgian Nuclear Research Centre SCK•CEN, B-2400 Mol, Belgium
[e]Christie Medical Physics and Engineering (CMPE), The Christie NHS Foundation Trust, Wilmslow Road, Manchester M20 4BX, UK

Email address of Corresponding Author: andrew.robinson@npl.co.uk

BACKGROUND

The aim of the EMPIR funded MRTDosimetry project (June 2016 – May 2019) [1] is to provide the metrology needed for the clinical implementation of absorbed dose calculations in Molecular Radiotherapy (MRT). The project builds on the results and outputs from the preceding EMRP JRP HLT11 MetroMRT, which took the first steps towards the provision of data, methods, protocols and guidance for MRT dosimetry [2], in collaboration with many European hospitals as well as radiopharmaceutical companies and camera manufacturers. The focus of this follow-on project is "clinical implementation" and it is strongly directed by the involvement of leading hospitals across Europe as well as building on metrology expertise.

METHODS

The specific objectives of this project are:

1. To determine branching ratios and emission probabilities for ^{90}Y and ^{166}Ho to enable improved quantitative imaging (QI) and absorbed dose calculation for these radionuclides.

2. To exploit new technologies for the development of a transfer instrument optimised for measurements of the activity of MRT agents in clinics and radiopharmaceutical companies.

3. To develop 3D printed quasi-realistic anthropomorphic phantoms containing compartments fillable radioactive solutions or sealed radioactive test sources.

4. To develop a protocol for traceable calibration of QI using Single Photon Emission Computed Tomography (SPECT) for ^{177}Lu and ^{131}I, and Positron Emission Tomography (PET) for ^{90}Y, validated by a multi-site comparison exercise using quasi-realistic anthropomorphic 3D printed phantoms.

5. To generate multimodal images from SPECT phantom measurements and Monte Carlo (MC) simulations to provide material for an open-access database of reference images to be used as reference data for commissioning and Quality Control of SPECT-CT QI.

6. To improve the accuracy and metrological traceability in the calculation of absorbed dose from time-sequences of QI measurements by optimisation of the time points, choice of measurement modality (imaging or non-imaging), refinement of absorbed dose standards, and validation of available absorbed dose calculation methods.

7. To determine uncertainties in relation to the full MRT absorbed dose measurement chain from a primary standard to a range of commercial and non-commercial dosimetry calculation platforms as part of a multi-site dosimetry comparison exercise.

RESULTS

Highlights from the project will be presented [3-7] with a focus on the results of two pan-European SPECT QI and dosimetry calculation comparisons. The potential for clinical translation of the project outcomes will be highlighted and new guidance documents will be presented.

CONCLUSIONS

The MRTDosimetry project has demonstrated that traceable dosimetry for MRT can be implemented in a clinical context. The key to the long-term success of this project will be to ensure that the methods and tools developed are taken up world-wide by the MRT community.

REFERENCES

[1] http://mrtdosimetry-empir.eu/ (accessed 11/12/18)
[2] http://projects.npl.co.uk/metromrt/ (accessed 11/12/18)
[3] BILLAS, I., SHIPLEY, D., GALER, S., BASS, G., SANDER, T., FENWICK, A., & SMYTH, V. (2016). “Development of a primary standard for absorbed dose from unsealed radionuclide solutions”. Metrologia, 53(6), 1259–1271; “Reply to Comment on “Development of a primary standard for absorbed dose from unsealed radionuclide solutions”. Metrologia, 54, 615–616.
[4] VILLOING, D., MARCATILI, S., GARCIA, M.-P., & BARDIÈS, M. (2017). “Internal dosimetry with the Monte Carlo code GATE: validation using the ICRP/ICRU female reference computational model”. Physics in Medicine and Biology, 62(5), 1885–1904.
[5] D’ARIENZO, M. AND COX, M. (2017). “Uncertainty Analysis in the Calibration of an Emission Tomography System for Quantitative Imaging”. Computational and Mathematical Methods in Medicine, Volume 2017, Article ID 9830386,
[6] SOLC, J., VRBA, T., & BURIANOVA, L. (2018). “Tissue-equivalence of 3D-printed plastics for medical phantoms in radiology”. Journal of Instrumentation, 13(09), P09018–P09018.
[7] GEAR, J. I. et al, (2018). “EANM practical guidance on uncertainty analysis for molecular radiotherapy absorbed dose calculations”. Eur J Nucl Med Mol Ima., 1–12.

Clinical Alpha-Particle Dosimetry

S. Palm[a]

[a]University of Gothenburg, Sahlgrenska Academy, Dept of Radiation Physics, SE-413 45 Gothenburg, Sweden

Email address of Corresponding Author: stig.palm@gu.se

BACKGROUND

Targeted alpha therapy (TAT), where alpha emitters are used for internal radiotherapy, is a rapidly expanding field with a promise, if successful, to cure disseminated cancers. A sense of urgency to develop new alpha-emitting compounds is therefore shared by both industry and academia. The first generation of TAT (^{223}Ra; Xofigo) is not targeted towards the tumor cells but incorporates in remodeling bone due to its chemical similarity to calcium. This approved drug does not offer cure [1] but has served to introduce the concept into the clinic.

For a next generation TAT, various combinations of targeting vectors and alpha-emitters ^{211}At [2], ^{212}Pb [3], and ^{213}Bi [4,5] have been evaluated in completed clinical phase I trials. However, alpha-particle-emitting radionuclides are also delivered as targeted alpha therapy to patients outside the scope of controlled clinical trials and without any type of optimization or radiation dosimetry being performed. As an example, the recent international meeting (TAT11; Ottawa; April 2019), informed that ^{225}Ac-PSMA617 has now been used for ~800 therapeutic applications in >300 patients, all delivered as an experimental therapy for compassionate use [6,7].

As with any other type of radiation therapy, dosimetry can and should guide optimizations also of novel alpha-particle therapies and thereby also fulfil the requirements set up by new regulations for patient-specific dosimetry. In addition to tumor, normal-tissue irradiation must also be considered. The dosage of the radiopharmaceutical must therefore be properly balanced, and should be based on individual, i.e. patient-specific, dosimetric calculations. This requires quantification of radionuclide content in various organs and tissues over time. For alpha-emitters this is particularly challenging since their distribution within organs are rarely or never homogeneous. To account for likely inhomogeneity, that affect the dose distribution, the radionuclide distribution needs to be determined on a scale of the same order as the range of the emitted alpha-particles in matter, i.e. <100 μm.

The ultimate goal for alpha-particle dosimetry is, therefore, to link true microscopic 3D dose distributions to biological effect on both tumor and healthy tissues. Current lack of such data for patients is an obstacle for a wider clinical use of alpha-emitting radionuclide therapies. While the accuracy of today's alpha-particle dosimetry is nowhere near that of external-beam radiation therapy, some estimates of dose can always be derived by using relatively simple equipment and computer modelling.

METHODS

Attempts to provide clinical alpha-particle dosimetry have included the full range from measuring whole-body retention using simple probes to microdosimetry on individual cells imaged by quantitative alpha-cameras. Typically for radiopharmaceuticals, distribution is determined by gamma-camera scintigraphy. For alpha emitters, however, the abundance of gammas or characteristic X-rays suitable for gamma-camera imaging are typically low. Any scintigraphy must therefore be complemented with tissue sampling. This can include blood,

urine and feces. For intraperitoneal (i.p.) therapy, sampling i.p. liquid can provide additional information on the biokinetics needed for proper dosimetry. If possible, biopsies can be analyzed *ex vivo* for uptake and microdistribution.

As an example, a retrospective dosimetric study has previously been presented [8] for patients treated intraperitoneally with ^{211}At-MX35 F(ab')$_2$. Mean absorbed doses to normal tissues were calculated from single photon emission computed tomography/computed tomography (SPECT/CT) images. In addition, blood, urine and and i.p. fluid were measured for activity. Extrapolation of pre-clinical biodistribution data combined with clinical blood activity data allowed an estimate of absorbed doses in additional tissues.

Disseminated tumors are often too small to be imaged. Dose to various micrometastases can, however, be estimated by modelling uptake and release of targeted alphas on single cancer cells and small cell clusters [9].

RESULTS

For the example of patients treated intraperitoneally with ^{211}At-MX35 F(ab')$_2$, relatively high absorbed doses (approximately 10 Gy) were calculated for microtumors with diameters up to ~200 μm [10]. For the normal organs, the urinary bladder, thyroid, and kidneys received the highest absorbed dose. All organ doses were less than 10% of the estimated tolerance dose.

CONCLUSIONS

Dosimetry can and should be used to predict therapeutic effect, but also for estimating possible risks. Such benefit/risk estimates can then be used to further optimize the various alpha-particle therapies that are now being introduced in the clinic.

REFERENCES

[1] PARKER, C., NILDDON, S., HEINRICH D., HELLE, S.I., O'SULLIVAN, J.M., FOSSA, S.D., et al. Alpha emitter radium-223 and survival in metastatic prostate cancer. N Engl J Med **369** (2013) 213-223.

[2] ANDERSSON, H., CEDERKRANTZ, E., BACK, T., DIVGI, C., ELGQVIST, J., HIMMELMAN, J., et al. Intraperitoneal alpha-particle radioimmunotherapy of ovarian cancer patients: pharmacokinetics and dosimetry of (211)At-MX35 F(ab')2--a phase I study. J Nucl Med **50** (2009) 1153-1160.

[3] MEREDITH, R., TORGUE, J., SHEN, S., FISCHER, D.R., BANAGA, E., BUNCH, P., et al. Dose escalation and dosimetry of first-in-human alpha radioimmunotherapy with 212Pb-TCMC-trastuzumab. J Nucl Med **55** (2014) 1636-1642.

[4] SGOUROS, G., BALLANGRUD, A.M., JURCIC, J.G., MCDEVITT, M.R., HUMM, J.L., ERDI, Y.E., et al. Pharmacokinetics and dosimetry of an alpha-particle emitter labeled antibody: 213Bi-HuM195 (anti-CD33) in patients with leukemia. J Nucl Med **40** (1999) 1935-1946.

[5] ROSENBLAT, T.L., MCDEVITT, M.R., MULFORD, D.A., PANDIT-TASKAR, N., DIVGI, C.R., PANAGEAS, K.S., et al. Sequential cytarabine and alpha-particle immunotherapy with bismuth-213-lintuzumab (HuM195) for acute myeloid leukemia. Clin Cancer Res **16** (2010) 5303-5311.

[6] MORGENSTERN, A. 225Ac-PSMA617 for Therapy of Prostate Cancer – Where Do We Stand? J Med Imaging Radiat Sci **50**(Suppl) (2019) s19.

[7] KRATOCHWIL, C., BRUCHERTSEIFER, F., RATHKE, H., HOHENFELLNER, M., GIESEL, F.L., HABERKORN, U., et al. Targeted Alpha-Therapy of Metastatic

Castration-Resistant Prostate Cancer with (225)Ac-PSMA-617: Swimmer-Plot Analysis Suggests Efficacy Regarding Duration of Tumor Control. J Nucl Med **59** (2018) 795-802.

[8] CEDERKRANTZ, E., ANDERSSON, H., BERNHARDT, P., BACK, T., HULTBORN, R., JACOBSSON, L., et al. Absorbed Doses and Risk Estimates of (211)At-MX35 F(ab')2 in Intraperitoneal Therapy of Ovarian Cancer Patients. Int J Radiat Oncol Biol Phys **93** (2015) 569-576.

[9] PALM, S., BACK, T., LINDEGREN, S., HULTBORN, R., JACOBSSON, L., ALBERTSSON, P. Model of Intraperitoneal Targeted Alpha-Particle Therapy Shows That Posttherapy Cold-Antibody Boost Enhances Microtumor Radiation Dose and Treatable Tumor Sizes. J Nucl Med **59** (2018) 646-651.

[10] HALLQVIST, A., BERGMARK, K., BACK, T.A., ANDERSSON, H., DAHM-KAHLER, P., JOHANSSON, M., et al. Intraperitoneal alpha-emitting radio immunotherapy with Astatine-211 in relapsed ovarian cancer; long-term follow-up with individual absorbed dose estimations. J Nucl Med **60** (2019) doi:10.2967/jnumed.118.220384.

Adaptive Biological Treatment Planning for Peptide Radionuclide Radiotherapy

C. F. Calderón Marín[a]
J. J. González González[a], **G. Sgouros**[b]

[a]Oncology and Radiobiology Institute, Nuclear Medicine Dept., 29 & E street, Vedado, La Habana, Cuba
[b]Johns Hopkins University, School of Medicine, 733 North Broadway, Baltimore, USA

Email address of Corresponding Author: cfcalder@infomed.sld.cu

BACKGROUND

Radiopharmaceutical therapy should follow patient-specific planning protocols [1]. Internal dosimetry based on multimodal SPECT/CT images will produce more accurate dose estimates compared to the planar approach become useful for personalized treatment planning in clinical applications of radiopharmaceutical radiotherapy [2, 3]. In this contribution are presented methods for adaptive biological treatment planning based on the linear-quadratic (LQ) model adapted to radiopharmaceutical radiotherapy. The treatment prescriptions are validated using the spatial distribution of Biologically Effective Dose (BED) for calculation of the distribution parameters mean BED, Uniform Biologically Effective Dose (EUBED) for Organs at Risk (OARs) and tumors. Biological planning was simulated for several conditions for Lu-177 peptide therapy based on real patient data. Inter-patient variations and influence of random errors on dose estimations are also included. Some of these results are developed under IAEA CRP E2.30.05.

METHODS

The input prescription data are: the injected activity per cycle (A_{inj}), the number of cycles (n) and the time interval between cycles (τ). The internal dose information could be provided as: dose-volume histogram (DVH) or dose rate profiles. Dose rate profiles in kidneys, spleen, bone marrow (BM), whole body (WB) and tumors were modeled as multiexponential functions. The figure 1 shows the flux diagram for iso-effective planning. Two stop-criteria were implemented: (a) BEDs limits for OARs, or (b) BEDs in tumor(s) indicate that control could be reached without overcome the limits for OARs. In order to evaluate the effect of random errors in dose estimation, bootstrapping sampling [4] was implemented where sets of dose rate profiles or DVH will be randomly generated.

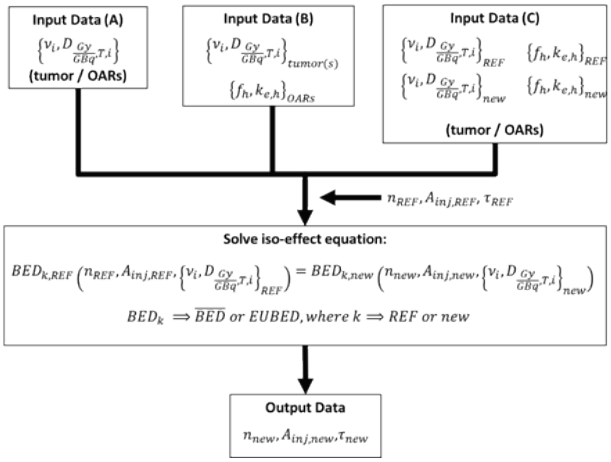

Figure 1. Diagram for iso-effective adaptive biological planning in molecular radiotherapy.

Two approach were used: (a) a mean dose rate profile or DVH for each OAR and tumor(s) were calculated, or (b) the process is repeated for each one. For tumors, the analysis was also done by grouping all tumors in a "single" volume of interest (VoI). The inter-patient variation of radiobiological data was considered by random sampling of alpha/beta values in the interval mean +/- standard deviation. The calculations are repeated for each simulated value.

RESULTS

In general, the main goal will be scaling up the total injected activity (injected activity per cycle x number of cycles). Criteria for plan evaluation and acceptance were incorporated based on iso-effective calculation for dose constraints in OARs and tumor control reference. If the interval between administration is too long dose accumulation will not be produced and the total effect after n cycles could be calculated as the summation overall partial effect (pE). Iso-effective relationships based on BED-like magnitude were obtained by solving:

$$n_{REF} \times pE_{REF}(A_{inj,REF}, D_{T,REF}) - K_{prol}(n_{REF} - 1)\tau_{REF} = n_{new} \times pE_{new}(A_{inj,new}, D_{T,new}) - K_{prol}(n_{new} - 1)\tau_{new} \quad (1)$$

where pE_k means the partial BED or EUBED reached in each cycle, $K_{prol}(n_k\text{-}1)\tau_k$ represents the loss in irradiation effect due to cell proliferation. The equation (1) could be used even for dose rate profiles or DVHs for OARs and tumor(s). The solutions of equation (1) let perform personalized treatment planning by determining an optimal prescription scheme (n,A_{inj},τ) or making adjustments during the course of the therapy considering the previous cycles (adaptive personalized planning). If spatial dose distribution in tumor (or dose rate profile) changes during the course of therapy (Figure 1) adaptive modification could be done. Inclusion of bootstrapping techniques for simulation of random error influence on dose estimation and the inter-patient variation of radiobiological parameters will produce flatter iso-effective profiles in comparison when constant parameters are used. The options for grouping several tumors in a "single volume" could help in the planning process in those cases where poor definition of tumors volume, or high-spread disease is observed. The formulation could be also used to compare different therapeutic schemes: dosing schemes, number of cycles, etc., or therapies with different radiopharmaceuticals or combined radiotherapy schemes.

CONCLUSIONS

The adaptive iso-effective biological planning could be used to establish personalized prescriptions (n, A_{inj}, τ) and also changing some of these parameters during the course of treatment. Bootstrapping techniques could be used to consider the influence random error on dose estimations and inter-patient variation of LQ parameters making predictions closer to real situations.

REFERENCES

[1] FLUX GD, O'SULLIVAN J, GAZE MN, PRISE KM, Opportunities for research in molecular radiotherapy, Br J Radiol **90** (2017) 20160921.
[2] INTERNATIONAL ATOMIC ENERGY AGENCY, Quantitative Nuclear Medicine Imaging: Concepts, Requirements and Methods, IAEA, Vienna, Austria (2014).
[3] SUNDLOV A et al., Individualised 177Lu-DOTATATE treatment of neuroendocrine tumours based on kidney dosimetry, Eur J Nucl Med Mol Imaging (2016).
[4] BARRETO H, HOWLAND F, Introduction to Econometrics - Using Monte Carlo Simulation with Microsoft Excel, Cambridge University Press, Cambridge (2006).

Parametric Optimization of Predictive Mathematical Model for the Final Thyroid Mass Determination, Assuming Heterogeneity of Thyroid Gland Mass Density

H. Weatherburn[a]
S. Fazlic[a]

[a]Cancer Centre London, 49 Parkside, Wimbledon, London SW19 5NB

Email address of Corresponding Author: henry.weatherburn@cancercentrelondon.co.uk

BACKGROUND

Administration of 131-I is a well-established technique for the treatment of thyroid disease [1]. Typical regimens used for Grave's disease (hyperthyroidism) have included low activities (80MBq), various fixed activities (185MBq, 370MBq, and 555MBq) and doses calculated on the basis of thyroid size, uptake of radioiodine and turnover of ^{131}I [2,3]. A range of activities between 3.7 GBq and 5.5 GBq [4] is typically administered for papillary and follicular thyroid carcinoma for ablation of thyroid remnants and for treatment of persistent or recurrent disease. Radioactive ^{131}I has been used to treat thyroid disease for more than six decades because it is clinically effective, safe, and cost effective in comparison with the therapeutic alternatives. Despite its widespread use, there remain many controversies surrounding use of radioiodine, including how clinicians should determine the optimal dose. Although internal radionuclide radiation dosimetry has been applied for many years, it continues to be a topic of discussion, due to uncertainties in thyroid uptake, biological half-life and thyroid mass [4,5].

METHODS

Traino et al., presented mathematical model which describes the thyroid mass reduction after the end of the clearance phase of ^{131}I from the thyroid **[6].** While this model incorporates a prediction of mass variation following the treatment, it actually considers volume variation with treatment which is based on the assumption that the thyroid mass density remains constantly 1g/cm^3 and ignores the possibility that this density may also be changing.

Traino et al. concluded their study by presenting an equation for calculation of final thyroid mass in patients with Grave's disease, assuming that thyroid tissue density is $1g/cm^3$:

$$m_{fin} = m_0 exp\left(-\alpha \frac{\Delta_{np} U A_0}{m_0}\left\{\frac{T_{max}}{2} + \frac{1}{\gamma A_0}\left[1 - \left(1 - 2\gamma \frac{A_0 T_{eff}}{ln(2)}\right)^{\frac{1}{2}}\right]\right\}\right)$$

In this paper we analyze the data available regarding the treatment of 37 patients published by Traino et al., using the same mathematical model for the reduction of Grave's disease patients after ^{131}I therapy to calculate final thyroid mass. However, unlike to other authors, we also consider the effect of actual mass density on the dose received by a thyroid as this has ramifications for the final dosimetric uncertainty. On this basis we then optimize the parameters in the mathematical model predicting the smallest deviation between the measured and calculated volume of a Grave's diseased thyroid. Two approaches were followed.

1. First premise is that the mass density is not changing during the treatment of Grave's diseased thyroid with ^{131}I, but it is different from 1 g/cm^3: $\rho_0 = \rho_{fin} \neq 1g/cm^3$.

2. Second premise is that the mass density is changing during the treatment of Grave's diseased thyroid with ^{131}I: $\rho_0 \neq \rho_{fin}$.

RESULTS

The results derived from both approaches don't significantly differ and demonstrate the possibility of obtaining better results with less uncertainty if we take in to account the mass density of thyroid tissue. While it is obvious that our results are not a real physical mass density, as mass density of $\rho_0 = 0.28 g/cm^3$ and $\rho_{fin} = 0.279 g/cm^3$ would correspond to a lung like tissue, it is therefore more likely that this result is a product of parameter *k* and real mass density ρ:

$$\rho \times k = 0.28 g/cm^3$$

CONCLUSIONS

Previous studies involving CT numbers showing that use of electron density as a proxy for specific gravity / physical density is possible and this approach could be used to study variations in thyroid mass during treatment with iodine and could be applied to improve dosimetry.

REFERENCES

[1] FLEMING, J.S., & PERKINS, A.C., Targeted radiotherapy (IPEM-R-83). United Kingdom (2000).

[2] GROSSO, M., Comparison of different thyroid committed doses in radioiodine therapy for Graves' hyperthyroidism, Cancer Biotherapy and Radiopharmaceuticals, Volume 20, Number 2, (2005).

[3] ALLAHABADIA A., et al., Radioiodine Treatment of Hyperthyroidism-Prognostic Factors of Outcome, The Journal of Clinical Endocrinology and Metabolism, 86(8):3611-3617.

[4] KLAIN M., et al., Radioiodine therapy for papillary and follicular thyroid carcinoma, Eur J Nucl Med (2002) 29 (Suppl.2):S479 S485.

[5] TRAINO, A.C., DIMARTINO, F., LAZZERI, M., A dosimetric approach to patient specific radioiodine treatment of Graves' disease with incorporation of treatment-induced changes in thyroid mass, Med. Phys. 31 (7), July 2004 pp.2121-2127.

[6] TRAINO, A.C., et al., A predictive mathematical model for the calculation of the final mass of Graves' disease thyroids treated with ^{131}I, Phys.Med.Biol.50 (2005) 2181-2191.

Patient Specific Dosimetry in Radiosynovectomy ^{153}Sm-HA

M. Takahashi [a]
J. Fernández-Varea[b], A. Santos[c], C. Cerqueira[c], C. Ramos[c], S. Brunetto[d]

[a]Instituto de Física "Gleb Wataghin", Universidade Estadual de Campinas, Campinas, Brasil.
[b]Facultat de Física (FQA and ICC), Universitat de Barcelona, Barcelona, Catalonia.
[c]Divisão de Medicina Nuclear, Departamento de Radiologia, Universidade Estadual de Campinas, Campinas, Brasil.
[b]Centro de Engenharia Biomédia, Universidade Estadual de Campinas, Campinas, Brasil.

Email address of Corresponding Author: mseren@ifi.unicamp.br

BACKGROUND

Radiosynovectomy (RS) is an invasive procedure that causes ablation of the inflamed synovial tissue through the intra-articular injection of radiotracers. Hydroxyapatite labeled with Samarium-153 [^{153}Sm-HA] are one of the options of radiotracer in RS, especially in countries where its commercial availability is superior to other isotopes, p.e. ^{90}Y [1,2]. ^{153}Sm emits β-particles with maximum energy of 808,2 keV and also a 103 keV γ-ray which is suitable to acquire images. Patient specific dosimetry for ^{153}Sm-HA RS can be a useful tool for individual treatment assessment and future determination of a standard injection activity. In the present work, we performed voxel dosimetry to calculate the 3D distribution of absorbed dose in four human articulations treated with ^{153}Sm-HA.

METHODS

To generate 3D dose distributions, it was assumed that all the activity in a given voxel is located in its centroid (point source). Given the range of β-particles in the continuous-slowing-down approximation (CSDA) and the size of the voxel, it is expected that a large fraction of the energy of the particles is deposited in the source voxel (self-dose). Adopting the MIRD formalism in this context, the source and target regions were the same voxel. The S-value, was determinate as $S_{voxel} = \sum n_i E_i \varphi_{i,voxel} / m_{voxel.}$ Here, n_i is the number of particles with energy E_i emitted per nuclear transition, $\varphi_{i,voxel}$ is the absorbed energy fraction in the source voxel and m_{voxel} is the mass attributed to the voxel.

$\varphi_{i,voxel}$ and m_{voxel} are dependent of the biological tissue of the voxel, which is determinated by the Hounsfiled scale (HU) of registered CT. For this, we defined four groups: dry air (HU<-200), adipose tissue (-200<HU<-20), soft tissue (-20<HU<+300) and compact bone (HU>+300). This four groups can better estimate voxel composition than assume that they were water or soft tissue.

Hydroxyapatite has a long biological excretion time compared to the physical half-life of these radionuclides, so ^{153}Sm-HA remains in the injected region, and no biodistribution calculation was needed. Accumlated activty in the treated area was dependent only of the calibration factor and decay time.

We built two matrices with the same dimensions as the SPECT image. One matrix had the S-values and the other had accumulated activity for each voxel. An element-wise multiplication was performed between the matrix, and the result was a 3D absorbed dose map. The steps used to calculate the 3D distribution of absorbed dose is show in Figure 1.

A volume of interest (VOI) was defined to be a volume inside an isocurve with 20% of the maximum accumulated activity in the image. Total Absorbed dose was defined as the energy deposited in the VOI divided by the total mass of the VOI.

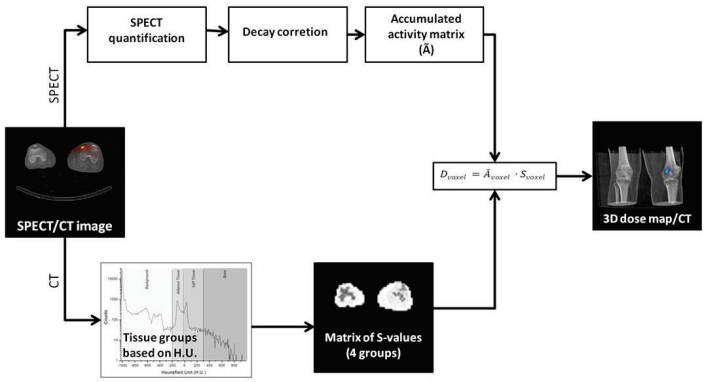

Figure 1. Steps used for patient specific dosimetry in RS using SPECT/CT images.

RESULTS

The proposed method for RS voxel dosimetry has been implemented in a in-house MATLAB [3] program. 3D absorbed dose map and total absorbed dose was calculated for total of four joints from two patients. Total absorbed dose, maximum absorbed dose for a voxel and the ratio of absorbed dose per unit of injected activity is shown in Table 1.

Table 1. Total Absorbed dose, Maximum absorbed dose in a voxel and absorbed dose per unit of injected activity.

Patient	Joint	Radiotracer	Injected Activty (MBq)	Total Absorbed Dose (Gy)	Maximum absorbed dose for a voxel(Gy)	Absorbed Dose/Activity (Gy/MBq)
1	Left knee	^{153}Sm-HA	551.3	20,6	49,52	0,037
2	Left elbow	^{153}Sm-HA	423.4	31,8	97,6	0,075
2	Right knee	^{153}Sm-HA	958.3	42,8	99,53	0,037
2	Left knee	^{153}Sm-HA	1135.9	48,5	106,8	0,051

CONCLUSIONS

The developed method for patient specific dosimetry enables the creation of 3D absorbed dose maps for ^{153}Sm-HA RS. This method allows a qualitative assessment of the treated volume extension and it can be used by the clinical staff as a tool to establish a connection between total absorbed dose and therapeutic effect.

REFERENCES

[1] CLUNIE, G. P., et al. "Changes in articular synovial lining volume measured by magnetic resonance in a randomized, double-blind, controlled trial of intra-articular samarium-153 particulate hydroxyapatite for chronic knee synovitis." Rheumatology (Oxford, England) 38.2 (1999): 113-117.

[2] CALEGARO, J., et al. "Comparison of the effect of knee synovectomy in haemophilic patients with 153Sm-and 90Y-labelled hydroxyapatite 1 year after." Haemophilia 20.6 (2014): 873-878.

[3] Guide, MATLAB User'S. "The mathworks." *Inc., Natick, MA* 5 (1998): 333.

Is Patient-Specific Dosimetry in Radionuclide Therapy Improving Patient Care?

Is Patient-Specific Dosimetry in Radionuclide Therapy Improving Patient Care? The Physicist Point-of-View

M. W. Konijnenberg[a]

[a]Dept. Radiology & Nuclear Medicine, Erasmus MC, Rotterdam, the Netherlands

Email address of Corresponding Author: m.konijnenberg@erasmusmc.nl

BACKGROUND

Targeted radionuclide therapies (TRT) have evolved from β-emitter ^{131}I therapy of thyroid diseases to highly sophisticated therapies to treat various types of metastasized cancer with targeted therapies using β-emitters, as ^{90}Y or ^{177}lu, and also with α-emitters, as ^{223}Ra and ^{225}Ac linked to a vector molecule, specific targeting the disease. Iodine uptake in thyroid tissue is very specific by the sodium/iodide symporter NIS channel and radio-iodine therapies could be administered with empirically derived fixed activities with reasonably good therapeutic efficacy and manageable low toxicity. This fixed activity administration posology has been replicated in many new targeted radionuclide therapies, including the activity 7.4 GBq (or 200 mCi) in the case of ^{177}Lu labeled compounds with a comparable half-life as ^{131}I. Several new therapies have been proven to result in prolonged progression-free and overall survival using this fixed activity protocol [1]. These results can be improved.

TRT form of course a new member in the radiotherapy family. Radiotherapy with external beams or brachytherapy are based on patient-specific treatment planning to ensure safe and efficacious therapies. Radionuclide therapies should be planned in the same manner [2]. Increasing evidence shows that also in radionuclide therapy applications dose-effect relations exist. It is possible to optimize and personalize radionuclide therapies by using dosimetry-based treatment planning [3, 4]. Normal organ toxicities can be prevented in organs with physiological uptake like kidneys and liver. Efficacy of the existing radionuclide therapies can be enhanced by treating to the absorbed dose required in target regions or to the maximum tolerable normal organ dose. Essential in all treatment planning for any type of RT is the therapeutic window concept, which also holds for TRT albeit that the absorbed dose is split into organ at risk and target dose, which are considered separately.

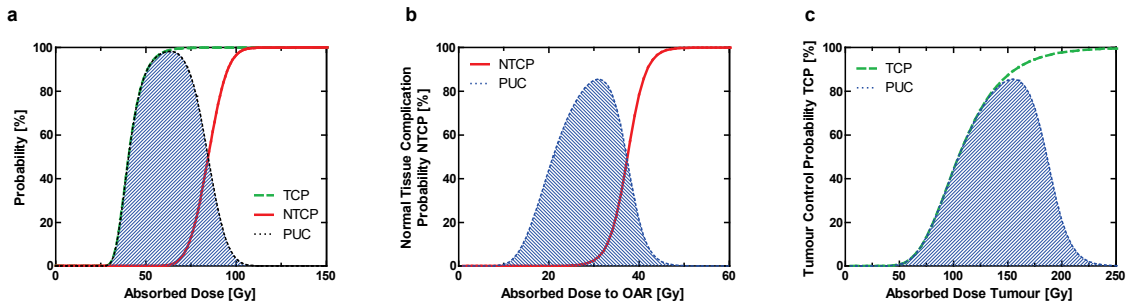

Figure 1. Therapeutic window between Tumour Control Probability (TCP), Normal Tissue Complication Probability (NTCP) leading to the Probability for Uncomplicated Cure (PUC), for external beam RT (a) and TRT (b and c).

Treatment planning models for TRT should form an essential part in the theragnostics approach. Theragnostics enables to image what you treat and dosimetry enables to predict its outcome. An overview of the options for prospective treatment planning will be presented and

the necessity to perform peri- or post- therapy dosimetry assessments. The level of accuracy in dosimetry can be variable between external probe monitor readings to full 3-D dose distributions. Practical constraints on dose reporting levels should be agreed upon as not all therapies will need the highest level of accuracy in dosimetry.

Uncertainties in the absorbed doses for TRT are much higher than the level achieved in external beam RT. These uncertainties follow from the chain of measurements involved and guidance on ways to take these uncertainties into account will help to improve the dosimetry [5]. A systematic uncertainty is contained in the targeting mechanism of TRT: radiation response of targeted cells or functional sub-units in organs at risk form a different radiobiology than with external beam RT. To enable further research in this field it is needed to know the absorbed doses from the small scale dosimetry for cells and organelles to whole organ and whole body macrodosimetry.

CONCLUSIONS

Dosimetry forms an essential part of the theragnostic approach in targeted radionuclide therapy. You see and know what you treat and how much you treat. This will improve patient care by personalized treatments with possibly better outcomes than standardized one-activity-fits-all TRT.

REFERENCES

[1] FLUX, G.D., et al., *Comparison of Empiric Versus Dosimetry-Guided Radioiodine Therapy: The Devil Is in the Details.* J Nucl Med, 2017. 58(5): p. 862.

[2] STOKKE, C., et al., *Dosimetry-based treatment planning for molecular radiotherapy: a summary of the 2017 report from the Internal Dosimetry Task Force.* EJNMMI Phys, 2017. 4(1): p. 27.

[3] STRIGARI, L., et al., *The evidence base for the use of internal dosimetry in the clinical practice of molecular radiotherapy.* Eur J Nucl Med Mol Imaging, 2014. 41(10): p. 1976-88.

[4] SJOGREEN GLEISNER, K., et al., *Variations in the practice of molecular radiotherapy and implementation of dosimetry: results from a European survey.* EJNMMI Phys, 2017. 4(1): p. 28.

[5] GEAR, J.I., et al., *EANM practical guidance on uncertainty analysis for molecular radiotherapy absorbed dose calculations.* Eur J Nucl Med Mol Imaging, 2018. 45(13): p. 2456-2474.

Out of Field Dosimetry

Dosimetric Inefficacy of Non Tissue Equivalent Commercial Optically Stimulated Luminescence Dosimeter for In Vivo Dosimetry of out of Radiation Field Exit Dose Measurements in External Beam Radiotherapy

G. K. Jain[a]
A. Chougule[b], **R. Verma**[b]

[a]Department of Radiation Oncology, MG Medical College & Hospital, Jaipur-302022, India
[b]Department of Radiological Physics, SMS Medical College & Hospital, Jaipur-302004, India

Email address of Corresponding Author: gourav108@gmail.com

BACKGROUND

The present study designed to evaluate entrance and exit doses for out of the radiation field in external beam radiotherapy (EBRT). The primary aim of this study was to investigate the efficiency of non tissue equivalent (NTE) commercially available optically stimulated luminescence dosimeters (OSLD) for in vivo dosimetry of out of the radiation field dose measurements in EBRT.

METHODS

All the measurements were performed in 10 head and neck patients (age range, 35–46 years; mean, 44 years) treated with two parallel opposed lateral fields on Bhabhatron-II TAW Telecolbalt unit (Panacea Medical Technologies, Bengaluru, India) using source to surface distance (SSD) technique. The OSLDs used in this study were from Landauer Inc., USA, Al_2O_3:C nanoDot^{TM} dosimeter (10 X 10 X 2 mm). TL dosimeters were from Nucleonics India Pvt. Ltd., LiF:Mg,Ti chips (3.2 X 3.2 X 0.89 mm). The OSL nanoDot^{TM} were placed at the level of the eyes of the patient for a single right lateral treatment field only. This methodology provided the set up to assess out of field entrance and exit radiation dose to eye. TLD-100 chips were also placed exactly in the identical places in the next treatment fraction of same patient. The physical data measured were separation distance at the level of eye, distance between radiation field edge and ipsilateral right eye at SSD. The distances were calculated for radiation beam exit from isocenter at the exit surface of the patient.

RESULTS

The distance between radiation field edge and ipsilateral eye at SSD was measured in the range of 2.0–4.0 cm with mean 3.3 cm. The distances of separation at the level of eye, entrance and exit of edge of beam from isocenter were in the range of 11cm-15cm, 7.0cm-8.5cm, 8.0cm-9.5cm respectively. It was obvious to observe with theoretical calculations using radiation divergence property that the primary radiation beam was not passing through contralateral eye. The contralateral eye was away from the exit of edge of radiation beam in all the cases and distances were found in the range of 0.5cm-2.8cm. However, when the doses were analyzed for non tissue equivalent OSL nanoDot^{TM} and it was surprising to note that the exit dose to contralateral eye (D_{exit}) were measured 1.2 to 2.0 times higher than the entrance dose to ipsilateral eye ($D_{entrance}$).

To investigate this over-response, the doses were measured with tissue equivalent TLD-100 chips in the identical conditions. It was found that D_{exit} were measured 15% to 20% less than $D_{entrance}$. Thus, the possible cause for this over-response in NTE dosimeter is increase in the

intensity of secondary electrons and low energy scattered photons reaching to dosimeter at the exit surface of the patient during out of field measurements.

The results of this study suggested that non tissue equivalent OSL nanoDot^{TM} were not the dosimeter of choice for out of field exit dose measurements. One should be precautious to use non tissue equivalent OSL nanoDot^{TM} for out of field exit dose measurements. Further study needs to be performed to deal this over-response using either appropriate correction factors or build up caps.

CONCLUSIONS

The non tissue equivalent dosimeters were not the promising dosimeters for out of field exit dose measurements. The research outputs of this study may be helpful for the selection of the appropriate in vivo dosimeter suitable for clinical use for out of the radiation field dose measurement conditions in radiotherapy.

Sensitivity Analysis to Neutron Dose at Patient's Organs According to Some Parameters in a LINAC in the Case of a Bladder Treatment

A. Alem-Bezoubiri[a,c]
H. Mazrou[b], A. C. Chami[c]

[a]Département de physique médicale, Division de Physique Radiologique, Centre de Recherche Nucléaire d'Alger-CRNA, 02 Boulevard Frantz-Fanon, BP 399 Alger-RP, 16000 Alger, Algérie.
[b]Division de l'Environnement, de la Sûreté et des Déchets Radioactifs (DESDR), CRNA, 02 Boulevard Frantz-Fanon, BP 399 Alger-RP, 16000 Alger, Algérie.
[c]Université des Science et de la Technologie Houari Boumediene, USTHB, BP 32 EL ALIA, BAB EZZOUAR ALGER, ALGERIE.

Email address of Corresponding Author: a.alem@crna.dz

BACKGROUND

The study of neutron contamination produced around medical linear accelerators was the focus of several research works, in the field, these last years [1-2]. These contamination neutrons lead to undesirable doses deposited at healthy tissues located at a distance from the target volume. As a consequence, there is an increased risk of developing secondary cancers in patients [3]. Consequently, an attempt has been made, through this work, to evaluate the photo-neutron doses at patient's organs by Monte Carlo (MC) simulation. To this purpose, a geometric MC model of the LINAC [4] was combined with a numerical MC model of the human body.

Then, a neutron contamination dose, in the organs of a female patient-specific analytical phantom, was evaluated in the case of a bladder treatment. Thereafter, a sensitivity study was performed to estimate the variation in the different organs of the patient. The achieved results were then compared to those published in the literature.

METHODS

The detailed geometry of the head of a VARIAN 2100C Linac operating in the mode of 18MV was simulated and validated using MCNP5 in a previous study [4]. In this study, we investigated the effect of some key components such as: the Primary Collimator (PC), Flattening Filter (FF), Multi Leaf Colimators (MLC), Jaws (SC), and the walls of treatment room (WR), on the production of neutron contamination, in patient' organs. To evaluate the effect of each component we kept the same geometry as it was in the initial one (without the perturbation) and removed the corresponding component. The patient anatomy was represented by MC model of an adult female MIRD phantom. The patient's bladder was placed in the isocenter and the irradiation ballistic of Bladder treatment was considered in these calculations.

RESULTS

The results are summarized in Figure1. As it can be seen, the maximum equivalent dose, in this therapy, was located at the adjacent organ (i.e. the uterus) at around 14 cm from the isocenter. And the total equivalent dose received by the mentioned organ is 53.24 mSv. While, the minimum equivalent dose is expected to be at organs located deeper from the target. From the sensitivity analysis, we presented the mean difference in dose equivalent due to removing any of FF, PC, SC, MLC and WS, the maximum difference achieved is 41%. The equivalent dose is found to be more sensitive to FF component. Finally, significant discrepancies with results

obtained by Khabaz et al [1] were found. We can say that this is due to the high dependence of secondary neutrons dose levels on the irradiation parameters.

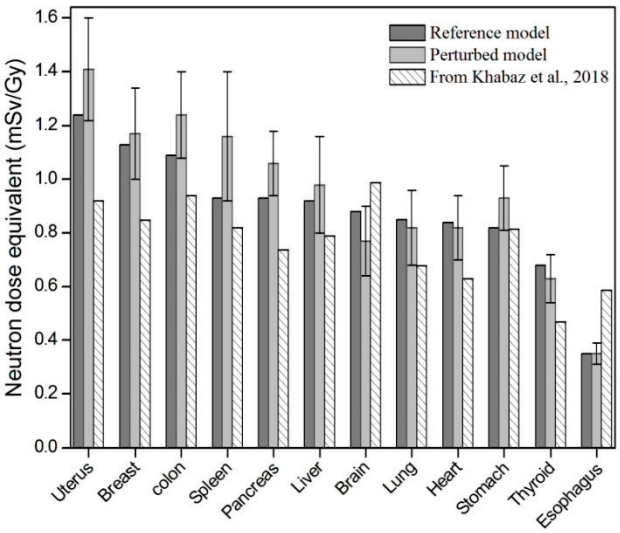

Figure 1. Equivalent dose of neutron in different organs for both models considered (Reference and perturbed models) compared with the results obtained by Khabaz et al. [1].

CONCLUSION

In this study, the photo-neutron equivalent doses were calculated at different patient's organs from a high energy LINAC. The MCNP5 Monte Carlo code was used. The treatment planning of urinary bladder was considered. As expected, the photo-neutron equivalent dose varies mainly according to the proximity of the organ considered to the target volume. The dose equivalent of photo-neutrons is more sensitive to FF components of the LINAC and to the shielding walls of the treatment room. In perspective this study will be enhanced using a more accurate human model phantom, and completed by the secondary cancer risk developing evaluation.

REFERENCES

[1] KHABAZ, R., BOODAGHI, R., BENAM, M. R., ZANGANEH, V., (2018). Estimation of photoneutron dosimetric characteristics in tissues/organs using an improved simple model of linac head. Applied Radiation and Isotopes 133: 88–94

[2] MONTGOMERY, L., EVANS, M., LIANG, L., MAGLIERI, R., & KILDEA, J. (2018). The effect of the flattening filter on photoneutron production at 10 MV in the Varian TrueBeam linear accelerator. Medical physics.

[3] BEZAK, E., TAKAM, R., YEOH, E., & MARCU, L. G. (2017). The risk of second primary cancers due to peripheral photon and neutron doses received during prostate cancer external beam radiation therapy. Physica Medica, 42, 253-258.

[4] ALEM-BEZOUBIRI, A., BEZOUBIRI, F., BADREDDINE, A., MAZROU, H., & LOUNIS-MOKRANI, Z. (2014). Monte Carlo estimation of photoneutrons spectra and dose equivalent around an 18 MV medical linear accelerator. Radiation Physics and Chemistry, 97, 381-392.

Imaging Dose from Different Imaging Modalities in Image Guided Radiotherapy of Head and Neck

A. Toutaoui
H. Mahmoudi, M. Belmessaoud, R. Louelh, S. Bencheikh

Hôpital Chahids Mahmoudi, Tizi-Ouzou, Algeria

Email address of Corresponding Author: abdelkader.toutaoui@gmail.com

BACKGROUND

Radiotherapy continues to be an essential part of a successful cancer treatment together with surgery and chemotherapy, with 50% of all patients receiving radiation therapy for the management of their cancers [1].

Modern radiotherapy relies on routine applications of imaging procedures for accurate tumor localization, real-time patient setup and margin reduction in the radio therapeutic management of cancers, a technique known as Image-Guided Radiotherapy (IGRT) [2]. The involved technologies include Digital Radiography (DR), Computed Tomography (CT), Magnetic Resonance Imaging (MRI), Positron Emission Tomography (PET), Electronic Portal Imaging (EPID), and Cone Beam CT (CBCT) etc., most of which utilizes ionization radiation [2]. Among them, Kilo-Voltage Cone Beam CT (kV-CBCT) has emerged as one of the most frequently applied techniques in the clinic.

With large therapeutic doses delivered to the tumor volume, it is not uncommon to think that there is no need to optimize our clinical practices to reduce the imaging doses to the patients from these routine imaging procedures during IGRT. Part of this view stems from the observation that the imaging doses merely accounted for a small fraction of the therapeutic doses if the imaging dose per procedure was compared to the therapeutic dose per fraction [3-6].

METHODS

In head and neck cancer treatment at Chahids Mahmoudi Hospital (Tizi-Ouzou, Algeria), treatment simulation is performed on PET-CT for better definition of target volumes. For IGRT procedures, EPID-based (electron portal imaging device) projection and cone-beam computed tomography (CBCT) imaging are used for patient positioning and verification. The need of evaluation of the contribution of imaging dose to the treatment plan is particularly pronounced since there exists a variety of different imaging systems using different photon energy (kV or MV), with 2D or 3D imaging, the dose of which is generally not included in the treatment planning system (TPS).

Our retrospective study focused on thirty patients who were treated in our department for head and neck cancer (nasopharynx, larynx, ...) and for whom a PET-CT simulation was performed. We undertook the evaluation of the dose received at different organ at risk during the PET- CT examination and the doses received from the CBCT procedures. The calculation of PET-CT effective dose includes both internal and external exposure as provided in ICRP publication 103 and 106. For Cone-beam CT, the effective dose and organ doses were estimated by using the ImPACT CT Patient Dose Calculator. The ImPACT Patient Dose Calculator, designed originally for fan beam CT, uses a library of Monte Carlo calculated dose calculations for organ doses in a humanoid mathematical phantom.

RESULTS

CT examination took the major role in contributing to the total effective dose of PET/CT imaging, corresponding to approximately 80.43%. The effective dose estimates from this investigation are similar to previous measures reported in the literature. Improved estimates of effective dose associated with the CT scan could be made by taking into account the recommended size specific dose estimates (SSDE) presented in the recently released American Association of Physicists in Medicine (AAPM) Report No. 204. The CT component of the total effective dose can be seen to increase steadily with patient weight due to automatic increases in the beam current to account for increased patient width. Alternatively, despite an increase in injected FDG activity to account for larger patients, a steady decrease in the PET component of the effective dose can be seen with increasing patient weight, which results in a lower estimated dose.

A maximum value of CBCT dose index of 182 mGy was recorded, with a number of CBCT procedures of 18 throughout the whole treatment. For all of the patients studied, the average dose index value is 55.80 mGy and the average number of CBCT procedures is 7.33. The average CBCT dose index per CBCT procedure is 8.79 mGy.

CONCLUSIONS

This work allowed a comparison of imaging dose with commonly accepted variations of the treatment beam, scatter, and leakage dose. It is assumed that the dose variations of the treatment beam which are accepted by the radiation oncologist and/or medical physicist in the spirit of the ALARA convention can also be applied to the additional imaging dose.

REFERENCES

[1] NATIONAL COUNCIL ON RADIATION PROTECTION AND MEASUREMENTS. Ionizing radiation exposure of the population of the United States: recommendations of the National Council on Radiation Protection and Measurements. Report no. 160. Bethesda, MD: NCRP, 2009.

[2] DAWSON LA, SHARPE MB. Image-guided radiotherapy: rationale, bene ts, and limitations. Lancet Oncol. 2006; 7: 848-858.

[3] ISLAM MK, PURDIE TG, NORRLINGER BD, ALASTI H, MOSELEY DJ, SHARPE MB, et al. Patient dose from kilovoltage cone beam computed tomography imaging in radiation therapy. Med Phys. 2006; 33: 1573-1582.

[4] WEN N, GUAN H, HAMMOUD R, PRADHAN D, NURUSHEV T, LI S, et al. Dose delivered from Varian's CBCT to patients receiving IMRT for prostate cancer. Phys Med Biol. 2007; 52: 2267-2276.

[5] DING GX, DUGGAN DM, COFFEY CW. Accurate patient dosimetry of kilovoltage cone-beam CT in radiation therapy. Med Phys. 2008; 35: 1135-1144.

[6] DING GX, COFFEY CW. Radiation dose from kilovoltage cone beam computed tomography in an image-guided radiotherapy procedure. Int J Radiat Oncol Biol Phys. 2009; 73: 610-617.

Out-of-Field Dosimetry in Proton Versus Photon Radiotherapy – An Outline of the EURADOS Working Group 9 Measurement Campaigns in Pediatric Phantoms

M. De Saint-Hubert[a]
Ž. Knežević[b], M. Majer[b], M. Romero-Expósito[c], I. Martínez-Rovira[c], N. Mojżeszek[d], L. Stolarczyk[d], O. Ploc[e], H. Hršak[f], L. Struelens[a], P. Olko[d], R. M. Harrison[g]

[a]Belgian Nuclear Research Center (SCK-CEN), Mol, Belgium
[b]Ruđer Bošković Institute (RBI), Zagreb, Croatia
[c]Universitat Autònoma de Barcelona (UAB), Bellaterra, Spain
[d]Institute of Nuclear Physics, PAN (IFJ-PAN), Krakow, Poland
[e]Nuclear Physics Institute (NPI), Řež, Czech Republic
[f]University Hospital Centre Zagreb, Croatia
[g]University of Newcastle upon Tyne, United Kingdom

Email address of Corresponding Author: mdsainth@sckcen.be

BACKGROUND

During radiotherapy out-of-field doses to normal tissue can lead to treatment associated side effects such as neurocognitive deficits, hypothyroidism, eyes disease, cardiac dysfunction, infertility and development of secondary neoplasms (SNs). Children are more sensitive to the effects of ionising radiation and due to their long life expectancy they have more chances to develop secondary cancer in their lifetime. Therefore, the assessment of the stray out-of-field doses is particularly important in radiation protection of child radiotherapy and forms an essential input for epidemiological studies on treatment associated side effects and the risk of SNs.

METHODS

The EURADOS working group 9 focusses on radiation dosimetry in radiotherapy and more specifically aims to assess out-of-field doses in pediatric radiotherapy treatments, using various photon and proton radiotherapy techniques. Child anthropomorphic phantoms are used that represent 5 year-old and 10 year-old children (CIRS, Inc., Norfolk, VA, USA). These phantoms allow insertion of various types of dosimeters to study the dose distribution inside the child and calculate average organ doses. Different passive dosimetry systems are used based on thermoluminescence (MTS-7, MTS-6, MCP-n) and radiophotoluminescence (GD-352M, GD-302M) while bubble detectors (BD) and polyallyldiglycol carbonate (PADC) track detectors are used to measure the neutron doses which contribute significantly to the out-of-field doses during proton therapy.

The out-of-field doses were assessed during brain irradiations because brain and central nervous system (CNS) tumours are second most common in children (accounting for 21%). The brain tumour was represented by a sphere of 6 cm diameter located on the left-anterior side of the 5 and 10 year old phantom heads. Different treatment modalities were applied during several measurements campaigns:

1. 3D-conformal radiotherapy **(3D-CRT)** - Varian Clinac 2300, Centre of Oncology Krakow
    - Measurement campaign 2013 in Krakow, Poland
2. Intensity modulated radiotherapy **(IMRT)** - Varian Clinac 2300, Centre of Oncology Krakow
    - Measurement campaign 2013 in Krakow, Poland
3. Gamma Knife (**GK**) – Leksell GK, University Hospital Zagreb

- Measurement campaign 2014 in Zagreb, Croatia

4. Proton therapy (**PT**) – Proteus 235 (IBA), Cyclotron Centre Bronowice in Krakow
    - Measurement campaign 2014 in Krakow, Poland

Furthermore, medulloblastoma treatment was studied which involves irradiation of the entire central nervous system, i.e craniospinal irradiations (CSI) which is associated with significant exposure of large volumes of healthy tissue and therefore a growing concern regarding treatment associated side effects. The entire brain and complete spine was irradiated to study the out-of-field doses using the following techniques:

1. **3D-CRT** – Siemens Artiste, University Hospital for Tumours, Zagreb
    - Measurement campaign 2014, Zagreb, Croatia
2. **Proton Therapy** - Proteus 235 (IBA), Cyclotron Centre Bronowice in Krakow
    - Measurement campaign 2017, Krakow, Poland

RESULTS

Brain irradiations with photon therapy techniques revealed most pronounced radiation to the out of-field organs using GK. The number of isocenters is an important factor defining the level of out-of-field doses during GK. IMRT, using coplanar fields, revealed the lowest out-of-field organ doses except for non-target brain and eye dose for which 3D-CRT, using non-coplanar fields, was somewhat lower. This was explained by the different treatment configurations while the use of mechanical wedges during 3D-CRT affects the out-of-field organ doses at larger distances. The out-of-field photon doses, as measured with TLDs and RPLs, are significantly lower using proton spot scanning technique compared to photon techniques. This difference becomes even larger with increasing distance from the brain, ranging from one order of magnitude, close to the brain, to more than two orders of magnitude further away from the target. In PT the neutron doses are lower than secondary photon doses close to the target while neutron dose becomes larger than secondary photon doses further away from the target. The neutron equivalent doses, as measured with BD and PADC, range from 1 mSv/Gy close to the field edge to 0.01 mSv/Gy at 20 cm from the field. Altogether still significantly reduced out-of-field doses are observed for PT spot scanning compared to photon therapy.

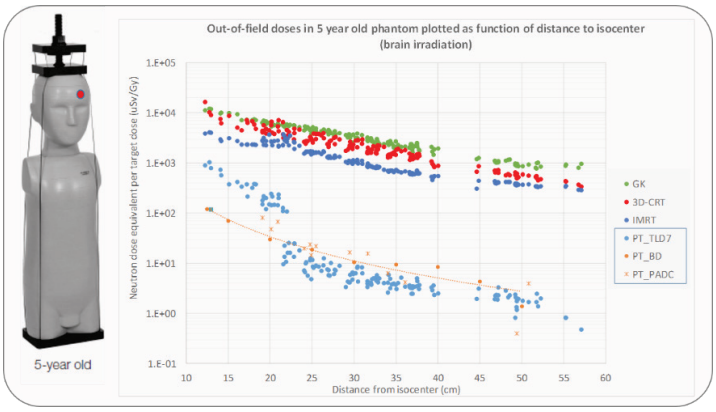

In case of CSI, 3D-CRT results in very high out-of-field doses (>800 mGy/Gy) mainly for organs that lie along the spinal cord such as thyroid, eyes, oesophagus, heart and thymus while organs such as breast, lungs and kidneys which lie more lateral in the body show significantly lower doses (<100mGy/Gy). Proton therapy data are still in progress, but the first results indicate reduced organ doses.

CONCLUSIONS

To conclude, PT reduces the out-of-field doses, but an accurate evaluation of the secondary neutron component is needed in the assessment of out-of-field doses during PT.

Dosimetry as a Tool in Optimization and Auditing

Dosimetry as a Tool in Optimization and Auditing

V. Tsapaki

Konstantopoulio General Hospital, 3-5 Agias Olgas Str, 14233, Nea Ionia, Greece

Email address of Corresponding Author: virginia@otenet.gr

BACKGROUND

The last years have witnessed immense improvements in medical imaging technology leading to a rapid increase in utilization of X-ray imaging. New digital detectors coupled with sophisticated, dedicated software and large advances in computing techniques that extract valuable clinical information within medical images have facilitated the expansion of applications of X-ray imaging not only in CT but also in mammography (breast tomosynthesis, contrast enhanced mammography, etc) and fluoroscopy. Digital imaging has improved workflow within the department and clinical outcome. The ability to easily view and store digital medical images using the Picture Archiving and Communications System (PACS) and modify them at request at any time, at any site or multiple sites at the same time, have boosted patient through-put in a medical department. Diagnostic as well as therapeutic X-ray techniques are becoming a routine in numerous centers around the world promising a successful clinical outcome and better patient safety. Focusing for example in interventional cardiology procedures, these are catheter based and do not require open surgery, extracorporeal circulation or lengthy stay within the hospital. Percutaneous Coronary Intervention considered in the past as a complex procedure and performed only in highly specialized laboratories for cardiovascular research, is now a routine technique in many hospitals. Once performed only in one occluded vessel, it is currently carried out in multivessel disease, multiple substenosis in the same vessel, or even complete occlusions in acute myocardial infarction; the technique has evolved so as to include more urgent, comorbid cases, despite achieving high success rates with significantly reduced need for repeat revascularization. Another example is catheter-guided radiofrequency (RF) ablation of cardiac arrhythmias which today is a generally accepted effective and safe procedure for the treatment of most supraventricular tachycardias, thus exhibiting rapid increase in frequency the last decade. Paediatric interventional procedures have also expanded recently due to the successful treatment of many congenital and structural heart problems. With evolving stent technology, they are currently applied in multiple areas, including pulmonary arteries, vena cavae, aortic and arch and descending aorta for coarctation. A recent concept, hybrid surgery, involves the close collaboration of the interventional cardiologist and the cardiac surgeon combining catheter-intervention and surgery in the surgical theatre, such as pulmonary artery stent implantation associated with pulmonary valve replacement.

Unfortunately, the use of X-ray equipment is inevitable in all these clinical problems. There is substantial increase of X-ray imaging utilization creating greater concern about radiation hazards. In this regard, radiation dose optimization has been given a great deal of attention the last years. Moreover, the increasing number of reports on adult radiation injuries during these procedures has raised various issues of patient radiation safety. Furthermore, most operators are unaware of the high patient radiation doses and possible radiation injuries even with the use of modern up to date equipment. Occasionally, these radiation burns can be chronically and severely painful, not to mention that both operators and hospitals may be subjected to legal actions. Despite the publicity and publications on radiation dose and harmful effects, the indexes of topics in major conferences still lack the dose optimization issue. Most operators use a “learn as you go” approach instead of formal instruction concerning radiological

equipment, or radiation dose optimization. The consequences of non-formal training in radiation protection are 1) that operators are unaware of possible dose descriptors that are currently displayed in all modern X-ray machines, 2) are not familiar with the level of radiation dose and associated risk imparted to the patient or 3) they are not aware of what are acceptable values of radiation dose.

The recent International Basic Safety Standards (BSS) [1] as well as the recent European (2013/59/Euratom) [2] both underline the need for patient dose optimization in all radiological practices. Both documents also state the need to establish typical, local, regional and national Diagnostic Reference Levels (DRLs) as a practical and important tool for dose optimization.

More specifically, International BSS clearly state at Requirement 38 entitled “Optimization of protection and safety” and under the section “Dosimetry of patients” that this must be performed and documented by or under the supervision of a medical physicist, using calibrated dosimeters and following internationally accepted or nationally accepted protocols.

The European BSS also clearly state that medical X-ray equipment must have a means to inform the practitioner of the relevant parameters for assessing the patient dose and even more important to have the capacity to transfer this information to the record of the examination (2013/59/Euratom) [2]. Finally, the European BSS introduce new requirements in relation to exposure of asymptomatic individuals, which either shall be part of an approved health-screening programme or shall require specific documented justification for that individual by the practitioner, in consultation with the referrer, following guidelines from relevant medical scientific societies and competent authorities.

Specifically, for DRLs and records of patients, International BSS provide detailed description of requirements regarding DRLs as followed: “Registrants and licensees shall ensure that:

(a) Local assessments are made at approved intervals for those radiological procedures for which DRLs have been established

(b) A review is conducted to determine whether the optimization of protection and safety for patients is adequate, or whether corrective action is required if, for a given radiological procedure:

- Typical doses or activities exceed the relevant DLR; or
- Typical doses or activities fall substantially below the relevant DRL and the exposures do not provide useful diagnostic information or do not yield the expected medical benefit to the patient.

European BSS state that ‘Diagnostic reference levels means dose levels in medical radiodiagnostic or interventional radiology practices, or, in the case of radio-pharmaceuticals, levels of activity, for typical examinations for groups of standard-sized patients or standard phantoms for broadly defined types of equipment’. Moreover, the European BSS state that ‘Member States shall ensure the establishment, regular review and use of diagnostic reference levels for radiodiagnostic examinations, having regard to the recommended European diagnostic reference levels where available, and when appropriate, for interventional radiology procedures, and the availability of guidance for this purpose’. The national DRLs should be compared with available European DRLs whenever either of the values have been established or updated. Whenever the national DRLs applied are consistently exceeded, appropriate investigations to identify the reasons, and corrective actions to improve the clinical practice, if necessary and feasible, should be undertaken without undue delay

Due to the large number of X-ray diagnostic and interventional procedures performed daily, patient dose collection can be a time consuming and complex task. Manufacturers have recently introduced sophisticated software (dose tracking software (DMS)) to the health market to assist staff on this task. Using this software, patient dose data can be easily and quickly archived using information from Digital Imaging and Communication in Medicine (DICOM) header of X-ray systems or from Picture Archiving and Communication System (PACS) of hospital and further analysed [3].

METHODS/RESULTS

Patient dose monitoring in diagnostic and interventional radiology has proved to be a well-established method to engage staff in dose optimization. Data of our continuous dose monitoring for the last years will be presented to show how these can be used to optimize patient exposure and "train" operators and staff in radiation protection.

Examples are provided in Figure 1 for Endoscopic Retrograde Cholangio-Pancreatography (ERCP) [4] and Figure 2 for Coronary Angiography (CA) [5]. The data in the Figures 1 and 2 correspond to data analysis during the years 2009 to 2016. Results are continuously discussed in our hospital with physicians (endoscopists, cardiologists, orthopedic surgeons, etc)

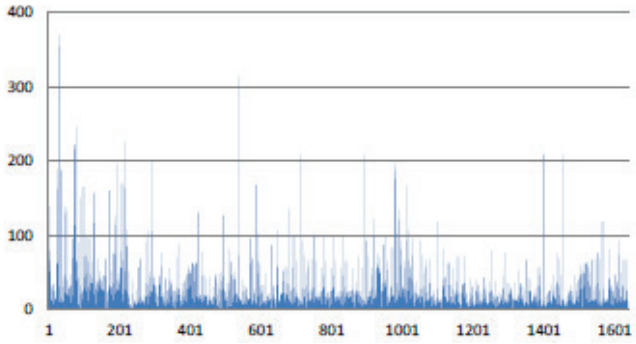

Figure 1. ERCP Patient dose in terms of P_{KA} in Gycm^2 values per procedure from year 2009 to 2016 (1632 cases). Y-axis is patient dose in P_{KA} and x-axis patient number

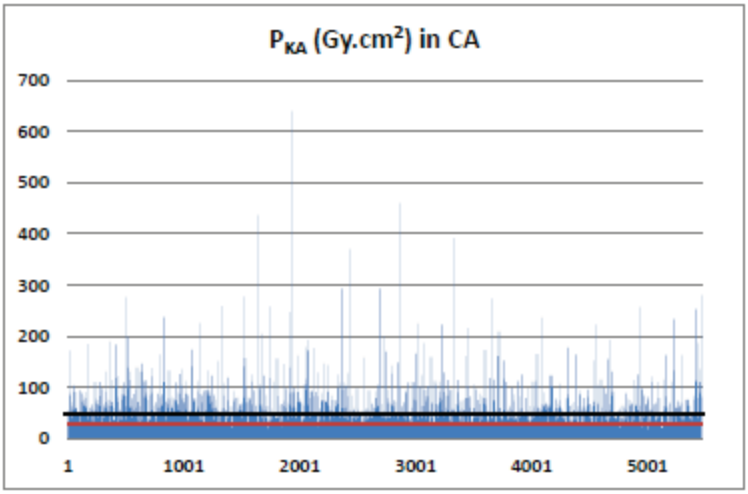

Figure 2. Patient dose in terms of P_{KA} in Gycm^2 during all Coronary Angiography (CA) procedures (5469) from January 2009 to May 2016. Red horizontal line corresponds to 45 Gycm^2 (European DRL) and black horizontal line corresponds to 55 Gycm^2 (Greek National DRL). Typical P_{KA} range was 24.5 - 30.5 Gycm^2 lower than national and European DRLs.

CONCLUSIONS

Patient dosimetry is a very important tool for exposure optimization and auditing. It also facilitates the engagement of different staff members (physicians, radiation technologists, nurses and other professional groups) to dose optimization and helps in strengthening radiation protection culture.

REFERENCES

[1] INTERNATIONAL ATOMIC ENERGY AGENCY (IAEA). Radiation Protection and Safety of Radiation Sources: International Basic Safety Standards General Safety Requirements International Atomic Energy Agency Safety Standards Series No. GSR Part 3, 2014, Vienna

[2] COUNCIL DIRECTIVE 2013/59/EURATOM 2014 Basic safety standards for protection against the dangers arising from exposure to ionising radiation and repealing Directives 89/618/Euratom, 90/641/Euratom, 96/29/Euratom, 97/43/Euratom and 2003/122/Euratom. Publications Office of the European Union, Luxembourg

[3] TSAPAKI V et al. Experience with the use of a dose management system in the everyday routine of a CT department. A touchstone or a millstone? Hell J Radiol, 3(1), 2018, 17-26.

[4] TSAPAKI V et al. (2017) Patient and Staff Radiation Exposure during Endoscopic Retrograde Cholangio-Pancreatography: Eight Years of Dose Monitoring. OMICS J Radiol 6, 2017, 253.

[5] TSAPAKI V et al. Interventional Cardiology - eight years of practice: do increased experience and technological evolution lead to undertaking more difficult cases and higher patient doses? OMICS J Radiol 6, 2017, 248.

Organ Dose Evaluation in Neck Computed Tomography Scans using a Male Anthropomorphic Phantom

F. Santos[a]
W. Abujaile[a], **A. Mourão**[a,b]

[a]Department of Nuclear Engineering, Federal University of Minas Gerais, Belo Horizonte, MG, Brazil
[b]Biomedical Engineering Center, Federal Center for Technological Education of Minas Gerais, Belo Horizonte, MG, Brazil

Email address of Corresponding Author: fernanda.stephaniebh@yahoo.com.br

BACKGROUND

Computed Tomography (CT) has been one of the most used imaging modalities in medicine. The increase of CT usage is a global concern due to high radiation doses involved [1]. Neck CT scans provide more details on neck injuries, tumors, and other diseases than other types of X-ray imaging [2]. The aim of this work is to investigate methods to reduce the absorbed dose in the neck CT with the use of bismuth shielding.

METHODS

An anthropomorphic male phantom (model Hamley Atom) was used in neck CT scans (Figure 1). Scans were carried out, covering a length ranging from the occipital to the first thoracic vertebra, using a Toshiba CT scanner (Prime Aquillion model with 80 channels). Radiochromic film strips were used to evaluate the doses in organs such as thyroid, lenses, hypophysis, spinal cord, breasts, salivary and parotid glands. Two neck CT scans were conducted using the same protocol, with the phantom in supine position with and without neck bismuth shielding.

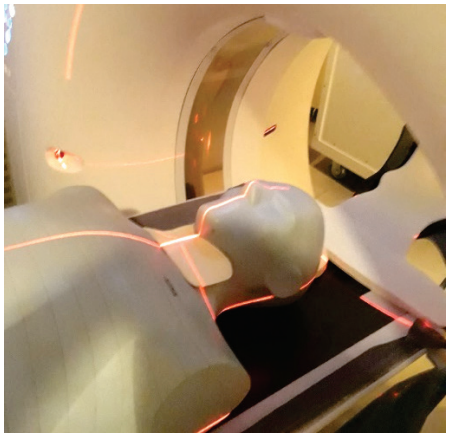

Figure 1. Hamley Atom phantom with bismuth shielding on the neck.

RESULTS

The results of this work show absorbed doses varying from 1.31 to 31.36 mGy. The highest dose of 31.36 mGy is absorbed by the thyroid without bismuth shielding (13.71 mGy with the use of bismuth shielding). The doses were lower with the use of bismuth shielding for all organs, mainly in the thyroid (Table 1). The analysis of noise in the central slice presented acceptable values for soft tissues, not exceeding 1%.

Table 1. Absorbed doses in the organs studied.

Organ position	Absorbed dose (mGy)	
	Without bismuth shielding	With bismuth shielding
Eye Lens	8.62 ± 0.69	3.29 ± 0.66
Thyroid	31.36 ± 0.96	13.71 ± 0.69
Pharynx	12.29 ± 0.78	11.47 ± 0.71
Parotid Gland	7.16± 0.62	4.49 ± 0.68
Salivary Gland	17.32 ± 0.65	13.52± 0.75
Hypophysis	7.85 ± 0.88	3.94 ± 0.78
Breast	1.81 ± 0.51	1.31 ± 0.53
Spinal Cord	11.16 ± 0.62	10.05 ± 0.72

CONCLUSIONS

Absorbed doses were determined during cervical CT scans with and without bismuth shielding on the neck of the phantom. Dose values were significantly reduced in all organs studied, suggesting that the use of bismuth shielding would, in some cases, be a proper radiation protection measure.

REFERENCES

[1] INTERNATIONAL COMMISSION ON RADIOLOGICAL PROTECTION ICRP, Statement on tissue reactions/early and late effects of radiation in normal tissues and organs-threshold doses for tissue reactions in a radiation protection context, Publication 118 (2012).

[2] ALONSO, T., MOURÃO, A., SANTANA, P., Assessment of breast absorbed doses during thoracic computed tomography scan to evaluate the effectiveness of bismuth shielding, Applied Radiation and Isotopes **117**, (2016) 55-57.

Evaluation of Lung and Thyroid Doses in Paediatric CT

P. Costa[a]
L. Giansante 1[a], D. Nersissian[a], E. Gebrim[b]

[a]Institute of Physics, University of São Paulo, São Paulo-SP, 05508-090, Brazil
[b]Institute of Radiology of the School of Medicine of the University of São Paulo, São Paulo-SP, 05403-010, Brazil

Email address of Corresponding Author: pcosta@if.usp.br

BACKGROUND

Estimation of organ doses imparted by CT procedures is not a trivial task. Three approaches have been adopted over the past decades: (a) direct measurements with different kinds of dosimeters, anthropomorphic phantoms, and postmortem subjects, (b) calculations using Monte Carlo methods combined with computational human phantoms, and (c) biological dosimetry based on blood samples [1]. Several advantages and disadvantages can be discussed regarding each approach. Anthropomorphic phantoms for dosimetry, for instance, have been in use for more than 30 years, and research indicates that there is ongoing development in the field of computational phantoms responding to to the development of new CT technologies [2].

METHODS

In the present study, an experimental methodology to evaluate organ doses in routine peadiatric chest CT protocols were implemented. The methodology uses TLD (LiF:Mg,Ti) chips embedded in a pediatric anthropomorphic phantom. Their small size provides accurate spatial localization of the dose inside the studied organs (lungs and thyroid). The phantom used was the CIRS ATOM® dosimetry verification phantom, model 705 (CIRS, Inc., VA, USA), which simulates a pediatric 5-year old patient. The irradiations were performed using a Philips Brilliance 64 CT scanner (Philips, Germany). The method for organ dose calculation from TLD signal distributions inside the target organs was previously published by the authors [3].

RESULTS

Lung and thyroid absorbed doses with respective uncertainties (*k = 1*) for the Chest protocols applied to the pediatric phantom, are presented in Table 1.

Table 1. Lung and thyroid absorbed doses with respective uncertainties (k = 1) for the Chest protocols a*pplied to the pediatric phantom*

		80 kV/146 mAs	120 kV/55 mAs
Mean absorbed dose (mGy)	Thyroid	5.93 ± 0.31	6.84 ± 0.25
	Lungs	4.58 ± 0.22	6.12 ± 0.27

CONCLUSIONS

Findings of the present investigation may pave the way to decrease radiation dose whereas the image quality could be potentially preserved. In particular, dose reduction of up to 28.7% on the absorbed dose was reported for pediatric protocols with a change from 120 to 80 kV.

Further investigations considering other radiosensitive organs and other protocols must be conducted as a step towards the implementation of optimization strategies.

REFERENCES

[1] KALENDER, W. A., Dose in x-ray computed tomography. Physics in Medicine and Biology, 2014. 59(3): p. R129-R150.

[2] COSTA, P. R., Computer Tomography Phantom Applications, in The Phantoms of Medical and Health Physics. 2014, Springer. p. 123-142.

[3] GIANSANTE, L., et al., Organ doses evaluation for chest computed tomography procedures with TL dosimeters: Comparison with Monte Carlo simulations. Journal of Applied Clinical Medical Physics (2019) 20(1): 308–320. doi: 10.1002/acm2.12505

Radiation Protection Dosimetry and Diagnostic Reference Levels for X-ray Imaging Procedures: An Excerpt from ICRP Publication 135

D. Joseph[a]
C. Nzotta[b], **M. Silas**[c], **N. Flavious**[c]

[a]Department of Medical Radiography, Bayero University Kano, Nigeria
[b]Department of Radiography, Nnamdi Azikiwe University, Nnewi Campus, Nigeria.
[c]Department of Medical Radiography, University of Maiduguri, Borno State,Nigeria

Email Address of Corresponding Author: josephdlama@gmail.com

BACKGROUND

Radiation protection and dosimetric protocols for establishing Diagnostic Reference Levels (DRLs) have been clearly outlined in ICRP Publication 135. Diagnostic Reference Levels have been proven to be an effective tool that aids in optimization of protection in medical exposures of patients for x-ray imaging procedures. The aim of this study is to establish dosimetric protocols for DRLs in medical imaging procedures and to provide guidelines from ICRP Publication 135, which will serve as a guide for practitioners globally.

METHODS

This work is a prospective cross-sectional study carried out to establish DRLs for adult radiological procedures in some selected teaching hospitals in North Eastern Nigeria. A total of 1080 patients were enlisted in this study, thirty patients for each of the 36 different procedures featuring common x-ray examinations, dental x-ray examinations, contrast examinations, mammography and computed tomography examinations. Thermoluminiscent dosimeter (TLD) chips and dose area product (DAP) meters were used to obtain the dose values (Entrance surface dose, Dose area product) using standard protocols. Exposures were made with TLDs placed at the central axis at point where the x-ray beam intercepts the patient's skin. Computed tomography dose index and dose length products were obtained from the computed tomography scanner console.

RESULTS

The DRLs for posterior anterior (PA) chest and lateral x-ray obtained in this work were 0.59 mGy and 1.02 mGy, respectively. For PA skull and lateral skull x-ray DRLs were 1.02 mGy and 1.01 mGy. The DRLs for PA elbow and lateral elbow were 0.57 mGy and 1.77mGy. For AP shoulder and lateral x-ray DRLs were 0.71 mGy and 0.83 mGy. The DRL for dorsi-plantar foot and dorsi-plantar oblique foot in this work were 0.58 mGy and 0.61. Dose values for contrast studies were 6.68mGy, 10.66mGy.cm^2 for IVU, 2.31 mGy, 3.67mGy.cm^2 for HSG, 2.66 mGy, 8.98mGy.cm^2 for barium meal, 12.78 mGy, 20.64 mGy.cm^2 for barium enema, 2.73 mGy and 6.56 mGy.cm^2 for barium swallow and 2.05 mGy, 7.77 mGy.cm^2 for RUG. Diagnostic reference levels for cranio-caudal and medio-lateral oblique were 0.63 and 1.04 mGy while CT head, chest and abdomen are 67.90 mGy, 18.38 mGy and 19.20 mGy.

Table 1. Median doses and 75th percentile (DRLs) for Radiographic examination

Examination	Median ESD (mGy) Hospital A	Median ESD (mGy) Hospital B	Median ESD (mGy) Both	DRL (mGy)
PA chest x-ray	0.34±0.05	0.55±0.43	0.45±0.36	0.59
Chest x-ray lateral	0.78±0.07	0.87±0.49	0.82±0.44	1.02
PA skull x-ray	0.79±0.32	0.74±0.50	0.77±0.41	1.02
Lateral skull	0.77±0.32	0.61±0.45	0.69±0.73	1.01
AP elbow	0.44±0.05	0.36±0.17	0.40±0.25	0.57
Lateral elbow	0.56±0.06	0.36±0.29	0.46±0.34	0.77
AP shoulder	0.29±0.03	0.71±0.27	0.50±0.24	0.71
Lateral shoulder	0.59±0.06	0.66±0.40	0.63±0.37	0.83
Dorsi plantar foot	0.34±0.03	0.56±0.24	0.45±0.21	0.58
Dorsi plantar oblique foot	0.36±0.03	0.45±0.25	0.41±0.23	0.61
Abdominal x-ray	0.87±0.46	0.43±0.35	0.83±0.31	1.01
Pelvic x-ray AP	0.62±0.05	0.80±0.34	0.60±0.30	0.82
Hand dorsi palmar oblique	0.21±0.03	0.58±0.28	0.25±0.20	0.59
Hand dorsi palmar	0.49±0.07	0.30±0.21	0.56±0.37	0.58

Table 2. Median doses received and 75th percentile (DRLs) for contrast radiographic examination

Examination	Median ESD (mGy) Hospital A	Median ESD(mGy) Hospital B	Median ESD (mGy) Both	DAP (mGy.cm^2)	DRL mGy	DRL mGy.cm^2
IVU	2.17±1.94	4.61±4.58	4.89±3.26	9.25±1.31	6.68	10.66
HSG	1.41±0.66	2.30±1.45	1.44±0.55	2.97±0.55	2.31	3.67
Barium meal	1.66±0.44	2.61±1.31	2.14±0.88	7.33±1.85	2.66	8.98
Barium enema	10.63±1.05	2.62±1.31	11.95±1.90	16.26±3.23	12.78	20.64
Barium swallow	1.62±0.35	2.62±1.45	2.12±0.90	7.62±2.01	2.73	6.56
RUG	1.18±0.65	1.82±1.19	1.50±0.92	5.91±1.24	2.05	7.55

Key- IVU- Intravenous urography, HSG- Hysterosalpingography, RUG- Retrograte-urethrography, ESD- Entrance skin dose, DAP-Dose area product

Table 3. Median doses received and 75 percentile (DRLs) for computed tomography examination

Examination	Median CTDI (mGy) Hospital A	Median CTDI (mGy) Hospital B	Median CTDI (mGy) Both	DLP (mGy.cm)	DRL (mGy)
CT Head	57.26±12.50	44.08±9.95	57.251±2.50	958.52±6.3	67.90
CT Chest	13.94±4.48	10.64±4.78	12.58±4.20	659.10±1.30	18.38
CT Abdomen	13.92±5.57	10.92±5.57	12.24±4.28	1290.07±1.71	19.20

Key- CT- Computed tomography, CTDIvol- Volumetric computed tomography dose index, DLP- Dose length product.

CONCLUSIONS

This study has followed the standard dosimetry requirements by ICRP to establish DRLs in two teaching hospitals in North Eastern Nigeria a low resource setting, which is useful for formulation of National DRLs.

REFERENCES

[1] BASIC SAFETY STANDARD 9 COUNCIL DIRECTIVE 96/29/EURATOM, Laying down Basic Safety Standards for the protection of the health of workers and the general public against the dangers arising from ionizing radiation, Official Journal of the European Communities, No L 159.

[2] BRENNAN P C., DONNELL M.C AND LEANLY D.O., Increasing FFD Reduces Radiation Protection, Dosimetry, Oxford University Press, (2004) 108 (3):263 -268.

[3] EGBE N.O, INYANG S. O., EDUWEM D. U., AND AMA I., Doses and Image Quality for Chest Radiograph in three Nigerian Hospitals, European Journal of Radiography, (2011), 1:30 – 36.

[4] EUR96 (1996) EUROPEAN GUIDELINES ON QUALITY CRITERIA FOR DIAGNOSTIC RADIOGRAPHIC IMAGES, European Commission, EUR 16260 EN, June 1996

[5] EUROPEAN COMMISSION. European Guidelines on Quality Criteria for Diagnostic Radiographic Images, EUR, 16260 EN, Luxembourg. Office for Official Publications of European Communities 1996.

[6] HART D, HILLER M C, SHRIMPTON P .C. Doses to patients from Radiographic and Fluoroscopic x-ray imaging procedures in the UK-2010 Review. Health Protection Agency Publication, (1996)1(2):716- 1416.

[7] INSTITUTE OF PHYSICS AND ENGINEERING IN MEDICINE. Recommended standard for routine performance testing of diagnostic x-ray imaging system. IPEM Report 91. York, UK: IPEM 2015.

[8] INTERNATIONAL COMMISSION ON RADIOLOGICAL PROTECTION. (ICRP 135) Diagnostic reference levels in medical imaging: review and additional advice. (2015) [http://www.icrp.org/docs/DRL_for_web.pdf. Accessed August 24, 2016]

[9] INTERNATIONAL ATOMIC ENERGY AGENCY, International Basic Safety Standards for Protection against Ionizing Radiation and for safety of radiation sources *IAEA Safety Series* No. 115-1, Vienna Austria.

[10] IONIZING RADIATION MEDICAL EXPOSURE REGULATIONS.2000. (IRMER). (2012). Guidance on the use of Diagnostic Reference Levels as the Term applies to Ionizing Radiation. Regulation 2000.

Protons and Beyond

The New ICRU Report on Prescribing, Recording and Reporting Light Ion Beam Therapy

O. Jäkel[a]
C. Bertb[b], P. Fossati[c], C. P. Karger[d], T. Kamada[e], N. Matsufuji[e], M. Scholz[f], P. M. DeLuca[g]

[a]German Cancer Research Center DKFZ, Heidelberg, Germany and Heidelberg Ion Beam Therapy Center HIT, Heidelberg, Germany.
[b]University Medical Center, Erlangen, Germany.
[c]Fondazione CNAO, Pavia, Italy and MedAustron, Wiener Neustadt, Austria.
[d]German Cancer Research Center, Heidelberg, Germany.
[e]National Institute of Radiological Sciences NIRS, Chiba, Japan.
[f]Gesellschaft für Schwerionenforschung GSI, Darmstadt, Germany.
[g] University of Wisconsin, Madison, USA.

Email address of Corresponding Author: o.jaekel@dkfz.de

BACKGROUND

The International Commission on Radiation Units and Measurements (ICRU) is currently in the final stage of publishing Report 93, Prescribing, Recording and Reporting Light Ion Beam Therapy.

Light ion beam therapy has been initially developed at Lawrence Berkeley National Laboratory (LBNL) and first patients were treated with helium beams there in 1954, the same year, when proton therapy started in Berkeley. In 1975, also at LBNL, heavier ions, like carbon, neon, silicon and argon ions were used in clinical trials. It has been shown in these trials, that light ions offer not only a beneficial absorbed depth dose curve, but in addition have an increased biological effectiveness in the Bragg peak as compared to entrance region, which makes them very attractive especially for treating radio-resistant tumors. The first clinical facility for carbon ion beam therapy was opened in 1994 in Chiba, Japan and the number of clinical centers has been increasing slowly, but steadily, with ten centers being in operation today.

The report is the result of a longstanding collaboration between the IAEA and ICRU and has been initiated after joint meetings in Vienna, Austria (2004) and Columbus, Ohio (2006) in an attempt to standardize the reporting of light ion beam radiotherapy [1].

METHODS

The report relies on concepts previously developed by the ICRU for reporting other therapies but with special emphasis on the use and reporting of RBE-weighted quantities [2]. Such harmonization will facilitate the comparison of therapeutic results obtained with ions not only between ion beam therapy centers but also with centers using other modern forms of radiation therapy, such as proton-RT and IMRT with photon beams.

The report outlines the different biological models used for calculating RBE weighted dose for light ion beam therapy and attempts to clarify their clinical use in order to enable a common understanding of clinical practice in various facilities. It gives detailed recommendations on how light ion beam therapy should be prescribed, recorded and reported. The physical and technical background of light ion beam therapy is explained. The recommendations on dosimetry were harmonized and updated according to the upcoming revision of IAEA's

International Code of practice based on standards of absorbed dose to water, TRS-398 [3] and the latest key data for ionizing-radiation dosimetry, ICRU report 90 [4].

RESULTS AND CONCLUSIONS

Consistent with previous ICRU Reports 78 [5] and 83 [6], this report outlines the fundamentals of radiotherapy with light ion beams and recommends a strict terminology for volumes and doses (absorbed dose and RBE weighted dose). Moreover, the current radiobiological models, used clinically to calculate RBE, are reviewed. Recommendations are given, as to how clinical treatments should be prescribed, recorded and reported, in order to facilitate a comparison of clinical results and avoid confusion among different centers.

We are convinced that this report will help to improve the terminology in the field of light ion therapy and help to communicate clearly about the clinical outcomes.

REFERENCES

[1] IAEA, International Atomic Energy Agency. *Relative Biological Effectiveness in Ion Beam Therapy*, Technical Reports Series No. 461 (International Atomic Energy Agency, Vienna).

[2] ICRU, International Commission on Radiation Units and Measurements. "Prescribing, recording, and reporting proton-beam therapy," ICRU Report 78, J. ICRU **7**(2).

[3] IAEA, International Atomic Energy Agency. *Absorbed Dose Determination in External Beam Radiotherapy: An International Code of Practice for Dosimetry Based on Standards of Absorbed Dose to Water*, IAEA TRS-398 (International Atomic Energy Agency, Vienna).

[4] ICRU, International Commission on Radiation Units and Measurements. "Key data for ionizing-radiation dosimetry: Measurement standards and applications," ICRU Report 90, J. ICRU **14**(1).

[5] ICRU, International Commission on Radiation Units and Measurements. "Prescribing, recording, and reporting proton-beam therapy," ICRU Report 78, J. ICRU **7**(2).

[6] ICRU, International Commission on Radiation Units and Measurements. "Prescribing, recording and reporting photon-beam intensity-modulated radiation therapy," ICRU Report 83, J. ICRU **10**(1).

Reference Dosimetry of Scanned Proton Beams – State of the Art

H. Palmans[a,b]
J. Medin[c], S. Vynckier[d], N. Kanematsu[e], S. Greilich[f], O. Jäkel[f], S. Vatnitsky[a]

[a]MedAustron, Wiener Neustadt, Austria
[b]National Physical Laboratory, Teddington, UK
[c]Skåne University Hospital, Lund, Sweden
[d]Université Catholique de Louvain, Brussels, Belgium
[e]National Institute of Radiological Sciences, Chiba, Japan
[f]German Cancer Research Center, Heidelberg, Germany

Email address Corresponding Author: hugo.palmans@medaustron.at

BACKGROUND

Modern high-energy proton therapy has shifted almost entirely to scanned beam delivery modalities. The recommendations for reference dosimetry in IAEA TRS-398 [1] were based on experience with passively-scattered proton beams but assumed to be applicable to scanned beams as well. Some peculiarities of scanned beam dosimetry were, however, not addressed [2, 3] and are to be taken care of in the revision of TRS-398 [4].

A key difference is that for passively scattered beams, the monitor is calibrated in terms of absorbed dose to water in the spread-out Bragg peak, while for most scanned beams the monitor is calibrated in terms of proton number in a single spot [2]. The latter can, in principle, be determined by a Faraday cup, but for consistency with other beam modalities the proton number is derived from the dose-area-product at shallow depth of a single spot.

Other important issues to consider are that recombination can be large due to high instantaneous dose rates, depth dose gradients can be present at shallow depths and operation of reference dosimeters can be different as in passively scattered beams. This paper presents current state-of-the-art knowledge and data on reference dosimetry of scanned proton beams.

METHODS

Two different methods have been proposed to determine dose-area-product at shallow depth [2]; the first using a reference-class Farmer or plane-parallel ionization chamber in a single-layer scanned field and the second using a large-area chamber in a single static pencil beam. An experimental comparison of both methods at MedAustron is presented by Osorio et al [5].

The depth dose gradient at shallow depth can be substantial for the lowest clinical proton energies. It is thus important to consider if the effective point of measurement, P_{eff}, should be used as reference point for Farmer type chambers or for which beam energy range the use of the center of the ionization chamber, as recommended in TRS-398, can be used with acceptable uncertainty. The displacement correction was quantified based on experimental data from two proton centers and experimental and simulated data on P_{eff} and its uncertainty.

Concerning the beam quality correction factor, k_Q, experimental and Monte Carlo simulated overall factors from the literature are compared with those tabulated in TRS-398 and those determined for scanned beams are compared with those for scattered beams. Also studies on the recombination correction factor for scanned protons beams are reviewed.

RESULTS

The analysis of depth dose gradients reveals that when using an effective point of measurement and considering its uncertainty, thimble chambers can be used without displacement correction for residual ranges above 5 cm with a relative standard uncertainty contribution not larger than 0.5%. When using the centre of the ionization chamber at the reference depth, an uncertainty of 0.5% or less on the assumption there is no displacement correction can only be achieved for residual ranges above 15 cm.

Experimental and Monte Carlo (MC) calculated beam k_Q values compared with TRS-398 data in Figure 1 show that for none of the reference-class chambers considered the deviations between literature data and TRS-398 or between scanned and scattered beams are significant.

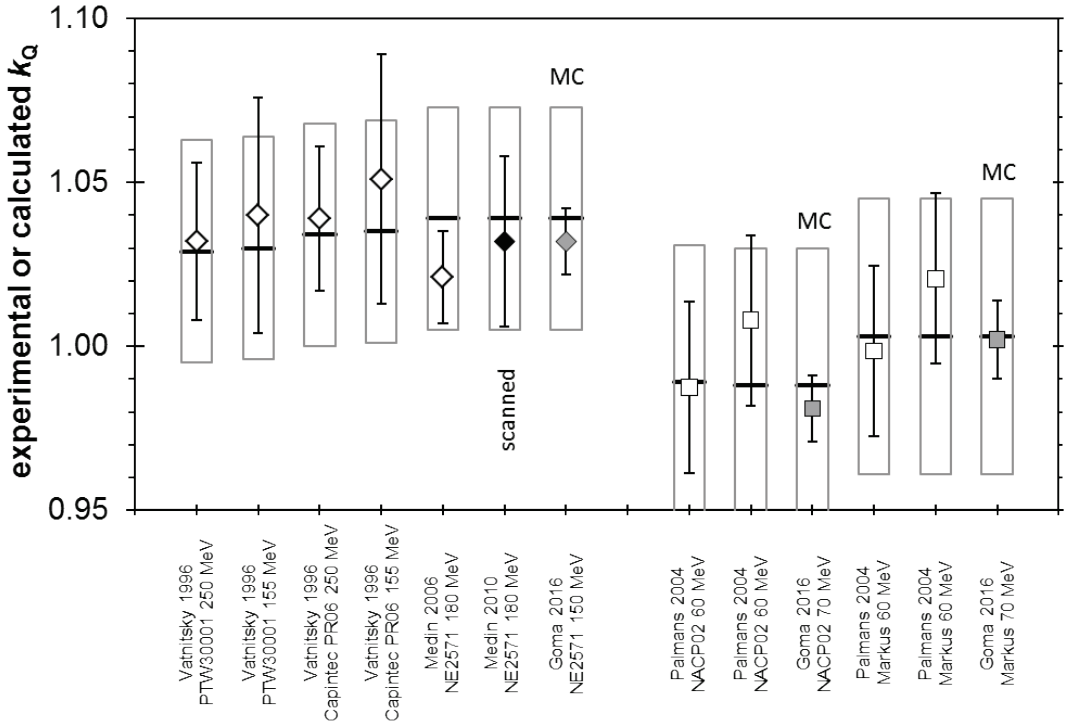

Figure 1. Experimental and MC calculated k_Q values (symbols with uncertainty bars) extracted from the literature [6-10] compared with k_Q values in TRS-398 (horizontal lines with boxes as uncertainty intervals) for Farmer type chambers (left group of data) and plane-parallel chambers (right group of data). MC calculated data points and those that pertain to scanned beams are marked. Uncertainties in this figure are expressed at 95% confidence level based on published information.

For cyclotron and synchrotron beams, ion recombination behaves as for continuous beams but synchrocyclotron beams behave as pulsed beams with substantial recombination losses [11]. Counteracting this by increasing the operating voltage brings the chamber in charge multiplication regime making the application of the two-voltage method invalid. One should thus be careful when applying this method and if necessary acquire a full Jaffé plot [11].

CONCLUSIONS

This contribution reviews information on calibration methods, beam quality correction factors, gradient corrections and ion recombination for scanned proton beams that contributes to the revision of the proton dosimetry chapter in the revision of TRS-398 [4].

REFERENCES

[1] ANDREO, P., BURNS, D. T., HOHLFELD, K., HUQ, M. S., KANAI, T., LAITANO, F., SMYTH, V. G., VYNCKIER, S., Absorbed Dose Determination in External Beam Radiotherapy: An International Code of Practice for Dosimetry based on Standards of Absorbed Dose to Water, Technical Report Series No. 398, IAEA, Vienna (2000).

[2] PALMANS, H., VATNITSKY, S. M., Beam monitor calibration in scanned light-ion beams, Med. Phys. **43** (2016) 5835–5847.

[3] GOMÀ, C., SAFAI, S., VÖRÖS, S. S., Reference dosimetry of proton pencil beams based on dose-area product: a proof of concept, Phys. Med. Biol. **62** (2017) 4991–5005.

[4] VATNITSKY, S. M., Update of Codes of Practice for Proton and Light-ion beam dosimetry, This Conference (2019).

[5] OSORIO, J., DREINDL, R., GREVILLOT, L., VATNITSKY, S., STOCK, M., KUESS, P., PALMANS, H., Dose monitor calibration for a synchrotron based scanned proton beam facility – methodology comparison and MedAustron experience, This Conference (2019).

[6] VATNITSKY, S. M., SIEBERS, J. V., MILLER, D. W., k_Q factors for ionization chamber dosimetry in clinical proton beams, Med. Phys. **23** (1996) 25–31.

[7] MEDIN, J., ROSS, C. K., KLASSEN, N. V., PALMANS, H., GRUSELL, E., GRINDBORG, J. E., Experimental determination of beam quality factors, k_Q, for two types of Farmer chamber in a 10 MV photon and a 175 MeV proton beam, Phys. Med. Biol. **51** (2006) 1503–1521.

[8] MEDIN, J., Implementation of water calorimetry in a 180 MeV scanned pulsed proton beam including an experimental determination of k_Q for a Farmer chamber, Phys. Med. Biol. **55** (2010) 3287–3298.

[9] PALMANS, H., THOMAS, R., SIMON, M., DUANE, S., KACPEREK, A., DUSAUTOY, A., VERHAEGEN, F., A small-body portable graphite calorimeter for dosimetry in low-energy clinical proton beams, Phys. Med. Biol. **49** (2004) 3737–3749.

[10] GOMÀ, C., ANDREO, P., SEMPAU, J., Monte Carlo calculation of beam quality correction factors in proton beams using detailed simulation of ionization chambers, Phys. Med. Biol. **61** (2016) 2389–2406.

[11] ROSSOMME, S. HORN, J. BRONS, S. JÄKEL, O., MAIRANI, A., CIOCCA, M., FLOQUET, V., ROMANO, F., RODRIGUEZ GARCIA, D., VYNCKIER, S., PALMANS, H., Ion recombination correction factor in scanned light-ion beams for absolute dose measurement using plane-parallel ionisation chambers, Phys. Med. Biol. **62** (2017) 5365–5382.

Monte Carlo Correction Factors for a Proton Calorimeter in Clinical Proton Beams

F. Romano[a]
D. Shipley[a], **H Palmans**[a,b]

[a]Metrology for Medical Physics, National Physical Laboratory, Hampton Road, Teddington, Middlesex, TW11 0LW
[b]Medical Physics, EBG MedAustron GmbH, A-2700 Wiener Neustadt, Austria

Email address of Corresponding Author: francesco.romano@npl.co.uk

BACKGROUND

Calorimetry is the only fundamental method for measuring the quantity absorbed dose according to its definition. A calorimeter directly measures the temperature rise resulting from irradiation in an absorber (core), assuming all the energy deposited in a material appears as heat [1]. The National Physical Laboratory (NPL) has considerable expertise in graphite calorimetry, which offers a number of advantages (such as higher sensitivity) compared to calorimetry in water [2, 3]. NPL is currently commissioning a new graphite calorimeter as a primary standard of absorbed dose to water for clinical proton beams that is robust and portable enough to be used in the end-user facility. The aim is to achieve an uncertainty on reference dosimetry for protons of around 2% (at 95% confidence level), which is approximately half the estimated uncertainty for calibrations based on IAEA TRS-398 [4]. In this work, Monte Carlo calculated correction factors required to obtain absorbed dose to graphite from a calorimeter measurement in a range of monoenergetic and clinical proton beams and their uncertainty are determined.

METHODS

Monte Carlo (MC) simulations were developed with TOPAS (v3.1) [5], based on the Geant4 toolkit, to determine the non-graphite ($k_{\text{non-g}}$), gap (k_{gap}) and volume averaging (k_{vol}) correction factors for the calorimeter using a series of simulation geometries. $k_{\text{non-g}}$ corrects for the presence of non-graphite materials in the core, k_{gap} for the presence of vacuum gaps and k_{vol} converts the mean absorbed dose in the graphite core to the absorbed dose in a point located at the centre of the core. k_{gap} and k_{vol} were determined for a range of monoenergetic proton energies between 60 MeV and 230 MeV, and for clinical SOBPs, such as, the standard test volume recommended in the draft IPEM Code of Practice for high energy scanned beams and for the fully modulated passively scattered beam (62 MeV) at the Clatterbridge Cancer Centre (CCC), UK. The STV in scanned beams for reference dosimetry is a 10x10x10 cm^3 dose volume centred at 15 g cm^{-2} depth in water. To create this volume, a MATLAB script was used to optimize the weight of the individual beamlets (previously obtained with TOPAS) to achieve the required depth profile (<0.5% uniformity in the SOBP region). A similar technique was used for the fixed energy passively scattered CCC beam but here the weights of individual beamlets obtained with energy degraders of different thickness were optimized to achieve the required fully modulated SOBP.

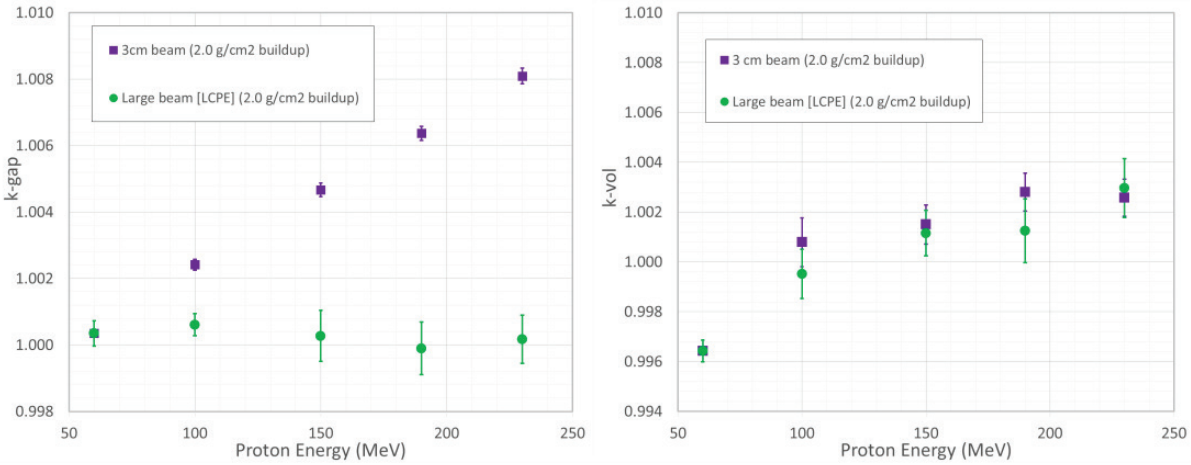

Figure 1. k_{gap} and k_{vol} corrections calculated for 5 monoenergetic proton energies

RESULTS

Figure 1 shows k_{gap} and k_{vol} corrections calculated for 5 monoenergetic proton energies at a measurement depth of 2.0 g cm^{-2}, for a 3 cm beam diameter and a larger beam diameter such that lateral charged particle equilibrium (LCPE) is achieved. k_{gap} increases with energy by up to 0.8% above unity for a 3 cm beam diameter, while with larger beam diameters k_{gap} is within 0.1% of unity for all energies. k_{vol} varies from 0.3% below unity at 60 MeV to 0.3% above unity at 230 MeV with no significant dependence on beam diameter. For the two clinical SOBPs, k_{gap} , k_{vol} and $k_{non\text{-}g}$ were found to be within 0.1% of unity in nearly all cases. However, k_{vol} for the CCC beam was found to be significantly larger in absolute terms (around 2.6% lower than unity), due to the presence of alignment cross-hairs and some radial beam non-uniformity.

CONCLUSIONS

For the new NPL proton calorimeter, k_{gap} is close to unity for monoenergetic proton beams when LCPE is achieved while k_{vol} is dependent on beam energy (changing by 0.6% between 60 and 230 MeV), which was found to be mainly a result of a perturbation of the distribution of secondary protons generated in non-elastic nuclear interactions. For clinical SOBPs, all correction factors are close to unity which is ideal for reference dosimetry. A detailed and validated MC model for the CCC beamline has also been developed. In particular for the CCC SOBP, larger values have been found for k_{vol} , whose value is sensitive to the spatial dose distribution non-uniformity due to the presence of passive elements in the beamline. These results will significantly contribute to the establishment of the NPL graphite calorimeter as a primary standard in proton therapy.

REFERENCES

[1] J. SEUNTJENS AND S. DUANE, "Photon absorbed dose standards", *Metrologia*, vol. 46, S39-S58, 2009

[2] H. PALMANS et al., "A small-body portable graphite calorimeter for dosimetry in low-energy clinical proton beams", *Phys. Med. Biol.*, vol. 49, p. 37-37-3749, 2004

[3] S. DUANE et al., "An absorbed dose calorimeter for IMRT dosimetry", *Metrologia*, vol. 49, p. S168-S173, 2012

[4] IAEA, Technical Report TRS -398, IAEA, Vienna, 2000

[5] J. PERL et al., "TOPAS: an innovative proton Monte Carlo platform for research and clinical applications.", *Med. Phys.*, vol. 39, n.11, p. 6818-6837, 2012

GATE/Geant4 as a Monte Carlo Simulation Toolkit for Light Ion Beam Dosimetry

M. Bolsa Ferruz[a]
H. Palmans[a,b], A. Carlino[a], M. Stock[a] and L. Grevillot[a]

[a]EBG MedAustron GmbH, Wiener Neustadt, Austria
[b]National Physical Laboratory, Teddington, UK

Email address of Corresponding Author: marta.bolsa-ferruz@medaustron.at

BACKGROUND

The growing interest in Light Ion Beam Therapy (LIBT) has fostered the efforts to raise the accuracy of ion beam dosimetry to the same level as conventional radiotherapy. Dosimetric measurements are mostly performed with ionization chambers due to their small energy and LET dependence. Solid-state detectors remain a good alternative due to the possibility of reducing the scoring volume down to sub-millimeter size, but specific methods must be implemented to account for their relative effectiveness (RE). Consistency in dosimetry is achieved by adopting water as a reference material, as well as by using a common formalism.

To derive dose to water from the detector signal, it is necessary to take into account the water-to-medium stopping power ratio ($s_{w,med}$) and the RE of the dosimeter. Both quantities need to be integrated over the complete particle spectrum. Monte Carlo (MC) codes are useful tools for the calculation of the $s_{w,med}$ and RE fluence-weighted integrals. The aim of this work is to determine those quantities in clinically relevant conditions for scanned proton and carbon ion beams. The following detectors have been considered: ionization chambers, alanine detectors, films and optically stimulated luminescent detectors (OSLD). In particular, this work intends to support end-to-end testing activities, where the entire clinical workflow is executed using homogeneous and anthropomorphic phantoms.

METHODS

The GATE [1] MC simulation platform based on GEANT4 [2] has been used. An analytical expression for the $s_{w,med}$ was determined as a function of the energy deposition scored by GATE/Geant4 and the water and medium mass stopping powers of the particle. This expression is equivalent to the Spencer-Attix equation [3]. The $s_{w,med}$ is calculated as the ratio of the computed dose to water and the dose to medium. A new tool for the computation of the RE was implemented. It makes use of the RE tables of the detector as a function of energy for the different particle types present [4]. The next step after the implementation of the simulation tools will be the comparison of the dose distributions corrected by the $s_{w,alanine}$ and $RE_{alanine}$ and the dosimetric data obtained with ionization chambers and alanine pellets during the medical commissioning and end-to-end testing activities of the proton beam line at MedAustron [5]. Additionally, $RE_{alanine}$ results from GATE simulations will also be compared with those from the RayStation v5.99.50 Treatment Planning System (TPS).

RESULTS

The distribution of $s_{w,air}$ was computed in a water volume for different radiation plans using scanned proton beam. An average value of 1.13 for $s_{w,air}$ was obtained with a systematic increase of 2% towards the distal edge. The $s_{w,det}$ was also computed for different detector media in water. For alanine and aluminium oxide (Al_2O_3), the $s_{w,med}$ is varying by up to 2%

and 10%, respectively, over the depth-dose profile. The RE for a homogeneous dose distribution in water was computed for alanine detectors to verify the capability of the new implemented GATE tool (Figure 1).

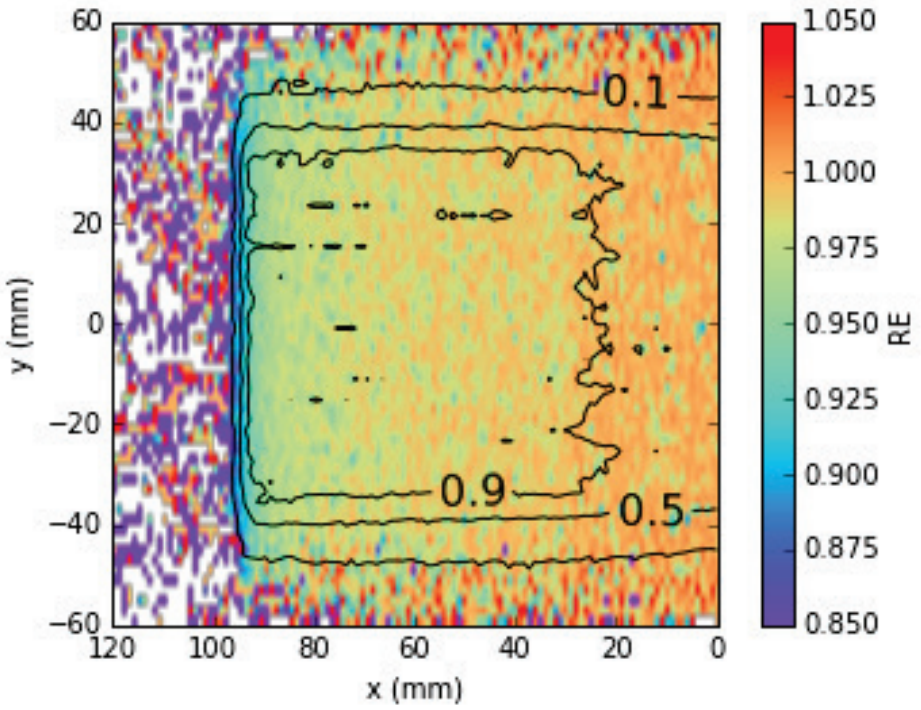

Figure 1. 2D distribution of the $RE_{alanine}$ *calculated with GATE for a homogeneous dose plan in water using scanned proton pencil beams. Continuous lines represent isodose levels.*

CONCLUSIONS

The capabilities of GATE/Geant4 for the determination of $s_{w,det}$ have been demonstrated. The method was shown to be equivalent to the Spencer-Attix cavity theory. The validation of the $s_{w,alanine}$ and $RE_{alanine}$ calculation for protons beams will be completed during the first quarter of 2019. By then, experimental data from the medical commissioning of the carbon ion beam line are expected to be available. A similar validation methodology as for proton beams will be applied.

REFERENCES

[1] SARRUT, D., BARDIES, M., ... & PAPADIMITROULAS, P., "A review of the use and potential of the GATE Monte Carlo simulation code for radiation therapy and dosimetry applications." Medical physics 41.6Part1 (2014).

[2] AGOSTINELLI, S., ALLISON, J., ... & BEHNER, F., "GEANT4—a simulation toolkit." Nuclear instruments and methods in physics research section A:Accelerators, Spectrometers, Detectors and Associated Equipment 506.3 (2003): 250-303.

[3] NAHUM, A. E., "Water/air mass stopping power ratios for megavoltage photon and electron beams." Physics in Medicine & Biology 23.1 (1978): 24

[4] HERRMANN, R., Prediction of the response behaviour of one-hit detectors in particle beams. Diss. PhD thesis, Aarhus University, Denmark (2012).

[5] CARLINO, A., GOULDSTONE, C., ... & PALMANS, H., "End-to-end tests using alanine dosimetry in scanned proton beams." Physics in Medicine & Biology 63.5 (2018): 055001.

The Preliminary Measurement for the Absorbed-Dose to Water of Carbon Ion Beam with Ion Chambers

J. Zhang[a]
K. Wang[a], S. J. Jin[a], Z. P. Wang[a]

[a]National Institute of Metrology, No. 18 of Bei San Huan Dong Lu, Chaoyang District, Beijing, China

Email address of Corresponding Author: jzh@nim.ac.cn

BACKGROUND

Radiotherapy with heavy ion beam is playing an important role in clinical therapy due to its physical characteristics [1]. The absorbed-dose to water of heavy ion beam is traced back to the ^{60}Co γ radiation standard based on the relevant technical protocol [2]. The uncertainty of correction for the beam factor k_Q between ^{60}Co γ and heavy ion beam is quite lager than that in other radiotherapy cases, such as high energy photon beam [3]. This is mainly owing to the lack of experimental result of the factor k_Q, therefore, only the theoretical calculation is applied [4].

Since 2014, the Linac dosimetry group in National Institute of Metrology of China (NIM) has been engaged in the absolute measurement study with a water calorimeter. The research for the absorbed-dose to water of the charged particles (electron, proton, heavy ion) is being put forward. In the present work, the absorbed-dose to water of a ^{12}C ion beam with the energy per atomic mass 400 MeV/u was studied based on a conventional ionometric method, the work reported here is motivated by the rapid-developing radiotherapy with heavy ion beams and as a pre-study for the upcoming absolute measurement.

METHODS

The experiment was carried out at a horizontal heavy ion terminal, where a ^{12}C ion beam was produced by a heavy ion research facility. The delivered energy to the terminal was (400±0.4) MeV/u and beam intensity was 1.5 nA, a typical heavy ion beam for radiotherapy.

A water phantom with the volume of 30 cm×30 cm×30 cm was installed at the iso-center position. The water phantom is made in PMMA and the front window is processed into a thickness of (2.6±0.1) mm. During the experiment, 4 ionization chambers were used to accumulate data one after another. The product number of the ionization chambers is FC65-G 1736, TW34001-2412, TW30013-4678 and TW30013-9166, among them FC65-G and TW30013 are cylindrical type chambers and TW34001 belongs to parallel-plate chamber. The calibration factors $N_{D,W}$ of the 4 chambers are traced back to the primary standard of absorbed dose to water of ^{60}Co γ radiation and the beam quality factors k_Q are currently recommended ones.

The polarity and recombination are the basic characteristics for the chambers under a certain beam condition. In heavy ion case, typical physical processes such as the space-charge effect can result in a more complicated scenario. Consequently, the above issues for the relevant chambers in the present work were evaluated under heavy ion beam condition.

RESULTS

The absorbed-dose to water *Dw* of heavy ion based on this work can be deduced through

$$D_w = M \cdot k_{elec} \cdot k_{TP} \cdot k_{pol} \cdot k_s \cdot k_s^{ini} \cdot N_{D,w} \cdot k_Q,$$

where *M* is the original result (the integrated charge from the 6517B electrometer), k_{elec} is the correction for the electrometer (since the main purpose of this work is to compare the results from the ionization chambers, it is feasible to consider k_{elec} as 1), k_{TP} corrects the air density refer to 293.15 K and 101.325 kPa. Other corrections including the polarization(k_{pol}), the recombination (k_s^{ins} and k_s) have been evaluated in this work. The normalized D_w from the FC65-G 1736 and other chambers are listed in Table 1, in which the number of incident ^{12}C ions is a simultaneous feedback from the heavy ion research facility.

The discrepancy of the results in Table 1 is approximately 0.7%, which is far smaller than the currently recommended uncertainty (3%) for the absorbed-dose to water of heavy ion.

Table 1. Absorbed dose to water of heavy ion measured by the chambers.

Chamber	**D_w (Gy/incident ^{12}C ions)**
FC65-G 1736	8.872×10^{-8}
TW30013-4678	8.855×10^{-8}
TW30013-9166	8.853×10^{-8}
TW34001-2412	8.737×10^{-8}

CONCLUSIONS

A study for the absorbed-dose to water of a 400 MeV/u ^{12}C heavy ion was conducted with the ionometric method. The corrections were also evaluated under the corresponding heavy ion condition. The results from different ionization chambers agree well within uncertainty, or in other words, the dissemination for the absorbed-dose to water of heavy ion by the different type of conventional dosimeters is basically stable.

REFERENCES

[1] KRAFT, G., Tumor therapy with heavy charged particles, Prog. Part. Nucl. Phys., 45, S473, 2000.

[2] ANDREO, P. et al., Absorbed dose determination in external beam radiotherapy: An international code of practice for dosimetry based on standards of absorbed dose to water, IAEA TRS-398(Vienna), 2000.

[3] ALMOND, P., R. et al., AAPM's TG-51 protocol for clinical reference dosimetry of high-energy photon and electron beams, Med. Phys., 26,1847,1999.

[4] LLACER, J. et al., On-line characterization of heavy-ion beams with semiconductor detectors, Med. Phys., 11, 266,1984.

Dose Monitor Calibration for a Synchrotron Based Scanned Proton Beam Facility - MedAustron Experience

J. Osorio[a]
R. Dreindl[a], L. Grevillot[a], S. Vatnitsky[a], M. Stock[a], P. Kuess[b], H. Palmans[a,c]

[a] EBG MedAustron GmbH, Marie-Curie Straße 5, 2700 Wiener Neustadt, Austria
[b] Medical University of Vienna, Waehringer Guertel 18-20, 1090 Vienna, Austria
[c] National Physical Laboratory, Teddington TW 11 0LW, United Kingdom

Email address of Corresponding Author: jhonnatan.osorio@medaustron.at

BACKGROUND

This work presents MedAustron's experience with two independent methods to calibrate the beam monitor in synchrotron-generated scanned proton beams [1]. One is based on a dose determination with an ionization chamber for a single-energy pencil beam using a single-layer scanned field. The second is based on the determination of dose-area-product to water (DAP_w) for a single-energy static spot using a large-area ionization chamber (LAIC).

METHODS

1. Beam monitor calibration in terms of number of protons

Unlike scattered particle beam systems, where the monitor is usually calibrated in terms of absorbed dose in a large field, in scanned beam monitors are calibrated in terms of the number of particles, N_p, or its dose equivalent, DAP_w [1,2]. N_p was derived from DAP_w dividing by the mean water stopping power at the reference depth per incident proton [1,6]. To guarantee measurements in a sufficiently low depth dose gradient, the reference depth was 1.4 cm for energies below 100 MeV and 2.0 cm depth for energies of 100 MeV and above.

2. Measurement in a single-energy pencil beam using a single-layer scanned field

A Roos-type plane-parallel ionization chamber was cross-calibrated in terms of absorbed dose to water against a Farmer-type chamber at 2 cm depth in a 179.2 MeV single-energy pencil beam using single-layer scanned field. The absorbed dose to water was determined in nine representative calibration energies, at the shallow reference depth with the cross-calibrated Roos chamber, by applying the formalism and data from IAEA TRS-398 based on the residual range of the measurement point [3]. DAP_w is derived from determined absorbed dose to water by multiplication with the product of the spot spacing in both scan directions [6].

3. Measurement with a LAIC in a single-energy static spot

LAIC - Bragg peak chamber (BPC) PTW 34070 was cross-calibrated in terms of absorbed water against Farmer-type chamber at 2 cm depth in a 179.2 MeV single-energy pencil beam using single-layer scanned field, large enough to cover the area of the BPC. A direct application of TRS-398 is not possible for the determination of DAP_w since no beam quality correction factors, κ_{Q,Q_0} has been reported for BPC chambers. In this work, κ_{Q,Q_0} for protons with respect to electron and photon beams was theoretically established [1] and experimentally validated [5]. To make both methods comparable, the same energies and calibration depths were used. The determination of the DAP_w with the BPC does not require the scanned beam, however, additional efforts need to be taken in the characterization of this type of chambers. In this particular case, a non-uniformity response correction factor over the area of the BPC of 3.2%

was applied [4]. This correction was needed because the BPC is cross-calibrated in a large field and used in a small field.

RESULTS

The total N_p per count of one of the beam monitors using both methods as a function of energy is shown in Figure 1. The total combined relative standard uncertainties on N_p were 2.5% and 4.1% for the single-energy layer and the single-energy spot methods, respectively. The differences between both methods were within 1.4%.

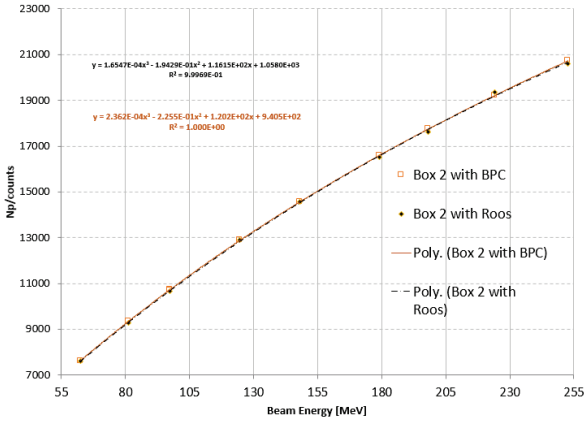

Figure 1. Number of particles per count as a function of nominal proton energy.

CONCLUSIONS

The large combined relative standard uncertainty (4.1%) for single-energy spot method with respect to single energy method is mainly coming from the inhomogeneity of BPC response, which was established in 3.2% [4] for the BPC used in this study. However, even considering the non-negligible inhomogeneity of BPC response, the two methods were compared and agreed within uncertainties showing that, both, the single-energy layer and single-energy spot methods can be applied. The advantage of the single-energy layer method is the use of well-characterized ionization chambers while the long irradiation time per reading and the required accuracy on the spot spacing are disadvantages. The single-energy spot method has the advantages of providing a direct determination of DAP_w and fast (spill-per-spill) measurements while it has the disadvantages of lacking the data in the literature, the unavailability of DAP_w calibrations at standards labs and the inherent non-uniformity of chambers over their sensitive detection area.

REFERENCES

[1] PALMANS, H., VATNITSKY, S.V., Beam monitor calibration in scanned light ion beams, Med. Phys. 43, (2016) 5835-5847.
[2] GOMA, C., Safai, S., et al, Reference dosimetry of proton pencil beam based on dose-area product: a proof of concept, Phys. Med. Biol. 62 (2017) 4991-5005.
[3] IAEA, Absorbed dose determination in external beam radiotherapy TRS-398. (2000)
[4] KUESS, P., PALMANS, H., et al, Lateral response heterogeneity of Bragg peak ionization chambers for narrow-beam photon and proton dosimetry. Phys. Med. Biol. 62 (2017) 9189-9206.
[5] OSORIO, J., PALMANS, H., ET AL, Response of Bragg peak ionization chambers in photon, electron and proton beams. PTCOG56 conference (2017) poster.
[6] JACKEL, O., HARTMANN, G.H, A calibration procedure for beam monitors in a scanned beam of heavy charged particles Med. Phys. 31 (2004) 1009-1013

Stopping-Power Ratios and Beam Quality Factors for Ion Carbon Beams – Impact of New ICRU90 Key Data

L. Burigo[a,b]
O. Jäkel[a,b], **S. Greilich**[a,b]

[a] German Cancer Research Center (DKFZ), Heidelberg, Germany
[b]National Center for Radiation Research in Oncology (NCRO), Heidelberg Institute for Radiation Oncology (HIRO) Heidelberg, Germany
[c]Heidelberg Ion-Beam Therapy Center (HIT), INF 450, D-69120 Heidelberg, Germany

Email address Corresponding Author: s.greilich@dkfz.de

BACKGROUND

Reference dosimetry for carbon ion beams relies on calibrated ionization chamber measurements and dose-to-water-based protocols. Since no primary standard for carbon beams exists, the most prominent code of practice – IAEA's TRS-398 [1] – defines the relation between dose to water and charge measured by an ionization chamber by means of beam quality correction factors k_Q.

The recent update of dosimetric key data by the 'International Commission on Radiation Units and Measurements' [2] impacts the computation of k_Q factors via changes of several key data, such as the the mean excitation energies I which enters the stopping power computation for water and air, the computation procedure itself, the average energy expended in the production of an ion pair in air, W/e, and the chamber perturbation factors. Andreo *et al.* [3] estimated the effect of the new key data on the beam quality correction factors to be -0.5 %, and on the stopping power ratios for carbon ions water to air $s_{w,air}$ -0.4 % - mainly due to the changes in I-values. An accurate assessment of $s_{w,air}$ in reference conditions with new recommendation is necessary to update the dosimetry protocols for carbon ion beams.

This contribution presents an evaluation of the impact of the updated key quantities on the stopping power ratio $s_{w,air}$ and the k_Q factors for carbon ion beams in different reference conditions. In addition, recommendation of new values of $s_{w,air}$ are presented.

METHODS

Monte-Carlo radiation transport simulations using the Geant4 toolkit [4] were used to compute stopping-power ratio water to air for carbon ion beams. In order to use the new recommendations of I values for water and air in the ICRU Report 90 [2], the published tables for protons, alpha particles and carbon ions were implemented in the Geant4. In addition, as carbon ions penetrating matter produce a variety of fragments, tables of stopping power for ion species not covered in the ICRU Report 90 were also generated.

Different reference conditions were considered for the calculation of $s_{w,air}$, namely, monoenergetic carbon ion beams with residual range in water varying from 3 to 30 cm, and spread-out Bragg peaks (SOBP) of different widths and depths in water. The stopping power ratios as a function of depth were computed by simulating the irradiation of a 50x50x50 cm^3 water phantom divided in 0.25 mm-thick slabs in depth. The residual range R_{res} of the beam was used as a beam quality specifier allowing to parametrize the dependence of $s_{w,air}$ on the beam quality. In particular, for monoenergetic carbon ion beams, the depth 1 g cm^{-2} was used

as reference condition to compute R_{res}, while the position of the center of the SOBP was used to compute R_{res} for the SOBP beams.

The stopping power ratio obtained with the updated key data was then applied to assess the impact on the beam quality correction factors k_Q available in the literature for a variety of ionization chambers.

RESULTS

The $s_{w,air}$ at the reference depth of 1 g cm^{-2} in water for the reference conditions of pristine carbon ion beams evaluated in this study fall into a (−0.07 %,+0.12 %) interval around $s_{w,air}$ = 1.1247. As for the reference conditions of the center of physically optimized SOBPs, $s_{w,air}$ fall into a (−0.09 %,+0.18 %) interval around $s_{w,air}$ = 1.1274.

However, if a single constant $s_{w,air}$ is used as recommended in TRS398, an average between the values representative for pristine and for physically optimized SOBP configurations should be used, which is 1.126. All values obtained in this study fall into a (−0.2 %, +0.3 %) interval around this value. The change of −0.4 % with respect to the recommended value of 1.130 in TRS398 is in agreement with the statements given in ICRU Report 90.

Eventually, a parameterization can be employed to model the dependence of $s_{w,air}$ on the specific beam situation.

The updated beam quality factors agreed better with experimental data for cylindrical chambers [5], especially where updated Co-60 perturbation factors were available. For plane-parallel chambers, however, discrepancies up to 2 % were found which require further investigation.

CONCLUSIONS

This contribution provides a detailed assessment of the impact of the update of dosimetric key data on the stopping-power ratio and beam quality correction factors.

REFERENCES

[1] INTERNATIONAL ATOMIC ENERGY AGENCY 2000 Technical Report Series 398
[2] INTERNATIONAL COMMISSION ON RADIATION UNITS AND MEASUREMENTS 2014 J. *ICRU* **14**(1)
[3] ANDREO P *et al* 2013 *Phys. Med. Biol.* **58** 6593–6621
[4] AGOSTINELLI S *et al* 2003 *Nucl. Instrum. Methods A* **506** 250–303
[5] OSINGA-BLÄTTERMANN AND KRAUSS 2018 *Phys. Med. Biol.* accepted manuscript doi: 10.1088/1361-6560/aaf5ac

Ionisation Chamber Intercomparisons in a Low-Energy Passively-Scattered and Two High-Energy Pencil Beam Scanning Proton Beams

A. Lourenco[a,b]
A. Kacperek[c], I. Patel[d], A. Vestergaard[e], H. Nyström[e], O. Nørrevang[e], H. Palmans[a,f], R. Thomas[a]

[a]Medical Radiation Science, National Physical Laboratory, Teddington TW11 0LW, United Kingdom
[b]Department of Medical Physics and Biomedical Engineering, University College London, London WC1E 6BT, United Kingdom
[c]The National Eye Proton Therapy Centre, The Clatterbridge Cancer Centre, Wirral CH63 4JY, United Kingdom
[d]Christie Medical Physics and Engineering, The Christie NHS Foundation Trust, Manchester M20 4BX, United Kingdom
[e]Aarhus University Hospital, Danish Centre for Particle Therapy, Aarhus, Denmark
[f] Medical Physics Group, EBG MedAustron GmbH, A-2700 Wiener Neustadt, Austria

Email address of Corresponding Author: ana.lourenco@npl.co.uk

BACKGROUND

The IAEA TRS 398 [1] has been adopted as the standard protocol for reference dosimetry in proton beams [2]. It recommends the use of an ionization chamber with a calibration coefficient in terms of absorbed dose to water traceable to standards laboratories. For proton beams, reference dosimetry is performed based on calibrations in cobalt-60 beams because primary standards laboratories have not yet established a calibration service for the direct determination of dose in proton beams. The aim of this study was to independently compare the response of user ionisation chambers against NPL reference ionisation chambers following recommendations of the IAEA TRS 398 [1] in a low-energy passively-scattered proton beam and in two high-energy proton scanned pencil beams.

METHODS

Measurements were performed at three clinical facilities: the 62 MeV proton cyclotron at the Clatterbridge Cancer Centre (CCC), UK, the 250 MeV proton cyclotron at The Christie, UK, and the Danish Centre of Particle Therapy (DCPT), Denmark. In the low-energy proton beam, measurements were made in a full-modulated beam, using a collimator size of 3 cm. The dose per monitor unit determined by seven NPL ionization chambers was derived. Additionally, six user ionization chambers were cross-calibrated in the proton beam against NPL reference chambers and calibrations were compared with those used in the clinic. In the high-energy proton facilities, measurements were performed using a single layer scanned field with a size of 10 x 10 cm^2, equidistant lateral spot spacing and equal number of MUs delivered for each spot, for 19 representative energies ranging from 70 MeV to 245 MeV. All ionisation chambers were positioned with their reference point at the isocentre and at a water-equivalent depth of 2 cm. Measurements were also performed in three composite fields of a 10 x 10 x 10 cm^3 homogenous dose volumes centred at a depth of 10 cm, 15 cm and 25 cm deep in water, respectively, centred at the isocentre, using two NPL PTW Roos ionisation chambers, and the determined dose was compared with the prescribed dose. Ionisation chamber readings were corrected for influence quantities, with particular attention to ion recombination corrections.

RESULTS

For the measurements performed in the CCC low-energy proton beam, the ratio between the dose per monitor unit derived for each individual chamber to that of the mean of all chambers was generally within 2%. There was good agreement between the ratio of the NPL cross-calibration coefficients and their individual calibration coefficients for protons derived from the IAEA TRS-398 [1] data. The ratio between the CCC calibration coefficients and the NPL cross-calibration coefficients was overall within 2% and differences were dependent on the type of cross-calibrated chamber used.

For the measurements conducted in the high-energy proton beams for the single-energy layers, the results performed by NPL and those calculated previously by the proton facilities agreed better than 1% and similar results were found in the homogenous dose volumes in comparison with the prescribed dose.

With regard to ion recombination corrections, the two-voltage method for continuous beams slightly underestimated the recombination correction because the effect of initial recombination is not included in the model, confirming earlier findings by Palmans *et al.* [3].

CONCLUSIONS

This ionisation chamber intercomparison study showed good agreement between the results acquired by NPL and the proton facilities where the use of a dedicated chamber type ensured consistency in the dosimetry between the different centres. It was found that centres apply ion recombination corrections differently and further clarification on how this should be done would be desirable in future codes of practices to ensure consistency between centres.

REFERENCES

[1] ANDREO, P., BURNS, D. T., HOHLFELD K., HUQ M. S., KANAI T., LAITANO F., SMYTH V. G., VYNCKIER S., "Absorbed dose determination in external beam radiotherapy: an international code of practice for dosimetry based on standards of absorbed dose to water", IAEA Technical Report Series 398, Vienna (2000)

[2] INTERNATIONAL COMISSION ON RADIATION UNITIS AND MEASUREMENTS, "Prescribing, Recording, and Reporting Proton-Beam Therapy", Report No 78, Bethesda, MD (2008)

[3] PALMANS, H., THOMAS, R., KACPEREK, A., Ion recombination correction in the Clatterbridge Centre of Oncology clinical proton beam, Physics in Medicine and Biology **51** (2006) 903-17

Dosimetry for Radiobiology Experiments

Study of the Electrons Range in Soft Tissue with the Energy of 50 keV

G. Joana[a]
B. Seniwal[b], **T. Fonseca**[b]

[a]Comissão Nacional de Energia Nuclear (CNEN) – CGMI/DRS, Rio de Janeiro, RJ, Brasil.
[b]Pós-Graduação em Ciências e Técnicas Nucleares – Escola de Engenharia (DEN/UFMG), Belo Horizonte, MG, Brasil.

Email address of Corresponding Author: georgia.joana@cnen.gov.br

BACKGROUND

Large number of studies have been conducted that examines the interdependence between energy and range for electrons with energies ranging from keV's to MeV's. However, the quantitative description of low-energy electron transport is a complex problem, especially due to the fact that there are not reliable data available for cross sections of the different possible types of electron interactions with matter [1]. Since the analytic models of electron transport are incomplete which presents difficulties to present any solution, Monte Carlo codes have been adopted as an alternative for these approaches and are used extensively nowadays [1-3]. Studies shown that the low-energy electrons particularly the Auger electrons and Coster-Kronig (CK) electrons from emitters located inside biological tissues may lead to severe damages in cellular and subcellular levels because as the energy of electron decreases the Linear Energy Transfer (LET) increases [4-7]. Thus, there is a special interest in the determination of the relationship between initial energy and range of electrons despite of the fact that the ionizing radiation transfer energy to the medium predominantly through the interaction of low-energy secondary electrons produced in the material [1]. The main goal of this work is to evaluate low-energy electrons range to future studies of the extent to which these electrons, set in motion around the radiation path, could induce direct damage to the DNA of living cells.

METHODS

This work investigated electrons with energy ranging from 1 and 50 keV. An isotropic monoenergetic source of electron was located inside a semi-infinite homogeneous equivalent tissue medium. Composition of tissue medium was taken similar to that provided by the International Commission on Radiation Protection (ICRP) as soft tissue [8]. The simulations were performed using the Monte Carlo PENELOPE code [9]. It is able to simulate the tracks of low energy electrons and photons up to 100 eV. According to AAPM Task Group 25 [10] on clinical electron-beam dosimetry different definitions of range are introduced to measure the quality of electron beam, since these definitions lose their meaning when it comes to low-energy electrons. Therefore, in this work we considered five parameters to measure the range of low energy electrons: the sum of all electron displacements, R; the sum of the displacements in which 90% of the initial energy of the electron is absorbed, R_{90}; and the same for 95% of its initial energy, R_{95}; the projection of the maximum distance reached by the electron on the incidence direction, R_{proj}; and the distance between the initial and final points, total displacement (TD). From the information about the history of each simulated particle, as the position in which interactions occurred, type of interaction, energy deposited in each event, direction of deflection, etc., these ranges were calculated.

RESULTS

The calculated ranges as defined in this work, R, R_{90} e R_{95}; projected range, R_{proj}, and total displacement, TD, is presented in Table 1.

Table 1 – 1 and 50 keV electron's range.

Energy (keV)	R (cm)	R_{90} (cm)	R_{95} (cm)	R_{proj} (cm)	DT (cm)
50	4.39E-03	2.44E-03	2.84E-03	1.70E-03	3.03E-03
1	5.19E-06	2.84E-06	3.37E-06	1.95E-06	3.42E-06

The path length, R, is greater than all other parameters. The R_{proj} is the least of them. The ranges TD and R_{95} have comparable values. The difference between the R_{proj} and the R ranges is approximately 60%, so the depth of electron penetration is approximately 40% of the electron trajectory size. The 50 keV path length, R, is approximately equal to the cell diameter. In search of the most appropriate concept for electron range that can relate the damage occurring at the cellular level, one has to look for electrons of lower energy. Such as 1 keV path length, R, which is of the order of one-hundredth of the cell diameter.

CONCLUSIONS

In this work, it was studied the range in biological tissue for electrons with 1 and 50 keV using Monte Carlo PENELOPE code. The path length, R, is a good estimate for the trajectory size. Being equal to the total length of the electron trajectory, R can be taken as an upper limit in determining ranges.

REFERENCES

[1] MEESUNGNOEN, J.; et al. Low-energy electron penetration range in liquid water. Radiation Research **158** (2002) 657.

[2] EVERHART, T. E.; et al. Determination of Kilovolt Electron Energy Dissipation vs Penetration Distance in Solid Materials. Journal of Applied Physics **42** (1971) 5837.

[3] EMFIETZOGLOU, D.; et al. Monte Carlo simulation of the energy loss of low-energy electrons in liquid water, Physics in Medicine and Biology **48** (2003) 2355.

[4] CHANDA, N.; et al. Radioactive Gold Nanoparticles In Cancer Therapy: Therapeutic Efficacy Studies Of Ga-198 AuNP Nanoconstruct In Prostate Tumor–Bearing Mice. Nanomedicine: Nanotechnology, Biology And Medicine **6** (2010) 201.

[5] NIKJOO, H.; et al. Modelling of Auger-Induced Dna Damage by Incorporated ^{125}I. Acta Oncologica **35** (1996) 849.

[6] INCERTI, S. et al. Simulation Of Auger Electron Emission From Nanometer-Size Gold Targets Using The Geant4 Monte Carlo Simulation Toolkit. Nuclear Instruments And Methods In Physics Research B **372** (2016) 91.

[7] PODGORSAK, E.B. Radiation oncology physics: A handbook for teachers and students, IAEA, Austria (2005) 657pp.

[8] WHITE, D.R.; et al. Report 46, Journal of the International Commission on Radiation Units and Measurements **24** (1992) NP.

[9] STEWART, R.D.; et al. Microdosimetric properties of ionizing electrons in water: a test of the PENELOPE code system. Physics in Medicine and Biology **47** (2002) 79.

[10] KHAN, F.M, et al. Clinical electron-beam dosimetry: Report of AAPM Radiation Therapy Committee Task Group No. 25. Medical Physics **18** (1991) 73-109.

Microdosimetric Calculations for I-123 Using Geant4-DNA

B. Seniwal[a,b]
T. C. F. Fonseca[a,b]

[a]Departamento de Engenharia Nuclear – UFMG BH/MG, Brasil
[b]Programa de Pos-graduacao em Ciencias e Tecnicas Nucleares - UFMG BH/MG, Brasil

Email address of Corresponding Author: bseniwal@eng-nucl.dout.ufmg.br

BACKGROUND

Since early 1960s computational and mathematical models are used to describe complex biophysical processes associated with radiation induced cell death, as the earliest applications of molecular biology techniques to radiation biology. Most of these studies focuses on radioactive isotopes of iodine, particularly I-123, I-125 and exploring the potential of Auger electrons [1, 2, 3]. From these studies it can be concluded as Auger electrons and Coster-Kronig (CK) electrons has LET value equivalent to heavy charged particles, which make them good candidate for targeted radiation therapy or tumor therapy using radioactive nanoparticles [4, 5]. Here, we have investigated various microdosimetric parameters for I-123 using GEANT4-DNA such as average energy deposited, S- value, and Dose Point Kernel (DPK) and compared them with literature [3]. I-123 is used mainly in nuclear medicine because of its ideal γ -ray energy (159 keV) and relatively short half-life (13 .2 h). The decay of I-123 is, however, also associated with the production of Auger electrons (14% decay by Electron Capture). These low energy particles (< 500 eV) have a very short range in tissue (< 25 nm) (International Commission on Radiological Protection 1983) and as a result induce biological damage similar to that of high linear energy transfer radiations such as 5 MeV α-particles, provided that the isotope is allowed to decay within the cell nucleus [6]. The main objective of this work is to reproduce the geometric model and results found on the H Fourie et al., 2014 [3]. This very first validation is as an exercise to learn the main features of GEANT4-DNA project and then go for more complex structures and simulations on the field of nanodosimetry.

METHODS

Geant4.10.04.p02 simulation toolkit, which inherits Geant4-DNA project in it, was used in this work. The geometry of cell was defined using *DetectorConstruction* initialization file. Cells with radius 6 μm (resembling Chinese hamster ovary (CHO-K1) cells) and with a nucleus of radius 5 μm (resembling human lymphocytes) were modeled. In order to keep the model realistic four spheres (cell envelope, cytoplasm, nucleus envelope and the nucleus core) were defined using G4Orb method. Cell envelope and nucleus envelope were composed of ICRU soft tissue equivalent ($G4\_TISSUE\_SOFT\_ICRU-4$) material while cytoplasm and nucleus core was composed of unit density water ($G4\ WATER$) and were placed inside spherical world volume filled with water. A neutral, stationary, unexcited $I53$ atom was randomly situated within the nucleus core, cytoplasm, cell or one neighbor cell away and microdosimetric quantities such as energy deposited, S-value and radial energy deposited (DPK) were study.

RESULTS

Maximum value to energy deposition, S-value and radial energy deposition was obtained when calculating them inside the nucleus. Due to the low energy the particles couldn't get outside of the nucleus or few of them reached the cytoplasm of the cell. Similar pattern of energy

deposition was obtained as quoted in literature. Underestimation in values was observed in comparison to the data available in literature.

CONCLUSIONS

This paper reports the validation of the geometry and simulation on *I*53 atom was randomly distributed in the nucleus of the cell by calculating the energy deposited, S-value and radial energy deposited. The results were compared to the literature and the variations are within the expected.

REFERENCES

[1] NIKJOO H., et. al. *Modeling of Auger-Induced Dna Damage by Incorporated I* . Acta Oncologia. 35(7):849-856, 1996.

[2] ANDRE T., et. al. *Comparision of Geant4-DNA simulation of S-values with other Monte Carlo codes*. Nucl. Instrum. Methods Phys. Res. B(319): 87-94, 2014.

[3] H. FOURIE, R. T. NEWMAN, AND J. P. SLABBERT. *Microdosimetry of Auger electron emitting I radionuclide using Geant4-DNA simulations* . Phys. Med. Biol, 60:3333-3346, 2015.

[4] BOUSIS C., EMfiETZOGLOU D. AND NIKJOO H. *Monte Carlo single-cell dosimetry of I-131, I-125 and I-123 for targeted radioimmunotherapy of B-cell lymphoma* . Int. J. Radiat. Biol. 88:908–15, 2012.

[5] EMfiETZOGLOU D., et al. *A Monte Carlo study of energy deposition at the sub-cellular level for application to targeted radionuclide therapy with low-energy electron emitters* . Nucl. Instrum. Methods Phys. Res. B(256):547–53, 2007.

[6] E. B. PODGORSAK. *International Atomic Energy Agency, Radiation oncology physics : a handbook for teachers and students*. Ed. Vienna, Austria: International Atomic Energy Agency, 2005.

Characterization of DoseWire Inorganic Scintillator for Relative Measurements in Small Animal Irradiators

I. Silvestre[a]
A. Westhorpe[b], M. Barry[a], G. Schettino[a], R. A. Sharma[b], A. Subiel[a]

[a]National Physical Laboratory (NPL). Hampton Road, Teddington. Middlesex. TW11 0LW
[b]UCL Cancer Institute. Paul O'Gorman Building. University College London. 72 Huntley Street. London WC1E 6BT

Email address of Corresponding Author: ileana.silvestre.patallo@npl.co.uk

BACKGROUND

Inorganic scintillation detectors (ISDs) are a source of interest for relative measurements in a wide range of X-ray beams [1]. Their small dimensions and the possibility to produce real-time readings, makes them attractive for measurements in small fields. A commercially available detector for *in vivo* dosimetry, DoseWire (DoseVue N.V, Belgium), was characterized with medium energy X-rays. The present study evaluates the possibilities of its use for relative measurements in small animal irradiators.

METHODS

Three DoseWire detectors with 5 m, 10 m and 1 m fibre length (Figure 1), were characterized. Several medium energy X-ray beam qualities, generated at the NPL's radiation facility, were used to asses a range of dosimetric characteristics of the detectors: dose rate and beam quality dependence, linearity, repeatability and short term reproducibility. Energy dependence of the detector was evaluated by comparison to measurements with a secondary standard ionization chamber by measuring dose at 2 cm depth in four different beam qualities. Detector's response with dose rate was evaluated by changing the beam fluence rate.

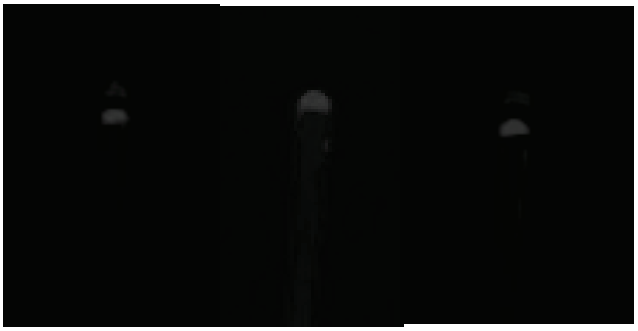

Figure 1. DoseWire detectors: 1 m, 5 m and 10 m fiber length.

A ^{60}Co Theratron 780 unit was used to evaluate the long term reproducibility associated with radiation damage effects, caused by the extended exposure to ionizing radiation. A similar procedure to the one for the W1 Exradin plastic scintillator [2] was developed. A PMMA plate, that allows for the detector to be accurately and reproducibly positioned, was designed with the objective to perform irradiations in repeatable reference conditions in the ^{60}Co unit at NPL.

The angular response of the detector was evaluated with a small animal radiation research platform (SARRP, Xstrahl). Directional dependence was characterized by rotating the detector along its longitudinal axis and also by varying the radiation incidence angle in the polar direction. SARRP Output Factors (OPF) for all the available collimators were measured. Additionally, a temperature controlled water bath was used to assess detector's response with varying temperature.

RESULTS

Signal for the more penetrating beam quality (HVL 4 mm Cu) shown the worse short term reproducibility, with the larger coefficient of variation for the given series of measurements (0.76%). A coefficient of regression, R=1.0, was found for a linear fitting of monitor units (MU) versus detector signal and for all beam qualities (dose levels ranging from 0 to 240 MU). The detector response (normalized at the largest dose rate for a given beam quality) varies less than 2% with respect to dose rate variation in the range from 2 cGy/min to 15 cGy/min.

The position of the detector inside the encapsulation is critical for the angular dependence of the detectors. There was a very small variation of the response of the scintillator with the gantry rotating perpendicular to the detector axis (less than 0.5%). Due to the semispherical shape of the detectors, there are limitations for its use when the gantry rotates parallel to the detector's polar axis outside the 290 to 70 degrees range.

There was no temperature dependence on the response of the scintillators (temperature range from 17 to 28 ºC).

For SARRP collimators down up to 3 mm equivalent square, OPFs agree with film measurements within 4%. For the smaller applicators (Ø 1 mm and 0.5 mm), difference with films are larger than 10%. Comparison with published data show large spread between institutions for the smaller collimators [3-4].

Table 1 summarizes the variation of the scintillator response with beam quality for the 1 m fibre detector. The results are presented as correction factors to the measured signal.

Table 1. Correction factors (kq) for DoseWire (1 m fibre).

kV	mA	HVL (mmCu)	kq x E+05 (Signal/Gy)
135	10.1	0.5	3.98±0.003
180	10.1	1.0	2.56±0.006
220	10.1	2.0	1.36±0.005
280	10.1	4.0	0.46±0.002

CONCLUSIONS

DoseWire is a suitable detector for relative measurements in small animal irradiators with collimators larger than 1 mm equivalent square. A cross calibration on the users beam quality is recommended.

REFERENCES

[1] KERTZSCHER, G., BEDDAR, S., Inorganic scintillation detectors based on Eu-activated phosphors for ^{192}Ir brachytherapy, Phys Med Biol. **62** (2017) 5046.

[2] DIMITRIADES, A., et al., Characterisation of a plastic scintillation detector to be used in a multicentre stereotactic radiosurgery dosimetry audit, Radiation Physics and Chemistry. 140 (2017) 373

[3] GUITA, M., et al., Small Field dosimetry for the small animal radiotherapy research platform (SARRP), Radiat Oncol. **12** 1 (2017) 204

[4] LINDSAY, P.E., et al., Multi-institutional dosimetric and geometric commissioning of image-guided small animal irradiators, Med Phys. **41** 3 (2014) 031714

Dosimetry Considerations in Pre-Clinical Radiation Research with Medium Energy X-rays

A. Subiel[a]
I. Silvestre[a], M. Barry[a], A. Tulk[b], G. Soultanidis[c], J. Greenman[c], V. Green[c], C. Cawthorne[d], G. Schettino[a]

[a] National Physical Laboratory, Hampton Road, Teddington, Middlesex, TW11 0LW
[b]Xstrahl Ltd, Riverside Way, Camberley, Surrey, GU15 3YL
[c]University of Hull, Cottingham Road, Hull, East Riding of Yorkshire, HU6 7RX
[d]Molecular Small Animal Imaging Centre (MoSAIC), KU Leuven, Leuven, Belgium

Email address of Corresponding Author: anna.subiel@npl.co.uk

BACKGROUND

The lack of suitable dosimetry protocols, coupled with the increasing complexity of pre-clinical irradiation platforms, undermines confidence in preclinical studies and represents a serious obstacle in the translation to clinical practice. To accurately measure output of a pre-clinical radiotherapy unit, appropriate Codes of Practice (CoP) for medium energy X-rays need to be used [1]. However, determination of absorbed dose to water (D_w) relies on application of backscatter factor (B_w) employing in-air method or carrying out in-phantom measurement at the reference depth of 2 cm in a full scatter condition. The full scatter conditions require the size of the phantom extending outside the beam edges and have been recommended to be at least 30 × 30 × 30 cm^3 [1]. In most of the instances in pre-clinical irradiators the full scatter conditions cannot be fulfilled and, moreover, are not adequate to geometries used in pre-clinical practice (Figure 1). Therefore, additional recommendations to the existing CoP are required to accurately determine the dose rate (beam output) relevant to irradiation configurations in pre-clinical radiation research.

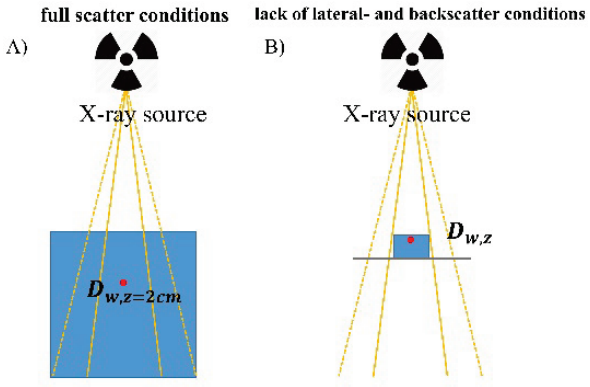

Figure 1. The conceptual difference between reference conditions recommended by the CoP (A) and the irradiation geometries typically used in pre-clinical research (B).

METHODS

Monte Carlo (MC) simulations employing the DOSRZnrc user code, that forms part of the EGSnrc system, were used to calculate the effects of lack of full lateral and backscatter conditions in pre-clinical irradiators. The photon and electron transport cut-off energies were both set to 10 keV. The low energy photon processes, i.e. bound Compton scattering, Rayleigh scattering and atomic relaxations were included in the simulations. Four different beam spectra, corresponding to 0.5, 1, 2 and 4 mm of Cu half-value layer (HVL) were simulated. The effect

of lack of lateral scatter has been accessed by modelling a cylindrical phantom and scoring the dose for decreasing the phantom diameter from 30 cm down to 1 cm. The lack of full backscatter has been assessed by decreasing the thickness of the underlying water from 30 cm down to 1 cm. The D_w has been assessed at 1 mm depth (i.e. $D_{w,z=1mm}$), rather than at the surface, to model typical irradiations of monolayer cell cultures, accounting for the presence of tissue culture medium. The lack of lateral- and backscatter on the calculated beam output has been assessed for various beam sizes. Additionally, the effect of SSD on the dose rate has been evaluated using the inverse-square law.

RESULTS

The MC simulations for investigated beam qualities (0.5 - 4 mm Cu) have shown that D_w quantity is highly dependent on the thickness of backscatter material (here water). Table 1 shows the change of the beam output ($D_{w,z=1mm}$) for 4 mm of Cu HVL as a function of the thickness of underlying material and field size. If the output of a 30 cm diameter field is assessed in full scatter conditions and irradiations of cell monolayers are performed under 1 cm backscatter, a 20% correction to the beam output is required to accurately account for the decrease of the dose rate. This correction decreases with HVL and field size. Similarly, the lack of full lateral scatter has an effect on $D_{w,z=1mm}$, particularly for a large field size and the required correction can reach a few percent when small samples are used.

Table 1. The effect of lack of full backscatter conditions on 4 mm Cu beam output ($D_{w,z=1mm}$).

Backscatter thickness [cm]	**Beam diameter**			
	5 cm	**10 cm**	**20 cm**	**30 cm**
	Output relative to full scatter condition [%]			
30	100.0	100.0	100.0	100.0
10	99.7	99.9	98.3	97.6
5	99.1	97.8	94.3	92.2
2	97.1	93.4	87.5	84.2
1	94.9	89.9	83.0	79.5

The source-surface distance (SSD) is also a critical parameter having an effect on the beam output. For instance, the change of SSD from 30 cm to 30.5 cm confers a > 3% decrease in the dose rate. It is therefore, important to carefully assess the distance of a source to the irradiated sample.

CONCLUSIONS

Measurement of the beam output in pre-clinical irradiators is often challenging due to the unfeasibility of achieving the full scatter conditions required to directly employ the CoP for the determination of D_w. Additionally, realization of full scatter conditions is often unrealistic as it is far from the irradiation setups used in practice. It is therefore essential to either (i) apply correction factors to account for the differences in the determination of the beam output between the full scatter and actual irradiation conditions or (ii) to carry out measurements in conditions that most closely represent experimental geometries employing a well-characterized detector. Datasets enabling accurate determination of correction factors together with a set of recommendations should be published to enable the research community to carry out accurate dosimetry in pre-clinical radiation research.

REFERENCES

[1] MA, C.M., AAPM protocol for 40-300 kV x-ray beam dosimetry in radiotherapy and radiobiology, Med. Phys. **28**(6) (2001) pp. 868-93

Occupational Dosimetry

ISO/TC 85/SC 2 Standards for Staff Radiation Protection in Medicine

C. Challeton-de Vathaire[a]
D. Bingham[b], J.-F. Bottollier-Depois[a], P. Cortes[c], R. Cruz Suarez[d], S. Derreumaux[a], C. Kim[e], F. Queinnec[a], L. Thomas[f], I. Gardin[g]

[a]IRSN, Fontenay-aux-Roses, France
[b]AWE, Reading, United Kingbom
[c]ITER, Saint-Paul Lez Durance, France
[d]AIEA, Vienna, Austria;
[e]Korea University, Seoul, South Korea
[f]AFNOR, Saint-Denis, France
[g]CHB et LITIS (EA4108), Rouen, France

Email address of Corresponding Author: cecile.challetondevathaire@irsn.fr

BACKGROUND

The international standardization organization ISO develops standards in the field of radiological protection for more than thirty years.

Within ISO/TC 85 Nuclear energy, nuclear technologies and radiological protection, subcommittee SC 2 develops standards to improve radiation protection for individuals (workers, patients, members of the public) and in the environment in various exposure situations to ionizing radiations, planned, existing or emergency situations, linked to medical, nuclear, industrial or research activities and natural radiation sources (radon, cosmic radiation).

In the medical field, the development of new standards meets the increasing need for guidelines and protocols. It includes standards for external and internal individual monitoring of the staff, for patient dosimetry and related protocols in clinical applications and for shielding systems.

STANDARDS FOR OCCUPATIONAL INTERNAL DOSIMETRY

Two general standards, developed for the monitoring of occupational internal dosimetry in all activities, are applicable to the staff involved in the medical use of ionizing radiation: ISO 20553:2006 “Radiation protection - Monitoring of workers occupationally exposed to a risk of internal contamination with radioactive material” and ISO 27048:2011 “Radiation protection - - Dose assessment for the monitoring of workers for internal radiation exposure”.

ISO 20553 offers guidance for the decision whether a monitoring programme is required for workers exposed to the risk of internal contamination by radioactive substances and how it should be designed. It establishes principles for the development of compatible goals and requirements for the programmes and specifies the minimum requirements for their design.

ISO 27048 presents procedures and assumptions for the standardised interpretation of monitoring data. Those procedures allow the quantification of exposures for the documentation of compliance with regulations and radiation protection programmes. The standard specifies the minimum requirements for the evaluation of data from the monitoring in order to achieve acceptable levels of reliability in internal dose assessment.

A standard has been specifically developed for the application of the general standard ISO 20553 to the staff of a nuclear medicine department: ISO 16637:2016 “Radiological protection - Monitoring and internal dosimetry for staff members exposed to medical radionuclides as unsealed sources”. It specifies the minimum requirements for the design of professional programmes to monitor workers exposed to the risk of internal contamination via inhalation by

the use of radionuclides as unsealed sources in nuclear medicine imaging and therapy departments.

Performance of internal dosimetry services including *in vitro* monitoring can be evaluated following ISO 28218:2010 “Radiation protection - Performance criteria for radiobioassay” and in the future, for *in vivo* monitoring, by a standard in development: ISO 23588 “Radiological protection - General requirements for performance testing for *in vivo* monitoring”.

ISO 28218 provides criteria for quality assurance and control, and evaluation of performance of radiobioassay service laboratories. It presents guidance for *in vivo* radiobioassay and *in vitro* radiobioassay. ISO 23588 will specifie minimum requirements for proficiency tests and intercomparison exercises that are offered to facilities operating *in vivo* detection systems. It will be applicable to programs that are meant to test the quality and capability of the participating laboratories. The standard will cover technical (e.g. selection of radionuclides and phantoms, traceability of activities), management (e.g. announcement, realisation of the measurements, transportation, reporting) and data analysis aspects.

STANDARDS FOR OCCUPATIONAL EXTERNAL DOSIMETRY

ISO 15382:2015 “Radiological protection - Procedures for monitoring the dose to the lens of the eye, the skin and the extremities” is applicable to the workers in the medical field which are particularly concerned by risk of exposition to the hand during injection of radiopharmaceuticals and interventional radiology procedure. External dosimetry service can be evaluated using ISO 14146:2018 “Radiological protection - Criteria and performance limits for the periodic evaluation of dosimetry services”.

ISO 15382 provides procedures for monitoring the dose to the skin, the extremities (hands, fingers, wrists, forearms, feet and ankles), and the lens of the eye in planned exposure situations. It covers practices which involve a risk of exposure to photons in the range of 8 keV to 10 MeV and electrons and positrons in the range of 60 keV to 10 MeV. This standard gives guidance for the design of a monitoring program to ensure compliance with legal individual dose limits. It refers to the appropriate operational dose quantities and specifies the type and frequency of individual monitoring and the type and positioning of the dosemeter according to the nature of the exposure. It gives guidance on how to decide if such dosemeters are needed and present different approaches to assess and analyse skin, extremity, and lens of the eye doses.

ISO 14146 specifies the criteria and the test procedures to be used for the periodic verification of the performance of dosimetry services supplying personal and/or area dosemeters (i.e. workplace or environmental dosemeters). The performance evaluation can be carried out as a part of the approval procedure for a dosimetry system or as an independent check to verify that a dosimetry service fulfils specified national or international type test performance requirements under representative exposure conditions that are expected or mimic workplace fields from the radiological activities being monitored. This document applies to personal and area dosemeters for the assessment of external photon radiation with a (fluence weighted) mean energy between 8 keV and 10 MeV, beta radiation with a (fluence weighted) mean energy between 60 keV and 1,2 MeV, and neutron radiation with a (fluence weighted) mean energy between 25,3 meV and 200 MeV. It covers all types dosemeters needing laboratory processing (e.g. thermoluminescent, optically stimulated luminescence, radiophotoluminescent, track detectors or photographic-film dosemeters) and involving continuous measurements or measurements repeated regularly at fixed time intervals (e.g. several weeks, one month). Active dosemeters (for dose measurement) may also be considered if treated as passive dosimeter (i.e.

the dosimetry service reads their indicated values and reports them to the evaluation organization).

OTHER STANDARDS FOR STAFF AND PUBLIC RADIOPROTECTION IN MEDICAL APPLICATIONS OF IONIZING RADIATION

Several standards deal with public and staff radioprotection in nuclear medicine, including two on radioactive waste management: ISO 19461-1:2018 “Radiological protection - Measurement for the clearance of waste contaminated with radioisotopes for medical application - Part 1: Measurement of radioactivity” and ISO 19461-2 (under development) “Part 2: Management of solid radioactive waste in nuclear medicine facilities” and two on the ambient dose equivalent from patients after treatment for thyroid cancer by ^{131}I: ISO 18310-1:2017 “Measurement and prediction of the ambient dose equivalent from patients receiving iodine 131 administration after thyroid ablation - Part 1: During the hospitalization” and ISO 18310-2 (Under development) “Part 2: After release from the hospital”.

The ISO 19461-1:2018 document establishes the method of radioactivity measurement and determination of the storage periods of the radioactive wastes produced as a result of medical application of the radioisotopes based on counting measurements using a detector and decay correction from the initial activity concentration of the radioisotopes contained in the waste stream. It provides a set of controls and measurements for the self-clearance of the radioactive wastes by which the medical facility can be assured to meet the clearance level. Part 2 of ISO 19461 addresses aspects of management of solid biomedical radioactive waste from its generation in nuclear medicine facilities to final clearance and disposal, as well as the manner to establish an effective program for biomedical radioactive waste management. It provides a list of the main radioisotopes used in nuclear medicine facility and their main physical characteristics, as well as the radioactive waste management program, from their sorting, collection, packaging and labelling, the radioactivity survey and decay storage, clearance levels, transportation if necessary, until their disposal or discharge.

Part 1 of ISO 18310 specifies suitable methods for the measurement of personal dose equivalent of the patient treated with radioiodine after thyroid ablation due to the adjacent patient receiving the same therapy procedures. It addresses the measurement methods, the calibration of ionization chamber and the uncertainty estimation for the measurement of the personal dose equivalent of the patient treated with radioiodine after thyroid ablation using the ionization chamber. Part 2 addresses the measurement methods, procedures and uncertainty estimation for the measurement of the effective dose equivalent to the caregiver in the vicinity of the patient treated with radioiodine to ablate the thyroid using a personal dosimeter, after release of the patient from the hospital.

Considering radiotherapy, a standard has been developed for the shielding of medical accelerators**:** ISO 16645:2016 “Radiological protection - Medical electron accelerators - Requirements and recommendations for shielding design and evaluation”.

CONCLUSIONS

ISO has developed different standards for occupational radioprotection in medicine including guidance for the monitoring of external and internal exposure. Others published ISO standards deal with clinical dosimetry for the patient as ISO 21439:2009 on beta radiation sources for brachytherapy or ISO 28057 on dosimetry with solid thermoluminescence detectors for photon and electron radiations in radiotherapy.

The published standards can be purchased via ISO/TC85/SC2 web site:
https://www.iso.org/committee/50280.html

Compulsory Use of Extremity Dosimetry in Nuclear Medicine Facilities

M. A. Rivera Cardona[1]
C. E. Ribeiro Alves[1]

[1]Comissão Nacional de Energia Nuclear, National Comissiono of Nuclear Energy, Divisão de Aplicações Médicas e de Pesquisa, Rua General Severiano, 90 - Botafogo - CEP: 22.290-901, Rio de Janeiro, RJ, Brasil

Email address of Corresponding Author: marissa@cnen.gov.br

BACKGROUND

During the last 20 years, extremity dosimetry (ED) has become a matter of concern for regulatory bodies. In 2010, less than 10% of nuclear medicine facilities (NMF) registered the use of ED. In 2013, the use of ED became compulsory for nuclear medicine workers who handled radionuclides.

According to international studies [1], [2], and [3], regarding hand exposure, the fingertips are the most exposed location (tip of the index finger and thumb) most commonly used during radiopharmaceutical manipulation procedures, having this in mind, whenever ED values exceed 20mSv per month (equivalent dose) the regulatory body shall be notified [4] and [5].

METHODS

In order to stablish compulsory use of ED, a previous study was accomplished from 2006 to 2008. A total of 12 NMF from the national territory were evaluated. As an example, the EW distribution with ED monitoring for all evaluated facilities is shown in Table 1 for the year 2006. A similar set of data was registered for the years 2007 and 2008. Table 1 presents the total of EW at a given facility, the percentage of those EW that used ED, the percentage of the ED that presented trustful values when compared to their respective chest dosimeter and the last column showed the quantity of ED whose values exceeded the respective chest values by a factor of 25.

Table 1. Extremity Dosimetry Distribution for the Year 2006.

NMF	Total EW	EW with ED (%)	Trusted ED (%)	ED/CD ≥ 25
1	49	25 (51%)	14 (56%)	0
2	14	0 (0%)	0 (0%)	0
3	0	0 (0%)	0 (0%)	0
4	5	1 (20%)	1 (100%)	0
5	56	10 (18%)	7 (70%)	1
6	8	1 (12%)	1 (100%)	0
7	13	4 (30,7%)	4 (100%)	0
8	17	0 (0%)	0 (0%)	0
9	55	45 (82%)	23 (51%)	2
10	6	3 (50%)	2 (66,6%)	0
11	22	4 (18,1%)	4 (100%)	0
12	5	0 (0%)	0 (0%)	0
Total	**250**	**88**	**42**	**3**

RESULTS

Of the 12 NMF evaluated and considering the three years of study, 5 (41.7%) presented at least one event in which the ED value was greater than a factor of 25 in relation to the respective chest dosimeter value (effective dose). Comparing the events found in relation to the number of EW with trusted ED values, these were ranging between 3.2% (2007) and 7.1% (2006).

CONCLUSIONS

Before 2013, enough evidences were found indicating that ED was not correctly used or not used at all even though it was available at NMF. From 2014 to 2016, an educational campaign of the regulatory body was done through audits and inspection for the appropriate use of ED. From 2017 until today, reinforcement measures have been applied in NMF that do not use ED. Another important thing to note is from a survey done with ED values notifications to the regulatory body in 2007 and then how it evolved until 2018 from almost none notifications at all to 5 notifications in 2018. For the following years we expect an increase in the number of notifications since EW is still learning to correctly use ED.

REFERENCES

[1] PANT, G.S., SHARMA, S.K., and RATH, G.K., "Finger Doses for Staff Handling Radiopharmaceuticals in Nuclear Medicine", Journal Of Nuclear Medicine Technology, **34,** No. 3 (2006.), 169-173.

[2] WRZESIEN, M., OLSZEWSKI, J. and JANKOWSKI1, J., "Hand Exposure to Ionising Radiation of Nuclear Medicine Workers", Radiation Protection Dosimetry, **130**, No. 3 (2008), 325–330.

[3] LECCHI, M., MALASPINA, S., and DEL SOLE, A., "Effective and equivalent dose minimization for personnel in PET procedures: how far are we from the goal?", European Journal of Nuclear Medicine and Molecular Imaging, **43** (2016), 2279–2282.

[4] Diretrizes Básicas de Proteção Radiológica, NORMA CNEN-NN-3.01, (2011).

[5] Requisitos de Segurança e Proteção Radiológica para Serviços de Medicina Nuclear NORMA CNEN-NN-3.05, (2013).

The UK Approach to Monitoring Finger Doses in Nuclear Medicine

C. Martin[a]
A. Hughes[b], **D. Temperton**[c], **T Jupp**[d]

[a]University of Glasgow, 27 Garngaber Avenue, Lenzie, Glasgow, G66 4LL
[b]Royal Preston Hospital, Sharoe Green Lane, Preston, PR2 9HT
[c]University Hospitals Birmingham NHS Foundation Trust, Selly Oak, Birmingham, B29 4NE
[d]Radiation Protection, Royal Surrey County Hospital, Egerton Road, Guilford, GU2 7XX

Email address of Corresponding Author: colin.j.martin@ntlworld.com

BACKGROUND

Nuclear medicine services prepare and administer radiopharmaceuticals to patients. The preparation stage is usually carried out in a Radiopharmacy, and regional services may dispense up to 100 GBq of ^{99m}Tc per day. Centres with positron emission tomography (PET) scanners handle high activity levels because of the short half-lives of ^{18}F and other PET radionuclides. The manipulation of radiopharmaceuticals with syringes and vials will lead to high doses to the fingers. Measures to protect the fingers include use of tungsten shields that support the vial and provide better protection than simple lead pots, and use of syringe shields for preparation, drawing up, and performing injections. These can reduce the doses to the finger by factors of 4-10 [1]. Automated dispensers provide good protection with PET radionuclides but are expensive. Obtaining accurate dose assessment from routine monitoring is difficult, as the dose gradients across the hands can be substantial and the maximum dose, which is usually at the fingertips, is underestimated by ring dosemeters worn at the bases of the fingers [2, 3].

METHODS

Different techniques are used for withdrawing radiopharmaceutical from a vial, to allow the tip of the needle to remain within the liquid (Figure 1). These influence the finger that will receive

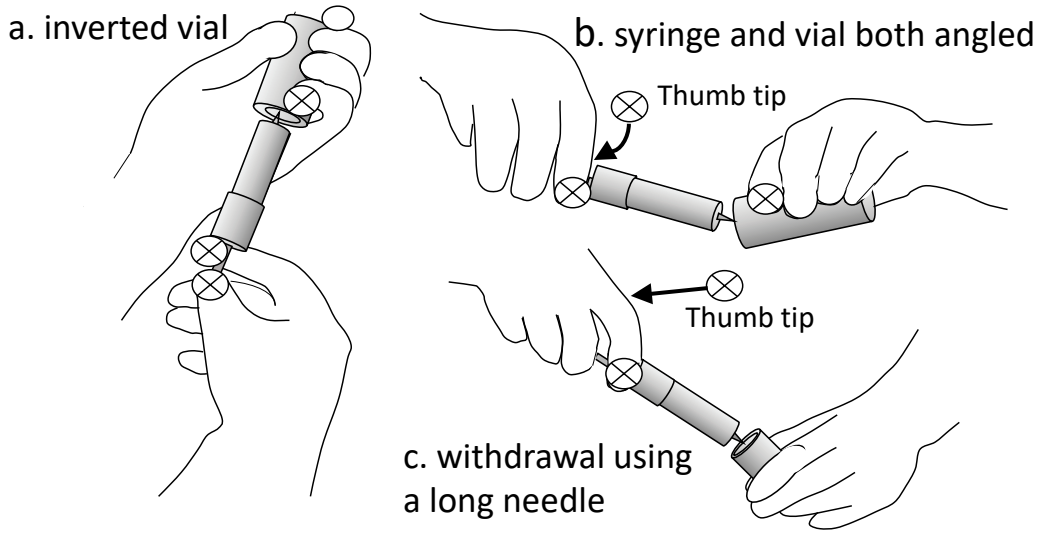

Figure 1. Hand positions used in withdrawing radiopharmaceutical from a vial with a syringe. The tips of the fingers more likely to be exposed are marked with ⊗.

the higher dose. The index finger and thumb of the hand holding the syringe are likely to be more exposed, but exposure of the hand holding the vial can vary. If the vial is inverted and activity withdrawn downwards (Figure 1a) the wrist and little finger of the hand holding the vial can receive a higher dose. Whereas if vial and syringe are both angled downwards (Figure

1b) the index finger receive may be more exposed. In nuclear medicine departments where the vial holding the activity is contained in a lead pot, the vial is supported by the syringe needle and the neck may protrude from the shield increasing the dose level. Occasionally a finger may touch the cap of the vial adjacent to the radiopharmaceutical, and so receive a higher dose and such exposures are virtually impossible to assess unless a dosemeter is worn at the fingertip.

For injections insertion of the needle into a vein requires careful positioning. Use of the index finger to guide the needle containing radiopharmaceutical gives a dose to the tip. A butterfly cannula is frequently inserted into a vein, prior to administration to avoid this. Nevertheless a survey of UK practices revealed that only 33% never touched a needle during injections [3]. Finger doses in a study of 30 nuclear medicine departments in six European countries recorded finger doses ranging from 0.02 to 0.8 mSv per GBq for both preparation and administration of ^{99m}Tc and 0.1 to 4 mSv per GBq for ^{18}F [2]. In these studies the tips of the index finger and thumb on the two hands were found to receive the highest doses. The wide range in recorded values make dose levels difficult to predict and careful training and observation of staff practices is required when determining dosemeter placement.

RESULTS

Guidance on personal dosimetry linked to revised UK regulations has been prepared [4]. If annual extremity doses are a few tens of mSv, ring dosemeters worn at the base of the finger could be used for routine monitoring, but an attempt should be made to determine how this dose relates to that at the most exposed region. If the dose to a fingertip is likely to approach 100 mSv, then finger stalls are recommended in order to measure the dose at the position considered to receive the highest dose. For small sources such as syringes and vials, the magnitude of the dose gradient is determined by the proximity of the fingertip to the unshielded source, so if fingertips are close to or may come into contact with the source, finger stalls provide the better option. But if the same manipulations are repeated many times, and doses do not approach 100 mSv, then ring dosemeters could be worn on the palmar side of the index fingers with a scaling factor to assess dose to the fingertip. Measurements at the tip should be carried out for a trial period to establish a ratio between doses to the tip and the dosemeter position that can subsequently be applied routinely. Scaling factors to estimate doses to the fingertips should be assessed individually for each worker. Values of 3-4 may be appropriate for most departments, but if a reliable factor is not available, a value of 6 should be used.

CONCLUSIONS

Doses to the hands should be monitored for radiopharmacy staff preparing and administering imaging radiopharmaceuticals regularly. Use of finger stalls to measure doses to the tips of the index fingers on both hands is recommended wherever there is a risk of the fingertip dose approaching 100 mSv. A scaling factor should be applied if ring dosemeters are employed.

REFERENCES

[1] WHITBY, M AND MARTIN, C J A multi-centre study of dispensing methods and hand doses in UK hospital radiopharmacies. Nucl. Med. Commun. 26, 2005, 49-60

[2] VANHAVERE F, CARINON E, GUALDRINI G E et al. ORAMED: Optimisation of Radiation Protection for Medical Staff. 7th EURADOS Report 2012-02 ISSN 2226-8057, ISBN 978-3-943701-01-2.

[3] MARTIN C J Strategies for assessment of doses to the tips of the fingers in nuclear medicine. Journal of Radiological Protection 36, 2016, 405–418

[4] MARTIN C J, TEMPERTON D H, HUGHES A AND JUPP T Guidance on the personal monitoring requirements for personnel working in healthcare. (York: IPEM) 2018.

Correlation Between the Dose Measured with Eye Lens Dosimeters and the Eye Lens Dose, when Lead Glasses are Used

E. H. Silva[a]
C. Martin[b], F. Vanhavere[a], N. Buls[c]

[a]Belgian Nuclear Research Centre, Boeretang 200, 2400 Mol, Belgium
[b]DCPB, University of Glasgow, Gartnavel Royal Hospital, Glasgow, G12 0XH, UK
[c]Department of Radiology - UZ Brussel, Laerbeeklaan 101, 1090 Jette, Belgium

Email address of Corresponding Author: ehdsilva@sckcen.be

BACKGROUND

The efficiency of different models of lead glasses in protecting the eye lenses of interventional clinicians has been assessed in a variety of ways: with phantoms [1], during clinical practice [2] and with computational simulations [3]. If the dosemeter is worn under the lead glasses, the measured dose is considered to be similar to that received by the eye lens [4], while if the unshielded dosemeter is worn outside the glasses, a correction factor may be applied to allow for the protection provided by the glasses. However, due to the complex radiation field to which interventional clinicians are exposed, there is the potential for both approaches to underestimate the dose to the eye lens [1,5].

METHODS

The arrangement used in interventional cardiology was simulated with MCNPX software and doses that would be measured with $H_p(3)$ dosemeters in various positions were compared to the dose in the sensitive region at the surface of the eye lens, $H_{lens,sensitive}$,

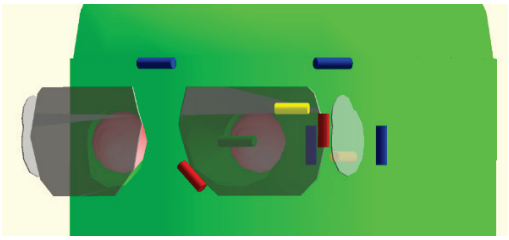

Figure 1: Lead glasses with simulated dosemeters: 4 blue unshielded dosemeters on the surface of the head of the phantom, 2 yellow dosemeters on the glasses under the lens, 2 red dosemeters on the glasses over the lens, and one reference green dosemeter, $H_p(3)_{ref}$, on the surface of the eye.

The patient and operator were modeled as stylized phantoms, without any internal organs, except for the presence of detailed model eyes within the operator's head [6]. The operator was modeled wearing a 0.5 mm lead apron and thyroid collar. Two realistic models of lead glasses were considered: one wraparound with lenses at an angle to the front of the head (0.75 mm Pb equivalent) and one with flat frontal lenses and side shielding (0.75 mm and 0.5 mm Pb, respectively). Eye lens dosemeters [7] were placed in 8 positions on the left side of the head of the operator, figure 1. A reference dosemeter was also placed on the surface of the left eye, to reproduce the setup used in experimental assessments of efficiency of lead glasses. The exposure from an interventional cardiology procedure with the x-ray tube positioned to the left of the operator was simulated using five standard projections and acquisition parameters. Procedures were simulated for two accesses routes via the brachial and femoral arteries.

RESULTS

The shielded dosemeters placed under the lens of the lead glasses (yellow, figure 1)

underestimated the eye lens dose, $H_{lens,sensitive}$, by 60% to 80%. For the unshielded dosemeters on the head (blue), $H_p(3)/H_{lens,sensitive}$ varied from 1.0 to 1.6, whereas for dosemeters worn outside the shielding of the lead glasses (red), $H_p(3)/H_{lens,sensitive}$ was 1.5 to 1.6. This indicates that a correction factor of 0.5 for unshielded dosemeters, considered to be conservative [4], could also underestimate the eye lens dose. Thus both approaches are likely to underestimate the true dose to the eye lens. The reference dosemeter placed on the surface of the eye (green), which represents the position normally used as the reference in phantom measurements $H_p(3)_{ref}$, received, on average, 40% less radiation dose than the sensitive volume in the eye lens, $H_{lens,sensitive}$. Therefore, a higher efficiency is inferred for lead glasses when $H_p(3)_{ref}$ is used for dose comparisons, with $H_p(3)/H_p(3)_{ref}$ varying from 2.2 to 3.5 for the dosemeters on the head and over the glasses. This occurs because the level of shielding for tissue or dosemeters from radiation incident from the side and from scatter improves as the measurement position is moved closer to the shielded lens.

CONCLUSIONS

Dosemeters worn by interventional clinicians under lenses of lead glasses may underestimate the eye lens dose by more than 60% due to the complex scatter field. The position used for the eye lens reference when protection from lead glasses is affects the result, so that measurements made in experiments on phantoms tend to overestimate actual levels of protection. In consequence, application of a correction factor of 0.5 to readings from a dosemeter worn on the surface of the head for staff wearing glasses also underestimates eye lens dose.

REFERENCES

[1] DOMIENIK, J., BRODECKI, M., The effectiveness of lead glasses in reducing the doses to eye lenses during cardiac implantation procedures performed using x-ray tubes above the patient table, Journal of radiological protection : official journal of the Society for Radiological Protection **36** 2 (2016) N19-25.

[2] DOMIENIK, J., et al., The impact of various protective tools on the dose reduction in the eye lens in an interventional cardiology-clinical study, Journal of radiological protection : official journal of the Society for Radiological Protection **36** 2 (2016) 309-318.

[3] KOUKORAVA, C., et al., Efficiency of radiation protection equipment in interventional radiology: a systematic Monte Carlo study of eye lens and whole body doses, Journal of radiological protection : official journal of the Society for Radiological Protection **34** 3 (2014) 509-528.

[4] INTERNATIONAL ORGANIZATION FOR STANDARDIZATION, Radiological protection - Procedures for monitoring the dose to the lens of the eye, the skin and the extremities, 2015.

[5] MARTIN, C.J., Protecting interventional radiology and cardiology staff: Are current designs of lead glasses and eye dosemeters fit for purpose?, Journal of radiological protection : official journal of the Society for Radiological Protection **38** 2 (2018) E22-e25.

[6] BEHRENS, R., DIETZE, G., ZANKL, M., Dose conversion coefficients for electron exposure of the human eye lens, Physics in medicine and biology **54** 13 (2009) 4069-4087.

[7] SILVA, E.H., et al., OPTIMIZATION OF A RADIOPHOTOLUMINESCENT GLASS DOSEMETER FOR OCCUPATIONAL EYE LENS DOSIMETRY IN INTERVENTIONAL RADIOLOGY/CARDIOLOGY, Radiat Prot Dosimetry **182** 2 (2018) 177-183.

Quantitative Imaging for Radionuclide Therapy

Calibration of Activity Meters (aka. Dose Calibrators) in Nuclear Medicine

H.-S. Jans[a]

[a]Department of Oncology, University of Alberta, 11560 University Avenue, Edmonton, Alberta, Canada T6G 1Z2

Email address of Corresponding Author: hans-sonke.jans@ahs.ca

BACKGROUND

Radiation dose received by patients either treated or diagnosed with unsealed sources in nuclear medicine directly depends on the amount of radiopharmaceutical administered to the patient. The rise of quantitative imaging [1-3] and rigorous accreditation requirements for clinical trials add to the importance of accurately measuring radioactivity administered to patients.

Prior to administration, radioisotope activity is measured with a well-type, re-entrant ion chamber, also known as a radionuclide calibrator or dose calibrator (DC). Standard of good practice in most countries calls for administered activity to be within 10% of the amount prescribed by a physician [4]. The measurement of radioisotope activity is therefore recommended to be performed with an accuracy between 2% and 10%, depending on isotope-specific factors (mode and energy of emission) and instrument class (clinical DC or secondary standard DC) [4-7]. Several studies show that these limits are not consistently met [8-13], demonstrating insufficient calibration accuracy of the DCs used in clinical practice.

The current generated in the ion chamber's sensitive volume for a given amount of activity is isotope-dependent. Therefore, a DC's calibration, i.e. the adjustment of its reading to correctly display the amount of activity present in its well, needs to be established separately for each isotope to be assayed with that DC. Besides being isotope-specific, calibration of DCs should also be carried out in a manufacturer-independent manner, traceable to a standards laboratory [4-6].

Traceability is established by cross-calibrating the DC to a standards laboratory. Several approaches to establish and maintain traceability are discussed. Besides simply relying on manufacturer settings, they can be classed into two groups: exchange of a radioisotope source of known activity and exchange of a calibrated measurement instrument. Advantages and drawbacks of each of these methods are presented, together with practical implementations recently proposed.

METHODS FOR CROSS-CALIBRATION

Reliance on manufacturer

The initial calibration of a new DC is set by its manufacturer. If this calibration were accurate, stable over time and encompass all isotopes of clinical interest, a simple constancy check with a long-lived radioisotope (see below) would suffice. But the inaccuracies in DC calibration found in several studies [8-13] suggest that reliance on the manufacturer alone is not a satisfactory approach. Furthermore, omission of manufacturer-independent checks is not considered good clinical practice and stands in contrast to quality assurance procedures commonly in place for other quantitative instruments. For example, the accuracy of survey meters, ion chambers and GM counters are regularly verified by independent 3rd parties.

Exchange of known radioisotope samples

If a radioisotope sample of known activity (i.e. traceable to a standards laboratory) is available, the DC's calibration *for that isotope* can be established (or verified) by simply measuring that sample in the DC, provided that confounding factors such as source position inside the DCs well, source volume and composition (e.g. glass vs. plastic enclosure, water vs. resin bulk material) are taken into account. Several variations of this method exist:

Shipping long-lived radioisotope samples: Long-lived sources of known activity are readily available, e.g. Cs-137, Ba-133 or Co-57 with half-lives from 9 months to 30 years. These isotopes, however, are *not* administered to patients. They are therefore useful for constancy checks over long time periods, but inadequate for establishing a DC's calibration for isotopes administered to patients. Because of its simplicity however, this method, together with reliance on the manufacturer's calibration settings (above), is often the default method for assessing DC calibration.

Shipping surrogate radioisotope samples: Here, a long-lived radioisotope is utilized, whose decay scheme is similar to that of a clinical radioisotope. The most prominent example of this approach is Ge/Ga-68 serving as a surrogate for F-18 [14, 15]. Though proven feasible in this case, this approach cannot be easily applied to other isotopes because of the incidental nature of decay scheme similarities [4]. In most cases, a long-lived isotope that sufficiently matches the decay properties of a clinical isotope does not exist.

Shipping clinically used radioisotope samples: Some countries maintain a program of regular exchange of select, clinically used isotopes (e.g. I-131, Tc-99m, Ga-67) between a standards laboratory and nuclear medicine clinics [5, 8, 16]. Despite their seeming simplicity, such programs are difficult to maintain as they depend on distance and efficiency of shipping and are feasible only for longer-lived clinical isotopes; in addition, repeat measurements at a later time are possible only within a few half-lives of the isotope in question. Canada terminated its program in 2000 [17, 18].

Exchange of measurement instruments

Shipping of the dose calibrator: Shipping a DC to a standards laboratory for calibration is not commonly pursued because of the bulk of the instrument and its installation, commonly built-in under a counter and behind heavy shielding. Moreover, a replacement instrument would need to be available in order to maintain clinical service while the DC is sent out for calibration.

Shipping of a dedicated transfer instrument: Sending a dedicated instrument to the standards laboratory for calibration has the advantages of a) enabling uninterrupted clinical service, b) allowing purpose-driven design to optimize e.g. sample positioning accuracy c) eliminating the problem of radioisotope decay during shipping and d) eliminating the radiation safety concerns and administrative overhead associated with shipping radioactive substances e) permitting repeat measurements beyond the limitation of radioisotope half-life. It does, however, presuppose adequate radioisotopic purity at each site. This approach mimics the procedure established in radiation therapy, where an ion chamber–electrometer pair is sent to a standards laboratory for calibration and is then used at the local clinic to calibrate e.g. linear accelerators, Co-60 teletherapy machines or brachytherapy systems.

To perform the calibration, samples of *clinical* radioisotopes are drawn from *local stock*. A sample at the standards laboratory is first measured in their calibrated setup (e.g. a DC dedicated to this purpose); afterwards, the sample of now-known activity is measured in the transfer instrument, which is then calibrated. The calibrated transfer instrument is now shipped

back to the local clinic and used to calibrate DCs there with radioisotope samples drawn from local stock. Several types of such dedicated transfer instruments have recently been proposed:

- *A dedicated dose calibrator:* A mock service was set up to test the accuracy of DCs in Canada [17]. Using a dedicated DC as transfer instrument has the advantage of ready availability, though the instrument shipped is still fairly bulky and heavy. Tests were carried out for Tc-99m with syringes of different volumes typically used clinically. Uncertainties of <0.5% (k=1) were reported, though limited shielding, timing inaccuracies, variations in sample volume and positioning inside the DC can add to calibration uncertainty in routine clinical practice.
- *Exposure of film:* Radiation emanating from a clinical radioisotope exposes film under reference conditions at the standards laboratory [19] and a film calibration curve is obtained. Reference conditions are replicated at the nuclear medicine clinic and sample activity inferred from the film's calibration curve. Tests with Tc-99m revealed an overall uncertainty of 2.0% (k=2). Disadvantages are the long expose time required (approximately one day) and the logistics of film storage/handling/scanning for the maintenance of the program.
- *A purpose-designed ion chamber:* An ion chamber has been manufactured to hold a syringe in a precisely defined position in its sensitive volume; the chamber itself fits inside the well of an existing DC, which ensures adequate shielding [20, 21]. The chamber's calibration factor for a given isotope is established at the standards laboratory. The calibrated chamber is then used at the nuclear medicine clinic to ascertain the activity of an isotope sample drawn from local stock, which is in turn used to calibrate the clinic's DCs. An uncertainty budget of <1% (k=1) has been reported. This concept envisions dedicated software to operate the electrometer, perform decay calculations and time-stamping (a necessity for short-lived isotopes) and store the isotope-specific calibration factors. Advantages are small size and weight for easy portability, good shielding and low measurement uncertainty.

The obvious use of these cross-calibration instruments is to enable traceability to a standards laboratory for absolute activity calibration of DCs. But cross-calibration would also be useful and possible for additional applications:

- Several clinical sites participating in multi-center trials could be cross-calibrated relative to each other in order to facilitate better agreement of radioactivity measurements and thus reduce quantitative uncertainties in those trials.
- When introducing novel radioisotopes into clinical use, these transfer instruments would allow cross-calibration of the clinical DCs with the ones of the radiopharmaceutical manufacturers, again to improve quantitative precision of clinical trial and follow-up data.
- The primary standardization for the clinically important isotope F-18 has been fluctuating at NIST by more than 4% since 1992 [22]; cross-calibration devices like the ones described here would allow precise intercomparison of such short-lived radioisotopes among national standards laboratories around the world.

CONCLUSIONS

Some of the approaches for DC cross-calibration are not independent of the manufacturer and others merely establish calibration for *not* clinically used radioisotopes; these cannot be recommended. The seemingly simple, but actually challenging problem of calibrating a DC i) accurately ii) isotope specific iii) manufacturer independent and iv) traceable to a standards laboratory is highlighted by studies demonstrating inconsistent DC calibration. This problem is exacerbated by the need to calibrate novel radioisotopes being researched and introduced into clinical practice and by some inconsistency over time of the primary standardization of F-

18. These challenges are being addressed by recent advances for DC calibration based on dedicated transfer instruments.

REFERENCES

[1] Clarke LP et al. “The quantitative imaging network: NCI’s historical perspective and planned goals,” Transl. Oncol. 7, 1–4 (2014)

[2] FDG-PET/CT Technical Committee, “QIBA Profile. FDG-PET/CT as an Imaging Biomarker - Measuring Response to Cancer Therapy”, Quantitative Imaging Biomarkers Alliance, Version 1.13, Technically Confirmed Version, QIBA November 18, 2016, Available from: RSNA.ORG/QIBA

[3] “IAEA Human Health Reports No. 9, Quantitative Nuclear Medicine Imaging: Concepts, Requirements and Methods”, published by the International Atomic Energy Agency (IAEA) in 2014 (ISBN: 978–92–0–141510–3)

[4] "The Selection, Use, Calibration, and Quality Assurance of Radionuclide Calibrators Used in Nuclear Medicine" American Association of Physicists in Medicine, Report of Task Group 181, June 2012

[5] Gadd R, et al. ”UK Measurement Good Practice Guide 93: Protocol for establishing and maintaining the calibration of medical radionuclide calibrators and their quality control" Middlesex, UK, National Physics Laboratory (2006), ISSN: 1368-6550)

[6] "IAEA Technical Report Series No. 454, Quality Assurance for Radioactivity Measurement in Nuclear Medicine", published by the International Atomic Energy Agency (IAEA) in 2006 (ISBN: 92–0–105306–1)

[7] American National Standards Institute (ANSI), "Calibration and usage of dose calibrator ionization chambers for the assay of radionuclides." ANSI N42.13-2004

[8] National Physical Laboratory Report DQL-Rn 003, "A review of Commercial Radionuclide Calibrators" by M. Baker et al., July 2005

[9] Zimmerman BE et al.: "Experimental determinations of commercial `dose calibrator' settings for nuclides used in nuclear medicine", Applied Radiation and Isotopes 52, 615-19, 2018

[10] Zimmermann BE et al. "Multicenter comparison of dose calibrator accuracy for PET imaging using a standardized source", Journal of Nuclear Med., 50(S2), 472, 2009

[11] Beattie BJ et al. " A Recommendation for Revised Dose Calibrator Measurement Procedures for Zr-89 and I-124", Plos One, 9(9), 1-8 (2014)

[12] Wooten AL et al. " Calibration setting numbers for dose calibrators for the PET isotopes Mn-52, Cu-64, Br-76, Y-86, Zr-89, I-124", Applied Radiation and Isotopes 113, 89–95, 2016

[13] Bailey DL et al. "Accuracy of Dose Calibrators for G-68 PET Imaging: Unexpected Findings in a Multicenter Clinical Pretrial Assessment", Journal of Nuclear Med. 59(4), 636-38, 2018

[14] Allberg K, “Simulated dose calibrator source standard for positron emission tomography radionuclides,” U.S. patent US7825372B2 (9 March 2009)

[15] Zimmerman BE et al. "Development of a Traceable Calibration Methodology for Solid 68 Ge/ 68 Ga Sources Used as a Calibration Surrogate for F-18 in Radionuclide Activity Calibrators", Journal of Nuclear Med. 51(3), 448-53, 2018

[16] Oropesa P et al. "Radionuclide Calibrator Comparisons and Quality Improvement in Nuclear Medicine", Applied Radiation and Isotopes (66) 3, 2008, 353-361. An overview is provided on DC calibration initiatives undertaken for various isotopes in different countries.

[17] Galea R et al. “Renewing the radiopharmaceutical accuracy check service for Canadian radionuclide calibrators”, Applied Radiation and Isotopes 109 (2016) 254–256

[18] Santry D “The Canadian Experience on Performing Accuracy Checks on Administered Doses of Radiopharmaceuticals”, Applied Radiation and Isotopes (49), 9-11, 1998, 1453-58
[19] Oliveira PA et al. "Innovative methodology for intercomparison of radionuclide calibrators using short half-life in situ prepared radioactive sources", Medical Physics 41 (7), 2015, 072507-1 - 8. An approach to cross-calibration using Gafchromic film.
[20] Jans H-S, "Activity cross-calibration of unsealed radionuclides utilizing a portable ion chamber", Medical Physics, 43(12): 6536-43, 2016
[21] Keyvanloo A et al., "Technical Note: Minimizing geometrical uncertainties of cylindrical well-type ionization chamber measurements: There is an optimal chamber length", Medical Physics, 45(8): 3962-68, 2018
[22] Bergeron DE et al. "A Review of NIST Primary Activity Standards for F-18: 1982 to 2013", Journal of Research of the National Institute of Standards and Technology 119, 371-96, 2014

Updates in Reference Dosimetry

The Contribution of the RTNORM EU Consortium to the Update of the $k_{Q,Q0}$ Factors for the International Dosimetry Code of Practice IAEA TRS 398

M. Pinto[a]
C. E. Andersen[b], F. Delaunay[c], L. De Prez[d], M. Donois[c], S. Duane[e], C. Gomà[f], A. Kosunen[g], J. Ojala[g], M. Pimpinella[a], J. Plagnard[c], B. Rapp[c], T. Siiskonen[g], L. Sommier[c], P. Teles[h], J. Tikkanen[g], K. Zink[i]

[a]ENEA-INMRI, National Institute for Ionizing Radiation Metrology, Santa Maria di Galeria Roma, Italy
[b]DTU Danish Technical University, Roskilde, Denmark
[c]CEA-LIST, LNE-LNHB, Gif-Sur-Yvette, France
[d]VSL, Delft, The Netherlands
[e]NPL National Physical Laboratory, Teddington, United Kingdom
[f]KU Leuven, Department of Oncology, Laboratory of Experimental Radiotherapy, Leuven, Belgium[1]
[g]STUK, Helsinki, Finland
[h]IST-ID, Instituto Tecnológico e Nuclear, Lisboa, Portugal
[i]Technische Hochschule Mittelhessen, Institute of Medical Physics, Giessen, Germany

Email address of Corresponding Author: massimo.pinto@enea.it

BACKGROUND

The International Atomic Energy Agency (IAEA) issued the TRS-398 radiation dosimetry Code of Practice (CoP) in 2000, [1], which is the *de facto* norm for radiotherapy dosimetry and is used on a worldwide basis. One of the essential contributions of the TRS 398 CoP is the ability to correct a radiation dosimeter response for differences between beam qualities, which relate to the energy distribution of the radiation fields, at the calibration laboratory (Q_0) and the beam qualities at the hospitals (Q). These corrections are called *beam quality correction factors* and are known as $k_{Q,Q0}$ (or k_Q, for short, when the Q_0 quality is that of radiation emitted from ^{60}Co sources). The datasets of the TRS 398 were prepared in the mid-1990s and include values of k_Q factors that were calculated for clinical radiotherapy beams over the entire range of beam modalities that were available at that time. Many technological advances have resulted since the first publication of the TRS 398: new models of ionization chambers, new radiation beam modalities (*e.g.* flattening filter free beams) and new recommendations [2] have emerged. Accordingly, the IAEA has recently issued two calls for new k_Q datasets, a first call aimed at experimental determinations, and a second call for Monte Carlo-calculated k_Q factors.

The European-Funded Joint Research Project "RTNORM" (funded from May 2017 until October 2019) is contributing towards the update of the TRS 398 by carrying out a series of concerted *measurements* and *calculations* of k_Q factors for numerous types of ionization chamber and a series of beam modalities, covering kV x-rays, MV photon beams including flattening filter-free (FFF) modalities, and scanned proton beams. One peculiar aspect of the RTNORM consortium is that both the experimentally determined k_Q factors and the Monte Carlo calculated k_Q factors are first validated within the consortium, by internal comparisons of datasets generated using a variety of Monte Carlo codes (EGSnrc, PENELOPE, PENH, Fluka) or by experimental comparisons based on measurements traceable to several different primary standards of air kerma and absorbed dose to water. A second round of data comparison across the two methods (experiments, Monte Carlo models) secures a stronger confidence in the

[1] From April 1, 2019, at IDIBAPS, Barcelona, Spain

datasets and in the estimated uncertainties, prior to final submission of the data to the IAEA for potential inclusion in the update of the TRS-398.

METHODS

kV x-rays

Until recently, dosimetry in radiotherapy treatments using kV x-ray beams was largely based on primary standards for air kerma. Codes of practice include conversion procedures from kerma-based calibrations, N_K, to absorbed dose to water, D_w, calibrations. This introduces additional uncertainties and leads to potential errors. In the field of kV x-rays dosimetry, RTNORM aims to realize a supporting framework based on the direct use of the quantity of interest, D_w, by means of $k_{Q,Q0}$ values. Experimental estimates of p_Q and $k_{Q,Q0}$ factors were obtained for a total of 24 ionization chambers of three different types (13 × NE2571, 7 × PTW 30013 and 4 × IBA FC 65-G) and in six filtered kV x-ray qualities, with all measurements traceable to several EU National standards of both air kerma and absorbed dose to water. In parallel, Monte Carlo-based estimates were pursued by running simulations with the well-established codes PENELOPE and EGSnrc.

MV photon beams

Dosimetry in radiotherapy treatment using high-energy photons is an area of metrology which is already underpinned by the availability of primary standards for absorbed dose to water. For MV photon beam dosimetry, RTNORM aims to deliver new absolute dosimetry measurements and to support Monte Carlo simulations for these very new beam modalities, using a range of calorimetric standards, and new datasets of k_Q values which expands beyond the current datasets. Experimental estimates of k_Q factors were obtained for different types of ionization chambers (Exradin A1SL, IBA CC13, IBA FC65-G, IBA FC65-P, NE 2571, PTW 30013, PTW 31010, PTW 31013 and PTW 31021) in beams with and without flattening filters, and Monte Carlo-based estimates of k_Q factors were obtained using the Monte Carlo code EGSnrc. Recommendations from the recently published ICRU n 90 report [2] were included in both cases.

Scanned proton beams

The use of scanned proton beams has emerged over the past several years and this is an area where the TRS-398 could benefit from significant updates. In RTNORM, experimental determinations of k_Q factors are sought using graphite calorimetry from the NPL. The Monte Carlo codes used in RTNORM for proton transport are PENH [3], Geant4/TOPAS, and FLUKA.

RESULTS

kV x-rays

Measurement results of the NE2571 ionisation chambers by LNE are illustrated in Figure 1, supporting the current dosimetric formalism where a calibration coefficient expressed in terms of the quantity air kerma (N_k) is converted to a calibration coefficient in terms of D_w upon application of an overall, chamber model-dependent, p_Q factor. Analyses of measurements on PTW 30013 and IBA FC65-G, as well as NE2571 chambers by ENEA-INMRI and VSL are in progress. Results of some Monte-Carlo calculations are also shown in figure 1 where the Q_0 quality was set to the CCRI-250 (based on EGSnrc, by ENEA-INMRI). Once all results have been finalised, datasets of measured calibration coefficients and Monte Carlo calculations will

be cross-compared and both the conversion of ionisation chamber N_K to N_{Dw} (supporting the current formalism) and the $k_{Q,Q0}$ factors (to support the future formalism) will be validated based upon these results.

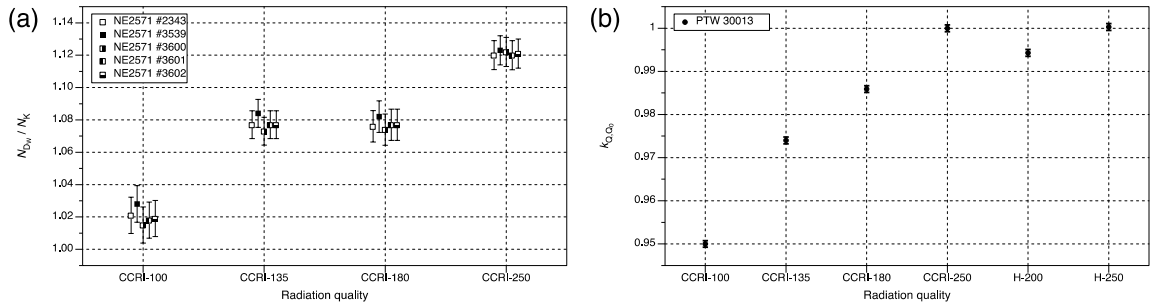

*Figure 1. **a**: experimental results of p_Q factors (convolved with (□□□) water to air ratios that were averaged over the x-rays photon spectra) for five ionization chamber model NE2571 in four radiation qualities (data provided by CEA-LIST LNE-LNHB, stated uncertainties indicate a coverage factor of 1). **b**: Monte Carlo calculations of $k_{Q,Q0}$ factors for the ionization chamber PTW 30013 in six radiation qualities (data provided by ENEA-INMRI and based on the code EGSnrc, uncertainties are type A only). Radiation qualities shown include four from the CCRI series [4] (a, b) and two qualities from the ISO 4037-1 norm (b).*

MV photon beams

Complex geometrical models of the ionization chambers have been developed based on detailed information from industry. $k_{Q,Q0}$ factors have been calculated for 9 different types of ionization chambers (Exradin A1SL, IBA CC13, IBA FC65-G, IBA FC65-P, NE 2571, PTW 30013, PTW 31010, PTW 31013 and PTW 31021) in beams with and without flattening filters using the Monte Carlo code EGSnrc and applying recommendations from the recently published ICRU n° 90 report. Calculations for ionization chambers where simulations were performed by several partners (3 types by two and 1 type by three) show good agreement with a maximum deviation in the results of 0.3 %. The volume-averaging corrections must be taken into account if the corrections are different between the water volume that was defined to calculate the absorbed dose to water and the cavity volume of the ionization chamber defined to calculate the absorbed dose to air (strong beam anisotropies or large difference between the ionization chamber cavity volume and the water volume). Figure 2 shows the overall results from the RTNORM consortium for the NE2571 chamber, including both experimental and Monte Carlo determinations, compared to the current dataset as published on the TRS-398.

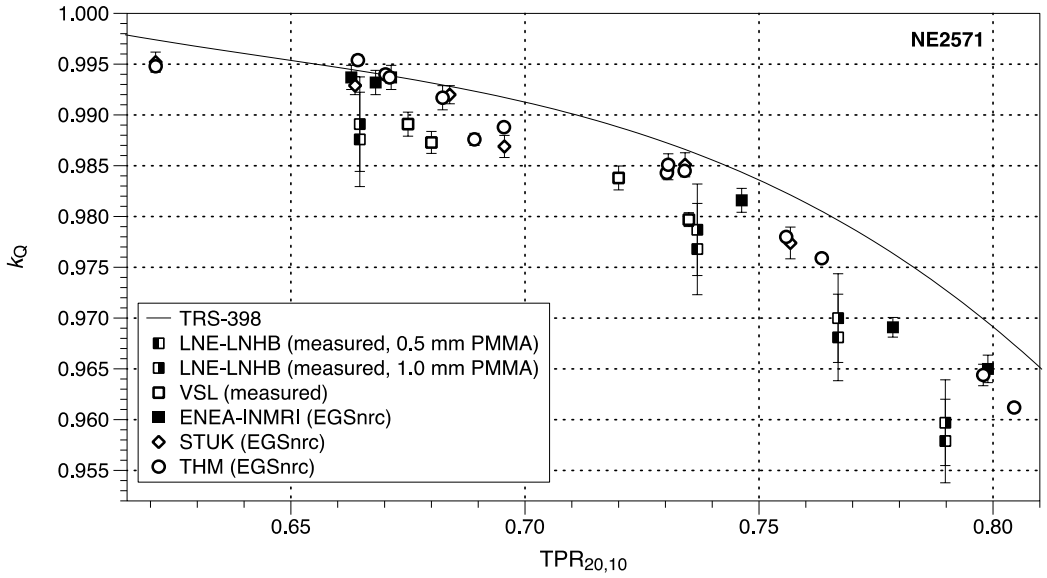

Figure 2. Experimental and Monte Carlo results of k_Q factors for the NE2571 ionization chamber. Uncertainties indicate a coverage factor of 1.

Scanned proton beams

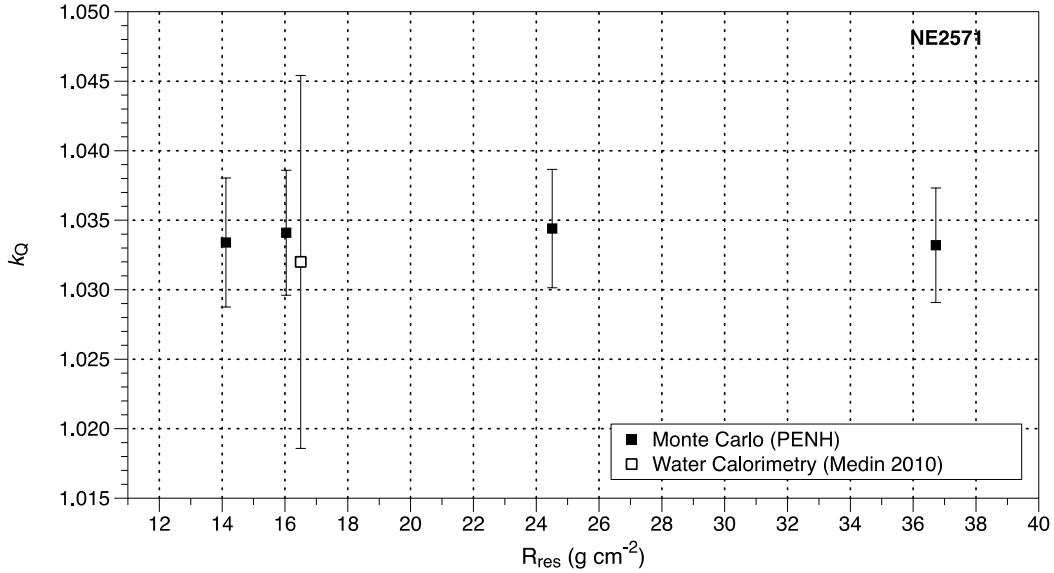

Figure 3. Results of k_Q factors for the NE2571 ionization chamber using the PENH Monte Carlo code [3]. Uncertainties indicate a coverage factor of 1. Also shown are the measurements using a water calorimeter adapted from [5].

CONCLUSIONS

The RTNORM collaboration has completed several planned tasks to date, by estimating $k_{Q,Q0}$ datasets through the use of both experimental and calculation methods for kV x-rays, MV photons including flattening filter-free beams, and scanned proton beams. Until October 2019, datasets will be expanded and compared across the two methods. In MV photon dosimetry, the maximum deviation of the results is 0.3%. Results from RTNORM may also help

understanding whether a k_Q-based formalism, accepted for most radiation modalities, could be considered reliable also in the field of kV x-rays dosimetry.

REFERENCES

[1] P. ANDREO, D. T. BURNS, K. HOHLFELD, M. HUQ, T. KANAI, R. F. LAITANO, V. SMYTH, AND S. VYNCKIER, Absorbed Dose Determination in External Beam Radiotherapy, an International Code of Practice for Dosimetry Based on Standards of Absorbed Dose to Water (International Atomic Energy Agency, Vienna, 2000), pp. 242.

[2] ICRU, ICRU Report No. 90: Key Data for Ionizing-Radiation Dosimetry: Measurement Standards and Applications (2016), pp. 1–118.

[3] F. SALVAT, A generic algorithm for Monte Carlo simulation of proton transport, Nuclear Instruments and Methods in Physics Research Section B: Beam Interactions with Materials and Atoms **316**, 144 (2013).

[4] CCEMRI(I), Qualités de Rayonnement, bipm.org, R15 (1972).

[5] J. MEDIN, Implementation of water calorimetry in a 180 MeV scanned pulsed proton beam including an experimental determination of k_Q for a Farmer chamber, Phys Med Biol **55**, 3287 (2010)

Monte Carlo Determination of Chamber Correction Factors for Medium Energy X-ray Beams Between 50 and 300 kV

J. Bancheri[a]
S. Ketelhut[b], **L. Büermann**[b], **J. Seuntjens**[a]

[a]McGill University, Medical Physics Unit, Cedars Cancer Centre, Montréal, QC, Canada
[b]Physikalisch-Technische Bundesanstalt (PTB), Bundesallee 100, Braunschweig, Germany

Email address of Corresponding Author(s): julien.bancheri@mail.mcgill.ca

BACKGROUND

Medium energy X-ray beams can be calibrated by determining the absorbed dose to water at a depth of 2 cm in a water phantom, $D_{w,z=2cm}$. With a corrected ionization chamber reading at the same point in water, M_w, and the chamber's air kerma calibration coefficient, $N_{K,a}$, $D_{w,z=2cm}$ can be determined according to the following equation [1]:

$$D_{w,z=2cm} = M_w N_{K,a} \left[\left(\frac{\mu'_{en}}{\rho}\right)_{w,a}\right]_{water} k_{ch} k_{sheath} \,. \quad (1)$$

In equation 1, $\left[(\mu'_{en}/\rho)_{w,a}\right]_{water}$ is the water to air mean mass-energy absorption coefficient ratio at a depth of 2 cm in water. The overall chamber correction factor, k_{ch}, accounts for the changes in chamber response due to the displacement of water by the chamber cavity, the presence of the stem and the change in incident photon energy and angular distribution in the phantom to that in air. The effects of a waterproof sheath (if required) are accounted for in k_{sheath}. For waterproof chambers, k_{sheath} is unity. By rearranging, the terms in equation 1, the product $k_{ch} \cdot k_{sheath}$ can be calculated by:

$$k_{ch} k_{sheath} = \left(\frac{D_{w,z=2cm}}{K_a}\right)\left(\frac{M_a}{M_w}\right) \Big/ \left[\left(\frac{\mu'_{en}}{\rho}\right)_{w,a}\right]_{water} . \quad (2)$$

In equation 2, $N_{K,a}$ has been written as the ratio of air kerma in air, K_a, to chamber air cavity reading in air, M_a (at the same point free in air).

In this work, in the context of a current effort to update the TRS-398 protocol, chamber correction factors are determined through Monte Carlo simulations. They are compared to experimental values obtained at PTB with their recently-developed water calorimetry-based absorbed dose to water primary standard [2].

METHODS

Simulations were carried out with EGSnrc [3]. Experimentally measured photon spectra with generating voltages between 50 and 300 kV were provided by PTB [2]. In the simulations, the photon source was modelled as a collimated point source 100 cm away from the point of measurement (at 2 cm depth for the in-phantom calculation) with a diameter of 10 cm. Photon fluence spectra at the point of measurement in a 30x30x30 cm^3 water phantom were generated using FLURZnrc. These spectra were used to calculate the water to air mean mass-energy absorption coefficient ratios. The user code egs_chamber was used to calculate $D_{w,z=2cm}$ and K_a. The same geometry setup was used as that above. For the dose to water simulations, the parameters ECUT and PCUT were set to 0.512 MeV and 0.001 MeV, respectively. For the air kerma simulations, ECUT was set to a large number so that electron transport was turned off. Thus, dose is equivalent to kerma (electronic kerma is equal to kerma due to small values of g). Chamber simulations were carried out for the PTW 30013, NE2571, A12, IBA FC65-G, IBA FC65-P and Exradin A12 chambers. All chamber models (except the NE2571) were based

on drawings provided from the respective manufacturers. For the in-phantom simulations, the midplane of the chambers was placed at 2 cm depth. One note of importance is that renormalized photoelectric cross sections were used for all simulations. The decision to use these data was based on the release of ICRU 90 and the disagreement between recent experiment and un-renormalized cross sections [4].

RESULTS

The simulated chamber correction factors for all chambers were within 2 % of unity. The magnitude increases with energy up to a certain point (between 120 - 150 KV) and then decreases. Figure 1 presents the simulated and measured chamber correction factors for the IBA FC65-G and FC65-P chambers.

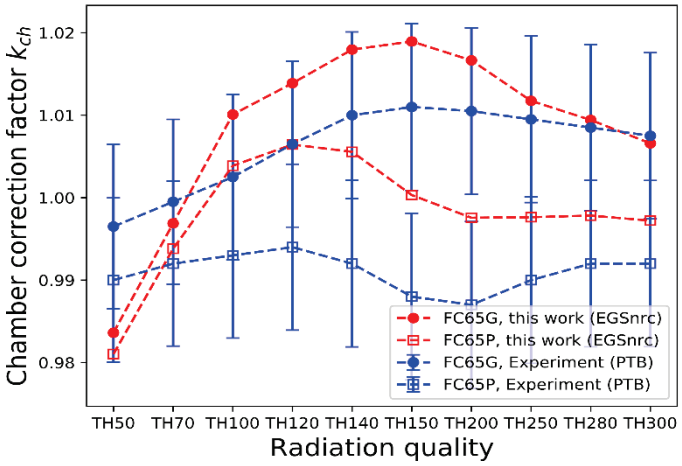

Figure 1. Chamber correction factors for the FC65G and FC65P chambers. Uncertainty bars represent 1% relative uncertainty. Type A uncertainties are less than 0.1% for simulated values.

CONCLUSIONS

Chamber correction factors for medium energy X-ray beams were determined through Monte Carlo simulations. Simulated values agree with experimental values to within 0.1-1.5 % for all chambers. Despite this, there is a trend in the comparison of measured and calculated chamber correction factors that merits further investigation.

REFERENCES

[1] MA, C.M., COFFEY, C.W., DEWERD, L.A., LIU, C., NATH, R., SELTZER, S.M., SEUNTJENS, J.P., AAPM protocol for 40-300 kV x-ray beam dosimetry in radiotherapy and radiobiology, Medical Physics **28** (2001) 868.

[2] KRAUSS, A., BÜERMANN, L., KRAMER, H.M., SELBACH, H.J., Calorimetric determination of the absorbed dose to water for medium-energy x-rays with generating voltages from 70 to 280 kV, Physics in Medicine and Biology **57** (2012) 6245.

[3] KAWRAKOW, I., MAINEGRA-HING, E., ROGERS, D.W.O., TESSIER, F., WALTERS, B.R.B., The EGSnrc Code System: Monte Carlo simulation of electron and photon transport, Technical Report PIRS-701, National Research Council Canada (2017).

[4] INTERNATIONAL COMMISSION ON RADIATION UNITS & MEASUREMENTS, Key Data For Ionizing-Radiation Dosimetry: Measurement Standards And Applications, ICRU Report 90, Bethesda, Maryland (2016).

A Study on the Monte Carlo Calculation of Kilovoltage X-ray Beam Backscatter Factors

R. Hill[a,b]
P. Andreo[c]

[a]Chris O'Brien Lifehouse, 119 – 143 Missenden Road, Camperdown NSW 2050, Australia
[b]Institute of Medical Physics, School of Physics, The University of Sydney NSW 2006, Australia
[c]Department of Medical Radiation Physics and Nuclear Medicine, Karolinska University Hospital, SE-171 76 Stockholm, Sweden

Email address of Corresponding Author(s): robin.hill@lh.org.au

BACKGROUND

Backscatter factors in water (B_w) are important dosimetric quantities used in reference and relative dosimetry of kilovoltage (kV) radiotherapy x-ray beams [1]. B_w is defined as the ratio of water kerma on the beam central axis at a point at the surface of a water phantom to the water kerma at the same point free in air [1-3]. It is not straightforward to measure B_w and data are typically determined from Monte Carlo (MC) calculations [2-4]; these are found in dosimetry protocols for kilovoltage x-ray beams [5]. Published values may, however, be for x-ray beams quite different from the beams found in the clinic or laboratory. In addition, the publication of ICRU Report 90 providing updated physics data, which may impact the values of B_w, has been one rationale for a new database of B_w values calculated by Andreo [6] for an extensive number of x-ray beam spectra, field sizes and source-to-surface distances. In this work, independent calculations of B_w for a broad range of x-ray beam qualities and field sizes using Monte Carlo techniques has been made for clinical beams generated by Pantak SXT150 and DXT300 generators. The results have been compared with those from the new database of Andreo, based on the Penelope MC system [7].

METHODS

The DOSRZnrc user code of the EGSnrc Monte Carlo System V2018 (NRC, Canada) has been used for the calculations of B_w in this study. The water kerma was scored in a voxel of water 0.1 mm thick and 10.0 or 20.0 mm diameter located at the surface of a full-scatter water phantom and free-in-air. Relevant options in EGSnrc for low energy x-ray calculations were switched on and photon and electron energy cut-off parameters were PCUT = 0.001 MeV and ECUT = 0.561 MeV. Primary beam spectra were calculated using the SpekCalc program for x-ray beams with combinations of kVp/HVL ranging from 30 kVp/0.33 mm Al to 280 kVp/3.8 mm Cu [8]. The total number of incident photons for each Monte Carlo simulated was selected to provide a type-A uncertainty in the value of kerma of less than 0.2%. The field diameters ranged from 2 to 20 cm all with an SSD of 30 cm. The calculated B_w were compared with the values from Andreo interpolated according to the clinical kVp, HVL and beam diameter.

RESULTS

The set of Monte Carlo calculated B_w values for clinical beams are presented in figure 1a for each beam as a function of field size; uncertainty bars are smaller than the size of the symbols. The comparison with the values interpolated from the Andreo database for the x-ray beams generated by a Pantak DXT300 unit are illustrated in figure 1b, where agreement to better than about ±0.7% for all the beam energies and field sizes considered was found.

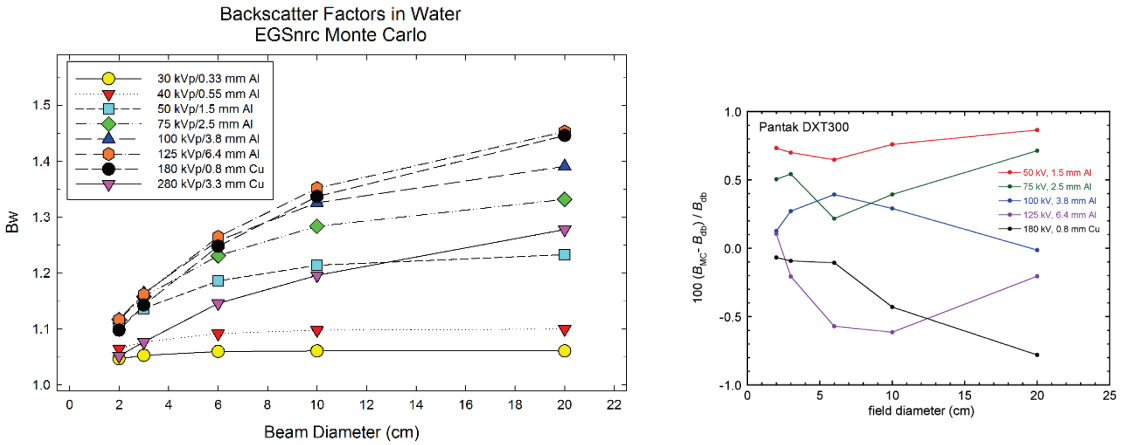

Figure 1. (a) Monte Carlo calculated values of backscatter factors for radiotherapy x-ray beams in the range 30 – 280 kVp. (b) Comparison of the MC results (B_{MC}) with those from the database of Andreo (B_{db}) for the beams from a Pantak DXT300 unit.

CONCLUSIONS

Monte Carlo calculations, using EGSnrc of B_w for dosimetry of radiotherapy kV x-ray beams have been performed for a broad range of clinical beam qualities and the results compared with a newly released database calculated with the Penelope MC system. Their agreement within better than about 1%, despite being based on different MC systems and methods, confirms the accuracy of both sets of values and provides a mutual quality assurance of the calculations.

REFERENCES

[1] HILL, R., et al., *Advances in kilovoltage x-ray beam dosimetry.* Physics in medicine and biology, 2014. **59**(6): p. R183.

[2] GROSSWENDT, B., *Backscatter factors for x-rays generated at voltages between 10 and 100 kV.* Physics in Medicine and Biology, 1984. **29**(5): p. 579-591.

[3] MA, C.M., SEUNTJENS J.P., *Mass-energy absorption coefficient and backscatter factor ratios for kilovoltage x-ray beams.* Physics in Medicine and Biology, 1999. **44**(1): p. 131-143.

[4] HEWSON, E., BUTSON M., and R. HILL, *Evaluating TOPAS for the calculation of backscatter factors for low energy x-ray beams.* Physics in Medicine & Biology, 2018. **63**(19): p. 195014.

[5] MA, C.M., et al., *AAPM protocol for 40-300 kV x-ray beam dosimetry in radiotherapy and radiobiology.* Medical Physics, 2001. **28**(6): p. 868-93.

[6] ANDREO, P., *Data for the dosimetry of low- and medium-energy kV x rays*. 2018, Karolinska University Hospital.

[7] SALVAT, F., FERNÁNDEZ-VAREA J., SEMPAU J., *PENELOPE—A code system for Monte Carlo simulation of electron and photon transport (Issy-les-Moulineaux: OECD Nuclear Energy Agency).* 2014.

[8] POLUDNIOWSKI, G., et al., *SpekCalc: a program to calculate photon spectra from tungsten anode x-ray tubes.* Physics in Medicine & Biology, 2009. **54**(19): p. N433.

Measurement of Chamber Correction Factors k_{ch} for Medium-Energy Therapeutic X-rays Between 70 kV and 300 kV Generating Voltage

S. Ketelhut[a]
L. Büermann[a], **J. Bancheri**[b], **J. Seuntjens**[b]

[a]Physikalisch-Technische Bundesanstalt (PTB), Bundesallee 100, Braunschweig, Germany
[b]McGill University, 845 Sherbrooke Street West, Montréal, Québec, Canada

Email address of Corresponding Author: steffen.ketelhut@ptb.de

BACKGROUND

Current medium-energy X-ray dosimetry protocols present a way to determine the calibration factor for absorbed dose to water N_{Dw} for suitable ionization chambers from the calibration factor for air kerma N_{Ka} [1,2]:

$$N_{D_w} = N_{K_a} \cdot \left(\frac{\bar{\mu}_{en}}{\rho}\right)^{d}_{w,a} \cdot k_{ch} \cdot k_{sheath}. \quad (1)$$

Here, $(\bar{\mu}_{en}/\rho)^{d}_{w,a}$ is the ratio of water to air for the mean mass-energy absorption coefficients, at a depth d in water. The chamber correction factor k_{ch} accounts for the change in the chamber response due to the displacement of water by the ionization chamber and its stem, and the change in energy and angular distribution of the incident photon fluence in water as compared to air. k_{sheath} is a correction factor for the effects of the waterproofing sheath used in the water phantom. For waterproof chambers, $k_{sheath} = 1$, and thus the chamber correction factor can be calculated as follows:

$$k_{ch} = \left(\frac{N_{D_w}}{N_{K_a}}\right) \Big/ \left(\frac{\bar{\mu}_{en}}{\rho}\right)^{d}_{w,a}. \quad (2)$$

Up to now, k_{ch} has been known with relative standard uncertainties between 1.5 % and 3.0 %. The purpose of this work was to measure k_{ch} for waterproof chambers according to Equation (2) with significantly lower uncertainties.

METHODS

At the Physikalisch-Technische Bundesanstalt (PTB), a primary air-kerma standard based on a free-air chamber and a primary absorbed-dose-to-water standard based on water calorimetry are maintained [3]. In this work, Farmer-type chambers of the type IBA FC65-G, IBA FC65-P, PTW TM30013, NE2571, and Exradin A12 were calibrated in terms of N_{Ka} and N_{Dw} against these primary standards at the same X-ray facility for the radiation qualities TH70 to TH300 generated with tube voltages between 70 kV and 300 kV. Ratios of $(\bar{\mu}_{en}/\rho)^{2cm}_{w,a}$ were calculated based on measured photon fluence spectra free-in-air and calculated spectra at a 2 cm depth in a water phantom. The calibration coefficients N_{Dw} were determined with relative uncertainties ranging from 0.46 % (for TH300) to 0.99 % (for TH70), and the calibration coefficients N_{Ka} were determined with a relative uncertainty of 0.26 %. The ratio of the mass-energy absorption coefficients at a water depth of $d = 2$ cm, $(\bar{\mu}_{en}/\rho)^{2cm}_{w,a}$, was calculated with an uncertainty of 0.3 %, giving a combined standard uncertainty of $u(k_{ch})$ between 0.6 % for TH300 and 1.0 % for TH70. The results are compared to Monte-Carlo simulations.

RESULTS

The correction factors k_{ch} are close to unity within about 1.5 % for all chambers despite significant variations of the N_{Ka}. For example, the calibration coefficient of the FC65G (with graphite walls) rises by more than 5 % from TH300 to TH70, and the calibration coefficient of the FC65P (with Delrin[2] walls) decreases by 10 % in the same range (see Figure 1). In comparison, k_{ch} deviates only by up to approximately 1 % from unity.

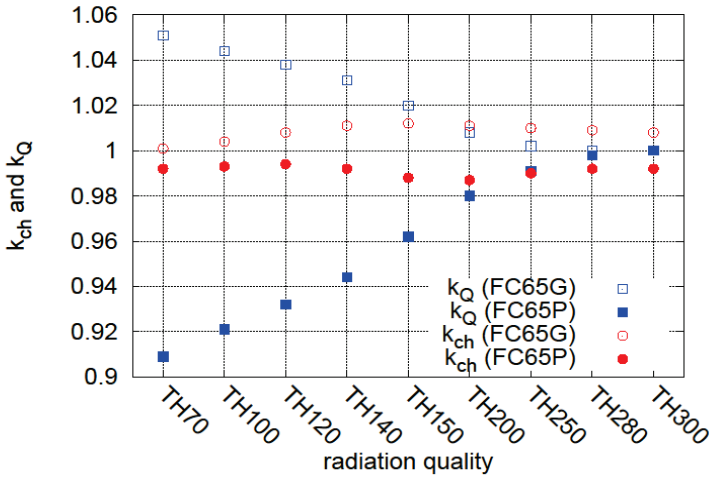

Figure 1. Chamber correction factor k_{ch} and radiation quality correction factor k_Q with respect to TH300 for the ionization chambers FC65G and FC65P.

CONCLUSIONS

In conclusion, k_{ch} is determined with relative standard uncertainties of less than 1 % for selected Farmer-type chambers. This is a robust correction which varies only slightly between chamber types although these reflect significant differences in their air-kerma response as a function of the radiation quality. These results will have an impact on the update of the international dosimetry protocol IAEA TRS 398 [4].

REFERENCES

[1] INTERNATIONAL ATOMIC ENERGY AGENCY, Absorbed Dose Determination in Photon and Electron Beams, Technical Reports Series (TRS) No. 277, Vienna (1997).

[2] MA, C.-M., COFFEY, C.W., DEWERD, L.A., LIU, C., NATH, R., SELTZER, S.M., SEUNTJENS, J.P., AAPM protocol for 40-300 kV x-ray beam dosimetry in radiotherapy and radiobiology, Medical Physics 28 (2001) 868.

[3] KRAUSS, A., BÜERMANN, L., KRAMER, H.-M., SELBACH, H.J., Calorimetric determination of the absorbed dose to water for medium-energy x-rays with generating voltages from 70 to 280 kV, Physics in Medicine and Biology 57 (2012) 6245.

[4] INTERNATIONAL ATOMIC ENERGY AGENCY, Absorbed Dose Determination in External Beam Radiotherapy, Technical Reports Series (TRS) No. 398, Vienna (2000).

[2] Delrin is the trade name of a type of polyoxymethylene (POM) = (CH_2O).

Phantom-Based Absorbed Dose Determination in Low Energy kV X Ray Beams

L. Büermann[a]

[a]Physikalisch-Technische Bundesanstalt, Bundesallee 100, 38116 Braunschweig, Germany

Email address of Corresponding Author: ludwig.bueermann@ptb.de

BACKGROUND

The Physikalisch-Technische Bundesanstalt (PTB) provides calibrations of plane-parallel ionization chambers mounted on the surface of a rectangular PMMA phantom (13 cm x 13 cm x 8 cm) in terms of absorbed dose to water at the surface of a water phantom (zero depth) in low energy kV X ray beams for the radiation qualities TW10 – TW100 (10 kV – 100 kV). Calibration results refer to reference conditions Q_0, d_0, a_0 (see below). To explain how the absorbed dose is obtained under non-reference conditions, the following symbols are needed:

Q, Q_0 radiation quality, reference TW 30

a, a_0 distance from the source to the chamber reference point, reference 30 cm

d, d_0 diameter of the circular beam at the surface of the phantom, reference 3 cm

M_P chamber reading when positioned at the surface of the phantom

k_Q correction for differences in the radiation quality with respect to the reference Q_0

k_g correction for differences in distance and beam diameter with respect to the reference.

The absorbed dose under non-reference conditions, $D_w(Q, d, a)$ is obtained according to

$$D_w(Q, d, a) = N_{D,w}(Q_0, d_0, a_0) M_P(Q, d, a)\, k_Q(Q, Q_0, d_0, a_0)\, k_g(Q, d, a) \qquad (1)$$

where $N_{D,w}$ is the absorbed dose calibration factor. The correction k_Q can be interpolated from values given in the certificate for TW10 to TW100. The correction k_g is given as

$$k_g(Q, d, a) = \frac{N_{K,P}(Q,d,a)}{N_{K,P}(Q,d_0,a_0)} \frac{B_W(Q,d,a)}{B_W(Q,d_0,a_0)} \qquad (2)$$

where $N_{K,P}$ is the air kerma calibration factor of the chamber when positioned in the PMMA phantom and B_W is the water-kerma-based backscatter factor. k_g is chamber-specific and was last determined at PTB about 30 years ago for the chamber types PTW M23342, M23344 and Capintec PS033, as published in [1]. The purpose of this work was to redetermine the corrections k_g for the most frequently used chamber types M23342 and M23344. The reasons for the redetermination were: (a) to see whether anything has changed with the chambers since 1989 and (b) to extend the data base of k_g to a more comprehensive data set.

METHODS

The ratios $\frac{B_W(Q,d,a)}{B_W(Q,d_0,a_0)}$ were obtained from calculations of Grosswendt [2]. $\frac{N_{K,P}(Q,d,a)}{N_{K,P}(Q,d_0,a_0)}$ were obtained from measurements at the PTB calibration facility. Three chambers of the type M23342 (SN 592, 2565, 2872) and two chambers of the type M23344 (SN 1058, 1059) were

examined. Measurements were done for the qualities ranging from TW10 to TW100 (8 qualities, see Table 1) at field diameters of 3 cm, 5 cm and 10 cm.

RESULTS

Geometry correction factors k_g obtained for the two examined chamber types are listed in Table 1. These values are mean values evaluated from the single results of the three M23342 chambers and the two M23344 chambers. The single results of each chamber type were consistent within 0.2 %. In general, the values listed in Table 1 agree with those published in [1] within the relative standard uncertainty of 1 %.

Table 1. Correction factors k_g for PTW M23342 and M23344 at the distance a=30 cm and beam diameters d=5 cm and 10 cm.

Radiation quality	Voltage (kV)	Filter (mm Al)	HVL (mm Al)	M23342		M23344	
				5 cm	10 cm	5 cm	10 cm
TW 10	10	-	0.030	1.00	1.00	1.00	1.00
TW 15	15	0.05	0.071	1.00	1.00	1.00	1.00
TW 20	20	0.15	0.113	1.00	1.00	1.00	0.99
TW 30	30	0.5	0.359	0.99	0.98	0.99	0.98
TW 40	40	0.8	0.741	0.98	0.97	0.98	0.96
TW 50	50	1.0	0.940	0.99	0.97	0.98	0.96
TW 70	70	4.0	2.94	0.97	0.93	0.96	0.92
TW100	100	4.5	4.41	0.97	0.94	0.96	0.93

CONCLUSIONS

The chamber-type-specific geometry correction factor k_g was redetermined for the plane-parallel chambers of the types PTW M23342 and PTW M23344 when used with the standard PMMA phantom. New values agreed with those published about 30 years ago within the relative standard uncertainty of 1 %. It can be concluded that the corrections k_g published in [1] can still be used. It is intended to extend the data set to more radiation qualities, distances and field diameters to provide a more comprehensive data set for users. These extended data sets will be suggested for adoption in the revised version of IAEA TRS 398 [3], the international dosimetry protocol.

REFERENCES

[1] ENGELKE, B.A., GROSSWENDT, B., Zur Bestimmung der Wasser-Energiedosis für Röntgenstrahlungen mit Erzeugerspannungen bis 100 kV, PTB-Mitteilungen 99, 3/89 (1989, in German only).

[2] GROSSWENDT, B., Dependence of the photon backscatter factor for water on source-to-phantom distance and irradiation field size, Phys. Med. Biol., Vol. 35, No. 9, 1233-1245 (1990).

[3] INTERNATIONAL ATOMIC ENERGY AGENCY, Absorbed Dose Determination in External Beam Radiotherapy, Technical Reports Series (TRS) No. 398, Vienna (2000).

The ARPANSA PSDL Measured and Calculated MV Photon k_Q Values for the Revision of IAEA TRS-398

C. Oliver
V. Takau, M. Hanlon, T. Bailey, J. Lye, D. Butler

The Australian Radiation Protection and Nuclear Safety Agency (ARPANSA), 619 Lower Plenty Road, Yallambie VIC 3085, Australia

Email address of Corresponding Author: chris.oliver@arpansa.gov.au

BACKGROUND

The ARPANSA Primary Standard Dosimetry Laboratory (PSDL) was invited by the IAEA to contribute to the update of IAEA TRS-398 for high energy photons. The ARPANSA PSDL has measured and calculated both experimental and Monte Carlo calculated k_Q factors.

METHODS

The ARPANSA PSDL has been measuring k_Q values of ionisation chambers since 2014 by measuring absorbed dose to water calibration factors in Co-60 gamma radiation, and 6X, 10X and 18X photon beams from an Elekta Synergy linear accelerator. These measurements are traceable to the graphite calorimeter which is the Australian primary standard for absorbed dose. k_Q have also been calculated with Monte Carlo simulations. The EGSnrc user code *egs_chamber* has been used to construct realistic models of a number of reference class ionisation chambers. Models of the Co-60 source and the linear accelerator photons beams were then used to calculate the doses to the sensitive volumes of the chambers and the dose to water to realise the theoretical k_Q value.

RESULTS

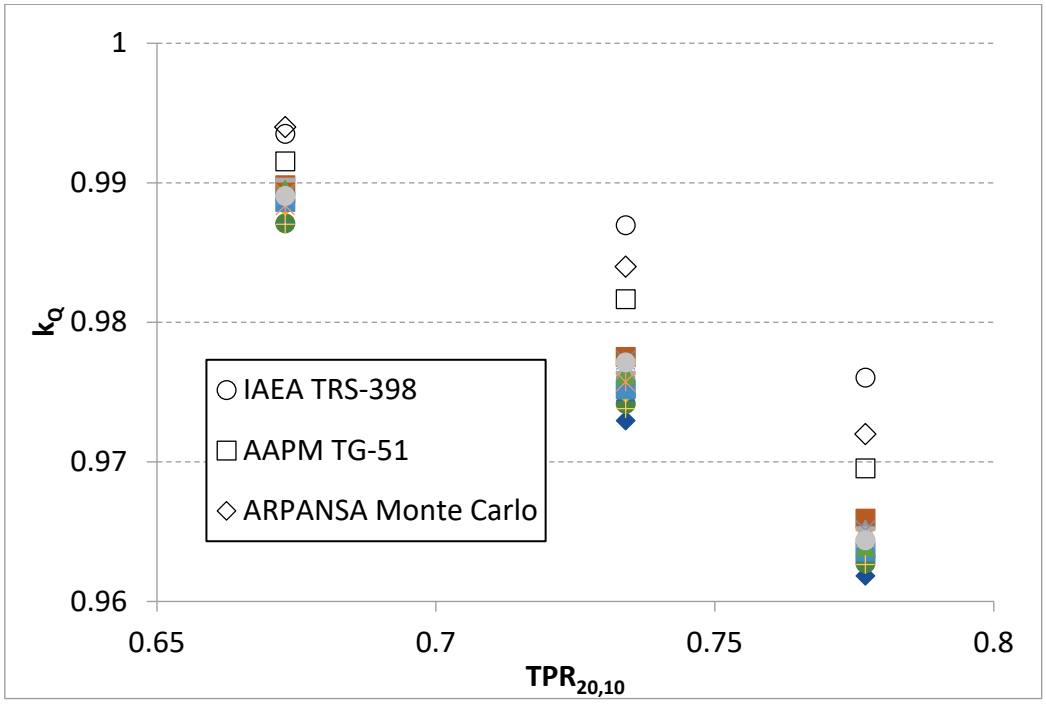

Figure 1. Experimental k_Q measured for twenty 2571 chambers (coloured) compared to two current protocols and Monte Carlo calculated values.

k_Q values have been measured for eight different types of ionisation chambers. The differences between IAEA TRS-398 k_Q values and those measured are shown in Figure 1 for the 2571 chamber along with comparison to those given in the updated AAPM TG-51 protocol.

Monte Carlo k_Q calculations for ten chamber types used for photon reference dosimetry have been determined with the 2571 chamber results shown in Figure 1. The differences between k_Q calculated using ICRU37 and ICRU90 data have been calculated to be approximately 0.2 % for all ten chamber types.

CONCLUSIONS

The ARPANSA PSDL has measured and calculated k_Q values for a range of reference ionisation chambers. These will contribute to the revision of the high-energy photon dosimetry update of IAEA TRS-398.

REFERENCES

[1] ANDREO, P. et. al., Absorbed dose determination in external beam radiotherapy: an international code of practice for dosimetry based on standards of absorbed dose to water. IAEA TRS-398 (2000).

[2] MCEWAN, M. et al., Addendum to the AAPM's TG-51 protocol for clinical reference dosimetry of high-energy photon beams, Medical Physics **41(4)** (2014) 041501-1-20.

Updating the TG-51 Protocol for Reference Dosimetry of High-Energy Electron Beams

B. Muir[a]
W. Culberson, S. Davis, G. Kim, S. Lee, J. Lowenstein, J. Renaud, A. Sarfehnia, J. Siebers, L. Tantot, N. Tolani

[a]National Research Council Canada, Ottawa, ON, Canada.

Email address of Corresponding Author: Bryan.Muir@nrc-cnrc.gc.ca

BACKGROUND

There is currently a major effort to revise protocols for calibration of external beams. The addendum to the AAPM TG-51 protocol for reference dosimetry of photon beams [1] was published in 2014. The joint AAPM/IAEA code of practice for dosimetry of small fields used in external radiation therapy [2] was published in 2017. The IAEA is updating the TRS-398 code of practice for absorbed dose determination for external beams and the AAPM working group on the review and extension of beam quality conversion factors (WGTG51) is working on an addendum to the TG-51 protocol for electron beam dosimetry.

METHODS

The focus of this work is on progress toward updating the TG-51 protocol for reference dosimetry of electron beams in terms of considerations for the ion chamber calibration beam quality and the selection of ion chamber type, shifts and corrections required for accurate reference dosimetry and new accurate data for electron beam quality conversion factors. A review of the literature is performed to compile a consistent set of data for accurate beam quality conversion factors and used to make recommendations to simplify and improve the accuracy of clinical electron beam dosimetry.

RESULTS

Three calibration routes produce satisfactory results for electron beam reference dosimetry. Reference-class cylindrical chambers calibrated in cobalt-60 can be used for calibration of all electron beams, even those with energy less than 6 MeV [3]. Variations of beam quality conversion factors for parallel-plate chambers are less dramatic than previously thought [4] so direct calibration of these chambers in cobalt-60 can be performed and a generic beam quality conversion factor can be used. Finally, cross-calibration of parallel-plate chambers against cylindrical reference chambers in a high-energy electron beam is still a viable option and this method will be more accurate with updated beam quality conversion factors described below.

The issue of the effective point of measurement and the treatment of gradient effects is revisited with data from the literature [5,6]. For depth-ionization measurements, optimal shifts, different from those recommended in current dosimetry protocols, are recommended for accurate R_{50} determination using both cylindrical and parallel-plate chambers. The same shift is recommended for point dose measurements for parallel-plate chambers as it allows more accurate determination of k_Q factors. For point dose measurements with cylindrical chambers, the point of measurement is taken as the center of the chamber cavity and the gradient correction is accounted for with Monte Carlo calculations of beam quality conversion factors, yielding acceptable results.

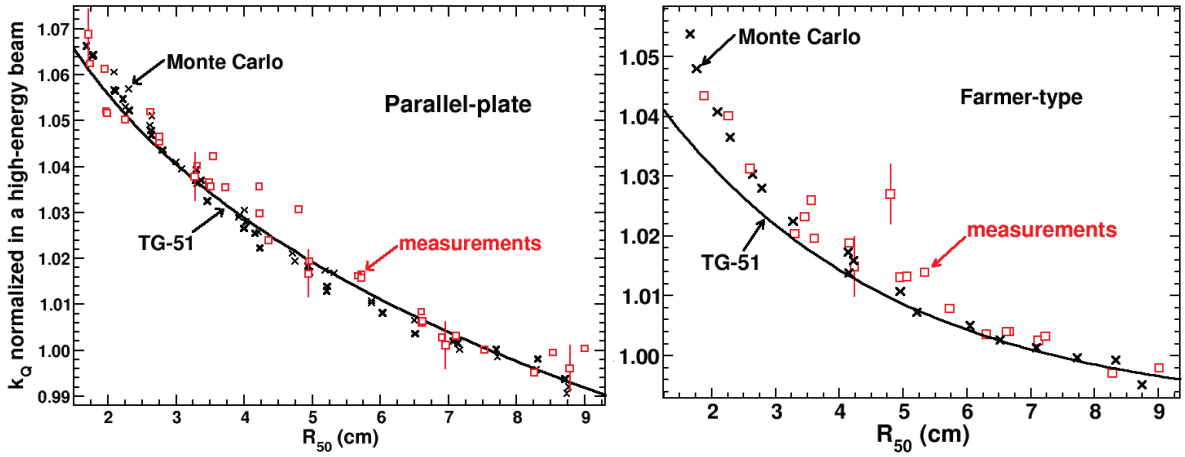

Figure 1. Normalized k_Q factors for parallel-plate (PTW Roos) and Farmer-type (NE2571 and Exradin A12) chambers. Error bars are shown for representative measurements.

Figure 1 shows beam quality conversion factors for commonly used ion chambers normalized in a high-energy beam with R_{50}=7.5 cm compiled from several publications (see [6] and references therein) that use Monte Carlo calculations or measurements performed at primary standards laboratories as well as those in the TG-51 protocol. For at least a few chamber types there are now several sources of high-quality data that provide a basis for updated beam quality conversion factors. Figure 1 shows variable agreement between TG-51 k_Q factors compared to high-quality compiled data depending on the chamber type with differences up to 2 % in low-energy beams, motivating the use of updated factors.

CONCLUSIONS

This work presents progress toward updating the TG-51 protocol for electron beam reference dosimetry to improve the accuracy of beam calibration by providing updated beam quality conversion factors and simplifying the calibration procedure (e.g., by removing the requirement for a measured gradient correction) with the goal of reducing errors in the clinic.

REFERENCES

[1] MCEWEN, M.R. ET AL., "Addendum to the AAPM's TG-51 protocol for clinical reference dosimetry of high-energy photon beams", Medical Physics **40** (2014) 041501.

[2] INTERNATIONAL ATOMIC ENERGY AGENCY, "Dosimetry of small static fields used in external beam radiotherapy", Technical Report Series no. 483, (2017).

[3] MUIR, B.R., MCEWEN, M.R., "Technical Note: On the use of cylindrical ionization chambers for electron beam reference dosimetry", Medical Physics **44** (2017) 6641.

[4] KAPSCH, R.P., GOMOLA, I., "Beam quality correction factors for plane parallel chambers in photon beams", Book of Extended Synopses for Symp. on Standards, Applications and Quality Assurance in Medical Radiation Dosimetry. IAEA; (2010) 35.

[5] MUIR, B.R., ROGERS, D.W.O., "Monte Carlo calculations for reference dosimetry of electron beams with the PTW Roos and NE2571 ion chambers", Medical Physics **39** (2013) 121722.

[6] MUIR, B.R., ROGERS, D.W.O., "Monte Carlo calculations of electron beam quality conversion factors for several ion chamber types", Medical Physics **40** (2014) 111701.

Dosimetry in Therapeutic Nuclear Medicine

Dosimetry for Radiopeptide Therapy

M. W. Konijnenberg

Dept. Radiology & Nuclear Medicine, Erasmus MC, Rotterdam, The Netherlands

Email address of Corresponding Author: m.konijnenberg@erasmusmc.nl

BACKGROUND

Dosimetry is an important asset in the therapy of neuro-endocrine tumours with radiolabelled peptides. Initially therapy was performed with ^{90}Y-DOTA-octreotide with good results [1, 2], but many cases of severe kidney damage have been observed due to the difficulty in performing accurate dosimetry for this pure β-emitter [3]. Therapy with ^{177}Lu-DOTA-octreotate does offer the possibility of performing dosimetry assessments by its emission of two γ-rays at 113 and 208 keV [4]. Nevertheless, this last product was granted worldwide market authorization on a fixed activity administration scheme after very successful grade 3 trials showing prolonged progression free and overall survival with good quality of life in comparison to conventional treatments [5, 6]. Peptide Receptor Radionuclide Therapy (PRRT) forms the second-line treatment for neuroendocrine tumours [7].

METHODS

Dose response curves have been found for the late (2-3 years after therapy) occurrence of kidney damage after therapy with ^{90}Y-DOTA-octreotate [2]. The dose limit depends strongly on the number of therapy cycles given and without additional risk factors for renal problems is set at 40 Gy Biologically Effective Dose (BED). The absorbed dose needed to reach reduction of tumour volume in PRRT with both ^{90}Y and ^{177}Lu is in the order of 200 Gy [8, 9]. PRRT with ^{177}Lu-DOTA-octreotate given in 4 cycles of 7.4 GBq lead to kidney absorbed doses in the range of 5-35 Gy (N=407) [10]. Despite this huge variation in absorbed dose additional cycles as salvage therapy does not lead to renal toxicity [11]. Hematologic toxicity is however observed after PRRT, 11% (sub-) acute toxicity and 4% late persistent toxicities [12, 13]. Disappointingly dosimetry does not form a predictive indicator for these events.

DISCUSSION

PRRT has been approved with a fixed dosing scheme and most centres follow this approach. Increasingly it is realized that PRRT should follow the regulations and procedures customary in other forms of radiotherapy; dosimetry guided treatment planning. Treating patients up to an absorbed dose to the kidneys of 23 Gy does not seem to lead to huge advantage in patient survival [14] in comparison to therapy without dosimetry [11]. Prospective clinical trials are ongoing to determine whether treatment to 40 Gy (BED) to the kidneys is more beneficial [15].

CONCLUSIONS

Despite the potential for performing dosimetry and the knowledge of dose response relations for PRRT dosimetry guidance is not fully exploited yet to design optimal treatments with possibly a shift from palliative care to complete cures.

REFERENCES

[1] JAMAR, F., et al., *86Y-DOTA0)-D-Phe1-Tyr3-octreotide (SMT487)--a phase 1 clinical study: pharmacokinetics, biodistribution and renal protective effect of different regimens of amino acid co-infusion.* Eur J Nucl Med Mol Imaging, 2003. 30(4): p. 510-8.

[2] WESSELS, B.W., et al., *MIRD pamphlet No. 20: the effect of model assumptions on kidney dosimetry and response--implications for radionuclide therapy.* J Nucl Med, 2008. 49(11): p. 1884-99.

[3] IMHOF, A., et al., *Response, survival, and long-term toxicity after therapy with the radiolabeled somatostatin analogue [90Y-DOTA]-TOC in metastasized neuroendocrine cancers.* J Clin Oncol, 2011. 29(17): p. 2416-23.

[4] LJUNGBERG, M., et al., *MIRD Pamphlet No. 26: Joint EANM/MIRD Guidelines for Quantitative 177Lu SPECT Applied for Dosimetry of Radiopharmaceutical Therapy.* J Nucl Med, 2016. 57(1): p. 151-62.

[5] STROSBERG, J., et al., *Health-Related Quality of Life in Patients With Progressive Midgut Neuroendocrine Tumors Treated With (177)Lu-Dotatate in the Phase III NETTER-1 Trial.* J Clin Oncol, 2018. 36(25): p. 2578-2584.

[6] STROSBERG, J., et al., *Phase 3 Trial of 177Lu-Dotatate for Midgut Neuroendocrine Tumors.* N Engl J Med, 2017. 376(2): p. 125-135.

[8] HICKS, R.J., et al., *ENETS Consensus Guidelines for the Standards of Care in Neuroendocrine Neoplasia: Peptide Receptor Radionuclide Therapy with Radiolabeled Somatostatin Analogues.* Neuroendocrinology, 2017. 105(3): p. 295-309.

[8] PAUWELS, S., et al., *Practical dosimetry of peptide receptor radionuclide therapy with (90)Y-labeled somatostatin analogs.* J Nucl Med, 2005. 46 Suppl 1: p. 92S-8S.

[9] ILAN, E., et al., *Dose response of pancreatic neuroendocrine tumors treated with peptide receptor radionuclide therapy using 177Lu-DOTATATE.* J Nucl Med, 2015. 56(2): p. 177-82.

[10] Bergsma, H., et al., *Nephrotoxicity after PRRT with (177)Lu-DOTA-octreotate.* Eur J Nucl Med Mol Imaging, 2016. 43(10): p. 1802-11.

[11] VAN DER ZWAN, W.A., et al., *Salvage peptide receptor radionuclide therapy with [(177)Lu-DOTA,Tyr(3)]octreotate in patients with bronchial and gastroenteropancreatic neuroendocrine tumours.* Eur J Nucl Med Mol Imaging, 2019. 46(3): p. 704-717.

[12] BERGSMA, H., et al., *Subacute haematotoxicity after PRRT with (177)Lu-DOTA-octreotate: prognostic factors, incidence and course.* Eur J Nucl Med Mol Imaging, 2016. 43(3): p. 453-63.

[13] BERGSMA, H., et al., *Persistent Hematologic Dysfunction after Peptide Receptor Radionuclide Therapy with (177)Lu-DOTATATE: Incidence, Course, and Predicting Factors in Patients with Gastroenteropancreatic Neuroendocrine Tumors.* J Nucl Med, 2018. 59(3): p. 452-458.

[14] GARSKE-ROMAN, U., et al., *Prospective observational study of (177)Lu-DOTA-octreotate therapy in 200 patients with advanced metastasized neuroendocrine tumours (NETs): feasibility and impact of a dosimetry-guided study protocol on outcome and toxicity.* Eur J Nucl Med Mol Imaging, 2018. 45(6): p. 970-988.

[15] SUNDLOV, A., et al., *Individualised (177)Lu-DOTATATE treatment of neuroendocrine tumours based on kidney dosimetry.* Eur J Nucl Med Mol Imaging, 2017. 44(9): p. 1480-1489.

Dosimetry in Radioembolization Therapy of Hepatic Malignancies: Value of Post-Therapy Imaging-Based Dose Estimates

Y. K. Dewaraja

Division of Nuclear Medicine, Department of Radiology, University of Michigan, Ann Arbor, MI 48109, USA

Email address of Corresponding Author: yuni@umich.edu

BACKGROUND

Radioembolization (RE) with Y-90 microspheres has gained acceptance as an alternative to chemoembolization for treatment of unresectable hepatocellular carcinoma and liver metastases [1]. For glass microspheres, the recommended administered activity is calculated to deliver 80 - 150 Gy to the treated lobe, while not exceeding 30 Gy to the lungs [2]. This calculation, which depends only on the treated liver mass and the lung shunt estimated from pre-treatment 99mTc-MAA imaging, assumes a uniform activity distribution in liver without differentiating absorbed doses (ADs) to lesions and parenchyma. Although the current approach to RE has led to high rates of tumor response with limited side effects, reported survival is in the range 8 - 30 months [1,3]. Thus, there is a strong incentive for employing dosimetry guided personalized therapy to achieve more durable responses. Ultimately, dosimetry guided treatment planning in RE requires robust relationships between the delivered dose metrics and pre-treatment prediction either by the traditional MAA study or recent [4] or future developments. However, post-therapy imaging also has value, potentially as an early predictor of toxicity and response and to plan subsequent REs or external beam radiation therapy (EBRT). Furthermore, direct estimates of the delivered dose metrics can be used to establish the dose – outcome models for predictive imaging-based treatment planning in the future. Because of the potential for different distributions of the MAA particles and the microspheres due to various factors, AD estimates from direct Y-90 imaging is expected to be more reliable for dose – outcome studies. The two options for post-therapy imaging in RE, Y-90 PET and bremsstrahlung SPECT, are both challenging, but PET offers higher spatial resolution and is generally considered to have higher quantitative accuracy especially if scatter correction is not available for SPECT. For glass microspheres, there have been a few recent reports on dose – response using Y-90 PET/CT-derived AD estimates [5-7].

METHODS

Time-of-flight Y-90 PET/CT was performed within a couple of hours of radioembolization in 24 patients (89 lesions) with primary (hepatocellular, cholangiocarcinoma) and metastatic (neuroendocrine, colon, pancreatic, rectal, melanoma, adrenal) liver lesions. Quantitative Y-90 imaging is challenging, hence clinically relevant phantom studies were first performed to determine optimal reconstruction parameters for the patient studies and to validate the quantification. Since the Y-90 PET image was available in units of Bq/mL, further calibration factors were not needed for quantification, but volume dependent recovery coefficients (RCs) were used for mean value partial volume correction. Voxel-level dosimetry was performed with the Dose Planning Method (DPM) Monte Carlo code [8] with the PET activity map coupled with the CT-derived density map as the input. The DPM dose-rate map was converted to an AD map accounting for physical decay. The voxel level BED was calculated using the reformulation of the linear quadratic model for Y-90 radioembolization therapy [9]. Lesions > 2 cc were outlined on baseline contrast enhanced CT or MRI by a radiologist and transformed to co-registered Y-90 PET/CT for dosimetry. Lesion specific shrinkage (percentage reduction

in largest diameter) at first follow-up was determined according to RECIST (available for all lesions) criteria that assesses physical size and mRECIST (available only for a subset) criteria that assesses the viable portions of the lesion. Lesions were also categorized as responding (CR, PR) and non-responding (PD, SD). For mRECIST response, logit regression tumor control probability (TCP) models were fit via maximum likelihood to relate lesion level binary response to the dose metrics. As an exploratory analysis, the non-tumoral liver absorbed dose – toxicity was also evaluated.

The Y-90 PET/CT based AD maps corresponding to some lesions showed necrotic regions that were under-dosed by the Y-90 therapy. These images were loaded on to an EBRT treatment planning system to explore the potential for boosting under-dosed areas with EBRT. Furthermore, for a subset of patients an exploratory analysis was performed to compare Y90 PET/CT based absorbed dose estimates with estimates from bremsstrahlung SPECT/CT that included previously developed [10] Monte Carlo based scatter correction in the OS-EM reconstruction.

RESULTS

In the phantom studies, the activity quantification errors for the liver, and 29 mL,16 mL, and 8 mL liver inserts were 8%, 21%, 27%, and 30%, respectively, without RCs and 1%, 5%, 5%, 14%, respectively when volume-dependent RCs were applied. In the patient studies, administered activities ranged from 0.5 to 5.8 GBq with a median value of 2.8 GBq. Analyzed lesion volumes at baseline ranged from 2 to 828 cc with a median value of 9 cc. For all lesions, the median PET-derived uptake was 5.4 MBq/mL (range 0.02 to 28.0) and the lesion-to-normal liver uptake concentration ratio was 4.2 (range 0.02 to 39.1) considering the treated liver lobe and 6.9 (range 0.03 to 93.9) considering the entire liver. Considering all lesions, the median AD was 268 Gy (range 1 to 1271) and the median BED was 404 Gy (range 1 to 4337). Considering all treatments, the median normal liver AD was 45 Gy (range 8 – 77). There was good agreement between lesion and liver AD estimates from Y-90 PET/CT and estimates from bremsstrahlung SPECT/CT when scatter correction was included in the reconstruction.

Treatment related toxicities were low and there was no correlation between non-tumoral liver AD and toxicity measures. Lesion specific response rates were 27% as assessed by RECIST for all 89 lesions and 57% by mRECIST for the subgroup of 42 lesions that had the required images for mRECIST analysis (RECIST response in this subgroup was 31%). For AD, the mean value among all responding lesions was 559 Gy and among non-responding lesions was 183 Gy ($p < 0.0001$). For BED, the mean value among all responding lesions was 1129 Gy and among non-responding lesions was 255 Gy ($p < 0.0001$). In the TCP analysis, both mean AD and BED metrics were significantly associated with the probability of response (AUC 0.87 to 0.90, $p<0.0001$). The AD yielding 50% TCP was 292 Gy, which is in between the value of 390 Gy reported by Chiesa et al [11] using pre-therapy Tc-99m MAA SPECT/CT based estimates and the value of 160 Gy reported by Kappadath et al [12] using bremsstrahlung SPECT/CT based estimates in RE with glass microspheres. The differences in the imaging modalities and activity quantification procedure as well as patient populations potentially contribute to the observed differences in the three studies.

CONCLUSIONS

Post-therapy Y-90 imaging with PET/CT or SPECT/CT is valuable for treatment verification and for establishing dose – outcome relationships in RE. The significant association between tumor dose metrics and response coupled with the low incidence of toxicity evident in the current study, demonstrates the potential for TCP guided treatment planning. However, these

results need to be confirmed in a larger cohort and robust relationships between pre- and post-therapy imaging-based estimates are also needed for treatment planning.

ACKNOWLEDGEMENTS

This work was supported by grant R01 EB022075 awarded by the National Institute of Biomedical Imaging and Biomedical Imaging, United States Department of Health and Human Services.

REFERENCES

[1] SALEM R, GABR A, RIAZ A, et al. Institutional decision to adopt Y90 as primary treatment for hepatocellular carcinoma informed by a 1,000-patient 15-year experience. *Hepatology.* 2018;68:1429-40.

[2] TheraSphere Ytrium-90 Glass Microspheres [package insert]. Available at: https://www.btg-im.com/BTG/media/TheraSphere-Documents/PDF/TheraSphere-Package-Insert_USA_Rev-14.pdf

[3] DOMINELLO M, BOWERS J, ZAKI M, KONSKI A. Radiotherapy and radioembolization for liver metastases. *Ann Palliat Med*. 2014;3:104-13.

[4] PRINCE JF, VAN DEN BOSCH MAAJ, NIJSEN JFW, et al.Efficacy of Radioembolization with (166)Ho-microspheres in salvage patients with liver metastases: A Phase 2 Study. *J Nucl Med*. 2018;59:582-588

[5] SRINIVAS SM, NATARAJAN N, KUROIWA J, et al. Determination of radiation absorbed dose to primary liver tumors and normal liver tissue using post-radioembolization (90)Y PET. *Front Oncol*. 2014;4:255.

[6] CHAN KT, ALESSIO AM, JOHNSON GE, et al. Prospective trial using internal pair-production positron emission tomography to establish the Yttrium-90 radioembolization dose required for response of hepatocellular carcinoma. *Int J Radiat Oncol Biol Phys.* 2018;101:358-65.

[7] ABADIE P, HESSE M, JAMAR F, LHOMMEL R, WALRAND S. (90)Y TOF-PET based EUD reunifies patient survival prediction in resin and glass microspheres radioembolization of HCC tumours. *Phys Med Biol.* 2018;63:245010.

[8] WILDERMAN SJ, DEWARAJA YK. Method for fast CT/SPECT-based 3D Monte Carlo absorbed-dose computations in internal emitter therapy. *IEEE Trans Nucl Sci* 2007;54:146.

[9] CREMONESI M, CHIESA C, STRIGARI L, et al. Radioembolization of hepatic lesions from a radiobiology and dosimetric perspective. Frontiers in Oncology (2014) 4:1-20(article 210); doi:10.3389/fonc.2014.00210.

[10] DEWARAJA YK, CHUN SY, SRINIVASA RN et al. Improved quantitative (90) Y bremsstrahlung SPECT/CT reconstruction with Monte Carlo scatter modeling. *Med Phys*. 2017;44:6364-76.

[11] CHIESA C, MIRA M, MACCAURO M et al. Radioembolization of hepatocarcinoma with (90)Y glass microspheres: development of an individualized treatment planning strategy based on dosimetry and radiobiology. *Eur J Nucl Med Mol Imaging*. 2015;42:1718-38.

[12] KAPPADATH SC, MIKELL J, BALAGOPAL A, BALADANDAYUTHAPANI V, KASEB A, MAHVASH A. Hepatocellular carcinoma tumor dose response after (90)Y-radioembolization with glass microspheres using (90)Y-SPECT/CT-based voxel dosimetry. *Int J Radiat Oncol Biol Phys*. 2018;102:451-461.

Selective Internal Radiotherapy Dose Calculation: A Pilot Study to Compare Lung Shunt Fraction on Planar and SPECT/CT Imaging

N. Poon-iad
A. Teyateeti, P. Chaudakshetrin

Division of Nuclear Medicine, Department of Radiology,
Faculty of Medicine Siriraj Hospital, Mahidol University, Bangkok, Thailand

Email address of Corresponding Author: Nucharee.poo@mahidol.ac.th

BACKGROUND

Yttrium-90 (^{90}Y) microspheres are commonly used for hepatic selective internal radiotherapy. Evaluation of a lung shunting fraction using ^{99m}Tc macro-aggregated albumin (MAA) scintigraphy is required to simulate the distribution pattern of the ^{90}Y therapeutic activity for selective internal radiotherapy treatment of liver malignancies. The lung shunt fraction (LSF) is defined as the ratio of radioactive counts in the lungs to the combined radioactive counts in the lungs and liver. Significant error in ^{90}Y microsphere treatment dose did occur if the regions of interest (ROIs) or volumes of interest (VOIs) were not defined properly in the lung shunting calculation. The purpose of this study was to compare the radiation dose calculation from different lung shunt fraction (LSF) for pre-treatment evaluation of selective internal radiotherapy)SIRT(between planar scintigraphy)PS(and SPECT/CT imaging.

METHODS

The lung shunting percentage (%LSF) on ^{99m}Tc macro-aggregated albumin (MAA) planar and SPECT/CT imaging of 16 hepatocellular carcinoma patients were retrospectively analyzed. In dosimetric calculations, all variables were derived from medical record. Activity administered was calculated using a body surface area (BSA) and partition model (PM) method.

RESULTS

Lung shunt percentage as calculated from planar scans was almost 2 times higher in all cases as compared to SPECT/CT results in the same patients, 8.68 ± 6.44 and 4.45 ± 4.20, respectively)p = 0.000(. Estimated treatment activity (TA) using BSA method in 81% (13/16 patients) whose %LSF on both imaging were less than 10%, PS-based TA were equal to SPECT/CT-based TA. In 2 of 16 patients whose PS-based %LSF were 10.04% and 18.43%, estimated PS-based TA using dose reduction factor, were less than SPECT/CT-based TA (with %LSF of 4.5% and 14%, respectively). In the rest 1 patients, SIRT is ineligible on PS (LSF 21.38%) but eligible based on SPECT/CT (LSF 13.8%). For PM method, mean of PS-based and SPECT/CT-based TA were significantly different, 2.55 ± 2.13 vs 2.46 ± 2.08 GBq (p = 0.000). With these given TA and %LSF, estimated lung absorbed dose is considerably higher on planar scans, 10.87 ± 8.24 and 5.32 ± 5.47 Gy, for PS and SPECT/CT respectively (p = 0.000).

CONCLUSIONS

PS-based %LSF was significantly higher than that of SPECT/CT-based, possibly from organ overlapping in 2D images. Care should then be taken in dose calculation, either with BSA and PM method, to prevent unintentional reduction of TA from overestimate of the LSF which possibly lead to underdosing. SPECT/CT can provide a more accurate measurement of LSF than planar imaging.

REFERENCES

[1] MURTHY R, NUNEZ R, SZKLARUK J, et al. Yttrium-90 microsphere therapy for hepatic malignancy: devices, indications, technical considerations, and potential complications. Radiographics (2005) 41–55.

[2] BURTON MA, GRAY BN, JONES C, COLETTI A. Intraoperative dosimetry of ^{90}Y in liver tissue. Int J Rad Appl Instrum B. (1989) 495–8.

[3] BURTONMA, GRAY BN, KLEMP PF, KELLEHER DK, HARDY N. Selective internal radiation therapy: distribution of radiation in the liver. Eur J Cancer Clin Oncol. (1989) 1487–91.

[4] BURTON MA, GRAY BN, KELLEHER DK, KLEMP PF. Selective internal radiation therapy: validation of intraoperative dosimetry Radiology. (1990) 253–5.

[5] HO S, LAU WY, LEUNG TW, CHAN M, NGAR YK, JOHNSON PJ, et al. Partition model for estimating radiation doses from yttrium-90 microspheres in treating hepatic tumours. Eur J Nucl Med. (1996) 947–52.

[6] HO S, LAU WY, LEUNG TWT, CHAN M, JOHNSON PJ, LI AKC. Clinical evaluation of the partition model for estimating radiation doses from yttrium-90 microspheres in the treatment of hepatic cancer. Eur J Nucl Med. (1997) 293–8.

[7] HO S, LAU WY, LEUNG TWT, CHAN M, CHAN KW, LEE WY, et al. Tumour-to-normal uptake ratio of ^{90}Y microspheres in hepatic cancer assessed with ^{99m}TC macroaggregated albumin. Br J Radiol. (1997) 823–8.

[8] POON-IAD N, TEYATEETI A, CHAUDAKSHETRIN P. Evaluation of Lung Shunt Fraction from Planar Scintigraphy and SPECT/CT Images.The 11th Annual Scientific Meeting, Thai Medical Physicist Society. (2019) 128-131.

[9] HELMUT DITTMANN, JUERGEN KUPFERSCHLAEGER, DIANA FEIL, et al. Quantitative SPECT/CT for evaluation of lung shunting prior to SIRT: Results of a pilot study. J NucI Med (2015).

[10] HOJJAT AHMADZADEHFAR, AMIR SABET, KIM BIERMANN, et al. The Significance of 99mTc-MAA SPECT/CT Liver Perfusion Imaging in Treatment Planning for 90Y-Microsphere Selective Internal Radiation Treatment. The journal of nuclear medicine. vol. 51, no. 8: august (2010) 1206-1212.

[11] DITTMANN HJMH, KOPP D, KUPFERSCHLAEGER J, et al. A prospective study of quantitative SPECT/CT for evaluation of hepatopulmonary shunt fraction prior to SIRT of liver tumors. J NucI Med (2015).

^{177}Lu Peptide Receptor Therapy: Dosimetric Experience in Uruguay

M. Terán[a]
S. Rodriguez[b], N. Niell[b,c], G. Dos Santos[b,c], J. Gaudiano[c], J.C. Hermida[b], O. Alonso[b,c]

[a]Universidad de la República, Facultad de Química, Área Radioquímica, Av. Gral. Flores 2124 Montevideo Uruguay.
[b]Centro de Medicina Nuclear e Imagenología Molecular. Hospital de Clínicas. Av. Italia s/n.
[c]Centro Uruguayo de Imagenología Molecular. Ricaldoni 2010. Montevideo Uruguay.

Email address of Corresponding Author: mterangretter@gmail.commailto:myemail@domain.com

BACKGROUND

In a collaborative work between the National Cancer Institute (INCA), the Centre of Nuclear Medicine and Molecular Imaging of the University Hospital (CMNIM), the Uruguayan Centre for Molecular Imaging (CUDIM) and the Faculty of Chemistry, Uruguay introduced in 2017 peptide receptor radiotherapy (PRRT) with both ^{177}Lu-DOTATATE and ^{177}Lu-PSMA. In this work, the quantification of planar images was chosen to establish the biokinetic profile over time and the data set was complemented with blood samples [1]. The calculations were made based on the MIRD methodology and the tool to estimate the doses was the OLINDA / EXM code.

METHODS

The work was performed with two groups of patients, four treated with ^{177}Lu PSMA and two treated with ^{177}Lu-DOTATE. The protocols were approved by the ethics committee in accordance with the national regulations and the Declaration of Helsinki principles. The average amount of ^{177}Lu-DOTATATE was 7.6 ± 0.4 GBq co-administered with an intravenous infusion kidney-protective of amino acids. ^{177}Lu PSMA average administered activity was 6.40 ± 0.25 GBq.

Attenuation corrections of planar scans was performed using a transmission image with flood source filled with ^{177}Lu (500-1000 MBq). The dosimetric protocol for ^{177}Lu PSMA required blood sampling (3mL) at 0.3,1, 2, 24, 48, 72 and 168 hours. Planar images at 2 (without micturition), 24, 48,72 and 168 hours (with previous micturition) post administration. SPECT CT at 48 hours.

The dosimetric protocol for ^{177}Lu DOTATATE required blood sampling (3mL) at 1, 2, 4, 24, 96 and 168 hours. Planar images at 1 (without micturition), 24, 96 and 168 hs (with previous micturition) post administration. SPECT CT at 96 hs.

All the images were acquired in a MEDISO AnyScan SC-SN-3-60R gamma camera of two heads with medium energies collimator at 208 KeV with 15% window. Planar images were corrected both for scatter using TEW method and for attenuation using the transmission scan according to Siegl et al [2]. Activity of the images was quantified according to the conjugate view method and time-activity curves plotted. For the conjugate view calculations, the injected activity was considered the 100% of the counts of the first whole body image, ROIs for whole body (WB) kidneys and liver were draw. Liver and kidneys thickness were determined by a high-resolution CT [3]. In order to determine red marrow (RM) dose, blood samples were weighed and activity measured in a Captus 3000 well detector NaI(Tl) 1x1'' associated to an

MCA. Both whole body and blood data were processed using OLINDA/EMX code to determine the accumulated activity profile and the doses of the critical organs.

RESULTS

The estimated doses in RM, kidneys, liver and WB for each patient treated with ^{177}Lu PSMA or ^{177}Lu DOTATATE are presented in table 1.

Table 1. Patients Doses (Gy)

^{177}Lu PSMA				
Patient	**RM (Gy)**	**Kidneys**	**Liver**	**WB**
1	0.27	1.98	7.46	0.42
2	0.95	4.44	0.50	0.56
3	0.64	3.15	0.50	0.20
4	2.01	8.75	1.06	0.37
Mean ±SD	**0.97±0.75**	**4.58±2.96**	**2.38±3.39**	**0.39±0.15**

^{177}Lu DOTATE				
Patient	**RM (Gy)**	**Kidneys**	**Liver**	**WB**
1 Masculine	1.31	6.11	7.21	1.33
2 Feminine	1.38	10.14	6.16	1.07
Mean ±SD	**1.34±0.05**	**8.12±2.85**	**6.68±0.74**	**1.20±0.19**

Although patient 1 showed a liver dose out of range, it was due to high uptake in liver metastases, not present in the rest of the patients of his group.

CONCLUSIONS

The method was robust, easy to implement in routine and patients showed doses in consonance with published data. Taking into account the total amount of therapies with ^{177}Lu is facing an important increase, these results embolden to further improvement of the method, aiming to increase the accuracy in the absorbed dose estimates and its correlation to haematological response.

Acknowledgements: Dra. H. Balter[c], Lic. Eugenia Demarco[b], Lic P.Grahambell[b].

REFERENCES

[1] SGOUROS G. Dosimetry of internal emitters. J Nucl Med (2005) 46 1:18s–27

[2] MIRD Pamphlet No. 16: Techniques for Quantitative Radiopharmaceutical Biodistribution Data Acquisition and Analysis for Use in Human Radiation Dose Estimates. J NucIMed (1999) 4037S-61S

[3] SVENSSON et al. A novel planar image-based method for bone marrow dosimetry in 177Lu-DOTATATE treatment correlates with haematological toxicity EJNMMI Physics(2016) 3:21.

Dosimetric Analyses of Critical Organs (Kidney, Liver and Spleen) of Patients with Neuroendocrine Tumors Treated with 177Lu-DOTATATE

S. K. Gupta[a]
P. Thakral[b], **P. K. Bajpai**[a]

[a]National centre for Accelerator Based Research, Guru Ghasidas University, Bilaspur, CG, India
[b]Department of Nuclear Medicine, Fortis Hospital, Gurugram, Haryana , India

Email address of Corresponding Author: santoshaiims@gmail.com

BACKGROUND

The aim of this work was to calculate the radiation absorbed dose to kidneys, liver and spleen of Patients with diagnosed neuroendocrine tumours (NETs) treated with 177Lu-DOTATATE.

METHODS

We enrolled 81 patients (male/female patients, 60/21) with mean age of 48.1±15.3 years affected by different types of NETs diagnosed with 68Ga-DOTANOC PET-CT and biochemical markers. For radiation protection of kidneys, amino acid mixture (lysine and arginine) was co-infused; 3.7 to 7.4 GBq (100-200 mCi) of 177Lu-DOTATATE was infused to each patient over 30 minutes. Each patient underwent a series of 9 whole-body scans at 30 minutes (pre-void) and 4, 24, 48, 96, 144, and 168 h. The organs included in dosimetric calculation were kidney, liver, spleen, pituitary gland, and NETs. All dosimetric calculations were done using the OLINDA/EXM 1.0 software.

RESULTS

Physiological uptake of 177Lu-DOTATATE was seen in all patients in kidneys, liver, spleen, and pituitary gland. Radiation absorbed doses were calculated: 0.54 ±0.1 mGy/MBq for kidneys, 0.23 T 0.05 mGy/MBq for liver and 1.27 ± 0.14 mGy/MBq for spleen.

CONCLUSIONS

The maximum cumulative activity of 177Lu-DOTATATE that can be safely administered to a patient within permissible renal threshold in our study was found to be 40 GBq (1100 mCi). However, there are considerable interpatient differences in absorbed doses of all organs requiring individualized dosimetry for optimizing tumour dose.

Pre Therapy Patient Dosimetry with ^{177}Lu-PSMA CC34 Indonesia Experience

N. R. Hidayati[a]
A. R. Dewi[b], E. Rosilawaty[b], R. Shintawati[b], W. Mailana[a], A. H. S. Kartamihardja[b]

[a]Center for Technology of Radiation Safety and Metrology, Jl. Lebak Bulus No.49, Cilandak Jakarta Selatan, Indonesia 12440
[b] Department of Nuclear Medicine and Molecular Imaging Hasan Sadikin General Hospital, Jl. Pasteur No.38, Pasteur, Sukajadi, Kota Bandung, Jawa Barat 40161 INDONESIA

Email address of Corresponding Author: inn98@batan.go.id

BACKGROUND

Based on WHO data in 2014, prostate cancer in Indonesia has been ranked as the 3rd place after lung and colorectal cancers. In the last few years, the management of prostate cancer in nuclear medicine in Indonesia has been evolved in diagnostic procedures. According to some references, ^{177}Lu has been used for theranostic procedures because it can be utilized as diagnosis and therapy agent. In addition, several clinical evaluations of ^{177}Lu-PSMA [1] have been carried out worldwide and the results have been satisfactory in prostate cancer patients. The individualized patient dosimetry in Radionuclide Therapy also has been considering as a global issue since the Bonn Call for Action in 2012 has stated that patient dosimetry in Radionuclide Therapy should be more developed to consider radiation protection of patient who undergo therapy using unsealed radionuclide (Radionuclide Therapy, RNT). Nevertheless, the implementation of dosimetry in RNT in Indonesia has not been applied before 2017. Hence, considering the benefits, Indonesia has initiated a pre therapy dosimetry study for prostate cancer patient who will be treated using ^{177}Lu-PSMA in the mid of 2017 with the support from IAEA-CRP E230005 “Dosimetry in Molecular Radiotherapy for Personalized Patient Treatments. The study is aimed to perform pre therapy dosimetry and investigate the radiation dose to kidney and liver as critical organs in radionuclide therapy using ^{177}Lu-PSMA, and establish the protocol for performing patient dosimetry for patients in radionuclide therapy in Indonesia.

METHODS

The study has been attributed by ethical approval no.LB.04.01/A05/EC/358/XII/2017. For initial study, twelve prostate cancer patients have been administered with 228.61±13.80 MBq of PSMA -CC34 labelled with ^{177}Lu. The selected patients are the prostate cancer patients who have negative result on bone scan. The quality of labelled product was determined by thin layer chromatography equipment with the purity about 95%. After 4,24, and 48-hour post injection, patients were scanned by Gamma Camera Infina Siemens with the scan speed of 10 cm / minute using a dual-head gamma camera equipped with a parallel-hole medium-energy collimator. Double peaks at 113 and 208 keV and 15% window settings are used for WBS acquisition. The results of image acquisition were analysed using View Conjugate Methods by following the protocol described on MIRD 16, for a pair of anterior and posterior images[2]. The result of analysis was in mCi or MBq of activity in organs. This value then has been calculated to the administered dose to get %ID of ^{177}Lu-PSMA. The %ID of organs has been used as the input of OLINDA/EXM to get the organ doses in mSv/MBq.

RESULTS

The result of this study has shown that kidneys and liver are the organs which receive the highest radiation dose from the administration of ^{177}Lu-PSMA. Moreover, similar to other studies in individualized patient dosimetry using ^{177}Lu, the kidney dose then can be used as organ limiting dose for the next therapy procedures using the ^{177}Lu-PSMA. Hence, it can be stated the radiation dose to kidneys will not receive more than 1 Gy, while the limit dose for kidney in most RNT procedures are 30 Gy.

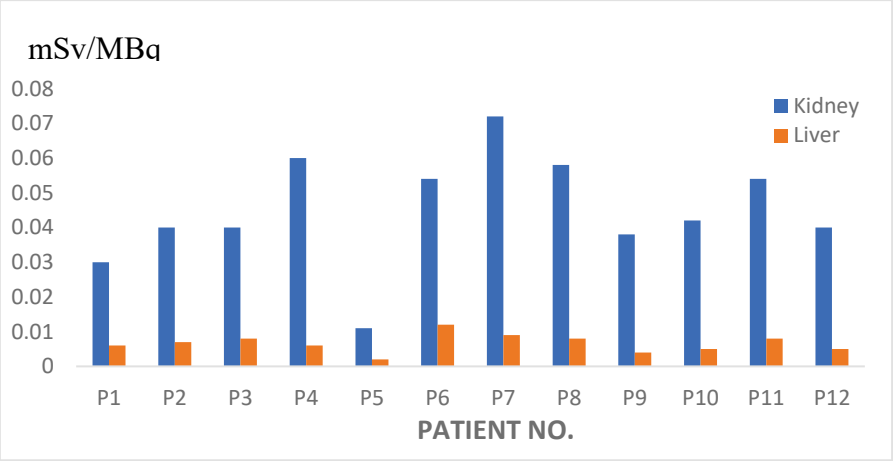

Figure 1. The kidney and liver doses after injection of ^{177}Lu-PSMA CC34 in prostate cancer patients.

Since there were some bone uptakes in few patients, it has been found the reference stating that PSMA-CC34 may have reacted to the blood serum and finally may result in the uptake of ^{177}Lu in bones. For this reason, an analysis for bone marrow dose needs to be done. However, since the acquisition process was only performed in planar studies, this study cannot give the information needed to determine bone marrow dose for the patients. In further studies, the SPECT/CT will be utilized to support the development on patient dosimetry in RNT in Indonesia.

CONCLUSIONS

The study has shown that kidneys and liver received the highest uptake in pretherapy dosimetry using ^{177}Lu-PSMA-CC34 with the dose of 0.045 ± 0.016 and 0.007 ± 0.003 mSv/MBq. In the future, the protocol for patient dosimetry in RNT in Indonesia can be developed based on the study with some improvements.

REFERENCES

[1] KABASAKAL, L., et al., Pre-therapeutic dosimetry of normal organs and tissues of (177)Lu-PSMA-617 prostate-specific membrane antigen (PSMA) inhibitor in patients with castration-resistant prostate cancer, European journal of nuclear medicine and molecular imaging **42** 13 (2015) 1976-1983.

[2] BAILEY, D.L., et al., In vivo quantification of 177 Lu with planar whole-body and SPECT/CT gamma camera imaging, EJNMMI physics **2** 1 (2015) 20.

Dosimetry Audits for New Technologies

Dosimetry Audits for Advanced Techniques: Challenges and Potential Solutions

N. Jornet[a]
C. Clark[b]

[a]Servei de Radiofisica i Radioprotecció. Hospital Sant Pau, Barcelona, Spain
[b]Medical Physics Department, Royal Surrey County Hospital, Guildford Surrey, UK

Metrology for Medical Physics, National Physical Laboratory, Teddington, Midd UK

Email address of Corresponding Author: njornet@santpau.cat

BACKGROUND

Dosimetry audits are an effective tool for quality improvement and patient safety in Radiation Therapy. Numerous examples show how dosimetry audits have played a key role in setting and improving treatment standards as well as in identifying issues which may cause harm to patients, such errors in reference dosimetry [1-3]. They also are crucial in supporting the implementation of complex techniques and in facilitating awareness of issues which may exist in specific combinations of equipment. External dosimetry audits are, without any doubt, an excellent safety net to trace inaccuracies that otherwise would not easily be detected.

During the last years there has been an explosion on the implementation of new technology and techniques. These techniques are implemented in large university centers as well as small hospitals. External dosimetry audits, in both scenarios, provide external validation of the dosimetry chain which not only results in ensuring safety but also improves treatment quality.

Dosimetry audits are part of institution credentialing for clinical audits [4,5]. However, even if the benefits of dosimetry audits are acknowledged by all professionals in Radiation Oncology, it is still not a routine practice in all radiotherapy centers across Europe.

METHODS

While the benefits of dosimetry audits are clear, the organization of those audits is challenging, both from the design and also from the economical sustainability. Therefore, innovative ideas to reduce the cost while keeping the potential in error or inaccuracies detection are being discussed. For instance, remote auditing using the detectors and phantoms from the institution with a central independent validation has been explored by EORTC Quality Assurance group [6]. The Australasian clinical trials group is testing a methodology using electronic portal devices [7]. Alternative approaches could include collection of log-files for continued assessment of quality [8], which could be of particular value in clinical trials. Alternative methods for efficiency of audit include the use of complexity metrics to pre-determine which plans should be investigated, however no metric appears to yet exist which gives a robust response across all planning and/or delivery systems [9].

Regional and national initiatives of audit networks are particularly interesting. These initiatives have the added value of promoting quality sensibility amongst radiation oncology teams and harmonizing the quality standards in the region [10-12].

The IAEA has played a key role in facilitating and conducting dosimetry audits all over the world [13]. For instance, it keeps an updated database of all dosimetry audit networks, regional, national and supranational [14]. It also has training programs for medical physicists who want

to implement dosimetry audits in their countries and lately has developed an end-to-end audit methodology using an anthropomorphic phantom (SHANE) for IMRT and VMAT. This phantom can be borrowed by different countries that want to launch a national audit on advanced techniques.

CONCLUSIONS

Dosimetry audits can support quality improvement through standardisation of radiotherapy practice across the world and should be an integral part of any quality management programmes in radiotherapy. There are multiple challenges in designing and running effective dosimetry audits in a time when new techniques and new equipment are being implemented in a large scale all over the world. Solutions such as audit networks with shared phantoms and methodologies could be an excellent solution for institutions that are implementing new technologies. The use of remote auditing using in-house phantoms and detectors with a centralised independent evaluation are also cost-effective methodologies that should be further explored to assess its sensitivity and specificity of the local detection of errors in comparison with independent measurements.

REFERENCES

[1] CLARK, C.H., Aird, E.G., Bolton, S., Miles, E.A., Nisbet, A., Snaith, J.A. et al. Radiotherapy dosimetry audit: three decades of improving standards and accuracy in UK clinical practice and trials. Br J Radiol. (2015) 88: 1055

[2] THWAITES, D. Accuracy required and achievable in radiotherapy dosimetry: have modern technology and techniques changed our views? J Phys Conf Ser. (2013); 444

[3] GERSHKEVITSH, E., Pesznyak C, Petrovic B, Grezdo J, Chelminski K, do Carmo Lopes M, et al. Dosimetric inter-institutional comparison in European radiotherapy centres: Results of IAEA supported treatment planning system audit. Acta Oncol (2014)5:628-36.

[4] CLARK, C.H., Hurkmans, C.W., and Kry, S.F. The role of dosimetry audit in lung SBRT multi-centre clinical trials. Phys Med. (2017) 44: 171–176

[5] KRON,T., Haworth, A., and Williams, I. Dosimetry for audit and clinical trials: challenges and requirements. J Phys Conf Ser. (2013) 444

[6] WEBER, D., Vallet, V., Molineu, A., Melidis, C., Teglas, V., Naudy, S. et al. IMRT credentialing for prospective trials using institutional virtual phantoms: results of a joint European Organization for the Research and Treatment of Cancer and Radiological Physics Center project. Radiat Oncol. (2014) 9: 123

[7] MIRI, N., Lehmann, J., Legge, K., Zwan, B.J., Vial, P., and Greer, P.B. Remote dosimetric auditing for intensity modulated radiotherapy: a pilot study. Phys Imag Radiat Oncol. (2017) 4: 26–31

[8] PASLER, M., Hernandez, V., Jornet, N., and Clark, C.H. Novel methodologies for dosimetry audits: adapting to advanced radiotherapy techniques. Phys Imag Radiat Oncol. (2018) 5: 76–84

[9] HERNANDEZ, V., Saez, J., Pasler, M., Jurado-Bruggeman, D., and Jornet, N. Comparison of complexity metrics for multi-institutional evaluations of treatment plans in radiotherapy. Phys Imag Radiat Oncol. (2018) 5: 37–43

[10] JORNET, N., Carrasco, P., Beltrán, M., Calvo, J.F., Escudé, L., Hernández, V. et al. Multicenter validation of IMRT pre-treatment verification: comparison of in-house and external audit. Radiother Oncol. (2014);112: 381–388

[11] JURADO-BRUGGEMAN, D., Hernandez, V., Saez, J., Navarro, D., Pino, F., Martinez, T. et al. Multicenter audit of VMAT planning and pre-treatment verification. Radiother Oncol. (2017); 124: 302–310

[12] THOMAS, R.A.S., Bolt, M.A., Bass, G., Nutbrown, R., Chen, T., Nisbet, A. et al. Radiotherapy reference dose audit in the United Kingdom by the National Physical Laboratory: 20 years of consistency and improvements. Phys Imag Radiat Oncol. (2017); 3: 21–27

[13] IZEWSKA, J., Georg, D., Bera, P., Thwaites, D., Arib, M., Saravi, M. et al. A methodology for TLD postal dosimetry audit of high-energy radiotherapy photon beams in non-reference conditions. Radiother Oncol. (2007) 84: 67–74

[13] IZEWSKA, J., Lechner, W., and Wesolowska, P. Global availability of dosimetry audits in radiotherapy: the IAEA dosimetry audit networks database. Phys Imag Radiat Oncol. (2018) 5: 1–4

IMRT Audit in Portugal: Results of an IAEA National Supported Project

T. Santos[a,b]
M. Carmo Lopes[b], E. Gershkevitsh[c], J. Izewska[d]

[a]Physics Dept., University of Coimbra, Rua Larga, 3004-516 Coimbra, Portugal
[b]Medical Physics Dept., IPOCFG, E.P.E., Av. Bissaya Barreto 98 3000-075 Coimbra, Portugal
[c]North Estonia Medical Centre, Tallinn, Estonia
[d]Dosimetry and Medical Radiation Physics Section, International Atomic Energy Agency, Vienna, Austria

Email address of Corresponding Author: taniafssantos@gmail.com

BACKGROUND

Intensity modulated radiation therapy (IMRT) is becoming commonly used in radiotherapy centres. Due to increased complexity of the IMRT planning and delivery, when compared to 3-dimensional conformal radiotherapy (3D-CRT), stringent quality assurance (QA) procedures are needed to safely implement and perform IMRT. To facilitate safe and efficient use of IMRT, the IAEA has developed an audit methodology for reviewing the physics aspects of IMRT Head and Neck (H&N) treatments through on-site visits. This audit was carried out in Portugal with the IAEA assistance. The results are presented in this work.

METHODS

All institutions presently performing IMRT treatments in Portugal (20/24) have volunteered to participate in the project. The audited radiotherapy equipment encompassed different treatment machines, treatment planning systems (TPS), dose calculation algorithms and IMRT delivery techniques, including volumetric modulated arc therapy (15), sliding window (3), step and shoot (1) and helical IMRT (1).

Following the IAEA methodology [1], the national auditor travelled through 20 centres between March and September 2018 taking with her the SHANE phantom (CIRS Inc, Norfolk, Virginia). This specially designed H&N phantom in combination with a DICOM RT structure set of target volumes and organs-at-risk were used to simulate all steps of a nasopharynx IMRT treatment as if it were a typical patient. To guide the planning process, a list of dose-volume objectives and constraints was provided. The national auditor spent two days at each centre. A CT scan of SHANE phantom and treatment planning were done in the first day. The second day was dedicated to the audit measurements. In total 20 H&N IMRT plans were created and verified using the same dosimetry system and evaluation metrics. The on-site measurements also included tests to evaluate the MLC performance – picket fence/band test – and small beam dosimetry, namely verification of the field size and penumbra width of a 2×2 cm^2 MLC shaped field using EBT3 film. Treatment machine daily output variation was also checked and taken into account. The comparison between TPS calculations and measurements with small volume ionization chamber at four positions inside the SHANE phantom corresponding to PTVs and spinal cord, was performed. Also, an EBT3 film was positioned in a coronal plane and irradiated with three treatment fractions. FilmQA Pro software (Ashland Inc., Covington, Kentucky) was used to evaluate the agreement between film measurements and TPS calculated dose distributions.

RESULTS

Analysis of MLC tests showed that leaf positioning accuracy was within ±0.5 mm in all institutions. Differences between field size and penumbra widths of the measured in-plane and cross-plane profiles for the 2 × 2 cm^2 field and the ones calculated in TPS were within ±2 mm.

All participants have generally met the proposed plan constraints despite the differences in technology, adopted planning strategies and dose calculation specificities. All plans were considered deliverable by the local medical physicists, using the local QA equipment, evaluation metrics and acceptability criteria. Considering ionization chamber measurements performed by the auditor in SHANE, differences between the calculated doses corrected for the daily output – D_{cal*} – and the measured doses were within the established tolerances of ±5% for PTVs and ±7% for the spinal cord, in all centres. One follow-up visit was required to resolve a major deviation in the spinal cord. A summary of percent differences per measurement point is presented in Figure 1.

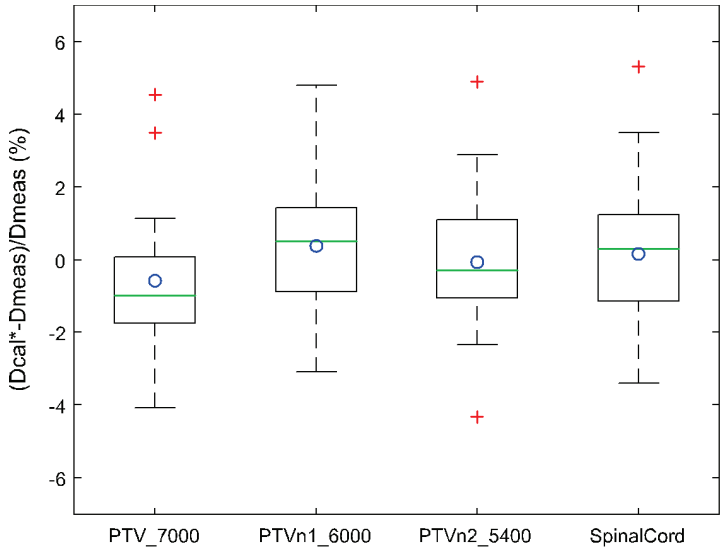

Figure 1. Boxplot summarizing the ionization chamber measurement percent differences for PTVs and spinal cord. The whiskers are defined as the largest and lowest data values within 1.5 times interquartile range. Points above/bellow those limits - outliers - are denoted by a '+'. Mean values are represented by a 'o'.

For film analysis, passing rates were on average 96.9 ± 2.9% (ranging from 90.3% to 99.1%). All above the acceptance limit of 90% for a criterion of 3% global dose/3mm, 20% threshold.

CONCLUSIONS

The audit results revealed that the status of TPS calculations and dose delivery for H&N IMRT in Portugal is within the specified tolerances with no major reasons for concern.

REFERENCES

[1] P. Kazantsev et al., "New IAEA end-to-end on-site IMRT audit methodology: Pilot test results," in Proceedings of the International Conference on Advance in Radiation Oncology (ICARO2), International Atomic Energy Agency (IAEA), Vienna, 2017.

Development of a Quality Control System for Intensity Modulated Radiotherapy

R. Souza[a]
L. da Rosa[b], **D. Braz**[c]

[a]Instituto Nacional de Câncer, Rua do Rezende, 128 sala 322, Rio de Janeiro, RJ – Brazil.
[b]Instituto de Radioproteção e Dosimetria, Av. Salvador Allende s/n, Rio de Janeiro, RJ – Brazil.
[c]Universidade Federal do Rio de Janeiro, Centro de Tecnologia Rua Horácio Macedo, Bloco G sala 206, Cidade Universitária - Rio de Janeiro, RJ – Brazil.

Email address of Corresponding Author: salomon@inca.gov.br

BACKGROUND

In radiotherapy, external auditing programs and the use of dose evaluation systems for quality control are not new. Radiological Physics Center (RPC) of the MD Anderson Cancer Center of the University of Texas since 1968 [1] and the International Atomic Energy Agency (IAEA) which since 1969 [2] have been conducting a dose postal program with thermoluminescent dosimeters (TLD). Several other societies and organizations around the world have developed their own evaluation systems [3,4], including Brazil [5], through the Quality Program in Radiotherapy (PQRT) of the National Cancer Institute (INCA). Currently, the only institution in Brazil that does quality control in radiotherapy through local and postal evaluations is INCA's PQRT, but limited to the physical parameters of the photon and electron beams and has not yet implemented a system for the evaluation of complex techniques - such as the IMRT. The main objective of this work was to develop a quality control system for intensity modulated radiotherapy (IMRT) with the use of thermoluminescent dosimeters and radiochromic films, which can be sent by post, which is valuable given the continental dimensions of Brazil.

METHODS

A phantom (figure 1a) was constructed to be irradiated by the institution evaluated in the external audit with 200 cGy in the PTV and consists of eight 15 cm x 15 cm polystyrene plates, two of them serving only as base and top. The central part is the heart of the system, composed of six 0.5 cm thick plates with 81 wells to accommodate the Harshaw TLD-100 chips in each plate and one cavity for the Gafchromic EBT2 radiochromic film. In these six plates five heterogeneities are inserted, representing various tissues of the body in a prostate treatment configuration as shown in figure 1b below.

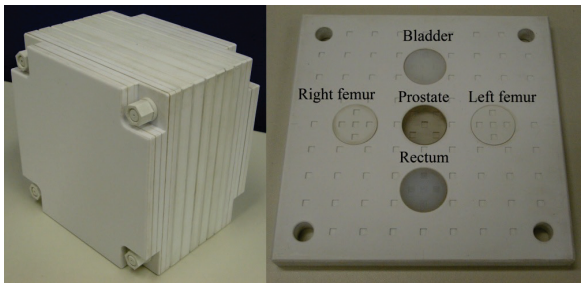

Figure 1. a. Phantom closed, b. Internal plate with heterogeneities.

The detectors are further evaluated in the PQRT dosimetry lab using a Fimel PCL3 reader (TLDs) and an Epson Perfection V850 PRO scanner and a home-built software (radiochromic

films) [7]. As a criterion for the analysis of the results of the doses measured with the TLDs, ±3% was chosen for the PTV and ±5% for the OARs. For the analysis of the gamma index of the radiochromic film the criterion 95% pass rate was chosen in 5% -3mm gamma index. The expanded uncertainty (U) for a 95% confidence interval of the results is 1.3% for the TLDs and 1.7% for the radiochromic film, which demonstrates the good accuracy of the present system for quality control in IMRT.

RESULTS

The results of the first 15 institutions evaluated are shown in Table 1.

Table 1. Results of the first 15 institutions evaluated.

Evaluation	In accordance	Not in accordance	% acceptance
TLD PTV	13	2	86,7%
TLD OARs	10	5	66,7%
Gamma Index 95%	12	3	80,0%

CONCLUSIONS

The system created for external audits of dose and dose distribution in treatments using the IMRT technique proved to be efficient in detecting nonconformities.

REFERENCES

[1] HANSON, W., AGUIRRE J.F., STOVALL, M., "Radiotherapy physics quality audit networks in the USA", IAEA TECDOC 989, Quality assurance in radiotherapy (1997).

[2] IZEWSKA, J., ANDREO, P., The IAEA/WHO TLD postal programme for radiotherapy hospitals, Radiotherapy and Oncology **54** (2000) 65.

[3] DERREMAUX, S., CHAVAUDRA, J., BRIDIER, A. *et al.,* A European Quality Assurance Network for Radiotherapy: Dose Measurement Procedure, Physics, Medicine and Biology **40** (1995) 1191.

[4] FERREIRA, I.H., DUTREIX, A., BRIDIER, A., CHAVAUDRA, J., SVENSSON, H., The ESTRO-QUALity assurance network (EQUAL), Radiotherapy and Oncology **55** (2000) 273.

[5] MARIN, A.V., in Portuguese - Desenvolvimento de um Sistema Dosimétrico Postal para Uso em Programas de Qualidade em Radioterapia com Feixes de Fótons em Condições de Não Referência. Dissertação de M.Sc., IRD/CNEN, Rio de Janeiro, Brasil (2003).

[6] ALVES, V.G.L., CARDOSO, S.C., SILVA, A.X., Gafchromic EBT2 Dosimetry via Robust Optimization, Computer Physics Communications **184** (2013) 1708.

Comparison of Alanine Dosimetry Systems at Radiation Therapy Levels

M. McEwen[a]
P. Sharpe[b], **I. Mansour**[a], **C. Gouldstone**[b]

[a]National Research Council Canada, Ottawa, ON Canada
[b]National Physical Laboratory, Teddington, UK

Email address of Corresponding Author: malcolm.mcewen@nrc-cnrc.gc.ca

BACKGROUND

Alanine is increasingly used at radiation therapy level doserates, the low atomic number of alanine, the size of dosimeters, the linearity of response and the non-destructive read-out are among the reasons why it is attractive for radiation therapy applications. A number of laboratories have previously demonstrated an alanine capability at doses below 100 Gy [1, 2] and the National Research Council of Canada has been developing such a capability over recent years [3]. The intention is for the NRC to provide a mailed audit dosimetry service to Canadian cancer centres, similar to mailed services offered by IROQ-Houston, the IAEA and the NPL. Some validation work has been done, comparing the NRC alanine measurements to doses derived using a calibrated ionization chamber (traceable to NRC) but an external validation is necessary to demonstrate international equivalence.

METHODS

A bi-lateral comparison was carried out during the period 2017-2018, between the NRC and the NPL. This was a reciprocal or symmetrical comparison: i) NPL alanine dosimeters were sent to NRC for irradiation, and then returned to NPL for read-out; ii) NRC alanine dosimeters were sent to NPL for irradiation, and then returned to NRC for read-out.

It is generally recommended that for delivered absorbed dose values lower than 15 Gy, an additional step in the alanine readout is required to remove the effect of background signals in the measured EPR spectrum. These background subtraction algorithms tend to be laboratory-specific and it is therefore not straightforward to evaluate the impact of them on the final measurement. To make the analysis of the comparison simpler, doses higher than 15 Gy were delivered at both laboratories, up to a maximum of 1 kGy. At these dose levels, the simple peak-to-peak analysis of the EPR spectrum is sufficient for the determination of the dose. An extended dose range also allowed investigation of possible non-linearities or systematic biases in the irradiation procedures and/or read-out protocols.

RESULTS

The results are shown in Figure1. There are two data sets corresponding to the NPL read-out system because that laboratory uses calibration curves with standard dose ranges and this comparison covered two such ranges. For the NRC read-out, a specific calibration curve was constructed for the entire dose range used in the comparison.

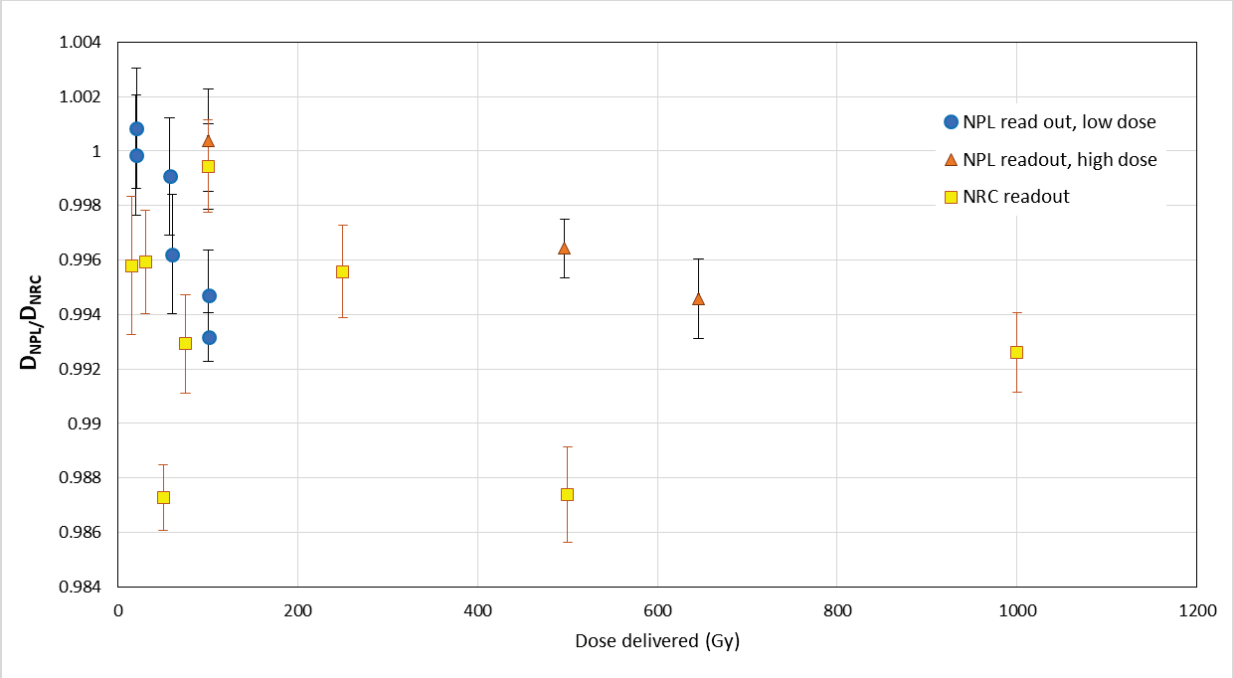

Figure 1. The value of the ratio ($Dose_{NPl}/Dose_{NRC}$) determined by both laboratories. Depending on the "direction" of the comparison the dose from a particular lab may refer to the stated delivered dose or that measured from the alanine pellets. The uncertainty bars only show the standard uncertainty of the alanine read-out.

Combining the results from the two comparisons gives D_{NPL}/D_{NRC} = 0.9954 with an estimated standard uncertainty of 0.7%. This is consistent with the same ratio as obtained from the BIPM KCDB (http://kcdb.bipm.org).

CONCLUSIONS

The results show that that the alanine dosimetry systems operated by the NPL and the NRC are equivalent within the uncertainties and also demonstrates that irradiations are consistent between therapy-style and self-shielded Co-60 irradiators. This comparison supports the use of alanine as an audit dosimeter for radiation therapy applications.

REFERENCES

[1] SHARPE, P.H.G., RAJENDRAN, K., SEPHTON, J.P., Progress towards an alanine/ESR therapy level reference dosimetry service at NPL. *Appl. Radiat. Isot.* 47, (1996) 1171.

[2] ANTON, M., Development of a secondary standard for the absorbed dose to water based on the alanine EPR dosimetry system, *Appl. Radiat. Isot.* 62 (2005) 779

[3] MANSOUR, I., Development of mailed dosimetric audit for external beam radiation therapy using alanine dosimeters, MSc thesis, Ottawa: Carleton University (2018)

Novel Dosimetry Audit Based on End-to-End Testing with Alanine Detectors in Proton Beam Therapy

A. Carlino[a]
H. Palmans[a,b], C. Gouldstone[b] , P. Trnkova[c,d], S. Vatnitsky[a], M. Stock[a]

[a]MedAustron Ion Therapy Center, Marie Curie-Straße 5, A-2700 Wiener Neustadt, Austria
[b]National Physical Laboratory, Hampton Road, TW11 0LW Teddington, United Kingdom
[c] HollandPTC, Huismansingel 4, 2629 Delft, The Netherlands
[d]Erasmus MC, Doctor Molewaterplein 40, 3015 GD Rotterdam, The Netherlands

Email address of Corresponding Author: antonio.carlino@medaustron.at

BACKGROUND

The purpose of end-to-end testing (E2E) is to confirm that the entire logistic chain of a radiation treatment, starting from CT imaging, treatment planning, patient positioning and verification to beam delivery, is adequately implemented resulting in sufficient accuracy of planned dose delivery. A novel methodology for dosimetric E2E based on customized anthropomorphic phantoms using alanine dosimetry, ionization chambers and radiochromic films was established at the light ion beam therapy facility MedAustron [1] (Wiener Neustadt, Austria). Based on this methodology an independent dosimetry audit was applied, for the first time, to the HollandPTC facility (Delft, The Netherlands) equipped with a scanned proton beam delivery system. We present results of both proton facilities comprising 4 different beam lines.

METHODS

A homogeneous polystyrene phantom and two anthropomorphic phantoms (pelvis and head phantom) have been customized to allocate different detectors such as radiochromic films, Farmer chamber and alanine pellets. During testing, the phantoms were moving through the workflow as real patients to simulate the entire clinical procedure. The CT scans were acquired with pre-defined scan protocols used at both proton therapy facilities, for cranial and pelvic treatments. All treatment planning steps were performed with RayStation (RS) v6.1 and v7.0 TPS available respectively at MedAustron and at HollandPTC. A physical dose of 10 Gy was planned to clinically shaped target volumes in order to achieve reproducibility better than 0.5% on the dose determined with alanine pellets. In the treatment rooms the plans were delivered to the phantoms loaded either with alanine pellets and radiochromic EBT3 films or a Farmer chamber. The alanine pellets (5.0 mm diameter and 2.4 mm thickness) and their read-out were provided by NPL. To bypass uncertainties related to the conversion from dose to water to dose to alanine in both the Co-60 calibration beam and the proton beam, alanine was cross-calibrated against a Farmer in a high-energy proton beam [2]. Corrections for the alanine “quenching” were derived by a Monte Carlo dose calculation platform implemented in a non-clinical version of RayStation [1].

RESULTS

The dose to water determined with the Farmer chamber in all delivered plans was within 2% of the TPS calculated dose. A maximum lateral homogeneity index of 3.5% inside the treatment field was measured with EBT3 films. Doses determined with the alanine pellets after correction for the quenching effect showed a mean deviation within 2% and a maximum deviation below 5% in the homogeneous and anthropomorphic phantoms (figure 1). Several audits are planned to be performed in the near future and more results coming from other proton therapy facilities may be available at the time of the presentation.

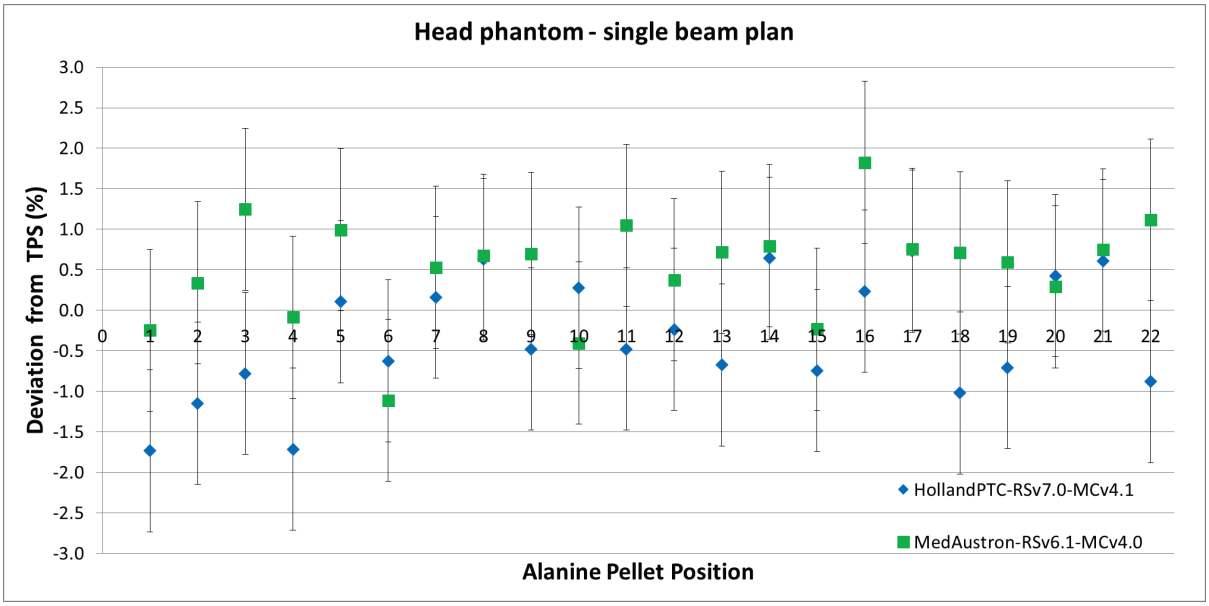

Figure 1. Relative differences between dose determined with alanine pellets and TPS planned dose for a single beam plan delivered to the head phantom. In blue symbols the comparison for the plan delivered at HollandPTC and in green symbols the comparison for the plan delivered at MedAustron.

CONCLUSIONS

Our experience shows that alanine pellets are suitable detectors for dosimetric E2E test based audits and the developed procedures can be used to support implementation of upcoming new proton beam therapy facilities in Europe and may also serve as dosimetric credentialing for clinical trials in the future.

REFERENCES

[1] CARLINO, A., et al. End-to-end tests using alanine dosimetry in scanned proton beams, Phys. Med. Biol. 63 (2018) 055001 (17pp).

[2] PALMANS, H., et al. Cross calibration of alanine for scanned proton beams, (2018) NPL Report IR 48

Proton Therapy QA Around the Globe: IROC Houston's Multi-Institutional Audit Program

P. Taylor
J. Lowenstein, P. Alvarez, S. Kry, D. Followill

UT MD Anderson Cancer Center – IROC Houston QA Center

Email address of Corresponding Author: PATaylor@mdanderson.org

BACKGROUND

The Imaging and Radiation Oncology Core (IROC) Houston QA Center is part of a cooperative that oversees the quality assurance of clinical trials funded by the National Cancer Institute (NCI) for radiation therapy and radiologic imaging. IROC Houston's mission is to ensure the NCI that participating institutions deliver clinically comparable and consistent dose so radiotherapy data from multi-institutional trials can be collected and compared. With the increasing use of proton radiation therapy, many multi-institutional clinical trials have begun to incorporate proton therapy as a delivery modality. The NCI tasked IROC Houston with developing a method of auditing participating proton therapy centers. To this end, IROC has established both a remote and on-site audit program for proton therapy that is the most comprehensive proton peer review program in the world.

METHODS

The proton therapy remote audit program mirrors IROC Houston's photon QA program. There is a facility questionnaire for proton facilities, annual monitoring of beam output performed using thermoluminescent dosimeters (TLD), and anthropomorphic phantoms. Each of these remote audit tools has been modified to accommodate the unique nature of proton therapy. IROC Houston's TLD system has been characterized in a proton therapy beam. The anthropomorphic phantoms had to be adapted as well, as many plastics used for photon phantoms are not tissue-equivalent in a proton therapy beam. For proton phantoms, old and new plastics were tested for their HU and relative linear stopping power (RLSP), and only those materials that fell within 5% of the clinical HU-RLSP conversion curve were deemed appropriate for phantom design. The phantoms each contain TLD and radiochromic film for absolute and relative dose measurements, respectively. Six anthropomorphic phantoms have been created for proton therapy audits, mimicking brain, head & neck, thoracic, prostate, liver, and spine disease.

Procedures have also been developed for on-site dosimetry audits, emulating IROC Houston audits of linear accelerators. The goal of the on-site visit is to ensure that each proton institution has accurate beam delivery that is comparable to other proton centers. The audits consist of thorough machine QA, such as beam calibration, reference and patient dosimetry, IGRT-proton coincidence, and CT HU-RLSP conversion, as well as a review of the institution's treatment planning and QA practices. The data and review are collated into a report, along with IROC Houston's recommendations on how to improve clinical and dosimetric practices.

RESULTS

IROC Houston has provided audit services to 44 proton facilities in ten countries. There have been over 650 TLD beam output checks performed. The mean TLD/institution ratio is 0.997 +/- 0.020. There have been 239 phantom irradiations analysed and the overall pass rate is 73%.

The pass rates for individual phantoms are as follows: brain (95%), head & neck (86%), liver (35%), lung (69%), prostate (83%), and spine (76%). Phantom failure rate correlates with number of targets (the liver phantom has two), and motion (the liver and lung phantoms are irradiated on moving platforms). Another trend observed with the proton phantoms is that the treatment planning systems overestimate dose to the target. As Monte Carlo algorithms are developed for proton therapy, some phantom plans have been recalculated using Monte Carlo. These results are particularly interesting for the lung phantom (Figure 1), which shows not only an improvement in the absolute dose agreement when switching from Pencil Beam to Monte Carlo calculations, but also better dose distribution shape agreement, particularly in the proton beam range direction. This data suggests that a Pencil Beam algorithm may not be appropriate for proton dose calculation in the lung.

IROC Houston has performed 35 on-site audits of 27 proton therapy centers – 10 for scattered beams, 7 for uniform scanning, and 18 for pencil beam scanning delivery. Several facilities with multiple delivery modalities have received two on-site audits. The mean number of recommendations that an institution receives is 4. Most of the recommendations from the on-site audits are for QA practices or for the HU-RLSP conversion curve. 21 of the 27 proton centers that received on-site audits have gone on to enrol patients in NCI-funded clinical trials.

CONCLUSIONS

IROC Houston has developed a robust audit program for proton therapy, including both remote and on-site audit tools. While beam calibration is very tight across institutions, there are still areas for improvement in clinical practice, such as the dose modelling for beam delivery in the lung and accuracy of HU-RLSP conversion. Proton institutions around the world can benefit from the in-depth peer review that IROC Houston's QA program provides.

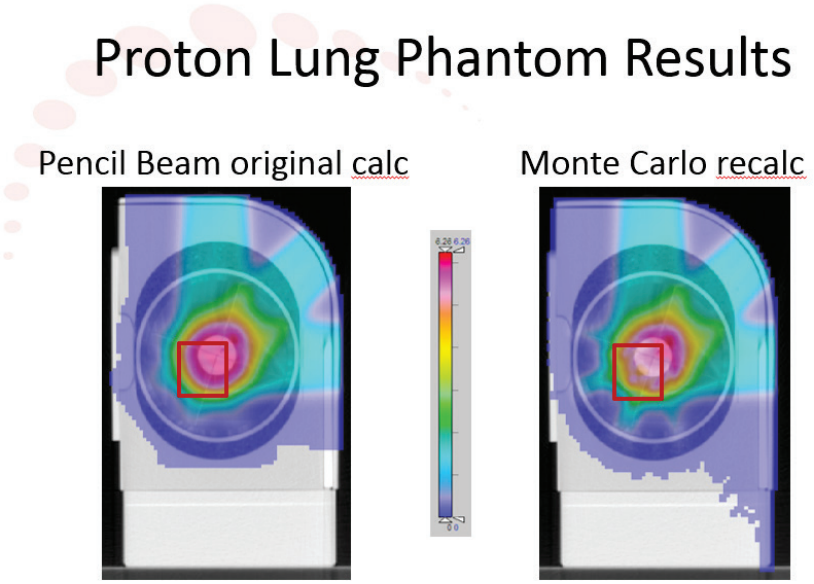

Figure 1. Comparison of proton lung phantom calculations with pencil beam and Monte Carlo dose algorithms. The pencil beam algorithm predicts a higher, uniform dose to the target.

Quality Assurance Activities for Multi-institutional Clinical Trial of Carbon-ion Radiotherapy in Japan

A. Fukumura[a]
H. Mizuno[a], N. Kanematsu[a], S. Yonai[a], T. Shirai[a], K. Yusa[b], T. Yanou[c], M. Suga[c], M. Mizota[d], S. Minohara[e], T. Kanai[f], T. Kamada[a]

[a]National Institute of Radiological Sciences (NIRS), QST, Chiba, Japan
[b]Gunma University Heavy Ion Medical Center, Gunma, Japan
[c]Hyogo Ion Beam Medical Center, Hyogo, Japan
[d]Ion Beam Medical Center, SAGA HIMAT Foundation, Saga, Japan
[e]Kanagawa Cancer Center, Kanagawa, Japan
[f]Osaka Heavy Ion Therapy Center, Osaka, Japan

Email address of Corresponding Author: mizuno.hideyuki@qst.go.jp

BACKGROUND

There are six carbon-ion radiotherapy (CIRT) facilities in operation and one facility under construction in Japan. Total patients of more than 17,000 have been treated with CIRT all over Japan. NIRS/QST marks the 25th years anniversary of CIRT at HIMAC in 2019.

From the viewpoint of public insurance coverage, nationwide multi-institutional clinical trial of CIRT has been started since 2014. [1, 2] To ensure that the results of the trial are meaningful, it is important that the dose reported by one facility is the same as the dose reported by the other facilities. Quality assurance (QA) activities for CIRT were carried out for credentialing facilities to participate in the trial, including dosimetry audit as well as investigations to harmonize medical physics processes among the CIRT facilities in Japan.

METHODS

The multi-institutional QA activities for CIRT mainly consist of questionnaires and the following site visit with peer review process.

The questionnaires contained 74 items, including beam calibration and verification (6 items), the irradiation system (18 items), treatment planning (27 items), patient immobilization (3 items), patient setup (11 items), and QA (9 items).

The site visit included an interview and dosimetry audit, which involved X-ray CT data acquisition, treatment planning, position alignment and ionization chamber dosimetry. For two beam energies of 290 and 400 MeV/u typically, auditors determined absorbed dose to water with ionization chamber measurement based primarily on the IAEA TRS 398. The measured dose was compared with the dose calculated independently by a host facility. The results obtained by the QA activities were reviewed and used for credentialing facilities to participate in the clinical trial. More detailed information on methods of the activities can been seen elsewhere. [3]

RESULTS

Table 1 summarizes the dosimetry audit results in the site visit of the QA activities. The average discrepancy between measurements and calculations for absorbed dose to water was 0.6 % with the standard deviation of 1.4 % among the facilities. The maximum absolute value of the discrepancy was 2.7 % within 3 %, which is adopted as optimal limit by the European

organization for research and treatment of cancer-radiation oncology group (EORTCROG) for the beam output audit of photon and electron beams [4].

Table 1. Summary of the dosimetry audit results

*One of the six participating institutions operates both passive and scanning beam facilities; the result of the scanning beam of the institution was tabulated as an independent facility.

Facility*	Plan 1 (high-energy) Difference between the Measured and Calculated doses	Plan 2 (low-energy) Difference between the Measured and Calculated doses
A	+1.0% (S.D. 0.2%)	+0.8% (S.D. 0.2%)
B	+2.1% (S.D. < 0.1%)	+2.6% (S.D. < 0.1%)
C	+1.4% (S.D. 0.1%)	+1.2% (S.D. < 0.1%)
D	-1.0% (S.D. 0.1%)	+1.1% (S.D. < 0.1%)
E	-2.7% (S.D. < 0.1%)	-1.4% (S.D. 0.1%)
F	0.0% (S.D. 0.1%)	-0.1% (S.D. 0.1%)
G	+1.0% (S.D. 0.2%)	+1.7% (S.D. < 0.1%)
Average	0.3%	0.8%
	Total average 0.6% (S.D. 1.4%)	

CONCLUSIONS

The inter-institutional QA activities including dosimetry audit have shown the consistency of dosimetry among CIRT facilities in Japan. The CIRT has been covered by public insurance for bone and soft tissue sarcoma, head and neck tumor and prostate cancer. The nationwide multi-institutional clinical trial of CIRT still continues to enlarge the public insurance coverage.

REFERENCES

[1] KOTO, M., et al. Multicenter study of carbon-ion radiation therapy for mucosal melanoma of the head and neck: subanalysis of the japan carbon-ion radiation oncology study group (J-CROS) study (1402 HN). Int J Radiat Oncol Biol Phys. 2017;97:1054–1060.

[2] NOMIYA, T., et al. A multi-institutional analysis of prospective studies of carbon ion radiotherapy for prostate cancer: a report from the Japan Carbon Ion Radiation Oncology Study Group (J-CROS). Radiother Oncol. 2016;121:288–293

[3] MIZUNO, H., et al. External dosimetry audit for quality assurance of carbon-ion radiation therapy clinical trials. Radiat Oncol Phys. 2018; DOI: 10.1002/acm2.12465

[4] HURKMANS, C.W., et al. Beam output audit results within the EORTC radiation oncology group network. Radiat Oncol. 2016;11:160

Monte Carlo in Diagnostic Radiology and Nuclear Medicine Dosimetry

OpenDose: An Open Database of Reference Data for Nuclear Medicine Dosimetry

M. Chauvin[a]
D. Borys[b], F. Botta[c], P. Bzowski[b], F. Cervenansky[d], J. M. Clavijo[e], M. A. Coca Pérez[f], M. Cremonesi[c], J. Dabin[g], A. M. Denis-Bacelar[h], A. Desbrée[i], Z. El Bitar[j], N. Falzone[k], J. M. Fernández-Varea[l], L. Ferrer[m], D. Franck[i], N. Lanconelli[n], B. Lee[k], A. Mairani[o], G. Mathieu[p], A. Malaroda[q], K. Matusik[b], E. McKay[r], M. Pacilio[s], I. Perseil[p], J. Pieter[b], S. Pop[d], A. P. Robinson[h], J. L. Rodríguez[t], D. Sarrut[d], L. Struelens[g], L. A. Torres Aroches[e], A. Vergara Gil[a], M. Bardiès[a]

[a]CRCT, UMR 1037, INSERM, Université Toulouse III Paul Sabatier, Toulouse, France
[b]Silesian University of Technology, Gliwice, Poland
[c]Istituto Europeo di Oncologia, Milano, Italy
[d]CREATIS, Centre Léon Bérard, Université Lyon, Lyon, France
[e]Centro de Isótopos, La Habana, Cuba
[f]MEDSCAN Nuclear Medicine and PET/CT Centre, Concepción, Chile
[g]Belgian Nuclear Research Centre, Mol, Belgium
[h]National Physical Laboratory, Teddington, United Kingdom
[i]Institut de Radioprotection et de Sûreté Nucléaire, Fontenay-aux-Roses, France
[j]Institut Pluridisciplinaire Hubert Curien, Strasbourg, France
[k]Oxford Institute for Radiation Oncology, Oxford, United Kingdom
[l]Facultat de Física, Universitat de Barcelona, Barcelona, Spain
[m]Institut de Cancérologie de l'Ouest, St Herblain, France
[n]University of Bologna, Bologna, Italy
[o]Centro Nazionale di Adroterapia Oncologica, Pavia, Italy
[p]INSERM, DSI, Coordination de l'Informatique Scientifique, Paris, France
[q]University of Wollongong, Wollongong, Australia
[r]Saint George Hospital, Sydney, Australia
[s]Azienda Ospedaliera Universitaria Policlinico Umberto I, Roma, Italy
[t]Clínica Las Condes, Santiago de Chile, Chile

Email address of Corresponding Author: manuel.bardies@inserm.fr

BACKGROUND

Dosimetry in Nuclear Medicine is based on a common formalism (MIRD) using pre-calculated reference S Values. For decades, S Values generated from mathematical models were the only available reference. The transition from mathematical to voxel-based and meshed-based models generates a need for new reference data.

The OpenDose project brings together resources and expertise through an international collaboration to generate, verify and disseminate reference dosimetric data to the Nuclear Medicine community.

METHODS

- Setting up a long-term international collaboration for Nuclear Medicine dosimetry based on Monte Carlo (MC) modelling of radiation transport.
- Implementing a distributed computation framework to get results within a reasonable timeline and ensure traceability of generated data.

- Generating Specific Absorbed Fractions for different computational models, for monoenergetic radiation (electrons, photons, alphas).
- Cross-checking the results between different codes for different energy/source/target checkpoints.
- Setting up an open database in SQL format with Isotope, Model and SAF value data.
- Integrating the SAFs over the emission spectra [1] to provide reference S values.
- As a first step, we decided to focus on the ICRP 110 reference humans [2] to prove the viability of the concept. The models comprise 140 segmented volumes (organs/tissues) allowing 19600 (target ← source) combinations, and 53 different media.

RESULTS

- The collaboration currently includes 14 research teams from 18 institutes and 5 of the most popular MC software used in radiopharmaceutical dosimetry: Geant4/GATE, Fluka, EGSnrc/EGS++, MCNP/MCNPX and Penelope.
- An initial exercise where all partners had to produce 28 simulations each allowed to set up a common computational framework and a unified result format.
- Each simulation (1 source, 1 radiation type, 1 energy) considers 140 targets
- A total of 14859 simulations were performed, representing SAFs for 81 sources, electrons and photons, 91 energy bins.
- SAF obtained from different codes were compared and allowed some partners to identify errors in their simulation setup.
- A PostgreSQL database was developed to handle all the data produced by the collaboration. This database is currently on a local server.
- A python program was developed to access the SQL database and integrate mono energetic SAF values over radioisotopes spectra to generate S values.
- A web interface to allow free access to the database and perform dosimetry is being developed and will be online soon.

REFERENCES

[1] ICRP. Nuclear Decay Data for Dosimetric Calculations. ICRP Publication 107. Ann. ICRP 38 (3), 2008.

[2] ICRP. Adult Reference Computational Phantoms. ICRP Publication 110. Ann. ICRP 39 (2) 2009.

DOSIS: A Patient-Specific MC Based Dosimetry Toolkit for Nuclear Medicine Procedures

P. Pérez[a,b]
M. Valente [a,b]

[a]IFEG - CONICET, Argentina
[b]FAMAF - UNC, Argentina

Email address of Corresponding Author: pedro.perez@unc.edu.ar

BACKGROUND

The use of radiolabelled molecules for tumor targeting proved to be very useful for the treatment of systemic malignancies, even when external radiotherapy is not applicable or appropriate. To this aim, radionuclides are labelled to carrier molecules for transporting them to the tumor region after patient infusion.

In order to achieve lethal damage to tumor cells and try to avoid exceeding tolerable dose levels in normal tissues, an accurate 3D patient-specific dosimetry assessment with millimeter resolution should be a relevant pre-requisite for these nuclear medicine procedures. Hereby, the development of dosimetry tools to asses *in vivo* radiopharmaceutical biodistribution for further estimation of 3D dose released to target and normal tissues has become in an increasing research line in the field of internal dosimetry.

The three most extended methods for calculating relevant dosimetry parameters in nuclear medicine are: S-values estimation [1], Dose Point Kernel (DPK) convolution [2] and Monte Carlo (MC) simulation of radiation transport and computation of absorbed energy [3]. These three methods have shown to be capable of dosimetry at voxel level, which is in fact desired in order to consider the non homogeneity for both activity and mass distributions based on patient specific images.

S-values are based on virtual mathematical phantoms calculations and some corrections based on patient characteristics, DPK convolution is able to achieve radial dose distributions in patient-specific conditions from activity distribution acquired from patient images (i.e. SPECT or PET) and MC simulations are accepted as the most accurate method of estimating radiation transport and absorbed dose in complex geometries [3].

Then, it is necessary to advance towards integrated solutions capable of performing patient-specific 3D dosimetry at voxel level based on anatomical and metabolic images by using at least one of the two last mentioned methods: DPK convolution and/or MC simulations; especially in a context of growth of the use of radionuclides for therapy and the energies involved.

METHODS

The DOSIS (Dose Optimization System and Integrated Software) computational toolkit was developed to perform patient-specific dosimetry based on personalized patient anatomy and biodistribution of radionuclides both obtained by currently available dual PET/CT or SPECT/CT facilities. Additionally, a 2D planar dosimetry module was incorporated aiming at considering time dependence of activity bio-distribution within regions of interest. DOSIS toolkit workflow is depicted in Figure 1.

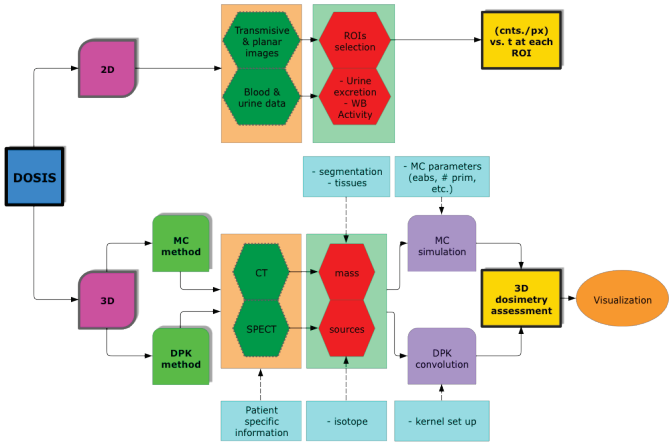

Figure 1. DOSIS workflow

This work is focused on comparing 3D dose distributions obtained with DOSIS by using full stochastic MC simulations versus the same distributions obtained with analytic approaches like DPK convolution and local energy deposition, when considering non-homogeneous activity or density distributions at different scales. Virtual phantoms were considered for this study. As example, the β^- emitters most commonly used for therapy (^{90}Y, ^{131}I, ^{177}Lu) were investigated accounting for emissions of β^--particles, conversion electrons, gamma radiation, and characteristic X-rays.

RESULTS

DOSIS successfully implemented novel tools devoted to managing radiation transport simulation by means of physics package of PENELOPE Monte Carlo general-purpose code applied to voxelized geometries defined by 3D mass and activity distributions obtained from dual scanning imaging.

CONCLUSIONS

The obtained results confirmed that DOSIS toolkit is a reliable and accurate tool for personalized internal dosimetry also highlighting advantages/drawbacks of the different calculation schemes proposed.

REFERENCES

[1] STABIN, M., Nuclear medicine dosimetry, Phys. Med. Biol. **51 No. 13**, (2006) R187.

[2] PAPADIMITROULAS, P., LOUDOS, G., NIKIFORIDIS, G. C., KAGADIS, G. C., A dose point kernel database using GATE Monte Carlo simulation toolkit for nuclear medicine applications: Comparison with other Monte Carlo codes, Med. Phys. **39 No. 8** (2012) 5238.

[3] BOTTA, F., et al., Use of the FLUKA Monte Carlo code for 3D patient-specific dosimetry on PET-CT and SPECT-CT images., Phys. Med. Biol **58 No. 22** (2013) 8099.

Clinical Dosimetry for Diagnostic and Interventional Radiology

Clinical Dosimetry for Diagnostic and Interventional Radiology

J. Damilakis[a]

[a]University of Crete, Faculty of Medicine, Department of Medical Physics, Iraklion, Crete, Greece

Email address of Corresponding Author: john.damilakis@med.uoc.gr

BACKGROUND

There is a need to optimize diagnostic and interventional radiology procedures to reduce radiation doses and develop dose evaluation tools that can be used in clinical practice to ensure adequate and improved radiation protection of patients and medical personnel. Clinical dosimetry is the corner stone of any dose optimization effort. To justify an X-ray examination, expected benefits should be weighed against the potential radiation risks. This means that clinical dosimetry is also an important tool for the justification of exposures. The aim of this article is to provide information about modern dosimetry methods available for everyday clinical use and to present research efforts for the development of advanced clinical dosimetry tools.

METHODS

CT is a valuable imaging modality. However, radiation dose associated with CT examinations and the potential adverse biological effects due to radiation is an issue of concern. To reduce doses, CT examinations should be optimized. Radiation doses are usually estimated using dosimeters such as thermoluminescent crystals and standardised physical phantoms or Monte Carlo simulation codes and mathematical phantoms. However, the optimisation of protocols in clinical routine and the prediction of diagnostic performance may not be adequately accomplished using phantoms representing only standard size patients of standard ages.

Monte Carlo approaches have been based on mathematical phantoms. Methods have mainly been described in the literature for the assessment of effective dose from examinations. Methods are needed to estimate organ and tissue doses based on models of real patients representing as many as possible human body anatomies and sizes and taking into account all parameters influencing patient dose.

Fluoroscopically-guided interventional procedures deliver high doses to the patients, particularly to the skin and during long procedures. Patient dose monitoring usually involves estimation of dose quantities such as kerma-area product and cumulative air kerma, which are poor indicators of skin dose. Thermoluminescent dosimeters and radiochromic films do not provide real time information and their use requires considerable expertise. Tools should be introduced in clinical practice for real time patient dose monitoring during interventional procedures.

Fluoroscopically-guided interventional procedures are also associated with relatively high occupational doses mainly due to high utilization, long fluoroscopy time and large number of cine acquisitions. Occupational dosimetry of healthcare personnel working in interventional suites is of paramount importance. Several recent studies have shown a significant association between long-term exposure to low-dose radiation and increased risk of cataract formation. It is evident that the eye lens is more radiosensitive that previously estimated and thus eye lens dose monitoring and protection of the eyes of occupationally exposed personnel is very important.

Diagnostic reference levels (DRLs) is an important dose optimization tool [1]. Since clinical indications dictate the main parameters that affect patient dose from CT such as scanning length, collimation and number of phases, DRLs should be specified for a given clinical indication. Similarly, DRLs should be set-up for fluoroscopically guided procedures. In Europe, only few national radiation protection authorities have defined a limited number of DRLs for different clinical indications [2]. National and local actions on establishing, updating and using DRLs are needed for effective dose optimization in diagnostic and interventional radiology.

Deep learning methods can be used for a large number of tasks in medical imaging. These tasks may cover image production steps such as dose optimization and image reconstruction. Dosimetry may also benefit from the development of artificial intelligence (AI) techniques. Medical physicists and radiologists should investigate the potential of using AI to support clinical dosimetry for diagnostic and interventional radiology.

RESULTS

MEDIRAD (Implications of Medical Low Dose Radiation Dose) is a Horizon 2020 European Commission (EC) research project that develops novel clinical dosimetry methods and dose optimization tools for CT, fluoroscopically-guided interventional procedures and hybrid systems. MEDIRAD methodologies are capable of reducing patient and staff radiation dose and potential radiation-related risks of cancer and non-cancer outcomes from imaging while maintaining or improving diagnostic information from existing and emerging techniques.

To avoid radiation overexposure accidents in interventional suites, interventional radiologists in cooperation with medical physicists should establish standard clinical protocols for each specific type of procedure performed. Cumulative absorbed dose to the skin should be limited to the minimum necessary for the clinical task. To avoid deterministic effects such as skin erythema, real-time dosimetry tools should be developed and used in everyday clinical practice [3]. To decrease occupational radiation doses, proper dose monitoring of exposed personnel is needed. PODIUM (Personal Online Dosimetry Using Computational Methods) is an EC research program to improve individual monitoring of exposed workers by developing an online dosimetry application based on computer simulations.

Individual monitoring of the eye lens dose is important for interventional radiology personnel. Typical scattered X-ray spectra vary between mean energies from about 20 keV to about 120 keV. It is recommended that dosimeters calibrated in terms of the dose quantities Hp(0.07) or Hp(3) are used in interventional suites. Proper position of dosimeters is of importance for accurate dose monitoring.

Although a large number of studies on doses from x-ray imaging are available, there is very limited information about clinical-indication specific DRLs. The EC launched the ‘European study on clinical diagnostic reference levels for x-ray medical imaging’ (EUCLID) project to provide up-to-date clinical DRLs. The main objectives of the project are to a) conduct a European survey to collect data needed for the establishment of DRLs for the most important, from the radiation protection perspective, x-ray imaging tasks in Europe and b) specify up-to-date DRLs for these clinical tasks. EUCLID started in August 2017 and the duration of the project is 33 months. A survey has been developed for collection of data needed for DRLs determination from 14 European countries. Data are collected for 10 CT clinical indications and 4 fluoroscopically guided interventional procedures. While the hospitals are collecting data and uploading them to a secure platform, literature is reviewed, and different methods of data analysis are investigated by EUCLID experts.

CONCLUSIONS

Clinical dosimetry is the corner stone of dose optimization and justification of exposures in diagnostic and interventional radiology. There is a need to develop state-of-the-art methodologies to determine patient organ and tissue doses accurately for all major modalities and especially for high-dose procedures such as CT and fluoroscopically-guided procedures. Moreover, novel tools are needed to improve occupational dosimetry.

REFERENCES

[1] INTERNATIONAL COMMISSION ON RADIOLOGICAL PROTECTION, Diagnostic reference levels in medical imaging, Publication 135, Pergamon Press, Oxford and New York (2017).

[2] DAMILAKIS, J., FRIJA G., Clinical diagnostic reference levels in medical imaging, Health Management **18** (2018) 402

[3] INTERNATIONAL COMMISSION ON RADIOLOGICAL PROTECTION, Avoidance of radiation injuries from medical interventional procedures, Publication 85, Pergamon Press, Oxford and New York (2000).

Steps Towards Personalized Dosimetry in Computed Tomography

L. Büermann[a]
S. Rosendahl[a], S. Ketelhut[a], M. Kortesniemi[b], V. M. Sundell[b], A. Kosunen[c], T. Siiskonen[c]

[a]Physikalisch-Technische Bundesanstalt, Bundesallee 100, 38116 Braunschweig, Germany
[b]HUS Medical Imaging Center, Helsinki University Central Hospital, Haartmaninkatu 4, 00290 Helsinki, Finland
[c]STUK - Radiation and Nuclear Safety Authority, Laippatie 4, 00880 Helsinki, Finland

Email address of Corresponding Author: ludwig.bueermann@ptb.de

BACKGROUND

Patient dosimetry in computed tomography (CT) is currently based on two quantities, which must be indicated by any CT scanner: the volume CT-dose index ($CTDI_{vol}$) and the dose-length product (DLP) [1]. The estimation of stochastic radiation risk, expressed in terms of the effective dose (E), is obtained by $E = E_{DLP} * DLP$, where E_{DLP} is a calculated region-specific normalized effective dose conversion coefficient. However, this type of CT-dose estimation has many shortcomings and is not suitable for CT-scanner and patient-specific dose estimates. Therefore, a procedure was developed that opens the gate to practical personalized CT dosimetry which is realized by a quick Monte-Carlo-based post-scan 3D dose simulation [2] as shown in the upper part of Figure 1. As a result, the patient- and scan-specific effective dose is obtained.

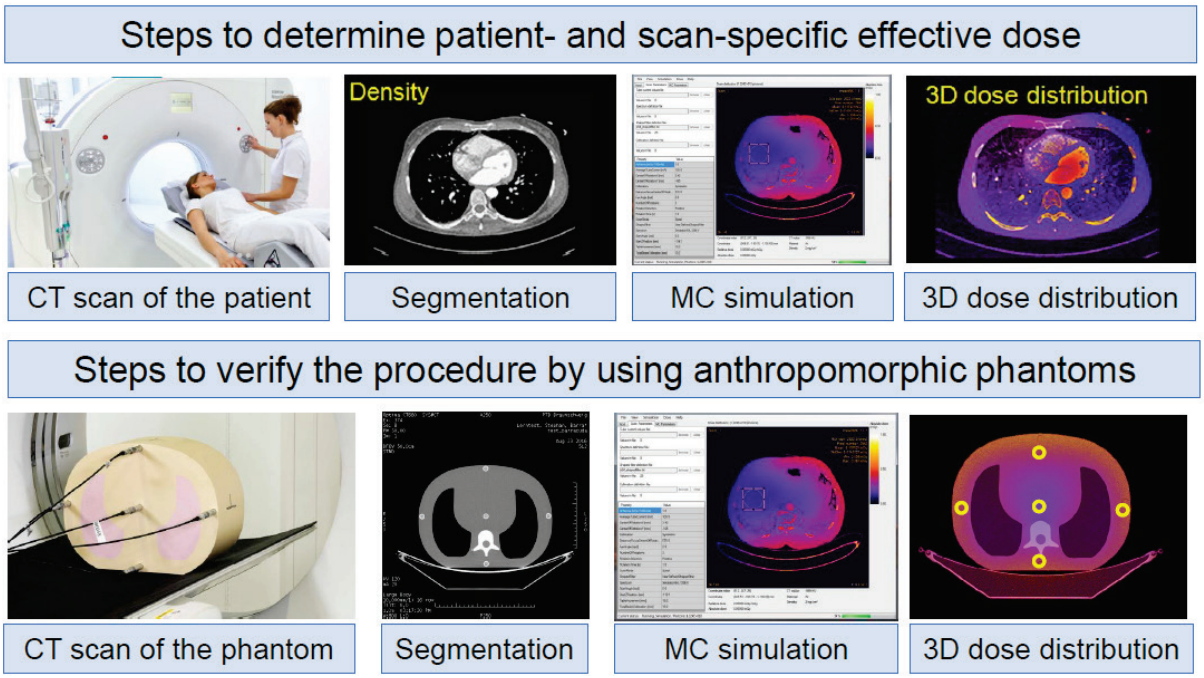

Figure 1. Illustration of the procedure for personalized CT dosimetry. The reconstructed CT image of the patient is segmented into anatomical regions and used as input geometry for a Monte Carlo simulation after the scan to obtain the 3D dose distribution. The procedure is verified by using anthropomorphic phantoms equipped with real-time dose probes.

The inputs that are needed for the simulations are: the equivalent CT-source model, the segmented 3D CT image of the patient taken from the DICOM file and the actual scan parameters. The quick and automatic segmentation of anatomical structures is still a challenge

but might be solved in the future by applying methods based on convolutional neural networks [3]. The purpose of this work was to develop viable procedures for the verification of personalized dosimetry in CT using Monte-Carlo-based simulations.

METHODS

Mobile equipment was developed and used for the rapid, non-invasive determination of equivalent source models of CT scanners under clinical conditions [4]. Standard CTDI head and body phantoms as well as anthropomorphic CT-dose phantoms were scanned. Inside the phantoms, real-time CT-dose probes were placed at five representative positions as shown in the lower part of Figure 1. The accumulated dose at the five positions was simultaneously measured during the scan. ImpactMC [2], a quick Monte-Carlo-based CT-dose software program, was used to simulate the scan. The necessary inputs were obtained from the scan parameters, the measured equivalent source models and the material-segmented CT images of the phantoms. Post-scan 3D dose distributions in the phantoms were obtained and dose values calculated at the five detector positions inside the phantom were compared with the measurements. To date, the procedure has been applied to scanner types GE Optima CT660, Toshiba Aquilion One, Siemens Somatom Definition Edge and Flash.

RESULTS

Measured and calculated dose values obtained in different phantoms with different scanner types generally agreed within the relative standard uncertainties of about 5 % – 10 % [5].

CONCLUSIONS

Viable, rapid procedures were developed that allow the post-CT-scan dose to be measured and calculated at five positions inside anthropomorphic phantoms. The procedures are applicable to any scanner type under clinical conditions. Results show that the procedures are well suited for verifying the applicability of personalized CT dosimetry based on post-scan Monte Carlo calculations.

ACKNOWLEDGEMENTS

This project has received funding from the EMPIR programme in the scope of the project entitled Metrology for multi-modality imaging of impaired tissue perfusion (15HLT05) co-financed by the EMPIR Participating States and by the European Union’s Horizon 2020 research and innovative programme.

REFERENCES

[1] ICRU, Radiation Dose and Image-Quality Assessment in Computed Tomography, ICRU Report 87, Journal of the ICRU Volume 12 No. 1 (2012).
[2] CHEN, W. et al., Fast on-site Monte Carlo tool for dose calculations in CT applications, Med Phys 39:2985-96 (2012).
[3] YAMASHITA, R. et al., Convolutional neural networks: an overview and application in radiology, Insights into Imaging 9, 611-629 (2018).
[4] ROSENDAHL, S., BÜERMANN, L., Dynamic determination of equivalent CT source models for personalized dosimetry, Current Directions in Biomedical Engineering, 3(2), 791-794 (2017).
[5] ROSENDAHL, S. et al., Verification of a comprehensive procedure for personalized dosimetry in computed tomography, submitted to PMB (2018).

Dosimetry in Head and Neck in Computed Tomography Scans

A. M. L. Gómez[a]
P. C. Santana[a] **; A. P. Mourão**[a,b]

[a]Department of nuclear engineering, Engineering school, Universidade Federal de Minas Gerais, Av. Antônio Carlos 6627, CEP: 31270-90, Pampulha, Belo Horizonte, MG, Brazil
[b]Biomedical Egineering Center, Centro Federal de Educação Tecnológica de Minas Gerais CEFET-MG, Av. Amazonas 5253 - Room 113, CEP: 30421-169, Nova Suiça, Belo Horizonte, MG, Brazil

Email address of Corresponding Author: amlgphys@gmail.com

BACKGROUND

Non-invasive methods of diagnostic, such as computed tomography (CT) have had a rapid growth in radiology services. There is a concern with the doses of radiation deposited in patients because the CT scans are those who contribute the most to the increase of the dose in the population. The legislation that regulates the levels of dose in a patient just imposes a high level according with to the type of exam, depending on the region of the body being irradiated. It is therefore necessary to determine the deposited dose values in patients depending on routine protocols used in the radiology services and propose an optimization protocols in accordance with the principles of radioprotection. Tests were performed to determine the dose profile deposited in routine of adult, using anthropomorphic phantom simulator male and female. Radiochromic film strips were introduced in the central region of the phantom for register the dose profile in head and neck and, thus, determine the amount of the dose deposited inside. We used a CT scanner of the General Electric of 64 channels programmed in helical scan mode were voltages of 80, 100 and 120 kV, and the automatic exposure control. Another programmed in helical scan mode were voltage of 120 kV and fixed current. Dosage values were found between 16.12 to 25.19 mGy on average for anthropomorphic male phantom and values of 12.75 to 17.75 mGy for anthropomorphic female phantom. Noise analyses were performed, finding that all are acceptable diagnostic parameters in Brazilian legislation.

METHODS

It was used adult anthropomorphic male and female phantom where was introduced in the area central radiochromic film strips GAFCHROMIC XR-AQ2 with dimensions of 0.5 x 32 cm^2. Scans of 25 cm of length were the GE CT scanner model Discovery of 64 channels. The CT scanner was programmed in helical mode for head scan with voltage of 80, 100 and 120 kV, automatic exposure control and voltage of 120 kV with fixed current of 200 mA. The film strips exposed were digitalized and processed using the software ImageJ to obtain the intensity values of darkening for exposition. The film strips were calibrated to convert the intensity values for dose in mGy to determine the dose profile. The noise analysis was performed for the images according to the protocol used by RadiAnt software.

RESULTS

They were found in the lowest average absorbed dose for protocol with voltage of 80 kV and automatic exposure control in relation to the routine radio-diagnostic service (120 kV and fixed current), with a reduction of 29.69%. Figure 1a represents the profiles of absorbed dose for each protocol used. The average values of absorbed dose for 100 kV had a 0.08% reduction

and 120 kV with automatic current control had an increase of 0.09%, compared to the routine used with fixed current for the anthropomorphic male phantom.

They were found in the lowest average absorbed dose for protocol with voltage of 120 kV and fixed followed by protocol with voltage of 80 kV and automatic exposure control. A variation found is 4%. Figure 1b represents the profiles of absorbed dose for each protocol used. The average values of absorbed dose for 100 kV had a 23.53% to increase and 120 kV with automatic current control had an increase of 39.21%, compared to the routine used with fixed current for the anthropomorphic female phantom.

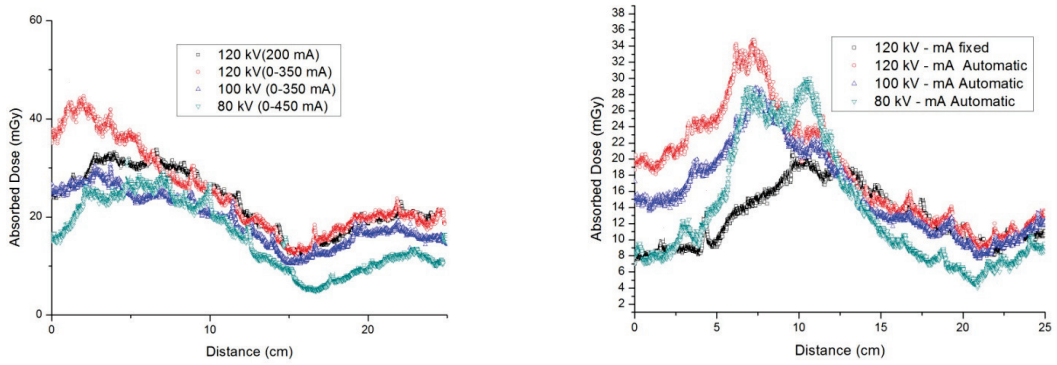

(a) (b)

Figure 1. Dose profile in head and neck CT scans.

CONCLUSIONS

The graphics represent higher values of dose in higher thickness of the object Simulator (head and neck regions). The dose values are recorded within the limits suggested by the brazilian legislation that is of 50 mGy for CT scan head [1], so it is possible to use protocols with different parameters of acquisition of CT images that put smaller values of dose in patients. The percentages of noise in the images are within the established parameters for diagnosis.

REFERENCES

[1] da Silva Ramos, F., de Souza Vasconcelos, R., dos Santos Gonçalves, M. and de Oliveira, M.V.L., 2015. Análise comparativa dos testes de controle de qualidade em tomografia computadorizada de acordo com as legislações nacional e internacional. *Brazilian Journal of Radiation Sciences*, *3*(1A).

Performance of Semiconductor Dosimeters for Air Kerma and Quality Control Measurements in Mammography

E. Salomon[a,b]
P. Homolka 1[b], I. Csete[a], P. Toroi[a]

[a]International Atomic Energy Agency, 1220 Vienna, Wagramerstraße 5
[b]Medical University of Vienna, 1090 Vienna, Waehringer Guertel 18-20

Email address of Corresponding Author: elisabeth.salomon@meduniwien.ac.at

BACKGROUND

For comprehensive quality control measurements in diagnostic radiography, ionization chambers and semiconductor-based dosimeters are used. Semiconductor dosimeters are easy to handle, and they provide several quantities of interest with one exposure. However, their inherent energy dependence of their response is influenced by the radiation quality and more pronounced than for ionization chambers [1-3]. Therefore, multiple compensation methods, based on the radiation quality, are developed by the manufacturers. To ensure the quality of dose measurements, it is essential that every dosimeter used for this purpose is calibrated regularly. It shall be possible to perform this calibration independent from the manufacturer in a local Secondary Standards Dosimetry Laboratory (SSDL).

Radiation conditions for use in the determination of characteristics are specified in IEC 61267 [4] and requirements for a satisfactory level of performance and standardized methods for the determination of compliance with these are defined in IEC 61674 [5]. For mammography radiation qualities based on Molybdenum (Mo) -anode and Mo-filtration are recommended to be used for the calibrations [6]. This does not reflect the large range of clinically used radiation qualities which includes for example radiation qualities based on tungsten (W) anode.

This study was performed to investigate the radiation quality dependence of commercial semiconductor dosimeters under calibration laboratory conditions, and to estimate errors and uncertainties related to different measurement and calibration scenarios.

METHODS

Calibration factors for air kerma measurements of eight semiconductor dosimeters were determined for five different anode-filter combinations (Mo-Mo, Mo-Rh. W-Al, W-Rh and W-Ag) and tube voltages from 25 kV to 35 kV. For dosimeters capable of measuring (half-value layer) HVL and tube voltage, calibration factors for these measurements were derived. The study was performed in the Dosimetry Laboratory of the IAEA following their calibration procedure as defined in [7]. In the course of this study a master´s thesis was prepared. More details can be found there [http://katalog.ub.tuwien.ac.at/AC15022933].

RESULTS

Maximum deviations from the reference values are shown for air kerma, tube voltage and HVL measurements in Table 1. Five dosimeters (D - H) complied within the ±5% as stated in IEC 61674 for air kerma measurements. The Expanded uncertainty (k=2) for the calibration factor for air kerma rate measurements determined according to [8] were in the range of 1.28% to 1.56%. Tube voltage and HVL measurements exhibited deviations up to 13% and 11%, respectively.

CONCLUSIONS

Eight semiconductor dosimeters were calibrated against the IAEA reference standard. Five dosimeters fulfilled the ±5% maximum deviation limit for air kerma measurement. No dosimeter tested complied with the accuracy limits stated by the manufacturer for tube voltage measurements; and only two dosimeters complied with the limits for HVL measurements. It is assumed that the performance of HVL and tube voltage measurements of semiconductor dosimeters is optimized for the quality control purpose and repeated relative measurements with a fixed radiation quality. However, uncertainty of these measurements should be carefully evaluated when these quantities are used for absolute measurements.

Table 1. Maximum deviations from the reference air kerma, tube voltage and half-value layer (HVL) measured with eight dosimeters (A – H).

	Maximum deviation in %		
Dosimeter	**Air kerma**	**Tube voltage**	**HVL**
A	-6 to 16	-1 to 13	—
B	-0.6 to -16	—	—
C	-1 to 6	—	—
D	-0.3 to 4	1 to 10	-3 to 11
F	-1 to 3	0.3 to 7	1 to 11
E	1 to 3	0.0 to 8	-4 to 7
G	-1 to 1	-9 to 8	-7 to 1
H	-1 to 3	-6 to -1	-4 to 3

REFERENCES

[1] M. Sekimoto, Y. Katoh, and T. Katoh, “Calibration coefficients of dosimeters used in mammography for various target/filter combinations,” *J. Appl. Clin. Med. Phys.*, vol. 16, no. 6, pp. 401–410, 2015.

[2] L. A. DeWerd, J. A. Micka, R. W. Laird, D. W. Pearson, M. O´Brien, and P. Lamperti, “The effect of spectra on calibration and measurement with mammographic ionization chambers,” *Med.Phys.*, vol. 29, no. 11, pp. 2649–2654, 2002.

[3] J. Witzani, H. Bjerke, F. Bochud, I. Csete, M. Denoziere, W. de Vries, K. Ennow, J. E. Grindborg, C. Hourdakis, A. Kosunen, H. M. Kramer, F. Pernicka, and T. Sander, “Calibration of dosemeters used in mammography with different X ray qualities: EUROMET project no. 526,” *Radiat. Prot. Dosimetry*, vol. 108, no. 1, pp. 33–45, 2004.

[4] INTERNATIONAL ELECTROTECHNICAL COMMISSION, “NORME INTERNATIONALE CEI/IEC 61267: Medical diagnostic X-ray equipment- Radiation condition for use in the determination of characteristics,” 2005.

[5] INTERNATIONAL ELECTROTECHNICAL COMMISSION, “IEC 61674: Medical electrical equipment- Dosimeters with ionization chambers and/or semiconductor detectors as used in X-ray diagnostic imaging,” 2009.

[6] INTERNATIONAL ATOMIC ENERGY AGENCY, *Dosimetry in Diagnostic Radiology: an Internacional Code of Practice- Technical Report Series No 457*. 2014.

[7] INTERNATIONAL ATOMIC ENERGY AGENCY, “APPENDIX TO IAEA CALIBRATION CERTIFICATE: Calibration of Reference Dosimeters for Diagnostic Radiology at the IAEA Dosimetry Laboratory Appendix 2 DOLP.013,” pp. 1–9.

[8] Joint Commitee for Guides in Metrology, *Evaluation of measurement data — Guide to the expression of uncertainty in measurement*, vol. JCGM 100:2. 2008.

Patient Specific Mean Glandular Dose Estimated from Full Field Digital Mammography and Digital Breast Tomosynthesis

S. Lau
Y. F. A. Aziz, K. H. Ng

Department of Biomedical Imaging, Faculty of Medicine, University of Malaya, 50603 Kuala Lumpur, Malaysia

Email address of Corresponding Author: ngkh@ummc.edu.my

BACKGROUND

As breast is radiosensitive, it is essential to carry out radiation dose monitoring during routine breast screening to avoid any unnecessary increase in mean glandular dose (MGD), while achieving high diagnostic image quality [1-4]. Widely practiced quality assurance programs (such as the one provided by the International Atomic Energy Agency) [1], includ recommendations for acceptable and achievable limits for MGD. Patient specific MGD measurement plays an important role in enabling the radiologists and radiographers to be aware of the MGD received by each individual woman during breast screening. In this study, we aimed to assess and compare the patient specific MGD in both full field digital mammography (FFDM) and digital breast tomosynthesis (DBT) based on a volumetric measurement approach.

METHODS

An automated volumetric breast density measurement software (Volpara, Version 1.5.1, Volpara Solutions Ltd. NZ) was used to compute the patient specific MGDs from FFDM and DBT images, including both craniocaudal (CC) and mediolateral oblique (MLO) views, for 206 women (mean age: 59±9 years). These images were acquired using the combo procedure on a DBT system (Hologic Selenia Dimensions, Hologic, Inc. US), which was able to capture both FFDM and DBT images of the same breast under the same compression, and hence eliminated the discrepancy in compressed breast thickness. The patient specific MGDs from FFDM and DBT images were then analyzed using statistical software (MedCalc, Version 15.4, Medcalc Software, BE). The MGDs reported by the DBT system manufacturer on the console display were also recorded for comparison with the patient specific MGDs computed by the automated software.

RESULTS

The box and whisker plot for patient specific MGDs estimated from FFDM and DBT images is shown in Figure 1.

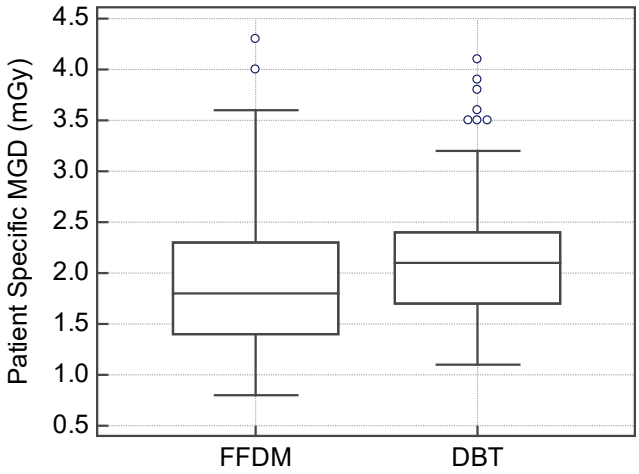

Figure 1. Box and whisker plot for patient specific MGDs estimated from FFDM and DBT images.

The mean patient specific MGD estimated from the FFDM and DBT images were 1.9±0.7 mGy and 2.1±0.6 mGy, respectively. Although patient specific MGDs estimated from FFDM and DBT images were strongly and positively correlated ($r=0.87$, $p<0.0001$), the patient specific MGD estimated from FFDM images was significantly lower than the one estimated from DBT images ($p<0.0001$). It was also observed that the MGDs reported by the manufacturer were generally lower than that computed by the automated software for both FFDM and DBT.

CONCLUSIONS

Our study showed that automated volumetric breast density measurement software can be used for dose monitoring in routine breast screening. The differences in MGDs reported by the manufacturer and the automated software were due to the different approaches used in computing the results. We expected the MGDs computed by the automated software for both FFDM and DBT to be more accurate and useful as they were patient specific, and based on volumetric approach.

REFERENCES

[1] INTERNATIONAL ATOMIC ENERGY AGENCY, Quality Assurance Programme for Digital Mammography, IAEA Human Health Series No 17 (2011). Available from: http://www-pub.iaea.org/MTCD/publications/PDF/Pub1482_web.pdf

[2] EUROPEAN COMMISSION, European Guidelines for Quality Assurance in Breast Cancer Screening and Diagnosis (2006). Available from: http://euref.org/european-guidelines/4th-edition

[3] FOOD AND DRUG ADMISSION, Mammography Quality Standards Act and Program (1992). Available from: http://www.fda.gov/Radiation-EmittingProducts/MammographyQualityStandardsActandProgram/default.htm

[4] Ng, K.H., Lau, S., Vision 20/20: Mammographic Breast Density and its Clinical Applications, Med Phys **42** (2015) 7059-7077.

Fibroglandular Tissue Distribution in Compressed Breasts for a New Breast Dosimetry Model

C. Fedon[a]
M. Caballo[a], **D. R. Dance**[b,c], **O. Diaz**[d], **I. Sechopoulos**[a,e]

[a]Department of Radiology and Nuclear Medicine, Radboud University Medical Center, PO Box 9101, 6500 HB Nijmegen, The Netherlands
[b]National Co-ordinating Centre for the Physics of Mammography (NCCPM), Guildford GU2 7XX, UK
[c]Department of Physics, University of Surrey, Guilford GU2 7XM, UK
[d]Computer vision and robotics institute, University of Girona, Campus Montilivi, 17071 Girona, Spain
[e]Dutch Expert Center for Screening (LRCB), PO Box 6873, 6503 GJ Nijmegen, The Netherlands

Email address of Corresponding Author: christian.fedon@radboudumc.nl

BACKGROUND

X-ray mammography remains the worldwide primary screening method for early breast cancer detection in millions of women. Being an x-ray examination, there is a risk, albeit small, of radiation-induced carcinogenesis. Thus, it is necessary to provide an accurate dose evaluation for optimization and assessment of screening.

Currently, the dose metric used in mammography is the average glandular dose [1]. This quantity estimates the amount of radiation dose absorbed by the fibroglandular tissue, which is considered the radiosensitive tissue in the breast. Recent studies have shown that current models tend to overestimate patient dose by up to 30% due to the assumption that fibroglandular tissue is uniformly distributed within the breast [2,3].

Therefore, new breast models based on non-uniform tissue distribution are encouraged.

Consequently, the goal of this work is to provide an accurate characterization of fibroglandular tissue distribution in compressed breast to aid the development of a new, accurate breast models for universal dosimetry evaluations.

METHODS

87 breast CT (BCT) images were acquired at our institution (RadboudUMC, Nijmegen, the Netherlands) with a dedicated BCT clinical prototype [4]. All images were reconstructed in a volume with isotropic voxel size of 0.273 mm. All voxels were automatically classified as skin, adipose or fibroglandular tissue [5], and then mechanically deformed using an open-source software (NiftySim) in order to simulate the craniocaudal breast compression during mammographic acquisition.

After the mechanical compression step, each compressed breast volume was divided into 50 regions for each main view (coronal, axial and sagittal), resulting in a 3D matrix with dimensions 50x50x50. For each of these views, the relative glandular fraction in the *i*-th region, RGF_i, was obtained as the ratio of the number of glandular voxels in the *i*-th region to the total number of voxels (i.e., adipose and glandular) in the *i*-th region.

This analysis was repeated for all 87 compressed breast models, and an average value for RGF_i was obtained for each region in each view. Fitting functions describing the fibroglandular tissue distribution were obtained using data analysis software (TableCurve 2D®).

RESULTS

It was observed that the fibroglandular tissue tends to be concentrated towards the nipple (Figure 1a), without any left-right preferred orientation (sagittal view, Figure 1c). In the axial view (Figure 1b), it is clearly visible that the fibroglandular tissue tends to be concentrated towards the bottom of the compressed breast (i.e., regions numbered 30-45), probably due to the effect of the force of gravity.

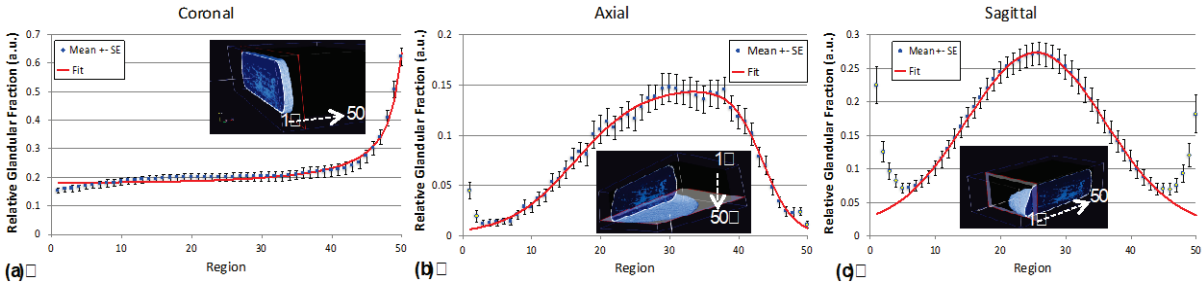

Figure 1. Relative glandular fraction for (a) coronal, (b) axial and (c) sagittal view.

CONCLUSIONS

For the first time, we observed that, in the axial direction, the fibroglandular tissue is not concentrated at the centre of the compressed breast. Although it is commonly assumed [3-4] that the fibroglandular tissue is more concentrated in the central part of the breast, our results suggest that this assumption might not be an accurate description of the fibroglandular distribution in compressed breasts. This bias of the glandular tissue distribution towards the bottom section of the breast could explain the over-estimation in average glandular dose of the current breast dosimetry models [1].

The data presented provides information about the internal fibroglandular breast structure, confirming the importance of updating the radiation dosimetry models, overcoming the limitation of the *average breast* model [1]. In this sense, the Task Group/Workgroup No. 282 recently formed by the American Association of Physicists in Medicine (AAPM) and the European Federation of Organization for Medical Physics (EFOMP), aims to develop a more universal breast dosimetry models for x-ray mammography and breast tomosynthesis.

REFERENCES

[1] DANCE, DR., SECHOPOULOS, I., "Dosimetry in x-ray-based breast imaging", Phys. Med. Biol. **61** (2016) R271-R304.

[2] SECHOPOULOS, I., BLIZNAKOVA, K., QIN, X., FEI, B., FENG, SSJ. "Characterization of the homogeneous tissue mixture approximation in breast imaging dosimetry" Med. Phys. **39** (2012) 5050-5059.

[3] HERNANDEZ, AM., SEIBERT JA., BOONE, JM. "Breast dose in mammography is about 30% lower when realistic heterogeneous glandular distributions are considered" Med. Phys. **42** (2015) 6337-6348.

[4] SECHOPOULOS, I., FENG, SSJ., D'ORSI, CJ., "Dosimetric characterization of a dedicated breast computed tomography clinical prototype", Med. Phys. **37** (2012) 4110-4120.

[5] CABALLO, M., BOONE, JM., MANN, R., SECHOPOULOS, I. "An unsupervised automatic segmentation algorithm for breast tissue classification of dedicated breast computed tomography images", Med. Phys. **45** (2018) 2542-2559.

Assessment of Entrance Skin Dose of Four Groups of Children Arising from Angiography Procedures

M. T. Bahreyni Toossi[a]
H. Zare[a], Z. Eslami[a], M. Mehrpouyan[b], B. Alizadeh[c], H. Birjandi[c], M. Sedighpour[a]

[a]Medical Physics Research Center, Mashhad University of Medical Sciences, Mashhad, Iran
[b]Sabzevar University of Medical Sciences, Sabzvar, Iran
[c]Department of Pediatric, Mashhad University of Medical Sciences, Mashhad, Iran

Email address of Corresponding Author: bahreynimt@mums.ac.ir

BACKGROUND

Congenital heart diseases (CHD) are a group of cardiovascular abnormalities that are present at birth but their cause are not known in 90% of cases. Congenital heart disease is the most common heart disease in children and infants. The incidence of congenital cardiac diseases is 8 cases per 1,000 [1,2]. There are several reasons to prescribe angiography for children and adults. In adults, angiography and angioplasty are often used for diagnosis and treatment of cardiovascular and coronary artery diseases, while in children it is mostly applied for children who suffer from inter ventricular hole or valve stenosis [3]. During the fluoroscopy procedure, the patient and the cardiologist are exposed. Many studies have focused on adult patients [4]. On average, the risk of early and late effects of exposure to radiation in infants and young children is higher than the older children. Therefore, attention to radiation protection of the infant and younger children seem to be very important [5]. According to the ICRP report No. 85 the threshold dose skin for effects of ionizing radiation should be 2 Gry, at the mean time it is emphasized that if a patient dose exceeds 2 Gy, the individual should be under clinical observation [6, 7].The aim of this study was to determine the coefficients obtained by the dose area product (DAP) used in angiographic procedures in various direction of X-ray tubes around the patient's body. The dose of the child's skin was calculated for four age groups. These coefficients were used to estimate maximum skin dose (MSD) of children who underwent from angiography and angioplasty. Also, DAP values acquired for each patient in combination with the above mentioned coefficients and the correlation between DAP values and dose enables us to compile a computer program in MATLAB or EXCEL in order to accurately estimate the patients dose.

METHODS

In this study, 66 patients underwent angiography in the catheterization laboratories (CATHLABs) department of Imam Reza hospital in Mashhad with Siemens AXIOM Artis Zee X ray C-arms. The Artis system is equipped with a DAP meter, consisting of an ionization chamber placed in front of the tube collimator. This system records DAP value for each imaging projection and saves all DAP values acquired throughout a complete procedure. DAP values include most clinical and geometric characteristics used in a radiological examination [8].The dosimeters used in this study were TLDs. TLD is a suitable dosimeter to measure maximum skin dose, as it provides very good accuracy, as well as the possibility of using multiple TLDs simultaneously on a wide surface. It should be noted that due to the high skin exposure, conventional film dosimeters could not be used. For each patient, 10 TLD chips were used. 6 TLD chips were placed at the back of the patient and 4 TLD chips were placed on both sides of armpit.In this study, four phantoms made of PMMA (Perspex) containing water, were used in different sizes representing four age groups and were considered as the patient on the bed. These phantoms were exposed to direct X-rays at various angles. For measuring the skin

dose on the phantom, an array of TLD dosimeters were placed on a 2.5 cm flat parabolic triangle. At each view, the phantom chest was exposed to X-ray for four seconds. And in the six most common views, each phantom was exposed for ten seconds.

RESULTS

Measured dose (skin dose) obtained from TLD values (placed on the phantom surface) and DAP values acquired from individual imaging angle $(DAP)_i$; recommended in this study were utilized and 29 coefficient were produced (X_i) Equation (1). In order to use recorded dosimetric quantities of individual patient to monitor his/her skin dose. Therefore, based on these coefficients and the DAP values, the patient skin dose can be estimated at the location of each array of TLDs for each patient.$X_i = \frac{(Skin\ Dose)_i}{(DAP)_i}$ (Obtained for a specific angle) (1), $(Skin\ Dose)_{total} = \sum_{i=1}^{n}\{\{X_i \times (DAP)_i\}$ (Total skin dose arising from a complete procedure) (2). We proposed these coefficients to create a computer program which enables us to use Siemens X-ray tube recorded data file so that we can use dosimetric information of patients to monitor his/her skin dose. For each patient, the coefficients were applied for different angles and the corresponding dose was calculated. Then, the results of the computational dose with the measured dose were compared for four phantoms.

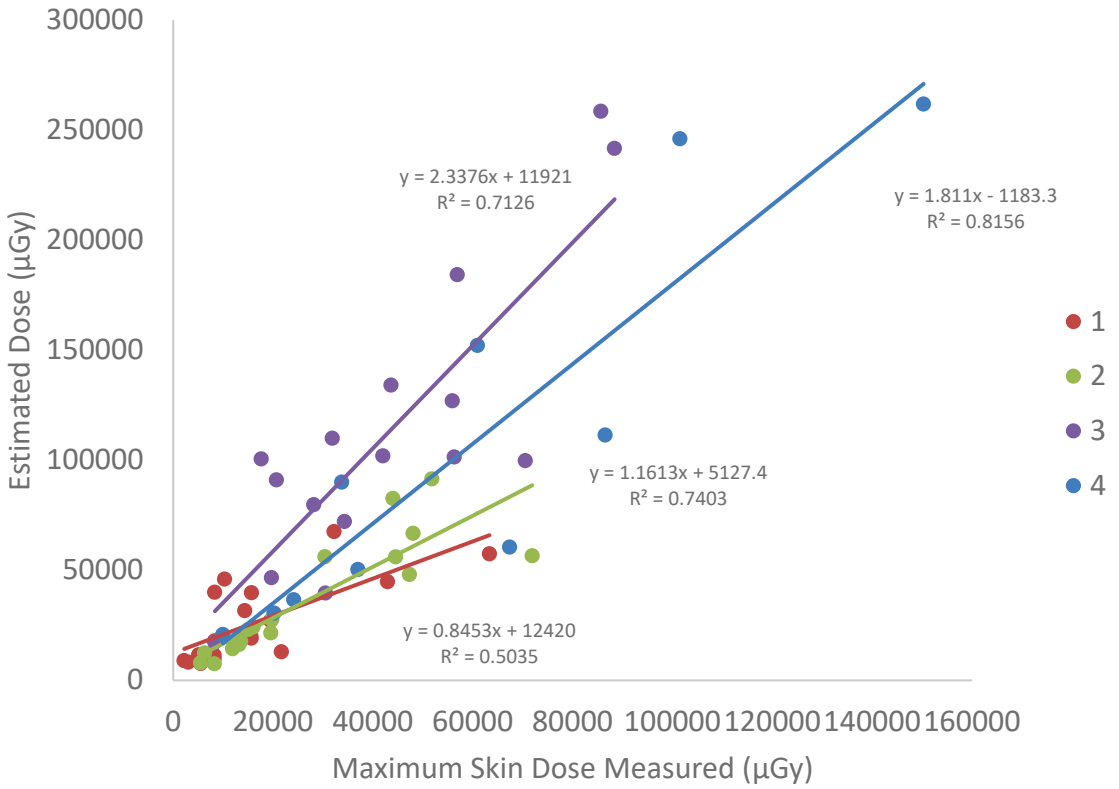

Figure 1. Scatter Plot shows relationship between maximum measured skin dose and estimated dose for different age groups

Average measured MSD patients for 1, 5, 10 and 15 age groups were, respectively, (µGy) 16550.4211 ± 15155.92725, 27485.1176 ± 19858.97947, 43169.2500 ± 23998.92050 and 59179.7000 ± 43739.87010. Estimated dose for Phantoms representing the four age groups were, respectively, 26409.1421 ± 18054.01557, 42542.2939 ± 34925.58975, 113416.7856 ± 63237.03966 and 119119.1500 ± 93909.77711.

CONCLUSIONS

According to our results, by increasing the size of the phantom, the correlations between the maximum skin dose and the estimation dose is increased. Comparison of correlation coefficient (R^2) of different age groups (Fig. 2) is indicating (R^2) for 1 year age group is less than the corresponding value for the other three age groups. It can be interpreted that the small size of this phantom causes more scattering of the data. According to the results of this study, Xi coefficient is influenced by the position of the tube relative to the patient, the experience and speed of the physician, the size of the patient, DAP, etc., and can be used to simply estimate patient dose incurred from cardiopulmonary vascular prescribed in diagnosis of children congenital diseases.

REFERENCES

[1] SALZER, H.R., HASCHKE, F., WIMMER, M., HEIL, M., SCHILLING R. Growth and nutritional intake of infants with congenital heart disease. Pediatr Cardiol [Internet]. 1989 Dec [cited 2018 Feb 4];10(1):17–23. Available from: http://www.ncbi.nlm.nih.gov/pubmed/2495525

[2] KNOWLES, R., GRIEBSCH, I., DEZATEUX, C., BROWN, J., BULL, C. "Newborn screening for congenital heart defects: a systematic review and cost-effectiveness analysis". (2005) [cited 2018 Feb 4]; Available from: https://www.ncbi.nlm.nih.gov/books/NBK62216/

[3] RAHIM, F., EBADI, A., SAKI, G., REMAZANI, A. "Prevalence of congenital heart disease in Iran: A clinical study". J Med Sci. (2008);8(6).

[4] TOOSSI, M. T. B, MEHRPOUYAN, M., NADEMI, H., FARDID, R., "Preliminary results of an attempt to predict over apron occupational exposure of cardiologists from cardiac fluoroscopy procedures based on DAP (dose area product) values." Australas Phys Eng Sci Med. (2015) ;38(1):83–91

[5] KHONG, P.L., RINGERTZ, H., DONOGHUE, V., FRUSH, D., REHANI, M., APPELGATE, K. et al. ICRP publication 121: radiological protection in paediatric diagnostic and interventional radiology. Ann ICRP. (2013) ;42(2):1–63.

[6] VALENTIN, J., Avoidance of radiation injuries from medical interventional procedures: ICRP Publication 85. In: Annals of the ICRP. (2000). p. 7–67.

[7] ICRP. ICRP 103: The 2007 Recommendations of the International Commission on Radiological Protection. Ann ICRP. 2007;37:330.

[8] HART, D.; JONES, D. G.; WALL B. F., "Estimation of effective dose in diagnostic radiology from entrance surface dose and dose-area product measurements" [Internet]. Chilton (United Kingdom); 1994. Available from: https://inis.iaea.org/search/searchsinglerecord.aspx?recordsFor=SingleRecord&RN=25049644

Dosimetry in the Presence of Magnetic Fields

Ion Chamber Dosimetry in a Magnetic Field for MR-Linac Applications

O. Jäkel[a]
B. K. Shukla[a], C. K. Spindeldreier[a], A. Pfaffenberger[a], S. Greilich[a], C. P. Karger[a]

[a]German Cancer Research Center (DKFZ), Heidelberg, Germany

Email address of Corresponding Author: o.jaekel@dkfz.de

BACKGROUND

Although the integration of magnetic resonance imaging (MRI) with a linear accelerator (LINAC) for radiotherapy has been suggested already in 2004 [1], the technical complexity is considerably. After the introduction of an integrated low field MRI into a Co-unit into clinical service in 2014 [2], it took until 2017 [3] until a low-field MR-Linac (0.35T) became clinically available [3]. In 2018 [4] another system with higher field strength (1.5T) became clinically available and both systems have become more and more widely available recently. These relatively recent developments ask for investigations of the perturbation of ion-chambers operated in a magnetic field.

METHODS

Before a dedicated MR-Linac became available in Heidelberg, an experimental electromagnet has been designed at the German Cancer Research Center for dosimetry investigations (Schwarzbeck AGEM 5520, Germany). The magnetic field strength is variable and at maximum 1.1 T is achieved. An integrated water cooling system limits heating of the magnet to less than 0.2 °C per measurement series. Ionization chambers can be positioned in the pole gap using a 3D-printed water tank with integrated chamber holders, fixing the chamber stem at the top of the water tank.

The magnet is transportable and was used together with a 6MV clinical linac (Artiste, Siemens Medical Solutions Inc., PA, USA). In Figure 1 the setup at the linac is shown.

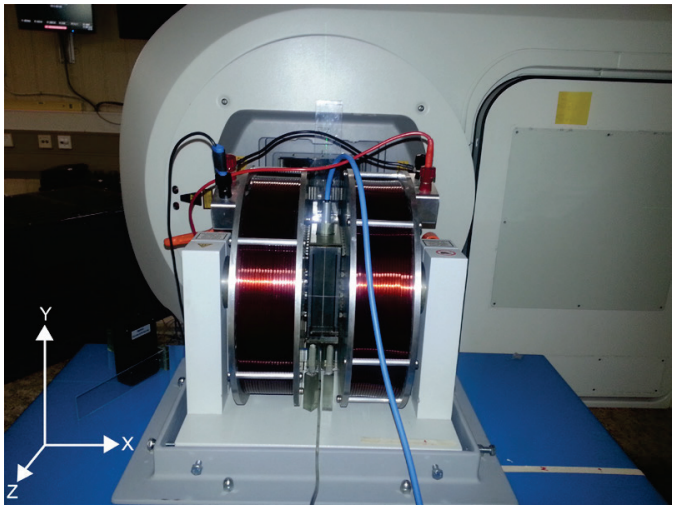

Figure 1. Setup of the electromagnet at the linac (Fig. from [5]).

With this system several measurement series have been performed and are already reported in [5] and [6]. In these series the effect of chamber size and orientation relative to the magnetic field and the beam orientation has been studied experimentally for various thimble type chambers. In order to understand the effects more systematically also Monte Carlo simulations have been carried out for the experimental setup using the EGS-4 code [7], which was recently

modified as to include the magnetic field effects and provided to us by I. Kawrakow. Also some investigations on polarity and recombination effects in the magnetic field were performed.

RESULTS

The largest increases in measurement signals of up to 8.6% were found experimentally for chambers with radii between 3 to 6mm at magnetic field strengths from 0.9T (for the 3mm inner radius) to 0.6T (for 6mm inner radius) for the magnetic field perpendicular to chamber and photon beam. The changes were significantly smaller for all chambers and field strengths (maximum around 1%) for the magnetic field parallel to the chamber axis and radiation beam.

The Monte Carlo simulations showed a very good agreement with the experimental data, when the chamber volume was corrected.

CONCLUSIONS

Magnetic field correction factors for Farmer-type chambers have been measured and calculated for different magnetic field strengths and field orientations. The response of the chambers depends on chamber radius, magnetic field strength and the orientation between radiation beam, chamber axis and magnetic field. The largest changes in response and thus in correction factors were observed for a magnetic field perpendicular to beam and chamber axis.

The exact definition of the sensitive volume of the chamber is important for the description of the measured data with Monte Carlo simulations, since the Lorentz force may deflect electrons towards or away from dead volume close to the guard electrode. It was found that a set-up with the magnetic field parallel to the chamber axis or parallel to the beam provides is more robust, since the correction factors as well as the influence of dead volumes are minimized.

REFERENCES

[1] LAGENDIJK J J W, RAAYMAKERS B W, VAN DER HEIDE U A, et al. (2002) MRI guided radiotherapy: MRI as position verification system for IMRT Radiother. Oncol. 64 (Suppl 1) 224 (Czech Republic European Society for Therapeutic Radiation Oncology)

[2] MUTIC S and DEMPSEY J F (2014) The viewray system: magnetic resonance-guided and controlled radiotherapy *Semin. Radiat. Oncol.* **24** 196–9

[3] https://www.henryford.com/news/2017/07/viewray-firstpatient

[4] RAAYMAKERS BW, JÜRGENLIEMK-SCHULZ IM, BOL GH, et al. (2017) First patients treated with a 1.5 T MRI-Linac: clinical proof of concept of a high-precision, high-field MRI guided radiotherapy treatment. Phys Med Biol. 62(23): L41-L50.

[5] SPINDELDREIER CK, SCHRENK O, BAKENECKER A, et al. (2017) Radiation dosimetry in magnetic fields with Farmer-type ionization chambers: determination of magnetic field correction factors for different magnetic field strengths and field orientations. Phys Med Biol. 62(16):6708-6728.

[6] SHUKLA BK, SPINDELDREIER CK, KARGER CP, et al. (2017) Magnetic field influence on the response of the exradin A1SLMR ionization chamber, Medical Physics in the Baltic states, Proceedings of the 13th International Conference on Medical Physics 11. November 2017. http://www.medphys.lt/medphys2017/images/MedPhys2017_Proceedings.pdf

[7] KAWRAKOW I, MAINEGRA-HING E, TESSIER F et al. (2009) The EGSnrc C++ class library *NRC Report* PIRS-898 (rev A) National Research Council, Canada

A Water Calorimeter for Absorbed Dose to Water Measurements in an MR-Linac

A. Krauss[a]
U. Ankerhold[a], K. Spindeldreier[b], S. Klüter[b]

[a] Physikalisch-Technische Bundesanstalt, Department of Dosimetry for Radiation Therapy and Diagnostic Radiology, 38116 Braunschweig, Germany
[b]Heidelberg University Hospital, Department of Radiation Oncology, 69120 Heidelberg, Germany

Email address of Corresponding Author: achim.krauss@ptb.de

BACKGROUND

MR-linacs combine magnetic resonance imaging (MRI) and a medical linear accelerator in one device and have the potential to further improve the outcome of radiation therapy by enabling online adaptive treatment planning [1]. Several devices which use 6 MV or 7 MV linacs with a magnetic field strength between 0.35 T and 1.5 T are already in clinical application. To enable accurate dosimetry with ionization chambers in the presence of magnetic fields, the influence of the magnetic field on the response of dosimetric detectors and on the dose distribution itself must be considered. Recently, several experimental and theoretical investigations on this issue have been performed [e.g. 2, 3, 4, 5]. The most direct method to investigate the influence of magnetic fields in dosimetry is realized by the application of an appropriate absorbed dose to water standard. At PTB, a new water calorimeter has been designed which is capable of determining D_w in an MR-linac. This is comparable to a development by de Prez *et al* 2016 [6]. The new device allows the direct calibration of ionization chambers in terms of absorbed dose to water for MR-linac irradiation conditions and hence the determination of their correction factor $k_{Q,B}$ which replaces the current radiation-quality dependent correction factor k_Q [7].

METHODS

As is common for other water calorimeters operated at PTB [8], the new water calorimeter is operated at a water temperature of 4 °C and is designed for horizontal irradiations. The use of metallic materials was avoided as far as possible during the construction of the calorimeter. To fit into the 70 cm diameter bore of an MR-linac, the outer edge length of the cubic calorimeter had to be limited to about 45 cm in height and depth. Simultaneously, the water phantom inside the calorimeter was downsized to about 22 cm x 30 cm x 24 cm (height, width, depth). The same type of detector as used in other PTB water calorimeters can be placed at a specified water depth inside the phantom. Ionization chambers can be directly calibrated inside the water phantom of the calorimeter at the same measurement position as the calorimetric detector was placed before. In the case of cylindrical ionization chambers, they can be mounted in the water phantom with the cylinder axis aligned perpendicular or parallel to the direction of the magnetic field. A large-area transmission ionization chamber is mounted in front of the radiation entrance window of the calorimeter to monitor the dose rate of the linac.

RESULTS

After assembling, measurements with the new water calorimeter were performed with 8 MV photon radiation at one of PTB's linacs and with ^{60}Co radiation to generally verify the long-term capability of the calorimeter for sensitive D_w determinations. A direct comparison with

PTB's primary standard water calorimeter at ^{60}Co radiation showed an agreement on a 0.1 % level. Furthermore, the set-up of the calorimeter was successfully tested at the 6 MV, 0.35 T Viewray MRIdian system at Heidelberg University Hospital.

CONCLUSIONS

The new water calorimeter allows direct measurements of $k_{B,Q}$ factors of ionization chambers. Within a collaboration between PTB and Heidelberg University Hospital, measurements with the calorimeter and with different cylindrical ionization chambers are in progress at the MRIdian system in Heidelberg. Preliminary results regarding $k_{B,Q}$ factors for different orientations of the chambers in respect to the direction of the magnetic field will be presented.

REFERENCES

[1] RAYMAKERS, B.W., LAGENDIJK, J.J.W., OVERWEG, J., KOK, J.G.M., RAAIJMAKERS, A.J.E., KERKHOF, E.M., VAN DER PUT, R.W., MEIJSING, I., CRIJNS, S.P.M., BENEDOSSO, F., VAN VULPEN, M., DE GRAAFF, C.H.W., ALLEN, J., BROWN, K.J., Integrating a 1.5 T MRI scanner with a 6 MV accelerator: Proof of concept, Phys. Med. Biol. **54** (2009) N229-N237.

[2] SMIT, K., VAN ASSELEN, B., KOK, J.G.M., AALBERS, A.H.L., LAGENDIJK, J.J.W., RAAYMAKERS, B.W., Towards reference dosimetry for the MR-linac: magnetic field correction of the ionization chamber reading, Phys. Med. Biol. **58** (2013) 5945–57.

[3] O'BRIEN, D.J., ROBERTS, D.A., IBBOTT, G.S., SAWAKUCHI, G.O., Reference dosimetry in magnetic fields: formalism and ionization chamber correction factors, Med. Phys. **43** (2016) 4915–27.

[4] SPINDELDREIER, C.K., SCHRENK, O., BAKENECKER, A., KAWRAKOW, I., BURIGO, L., KARGER, C.P., GREILICH, S., PFAFFENBERGER, A., Radiation dosimetry in magnetic fields with Farmer-type ionization chambers: determination of magnetic field correction factors for different magnetic field strengths and field orientations, Phys. Med. Biol. **62** (2017) 6708–28.

[5] POJTINGER, S., DOHM, O.S., KAPSCH, R.-P., THORWARTH, D., Ionization chamber correction factors for MR-linacs, Phys. Med. Biol. **63** (2018) 11NT03.

[6] DE PREZ, L., DE POOTER, J., JANSEN, B., AALBERS, T., A water calorimeter for on-site absorbed dose to water calibrations in ^{60}Co and MV-photon beams including MRI incorporated treatment equipment, Phys. Med. Biol. **61** (2016) 5051-76.

[7] VAN ASSELEN, B., WOODINGS, S.J., HACKETT, S.L., VAN SOEST, T.L., KOK, J.G.M., RAAYMAKERS, B.W., WOLTHAUS, J.W.H., A formalism for reference dosimetry in photon beams in the presence of a magnetic field, Phys. Med. Biol. **63** (2018) 125008.

[8] KRAUSS, A., The PTB water calorimeter for the absolute determination of absorbed dose to water in ^{60}Co radiation, Metrologia **43** (2006) 259-72.

Calorimetry-Based Clinical Reference Dosimetry of a 1.5 T MRI-Linac in Water and Solid Phantoms Using Aerrow

J. Renaud[a]
A. Sarfehnia[a,b], **J. Bancheri**[a], **J. Seuntjens**[a]

[a]McGill University, Medical Physics Unit, 1001 Decarie Blvd., Montreal, Quebec, Canada
[b]University of Toronto, 27 King's College Circle, Toronto, Ontario, Canada

Email address of Corresponding Author: james.renaud@mail.mcgill.ca

BACKGROUND

As a more direct alternative to ion chamber-based clinical reference dosimetry, a probe-format graphite calorimeter – herein referred to as Aerrow – has been developed in-house with the goal of measuring absolute dose in the clinic with a minimum disruption to the existing clinical workflow [1-2]. Similar in size and shape to a 0.6 cm^3 cylindrical ion chamber, Aerrow has been developed to help meet the clinical need for dosimetry in non-standard fields while exceeding the dosimetric accuracy currently achievable with calibrated ion chambers, currently the gold standard of clinical reference dosimetry. The purpose of this study was to build and to evaluate the possible use of Aerrow as a practical absolute clinical dosimeter (*e.g.*, use in solid phantoms) of high-energy photon beams while in the presence of a 1.5 T magnetic field.

METHODS

Based on a numerically-optimized design obtained in previous work [2], an Aerrow prototype capable of isothermal operation was constructed in-house using a new mechanically-rigid formulation of aerogel-based material (Airloy® X103, Aerogel Technologies LLC.) [3]. In isothermal mode, the sensitive volume is subject to thermal control and the measurand is the power required to maintain a stable temperature during irradiation. The ratio of the power and absorber mass is a direct measure of the dose rate.

Aerrow was used to perform comparative reference dosimetry in the 7-MV FFF photon beam of an MRI-linac (Elekta Unity clinical prototype) with and without the presence of the 1.5 T magnetic field against two calibrated reference-class ion chambers (Exradin A19 & Exradin A1SL, Standard Imaging Inc.). The measurements were carried out both in water and in water-equivalent solid phantom (Solid Water HE, Sun Nuclear Corp.) at a depth of 10 cm, an extended SAD of 143.5 cm, and otherwise standard conditions for two detector orientations (parallel and perpendicular to the magnetic field). Dose conversions and magnetic field perturbations, k_B, were calculated using the EGSnrc Monte Carlo code system [3-4].

RESULTS

Calculated values of k_B (B = 1.5 T) for the prototype Aerrow were found to be unity to within 0.1 % for all detector orientations and phantom mediums considered in this study. This result contrasts with air-filled ion chambers, which tend to exhibit correction factors of several percent when the detector major axis is oriented perpendicular to both the magnetic and radiation fields [5-6]. Table 1 summarizes the results of the reference dosimetry measurements. Doses to water determined in water and solid phantoms were shown to be equivalent for both orientations when using Aerrow. Ion chamber measurements in solid phantom were found to be unreproducible (with variation greater than 2 %) depending on the positioning of the ion chamber with respect to its major axis inside the phantom. This behavior is in accordance with the results observed by other groups and is related to non-symmetric air gaps present between the ion chamber and the solid phantom and their effect on the cavity response [7]. In contrast,

variations in Aerrow response as a function of detector rotation about its major axis in the solid phantom was on the order of 0.2 %, both with and without magnetic field present.

Table 1. Summary of reference dosimetry comparison performed in the MRI-linac. Stated uncertainty represents combined standard uncertainty on absorbed dose to water (k=1).

Detector type	Detector orientation & phantom	Magnetic field magnitude (T)	Measured dose to water (cGy per 100 MU)
Aerrow	Parallel & water	0	80.2±0.6
Exradin A19	Parallel & water	0	80.3±0.7
Exradin A1SL	Parallel & water	0	79.6±0.7
Aerrow	Parallel & water	1.5	79.5±0.6
Exradin A19	Parallel & water	1.5	79.2±0.6
Exradin A1SL	Parallel & water	1.5	78.8±0.6
Aerrow	Perpendicular & water	1.5	79.5±0.6
Exradin A19	Perpendicular & water	1.5	80.6±0.6
Exradin A1SL	Perpendicular & water	1.5	80.2±0.6
Aerrow	Parallel & solid	1.5	78.6±0.6
Aerrow	Perpendicular & solid	1.5	78.6±0.6

CONCLUSIONS

Within combined standard uncertainty, all absorbed doses to water determined using Aerrow agreed with corresponding ion chamber reference measurements. Results of this study suggest that applying k_B is unnecessary when using Aerrow, and that the accurate use of solid phantoms in the presence of a 1.5 T magnetic field is feasible.

REFERENCES

[1] RENAUD, J., MARCHINGTON, D., SEUNTJENS, J., SARFEHNIA, A., Development of a graphite probe calorimeter for absolute clinical dosimetry, Medical Physics 40 (2013) 020701-1.

[2] RENAUD, J., SARFEHNIA, A., BANCHERI, J., SEUNTJENS, J., Aerrow: A probe-format graphite calorimeter for absolute clinical dosimetry of high-energy photon beams, Medical Physics 45 (2018) 414.

[3] BANCHERI, J., SEUNTJENS, J., SARFEHNIA, A., RENAUD, J., Density effects of silica aerogel insulation on the performance of a graphite probe calorimeter, Medical Physics (2018) [*Accepted*]

[4] KAWRAKOW, I., ROGERS, D.W.O, The EGSnrc code system: Monte Carlo simulation of electron and photon transport, NRC Technical Report No. PIRS-701 v4-2-2-5 (National Research Council of Canada, Ottawa, Canada, 2007).

[5] O'BRIEN, D.J., ROBERTS, D.A., IBBOTT, G.S., SAWAKUCHI, G.O., Reference dosimetry in magnetic fields: formalism and ionization chamber correction factors, Medical Physics 43 (2016) 4915.

[6] MALKOV, V.N., ROGERS, D.W.O., Monte Carlo study of ionization chamber magnetic field correction factors as a function of angle and beam quality, Medical Physics 45 (2018) 908.

[7] HACKETT, S.L., VAN ASSELEN, B., WOLTHAUS, *et. al.*, Consequences of air around an ionization chamber: Are existing solid phantoms suitable for reference dosimetry on an MR-linac? Medical Physics 43 (2016) 3961.

Design and Performance of an MR-Compatible Calorimeter

M. Dsouza[a]
H. Nusrat[a], J. Renaud[b], G. Peterson[a], N. Entezari[a], A. Sarfehnia[a,c]

[a]Ryerson Department of Physics, Toronto, Canada
[b]National Research Council Canada, Ottawa, Canada
[c]University of Toronto Department of Radiation Oncology, Toronto, Canada

Email address of Corresponding Author: mark.dsouza@ryerson.ca

BACKGROUND

Absorbed dose water calorimetry has been a standard method for obtaining absolute dose to water. By measuring the radiation induced milli-kelvin temperature rise in water and taking into account the specific heat capacity of water, the accurate dose at the point of measurement can be determined [1]. Although water calorimetry has been established and used in high energy photon beams, its application to other particle types and/or novel radiotherapy delivery technologies has been limited.

With the recent advancements in image-guided radiotherapy, and the emergence of MR-integrated linear accelerators, the application of water calorimetry directly in an Elekta MR-linac (1.5 T, 7.2 MV) was studied. The aim of this work was to construct an MR-compatible portable 4 ºC cooled stagnant water calorimeter and use this to measure absolute dose in the presence of a magnetic field.

METHODS

Finite Element Method (FEM) software (COMSOL Multiphysics 4.4) was used to optimize the design of a water calorimeter (FIG1a,b). A systematic approach was taken where several water tank overall wall designs, wall thicknesses, and insulator materials (Cryogel (Aspen Aerogels, Northborough, USA), air, and Styrofoam) were simulated in order to minimize non-radiation induced temperature fluctuations within the calorimeter itself. All photon dose distributions used in the FEM analysis were simulated using Monte Carlo simulation (GEANT4.10.3). In order to minimize heat conduction at the point of measurement (i.e. thermistors), several simulations were carried out to look at the effects of various parameters related to glass vessel (vessel radius, glass thickness and separation, thermistor position inside the glass vessel, etc.) on conduction at the level of thermistors. This simulation-driven calorimeter design was based on choosing tank and vessel designs and materials that resulted in the most robust thermal stability inside the tank (in face of realistic simulated ambient thermal variations) and yielded least heat conduction in the vicinity of the thermistors.

Construction of the calorimeter was performed in-house using only plastic and ceramic components, making it MR-compatible. A preliminary performance evaluation of the calorimeter was done experimentally both in a conventional Elekta Agility linac as well as in an Elekta MR-linac (Elekta AB, Stockholm, Sweden). By analyzing the change in resistance of the thermistors using midpoint extrapolation, the temperature was determined. The two thermistors inside the vessel were then removed and replaced with an NRC calibrated A1SL ion chamber.

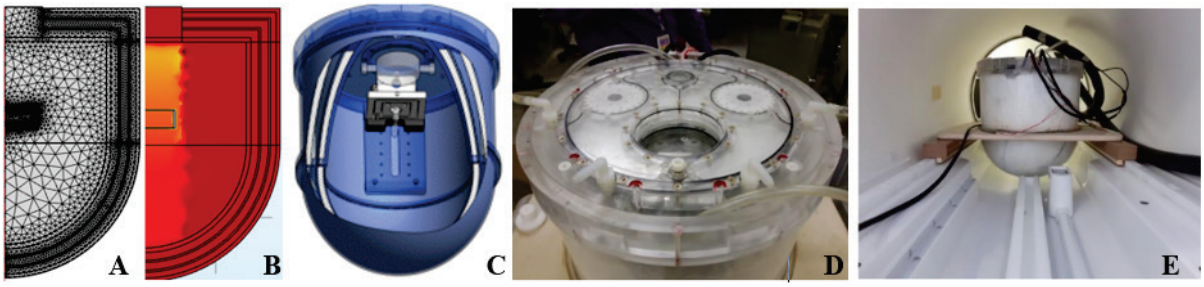

Figure 1. Methodology from A) 2D axial resolution slice of initial design of calorimeter in FEM software with meshing B) a sample 2D axial slice of calorimeter design with thermal distribution C) Calorimeter design in CAD software D) Final constructed lid design E) Final constructed design placed in Bore of the MR-linac

RESULTS

The calorimeter lid turned out to be the most complicated component of the calorimeter. It consisted of several layers that ensured pathways for coolant to evenly cool the calorimeter lid, as well as separate pathways for hydraulically driven stirrers. Furthermore, FEM analysis showed that a three acrylic shell system using Cryogel as insulation between the shells provided protection against both ambient temperature fluctuations of up to 2 ºC, as well as any periodic or random coolant temperature variations of up to 0.3 ºC. In order to accommodate measurements in Gamma Knife (Elekta AB, Stockholm, Sweden) and any volumetric delivery techniques, a secondary goal of the project, the final calorimeter design had a cylindrical top for beam irradiation from top using conventional linac geometry, and a hemispherical bottom for irradiations from the side (FIG 1).

FEM analysis showed that conduction sensitivity was most dependent on glass vessel wall thickness. The final water calorimeter was shown to be not only fully MR compatible, but it was also experimentally verified that the thermistors were visible in both MR and kV images. As such, our water calorimeter can be positioned in place for measurement using modern high-resolution imaging alone. Initial measurements (n=31) inside the MR-linac in the absence of the magnetic field were performed and yielded a 1.7% standard error, and the measured dose agreed to within 2% of that measured with a calibrated A1SL ion chamber. Based on these results, the insulation for the lid of the calorimeter was increased to improve thermal stability, and measurements under the MR-linac in the presence of the magnetic field are underway.

CONCLUSIONS

A water calorimeter was optimized and then constructed that is MR-compatible and can be imaged by kV x-rays or MRI for accurate positioning. Absolute dose measurements under a 7.2MV beam in the absence of magnetic field were carried out. The calorimeter lid has since been further insulated to minimize heat loss, and measurements in MR-linac are underway.

REFERENCES

[1] SEUNTJENS, J., DUANE, S., Photon absorbed dose standards, Metrologia **46** 2 (2009) 39.

[2] SEUNTJENS, J., DUSAUTOY, AR., Review of calorimeter-based absorbed dose to water standards, IAEA-CN- 96-3, Vienna, Austria, IAEA (2003) 37.

FEM Corrections for Monte Carlo Simulations of Ionization Chambers in Magnetic Fields

S. Pojtinger[a,c]
R.-P. Kapsch[a], O. Dohm[b], D. Thorwarth[c]

[a]Physikalisch-Technische Bundesanstalt, Braunschweig, Germany
[b]Department for Radiation Oncology, University Hospital Tübingen, Tübingen, Germany
[c]Section for Biomedical Physics, Department for Radiation Oncology, University Hospital Tübingen, Tübingen, Germany

Email address of Corresponding Author: stefan.pojtinger@ptb.de

BACKGROUND

Recent advances in the development of MR-linacs in which medical linacs are combined with an MR component for online imaging have generated interest in Monte Carlo simulations of the response of dosimetric detectors in magnetic fields. In early publications, significant deviations were found between experimental results and Monte Carlo simulations of the response of ionization chambers in magnetic fields [1], [2]. In a more recent work, it has been shown that this deviation becomes smaller if the sensitive volume of the ionization chamber is changed in a semi-empirical way [3].

In the work presented here, it is shown that agreement between the measurement and simulation results of better than 0.25 % can be achieved by combining Monte Carlo (MC) with Finite Element Methods (FEM) using a purely theoretical approach.

METHODS

COMSOL Multiphysics was used to simulate the electric field inside a PTW 30013 Farmer ionization chamber by means of finite element methods. The approach of Ross [4], who describes the sensitive volume of an ionization chamber as the volume in which the electric field lines reach from the wall to the central electrode of the ionization chamber, was followed to adjust the sensitive volume of the simulated chamber model. This approach involves discarding a large part of the volume near the ionization chamber's guard ring, where the electric field lines land in the guard of the ionization chamber instead of the central electrode. A script was written that, based on electric field lines calculated in COMSOL, creates an input file describing the adjusted sensitive volume geometry of the ionization chamber for the Monte Carlo code EGSnrc. The egs_chamber EGSnrc usercode was used to simulate this FEM adjusted ionization chamber geometry for magnetic flux densities up to 1.5 T in a setup in which all pairwise orientations between the ionization chamber axis, the magnetic field vector and the beam direction are perpendicular. This orientation features the greatest dominance of the magnetic field effect on the chamber's response and the largest deviations between the simulations and the experiments. To simulate the beam, an Elekta medical accelerator was modeled in BEAMnrc and the ionization chamber was put in a 30 x 30 x 20 cm^3 water phantom at a depth of 10 cm. All simulation parameters were set in accordance with ICRU 90. A similar setup was established in an experiment at the Metrological Accelerator Facility (MELAF), at PTB in Braunschweig [5]. To this end, a large electromagnet (Bruker E073) was placed in front of an Elekta medical accelerator. As the space between the pole shoes of the electromagnet was 6 cm throughout the experiment, a 20 x 20 x 6 cm^3 water phantom was used for measurements. The measurement of the ionization chamber was repeated on three different days, including a full repositioning of the chamber. The chamber was preirradiated with at least

1000 MU and the beam was active during the whole measurement to maintain a stable output; this output was monitored by an onsite transmission monitor chamber [6] mounted on the accelerator's head. For the measurement of the relative response of the ionization chamber in magnetic fields, the magnetic flux density between the pole shoes was controlled up to 1.5 T in steps of 0.15 T. The ionization current was measured for the Farmer ionization chamber as well as for the monitor chamber, for each magnetic flux density. Measurements at 0 T were taken in between these measurements. For the calculation of the relative response of the ionization chamber, the mean ionization current of the Farmer ionization chamber was normalized to the mean ionization current of the monitor chamber for each magnetic flux density. Later, these values were divided by the normalized mean ionization current of the Farmer ionization chamber at 0 T, resulting in the relative response.

RESULTS

The results of the simulations as well as those of the experiments are shown in Figure 1. Negative magnetic flux densities are used if the secondary electrons are deflected to the ionization chamber's tip; a positive sign is given if the electrons are deflected to the stem. While there are deviations of more than 1 % for the simulation without FEM adjustments the FEM adjusted simulation matches the experimental values within the uncertainty. The mean squared deviation between the simulated and experimental results with and without FEM adjustments is 0.21(34) % and 1.03(32) %, respectively.

CONCLUSIONS

The adjustment of the sensitive volume of ionization chambers is mandatory for Monte Carlo simulations in magnetic fields. To maintain the theoretical character of Monte Carlo simulations, it is possible to calculate the adjustments needed based on FEM simulations without relying on experimental data. This results in excellent agreement between measurements and simulations of the response of a Farmer ionization chamber.

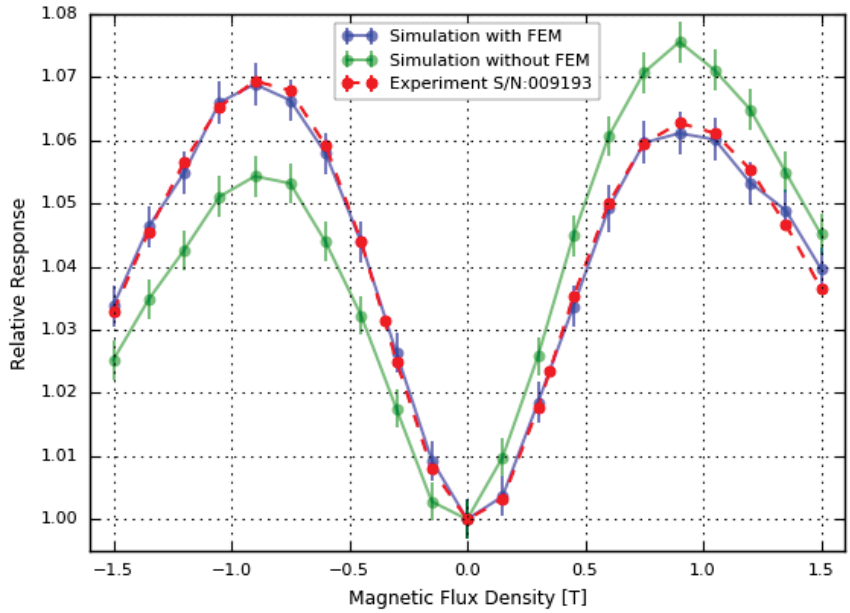

Figure 1. Relative response of a PTW 30013 Farmer ionization chamber in a magnetic field. The experimental results are compared to the results of the Monte Carlo simulation with and without FEM adjustments of the sensitive volume

REFERENCES

[1] I. MEIJSING *et al.*, “Dosimetry for the MRI accelerator: the impact of a magnetic field on the response of a Farmer NE2571 ionization chamber,” *Phys. Med. Biol.*, vol. 54, no. 10, pp. 2993–3002, May 2009.

[2] V. N. MALKOV AND D. W. O. ROGERS, “Charged particle transport in magnetic fields in EGSnrc,” *Med. Phys.*, vol. 43, no. 7, pp. 4447–4458, Jun. 2016.

[3] C. K. SPINDELDREIER *et al.*, “Radiation dosimetry in magnetic fields with Farmer-type ionization chambers: Determination of magnetic field correction factors for different magnetic field strengths and field orientations,” *Phys. Med. Biol.*, vol. 62, no. 16, pp. 6708–6728, Aug. 2017.

[4] C. K. ROSS, “Comments on ‘Ionization chamber volume determination and quality assurance using micro-CT imaging,’” *Phys. Med. Biol.*, vol. 54, no. 6, pp. 23–27, Mar. 2009.

[5] A. SCHÜLLER, S. POJTINGER, M. MEIER, C. MAKOWSKI, AND R. P. KAPSCH, “The metrological electron accelerator facility (MELAF) for research in dosimetry for radiotherapy,” in *IFMBE Proceedings*, 2019, vol. 68, no. 3, pp. 589–593.

[6] R. P. KAPSCH AND A. KRAUSS, “On the performance of monitor chambers to measure the output of medical linear accelerators for high-precision dosimetric investigations,” in *IFMBE Proceedings*, 2009, vol. 25, no. 1, pp. 85–88.

Developing a Dosimetry Audit for MRI-Linacs

R. Brown[a]
U. Jelen[b], **J. Begg**[b,c,d], **J. Lye**[a]

[a]Australian Radiation Protection and Nuclear Safety Agency, Melbourne, Vic, Australia
[b]Ingham Institute for Applied Medical Research, Liverpool, NSW, Australia
[c]Department of Medical Physics, Liverpool and Macarthur Cancer Therapy Centre, Sydney, NSW, Australia
[d]South Western Sydney Clinical School, University of New South Wales, Liverpool, NSW, Australia

Email address of Corresponding Author: rhonda.brown@arpansa.gov.au

BACKGROUND

MRI guided radiotherapy incorporates a linear accelerator with an on-board MRI scanner. An MRI-linac provides enhanced soft-tissue image contrast in real time during a patient's treatment. The strong advantages of improved targeting have led to implementation of MRI-linacs around the world. The new technology comes with new quality challenges, and independent dosimetry audit is a useful tool to assess the commissioning of these new treatment deliveries.

METHODS

The Australian clinical dosimetry service (ACDS) is developing both reference dosimetry and end-to-end audits. As part of the audit development, the ACDS performed a multichamber comparison in the Australian MR Linac (AML) located in Sydney, Australia, and imaging tests on an anthropomorphic phantom composed of CIRS solid water, CIRS inhale lung, and custom MR visible inserts, as shown in Figure 1.

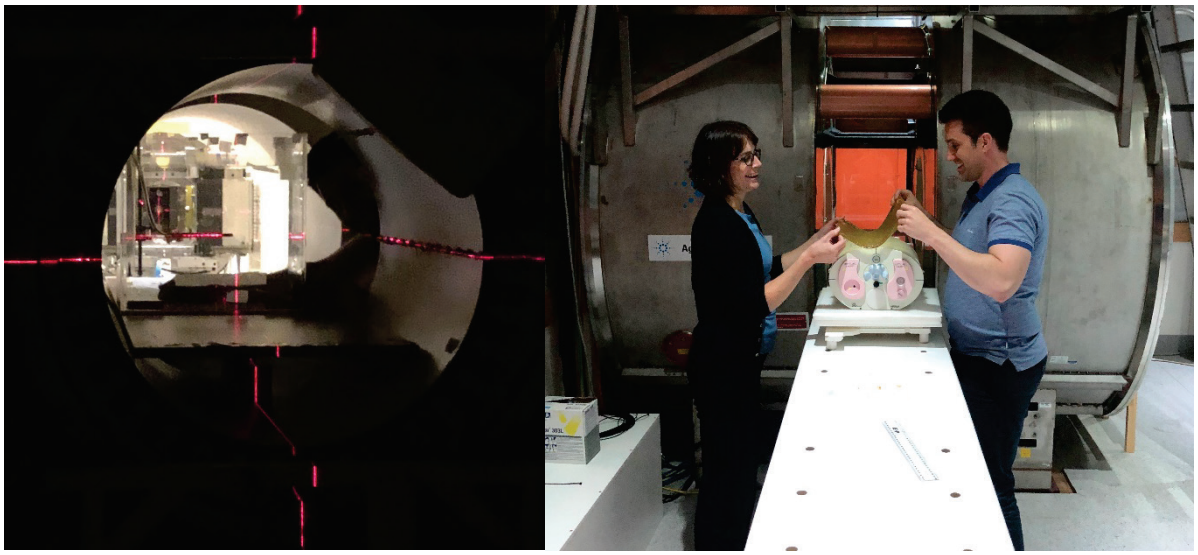

Figure 1. On left, Farmer type chamber in water tank with horizontal beam, chamber perpendicular to the magnetic field which is in-line with radiation beam. On right the anthropomorphic phantom is prepared for imaging.

The multichamber comparison was performed between two waterproof Farmer type chambers, FC-65G and PTW30013, a CC13, and a PTW 60019 microDiamond. The calibration of the FC-65G is traceable to the National Physical Laboratory (NPL), while the other three chambers

are traceable to the Australian Radiation Protection and Nuclear Safety Agency (ARPANSA). A 1% magnetic field correction is applied to the three ionization chambers, and no magnetic field correction is applied to the microDiamond. The 1% magnetic field correction was measured by the NPL for the FC-65G in the AML using alanine as the transfer. All chambers, including the microDiamond, are placed perpendicular (side-on) to the radiation beam.

RESULTS

Figure 2 shows the results of the multichamber comparison performed in a water tank and in a solid water slab phantom. All results are normalized to the dose measured by the FC-65G chamber in the water tank. The standard ACDS optimal level for a photon reference level dosimetry audit is agreement of 1.4 % (2σ) between the facility and ACDS measurement of dose in a 10cm×10cm field. All measurements agree at the ACDS optimal level. Water was injected into the 30013 and CC13 cavities in the solid water phantoms. The dosimetry was repeated and differences of 0.48% and -0.15% were observed respectively between the dry and wet solid water setup.

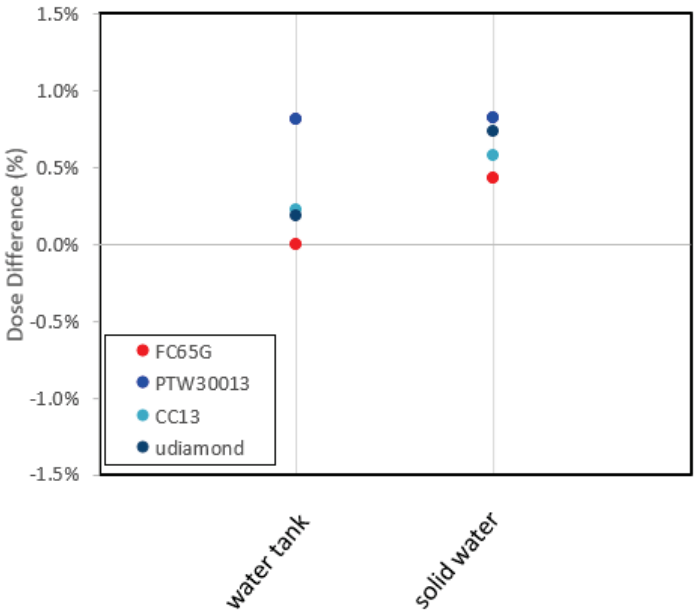

Figure 2. Multi-chamber dosimetry comparison with an in-line magnetic field configuration, performed both in water tank, and also in solid water (dry).

CONCLUSIONS

A multichamber comparison in reference conditions in an inline MR Linac configuration showed optimal agreement for all chambers, including a side-on microDiamond. MR visible inserts into a heterogeneous solid water and lung phantom provided sufficient signal for image-guided setup. This phantom would not be suitable for MR-only planning and a CT would be required for this type of end-to-end audit.

QA Detectors and Dosimetry Processes

QA: Detectors and Dosimetry Methods

N. Jornet[a]

[a]Servei de Radiofisica i Radioprotecció. Hospital Sant Pau, Barcelona, Spain

Email address of Corresponding Author: njornet@santpau.cat

BACKGROUND

One of the most critical steps in Radiation Oncology is the accurate commissioning and periodic Quality Assurance of treatment units and treatment planning systems. A clear understanding of the operating principles of the different radiation detectors and in particular of their limitations is fundamental to choose the correct detector for a particular measurement.

METHODS

Clear guidance of how reference dosimetry for high, medium and low energy X-ray beams, electron and particles beam has been provided by Reference Dosimetry Codes of Practice (CoP) [1-3]. Dosimetry audits have shown that centers that strictly follow a CoP present results within tolerance limits and therefore reduce the variability between centers [4-5]. CoP clearly state the detector that should be use and give guidance on the measuring methodology.

However, when we move away from reference conditions these CoP do not apply and therefore is up to the Medical Physicist to decide on the detector to use and also on the measuring methodology. For instance, when measuring output factors for large field x-ray beams difference up to 5% when using different detectors can be found. When increasing field size there is a higher contribution of scattered radiation to the detector response, therefore the energy dependence of the used detector has to be considered. Otherwise, we risk to over or underestimate the absorbed dose.

Small field dosimetry is probably the clearest case in which the understanding of the limitations of the different available detectors, as well as an exquisite measuring methodology is of outmost importance. Detector volume, energy dependence, perturbation effects have to be accounted for when choosing and using a detector for output factor determination in small field. Accidents affecting patients have been reported in cases in which a wrong detector has been used [6]. As the use of small fields has been expanding in the last years and aware of the challenges in performing a correct dosimetric characterization of those fields, IAEA and AAPM have recently published a code of practice [7] on small field dosimetry. Still, the accurate modelling of small fields and how the correct detector is used to collect the commissioning data is still challenging.

2D and 3D detectors passive and active are used in routine for daily output and beam symmetry and flatness constancy checks, patient specific pre-treatment verifications for IMRT and VMAT techniques. Most of those dosimetry systems are associated with a commercial software that is used both for the system calibration and measuring processes and also for the evaluation of measurements. Understanding of how these systems work is fundamental, otherwise inaccurate measurements could lead to suboptimal or even wrong patient treatments. AAPM has published guidelines on best practice when using these devices for IMRT/VMAT commissioning and pre-treatment verifications [8].

Most of the detectors used for beam characterization, 1D and 2D, can also be used for in vivo dosimetry. In vivo dosimetry constitutes the last check on the dosimetry chain, as it is

performed on the patient while he or she is being treated. The design of the detectors as well as the calibration has to be adjusted for this purpose.

CONCLUSIONS

Clinical Medical Physicists need an in depth understanding of radiation detectors and dosimetry methods in order to guarantee the quality and safety of radiation oncology treatments.

REFERENCES

[1] ANDREO, P, Burns DT, Hohlfeld K, Huq MS, Kanai T, Laitano F et al. Absorbed dose determination in external beam radiotherapy: an international code of practice for dosimetry based on standards of absorbed dose to water: IAEA Proc Ser Stand Codes Pract Med Radiat Dosim IAEA – TRS 398 (ISBN 92-0-102200-X) (2000).

[2] ALMOND, PR, Biggs PJ, Coursey BM, Hanson WF, Huq MS, Nath R et al. Protocol for clinical reference dosimetry of high-energy photon and electron beams. AAPM TG51 (1999):1847–70.

[3] AALBERS AHL, Hoornaert M-T, Minken A, Palmans H, Pieksma MWH, Prez LA de, et al. NCS report 18 – Code of Practice for the absorbed 403 Dose determination in high energy photon and electron beams, (2008).

[4] GERSHKEVITSH, E., Pesznyak C, Petrovic B, Grezdo J, Chelminski K, do Carmo Lopes M, et al. Dosimetric inter-institutional comparison in European radiotherapy centres: Results of IAEA supported treatment planning system audit. Acta Oncol (2014)5:628-36.

[5] IZEWSKA J, Andreo P. The IAEA/WHO TLD postal programme for radiotherapy hospitals. Radiother Oncol (2000) 54:65–72.6

[6] BOURGUIGNON, M., Krembel, D., Simon, J.M., & Peiffert, D.. Radiation therapy: the lessons from Epinal and Toulouse accidents. Radioprotection, (2009) 44(4), 417-429.

[7] IAEA. Dosimetry of small static fields used in external beam radiotherapy: an international code of practice for reference and relative dose determination. TRS 483 (2017).

[8] LOW,D., Moran J.M. , Dempsey J.F., et al. Dosimetry tools and techniques for IMRT. (2011) 38(3): 1313-1338

Updates and Challenges in Detector Technology

Ionisation Chamber Dosimetry – Updates and Challenges

M. McEwen

National Research Council Canada, Ottawa, ON Canada

Email address of Corresponding Author: malcolm.mcewen@nrc-cnrc.gc.ca

BACKGROUND

Air-filled ionisation chambers have remained the workhorse for reference dosimetry in radiation therapy clinics for many decades, despite the emergence of various other detector technologies. This is due to the well-established characteristics of ease-of-use, long term stability, high signal-to noise, linearity and small energy dependence. However, despite expert guidance in the form of dosimetry protocols, the literature shows that the application of ion chambers to new beam modalities and/or treatment deliveries has often led to dosimetric errors. This presentation will review the types of ion chambers available for external beam radiation therapy and discuss the pitfalls and challenges that must be met and overcome to achieve high accuracy dose measurements in a range of situations.

The questions that will be addressed include:

1) How does ion chamber size impact reference dosimetry?

2) What issues need to be considered when applying ion chambers to new modalities?

3) Is there an ideal chamber that can be used in all situations?

4) What should be the respective roles of the manufacturer and the medical physicist in choosing an ion chamber and correctly using it?

DISCUSSION

For almost three decades the Farmer-type cylindrical ion chamber was the most widely-used ion chamber in external beam reference dosimetry, but with the development of increasingly conformal treatments, smaller ion chambers have been produced, offering better determination of point dose in small radiation fields. However, it has been demonstrated that a micro-chamber (i.e., volume < 0.1 cm^3) cannot be simply viewed as a Farmer chamber with a lower sensitivity and assumptions valid for larger-volume chambers in large fields (e.g., 10 cm x 10 cm) do not necessarily apply in these small-field situations.

Parallel-plate chambers are recommended by several protocols for low-energy x-ray and low-energy electron beams. These thin-windowed chambers can show anomalous behaviors that do not follow theoretical predictions, and long-term drifts in response can be larger than for cylindrical chambers, requiring more detailed characterisation to ensure accurate use. Non-zero perturbation corrections in electron beams have also meant a revisiting of the recommendations regarding the “best” type of ion chamber for this modality.

Several new beam modalities have become available for the delivery of radiation therapy. These include proton (and heavy ion) beams, robotic or mobile linear accelerators, and, perhaps most recently, MR-linac hybrid systems. These systems all need calibration but introduce measurement challenges not seen previously, including larger ion recombination corrections, the effect of small air gaps, and the equivalence (or not) of solid versus water phantoms.

Ionisation chambers are still often the most appropriate detector but in the new situations additional measurement procedures or modified dosimetry protocols are likely required.

It should be remembered that it is the role of the medical physicist in the cancer centre to ensure that any piece of equipment is fit for purpose. It is therefore essential that they perform sufficient measurements and investigations in their particular situation to determine that the detector can be used in the specific radiation beam and achieve the necessary precision and accuracy. Equipment manufacturers are an excellent technical resource, as are international dosimetry protocols such as IAEA TRS-398 and IAEA/AAPM TRS-483, but the medical physicist is the qualified person on-site with the ultimate responsibility.

CONCLUSION

Ionisation chambers remain the detector of choice for clinical reference dosimetry, but care is required and assumptions in their use always come with associated uncertainties that need to be considered and mitigated for their correct use.

Non-Invasive X-ray Multimeters used in Diagnostic Radiology

L. Büermann[a]

[a]Physikalisch-Technische Bundesanstalt, Bundesallee 100, 38116 Braunschweig, Germany

Email address of Corresponding Author: ludwig.bueermann@ptb.de

Summary

This review briefly presents the status of **n**on-**i**nvasive **X**-ray **m**ultimeters (NIXMs), which are used for quality control (QC) measurements in the useful beams of diagnostic X-ray devices. NIXMs are designed to measure multiple X-ray beam parameters such as the X-ray tube voltage, the dose, the dose rate, the dose per pulse, the irradiation time, the tube current-time (mAs) product, the waveform, the half-value layer (Quick-HVL) and the total filtration (TF) in a single exposure. NIXMs are mainly used in general radiography, fluoroscopy and mammography. Some instruments have been developed for applications in computed tomography (CT). This review includes basic principles, general components, instrument examples, typical specifications, calibrations, international standards and independent performance tests, as well as future challenges.

Basic principles

NIXMs are based on at least two semiconductor sensors covered with metal filters of different thicknesses [1]. If irradiated with X-rays of a certain quality generated with conventional X-ray tubes, the sensor signals are proportional to the energy fluence rates ("beam intensities") transmitted. Thus, ratios of the different sensor signals are directly correlated to parameters that characterize the X-ray quality such as peak tube voltage (kVp) and TF. Knowledge of the X-ray quality makes it possible to correct the signal measured for the non-ideal energy dependence of the semiconductor sensors with respect to the quantity of air kerma. High signal sampling rates (kHz range) enable the system to record kVp as a function of time (waveform), from which the quantity practical peak voltage (ppV) is deduced. Furthermore, it is possible to measure the exposure time as well as other quantities derived from it such as the dose per pulse and the mean pulse dose rate.

General components, instrument examples, typical specifications, calibrations

A typical modern NIXM is composed of one or more detector units, a signal processor unit, system software and an indicator unit. These components can be combined to form a single instrument. It is also possible to use other general electronic devices (desktop/laptop computers or handheld devices) as alternatives to customized indicator units or as supplements to them. Different devices (or detector units) may be offered for special applications in radiography, fluoroscopy, mammography and computed tomography. Some examples of instruments currently available on the market (as of 2019) will be described below, including their typical specifications and uncertainties. Calibrations are usually performed at the manufacturer site or at accredited calibration laboratories over periods of one or two years.

International performance standards

There is no general international performance standard for NIXMs. Instead, one standard defines requirements concerning the dose and dose rate measuring channels of a given NIXM (IEC 61674 [2]), while another standard defines requirements concerning the measuring channel for the non-invasive measurement of the tube voltage (IEC 61676 [3]). There are no performance standards for non-invasive measurements of TF, Quick HVL or exposure time.

Standard X-ray qualities for testing NIXM devices are defined in IEC 61267 [4]. Increasing attention is being devoted to requirements concerning the system software where NIXMs are used to perform measurements that are subject to legal regulations (e.g. WELMEC Guide 7.2 [5] of the European cooperation in legal metrology).

Independent performance tests

In most cases, manufacturers indicate the compliance of their NIXMs with two standards: IEC 61674 (dose/dose rate) and IEC 61676 (tube voltage). However, no international standards exist for the other quantities measured by these devices. Only a small number of publications exist in which independent performance tests of NIXMs have been conducted; most of these publications deal with the performance of the dose/dose rate or tube-voltage indications as a function of different influence parameters [6]. In Germany, diagnostic dosimeters are covered by the Verification Act if used for legal dose measurements such as acceptance tests of medical X-ray devices. For this reason, such dosimeters need to be type tested by the Physikalisch-Technische Bundesanstalt (PTB). Such type tests are based on the requirements in the IEC 61674 standard and the WELMEC Guide 7.2.

Future challenges

Within the field of future NIXM developments, one of the most potentially challenging issues is finding a way to adapt them to accommodate the continual improvements and occasional technical changes to X-ray imaging modalities (e.g. digital breast tomosynthesis, contrast-enhanced dual energy mammography and cone beam CT). Adaptation to new radiation qualities and improvements in the angular response will be necessary. Real-time in-phantom dose probes based on semiconductors may also be a topic for future applications.

REFERENCES

[1] The non-invasive X-ray Multimeter. Principles, Advantages, Drawbacks and Uncertainties. Booklet for the Course “Physics of Diagnostic Radiology”. V 4.0 Jan Lindström (Karolinska University). Available only online: https://es.scribd.com/document/354394696/kVp40 (last visited: 2 April 2019)

[2] IEC. (1997) International Electrotechnical Commission. Medical Electrical Equipment—Dosimeters with Ionization Chambers and/or Semiconductor Detectors as Used in X-ray Diagnostic Imaging. IEC Publication 61674 (Geneva: International Electrotechnical Commission).

[3] IEC. (1996) International Electrotechnical Commission. Medical Electrical Equipment—Dosimetric Instruments for Non-Invasive Measurements of X-ray Tube Voltage in Diagnostic Radiology. IEC Publication 61676 (Geneva: International Electrotechnical Commission).

[4] IEC. (2005) International Electrotechnical Commission. Medical Diagnostic X-ray Equipment—Radiation Conditions for Use in the Determination of Characteristics. IEC Publication 61267 (Geneva: International Electrotechnical Commission).

[5] European cooperation in legal metrology, Software Guide 7.2, https://www.welmec.org/fileadmin/user_files/publications/WG_07/Guides/WELMEC_Guide_7.2_Software_Guide_2018.pdf

[6] Büermann, L., Böttcher, R.: *Performance test of multi-parameter measuring devices used for quality assurance in diagnostic radiology.* Proceedings of an International Symposium on Standards, Applications and Quality Assurance in Medical Radiation Dosimetry (IDOS 2010). Vol. 2, p. 33 https://inis.iaea.org/search/search.aspx?orig_q=RN:43009142

Novel Dosimetry

Ion Recombination in Ultra-Short High Dose-Per-Pulse Very High Energy Electrons (VHEEs)

M. McManus[a, b]
A. Subiel[a], **F. Romano**[a], **H. Palmans**[a, c]

[a] National Physical Laboratory, Hampton Road, Teddington, Middlesex, TW11 0LW, UK
[b] University College London, Gower Street, London, WC1E 6BT, UK
[c] MedAustron, Marie Curiestraße 5, A-2700 Wiener Neustadt, Austria

Email address of Corresponding Author: michael.mcmanus@npl.co.uk

BACKGROUND

Recent Monte Carlo (MC) studies have shown that the use of Very high Energy Electrons (VHEEs), with energies up-to 250 MeV, can provide more favourable dose distributions in comparison to current photon and electron therapy [1]. Ionisation chamber response and correction factors, in particular for ion recombination, are typically small at clinical energies and can be accounted for with high precision according to an electron beam dosimetry Code of Practice [2]. In high dose-per-pulse beams, ion recombination is a larger concern with a correction of approximately 20% being observed for Intraoperative Radiotherapy (IORT) beams [3]. For the case of ultra-short VHEEs the dose-per-pulse can be orders of magnitude higher than that of IORT. Therefore, the ability to correct accurately for ion recombination will play a crucial role in dose determination using ionisation chambers. Current recombination models are quoted to be accurate for the high saturation region where more than 70% of the charge is being collected by the chamber. Those models are expected to be invalid for the ultra-short VHEEs and a new ion recombination correction procedure may be required.

METHODS

The measurements were performed at a user facility at CERN, known as CLEAR, which generates electron bunches with energies up to 220 MeV. Each bunch can contain a charge between 0.001 and 1.5 nC, and a selectable number of bunches can be grouped into a larger pulse with bunch frequency of 1.5 GHz [4]. With high charge-per-bunch, and a large number of bunches-per-pulse, it is possible to investigate extremely high dose-rates in beam delivery. Two Roos® Type (PTW-34001) plane-parallel chambers were employed, one as a test chamber with variable collecting voltage spanning 25 to 600 V, and one as the monitor which was kept constant at the recommended chamber voltage of 200 V. The chamber response was investigated for charge-per-pulse values ranging from 30 to 10000 pC per-pulse. The effective point of measurement of the test chamber was placed at approximately 10 cm depth in a 30 x 30 x 30 cm^3 water phantom, with the monitor chamber attached to the test chamber with their entrance windows touching. The distance from the vacuum window to the surface of the phantom was approximately 50 cm. The NPL's Elekta Synergy® LINAC was also used for chamber response comparisons. The setup in the NPL beam was similar, however the chambers were exposed to a 12 MeV electron beam.

RESULTS

For the lowest charge-per-pulse, it was observed that the Roos® chamber responded similarly to that seen in clinical electron beams, with a distinct plateau region and saturation charge being reached when a collecting voltage of 600 V was applied. The collection efficiency, determined by the two-voltage analysis (TVA) method with voltages of 200 V and 100 V, for the 30 pC

per-pulse case, was calculated to be approximately 93%. As the charge-per-pulse in the beam was increased, a very significant reduction in the collection efficiency of the chamber was observed. Quantification of this effect in the high dose-per-pulse regime is challenging as the available models are inaccurate for such an extreme case. The saturation curve for 10000 pC per-pulse was close to linear over the whole voltage range. In this regime, a much larger collecting voltage could be required in order to reach saturation. However, as the chamber is not designed for such high voltages, this may induce other non-dosimetric artefacts such as charge multiplication. For the 30 pC per-pulse case, the recommended 200 V applied voltage is effective in collecting close to 100% of the produced charge. In contrast, for the 10000 pC regime, the chamber collects more than twice the charge for a 600 V collecting voltage, relative to the monitor chamber at 200 V. This indicates that the recommended voltage of the Roos® chamber is insufficient for an accurately correctable charge collection efficiency in high dose-per-pulse VHEEs.

CONCLUSIONS

It is clear that as the charge-per-pulse in the beam is significantly increased, the ability of the chamber to collect the produced charge decreases. This is due to the increase of the general recombination factor as the charge density in the chamber increases. Due to this extreme charge density, the space charge screening effect may also become significant. This screens the charged particles from the electric field causing them to move slower and therefore increase the probability of recombination. The large deficiency in charge collection due to recombination cannot be accounted for accurately using currently available models. These data will be useful for the characterization of ion chamber response through the comparison of measurements with dose-rate independent detectors, such as calorimeters and alanine. In turn, this should provide the foundations for the development of a new recombination correction procedure which will be valid for high dose-per-pulse beams.

REFERENCES

[1] BAZALOVA-VARTER AND OTHERS, “Treatment planning of radiotherapy with very high-energy electron beams and comparison of VHEE and VMAT plans”, *Am. Assoc. Phys. Med.,* **42,** (2015) 5.

[2] THWAITES, D.I., (CHAIR) ET. AL., “The IPEM code of practice for electron dosimetry for radiotherapy beams of initial energy from 4 to 25 MeV based on an absorbed dose to water calibration”, *Phys. Med. Biol.,* **48,** p. 2929, (2003) 18.

[3] DI MARTINO, F., GIANELLI, M., TRAINO, A. C., AND LAZZERI, M., “Ion recombination correction for very high dose-per-pulse high-energy electron beams”, *Med. Phys.*, **32**, pp. 2204-2210, Jul. (2005) 7.

[4] GAMBA, D. ET. AL., “The CLEAR user facility at CERN”, *Nucl. Instrum. Methods Phys. Res. Sect. Accel. Spectrometers Detect. Assoc. Equip.*, Dec. (2017).

Assessing the Contribution of Cross Sections to the Uncertainty of Monte Carlo Simulations in Micro- and Nanodosimetry

H. Rabus[a]
C. Villagrasa[b], G. Baiocco[c], M. C. Bordage[d], M. U. Bug[a], S. Chiriotti[e,f], W. Friedland[g], E. Gargioni[h], B. Heide[i], H. Nettelbeck[a], A. Parisi[e]

[a]Physikalisch-Technische Bundesanstalt, Bundesallee 100, 38116 Braunschweig, Germany
[b]Institute de Radioprotection et Sûreté Nucléaire, BP-17, 92262 Fontenay-aux-Roses, France
[c]Physics Department, University of Pavia, Via Bassi 6, 27100 Pavia PV, Italy
[d]INSERM, Université Toulouse III-Paul Sabatier, UMR 1037 CRCT, Toulouse, France
[e]Belgian Nuclear Research Centre (SCK-CEN), Boeretang 200, 2400 Mol, Belgium
[f]Paul Scherrer Institut, Forschungsstrasse 111, 5232 Villigen, Switzerland
[g]Helmholtz Zentrum Muenchen, Ingolstaedter Landstr. 1, 85764 Neuherberg, Germany
[h]Universitätsklinikum Hamburg-Eppendorf, Martinistrasse 52, 20246 Hamburg, Germany
[i]KIT, Hermann-von-Helmholtz-Platz 1, 76344 Karlsruhe, Germany

Email address of Corresponding Authors: hans.rabus@ptb.de, carmen.villagrasa@irsn.fr

BACKGROUND

Monte Carlo (MC) simulation is often used to study particle track structure (i.e. the micro- and nanoscopic pattern of energy deposition) of different radiation qualities to elucidate their relative biological effectiveness. For this purpose, several general-purpose MC radiation-transport codes have been recently upgraded to enable the step-by-step simulation of charged particle transport, which was previously the domain of dedicated track-structure MC codes. However, results of track structure simulations depend heavily on the cross-section data used in the codes, particularly those for inelastic interactions of electrons of very low energy (below 1 keV) [1]. Since different MC codes use different tables or models of cross-section data, a systematic investigation into the uncertainty of microdosimetric or nanodosimetric spectra arising from the use of different cross-section data is needed.

METHODS

To assess this uncertainty, Working Group 6 “Computational Dosimetry” of EURADOS has launched an exercise inviting participants to use a MC code of their choice to calculate microdosimetric spectra and nanodosimetric ionization cluster size distributions (ICSD) for electrons of a given energy spectrum (related to ^{125}I decay, maximum energy 34.7 keV). For microdosimetric calculations, the target was a 10 µm-diameter liquid-water sphere and three spatial distributions of the source were considered. ICSD were to be determined in 3 nm and 8 nm spherical volumes within this target at different distances from a source located in the center of the 10 µm sphere.

RESULTS

For a point source at the center of the 10 µm sphere and a source uniformly distributed within the sphere, the reported microdosimetric spectra are in good agreement with a standard deviation below 2% in the resulting frequency-mean specific energy values [2].

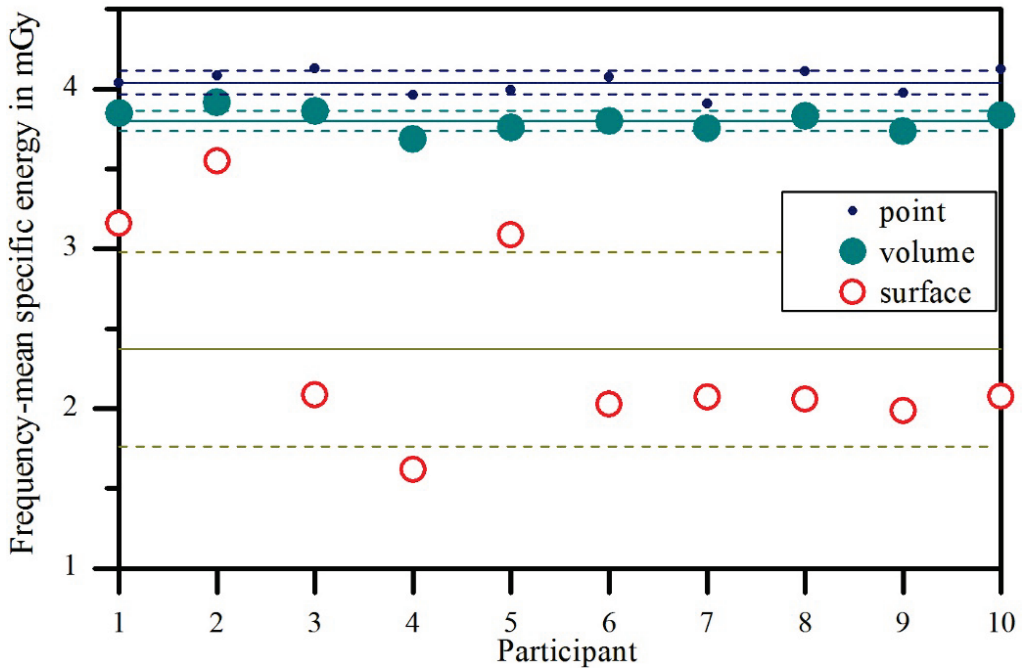

Figure 1. Microdosimetric frequency-mean specific energy values reported by the different participants (symbols), the respective average over all participants (solid lines), and uncertainty bands corresponding to one standard deviation (dashed lines).

For the case where the source was contained on the 10 µm sphere's surface, much larger discrepancies in the shape and the frequency-mean values of the microdosimetric spectra reported by the participants could be observed (see Figure 1).

Similarly, significant variations in the nanodosimetric ICSD reported by the participants were found, with up to 40% difference in the mean values of the ICSD.

CONCLUSIONS

The origin of the large discrepancies observed for the microdosimetric results with the surface source is still under investigation. In the next step of the exercise, a sensitivity analysis will be performed by studying the dependence of the simulation results on changes in the cross-section data. A preliminary sensitivity analysis was performed with the Geant4-DNA MC code using different available cross-section data tables. The results indicate that if the tremendous differences in the nanodosimetric ICSD were only due to uncertainties in the interaction cross sections for low-energy electron interactions, then these uncertainties would have to be around 100%.

REFERENCES

[1] LAZARAKIS, P., BUG, M. U., GARGIONI, E., GUATELLI, S., RABUS, H., ROSENFELD, A. B., Comparison of nanodosimetric parameters of track structure calculated by the Monte Carlo codes Geant4-DNA and PTra, Physics in Medicine and Biology **57** (2012) 1231–1250.

[2] VILLAGRASA, C., BORDAGE, M.-C., BUENO, M., BUG, M., CHIRIOTTI, S., GARGIONI, E., HEIDE, B., NETTELBECK, H., RABUS, H., Assessing the contribution of cross sections to the uncertainty of Monte Carlo calculations in micro and nanodosimetry, Rad. Prot. Dosim. **183** (2018) in press, doi: 10.1093/rpd/ncy240.

Nanodosimetric Track Analysis in a Spread-Out Proton Bragg Peak

S. Ngcezu[a,b,c]
H. Rabus[c]

[a]National Metrology Institute of South Africa (NMISA), CSIR Campus, Building 6, Meiring Naude Road, Brummeria, 0182, South Africa
[b]Physics Department, University of the Witwatersrand, 1 Jan Smuts Avenue, Johannesburg, South Africa
[c]Physikalisch-Technische Bundesanstalt (PTB), Bundesallee 100, 38116 Braunschweig, Germany

Email address of Corresponding Authors: sangcezu@nmisa.org, hans.rabus@ptb.de

BACKGROUND

A key finding of the BioQuaRT project [1] was a simple relation between radiobiological cross sections for cell inactivation by ion beams and nanodosimetric characteristics of the particle track structure of these beams [2]. Options for translating nanodosimetric information at the voxel level have also been investigated [3]. This work carries these approaches further by using nanodosimetric track structure analysis for estimating RBE variation in a clinical spread-out Bragg peak (SOBP) of protons.

METHODS

For 100 MeV protons entering a water phantom, the track structure has been simulated using Geant4-DNA for a number of positions along the pristine Bragg peak. Ionization cluster size distributions (ICSDs) were scored for targets of size corresponding to a 10 base-pairs segment of DNA was obtained for a set of radial distances from the proton trajectory and positions along the proton path. The functional dependence of nanodosimetric parameters on radial distance was analyzed using simple model functions and afterwards convolved with weighted distributions of the range taken from literature [4] to construct a SOBP.

RESULTS

For the track core, the radial dependence of ICSDs could be well reproduced assuming a superposition of a term proportional to the chord of the proton track and a contribution of electrons growing with the square of the radial distance. In the penumbra region, an inverse power law provided good fits in the entrance region while an exponential dependence was found within the last few tens of μm of the track. Integrating the radial dependence of the nanodosimetric cumulative probabilities for at least 2 or more ionizations in the target gave a quantity that an increase over the SOBP that is in in qualitative agreement with observations of enhanced relative biological effectiveness (RBE) in this region [5].

CONCLUSIONS

These encouraging preliminary results show the potential of using nanodosimetric track characteristics for predicting the variation of RBE for lethal lesions in cells in clinical situations. In ongoing further analysis, the influence of range straggling of the protons and of a non-homogenous spatial distribution of targets (DNA is only found within cell nuclei) and of the influence of on the outcome of the nanodosimetric prediction in investigated. The final goal is to arrive at a quantitative reproduction of the radiobiological findings, for which purpose it

may also be necessary to consider other target sizes and perhaps also correlations of nanodosimetric ICSDs in neighboring targets [6].

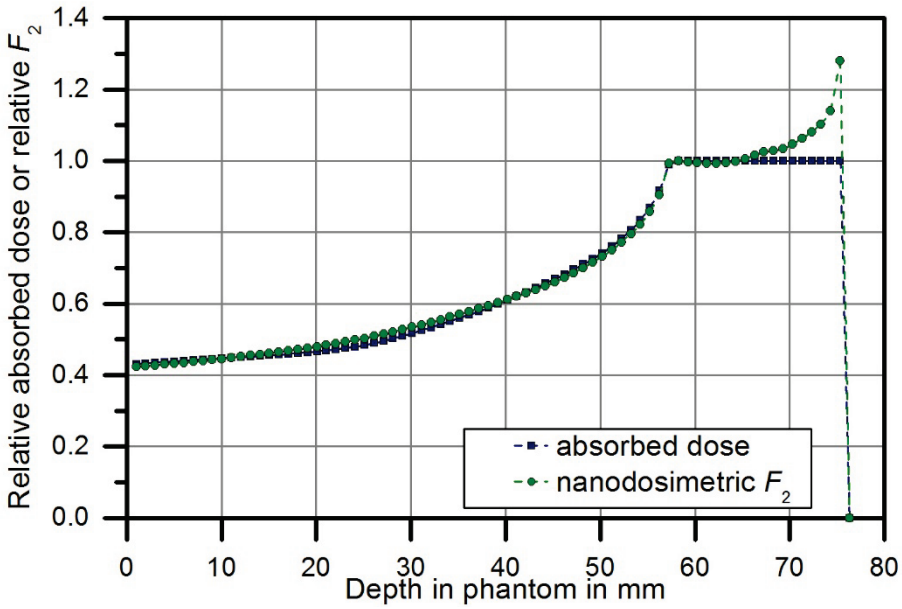

Figure 1. Normalized depth-dose curve and depth-dependence of the radially integrated nanodosimetric F_2 parameter. The data have been obtained without taking range straggling into account and therefore the weighting of the pristine Bragg peaks had to be adjusted as compared to the values given by Jette and Chen [4].

REFERENCES

[1] PALMANS, H., RABUS, H., BELCHIOR, A. L., BUG, M. U., GALER, S., GIESEN, U., HILGERS, G., MORO, D., NETTELBECK, H., PINTO, M., POLA, A., PSZONA, S., SCHETTINO, S., SHARPE, P. H. G., TELES, P., VILLAGRASA, C., WILKENS, J. J., Future development of biologically relevant dosimetry, Br. J. Radiology **88** (2015) 20140392.

[2] CONTE, V., SELVA, A., COLAUTTI, P., HILGERS, G., RABUS, H., Track structure characterization and its link to radiobiology, Radiat. Meas. 106 (2017) 506.

[3] ALEXANDER, F., VILLAGRASA, C., RABUS, H., WILKENS, J. J., Local weighting of nanometric track structure properties in macroscopic voxel geometries for particle beam treatment planning, Phys. Med. Biol. **60** (2015) 9145.

[4] JETTE, D., CHEN, W., ICreating a spread-out Bragg peak in proton beams, Phys. Med. Biol. **56** (2011) N131.

[5] LÜHR, A., VON NEUBECK, C., KRAUSE, M., TROOST, E.G.C., Relative biological effectiveness in proton beam therapy – Current knowledge and future challenges, Clin. Transl. Radiat. Oncol. **9** (2018) 35.

[6] PIETRZAK, M., STANISŁAW PSZONA, S., BANTSAR, A., Measurements of spatial correlations of ionisation clusters in the track of carbon ions—first results, Radiat. Prot. Dosim. **180** (2018) 162.

Novel radiation Detectors for X-ray Imaging and Radiation Therapy

J. Tikkanen[a]
T. Siiskonen[a], V. Litichevskyi[b], P. Luukka[b], E. Brücken[b], S. Kirschenmann[b]

[a]Radiation and Nuclear Safety Authority (STUK)
[b]Helsinki Institute of Physics (HIP)

Email address of Corresponding Author: joonas.tikkanen@stuk.fi

BACKGROUND

In x-ray imaging, the information about the energy of the detected photons can be used to extract additional information about the anatomical structures inside the patient and hence to decrease the dose. However, detectors that utilise spectral information in full capacity do not yet exist in commercial diagnostic equipment. Discrimination between energies is used only to some extent in dual CT.

Novel techniques in radiation therapy, such as volumetric modulated arch therapy and intensity modulated radiation therapy, have improved the efficacy of treatment. However, dose gradients in these fields can be significant and position resolution of ionisation chambers may be too poor to measure the dose variation within the irradiated area. A new type of 2D detector with high spatial resolution would make transition from reference to clinical field size according to IAEA TRS 483 more practical and would also benefit e.g. the quality assurance measurements at the clinics leading to better patient safety.

A read out chip for semiconductor chips capable of recording spectral information in each pixel has been developed for the CMS experiment at CERN. Detectors based on this technology are being developed in collaboration between Radiation and Nuclear Safety Authority of Finland and Helsinki Institute of Physics for use in imaging and dose profile measurements in MV photon beams.

METHODS

Silicon diodes optically coupled with GAGG:Ce and GOS:Tb scintillation materials were tested in RQR quality x-ray beams [1]. The RQR spectra measured with a HPGe spectrometer were converted, by modelling the spectrometer response with MCNP 6.1 software [2], to fluence spectra. The fluence was used in the characterisation of the scintillator coated detectors vs. bare diodes as reference samples. The purpose of the scintillator coating is to increase the detection efficiency of the silicon detectors limited by the effective atomic number.

A GBX200 Co-60 irradiator at the SSDL laboratory of STUK was modelled with EGSnrc for investigating the behaviour of silicon detectors and detector casings [3]. The field size was 10 x 10 cm^2. Simulated depth dose curve, dose profile and air-kerma to dose-to-water ratio were compared with measured values.

RESULTS

The scintillator coated diodes demonstrated higher currents from RQR4 onwards (mean energy 36.4 keV). For the GBX200 irradiator, the simulated and measured values agreed within 0.6%.

CONCLUSIONS

Use of the scintillator coating on the silicon diodes was shown to increase the detection efficiency. Pulse mode operation will be investigated in the near future. The model of the GBX200 irradiator can be considered accurate on the basis of agreement between the simulated and measured values. The model has applications also in other aspects of dosimetry, such as quality correction factor calculations. Further development of the detectors for dosimetry and imaging purposes will continue on the basis of these tests.

REFERENCES

[1] Medical diagnostic X-ray equipment - Radiation conditions for use in the determination of characteristics, IEC 61267:2005

[2] T. GOORLEY, et al., "Initial MCNP6 Release Overview", Nuclear Technology, 180, pp 298-315 (Dec 2012).

[3] I KAWRAKOW, E MAINEGRA-HING, DWO ROGERS, F TESSIER, BRB WALTERS. The EGSnrc Code System: Monte Carlo simulation of electron and photon transport. Technical Report PIRS-701, National Research Council Canada (2017).

Use of Effective Dose as an Indicator of Patient Risk

ICRP Proposals for the Application of Effective Dose in Medicine

C. Martin[a]
J. Harrison[b]

[a]Department of Clinical Physics and Bio-Engineering, University of Glasgow, UK
[b]Oxford Brookes University, Oxford, UK

Email address of Corresponding Author: colin.j.martin@ntlworld.com

BACKGROUND

Effective dose has been developed by the International Commission on Radiological Protection (ICRP) as a dose quantity related to detriment from radiation-induced stochastic effects, principally cancer, that can be used in the optimization of protection from all sources of exposure. Effective dose is the sum of equivalent doses (mean absorbed doses weighted for differences in biological damage produced by radiations) to each radio-sensitive organ or tissue, multiplied by tissue weighting factors that account for differences in their radiosensitivity [1]. The use of effective dose in optimization of protection relies on the assumption of a linear non-threshold (LNT) dose-effect relationship. Epidemiological data from a number of studies demonstrate significant excesses of cancer down to doses of less than 50 mSv [2] and suggest that the LNT model is the best interpretation of current scientific knowledge. Effective dose equates to health detriment from uniform whole body exposures, and can be applied to all exposures regardless of differences in distribution of doses between organs and tissues. However, it is calculated for reference persons, and nominal detriment values are calculated as averages over populations of all ages and both sexes. Effective dose was designed originally for use in the evaluation of occupational and public exposures. In the last two decades, effective dose has also been applied to medical exposures, and these applications have sometimes gone beyond the intended purposes of the quantity.

METHODS

ICRP established a Task Group to prepare a comprehensive report to provide guidance on the application of effective dose. A public consultation on the draft publication was held during summer 2018 and a revised version has been produced.

RESULTS

The report recommends that equivalent dose should not be regarded as a separate protection quantity. That is, dose limits applying to tissue reactions would be more appropriately set in absorbed dose (Gy) rather than equivalent doses (Sv), while dose criteria (constraints, reference levels, limits) for stochastic effects would continue to be set in effective dose (Sv).

Stochastic risks estimated for different medical procedures vary according to the organs and tissues irradiated. Values for effective dose can be derived from measured quantities such as kerma-area product for radiography, dose length product for computed tomography, and injected activity for nuclear medicine using conversion coefficients. Effective dose provides a tool with enough information about radiation exposure levels linked to health detriment for making everyday decisions. Some tasks for which it can be used are listed below:

- Providing information for use in selecting the appropriate technique for imaging
- In the justification of imaging exposures for individual patients
- Research studies: Summing the doses that may accrue from procedures performed

- Optimisation of technique: where the distribution of dose within body is different
- Reporting of unintended exposures, where the dose level is low
- Assessing doses to carers incurred willingly by those supporting patients
- Use of typical effective doses from common procedures in education and training.

These applications rely implicitly or explicitly on the assumption of a direct relationship between effective dose and stochastic risk. The ICRP report recommends that effective dose can be used as an approximate estimate of the risk that may be incurred as a result of radiation exposures. The report also considers the dependence of risk on age at exposure and differences between males and females, concluding that overall cancer risks are a factor of 2 – 3 higher for young children than young adults, with lower values for older adults. However, uncertainties in risk estimates at low doses should be recognized, with small contributions from the use of reference phantoms to calculate doses, and larger contributions from lack of knowledge of risks (per Gy or Sv) of individual cancer types at low doses. As well as recognized differences in risk between individuals of different ages and sex, there will also be genetic variations in risk within a population; the latter topic is the subject of a new ICRP Task Group. While it is reasonable to use effective dose as an approximate indicator of possible risk, best scientific estimates of risks to individuals should be calculated on the basis of estimates of organ doses, using age- and sex- specific risk estimates, with consideration of uncertainties. Generic terms that may be applied to potential risks from medical procedures are shown in Table 1. Applications for which use of effective dose is not recommended include:

- Assessing dose where all the exposure is predominantly to one organ
- Comparing doses for similar techniques in different departments or institutions
- Setting diagnostic reference levels for which measurable quantities should be used
- Providing patient dose information in reports for medical radiological procedures
- Calculation of stochastic risk for individual patients.

Table 1. Dose ranges and terminology for describing risks from medical procedures for adult patients age 30y-39y.

Effective dose (mSv)	Risk of cancer	Risk term	Examples of medical radiation procedures
< 0.1	No direct evidence	Negligible	Radiographs of chest, limbs and teeth.
0.1–1	No direct evidence	Minimal	Radiographs of spine, abdomen, and head
1–10	No direct evidence	Very low	CT scans of head and trunk, angiography
10–100	10^{-3}–10^{-2} with LNT	Low	CT scans trunk and interventional rad.
100s	$>10^{-2}$	Moderate	Multiple procedures and follow-up.

CONCLUSIONS

Effective dose is a useful indicator of harm that may result from a radiation dose received. Generic values can be used in referral guidelines and justification, in evaluating detriment in research studies, incident reporting, and doses to carers. However, the age, sex and health status must be taken into account when considering risks to individuals and uncertainties associated with estimates of risk at low doses should also be recognized.

REFERENCES

[1] INTERNATIONAL COMMISSION ON RADIOLOGICAL PROTECTION. The 2007 Recommendations of the International Commission on Radiological Protection. ICRP Publication 103. Ann. ICRP 37(2–4), Elsevier, Amsterdam, Netherlands (2007).

[2] NATIONAL COUNCIL ON RADIATION PROTECTION AND MEASUREMENTS. Implications of recent epidemiological studies on the linear nonthreshold model and radiation protection. NCRP Comm. 27, Bethesda, US (2018).

[3] MARTIN, C.J. Effective dose: how should it be applied to medical exposure? Brit. J. Radiol. 80, (2007) 639-647.

Comparison of Effective Dose Received by Patients Undergoing Whole-body PET-CT Procedure Using 18F-FDG and 68Ga-DOTATATE

M. A. Said[a]
M. Z. Zaini[a], Ali. N[a]

[a]Department of Nuclear Medicine,National Cancer Institute, 62250 Putrajaya, Malaysia

Email address of Corresponding Author: aminhpj@gmail.com

BACKGROUND

Patients who undergo PET/CT use different radiopharmaceuticals according to their diseases. Mostly 18F-FDG and 68Ga-DOTATE are used in the protocol of PET/CT imaging. The objective of this study is to estimate and compare the effective dose received by 50 18F-FDG patients and 50 68Ga-DOTATATE patients undergoing PET/CT procedure at Institut Kanser Negara in Malaysia.

METHODS

Effective dose from PET scans were calculated based on the dose coefficient reported in International Commission on Radiological Protection (ICRP) Publication 106 and activity of 18F-FDG and 68Ga-DOTATATE. Effective dose from CT scans were determined using k coefficient reported in ICRP Publication 102 and dose-length product (DLP) value.

RESULTS

The average effective dose from PET and CT scans for 18F-FDG was found to be 10.34 mSv and 6.90 mSv, respectively. Meanwhile for 68Ga-DOTATATE, the average effective dose from PET and CT scans was found to be 10.88 mSv and 4.52 mSv, respectively. The mean whole-body effective dose received by 18F-FDG and 68Ga-DOTATATE patients undergoing the combined PET/CT procedure was 18.15 mSv and 14.76 mSv.

CONCLUSIONS

These results could be used as reference for the dosimetry of patients undergoing PET/CT procedures in Malaysia.

REFERENCES

[1] Dhalisa, H., Mohamad, A.S., Rafidah, Z., Radiation Dose Assesment to the Adult Patient Undergo Whole-body PET/CT Examination After PET/CT machine Upgraded. Kluster Oncology Science and Radiology, Advanced Medical Dental Institute, Universiti Sains Malaysia (USM), Bertam, Penang, Malaysia

[2] Tatsumi M, Miller J.H, Wahl R.L, FDG PET/CT in evaluating pediatric malignancies. J Nucl Med (2007) 48:1923–1931Z.

[3] Marguerite T.H et.al, MIRD dose estimate report no 19: radiation absorbed dose estimates from F18FDG. Journal of Nuclear Medicine, 2002.43(2):p. 200-204

[4] Kitiwat, K., Anchali, K., et al. 2010. The determination of patient dose from F18-FDG PET-CT examination. Oxford Journals. Radiation Protection Dosimetry. Vol. 141(1): 50-55.

[5] Brix, G., Lechel, U., et al. 2005. Radiation exposure of patients undergoing whole-body dual modality F18-FDG PET-CT examinations. Journal of Nuclear Medicine. 46: 608-613.
[6] Naswa, N., Sharma, P., Kumar A., Gallium-68-DOTA-NOC PET/CT of Patients With Gastroenteropancreatic Neuroendocrine Tumors: A Prospective Single-Center Study. American Roentgen Ray Society.
[7] Mojtahedi, A., Thamake S. The Value of 68Ga-DOTATE PET/CT in Diagnosis and Management of Neuroendocrine tumors compared to current FDA approved imaging modalities. American Journal of Nuclear Medicine and Molecular Imaging.
[8] Shrimpton, P.C, Jessen K.A, Gelejins, J., Panzer, W., Tosi, G., References Doses in Computed Tomography. Radiat. Prot Dosim, 1998. 80(1-3):p. 55-59
[9] International Commission on Radiological Protection, ICRP, 1990 Recommendations of the International Commission on Radiological Protection. ICRP Publication 60. Ann ICRP 1991.21(1-3)
[10] International Commission on Radiological Protection, ICRP, Managing Patient Dose in Multi-Detector Computed Tomography(MDCT). ICRP Publication 102. Ann ICRP, 2007.37(1)
[11] International Commission on Radiological Protection, ICRP, Recommendations of the International commission on Radiological Protection). ICRP Publication 103. Ann ICRP, 2007.37(2-4)EPHENSON, R., Introduction to Nuclear Engineering, 2nd edn, McGraw-Hill, New York (1958) 491 pp.

Using the National Diagnostic Reference Levels for Estimation of Effective and Equivalent Organ Doses of Patients in Conventional Diagnostic Radiology

L. Stadnyk
O. Nosyk, O. Shalopa

Grigorev Institute for Medical Radiology, Pushkinskaya str., 82, Kharkiv, 61024, Ukraine

Email address of Corresponding Author: Lstadnyk@ukr.net

BACKGROUND

Assessing patient dose levels in diagnostic radiology for the most common types is very important for developing measures to optimize them in order in order to reduce the risk of radiation effects. Radiation risks can be assessed based on a study of effective doses for various types of X-ray studies, as well as knowledge of the distribution of equivalent doses in organs / tissues for the assessment of effective doses. At the same time, equivalent organ doses and effective dose cannot be determined by direct measurements, but are estimated only on the basis of modelling exposure conditions using physical or mathematical phantoms. The work is devoted to the determination of conversion factors from entrance surface doses (ESDs) to equivalent organ / tissues doses and effective doses from various types of radiographic examinations.

METHODS

For determination of the distribution of absorbed doses in the organs / tissues of the “standard” patient and estimation of the effective dose, phantom simulations were performed on anthropomorphic phantom Alderson-Rando (adult) with a given geometry and patient exposure conditions. The TL-detectors type MTS-P (LiF: Mg, Ti) were used.

There were simulated the exposure conditions for 6 types of radiography examinations and fluorography (film and digital) under the working parameter's ranges of the X-Ray diagnostic units of various models with standard irradiation geometry. The entrance and exit doses on the phantom surface also were measured.

A total of 116 phantom simulations of patient exposure conditions were carried out taking into account 2 to 3 measurement cycles for each irradiation regime. From phantom simulations, equivalent doses were estimated for the 12 most radiosensitive organs and tissues.

According to the results of comparison of the values of entrance surface doses (ESDs) which were measured in the center of the radiation field on the surface of the phantom with the values of equivalent organs/ tissues doses and calculated effective doses the conversion factors were determined for selected groups of X-ray machines and for different parameters of X-Ray investigations.

To assess the equivalent organ doses and effective doses, the data of national survey of patient's ESDs which were carried out for establishment of national diagnostic reference levels of different types of radiography studies were used. For calculation of equivalent and effective doses, average values of ESDs of studied arrays of measurements and calculations for each type of X-ray diagnostic studies were used.

RESULTS

The results of phantom simulations of patient exposure for most common radiography examinations and fluorography (film and digital) are shown in Table 1.

Table 1. Entrance surface doses and appropriate equivalent organ and effective doses for most common types of X-Ray diagnostic examinations.

Average value	**Fluorography**		**Radiography procedures**					
	Film	**Digital**	**Chest**	**Skull**	**Cervical spine**	**Thoracic spine**	**Lumbar spine**	**Pelvis**
ESDs, mSv (PA/PA)	4,3	0,6	1.1	4.1	2.0	8.8	13.0	13
ESDs, mSv (LAT)	-	-			1.9	10.0	22.0	-
Organs/Tissues	Total equivalent dose, mSv							
Thyroid	0.69	0.13	0.09	0.27	3.88	0.84	0.05	0.00
Breast	0.87	0.16	0.06	0.00	0.00	1.60	0.12	0.00
Oesophagus	1.71	0.31	0.10	0.13	0.63	2.01	0.18	0.00
Lung	3.77	0.69	0.26	0.21	0.37	3.00	0.31	0.00
Liver	1.09	0.20	0.06	0.00	0.00	5.02	3.45	0.44
Colon	0.05	0.01	0.02	0.00	0.00	0.00	4.78	2.36
Stomach	0.73	0.13	0.04	0.00	0.00	7.00	10.30	1.53
Bladder	0.06	0.01	0.02	0.00	0.00	0.00	2.45	2.87
Gonads	0.02	0.00	0.02	0.00	0.00	0.00	0.92	7.22
Skin	0.57	0.10	0.07	0.30	0.33	1.18	2.28	0.84
Bone marrow	1.51	0.28	0.12	0.32	0.66	0.88	1.36	0.93
Bone surface	1.54	0.28	0.12	0.40	0.94	2.02	0.66	0.43
Remainder	2.50	0.46	0.15	0.00	0.58	0.22	0.98	0.06
Effective dose	**1.10**	**0.20**	**0.08**	**0.09**	**0.39**	**2.54**	**2.59**	**2.20**

CONCLUSIONS

The modelling exposure conditions of patients on the phantom Alderson-Rando made a possibility to study the distribution of equivalent organ doses, to estimate the effective doses according to the average values of entrance surface doses for each selected type of diagnostic examinations which were obtained from the results of national survey of parameters of X-Ray diagnostic investigations and data of direct and indirect dose measurements of ESDs. These results can be used to the refined assessment of collective effective doses and radiation risks of the population of Ukraine from X-ray diagnostic examinations.

Assessment of Collective Effective, Equivalent Organ Doses and Radiation Risks for Ukrainian Population Due to Conventional X-Ray Diagnostic Examinations

L. Stadnyk
O. Nosyk, O. Shalopa

Grigorev Institute for Medical Radiology, Pushkinskaya str., 82, Kharkiv, 61024, Ukraine

Email address Corresponding Author: Lstadnyk@ukr.net

BACKGROUND

Currently in the field of radiation protection the optimization of most common X-Ray diagnostic procedures have a priority, since there is significant potential to reduce the medical exposure doses and radiation cancer risk. The purpose of this investigation is the estimation of collective equivalent organs/tissues doses and collective effective doses of the Ukrainian population using updated data on the mean values of equivalent organ and effective doses from phantom simulation, taking into account data on the average parameters of examinations and average values of entrance surface doses (ESDs). Determination of radiation risks of cancer for collected most common diagnostic procedures in according with risk coefficients from ICRP Pub.103.

METHODS

The equivalent organs/tissues doses and effective doses for all radiographic procedures and chest fluorography (film and digital) have been estimated from the results of phantom modelling using the standard phantom Alderson-Rando and the method of TL-dosimetry. The values of equivalent organs/ tissues doses for 'standard' patient and effective doses were determined from the data about the average values of entrance surface doses for selected X-Ray diagnostic procedures with using the conversion factors for every organ or tissue from the parameters of exposure conditions for each examinations.

Collective dose (Si) for the particular type of study was calculated by the formula:

$$S_i = \sum E_{ij} \cdot N_{ij}$$

where E_{ij} is the average effective dose and N_{ij} is the number of X-ray diagnostic studies from the i-type of X-ray examination on j-model of X-ray machine.

The assessment of absolute cancer radiation risks from radiography examinations and fluorography were carried out using data about numbers of conducted x-ray diagnostic studies in 2014 and radiation risk coefficients for adults (male and female) for the most radiosensitive organs and tissues from the ICRP Pub.103 [1].

RESULTS

Table 1 presents data of the frequency for most common X-ray diagnostic examinations, the average effective dose per procedure and the collective effective doses for selected types of X-ray procedures. Table 2 presents absolute cancer radiation risks from radiography examinations and fluorography.

Table 1. The collective effective doses for common X-ray procedures

X-ray procedures	Total number per year (thousand)	Average effective dose (mSv)	Annual collective effective dose (man-Sv)
Film fluorography	11199.2	1.10	12319.1
Digital screening radiography of chest	7466.2	0.20	1493.2
Chest / Thorax	6374.5	0.08	5210.0
Skull	906.7	0.09	81.6
Cervical spine	665.4	0.39	259.5
Thoracic spine	776.3	2.54	1971.8
Lumbar spine	1441.7	2.59	3734.0
Pelvis and hip	1330.8	2.20	2927.8

Table 2. The absolute cancer radiation risks from radiography examinations and fluorography (numbes of cases per year)

Organs/ Tissues	Fluorography		Radiography procedures						
	Film	Digital	Chest	Skull	Cervical spine	Thoracic spine	Lumbar spine	Pelvis	Total
Thyroid	5.6	0.3	0.2	0.1	1.9	0.3	0.0	0.0	8.4
Breast	64.5	3.3	1.5	0.0	0.0	57.0	1.0	0.0	127.3
Oesophagus	41.8	2.1	0.9	0.2	1.0	2.3	0.5	0.0	48.8
Lung	850.0	43.6	20.7	2.4	5.4	32.3	8.0	0.0	962.4
Liver	40.9	2.1	0.8	0.0	0.0	9.1	15.4	0.8	69.1
Colon	3.6	0.2	0.5	0.0	0.0	0.0	42.6	9.5	56.4
Stomach	69.8	3.6	1.3	0.0	0.0	32.4	112.1	7.1	226.3
Bladder	2.0	0.1	0.2	0.0	0.0	0.0	8.7	4.9	15.9
Gonads	0.6	0.0	0.2	0.0	0.0	0.0	2.6	10.2	13.6
Skin	2.7	0.1	0.1	0.1	0.1	0.3	1.3	0.2	4.9
Bone marrow	64.6	3.3	1.7	0.8	1.8	1.8	6.6	2.1	82.7
Bone surface	9.3	0.5	0.3	0.1	0.4	0.6	0.5	0.2	11.9
Remainder	339.2	17.4	7.3	0.0	5.4	1.4	14.0	0.5	385.2
Summary	**1494.6**	**76.6**	**35.8**	**3.7**	**16.0**	**137.6**	**213.2**	**35.6**	**2012.9**

CONCLUSIONS

Among the most common X-ray radiography procedures film fluorography gives the maximum contribution to the collective effective dose of the population of Ukraine and into the absolute risk of radiation effects.

Primary Standards Dosimetry Laboratories

Absorbed Dose to Water Measurements in the SOBP of a Clinical Carbon Ion Beam Using Water Calorimetry

K. Holm[a,b]
U. Weber[c], Y. Simeonov[d], S. Brons[e], O. Jäkel[b,e], U. Ankerhold[a], S. Greilich[b], A. Krauss[a]

[a]Department 6.2 Dosimetry for Radiation Therapy and Diagnostic Radiology , Physikalisch Technische Bundesanstalt (PTB), Bundesallee 100, 38116 Braunschweig, Germany
[b]Division of Medical Physics in Radiation Oncology, German Cancer Research Center (DKFZ), Im Neuenheimer Feld 280, 69120 Heidelberg, Germany
[c]Department for Biophysics, GSI Helmholtzzentrum für Schwerionenforschung GmbH, Planckstraße 1, 64291 Darmstadt, Germany
[d]Institute for Medical Physics and Radiation Protection, Technische Hochschule Mittelhessen, Gießen, Germany
[e]Heidelberger Ion Beam Therapy Center (HIT), Im Neuenheimer Feld 450, 69120 Heidelberg, Germany

Email address of Corresponding Author: kim.holm@ptb.de

BACKGROUND

Currently ionization chamber based dosimetry still shows significantly higher uncertainty in ion-beam therapy than in high-energy photon therapy. This fact is mainly due to a lack of experimental data and to the high uncertainty (about 3%) of the theoretically calculated values for the kQ-factors of ionization chambers.

In a previous work [1], kQ-factors for two Farmer-type ionization chambers were determined directly and successfully in experiments in the low-energy region of a clinical 429 MeV/u carbon-ion beam. Based on this, kQ-factors for a further eight different cylindrical ionization chambers and three different plane-parallel ionization chambers were determined by means of cross-calibration [2]. The standard uncertainties achieved were 0.8% for the directly determined factors and 1.1% for the factors of cross-calibrated chambers. This threefold reduction in the uncertainty compared to calculated values will lead to a decreased overall-uncertainty in dosimetry for ion beam therapy.

In a continuation of this project, kQ-factors will now be determined in a spread-out Bragg peak (SOBP) of a carbon ion beam. It is possible that a change in the values due to the higher LET will be observed.

METHODS

To determine kQ-factors, the absorbed dose to water must first be determined using the water calorimeter developed by PTB [3]. The calorimeter consists of an actively cooled water phantom in which the calorimetric detector or ionization chamber of interest can be positioned at a certain depth. The calorimetric detector is a glass cylinder filled with purified water that contains two thermistors that measure the radiation-induced temperature rise of the surrounding water. To ensure that the uncertainty due to heat dispersion remains low, a homogeneous irradiation field is needed.

In contrast to previous studies, full active scanning of the volume of interest would lead to high uncertainty due to the long scanning time needed for a three-dimensional volume. Therefore,

the SOBP will be created by in-depth passive scattering using a 3D-printed range modulator consisting of many pyramid-shaped pins [4].

RESULTS

Depth dose curves of carbon-ion beams in water modulated with the range modulator clearly show the formation of a SOBP with a relative standard deviation of 0.5% between the dose values in the plateau region, as shown in Figure 1. Furthermore, two peaks can be seen at the beginning and at the end of the plateau. These are caused by inaccuracies during the printing process but will not affect the calorimetric measurements, as they are far enough away from the calorimetric measurement position in the middle of the plateau. The lateral dose distribution measured with an ionization chamber array shows a 6x6 cm2 plateau with a relative standard deviation of the dose values from the central chamber of 2.0%.

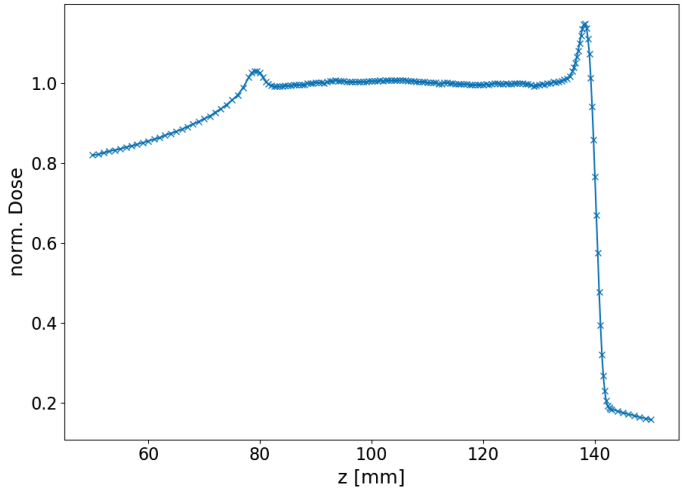

Figure 1. Depth dose curve of a 273 MeV/u carbon-ion beam in water modulated with the range modulator.

CONCLUSIONS

Further optimizing the range modulator as well as the irradiation parameters will create an irradiation field that is as homogeneous as possible. To measure the three-dimensional dose distribution more efficiently, a device is being developed at PTB that will move the ionization chamber array in a water phantom along the beam.

The reproducibility and time stability of the irradiation field will be investigated. Thereafter the absorbed dose to water under these irradiation conditions and from that the kQ-factors will be determined. Preliminary results regarding new kQ-factors will be presented.

REFERENCES

[1] OSINGA-BLÄTTERMANN, J.-M., et al, Direct determination of kQ for Farmer-type ionization chambers in a clinical scanned carbon ion beam using water calorimetry, Phys. Med. Biol. 62 (2017), 2033–2054

[2] OSINGA-BLÄTTERMANN, J.-M., KRAUSS, A., Determination of kQ factors for cylindrical and plane-parallel ionization chambers in a scanned carbon ion beam by means of cross calibration, Author submitted manuscript, Phys. Med. Biol. 107683.R1 (2018)

[3] KRAUSS, A., The PTB water calorimeter for the absolute determination of absorbed dose to water in 60Co radiation, Metrologia 43 (2006), 259-272
[4] SIMEONOV, Y., et al, 3D range-modulator for scanned particle therapy: development, Monte Carlo simulations and experimental evaluation, Phys. Med. Biol. 62 (2017), 7075-7096

Development of a Water Calorimeter as the Absorbed Dose-to-Water Primary Standard of High Energy Photon and electron Beams for China

K. Wang
S. Jin, Z. Wang, J. Zhang

National Institute of Metrology, Beijing, P. R. China

Email address of Corresponding Author: wangkun@nim.ac.cnmailto:myemail@domain.com

BACKGROUND

There are more than 2000 linear accelerators used for radiotherapy and the number increases by 100 per year in China. In order to supply the calibration service to the radiotherapy centers, National Institute of Metrology (NIM) developed the standard of the absorbed dose to water for high-energy photon and electron beams based on the national research center (NRC) of Canada designed [1]. After the measurement of absorbed dose to water for 6, 10, and 25 MV photons of accelerator by a water calorimeter, NIM took part the BIPM.RI(I).K6 comparison with Bureau International des Poids et Mesures (BIPM) on November 2016.

METHODS

The NIM water calorimeter with horizontal photon beams from the accelerator. This apparatus is composed of three parts, a calorimeter core and temperature rise data acquisition unit, a cooling and temperature control unit, a water phantom and support stable.

A cylindrical calorimeter core was used to measure water absorbed dose for photons of the accelerator and calibrate the transfer chamber for the international comparison. A parallel plate calorimeter core was fabricated with the measurement depth of 15 mm, so it can measure the water absorbed dose for 6 MeV electron beam.

RESULTS

The absorbed dose to water is measured by water calorimeter with output of 620 MU of the accelerator. Figure 1 summarize the results carried out on 10 MV photon beams. After calibrating thermistor and bridge separately, absorbed dose to water is absolutely measured with the combined standard uncertainty of 0.35%. The discrepancy of absorbed dose to water measured separately by N2-filled and H2-filled vessel is 0.2% at 10MV. The same results were obtained by Medin [2] with the measurement for ^{60}Co radiation.

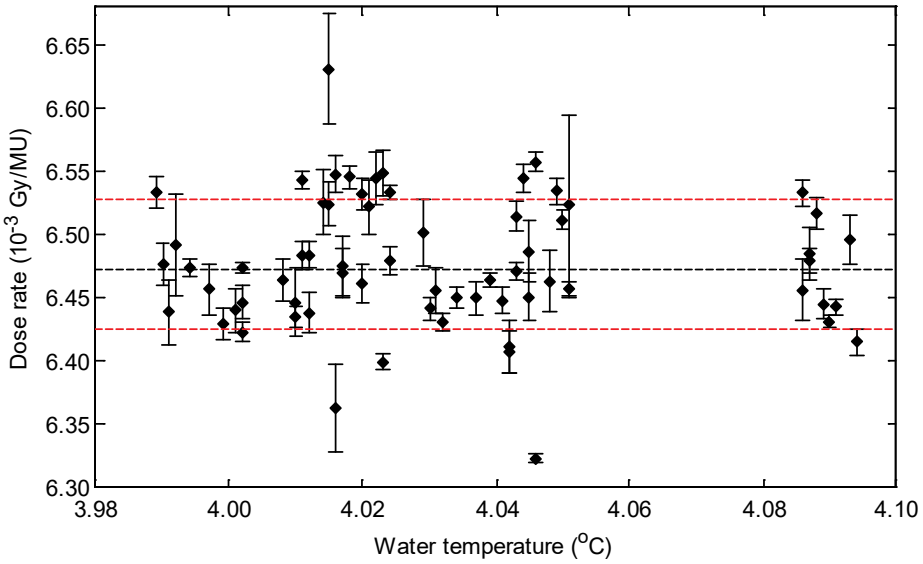

Figure.1. Results obtained using 10 MV photon beams of the Elekta Synergy at NIM. The uncertainly bars show the type A standard uncertainty.

The results of the BIPM.RI(I).K6 comparison reported as ratios of the NIM and the BIPM evaluations (and with the combined standard uncertainties given in parentheses), are 0.9917(60) at 6MV, and 0.9941(59) at 10MV [3]. The quality correction factors K_Q of commonly-used chambers were measured directly, which were 0.3% to 0.7% smaller than the recommended data in the IAEA TRS-398 protocol. The variations are between 0.1% and 0.8% for the results based on the methods recommended in IAEA TRS-398 and the chambers calibrated by megavoltage photons, in terms of the absorbed dose to water for the high-energy photon beams from clinical accelerator.

The water absorbed dose for 15 MeV electron beam was measured by parallel plate calorimeter core, the results were consistent with the absorbed dose calibrated by the ionizing chamber which traced to the water absorbed dose of ^{60}Co gamma radiation.

CONCLUSIONS

The primary standard of water absorbed dose for photon radiation of 6 MV, 10 MV and 25 MV is established, and took part the BIPM.RI(I)-K6 comparison. The new standard will instead the air-kerma based standard, to update the traceability system and reduce the uncertainty of ion chamber calibrations for accelerator radiotherapy.

REFERENCES

[1] SEUNTJENS, J P, ROSS, C K, KLASSEN, N V, & SHORTT, K R 1999 A Status Report on the NRC Sealed Water Calorimeter, *Rep. PIRS-0584, National Research Council*, Ottawa.

[2] MEDIN, J, ROSS, C K , STUCKI, G , KLASSEN, N V , & SEUNTJENS, J P 2004 Commissioning of an NRC-type sealed water calorimeter at METAS using ^{60}Co γ-rays. *Phys. Med. Biol*. 49(17), 4073–4086.

[3] SEUNTJENS, J P, ROSS, C K, KLASSEN, N V, & SHORTT, K R 1999 A Status Report on the NRC Sealed Water Calorimeter, Rep. PIRS-0584, National Research Council, Ottawa.

Experimental MV $k_{Q,Q0}$ from RTNORM EMPIR Project

F. Delaunay[a]
C. Andersen[b], **L. de Prez**[c], **S. Duane**[d]

[a]CEA- LIST, Laboratoire National Henri Becquerel LNE-LNHB, F-91191 Gif-sur-Yvette, France
[b]DTU, Center for Nuclear Technologies, Kongens Lyngby, Denmark
[c]VSL, Dutch Metrology Institute, Delft, the Netherlands
[d]National Physical Laboratory, Chemical- Medical & Environmental Science Department, Teddington, United Kingdom

Email address of Corresponding Author: franck.delaunay@cea.fr

BACKGROUND

The data in IAEA TRS-398 [1] for MV beams was prepared in the mid-1990s, and since that date a number of new developments have taken place, such as the publication of ICRU 90 on key data for measurement standards in the dosimetry of ionizing radiation [2], free flattening filter beams, new detectors and dosimetry for small fields. IAEA decided to update its protocol and by the end of 2015 asked for volunteers to measure (based on primary standard dosimeters) and calculate (with Monte Carlo codes) updated $k_{Q,Q0}$ values for reference-class ionization chambers (IC).

Following IAEA demand, EURAMET decided to launch the EMPIR project 16NRM03 RTNORM in mid-2017 to provide $k_{Q,Q0}$ factors to the IAEA. In the MV photon beams workgroup, DTU (Denmark), LNE-LNHB (France), NPL (United Kingdoms) and VSL (the Netherlands) were to measure $k_{Q,Q0}$ factors for 6 IC types in 10 cm x 10 cm linac x-ray beams with and without flattening filters [3].

METHODS

Primary standard dosimeters for absorbed dose to water are water and graphite calorimeters [4, 5, 6]. IAEA requested primary and secondary standard dosimetry laboratories to measure $k_{Q,Q0}$ values for at least 5 ICs of the same type, ideally from different manufactured batches and to include one chamber with well-known $k_{Q,Q0}$ values such as NE 2571.

RESULTS

The results of the different partners will be compared between themselves and to the values expected from previous comparisons [7, 8, 9]. Some of these results are given as examples on figure 1 for the PTW 30013 ionization chamber type.

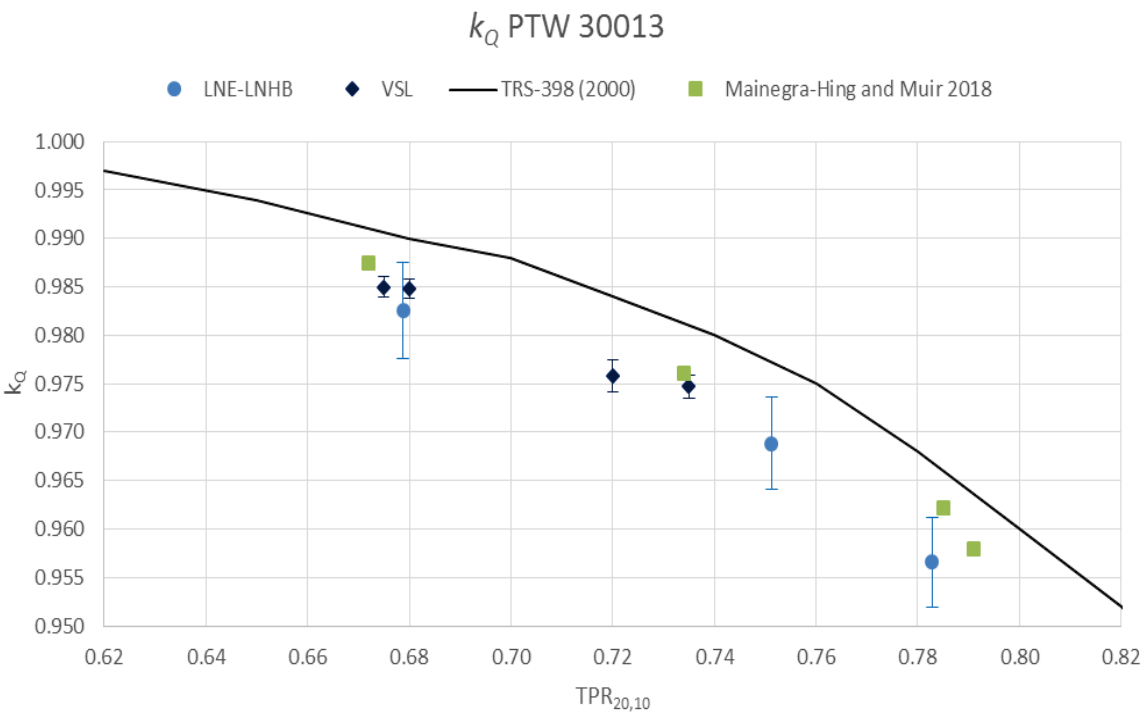

Figure 1. Experimental k_Q for PTW 30013 ionization chambers from VSL (dark blue diamonds) and LNE-LNHB (light blue discs) compared to values from the TRS-398 [1] (black continuous curve) and EGSnrc calculated k_Q from NRC [10] (light green squares). Shown uncertainties correspond to one standard deviation (k=1). VSL points correspond to 6 and 10 MV beams without and with flattening filters of an Elekta Versa HD while LNHB points correspond to 6, 12 and 20 MV beams with flattening filters of a GE Saturne 43.

CONCLUSIONS

The measured $k_{Q,Q0}$ values for Exradin A1SL (1 partner), IBA FC65-G (2 partners), NE 2571 (4 partners), NE 2611 (1 partner), PTW 30013 (3 partners) and PTW 31021 (1 partner) are being sent to IAEA for evaluation before acceptance or rejection to feed the TRS-398 update.

REFERENCES

[1] ANDREO, P., BURNS, D. T., HOHLFELD, K., HUQ, M. S., KANAI, T., LAITANO, F., SMYTH, V. G., VYNCKIER, S., IAEA TRS-398: absorbed dose determination in external beam radiotherapy Technical Report Series (Vienna: IAEA) (2000).

[2] INTERNATIONAL COMMISSION ON RADIATION UNITS & MEASUREMENTS REPORT 90, Key data for ionizing-radiation dosimetry: measurement standards and applications (2016).

[3] DE PREZ, L., DE POOTER, J., JANSEN, B., PERIK, T., WITTKAMPER, F., Comparison of k_Q factors measured with a water calorimeter in flattening filter free (FFF) and conventional flattening filter (cFF) photon beams, Phys. Med. Biol. 63 (2018) 045023.

[4] DE PREZ, L, DE POOTER, J., JANSEN, B., AALBERS, T, A water calorimeter for on-site absorbed dose to water calibrations in Co-60 and MV photon beams including MRI incorporated treatment equipment, Phys. Med. Biol. 61 (2016) 5051–76.

[5] PEARCE, J. A. D., SHIPLEY, D. R., DUANE S., Transfer of the UK absorbed dose primary standard for photon beams from the research linac to the clinical linac at NPL, Metrologia 48 (2011) 365.

[6] DELAUNAY, F., GOURIOU, J., DAURES, J., LE ROY, M., OSTROWSKY, A., RAPP, B., SOREL, S., New standards of absorbed dose to water under reference conditions by graphite calorimetry for ^{60}Co and high-energy x-rays at LNE-LNHB, Metrologia 51 (2014) 552.

[7] PICARD, S., BURNS, D. T., ROGER, P., DE PREZ, L., JANSEN, B., DE POOTER, J., Key comparison BIPM.RI(I)-K6 of the standards for absorbed dose to water of the VSL, Netherlands and the BIPM in accelerator photon beams, Metrologia **54** (2017) 06005

[8] PICARD, S., BURNS, D. T., ROGER, P., DUANE, S., BASS, G.A., MANNING, J.W., SHIPLEY, D. R., Key comparison BIPM.RI(I)-K6 of the standards for absorbed dose to water at 10 g cm^{-2} of the NPL, United Kingdom and the BIPM in accelerator photon beams, Metrologia **52** (2015) 06021

[9] PICARD, S., BURNS, D. T., ROGER, P., DELAUNAY, F., GOURIOU, J., LE ROY, M., OSTROWSKY, A., SOMMIER, L., VERMESSE, D., Key comparison BIPM.RI(I)-K6 of the standards for absorbed dose to water of the LNE-LNHB, France and the BIPM in accelerator photon beams, Metrologia **50** (2013) 06015

[10] MAINEGRA-HING, E., MUIR, B. R., On the impact of ICRU report 90 recommendations on k_Q factors for high-energy photon beams, Med. Phys. **45** (2018) 3904

Primary Standards and Measurement Methods for X-ray Emitting Electronic Brachytherapy Devices – EMPIR Project: PRISM-eBT

T. Schneider

Physikalisch-Technische Bundesanstalt, Bundesallee 100, 38116 Braunschweig, Germany

Email address of Corresponding Author: Thorsten.Schneider@ptb.de

BACKGROUND

In the past decade, electronic brachytherapy (eBT) has evolved as an attractive modality for the treatment of skin lesions, intraoperative partial breast irradiation and applications in intracavitary and interstitial sites, brain tumours and kypho-IORT. Operating at low kilovoltage energies, eBT has many of the advantages of established radiotherapy approaches, but with further benefits [1]: eBT is considered a cost-effective treatment application, since little or no capital expenditure on shielding is required and normal operating rooms can be used. The shorter treatment schedule reduces hospital bed time and costs. For some treatment modalities (e.g. rectum) it reduces surgical expense. In some clinics the use of eBT frees time for more expensive conventional linear accelerators allowing increased capacity without an additional high investment. And finally, since no radioactive sources need to be handled, the effort for radiation protection, transportation and safety are reduced.

The delivery and dosimetry technologies for eBT are often developed and marketed by the vendor of the device. Most of the systems come pre-calibrated by the manufacturers with pre-commissioned sets of dosimetric data and the dose values are only valid within a specific system. This makes it difficult to adopt a clinically established treatment plan from one system to another and to verify dosimetry independently, contrary to the core requirement of clinical medical physics that dosimetry should be subject to independent and traceable verification [2]. In almost all cases these eBT systems are not directly traceable to a National Metrology Institute and rely on indirect methods with uncertainties larger than clinically acceptable. Harmonised and simplified dosimetric procedures will improve the safety of use and will enable the full utilisation of this modality.

METHODS

Within the framework of an European Metrology Programme for Innovation and Research (EMPIR), six European National Metrology Institutes (NMIs) together with partners from universities and clinics will collaborate in a joint research project with the aim to establish a harmonised, simplified and traceable dosimetry for eBT. All activities together will reduce the uncertainties in dose, dose distribution and dose-effect-relation to a level recommended in [3] and improve the efficacy of eBT treatment. These activities will enable better confidence in the therapeutic and clinical benefit of these radiotherapy modalities through improved data and this, in turn, will increase uptake.

RESULTS

The specific objectives of the EMPIR project PRISM-eBT (June 2019 – May 2022) are:

1. To establish primary standards for the absorbed dose rate to water for eBT devices at 1 cm depth of water for internal radiotherapy, to evaluate currently used transfer instruments and corresponding measurement procedures and to establish simple and robust tools for dissemination of the absorbed dose rate to water to clinical practice.

2. To establish a dosimetric methodology for superficial eBT aligned with or similar to the recommendations for superficial (skin) external radiotherapy given in TRS 398 [4], DIN 6809-4 [5], NCS-10 [6] and IPEM [7].

3. To characterise detectors and measurement instruments suitable for the determination of 3D dose distributions in water by eBT devices. To develop a standardised traceable calibration process for these detectors, allowing a reduction in the uncertainties in dose, dose distribution and dose-effect-relation to a level recommended in IAEA Human Health Report No 31 [3].

4. To provide traceable dosimetry for 3D dose distribution measurements for eBT systems such as INTRABEAM, Axxent or Esteya for which no dosimetry system currently exists and to make them available for the end user community.

5. The data provided in this project will be compiled in Good Practice Guides and submitted to IAEA and Standards Developing Organisatios (SDOs) for uptake in their written standards.

CONCLUSIONS

An outline of the PRISM-eBT project will be presented to make the eBT user community aware of the work planned for the next three years (mid-2019 to mid-2022) and to enable end-users to comment on the proposed objectives. The results of this European Joint Research Project with contributions from six National Metrology Institutes, two University Hospitals and several external stakeholders will enable SDOs to draft a new standard for harmonized dosimetry of eBT devices which will increase the treatment efficacy of eBT.

ACKNOWLEDGEMENT

The research within this EURAMET joint research project receives funding from the European Community's Seventh Framework Programme, ERA-NET Plus, under Grant Agreement No. 217257.

REFERENCES

[1] INSTITUTE OF PHYSICS AND ENGINEERING IN MEDICINE; Medical and dental guidance notes. York, UK: IPEM; 2002.

[2] HENSLEY F, Present state and issues in IORT Physics, Radiation Oncology (2017) 12:37, DOI 10.1186/s13014-016-0754-z

[3] INTERNATIONAL ATOMIC ENERGY AGENCY, Accuracy Requirements and Uncertainties in Radiotherapy, IAEA Human Health Series No. 31, IAEA, Vienna (2016).

[4] INTERNATIONAL ATOMIC ENERGY AGENCY: Absorbed Dose Determination in External Beam Radiotherapy Based on Absorbed-Dose-to-Water Standards: An International Code of Practice for Dosimetry. IAEA, Technical Report Series No. 398. IAEA, Vienna, 2000

[5] DIN 6809-4:2016-06: Klinische Dosimetrie - Teil 4: Röntgentherapie mit Röntgenröhrenspannungen zwischen 10 kV und 300 kV / Clinical dosimetry - Part 4: X-ray therapy with X-ray tube voltages between 10 kV and 300 kV, in press

[6] NEDERLANDSE COMMISSIE VOOR STRALINGSDOSIMETRIE (NCS), Dosimetry of low and medium energy x-rays: A code of practice for use in radotherapy and radiobiology, NCS Report 10, NCS, Delft (1997)

[7] KLEVENHAGEN S C, AUCKETT R J, HARRISON R M, MORETTI C, NAHUM A E AND ROSSER K E 1996 The IPEMB code for practice for the determination of absorbed dose for x-rays below 300 kV generating potential (0.035 mm Al–4 mm Cu HVL; 10–300 kV generating potential) Phys. Med. Biol. 41 2605–25

p_Q and $k_{Q,Q0}$ Factors for Medium Energy X-rays from the RTNORM EMPIR Project

M. Pinto[a]
M. Pimpinella[a], B. Rapp[b], J. Plagnard[b], L. de Prez[c], B. Jansen[c], P. Teles[d], K. Zink[e]

[a]ENEA-INMRI, Istituto Nazionale di Metrologia delle Radiazioni Ionizzanti, Via Anguillarese 301, 00123 Santa Maria di Galeria (RM), Italy
[b]CEA-LIST, Laboratoire National Henri Becquerel (LNE-LNHB), F-91191 Gif-sur-Yvette, France
[c]VSL, Dutch Metrology Institute, Thijsseweg 11, 2629 JA Delft, The Netherlands
[d]IST-ID Associação do Instituto Superior Técnico para a Investigação e Desenvolvimento, Avenida Rovisco Pais 1, 1049-003 Lisboa, Portugal
[e]THM, Technische Hochschule Mittelhessen - University of Applied Sciences - Institut für Medizinische Physik und Strahlenschutz, Wiesenstr. 14, 35390 Gießen, Germany

Email address of Corresponding Author: massimo.pinto@enea.it

BACKGROUND

The data in IAEA TRS-398 [1] for medium-energy x-ray beams was prepared in the mid-1990s, and since that date a number of new developments have taken place, such as the publication of ICRU 90 on key data for measurement standards in the dosimetry of ionizing radiation [7], new detectors, and notably the availability of primary standards of absorbed dose to water that were not available at the time. The IAEA decided to update the TRS-398 protocol and by the end of 2015 asked for volunteers to measure (based on primary standard dosimeters) updated p_Q and $k_{Q,Q0}$ values for reference-class ionization chambers (IC).

Following the demand of the IAEA, EURAMET approved the EMPIR project 16NRM03 RTNORM in mid-2017 to provide both p_Q and $k_{Q,Q0}$ factors to the IAEA. In the kV x-rays photon beams workgroup, ENEA-INMRI (Italy), LNE-LNHB (France), IST-ID (Portugal), THM (Germany) and VSL (the Netherlands) were to measure and calculate both p_Q and $k_{Q,Q0}$ factors for 3 IC types in medium-energy x-ray beams of eight filtered radiation qualities.

METHODS

Primary standard dosimeters for absorbed dose to water are water and graphite calorimeters [6, 8, 9] and primary standards of air kerma are free-air chambers [2-4]. IAEA requested primary and secondary standard dosimetry laboratories to measure p_Q and $k_{Q,Q0}$ values for at least 5 ICs of the same type, ideally from different manufactured batches and to include one chamber with well-known p_Q and $k_{Q,Q0}$ values such as the NE 2571chamber.

RESULTS

For the PTW30013 chamber model, N_{Dw} from Monte Carlo simulations using EGSnrc were aligned to experimental measurements reported in a recent key-comparison [5]. New experimental determinations of $k_{Q,Q0}$ factors for the chamber model NE2571, using the CCRI-250 quality as Q_0, indicate $k_{Q,Q0}$ factors down to about 0.93 for the beam qualities with mean energy down to ~40 keV and an uncertainty of ~1.3% (k=1).

CONCLUSIONS

This work groups together independent Monte Carlo calculations and experimental determinations of both p_Q and $k_{Q,Q0}$ values from European National Metrology Institutes and Universities, using chamber models IBA FC65-G, PTW 30013, and NE 2571. Part of these data are being prepared for submission to the IAEA for inclusion in the update of the TRS 398.

REFERENCES

[1] ANDREO P., BURNS D.T., HOHLFELD K., HUQ M., KANAI T., LAITANO R.F., SMYTH V., VYNCKIER S., Absorbed Dose Determination in External Beam Radiotherapy, An International Code of Practice for Dosimetry Based on Standards of Absorbed Dose to Water IAEA TRS-398 (2000)

[2] BURNS D.T., KESSLER C., DE POOTER J.A., JANSEN B.J., Key comparison BIPM.RI(I)–K3 of the air-kerma standards of the VSL, The Netherlands and the BIPM in medium-energy x-rays, Metrologia **53** (2016) 06016–6

[3] BURNS D.T., KESSLER C., DENOZIERE M., KSOURI W., Key comparison BIPM.RI(I)–K3 of the air-kerma standards of the LNE-LNHB, France and the BIPM in medium-energy x-rays (2008)

[4] BURNS D.T., KESSLER C., PINTO M., CAPPADOZZI G., SILVESTRI C ., TONI M.P., Key comparison BIPM.RI(I)–K3 of the air-kerma standards of the ENEA, Italy and the BIPM in medium-energy x-rays Metrologia **51** (2014) TechSuppl06020

[5] BURNS D.T, KESSLER C., BÜERMANN L., KETELHUT S., Key comparison BIPM.RI(I)-K9 of the absorbed dose to water standards of the PTB, Germany and the BIPM in medium-energy x-rays Metrologia 55 (2018) 06006–6

[6] DE PREZ L.A., DE POOTER J.A., JANSEN B., AALBERS T.A., A water calorimeter for on-site absorbed dose to water calibrations in ^{60}Co and MV-photon beams including MRI incorporated treatment equipment, Phys Med Biol **61** (2016) 5051–76

[7] ICRU Report No. 90*:* Key Data for ionizing-radiation dosimetry: measurement standards and applications vol 14 (2016) no. 1.

[8] PINTO M., PIMPINELLA M., QUINI M., D'ARIENZO M., ASTEFANOAEI I., LORETI S., GUERRA A.S, A graphite calorimeter for absolute measurements of absorbed dose to water: application in medium-energy x-ray filtered beams, Phys Med Biol **61** (2016) 1738–64

[9] RAPP B., PERICHON N., DENOZIERE M., DAURES J., OSTROWSKY A. AND BORDY J.-M., The LNE-LNHB water calorimeter for primary measurement of absorbed dose at low depth in water: application to medium-energy x-rays, Phys Med Biol **58** (2013) 2769–86

Designing a State-of-the-Art Dosimetry Laboratory for Accelerator-Based Megavoltage Photon Beam Calibrations and Research

C. E. Andersen[a]

[a]Center for Nuclear Technologies, Technical University of Denmark, Build. 201, 4000 Roskilde, Denmark

Email address of Corresponding Author: clan@dtu.dk

BACKGROUND

To advance medical dosimetry research in Denmark and to support Danish hospitals in offering the most advanced treatment modalities available, a state-of-the-art dosimetry laboratory has been established by the Technical University of Denmark. The laboratory is currently used in an EURAMET EMPIR research project (www.RTnorm.eu) entitled: "kQ factors in modern external beam radiotherapy applications to update IAEA TRS-398", and data from this project will be used to demonstrate the capabilities of the laboratory. However, the main purpose of this contribution is to communicate how the laboratory has been designed with the view that this potentially could be of relevance for others within this field.

METHODS

The laboratory has two radiation sources: A medical linear accelerator (Varian Truebeam, Varian Medical Systems, USA) and a ^{60}Co source (Terabalt, UJP Praha, Czech Republic). An important feature of the accelerator is its ability to deliver five different qualities of megavoltage photon beams (4, 6, 10, 15, and 18 MV) plus two qualities without fattening filter (6 and 10 MV FFF). The laboratory is air-conditioned with a total air circulation flow of up to 21000 m^3/h, and the temperature stability (maximum deviation from the mean) over 24 h is better that 0.3°C at the isocenter of the accelerator and 0.15°C at the cobalt source. The stability of the humidity is better than 5%RH. Two Keithley 6517 electrometers with 1 nF external air capacitors and an external time base are used for traceable charge and current measurements, and these electrometers are calibrated in situ using a dedicated calibration system partly based on the one developed by Downton and Walker (2012). The laboratory is equipped with a closed local area network, and all instruments (including the cobalt source) can be controlled remotely using this network and any computer connected to it.

RESULTS

Ionization chambers are positioned free in air both in the cobalt and in the linear accelerator system using a combination simple alignment telescopes, micometers, digital indicators, and special gauge blocks. A special lift is used to submerge the ionization chamber into water. Important elements in this optical positioning system are based on procedures in used at the IAEA laboratories in Seibersdorf (Czap, 2017). The reproducibility of ionization chamber positioning influences absorbed dose to water measurements in the 30x30x30 cm^3 water tank by less than 0.03% (one standard deviation). Using an external transmission monitor chamber (PTW 7862, Germany) the output variability from the accelerator can be reduced to less than 0.05% (one standard deviation) over an extended period of time (weeks). This facilitates calibration of ionization chambers relative to a reference ionization chamber calibrated at a primary standards laboratory.

Data acquisition is carried out using a general-purpose software (Andersen, 2018) with a text-based scripting language that can communicate with instruments using different protocols (e.g. RS-232, GPIP and TCP) in their native command language. In particular, the software can handle buffered acquisitions obtainded by Keithley electrometers triggered by an external time base. The software is highly flexible, and the use of this software has been instrumental in the development and testing of all the various calibration and measurement procedures used in the laboratory. All data analysis and visualizations are carried out using standardized procedures programmed in R (R Core Group, 2018).

CONCLUSIONS

A new dosimetry laboratory for accelerator-based megavoltage photon beam calibrations and research has been established. Several systems and solutions have been developed along the way. Sorted by the time consumption required to reach those solutions, the following issues should be highlighted: to tune the air-conditioning system to be stable, to have a linear electrometer calibration system without the need for significant leakage corrections, to be able to position ionization chambers in a highly reproducible way, to account for accelerator output variability using an external monitor chamber positioned under stable thermal conditions, and to develop software for semi-automated data acquisition and analysis.

REFERENCES

[1] ANDERSEN, C.E., Guide to the MELab software (2018), DTU Nutech internal report, Denmark 155 pp.
[2] CZAP,L., Personal communication, 2018.
[3] DOWNTON, B., WALKER, S., Humidity effects on calibrations of radiation therapy electrometers, Medical Physics 39 (2012) 984-987.
[4] R CORE TEAM, R: A language and environment for statistical computing. R Foundation for Statistical Computing, Vienna, Austria. 2018, URL https://www.R-project.org/.

Secondary Standards Dosimetry Laboratories

Calibration of Radiation Protection Medical Monitoring Instruments Using Caesiumn-137 Gamma Calibration System

C. Omondi[a]

E. Cheruiyot[b], **W. Adwet**[b], **M. Nguli**[b]

[a]Kenya Bureau of Standards (KEBS)

[b]University of Nairobi (UoN)

Email address of Corresponding Author: collinsyallar@yahoo.co.uk

BACKGROUND

Radiation workers and the public in general need to be protected from the effects of ionizing radiation and this is the concern of every country's radiation protection agency. This can be realized by monitoring the radiation levels encountered by using radiation dosimeters and survey meters. The monitoring instruments should have a known level of accuracy and precision to avoid wrong dose or dose rate readings that could lead to overexposure. For this reason, it is a requirement for these instruments to be periodically calibrated to ensure that they are working properly and suitable for radiation monitoring purposes. The objective of this research is to demonstrate the importance of calibration of monitoring instruments using Caesium-137 gamma calibration system and compare the developed reference standards with existing standards.

METHODS

The k_{air} rate was deduced by applying the correction factor for pressure and temperature ($K_{P,T}$) and the calibration factor for the whole system (N_k) as in the following equation:

$$\boldsymbol{K_{air} = Q.\mathrm{K}_{P,T}.N_K}$$

where

$$\boldsymbol{K_{P,T} = P_0.T/P.T_0}$$

The calibration factor (C.F) was then obtained by:

$$\boldsymbol{C.F = \frac{reference\ reading}{observed\ value}}$$

RESULTS

Beam profile and homogeneity:

The ionization chamber was connected to PTW UNIDOS electrometer which was used to scan the beam horizontally in steps of 2.5 to 5 cm at Source-Chamber Distance (SCD) of 50, 100,115, 141,200, 300, 400 and 500 cm. The charge measurement at each point was taken after 60 seconds at Integration Current Mode of the electrometer after which a plot was made of the relative charge (Q) against the horizontal distance for different SCDs.

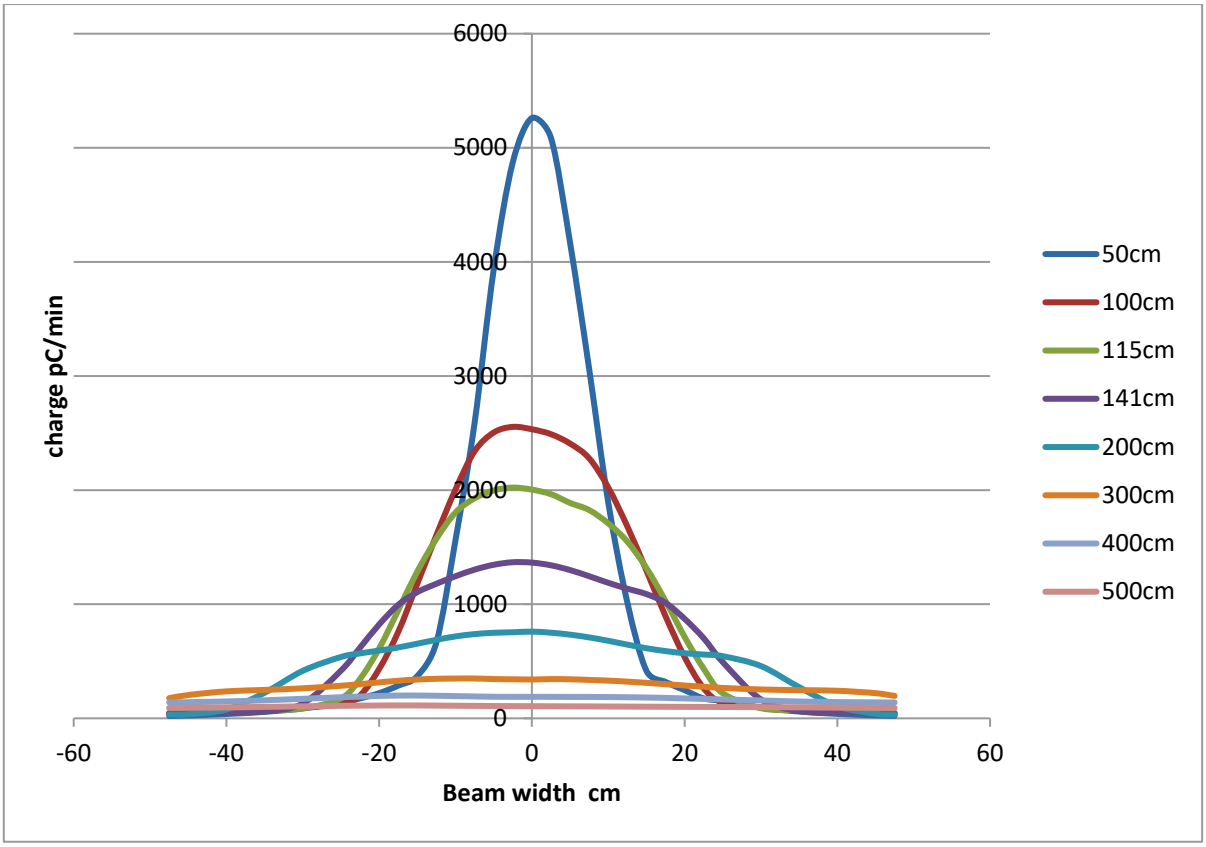

CONCLUSIONS

The beam width increased with increase in SCD while the charge decreased with increase in SCD following the inverse square law.

The shoulders of the beam were not well defined because the ionization chamber used was larger in diameter (140mm).

There were shifts in the position central beam axis (CBA) at each SCD which could have been caused by the misalignment of the laser and inaccurate positioning of the horizontal plane ruler. The misalignment of wall laser was noted during the experiment. Therefore, the wall laser divergence was determined and included in the uncertainty budget.

An ionization chamber with a smaller diameter is recommended for a well-defined beam profile.

REFERENCES

[1] IAEA. (2000). Safety Reports Series No. 16: Calibration of Radiation Protection Monitoring Instruments . Vienna: IAEA.

[2] IAEA. (2009). Technical Report Series No. 469: Calibration of Reference Dosimeters for External Beam Radiotherapy. Vienna: IAEA.

[3] Peter Sharpe, A. M. (1999). Guidelines for the Calibration of Dosimeters for use in Radiation Processing. UK: National Physical Laboratory.

[4] Stanslus, A. M., & Collins, Y. O. (1999). Cs-137 Gamma Quality Control Procedures. Nairobi: Kenya Bureau of Standards.

Improved Calibration Service in the Field of Diagnostic Radiology

O. Ciraj-Bjelac
M. Zivanovic, N. Krzanovic

Vinca Institute of Nuclear Sciences, University of Belgrade, M.P. Alasa 12-14, Vinca, Serbia

Email address of Corresponding Author: ociraj@vinca.rs

BACKGROUND

Health protection has been recognized as the most important goal and obligation of ionising radiation metrology. Dissemination of standards obtained with improved measurement capability to medical institutions certainly leads to better health protection. This requirement is important in diagnostic and interventional radiology, owing the fact that these procedures are the largest contributing factor to the population dose form man-made sources of radiation. In addition, the International Basic Safety Standards stress the importance of accurate dosimetry and require calibration of all measuring equipment related to application of ionising radiation in medicine.

For more than 4 decades, Secondary Standard Dosimetry Laboratory (SSDL) of Vinca Institute of Nuclear Sciences, a member of IAEA/WHO network of SSDLs, provides calibrations of dosimeters in radiotherapy, radiation protection and partially in the field of diagnostic radiology. Since 2014, SSDL is formally recognized by national metrology institution as a part of the national metrology infrastructure, with status of a Designated Institute (DI) for metrology of ionising radiation. Laboratory is accredited according to the standard ISO/IEC 17025. The service of the Laboratory was significantly improved through the IAEA Technical Cooperation project SRB/6/012 (2016-2017). The goal of the project was achieved through: a) improved accuracy in dosimetry for x-ray beam qualities and newly developed calibration service for diagnostic radiology and low energy x-rays; b) improved reliability of ionizing radiation measurements in radiotherapy, including dosimetry audits. The objective of this work is to present conditions used for the establishment of the radiation beam qualities and calibration procedures in the field of diagnostic radiology.

METHODS

Requirements for calibration facilities, in particular for the SSDL are given in terms of necessary equipment for generation of beam qualities, dosimetry and auxiliary equipment necessary for operation of SSDL. All equipment used for calibration in SSDL is of a reference class and includes: ionization chambers, electrometers, thermometers, barometers and a device to measure the relative humidity of air [1]. Radiation beam quality is the indication of photon fluence spectrum. In practice, it is determined by the tube voltage, first and second half-vale layer (HVL) and total filtration [1,2]. Required radiation qualities were established in accordance with recommendations given in the standards of International Electrotechnical Commission (IEC) according to the procedure described in IAEA TRS 457 [1.2]. For generating X ray beams, a dedicated X ray unit Hopewell Design 225 kV was used, whereas a ion chamber Exradin A3 (Standard Imaging, USA) with electrometer Unidos (PTW, Freiburg Germany) was used as a dosimetry standard.

RESULTS

The qualities used for the calibration of dosimeters for different applications are shown in the Table 1.

Table 1. Radiation beam qualities with first and second HVLs

Radiation beam quality	Tube voltage (kV)	First HVL (mm)	Second HVL (mm)	First HVL in TSR 457 (mmAl)
RQR2	40	1.42 Al	1.75 Al	1.42
RQR3	50	1.78 Al	2.34 Al	1.78
RQR4	60	2.19 Al	3.22 Al	2.19
RQR5	70	2.58 Al	3.85 Al	2.58
RQR6	80	3.01 Al	4.36 Al	3.01
RQR7	90	3.48 Al	5.19 Al	3.48
RQR8	100	3.97 Al	5.92 Al	3.97
RQR9	120	5.00 Al	7.46 Al	5.00
RQR10	150	6.57 Al	9.12 Al	6.57
RQT8	100	0.32 Cu	0.49 Cu	6.9
RQT9	120	0.47 Cu	0.701Cu	8.4
RQT10	150	0.68 Cu	1.12 Cu	10.1
W+Al28	28	0.31 Al	-	0.31 (RQR-M 2)

The general principles for the calibration of dosimeters used in diagnostic and interventional radiology described in the IAEA TRS 457 are followed in the laboratory's calibration procedures [1]. The SSDL provides a calibration coefficient in terms of air kerma or air kerma-length product or air kerma-area product. The uncertainty budget was updated, following laboratory upgrade. The uncertainty for diagnostic radiology calibrations is reduced 2.2 % to 1.6 % for diagnostic radiology.

CONCLUSIONS

Newly commissioned x ray unit, equipped with monitor chamber, dosimetry and auxiliary equipment enabled extension of the calibration services to mammography dosemeters and improved service for other diagnostic radiology dosemeters. Importantly, the new set up significantly improved overall accuracy measurements.

REFERENCES

[1] INTERNATIONAL ATOMIC ENERGY AGENCY. Dosimetry in diagnostic radiology: an international code of practice. Technical Reports Series No 457. Vienna: IAEA; 2007

[2] INTERNATIONAL ELECTROTECHNICAL COMMISSION. Medical diagnostic X-Ray equipment—radiation conditions for use in the determination of characteristics. Report IEC-61267 (2005).

High Energy Beams Dosimetric Intercomparison Study at Institute of Nuclear Medicine and Oncology (INMOL) Lahore, Pakistan

S. Shahid[a]
K. Masood[b], M. Riaz[b], A. Masood[c], A. Waheed Khan[b], A. Shahid[b], K. Mahmood[d]

[a]National University of Computer and Emerging Sciences, Lahore, Pakistan.
[b]Institute of Nuclear Medicine and Oncology, Lahore, Pakistan.
[c]Government College University, Lahore, Pakistan.
[d]Pakistan Institute of Nuclear Science & Technology, Islamabad, Pakistan.

Email address of Corresponding Author: drshahidsaman@gmail.com

BACKGROUND

This study involved the measurement of high energy photon beams output from high energy linear accelerator to ensure Quality Assurance (QA) by INMOL. The dosimetric research study enabled us to use combinations of ionization chambers and electrometers to measure the absolute output of various high energy beams i.e., 6MV and 15MV photon beams using the TRS 398 absorbed dose-to-water dosimetry [1-2].

METHODS

Absorbed dose to water was determined with SSDL dosimetry system using 6MV and 15MV energy beams and measurements parameters at field size of (10x10) cm^2, 100cm source to water phantom surface distance (SSD), while 10cm and 110cm source to ionization chamber distances (SCD) for respective radiation energy beams. IAEA water phantom of (30x30x30) cm^3 dimension having (10x10) cm^2 window with 3mm thick Perspex sheet and Perspex inserter of 2mm thick at wall position of thimble of farmer ionization calibrated chambers was used. Depth in water was 5cm and 10cm at respective high energy beam output real time measurement. Ionization chambers were being aligned by using cross laser beams fixation on front walls, cross wires of beam collimator and scale lighted on phantom surface.

RESULTS

This study demonstrated overall consistency in beam output measurement of dosimetric results for megavoltage photons beam. During these beam calibrations, there was not even a single beam lied outside the intercomparison tolerance level of ±2% [2]. Mean ratios were measured to calculate accelerator output which was in the range from 0. 999 to 1.003 (1 SD) with deviation (%) was from 0.05% to 1.00%. Ratio of measured accelerator output to locally established output are as: 0.98, 1.02; action: within tolerance, within range 0.97, 0.98 or 1.02, 1.03; action: with measurement repeated once and outside tolerance range 0.97, 1.03; action: investigated until resolved. For 6MV, (with field 10×10 cm, STD 100cm and depth 10cm), the calculated MU was 124.6, irradiated MU was 125 and calculated dose [A] was 1.003 (Gy), whereas, for 15MV, with same field, STD and depth) calculated MU was 108.1, irradiated MU was 108 and calculated dose [A] was 0.999Gy. For 6MV, measured dose by glass dosimeter [B] was 1.007 Gy with deviation +0.3% ([C]: (1 – A/B) x 100 %), whereas, for 15MV, measured dose by glass dosimeter [B] was 0.996 Gy with deviation -0.4% ([C]: (1– A/B) x 100%). The uncertainty in dose measured by glass dosimeter measurement of dose is about 1.6% (1 SD). Table 1 presents absorbed dose rate measurements at 5cm,10cm depth in water at SSD100cm.

Table 1. Absorbed dose rates (ADR) measurements

ADR measured at 5cm depth in water at SSD = 100cm			
Horizontal Beam 6MW, SSD=100 cm**,** Water-Depth =10cm, SCD=110cm, $TRP_{20/10}$ =0.68			
Field Size (cm²)	***ADR (cGy/MU) by SSDL***	***ADR (cGy/MU) by INMOL***	***% Deviation***
5 x 5	79.84	90.49	0.5
10 x 10	86.67	87.46	0.9
15 x 15	90.39	90.17	0.7
5 x 5	70.42	71.16	0.7
10 x 10	76.66	77.48	1.0
15 x 15	80.33	80.81	0.9
ADR measured at 10cm depth in water at SSD = 100cm			
Horizontal Beam 15MW**,** SSD=100 cm**,** Water Depth=10cm, SCD=110cm, $TRP_{20/10}$ =0.77			
Field Size (cm²)	***ADR (mGy/300MU) by SSDL***	***ADR (mGy/300MU) by Physicist***	***% Deviation***
5 x 5	1831.5	1811.1	-1.11
10 x 10	2059.1	2016.8	-2.05
15 x 15	2189.0	2137.8	-2.34
5 x 5	3608.7	3531.2	-2.15
10 x 10	3938.3	3851.2	-2.21
20 x 20	4108.4	4011.8	-2.35

CONCLUSIONS

Study established a methodology protocol for subsequent ongoing routine radiotherapy dosimetry audits and set baseline of results and produced a set of reference data. The intercomparison enhanced the investigation level for the identification of different possible sources of errors and provided a basis for precise clinical delivery of higher energy radiation beams for radiotherapy treatment [3].

REFERENCES

[1] IAEA, Absorbed dose determination in external beam radiotherapy: An international code of practice for dosimetry based on standards of absorbed dose to water, Report Series No.398, Vienna.

[2] EBERT, M. A., HARRISON, K., CORNES, D., HOWLETT, S., JOSEPH, D. J., Kron, T., HAMILTON, C. S. and DENHAM, J. W., A comprehensive Australasian multi-centre dosimetric intercomparison -issues, logistics and recommendations, Journal of Medical Imaging and Radiation Oncology (2008).

[3] CASTRO, P., GARCIA- VICENTE, F., MINGUEZ, C., FLORIANO, A., SEVILLANO, D., PÉREZ, L. and TORRES, J. J., Study of the uncertainty in the determination of the absorbed dose to water during external beam radiotherapy calibration, Journal of Applied Clinical Medical Physics, **9** (2008) 70.

Establishment of IEC-61267 RQR X-ray Qualities at SSDL of Algiers

A. Herrati[a]
K. Khalal-Kouache[b]

[a]Département de Dosimétrie des Rayonnements Ionisants (DDRI), Centre de Recherche Nucléaire d'Alger (CRNA), 2 Boulevard Frantz Fanon BP399 Alger-RP 16000 Algiers, Algeria
[b]Faculté de Physique, Université des Sciences et de la Technologie Houari-Boumediene (USTHB), BP32 El-Alia 16111 Bab Ezzouar Alger, Algiers, Algeria

Email address of Corresponding Author: ammar.herrati@yahoo.fr

BACKGROUND

The Secondary Standard Dosimetry Laboratory (SSDL) of Algiers was established in 1989 and is a member of IAEA/WHO SSDL network since 1990. He is in charge for calibration in radiotherapy and radiation protection. For more than two decades he assured the calibration of instruments used in radiotherapy using a Cobalt-60 source (ELDORADO 78 unit), and calibration of instruments for radiation protection purposes using Cesium-237 and Cobalt-60 sources (BUCHLER irradiator).

The SSDL of Algiers has already established X-ray qualities recommended by the ISO-4037_Part 1 [1] standard for the calibration of instrument used in radiation protection, namely the Narrow spectra series [2].

The SSDL of Algiers decided to extend its capability to encompass the calibration of instruments used in the field of conventional diagnostic radiology, by developing the recommended X-ray qualities by the IEC-61267 [3] and TRS-457 [4] standards.

METHODS

To develop the RQR X-ray qualities we have used an X-ray generator (PHILIPS MG-320), a dosimetry system (A3 Spherical ionization chamber associated to an UNIDOS electrometer), a monitor chamber (PTW Type 34014) and high purity Aluminum filters.

The RQR X-ray qualities were developed following the procedure described in IEC-61267 Standard, by determining the needed added filtration to obtain a Half Value Layer (HVL) in Aluminum equivalent with that specified in IEC-61267 Standard. This was done by trial and error method and by studying the variation of HVL versus the added filtration for each RQR quality. The setup used for HVL measurement is given in Figure 1.

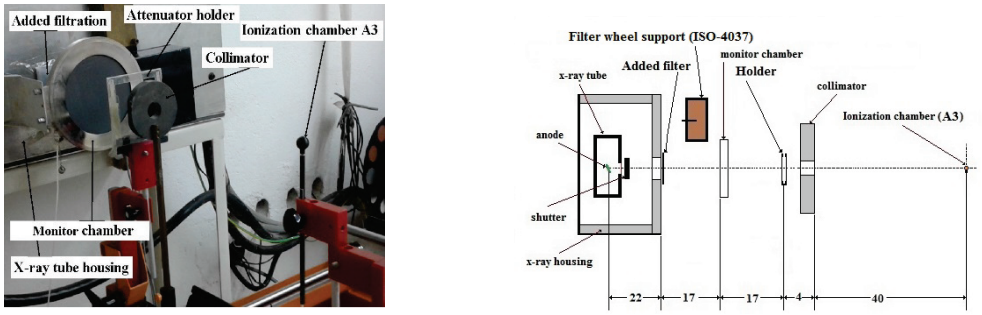

Figure 1. Setup for RQR X-ray qualities HVL measurement.

RESULTS

Characteristics of developed RQR qualities are summarized in Table 1, together with characteristics of reference X-ray qualities defined in IEC-61267 or TRS-457.

Table 1. Characteristics of RQR qualities developed at SSDL Algiers.

RQR Quality	kV	Added filter (mmAl)	HVL SSDL (mmAl)	HVL IEC (mmAl)	Std. Dev.* (%)	$\frac{HVL_{SSD}}{HVL_{IEC}}$
RQR2	40	2.70	1.44±0.04	1.42	1.61	1.014
RQR3	50	2.55	1.75±0.04	1.78	-1.79	0.978
RQR4	60	2.70	2.12±0.05	2.19	-3.20	0.968
RQR5	70	2.80	2.55±0.06	2.58	-1.01	0.988
RQR6	80	3.00	2.99±0.07	3.01	-0.75	0.993
RQR7	90	3.15	3.43±0.09	3.48	-1.33	0.986
RQR8	100	3.30	3.90±0.10	3.97	-1.83	0.982
RQR9	120	3.65	4.96±0.12	5.00	-0.80	0.992
RQR10	150	4.30	6.54±0.16	6.57	-0.39	0.995

*: Std. Dev. (%) = $100*(HVL_{SSDL}-HVL_{IEC})/HVL_{IEC}$

The measured HVLs for each developed X-ray quality are in good agreement with the reference values of IEC-61267 [3] and TRS-457 [4]. Indeed, from Table 1, we can see that the maximum deviation on HVL (3.20%) is less than 5%. All developed qualities at our SSDL meet the alternative criterion:

$$0.957 \leq \frac{\mathrm{HVL}(SSDL)}{\mathrm{HVL}(IEC)} \leq 1.044$$

CONCLUSIONS

In this work, we have developed some reference X-ray spectra recommended by the IEC-61267 standard, namely the RQR series. The obtained RQR Qualities are in good agreement with reference beams and are ready to be used for calibration of instruments used in conventional radiology.

REFERENCES

[1] INTERNATIONAL ORGANIZATION FOR STANDARDIZATION. X and gamma reference radiation for calibrating dose meters and dose rate meters and for determining their response as a function of photon energy- Part 1: Radiation characteristics and production methods. International Standard ISO 4037-1 (1997).

[2] HERRATI, A., ARIB, M., SIDAHMED, T. AND KHALAL-KOUACHE, K. Establishment of ISO 4037-1 X-ray Narrow-Spectrum Series at SSDL of Algiers, *Radiat. Prot. Dosim. (2016) doi: 10.1093/rpd/ncw093*

[3] INTERNATIONAL ELECTROTECHNICAL COMMISSION. *Medical diagnostic X-ray equipment, Radiation conditions for use in the determination of characteristics*. International Standard IEC 61267 (2005).

[4] INTERNATIONAL ATOMIC ENERGY AGENCY. *Dosimetry in Diagnostic Radiology: An International Code of Practice, Technical Report Series N°.457, IAEA, Vienna (2007).*

The SSDL-ININ Calibration and Measurement Capability (CMC) for Reference Air Kerma Rate $\dot{K}_R$ in LDR ^{137}Cs and HDR ^{192}Ir for Well Chambers

D. De la Cruz[a]
J. Álvarez[a], **M. Cabrera**[a]

[a]SSDL, Ionizing Radiation Metrology Department, ININ, Carretera Federal México Toluca S/N. La Marquesa, Ocoyoacac, Estado de México, México. C.P. 52750.

Email address of Corresponding Author: daniel.delacruz@inin.gob.mx

BACKGROUND

The SSDL of the Ionizing Radiation Metrology Department of ININ, since 1970, belongs to the IAEA and WHO (World Health Organization) networks of secondary laboratories, whose objective is to improve the accuracy in radiation dosimetry, trough: calibration services and quality control support for dosimetric evaluation at the hospital.

In Mexico, uterine cervical cancer is one of the important causes of death in women´s. This neoplasm is usually treated with surgery and/or high and low dose rate brachytherapy (BT), with ^{192}Ir sources and sets of ^{137}Cs sources, respectively. However, to achieve success in tumor control using external beam radiotherapy (RT) and/or brachytherapy (BT), the restrictions on accuracy and precision are that the absorbed dose given to the tumor volume has an expanded uncertainty $U(k=2) \leq 5\%$ for RT and $U(k=2) \leq 10\%$ for BT. In particular, we are given a semblance of several activities on reference dosimetry and comparisons in brachytherapy developed by the SSDL since 2005 until today, to set up the CMC for $\dot{K}_R$ in LDR ^{137}Cs and HDR ^{192}Ir for Well Chambers.

METHODS

The determination of $\dot{K}_R$, according NPL code of practice, it is realized by:

$$\dot{K}_R = N_{K_R} \cdot (Q/t) \cdot k_{el} \cdot k_{P,T} \cdot k_{pol} \cdot k_{rec} \cdot k_g \cdot k_{dec} \quad (1)$$

Where the meaning of each term is given in [1]. Therefore, the calibration coefficient for a well chamber is:

$$N_{\dot{K}_R} = \frac{\dot{K}_R}{(Q/t) \cdot k_{el} \cdot k_{PT} \cdot k_{rec} \cdot k_{dec}} \quad (2)$$

RESULTS

The SSDL-ININ has two secondary standard chambers for the realization of $\dot{K}_R$: the SI, HDR 1000 PLUS serial A963391 and A941755, the first calibrated at the NPL with a combined uncertainty u_c of 0.40% in HDR ^{192}Ir and the traceability for LDR 137Cs is given by the NIST through UW. Additionally, the QMS for this and other CMC was approved on September 2018 under the SIM-QSTF, and we are in process of the interregional RMO for the publication of these CMC's on the KCDB. The results obtained for the bilateral comparison ININ-CPHR are given in table 1 [2, 3]. Also, the SSDL-ININ had realized activities for the quality control in brachytherapy for the verification of the calibration of the sources and delivered dose in terms of *Dw*, requesting to the RT center for a reference dose of 2 Gy, with the use of TLD technique. Similar to external beam photons verification, [4, 5].

Table 1. Summary of the results of the bilateral comparison ININ CPHR for $\dot{K}_R$ to ^{192}Ir and ^{137}Cs

Well Chamber	N_{K_R} 10^5/Gy.A^{-1}h^{-1} $\pm U\%(k=2)$ ININ	CPHR	$\dot{K}_R$/mGy h^{-1} $\pm U\%(k=2)$ ININ (NPL)	CPHR (PTB)	Δ%	$R_{ININ/CPHR} \pm u_c$	E_n
A002423	4.645±1.25	4.701±2.60	24.256±1.20	24.537±2.58	-1.19	0.988±0.008	0.440
A941755	5.041±1.25	5.099±2.60	24.256±1.20	24.537±2.58	-1.14	0.989±0.009	0.393
A973052	4.627±1.25	4.679±2.60	24.256±1.20	24.537±2.58	-1.11	0.989±0.008	0.384

Well Chamber	$N_{K_R} \pm U\%(k=2)$ / GyA-1 h^{-1} x 10^5 ININ	CPHR	$\dot{K}_R \pm U\%(K=2)$/ mGy h^{-1} [1]CDSM4/EB711 2016 08 15 ININ (UW/NIST)	CPHR (IAEA/PTB)	Δ%	$R_{ININ/CPHR} \pm u_c$	E_n
A002423	5.084±2.48	5.079±2.56	96.14±2.36	96.05±2.44	-0.10	1.0010±0.0338	-0.028
A963391	5.015±2.47	5.012±2.59	96.14±2.36	96.05±2.44	-0.06	1.0006±0.0338	0.017
PTW 154	10.44±2.49	10.45±2.48	96.14±2.36	96.05±2.44	0.10	0.9990±0.0338	0.027

CONCLUSIONS

The SSLD-ININ has demonstrated its technical competence in the measurement and calibration of sources and well chambers in terms of $\dot{K}_R$ for the ^{137}Cs and ^{192}Ir. However, it was found the application of the air density correction $k_{P,T}$ fails due to the nonequivalence to air of the well chamber walls, [2].

REFERENCES

[1] BIDMEAD, A. M., SANDER, T., LOCKS, S. M., LEE, C. D., AIRD, E. G. A., NUTBROWN, R. F. and Flynn, A. Phys. Med. Biol. 55, 3145–3159 (2010).

[2] ÁLVAREZ, J.T., CABRERA, M.R., GUTIERREZ, S., TAMAYO, J.A., WALWYN G., DE LA CRUZ, D. Radiation Protection Dosimetry (2018), pp. 1–14 doi:10.1093/rpd/ncy053

[3] ÁLVAREZ, J.T., CABRERA, M.R., GUTIERREZ, S., DE LA CRUZ, D., TAMAYO, J.A., WALWYN G., Test proficiency of the SSDL-ININ-MEXICO for the calibration and measurement capability (CMC) of reference air kerma rate $\dot{K}_R$ in ^{137}Cs. Simposio de Metrologia 2018, (2018)

[4] LOAIZA, S.P., ÁLVAREZ, J.T.,. Revista Mexicana de Fisica 52 (5) pp. 413-421 (2006)

[5] ÁLVAREZ, J.T., TOVAR, V.M., SALINAS, B., HERNANDEZ, O., SANTILLAN, L., MOLERO, C., MONTOYA, J., Radiat Prot Dosimetry. 2006; 120(1-4): 95-9. Epub Apr 27 (2006).

Establishment of PTB Mammography Qualities Based on W-Anode and Al-Filtration at SSDL of Algiers

A. Herrati

Département de Dosimétrie des Rayonnements Ionisants (DDRI), Centre de Recherche Nucléaire d'Alger (CRNA), 2 Boulevard Frantz Fanon BP399 Alger-RP 16000 Algiers, Algeria

Email address of Corresponding Author: ammar.herrati@yahoo.fr

BACKGROUND

Mammography is an X-ray radiology of the breasts. It aims to detect abnormalities, sometimes signs of breast cancer, even before they have caused clinical symptoms. In order to obtain better diagnostics, several pictures of the breasts are taken from different angles. Although the limitation principle does not apply to doses received by patients, the other principle of radiation protection, namely optimization, remains applicable. In order to be able to correctly estimate the doses received by patients undergoing a mammography examination, it is necessary to follow an adequate dosimetric protocol, and to use calibrated dosimeters from recognized calibration laboratories.

The SSDL of Algiers has already established X-ray qualities recommended by the ISO-4037_Part 1[1] standard for the calibration of instrument used in radiation protection, namely the Narrow spectra series [2], and X-ray qualities recommended by the IEC-61267[3] and TRS-457[4] standards for the calibration of instruments used in the field of conventional diagnostic radiology.

In this work, we will develop at SSDL Algiers, X-ray qualities (denoted by WAV and WAH series) were developed at the German Primary Laboratory (PTB). These X-ray qualities are produced by an X-ray tube with Tungsten anode and Aluminum filtration.

METHODS

The WAV X-ray qualities were developed by determining the needed added filtration to obtain a Half Value Layer (HVL) in Aluminum equivalent with that specified in [5]. This was done by trial and error method and by studying the variation of HVL versus the added filtration for each WAV quality. The setup used for HVL measurement is given in Figure 1.

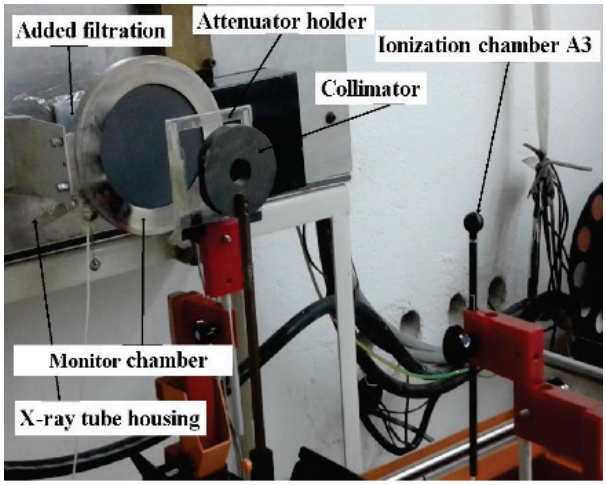

Figure 1. Setup for WAV and X-ray qualities HVL measurement.

The same method and setup was used to develop the WAH X-ray series.

RESULTS

Characteristics of developed WAV X-ray qualities are summarized in Table 1, together with characteristics of reference X-ray qualities defined in [5].

Table 1. Characteristics of WAV qualities developed at SSDL Algiers.

X-ray Quality	kV	Added filter (mmAl)	HVL SSDL (mmAl)	HVL PTB (mmAl)	Std. Dev.* (%)
WAV20	20	0.55	0.254	0.26	**-2.31**
WAV25	25	0.55	0.352	0.35	0.57
WAV28	28	0.55	0.399	0.40	-0.25
WAV30	30	0.55	0.422	0.43	-1.86
WAV35	35	0.55	0.510	0.51	0.00
WAV40	40	0.55	0.574	0.58	-1.03
WAV50	50	0.55	0.70	0.70	-1.29

*: Std. Dev. (%) = $100*(HVL_{SSDL}-HVL_{PTB})/HVL_{PTB}$

The measured HVLs for each developed X-ray quality are in in good agreement with the reference values. The maximum difference between HVL of the reproduced and reference series does not exceed 2.31% for the WAV series (results for WAH series are not reported in this synopsis, but maximum difference between HVL of the reproduced and reference series does not exceed 1.9%).

CONCLUSIONS

In this work, we have developed some reference X-ray spectra (WAV and WAH PTB X-ray qualities). The obtained X-ray Qualities are in good agreement with reference beams and are ready to be used for the calibration of instruments used in mammography.

REFERENCES

[1] INTERNATIONAL ORGANIZATION FOR STANDARDIZATION. X and gamma reference radiation for calibrating dose meters and dose rate meters and for determining their response as a function of photon energy- Part 1: Radiation characteristics and production methods. International Standard ISO 4037-1 (1997).

[2] HERRATI, A., ARIB, M., SIDAHMED, T. AND KHALAL-KOUACHE, K. Establishment of ISO 4037-1 X-ray Narrow-Spectrum Series at SSDL of Algiers, *Radiat. Prot. Dosim.* (2016) *doi: 10.1093/rpd/ncw093*

[3] INTERNATIONAL ELECTROTECHNICAL COMMISSION. *Medical diagnostic X-ray equipment, Radiation conditions for use in the determination of characteristics*. International Standard IEC 61267 (2005).

[4] INTERNATIONAL ATOMIC ENERGY AGENCY. *Dosimetry in Diagnostic Radiology: An International Code of Practice, Technical Report Series N°.457, IAEA, Vienna (2007).*

[5] Physikalisch-Technische Bundesanstalt (PTB). Untitled document downloaded from: https://www.ptb.de/cms/fileadmin/internet/fachabteilungen/abteilung_6/6.2/6.25/ptb_rad_qual_2015_01_07.pdf

Stability Checks of Secondary Standards Used for Calibrations in Diagnostic Radiology

M. Zivanovic[a]
N. Krzanovic[a], O. Ciraj Bjelac[a]

[a]Vinca Institute of Nuclear Sciences, University of Belgrade

Email address of Corresponding Author: milosz@vinca.rs

BACKGROUND

Safe use of radiation sources requires use of appropriate radiation detectors and dosemeters. Dosimetry equipment needs to be calibrated in order to obtain accurate radiation dose measurements. Calibrations are performed in standards laboratories, which use primary, secondary or reference standards traceable to International System of Units [1, 2]. Secondary standards used for calibrations must be stable between two calibrations, and the stability checks are performed within this period. Requirements for reference class dosemeters, as set by IAEA TRS 457, are for the stability of chamber response to be within ±0.5 %, and for secondary standards to be within ±0.3 %. Monitor chambers can be used as reference instruments if they fulfill the same requirements that are set for the reference chambers [3].

METHODS

Stability checks are performed routinely in Vinca Institute of Nuclear Sciences (VINS) Secondary Standards Dosimetry Laboratory (SSDL) at least once quarterly for each ionization chamber. Stability checks for new chambers, as well as the chambers that had a malfunction or repair, are performed in shorter intervals, until a confidence in chamber performance can be achieved.

Recently, new equipment was obtained, including an X-ray generator Hopewell Designs X80-225 kV-E. The superior short and long term stability of the new X-ray generator allowed using a simplified procedure for stability checks. According to the new procedure, chambers are positioned at 1 m in the reference RQT9 beam quality and 10 measurements are performed without using monitor chamber. Suitability of using monitor chamber as a reference instrument is also evaluated by performing stability checks. In this case, stability checks are performed by periodical comparisons with a secondary standard.

RESULTS

Results of the stability checks for two secondary standards (Exradin A3), a tertiary standard (Exradin A650) and a monitor chamber (PTW 34014) are shown in Figure 1.

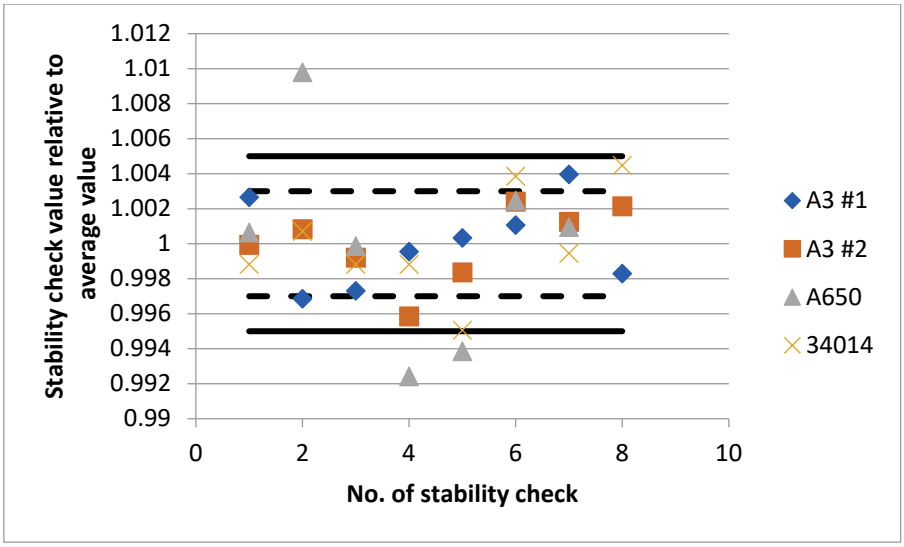

Figure 1.

Stability checks of Exradin A3 chambers have shown that 7 out of 8 measurements are within ± 0.3 % of the average value. Result of one stability check for each chamber does not meet the condition for the secondary standard and is approximately 0.4 % removed from the average value. However, repeated stability checks in both cases are within the requirements. A possible reason for increased deviation in these cases is chamber positioning. Positioning uncertainty is estimated at ± 1 mm, which can influence the stability check result by as much as 0.2 %, due to the fact that the dose rate decreases approximately with the square of the distance.

Stability checks for Exradin Magna A650 chamber have shown that this chamber is not within the requirements set by IAEA TRS 457 [3]. Stability checks results deviate by as much as 1 % from the average value, which cannot be explained by chamber positioning. Further investigation is needed, to exclude possible influence of connector cables and human error.

Monitor chamber stability tests have shown that it meets the requirement of response stability within ±0.5 %. The performance is also within the requirements for calibration of radiation protection equipment – ±0.5 % [4, 5].

CONCLUSIONS

Stability checks in VINS SSDL have shown that two secondary standards and monitor chamber meet the requirements for reference class dosemeters used for calibrations in diagnostic radiology. One chamber used as tertiary standard does not meet the requirements, and additional tests are warranted.

REFERENCES

[1] CIPM-MRA, Mutual recognition of national measurement standards and of calibration and measurement certificates issued by national metrology institutes, BIPM, Paris, 1999

[2] IAEA, SSDL Network Charter, International Atomic Energy Agency, Vienna, 2017.

[3] IAEA, Technical Report Series No. 457, Dosimetry in Diagnostic Radiology: An International Code of Practice, International Atomic Energy Agency, Vienna, 2007.

[4] IAEA, Safety Report Series No. 16 Calibration of Radiation Protection Monitoring Instruments, International Atomic Energy Agency, Vienna, 2000.

[5] ISO, ISO 4037-2, X and gamma reference radiation for calibrating dosemeters and doserate meters and for determining their response as a function of photon energy — Part 2: Dosimetry for radiation protection over the energy ranges from 8 keV to 1,3 MeV and 4 MeV to 9 MeV, International Organization for Standardization, 1997.

A Determination of a Correction Factor from ^{60}Co to ^{192}Ir Obtained by a Monte Carlo Simulation

L. Campos[a]
L.A.Magalhães[b]

[a]Departamento de Física Aplicada e Termodinâmica (DFAT/UERJ),Rua São Francisco Xavier, 524, Maracanã, CEP: 205550, Rio de Janeiro, Brasil
[b]Laboratório de Ciências Radiológicas (LCR/DBB/ UERJ),Rua São Francisco Xavier, 524,Maracanã, CEP: 205550, Rio de Janeiro, Brasil

Email address of Corresponding Author: tc_luciana@yahoo.com.br

BACKGROUND

Radiation dosimetry is an integral part of the radiation therapy process. The ultimate goal of radiation dosimetry is to determine the dose delivered to the tumour and to the normal tissues in a patient undergoing radiotherapy. The importance of HDR ^{192}Ir brachytherapy as the main mode of treatment calls for an accurate dosimetry standard. A dosimetry standard for the direct measurement of absolute dose to water in ^{192}Ir sources is not available.

In this work, we proposed an absorbed dose conversion by determination of a beam quality factor (k_Q) with an ionization chamber. Ideally, the k_Q should be measured directly for each chamber at the same quality as the user beam. However, this is not achievable in most standards laboratories. When no experimental data are available, or it is difficult to measure k_Q directly to realistic beams, in many cases the correction factors can be calculated theoretically with Monte Carlo method.

METHODS

In this study a dosimetric evaluation of GammaMed HDR Plus sources manufactured by Mallindkrodt was done. The calculations were performed according the information provided by MDS Nordion Haan GmbH. The core is encapsulated in a stainless steel wire (AISI 316L). The extension of the proximal end of the wire was modeled as a 60 mm long stainless steel cylinder (AISI 304) with an effective density of ρ=5.6 g/cm^3 [1]. To obtain the air-kerma and absorbed dose for the ^{192}Ir source, bare iridium source file was used as spectra for simulation. ^{192}Ir radionuclide was considered to be uniformly distributed in the active core of length L=3.5 mm. To obtain the dose and kerma, one code in the *EGSnrc* package was used: *cavity*. For this estimation, the ^{192}Ir source was located in the center of a 2.5x2.5x2.5 m^3 air cube. The air-kerma was scored to 0.25 cm up to 100 cm on the transverse axis in a cylindrical ring cell. In addition, 10^9 photon histories were required to obtain an uncertainty below 0.5%. The dose rate constant Λ was calculated by extrapolation technique. The air kerma per history in this study was calculated in air on the transversal axis at 100 cm from the source, as previously described.

The PTW Farmer ionization chamber type 30013 was used in this work and the geometry was constructed in according with the manufacturer specifications. A ^{60}Co spectrum published by Mora *et al.* [2] was employed and a standard ^{60}Co calibration setup was simulated. In this way, an ionization chamber was positioned in the 30x30x30 cm^3 water phantom at 5 cm with 80 cm of source surface distance. The reference field was 10x10 cm^2. In this work the ratio of absorbed water dose and the air cavity dose was obtain to egs_chamber by using the variance reduction techniques. The ratio between the two absorbed doses could be compared follow the dosimetry TRS-398 [3] protocol descriptions. Another calculation was done with the ionization

chamber and the ^{192}Ir GammaMed Plus at 2 cm to calculate $[D_w/D_{air}]^{192}$Ir that is the factor corresponding to the ratio dose scored in water, D_w, and the dose scored inside the chamber's collecting volume at the same point with water effectively replaced with the chamber, D_{air}.

RESULTS

A value of 1.109±0.003 for the dose to the chamber to dose to water ratio was determined for PTW 30013 ionization chamber. The uncertainty quoted is only of type A (1 standard deviation). In order to compare our calculation results to published data, from the Technical Report Series no. 398 (TRS-398), one could find a similar relation as equation 1 with slightly different notations than those used by the AAPM Task Group. The beam quality correction factor, k_Q, was obtained at 2 cm for PTW 30013 using the modeled ^{192}Ir source was 1.002±0.004.

CONCLUSIONS

The accuracy of source modeling was confirmed by comparing calculated results for the radial dose function with previous Monte Carlo data. The dose rate constant is consistent with the results of Ballester *et al.* [1] and Taylor&Rogers [4]. The ionization chamber PTW 30013 was modeled in detail according to the manufacture's specification. It was also possible to determine the ratio of the value of the absorbed dose in the cavity in relation to the dose in water to a depth with a good agreement with the TRS-398.

REFERENCES

[1] BALLESTER et al. Monte-Carlo dosimetry of HDR 12i and Plus 192IR sources. Med. Phys. 2001; 28:2586-2591.

[2] MORA et al. Monte Carlo simulation of a typical ^{60}Co therapy source. Med. Phys. 1999; 36:2494-2502.

[3] IAEA, 2001. Absorbed Dose Determination in External Beam Radiotherapy: An International Code of Practice for Dosimetry Based on Standards of Absorbed Dose to Water, Volume 398 of Technical Report Series IAEA, Vienna.

[4] TAYLOR REP; ROGERS, DWO. An EGSnrc Monte Carlo-calculate database of TG-43 parameters. Med. Phys. 2008; 35:4228-4241.

The SSDL-ININ-MEXICO CMCs for Dosimetry

M.A Montes R[a]

H. J. Mendoza N[a], D. De la Cruz H[a], M. R. Cabrera V[a], J. T. Alvarez R[a]

[a]SSDL, ININ, carretera Federal Mexico Toluca S/N, La marqueza, Ocoyoacac, Mexico, 52750

Email address of Corresponding Author: angeles.montes.servicios@inin.gob.mx

BACKGROUND

In 2002, in the context of the Mutual Recognition Agreement CIPM-MRA, the Instituto Nacional de Investigaciones Nucleares ININ, (through the SSDL of the Ionizing Radiation Metrology Department ME) is appointed as *institute designated* DI by the National Center of Metrology CENAM (The NMI of Mexico), to develop and maintain national standards in the area of ionizing radiation metrology in the country.

METHODS

The SSDL ININ indicates the need to develop and maintain your CMCs for calibration services in external beam radiotherapy and brachytherapy of high and low dose rate, in addition to implementing the ICRU operational quantities system for compliance with national regulations and international recommendations; finally also develop the CMCs for support the diagnostic radiology measurements in the country.

RESULTS

Initially, the QMS is established for 12 CMCs of dosimetry based on the ISO/IEC 17025: 2005, [1], and its approval is achieved in 2007. However, it is not reapproved until 2013 with only 6 CMCs, which is one reduction of 6 CMCs due to lack of comparisons. On the other hand, in this same year it has achieved the approval of 45 radioactivity CMCs.

In the month of September 2018, the SSDL-QMS that supports the CMCs is re-approved by the QSTF-SIM, with a total of 14 CMCs in Dosimetry and 45 radioactivity CMCs, which 6 dosimetry CMCs and 45 for radioactivity has been published at KCDB in 2016 and 2014 respectively, where we are in the process of publishing 4 CMC in dosimetry.

CONCLUSIONS

The demonstration of the competence of SSDL-ININ is achieved through key, supplementary, and bilateral comparisons; where the establishment of a QMS to support our CMC under the ISO 17025: 2005, for their publication at KCDB of the BIPM.

Table 1 Shows the 10 dosimetry CMCs of the SSDL-ININ-Mexico: 6 published on 2016 and 4 in process of publication on 2018 at KCDB.

N	Quantity	Minimum value	Maximum value	Units	Energy	$U\%$ $(k = 2)$	Source of traceability
1	$\dot{K}_a$	1.5E-03	3.1E-03	Gy s^{-1}	Co-60	1.0	ININ
2	$\dot{D}_w$	1.5E-03	3.1E-03	Gy s^{-1}	Co-60	2.5	BIPM
3	$\dot{K}_a$	1.4E-05	3.6E-04	Gy s^{-1}	Cs-137	1.2	ININ
4	$\dot{K}_a$	9.2E-04	1.4E-03	Gy s^{-1}	X-ray, 100 kV to 250 kV	2.6	NIST
5	$\dot{H}^*(10)$	1.7E-05	4.3E-04	Sv s^{-1}	Cs-137	5.0	ININ
6	$H_p(10)$	1.0E-03	1.0E-01	Sv	Cs-137	5.0	ININ
7	$\dot{K}_R$	1.0E-02	6.0E-02	Gy h^{-1}	Ir-192	1.5	NPL
8	$\dot{K}_R$	3.0E-05	3.0E-04	Gy h^{-1}	Cs-137	2.5	NIST
9	$\dot{H}'(10)$	1.6E-05	4.1E-04	Sv s^{-1}	Beta radiation	5.0	ININ
10	$H_p(0.07)$	1.0E-03	3.0E-01	Sv	Beta radiation	10.0	ININ

REFERENCES

[1] INTERNATIONAL ORGANIZATION FOR STANDARDIZATION, General Requirements for the Competence of Testing and Calibration Laboratories, ISO/IEC 17025, ISO, Geneva (2005).

Geometry Correction Factors for Rectangular Neutron Devices

N. Q. Nguyen[a]
N. T. Le[a], B. D. Ky[a], H. Q. Nguyen[a]

[a]Institute for Nuclear Science and Technology, 179, Hoang Quoc Viet st., Hanoi, Vietnam

Email address of Corresponding Author: nnquynh.inst@gmail.com

BACKGROUND

In order to calibrate a neutron measurement device, methods described in the ISO 8259-2 standard [1] implies the geometry correction applied to the device reading. However, regarding the non-spherical device (*i.e.* rectangular devices), the ISO 8529-2 gives only a guidance that the distance should be greater than twice the diameter of the device. In this work, the geometry correction factors for rectangular devices were simulated by the MCNP6 code [2]. The Ludlum 41-42L neutron device was then calibrated using these calculated geometry correction factors.

METHODS

Consider a cylindrical device irradiated by an isotropic point source (fig. 1.a) and a planar rectangular source (fig. 1.b).

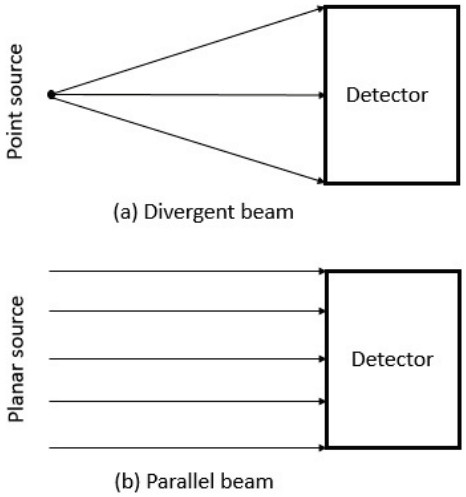

Figure 1. Rectangular neutron device irradiated by different geometrical sources.

The model of rectangular neutron devices consists of a 4 x 4 mm cylindrical ^{6}LiI(Eu) scintillator crystal placed at the center of the rectangular polyethylene moderator (density of 0.95 g/cm^3). The material composition of the scintillator crystal is assumed to be 4.43% ^{6}Li, 0.21% ^{7}Li and 95.45% ^{127}I, with mass density of 3.84 g/cm^3. 29 rectangular moderators of different length, width and height were used in simulation.

The neutron spectrum of the ^{241}Am-Be source was taken from ISO 8529-1 [3]. The ENDF/B-VII.1 nuclear data files packaged with MCNP6.1 were used. The new S(α; β) thermal cattering data of hydrogen in polyethylene (poly.20t) were used to take into account the chemical binding and crystalline effects on thermal neutron scattering at room temperatures.

Geometry correction factor was evaluated by the ratio of the response functions of parallel beam to one of divergent beam. The response function could be calculated by the number of reaction (n,α) in the ^{6}LiI(Eu) scintillator crystal.

RESULTS

As expected, the geometry correction factors decreases with increasing source-detector's center distance l, as well as toward the value 1 when the distance is much larger than the size of the device. For each detector, the geometry correction factors have a maximum value when the detector was close to the source. However, these maximum values vary from 1.0995 to 2.1960.

The Ludlum 41-42L neutron device was calibrated using 3 methods recommended by ISO 8529-2. The results were presented in Table 1.

Table 1. Correction factors of the Ludlum 41-42L

	Generalized fit method	Semi-empirical method	Reduced-fitting method
Correction factor	1.09 ± 0.03	1.11 ± 0.03	1.06 ± 0.02

CONCLUSIONS

In this work, the geometry correction factor of rectangular neutron devices in ^{241}Am - Be neutron field was simulated using MCNP6 code. The simulated results were also used to calibrate the Ludlum 41-42L neutron devices. It is suggested that the reduced-fitting method can be the method of choice to calibrate the neutron devices.

REFERENCES

[1] ISO 8529-2, Reference neutron radiations – Part 2: Calibration fundamentals of radiation protection devices related to the basic quantities characterizing the radiation filed (2000)

[2] T. GOORLEY *et. al*, Initial MCNP6 release overview – MCNP version 1.0, LA-UR-13-22934 (2013).

[3] ISO 8529-1, Reference neutron radiations – Part 1: Characteristics and methods of production (2000).

Personal Dose Equivalent of Neutron Radiation at Radiation Metrology Laboratory of STUK

J. Huikari
T. Siiskonen, A. Kosunen, P. Pousi

Radiation and Nuclear Safety Authority-STUK, Laippatie 4, FI-00880, Helsinki, Finland

Email address of Corresponding Author: jussi.huikari@stuk.fi

BACKGROUND

Increasing demand on calibrations of neutron personal dose meters and to test the neutron sensitivity of photon personal dose meters has been noticed at STUK. Up to now, Radiation Metrology Laboratory of STUK (SSDL) have had calibration capability for ambient dose equivalent ($H^*(10)$) by non-moderated ^{252}Cf and ^{241}AmBe neutrons. Therefore, this study was started to characterize neutron fields produced by STUK calibration neutron sources with measurements and simulations in order to investigate if the STUK facility is suitable for $H_p(10)$ personal neutron dosimeter calibrations. Evaluation is to be made in respect to international standards and the achieved uncertainty of the calibrations.

METHODS

Neutron field characteristics measurements were performed using non-moderated ^{252}Cf and ^{241}AmBe neutron sources. The room return was investigated applying a shadow cone method described in ISO 8529-2 standard [1], using a secondary standard Berthold LB 6411 traceable to PTB, Germany. For each measurement point, two measurements were made. First, measurement of total ambient dose equivalent rate produced by primary and scattered neutrons. Second, measurements behind a shadow cone having only contribution of scattered neutrons. Repeated measurements were made in cps mode in order to get the reliable value of the count rate and to reduce the standard deviation below 2%. These measurements were made source-to-detector distances from 77.5 to 155.5 cm with and without the shadow cone. The shadow cone used is made of polyethylene and its frame is of aluminum. The cone is 50 cm long and its end diameters are 11 cm and 26 cm. The calculations of dose equivalent rates and room return were performed using MCNPX 2.7.0 code package [2]. The initial neutron energy distributions for ^{252}Cf and ^{241}AmBe sources were taken from ISO 8529-1 standard [3]. MCNPX default libraries were used in the calculations. Simulations were carried out in the same source-detector distances as in measurements. To record results, tallies 2 and 5 were used. Tally 2 is particle flux averaged over a surface and tally 5 is a particle flux at a point detector. Tally 2 was 30*30 cm surface centered in air at the reference distance. Tally 5 were also in air centered at the reference distance. In order to get the dose rate, dose function was used to modify tally 5. The coefficients were taken from ICRP 74 [4]. Tally 5 totals for all neutron and uncollided neutron spectra were used to obtain the room return. In addition, albedo type dosimeters (^{6}Li and ^{7}Li) were irradiated to dose of 0.5 mSv $H_p(10)$. Irradiations were performed on ISO slab phantom at 50 and 75 cm distance. TLDs were provided by Doseco company, Finland with calibrations of TLDs traceable to PTB.

RESULTS

Results of the irradiation of dosimeters are shown in Table 1. The ISO 8529-2 states that the reading of the instrument must not change more than 40% due to room return [1]. With ^{252}Cf, this is fulfilled, while with ^{241}AmBe it is not fulfilled. However, simulation results for ambient

dose equivalent rate and measured values agree very well. Measured and calculated values for room return do not agree perfectly, which is interpreted to mean that model has some shortcomings. The discrepancy with ^{241}AmBe personal dose equivalent emphasizes that as well. STUK is aiming to a direct calibration comparison of personal dosimeters with primary laboratory.

Table 1. Neutron dosimeter irradiation results. Thermoluminescence dosimeters were irradiated to 0.5 mSv $H_p(10)$.

Source	Dose at 50 cm (mSv)	Dose at 75 cm (mSv)
^{241}AmBe	0.68	0.81
^{252}Cf	0.56	0.51

CONCLUSIONS

The calculated and measured ambient dose equivalent rates are in good agreement. Also, irradiation results with ^{252}Cf shows good agreement. Further measurements and irradiations as well as calculations are needed to solve the disagreement in room return values. This information will clarify the situation with ^{241}AmBe personal dose equivalent as well.

REFERENCES

[1] International Organization for Standardization. *Reference neutron radiations- Part 2: Calibration fundamentals of radiation protection devices related to the basic quantities characterizing the radiation field.* International standard ISO 8529-2, Geneva, Switzerland, 2000.

[2] T D. B. Pelowitz, ed., MCNPX User's Manual, Version 2.7.0, Los Alamos National Laboratory report LA-CP-11-00438, 2011.

[3] International Organization for Standardization. *Reference neutron radiations- Part 1: Characteristics and methods of production.* International standard ISO 8529-1, Geneva, Switzerland, 2001.

[4] Conversion Coefficients for use in Radiological Protection against External Radiation. ICRP Publication 74. Ann. ICRP 26 (3-4) 1996.

Calibrations of Neutron Survey Meters Used at a Medical Linear Accelerator Facility

L. N. Thiem[a]
N. N. Quynh[a], P. D. Khue[a], N. H. Quyet[a]

[a]Institute for Nuclear Science and Technology; 179 Hoang Quoc Viet, Hanoi, Vietnam

Email address of Corresponding author: Thiem.LNT@gmail.com

BACKGROUND

The Institute for Nuclear Science and Technology (INST) is a sub-institute of the Vietnam Atomic Energy Institute (VINATOM) responsible for calibrations of ionizing radiation measuring devices. Some neutron standard fields have been established at INST since 2015 [1,2] for this purpose of calibrations which are necessary before a neutron meter to be used in radiation measurements for safety assessment.

The reading of a neutron survey meter in a neutron field is the total component consisting of both the neutrons coming directly from the source to the meter and the neutrons scattered from air, concrete walls and other objects in the calibration room. However, different neutron meters could have different readings in the same total neutron field. The calibration factor, CF, of a neutron meter can be determined as the ratio between the conventional true value of neutron ambient dose equivalent rate in a free field, $H^*(10)_{FF}$, and the direct component of neutron ambient dose equivalent rate measured by a neutron meter, $H^*(10)_{dir}$.

This paper presents the calibration process of three neutron meters used at medical linear accelerator facilities, i.e. Aloka TPS-451C (Hitachi), KSAR1U.06 (Baltic Scientific Instruments) and Model 12-4 (Ludlum). The calibrations were done using a standard field of $^{241}Am-Be$ source following the recommendations of ISO 8529-2 series [3]. The CFs of these three neutron meters were evaluated and presented together with their uncertainty budgets.

METHODS

The total component of neutron ambient dose equivalent rate measured by a neutron meter, $H^*(10)_{tot}$, can be fitted as functions of distances from the source as shown in Eq. (1,2,3) corresponding to General Fit Method (GFM), Semi-Empirical Fit Method (SEM), and Reduced Fit Method (RFM), respectively [3].

$$H^*(10)_{tot}(l) = \frac{k}{l^2}\left[\frac{1+\delta.(\frac{r_D}{2l})^2}{1+\bar{\Sigma}(E).l} + A'.l + s.l^2\right] \quad (1)$$

$$H^*(10)_{tot}(l) = \frac{k}{l^2}\left[1 + \delta.\left(\frac{r_D}{2l}\right)^2\right].(1+A.l).(1+R.l^2) \quad (2)$$

$$H^*(10)_{tot}(l) = \frac{k}{l^2} + R_{sct} \quad (3)$$

RESULTS

In Eq. (1,2,3), the component of $\frac{k}{l^2}$ represents for the $H^*(10)_{dir}$ measured by neutron meters. The value of $H^*(10)_{FF}$ can be calculated as Eq. (4)

$$H^*(10)_{FF}(l) = \frac{B.F_1(\theta)}{4\pi l^2}.h_\Phi \quad (4)$$

Based on Eq. (1,2,3) and Eq. (4); the CF can be deduced as shown in Eq. (5). CFs and their uncertainties are shown in Fig.1.

$$CF = \frac{B.F_1(\theta)}{4\pi k}.h_\Phi \quad (5)$$

In those Eq. (1,2,3,4,5), k is the characteristic constant; l is the distance from the center of the source to the device center; A' in Eq.(1) is the air in-scatter component, which has the equivalent meaning with A in Eq. (2); and s in Eq. (1) is the factor accounting for the contribution of all other in-scattered neutrons, which has the same meaning with R in Eq. (2); r_D is the detector radius of a spherical meter or it is considered as half of the meter minimum dimension for non-spherical one; δ = 0.5 is the neutron effectiveness parameter and $\bar{\Sigma}$(E) = 890× 10^{-7} cm^{-1}; R_{sct} is the neutron ambient dose equivalent rate due to the room-scattered component.

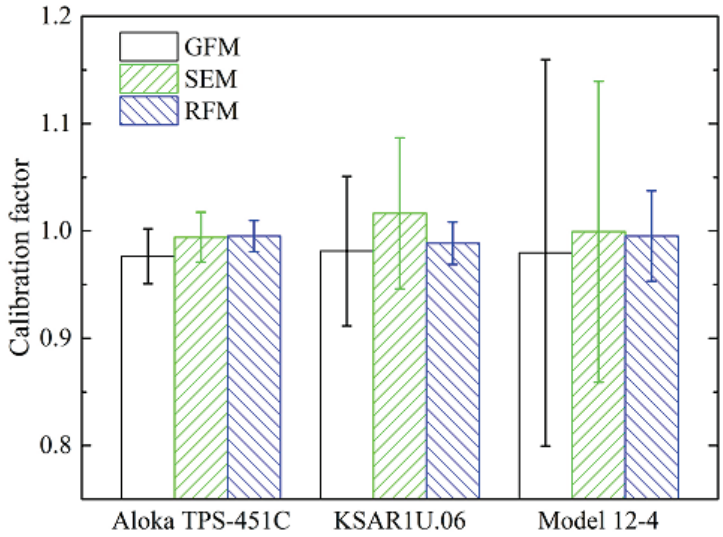

Figure 1. Calibration factors and their standard uncertainties of the neutron ambient dose equivalent rate meters obtained with the three fit methods

CONCLUSIONS

The averaged CFs of the three neutron meters are 0.99, 1.00 and 0.99, respectively with the deviation within 4% for each meter. The CF uncertainties obtained with different methods are ranged from 1.47% to 18.38% depending on the neutron meter and fit methods applied. The RFM method should be more preferably applied in the routine calibrations.

REFERENCES

[1] Thiem Ngoc Le et al.; Characterization of a Neutron Calibration Field with ^{241}Am-Be Source using Bonner Sphere Spectrometer; Applied Radiation and Isotopes; Vol.133 (2018), pp. 68-74.

[2] Thiem Ngoc Le et al.; Neutron Calibration Field of a Bare ^{252}Cf Source in Vietnam; Nuclear Engineering and Technology; Vol 49 (2017), pp. 277-284.

[3] ISO 8529-2:2001 (E); Reference Neutron Radiations - Part 2: Calibration Fundamentals of Radiation Protection Devices Related to the Basic Quantities Characterizing the Radiation Field; Switzerland; p.38. (2000).

Determination of Eye Lens Dose, Hp(3) Using TLD-700H at PTKMR-BATAN

N. Kartubi[a]
A. F. Firmansyah[a], Pardi[a], C. Tuti Budiantari[a]

[a]Center for Safety Technology and Radiation Metrology - National Nuclear Energy Agency (NNEA), Jl. Lebak Bulus Raya No. 49, Kotak Pos 7043 JKSKL, Jakarta Selatan 12070

Email address of Corresponding Author: nazaroh_s@batan.go.id

BACKGROUND

The use of ionizing radiation in medical institutions is increasing year by year. But the negative impact of radiation on the eye lens is increased, especially in interventional radiology, reported by Chodick et al, 2008 [1] and Vano et al, 2010 [2].

“Lens of the Eye Dosimetry has become increasingly important with the changes recommended by ICRP 103/2007 [3] (Statement on Tissue Reaction). The ICRP issued new recommended limits for radiation dose to the lens of the eye, Hp(3) due to concerns over cataracts in April 2011 [4]. This reduction of annual dose limits to the lens of the eye from 150 to 20 mSv (2 rem) has created the need for enhanced monitoring using dosimetry as close as possible to the eye.

In Indonesia, based on the Government Regulation of the Republic of Indonesia No.63/2000 [5] concerning Safety & Health of Ionizing Radiation, "In every utilization of ionizing radiation, the safety factor of the workers must be given on the highest priority". Acceptance of radiation doses by radiation workers must kept as low as possible so as not to exceed the dose limit value permitted by the Supervisory Board and based on the Government Regulation of the Republic of Indonesia No. 33/ 2007 [6] concerning Safety of Ionizing Radiation and Radioactive Source Security, "Safety measures are needed to protect workers, community members and the environment from radiation hazards".

Based on the Regulation of BAPETEN Head No. 4/2013 [7] article 56 (paragraph 1), “Monitoring of eye lens dose should be implemented starting from March 13, 2016, especially for radiation workers who work in special places that requires monitoring dose more intensive around the eye lens.

Based on the Regulation of BATAN Head No. 21/2014 [8] concerning Job description of working group in BATAN, PTKMR-BATAN has the responsibility to study the response of dosimeter which can be used as an accurate eye-lens dosimeter in Indonesia, to monitor the eye lens doses accepted by the radiation worker in the interventional radiology, nuclear medicine, and production of radioisotopes. Goals and objectives of this study is to obtain the calibrated dosimeter which is traceable to the international system (SI) through the national reference.

METHODS

TLD-700H used in this study was LiF: Mg, Cu, P (Figure 1). It has Z_{eff} of 8.3, main peak of 210ºC, maximum emission of 400 nm, relative sensitivity of 25% and fading at 25ºC can be ignored. This dosimeter can monitor beta radiation, gamma and X-rays. The chip for TLD-700H is XD-707H, it has a density of 7 mg/cm^2.

The uniformity of 30 TLD-700H were studied by irradiating the dosimeters attached on the surface of cylindrical phantom (Figure 2) against ^{90}Sr. After 24 hours, the dosimeters were read by using TLD Reader type 6600. The stability testing of TLD were done by irradiating the dosimeters against ^{90}Sr at different time. After 24 hours, the dosimeters were read, and the uniformity and stability test results were obtained.

The dosimeter responses against energy and doses were studied. The dosimeters (Figure 1) were inserted in the available chipstrate bag on the headband then attached on the surface of cylindrical phantom (Figure 2), at SDD (SDD = source detector distance) of 200 cm from the X-ray (Figure 3). The TLD were irradiated with X-ray on (80, 100 and 120) kV, at the Secondary Standard Dosimetry Laboratory (SSDL), in Mampang Prapatan, South of Jakarta, with 7 dosage variations (0.1; 0.5; 1; 5; 10; 15; 20) mSv. It was used 3 dosimeters for irradiating one dose. After being stored for 24 hours, the TLD were read by using TLD Reader (Figure 4). The data were plotted and the response of TLD-700H against doses and energy were obtained.

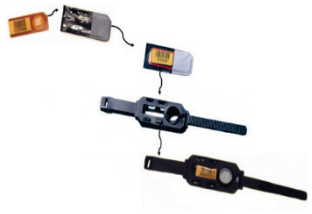

Figure 1. TLD-700H

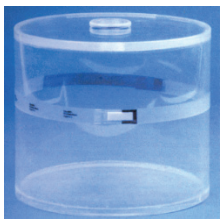

Figure 2. TLD-700H with head band on the surface of Cylindrical phantom

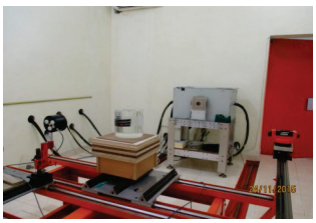

Figure 3. YXLON-MG325 X-Ray

Figure 4. TLD-Reader

RESULTS

The uniformity of TLD-700H were good enough, with 1σ: 1,65% (CL: 67%).

The stability of TLD-700: with 1σ: 2 % (CL: 67%).

The TLD's Response against the angles of X-ray incidence, R (Θ):

$$R(\Theta) = -0.0939\Theta^2 + 0.3893\Theta + 324.14;\ R^2 = 0.9987$$

The Response of TLD-700H against X-Ray doses were:

X-Ray (80 kV) → $R(E_2) = 34.549 *(D) + 0.0829,\ R^2 = 0.9986$
X-Ray (100 kV) → $R(E_2) = 24.725 * (D) + 13.103,\ R^2 = 0.9996$
X-Ray (120 kV) → $R(E2) = 27.929 *(D) - 2.4538,\ R^2 = 0.9974$

The TLD Response against X-Ray energy:

$$R(E) = 0.0939\ E^2 - 20.311\ E + 1222.2;\ R = 0.914$$

CONCLUSIONS

PTKMR-BATAN is ready to determine or evaluate the eye lens dose, Hp(3), provided with the uncertainty of measurement.

REFERENCES

[1] CHODICK, et al., Risk of Cataract after exposure to low dose of ionizing radiation: a 20 - year prospective cohort study among US radiologic technologists, Am. J. Epidemiol. 168,620-631, (2008).
[2] VANO, E, et al, Radiation cataract risk in interventional cardiology personnel, Radiation Res.174, 490-495, (2010).
[3] INTERNATIONAL COMMISSION ON RADIOLOGICAL PROTECTION (ICRP-103-2007), The 2007 recommendations of the international commission on Radiological Protection ICRP Publication 103, Ann. ICRP Vol. 37, Elsevier, Amsterdam, (2007).
[4] ICRP, "Statement on Tissue Reactions", ICRP ref 4825-3093-1464, Vienna, (2011)
[5] MADAN M. REHANI, AAPM-2013, Lens of the Eye Dosimetry, European Society Radiology and IAEA, 2013.
[6] PERATURAN PEMERINTAH (PP) RI No. 33/2007 tentang Keselamatan Radiasi Pengion dan Keamanan Sumber Radioaktif, Jakarta, (2007).
[7] PEMERINTAH (PP) RI No.63/2000 tentang Keselamatan & Kesehatan terhadap Radiasi Pengion, Jakarta, (2000).
[8] PERATURAN KEPALA BAPETEN No. 4, 2013 tentang Proteksi dan Keselamatan Radiasi dalam Pemanfaatan Tenaga Nuklir, Jakarta, (2013).
[9] PERATURAN KEPALA BATAN No. 21/2014 tentang Uraian Tugas Unit kerja di BATAN, Jakarta, (2014).

The Performance of TLD-BARC's PTKMR-BATAN on the Intercomparison of Hp(10) in the Year of 2016-2018 Held by SSDL Jakarta

N. Kartubi[a]
R. Syaifudin[a], S. Subandini Lolaningrum, A. Firnando Fb

[a]Center for Safety Technology and Radiation Metrology –National Nuclear Energy Agency, Jl. Lebak Bulus Raya No. 49, Kotak Pos 7043 JKSKL, Jakarta Selatan 12070.

Email address of Corresponding Author: nazaroh_s@batan.go.id

BACKGROUND

For accreditation requirements, laboratories are required to take part in an intercomparison program based on ISO / IEC-17025:2017. Testing or calibration laboratories that apply for accreditation to National Accreditation Committee (NAC) must have followed at least one intercomparison program. If there is no intercomparison program available, the laboratory must prove its capabilities as in ISO / IEC-17025 item 5.9.a [1].

Laboratories that have been accredited by (NAC) are required to take part in the comparison of measurements at least once a year. For the main scope of accreditation, the laboratory must take the proficiency test once in its accreditation period. In Indonesia, non-radiation intercomparison is usually managed by NAC, while the radiation intercomparison, such as dose quality audit of Hp (10) is managed by the Secondary Standard Dosimetry Laboratory (SSDL) - Jakarta.

As we know, the performance of a dosimetry material or equipment can change or decrease due to the time function (aging) or because of the frequency of use. For this reason, observations have been made on the performance of TLD-BARC from the results of Hp(10) intercomparison during 2016-2018. It was used ANSI (American National Standard Institute) criteria for the assessment [2]. This paper presents the performance of TLD-BARC's PTKMR-BATAN on the intercomparison of Hp(10) in the year of 2016-2018, held by SSDL-Jakarta.

METHODS

TLD-BARC [3] used in this intercomparison consisted of 3 disk dosimeter elements from Teflon BARC CaSO4: Dy materials, with Z_{eff}: 15.1 and disk TLD density: 2.52 g / cm^3. Softening Point of Teflon: 330 ^oC and Main Glow Peak Temperature: 230^oC, with a sensitivity of TLD disk: 30-40 x from LiF (TLD-100). Fading: (2-3) % in 6 months. Linear dose range: 0.1-20 mSv (within ± 10%). Energy response of CaSO4: Dy is very dependent on the energy of the photon, especially at 30 keV energy to 200 keV, while the energy above 200 is relatively flat.

QA for TLD-BARC's PTKMR-BATAN was carried out by implementation of QC test and participation in dose quality audit of Hp (10), held by SSDL-Jakarta. To assess the performance of TLD-BARC, it was used ANSI criteria and JCGM 100:2008 [4].

In this paper, the implementation of QC on new TLD-BARC was carried out by irradiating of 29 TLDs at a dose of 3 mSv, and QC of TLD-Reader by observations on Light Source and EHT (Extra High Tension).

TLD-BARC was calibrated against ^{137}Cs gamma source (OB-85) and X-Ray/YXLON-MG325. The calibration of TLD-BARC in 2015; 2016 and 2017 were presented. To guarantee the

quality of TLD services, Subdivision of Work Safety and Radiation Protection- PTKMR-BATAN participates in the intercomparison of Hp(10) [5], held by SSDL-Jakarta every year. By using these Calibration Curves, PTKMR-BATAN evaluates the personal dose equivalents, Hp(10), for more than 40,000 TLD's in the year of 2015.

RESULTS

The QC test on new TLDs was 2.8%, at a 95% confidence level.

Calibration Curves of TLD-BARC against ^{137}Cs were:

$2015 \rightarrow D_m = [0.001*R(D_1') - 0.0185] \pm 9.2\%, R^2 = 1.$
$2016 \rightarrow D_m = [0.0011*R(D_1') - 0.343] \pm 11.1\%, R^2 = 0.994$
$2017 \rightarrow D_m = [0.0011*R(D_1') + 0.1528] \pm 9.8\%, R^2 = 0.996$

Calibration Curve of TLD-BARC against X-ray N(80) was:

$D_m = [0.0006*R(D_1') - 0.3121] \pm 12.3\%$ (CL=95%)

The performance of TLD-BARC's PTKMR-BATAN on the intercomparison of Hp(10) in the year of 2016 to 2018 is presented in Table 1.

Table 1. Performance of TLD-BARC's PTKMR-BATAN intercomparison of Hp(10) in the year of 2016-2018.

Dosimeter Code	SSDL* Hp(10) (mSv)	PTKMR Hp(10) (mSv)	$\frac{PTKMR}{SSDL*}$	ANSI (H_{LL}-H_{UP})	Radiation	Year
16/Cs-CT-one-1	1	0.99	0.99	0.22-1.88	^{137}Cs	2016
16/Cs-CT-one-2	6	5.54	0.92	0.56-1.61		
16/XR-T-E-one-1	1	0.90	0.90	0.22-1.88	N80	
16/XR-T-E-one-2	6	6.92	1.15	0.56-1.61		
E17-B-X-1	1.5	1.321	0.88	0.53-1.64	N80	2017
E17-B-X-2	4.5	3.367	0.75	0.62-1.55		
E17-B-Cs-1	1.5	1.559	1.04	0.53-1.64	^{137}Cs	
E17-B-Cs-2	4.5	5.051	1.12	0.62-1.55		
E-18-Cs-B-a	5	5.22	1.04	0.62-1.55	^{137}Cs	2018
E-18-Cs-B-b	2	1.99	1.00	0.56-1.61		
E-18-X-B-a	5	4.38	0.88	0.62-1.55	N80	
E-18-X-B-b	8	7.46	0.93	0.64-1.53		

CONCLUSIONS

Based on ANSI criteria, the performance of TLD-BARC's PTKMR-BATAN was in good agreement (in the range of trumpet curve).

REFERENCES

[1] ISO-17025: 2017, General requirements for the competence of Testing and Calibration Laboratories, Vienna, (2008).

[2] ANSI: 2011, American National Standard for Dosimetry Personnel Dosimetry Radiation Performance – Criteria for Testing, New-York, (2011).
[3] A. S. PRADHAN, M. M., ADTANI, G. VARADHARAJAN, A.K .BAKSHI, Handbook on The Use of TLD BADGE Based on CaSO4:Dy Teflon TLD Disk for Individual Monitoring, BABHA Atomic Research Center, India, (2002).
[4] JCGM 100:2008, Evaluation of measurement data, Guide to the expression of uncertainty in Measurement, (2008).
[5] IAEA-TECDOC 1126: 1999, Intercomparison for individual monitoring of external exposure from photon radiation, Vienna, (1999).

Dosimetry Audits

Independent Dosimetry Audits as Best Practice in Radiotherapy

C. Trauernicht[a]
M. du Toit[a], M. Mohlapholi[a], T. Mkhize[a], D. Duprez[b], R. Bester[b]

[a]Tygerberg Hospital and Stellenbosch University, Division of Medical Physics, Gene Louw Building, Tygerberg Hospital, Francie van Zijl Drive, 7505 Tygerberg, South Africa
[b]Tygerberg Hospital, Division of Medical Physics, Gene Louw Building, Francie van Zijl Drive, 7505 Tygerberg, South Africa

Email Address of Corresponding Author: cjt@sun.ac.zamailto:myemail@domain.com

BACKGROUND

Tygerberg Hospital is an AFRA Regional Designated Center for Radiation Oncology and Medical Physics. The hospital requested a full IAEA QUATRO audit [1], which was done in November 2018. A dosimetry audit forms part of a fully comprehensive audit.

METHODS

A dosimetry audit was carried out on a sample of photon and electron beams in the department. This was done using equipment that was made available for use by the National Metrology Institute of South Africa (Farmer and Markus type ionisation chambers plus electrometer). The QUATRO audit team measured the doses according to the IAEA TRS 398 protocol [2]. Apart from the beam quality correction factors, corrections were also done for temperature and pressure, polarisation and ion recombination.

The previous independent dosimetry audit was done in December 2016. This audit was done using the Nano Dot Optically Stimulated Luminescence Dosimeters (OSLDs) from the Imaging and Radiation Oncology Core (IROC) of the MD Anderson Cancer Center in Houston, Texas. The OSLD dose was evaluated using the TG-51 Dosimetry Calibration Protocol [3]. The OSLD sample has an uncertainty of 5 % at a confidence level in excess of 90 %. Agreement within 5 % is considered a satisfactory check.

RESULTS

The results are shown below in Table 1.

Table 1. Dosimetry Audit Results.

Audit	Linac	Energy	Tygerberg Dose [Gy/100MU]	Audit Dose [Gy/100MU]	Difference [%]
QUATRO – Nov 2018 (TRS 398)	2	6 MV	0.988	1.005	1.7
	5	6 MV	1.015	1.008	-0.7
	5	10 MV	1.009	1.014	0.5
	5	18 MV	1.010	1.016	0.6
	4	10 MeV	1.009	1.008	-0.1
	4	12 MeV	1.012	1.010	-0.2
IROC – Dec 2016 (OSLD)	2	6 MV	1.000	1.017	1.7
	4	6 MV	1.000	1.002	0.2
	4	8 MV	1.000	1.038	3.8*
	4	18 MV	1.000	1.004	0.4
	4	6 MeV	1.000	1.028	2.8*
	4	8 MeV	1.000	1.017	1.7
	5	6 MV	1.014	1.012	-0.2
	5	10 MV	1.000	1.004	0.4
	5	18 MV	0.984	1.022	3.9*
	5	6 MeV	1.000	1.014	1.4
	5	8 MeV	1.000	1.003	0.3

* Agreement within 5 % is considered a satisfactory check for the IROC audit

CONCLUSIONS

Beam outputs were well within tolerance levels and no output adjustments were necessary. A regular dosimetry audit forms part of best practice in radiotherapy. This could take the shape of an independent medical physicist checking the beam output with his/her measuring equipment, or it could be an IAEA TLD dosimetry audit, which is provided free of charge by the IAEA. Two other alternatives were taken advantage of in this work. Future work could and should include full end-to-end testing.

REFERENCES

[1] INTERNATIONAL ATOMIC ENERGY AGENCY, Comprehensive Audits of Radiotherapy Practices: A Tool for Quality Improvement, STI/PUB/1297, Vienna (2007)

[2] INTERNATIONAL ATOMIC ENERGY AGENCY, Technical Report Series No. 398, Absorbed Dose Determination in External Beam Radiotherapy, STI/DOC/010/398, Vienna (2000)

[3] ALMOND, P.R., BIGGS, P.J., Coursey, B.M., HANSON, W.F., SAIFUL HUQ, M., NATH, R., ROGERS, D.W.O., AAPM's TG-51 protocol for clinical reference dosimetry of high-energy photon and electron beams, Med. Phys. 26 (9) (1999) 1847 - 1870

Development of a Dosimetry Audit Methodology for Advanced Radiotherapy

H. V. Maselesele[a]
Z. N. Msimang[b]

[a]Steve Biko Academic Hospital, Dr Savage Road, Pretoria, South Africa
[b]National Metrology Institute of South Africa**,** Meiring Naude road, Brummeria, Pretoria 0001

Email address of Corresponding Author: maselesele@webmail.co.za

BACKGROUND

Dosimetry audits have been used in verifying radiotherapy treatment in medicine. Radiotherapy treatment modalities are advancing rapidly and hence the need to develop dosimetry audit methodologies [1]. The IAEA/WHO and other institutions have well-developed systems to audit radiotherapy activities mostly focusing on reference beam output to minimize radiological incidences [2-3]. NMISA has recently established a similar postal dosimetry audit programme. This work seeks to develop a dosimetry audit methodology that will focus on advanced radiotherapy.

Advanced radiotherapy applications often use application of small field radiotherapy beams combined to produce required dose coverage to the cancer tumour. Quality assurance on treatment panning systems (TPS) and treatment delivery units is not an adequate tool to ensure accurate delivery of dose [4]. This methodology focuses on small field audits using EBT 3 films, treatment planning systems (TPS) audits and end to end audits for advanced radiotherapy.

METHODS

In phase 1, EBT3 films stripes were irradiated on a linear accelerator to generate a calibration curve using PTW film software. The beam output is calibrated using the TRS 398 protocol [5]. A standard field of 10 cm x 10 cm and a small field of 4 cm x 4 cm were chosen and used to irradiate the film. Different hospitals were requested to perform similar irradiation and the films were returned for analysis. This was to develop an average calibration curve based on data collected from selected centers.

Phase 2, involved scanning of Shane CIRS Phantom. The scans were used to generate a plan using the supplied instructions. In the instruction the tumor site was described and the Oncologist was expected to draw the relevant contours for the tumor and all the organs at risk associated with the treatment site. After approval, specified report parameters were requested to evaluate the plan [6-7].

RESULTS

Films calibration was successfully carried out for determining the dose. Film dosimetry audit doses where measured and compared with the expected given dose. The results for film dosimetry amongst the participating centers were in agreement within 5 %. However, the dose comparison with expected doses was more than 10 % and further investigations are being done. All structures drawn by the oncologist and the prepared plans were evaluated and doses where measured using Shane phantom. Ionization chambers and RPLD were used for dose

measurements. More results for TPS using Shane phantom were still being evaluated from the hospitals since this require more time.

CONCLUSIONS

This is an ongoing study and the results obtained for film dosimetry need thorough investigation. TPS and treatment delivery measurement data and investigation will be needing statistical analysis and further methodology development.

REFERENCES

[1] WAZIR, M., ASAD, U. (Eds), Assessment of national dosimetry quality audits result for teletherapy machines from 1989 to 2015, Journal of applied clinical medical physics, volume 7, No 2 (2016).

[2] IZEWSKA J., SVENSSON H. (Eds), Worldwide QA networks for radiotherapy dosimetry, Vienna, International Atomic Energy Agency, IAEA-CN-96-76 (2001).

[3] INTERNATIONAL COMMISSION ON RADIOLOGICAL PROTECTION 39 (4), Preventing accidental exposures from new external beam radiation therapy technologies. ICRP Publication 112 (2009).

[4] TECHNICAL REPORT SERIES NUMBER 430, Commissioning and Quality Assurance of Computerized Planning Systems for Radiation Treatment of Cancer, Vienna, International Atomic Energy Agency (2004).

[5] TECHNICAL REPORT SERIES NUMBER 398, Absorbed dose determination in external beam radiotherapy, Vienna, International Atomic Energy Agency (2000).

[6] TECHNICAL DOCUMENT 1583, Commissioning of radiotherapy treatment planning systems, testing for typical external beam treatment techniques, Vienna, International Atomic Energy Agency, (2008).

[7] COMPUTERIZED IMAGE REFERENCING SYSTEM INC., Intensity Modulated Radiotherapy thorax phantom manual, Model 002LFC, Tissue simulation & phantom Technology, Norfolk, Virginia, USA, (2017, www.cirsinc.com).

Dosimetric Comparison Between an External National QUATRO Audit and an Internal QA Results: The Ghana Experience

G. F. Acquah[a]
P. O. Kyeremeh[a], F. Hasford[b, d], E. Addison[c], S. Tagoe[d], E. K. Sosu[e], M. Boadu[e]

[a]Sweden Ghana Medical Centre, Medical Physics Department, Accra, Ghana.
[b]School of Nuclear and Allied Sciences, Department of Medical Physics, Accra, Ghana.
[c]Komfo Anokye Oncology Directorate, Medical Physics Department, Kumasi, Ghana.
[d]National Center for Radiotherapy and Nuclear Medicine, Physics Department Accra, Ghana.
[e]Radiological and Medical Research Institute, Ghana Atomic Energy Commission, Accra, Ghana.

Email address of Corresponding Author: gacquah.felix@gmail.com

BACKGROUND

Independent external audits are vital components of comprehensive quality assurance (QA) programme in radiotherapy [1]. The Ghana Society for Medical Physics (GSMP) provided a Quality Assurance Team for the Radiation Oncology (QUATRO) in accordance with the IAEA-TECDOC 1543 publication [2] and QUATRO guidelines for comprehensive audits conducted an external national audit. This exercise was to ensure credibility of the quality of radiation treatment being offered to patients who patronize these facilities. This study is to analyze the QUATRO's dosimetric results with that of the internal QA results of the facility during the audit period to help strengthen its QA programme.

METHODS

The QUATRO dosimetry audit included the beam output calibration, beam constancy check, output constancy with varying gantry angles and 3D end-to-end test using a CIRS (Model 002LFC) IMRT thorax phantom shown in Figure 1. Other measurements included wedge factors, in vivo dosimetry and monitor unit linearity test. The expert or external audit measured results and deviations were then compared with the local medical physicist to verify the institution's QA programs.

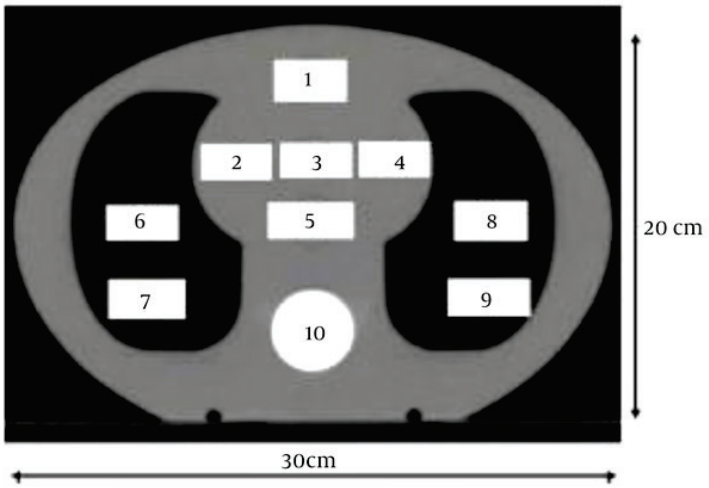

Figure 1. Scanned CIRS (Model 002LFC) IMRT thorax phantom for the end-to-end test

RESULTS

Figure 2 presents the results of the dosimetry audits performed during the QUATRO with that from the local facility's QA program. The QUATRO audit results were presented in a report consisting of a summary and an in-depth report of the safety, mechanical and dosimetry results.

Figure 2. Relative deviations during the QUATRO audit and QA.

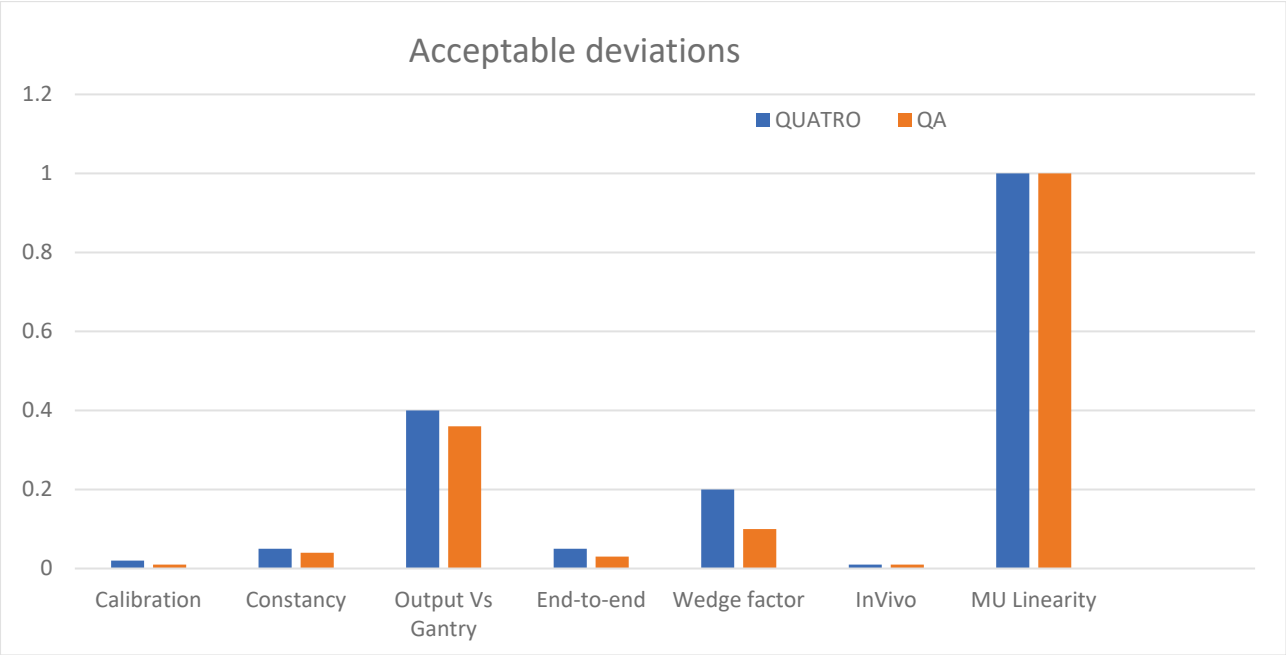

CONCLUSIONS

Each bar represents percentage deviations as assessed by the two dosimetry quality checks in relation to the acceptable levels or tolerance limits. It clearly shows the similarity in terms of deviations between the QUATRO results and the QA results. There is a good agreement between the external audit and the local QA regarding the dosimetry parameters measured. It has also shown that the dosimetry procedures at the facility are performed at a high quality and should be maintained while being encouraged to participate in other external audits.

REFERENCES

[1] LEER, J.W., McKENZIE, A., SCALLIET, P., THWAITES, D.I., Practical Guidelines for the Implementation of a Quality System in Radiotherapy, ESTRO Physics for Clinical Radiotherapy Booklet No. 4, European Society for Therapeutic Radiology and Oncology, Brussels (1998).

[2] INTERNATIONAL ATOMIC ENERGY AGENCY, On-site Visits to Radiotherapy Centres: Medical Physics Procedures, Quality Assurance Team for Radiation Oncology (QUATRO), IAEA-TECDOC-1543, IAEA, Vienna (2007)

Follow Up of Medical Physics Audit of Radiotherapy Centres in Ghana

F. Hasford[a,c]
E. K. Addison[b], E. K. Sosu[a,c], S. Inkoom[a,d], M. Boadu[a,c], G. F. Acquah[e], S. N. Tagoe[a,f], M. Pokoo-Aikins[a,c], T. Dery[c]

[a]Medical Physics Department, School of Nuclear and Allied Sciences, University of Ghana, Accra, Ghana.
[b]Oncology Directorate, Komfo Anokye Teaching Hospital, Kumasi, Ghana.
[c]Radiological and Medical Sciences Research Institute, Ghana Atomic Energy Commission, Accra, Ghana.
[d]Radiation Protection Institute, Ghana Atomic Energy Commission, Accra, Ghana.
[e]Medical Physics Department, Sweden Ghana Medical Centre, Accra, Ghana.
[f]National Centre for Radiotherapy and Nuclear Medicine, Accra, Ghana.

Email address of Corresponding Author: haspee@yahoo.co.uk

BACKGROUND

Ghana's population is estimated at 29 million, with three radiotherapy centres handling a variety of cancerous conditions. The three centres are located at Korle-Bu Teaching Hospital, the Komfo Anokye Teaching Hospital and Sweden Ghana Medical Centre. At present more than 8,000 new and follow-up patients suffering from a variety of cancerous and other degenerative diseases report to the three radiotherapy centres annually. In many developed countries, auditing in radiotherapy is well established resulting in safe application of radiation and improved treatment outcomes, however in Africa, the reverse case is observed.

METHODS

Ghana implemented a national QA audit programme for coordinated and sustainable audits of radiotherapy centres in 2016, with support from IAEA. Three audit teams comprising of medical physicists selected from among the radiotherapy centres were put together for the project. A CIRS thorax phantom was loaned from IAEA for performance of end-to-end testing as part of the dosimetry audit. Checks conducted by the audit teams in the radiotherapy centres include end-to-end tests, absorbed dose to water under reference conditions, room entrance interlock, manual door opening, audio video monitor, beam on indicators, beam terminate switch, emergency off switches, beam indicators, touch guards, table locking brakes, deadman's switches, tray, wedges, blocks and electron applicators. Also, mechanical and geometric tests such as collimator rotation, gantry rotation and couch table movement were undertaken for system performance as well as output factor measurements. Two years after the audit exercise, follow up is being conducted to assess the level of implementation of the recommendations.

RESULTS

Results from the audit exercises showed that the three radiotherapy centres were generally operating at desirable levels with a few identified anomalies needing corrective actions. Recommendations for the corrective actions on the identified anomalies were suggested to management of the radiotherapy facilities. The follow up conducted after two years indicates that over 80% of the recommendations made by the audit teams have been addressed by the radiotherapy centres, indicating high compliance rate.

CONCLUSIONS

In countries with sustainable dosimetry audits, significant improvements in patient safety and dosimetry have been recorded. With implementation of the QA audit programme in Ghana, internal and external audits are anticipated to be sustained as part of a comprehensive quality management system in radiotherapy services in the country.

REFERENCES

[1] INTERNATIONAL ATOMIC ENERGY AGENCY. Comprehensive Audits of Radiotherapy Practices: A Tool for Quality Improvement, Vienna, (2007).
[2] INTERNATIONAL ATOMIC ENERGY AGENCY. Comprehensive Clinical Audits of Diagnostic Radiology Practices: A Tool for Quality Improvement, Vienna, (2010).
[3] INTERNATIONAL ATOMIC ENERGY AGENCY. Quality Management Audits in Nuclear Medicine Practices, 2nd Edition, Vienna, (2015).
[4] HAWORTH, A., et al., Assuring high quality treatment delivery in clinical trials–results from the Trans-Tasman Radiation Oncology Group (TROG) study 03.04 "RADAR" set-up accuracy study, Radiotherapy and Oncology **90** 3 (2009) 299-306.
[5] OTTEVANGER, P., et al., Quality assurance in clinical trials, Critical reviews in oncology/hematology **47** 3 (2003) 213-235.
[6] WORLD HEALTH ORGANIZATION (WHO). Quality Assurance in Radiotherapy. Geneva: WHO, 1988.

Influence of Film Dosimetry Protocols on IMRT Audit Results

T. Santos[a,b]
T. Ventura[b], M. Capela[b], J. Mateus[b], M. Carmo Lopes[b]

[a]Physics Dept., University of Coimbra, Rua Larga, 3004-516 Coimbra, Portugal
[b]Medical Physics Dept., IPOCFG, E.P.E., Av. Bissaya Barreto 98 3000-075 Coimbra, Portugal

Email address of Corresponding Author: taniafssantos@gmail.com

BACKGROUND

Within the framework of a recent intensity modulated radiation therapy (IMRT) audit project carried out in Portugal in collaboration with the IAEA, two film dosimetry protocols have been used. The aim of this work was to explore the correlations of film analysis results, in terms of gamma passing rates between both protocols.

METHODS

Film irradiations were performed in 20 participating centres using Gafchromic EBT3 films (Ashland Inc., Covington, Kentucky) from a single batch (LOT #10241701). Following the audit methodology [1] – **Protocol A** – a film was placed at a coronal plane of the specially designed head and neck (H&N) and shoulders phantom – SHANE (CIRS Inc., Norfolk, VA) – and three treatment fractions were delivered to a dose of about 7 Gy in 6 MV photon mode. The agreement between film and treatment planning system (TPS) calculated dose distributions was evaluated with FilmQA Pro software (Ashland Inc., Covington, Kentucky) using triple channel correction, and considering TPS dose distribution as the reference. For **Protocol B** a second film was irradiated in the same setup with only one fraction and analysed following a well-established methodology developed and clinically employed at the national pilot centre. An in-house Matlab 2010a software, based on published work [2-4] was used for film processing considering triple channel correction. The dose maps were imported in RIT113 software (Radiological Imaging Technology Inc., Colorado Springs, CO) to perform gamma analysis, taking the film dose distribution as reference.

For dose calibration in both protocols, film strips were irradiated to known doses ranging from 0 to 9 Gy, in a 10×10 cm^2 field. To analyse a given application film, the generic calibration curve was then rescaled by means of two reference strips [2].

All films were scanned by the national auditor at least 48 hours after irradiation at the pilot centre, using a flatbed scanner Epson Expression 10000 XL. RGB images were acquired in transmission mode, landscape orientation, 48 bits colour depth, at 72 dpi, with all colour correction options disabled. A glass compression plate was used to ensure film flatness. Relative dose comparisons were performed with normalization done to a high dose low gradient region. Gamma analysis with a criterion of 3% global dose/3 mm, and 20% threshold was done. The audit passing rate defined acceptance limit was 90%.

Correlations between **Protocol A** and **Protocol B** have been explored. Results were considered in agreement when passing rates were above or below 95% (the most commonly used clinical acceptance limit) for both protocols and in disagreement when passing rates were above 95% for one protocol and below for the other.

As a complement to these protocols, also some interchanges have been introduced to further explore the results – i) films for one and three fractions have been analysed both in RIT and

FilmQA Pro softwares using the corresponding processing methods; ii) in RIT the TPS dose distribution was taken as reference to compare the results with the standard procedure of considering film as reference; iii) also in RIT all films have been analysed considering both single and triple channel dosimetry.

RESULTS

Using **Protocol A**, the overall average passing rate for three fractions films was 96.9 ± 2.8%. For **Protocol B**, gamma passing rates for one fraction films were on average 97.7 ± 3.5 %. Overall, a good agreement was found between **Protocols A** and **B**, with only 3/20 results having a passing rate above 95% for **Protocol B** and bellow it for **Protocol A**. Films irradiated with one fraction and analysed in FilmQA Pro, improved gamma passing rates when comparing to 3 fractions, 98.9 ± 1.6 % on average, ranging from 94.0% to 99.9%.

Analysis of the impact of choosing either film or TPS as reference dose distribution in RIT, showed that for films irradiated with one fraction, differences in gamma passing rates were negligible (less than 0.5% on average). Regarding EBT3 films irradiated with three fractions and analysed as per **Protocol B** (with triple channel correction and considering film distribution as reference), gamma passing rates for the adopted evaluation criteria were unexpectedly poor, being less than 90% in 10/20 institutions. The results significantly improved (~ 4%) when TPS dose was used as reference. Red channel analysis gave better results in both situations with only 2/20 centres not complying with the tolerance of 90% when taking film as reference, and 1/20 when considering TPS as reference.

CONCLUSIONS

Taking advantage of the large pool of data available in a national IMRT audit project, the results of this study revealed that the use of different film dosimetry protocols can lead to differences in gamma passing rates due to their inherent specificities. Nonetheless a good global agreement was found between the two used protocols. For the established tolerance levels and using relative dosimetry, the audit results based on film dosimetry for H&N IMRT treatments would be the same regardless the chosen protocol.

REFERENCES

[1] Kazantsev, P., et al., “New IAEA end-to-end on-site IMRT audit methodology: Pilot test results” in Proceedings of the International Conference on Advance in Radiation Oncology (ICARO2), International Atomic Energy Agency (IAEA), Vienna (2017).

[2] Lewis D., et al., An efficient protocol for radiochromic film dosimetry combining calibration and measurement in a single scan, Med. Phys. 39 (2012) 6339-50.

[3] Mayer, R.R., et al., Enhanced dosimetry procedures and assessment for EBT2 radiochromic film, Med. Phys., 39 (2012) 2147–55.

[4] Ferreira B. C., Lopes M. C., and Capela M., Evaluation of an Epson flatbed scanner to read Gafchromic EBT films for radiation dosimetry, Phys. Med. Biol., 54 (2009) 1073–85.

10 Years RPLD Postal Dose Audits for Radiotherapy in Japan

H. Mizuno[a]
A. Fukumura[a], W. Yamashita[b], S. Fukuda[a], N. Takase[b]

[a]National institute of Radiological Sciences, QST, 4-9-1 Anagawa, Inage-ku, Chiba-shi, Japan
[b]Association for Nuclear Technology in Medicine, 3-9-19 Kurosunadai, Inage-ku, Chiba-shi, Japan

Email address of Corresponding Author: mizuno.hideyuki@qst.go.jp

BACKGROUND

In 2007, a postal dose audit of an external radiation therapy unit was initiated in Japan using radiophotoluminescent glass dosimeters (RPLD). The methodology was developed by National Institute of Radiological Sciences and was operated by the Association for Nuclear Technology in Medicine. Audits are performed according to the request of the hospitals and the fee is about 700 € for 4 X-ray beam conditions.

METHODS

RPLD and solid phantom are used in the audit. RPLD is silver activated phosphate glass and the density is 2.61 g/cm^3. RPLD characteristics such as repeatable readout and negligible fading effect is suitable for the postal dose audit. Audit began with a reference condition and expanded its application to beams of different field size and wedged beams in 2010. In addition, in 2016, the modern type treatment units such as a flattening filter free linear accelerator, Tomotherapy unit, and Cyberknife unit could also be applied to audit.

RESULTS

By the end of October 2017, 4,579 beams were checked. Regarding the reference condition (2,326 beams), mean and standard deviation of the ratio of the measured dose to the intended dose (deviation) were +0.3% and +1.1%, respectively. This result indicates that the audit system was maintained well, and the dose was successfully evaluated. Regarding the variation in audit results, 99.9% of the beams was within tolerance level (Deviation should be within the 5%). However, 5 beams exceeded the tolerance level of 5%. In most cases, there was a clear mistake in the contents of the entry sheet of the audit. Hearing was done to the hospitals to clarify the cause, and in almost every case the cause was identified.

Table 1. The statistics of the 10 years postal dose audit.

	Side length of square field [cm]						**Wedge angle [°]**				
Energy [MeV]	**5**	**10**	**15**	**20**	**25**	**others**	**15**	**30**	**45**	**60**	**All**
4	99	509	36	104	20	-	78	62	24	28	960
6	263	760	70	180	29	4	111	103	38	45	1603
8	4	18	1	2	1	-	1	1	1	1	30
10	219	873	74	251	48	1	78	105	46	37	1732
14~18	5	46	-	9	-	-	2	1	0	1	64

6, 7 FFF	16	66	2	4	-	-	-				88
10, 11 FFF	16	54	3	4	-	-					77
Tomotherapy						17					17
Cyberknife						8					8
All	622	2326	186	554	98	30	270	272	109	112	4579

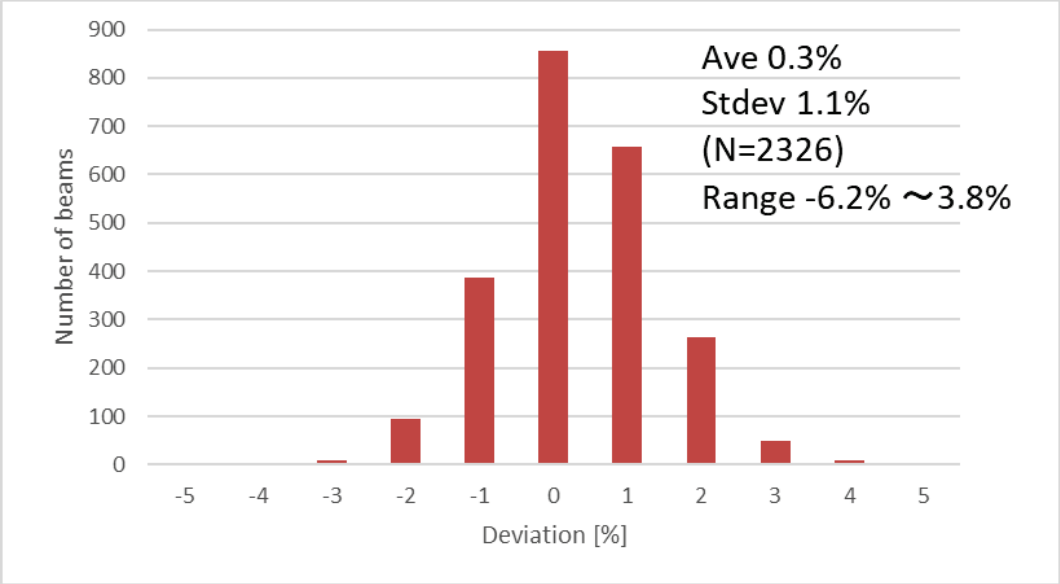

Figure 1. Distribution of the results of the audits of radiotherapy hospitals for the delivery of absorbed dose to water under reference condition during 2007-2017.

CONCLUSIONS

This activity has certainly improved the quality of the radiation therapy in Japan. More efforts are underway, such as application to electron beams or intensity modulated radiation therapy.

REFERENCES

[1] MIZUNO, H., et al., Feasibility study of glass dosimeter postal dosimetry audit of high-energy radiotherapy photon beams, Radiotherapy and Oncology **86** 2 (2008) 258-263.

[2] MIZUNO, H., et al., Application of a radiophotoluminescent glass dosimeter to nonreference condition dosimetry in the postal dose audit system, Medical physics **41** 11 (2014) 112104.

[3] MIZUNO, H., FUKUMURA, A., Establishment of a postal dose audit system in Japan using a radiophotoluminescent glass dosimeter, (2010).

National Dosimetry Quality Audits in Radiotherapy

H. Kim
J. Lee, M. Song

Korea Institute of Nuclear Safety, 62 Gwahak-ro, Yuseong-gu, Daejeon, Republic of Korea

Email address of Corresponding Author(s): hikim@kins.re.kr

BACKGROUND

Systematic quality control of radiotherapy is required to minimize the errors that can occur as a result of complicated radiotherapy and to deliver accurate doses. In addition, it is necessary to secure the reliability of the quality control performed by itself through independent dosimetry quality audits. In Korea, the Nuclear Safety Commission, which is a regulatory body for the use of radiotherapy, has established the postal audit system to guarantee the quality of radiotherapy and is carrying out the project from 2017. In this study, the results of the national dosimetry quality audit system are introduced.

METHODS

The quality audit program consists of two stages. The First step is to develop standard procedure for postal audit and establishment of calibration and technical accuracy of the inspection system. The second step is to verify the photon beam output of the LINAC used in hospitals using glass dosimeters. The number of hospitals using LINACs in Korea is 92, and the whole number of LINACs (163 Units) has been verified for two years from 2017 to 2018. The standard phantom for dose measurement was made of ABS(Acrylonitrile Butadiene Styrene Copolymer) resin, which has a similar attenuation coefficient to water and is less susceptible to shock and temperature. As recommended by the technical report series 398 of IAEA, the size of phantom was designed to be $20cm^3$, allowing the glass dosimeter to be positioned 10cm below the surface to take scatter into account. The acceptable level of output doses is ±5% as recommended by the ICRU, and the optimal level of those is ±3%.

RESULTS

To ensure traceability of the glass dosimeter and reliability of the domestic postal audit system, the reading dose of the dosimeter for the Co-60 beam was compared by taking part in the DAN (Dosimetry Audit Networks) program of IAEA SSDL (Seibersdorf, Vienna, Austria). Table 1 shows the intercomparison result for the dose difference between the KIRAMS(Korea Institute of Radiological Medical Sciences) SSDL in charge of the dose reading about Korea audit system and the IAEA SSDL.

Table 1. Difference in dose of glass dosimeter between internal and external audit system

Dose	Difference	Dose	Difference
1.50Gy	-0.52%	2.25Gy	0.92%
1.75Gy	0.61%	2.50Gy	0.33%
2.00Gy	-0.70%		

According to the difference less than ±1%, the reliability of dose reading of the domestic audit system was secured. Figure 1 shows the final result of photon output(114 beams) of 163 Linacs, and relative measurement uncertainty is 2.98%(k=1).

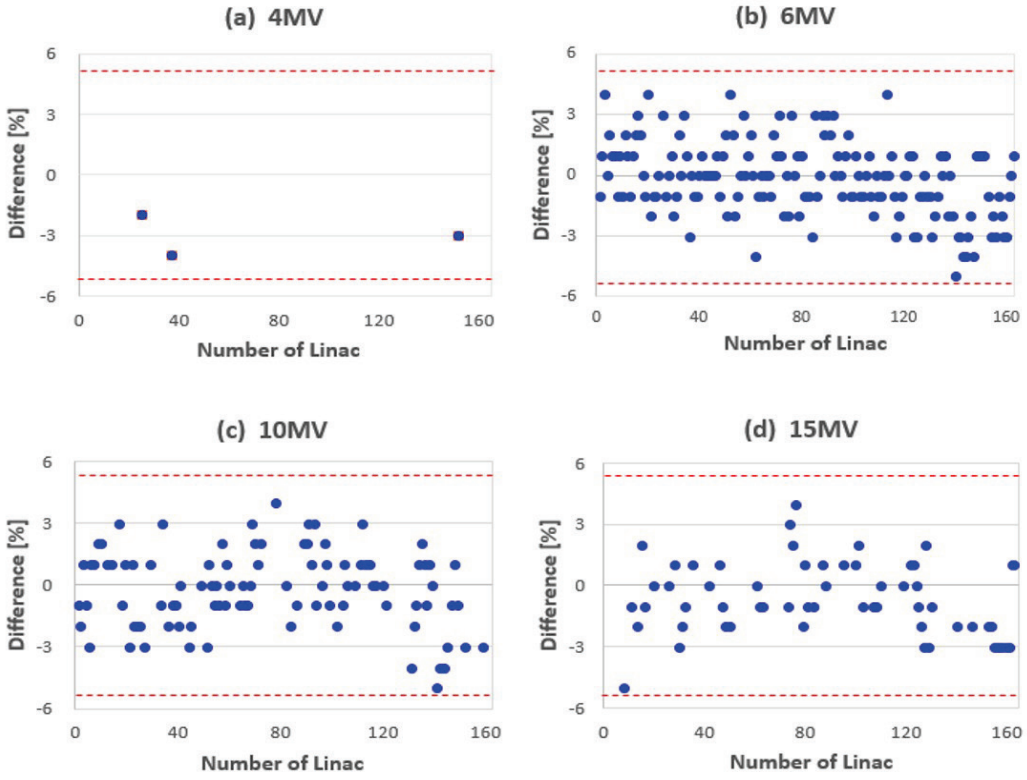

Figure 1. Results of glass dosimeter check of photon beam output

All output doses were within ±5% acceptable level. In the first verification of postal audit, there were two hospitals whose output exceeded the acceptable level due to setup errors. In this case, after hospital checked the procedure by itself, the postal audit was carried out again. And furthermore, On-site audit of the experts was carried out, at a more precise level of verification such as the measurement of PDD(Percentage Depth Dose) and mechanical check. Finally, the suitability of quality control was verified with this.

CONCLUSIONS

The output doses of Linacs were confirmed to be at acceptable levels by the domestic postal audit system. In 2019, the postal audit of tomotherapy and cyber-knife units would be performed to verify the output dose of those. It would be possible to reduce the deviation in quality control between hospitals by independent audit for radiotherapy and accumulate data related to domestic quality control level.

REFERENCES

[1] INTERNATIONAL COMMISSION ON RADIOLOGICAL PROTECTION, Prevention of Accidents to Patients Undergoing Radiation Therapy, ICRP Publication 86., Ann, ICRP 30.3 (2000)

[2] INTERNATIONAL ATOMIC ENERGY AGENCY, Comprehensive a Audits of Radiotherapy Practices: a Tool for Quality Improvement: Quality Assurance Team for Radiation Oncology(QUATRO), Vienna (2007)

10 Years Dosimetric Quality Audit of Radiotherapy Centers in Iran: SSDL's On-Site Visit Program during 2007-2017

K.Arbabi[a]
A. Rajabi[b], **M. Akbari**[b], **A. Alipoor**[a]

[a]Secondary Standard Dosimetry Laboratory (SSDL), Radiation Application Research School, Nuclear Science and Technology Research Institute (NSTRI), Karaj, Iran.
[b]Therapy Level Laboratory, Secondary Standard Dosimetry Laboratory (SSDL), Pars Isotope Co., Atomic Energy Organization of Iran (AEOI), Karaj, Iran.

Email address of Corresponding Author: k.arbabi@parsisotope.com

BACKGROUND

A dosimetric audit of radiotherapy centers is a quality control process that allows the accuracy of dosimetric and geometric precision of dose delivery to the patient. It can be used to evaluate the accuracy of dose delivery to the tumor during radiotherapy at various treatment centers. Differences in prescriptive dose, depending on the severity, have potential consequences not so important, severe and even fatal. Measuring the absolute output of linear accelerators (LINACs) under reference conditions is a gold standard method for verifying the accuracy of the radiotherapy dose delivery [1]. Radiotherapy centers in Iran have been auditing by the Secondary Standard Dosimetry Laboratory (SSDL) since 1991. In this study, in accordance with TRS 398 [2] and inspection instructions from the International Atomic Energy Agency's QUATRO Group [2], the dosimetric audit for 10 years during 2007-2017, was performed and the differences between SSDL and the inspected center were reported.

METHODS

The absolute photon output of the accelerators and some of the relative factors such as wedge factor, shield tray factor, total scatter factor were measured using a Farmer chamber and the results were compared with the reported values by the centers. Measurements were performed at 178 on-site visits from 61 radiotherapy centers (including 98 single and multi-energies LINACs) between March 2007 and October 2017. Some participating centers were visited more than once. Since in this work transportation of the equipment by ground or air (for large distances), were needed, it was required that the equipment was light and robust. A specific box was provided to transport the water phantom, electrometer, cable, and chamber. This box was checked in as personal luggage on flights. The chamber itself was carried in its vendor-supplied box in the mentioned specific provided box. Absolute photon dose measurements were carried out according to TRS-398 protocol [2] using Farmer ionization chamber (PTW TW30013). The PTW Farmer-type chamber was calibrated against a reference chamber at approximately three to six month intervals (depending on the frequency of site visits) throughout the entire study, following the method described in TRS 398 [2] using a fixed SSD arrangement. The reference chamber was a Farmer-type 30001 thimble chamber and with an absorbed dose-to-water calibration coefficient from a ^{60}Co beam ($N_{D,w}$) traceable to the SSDL of the IAEA. Action levels were determined within ±3% for absolute dose and ±2% for relative factors.

RESULTS

Absolute dose differences between SSDL and local centers were in the range of -3.5% up to 4%. As an example, Figure 1 indicates the output percentage of difference between SSDL and hospital measurements in 6 MV beam energy visited by SSDL during the dosimetric audit. The protocol applied was the IAEA TRS 398 [2].

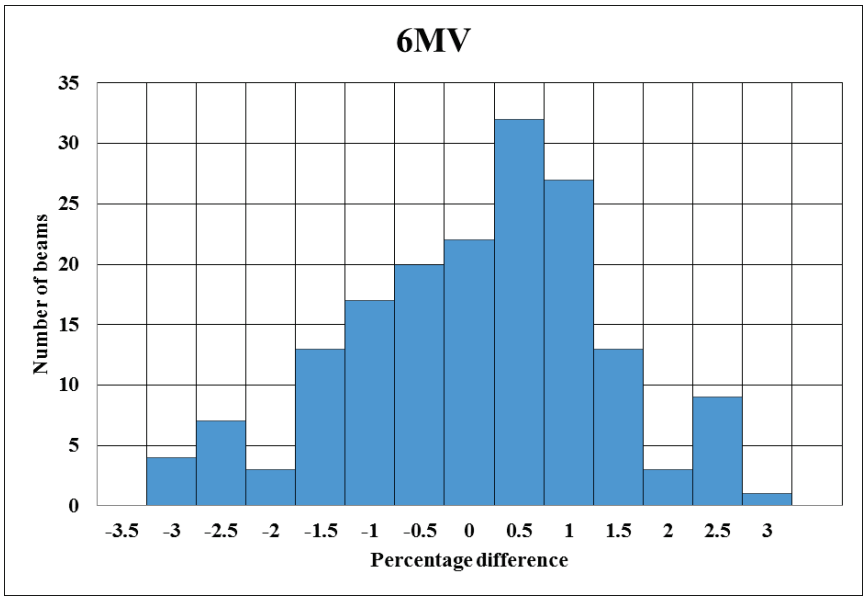

Figure 1. Percentage of difference in Output measurements between SSDL and hospitals in 6 MV beam energy audited by SSDL of Iran.

The maximum differences in the values of the relative dosimetry parameters between the amounts measured by SSDL and the local centers were -3.4% up to 3.7%. The difference between SSDL and radiotherapy centers at the reported absolute dose values in 11 beams measurements from 310 total beams was greater than the permissible limits.

CONCLUSIONS

The distribution of output measurements suggest the influence of some systematic error (outside of measurement uncertainty) which could potentially be introduced from multiple sources. It should also be noted that action limits warranting investigation were never exceeded. Differences in measurements between SSDL and radiotherapy centers could be due to the following: 1. Lack of qualified medical physicists in some radiotherapy centers, 2. Error in calculating beam quality factor (k_Q) for some chambers, 3. Mistake in the report of the reference depth and reference source to surface distance (SSD).

REFERENCES

[1] IAEA-TRS 398, 2000, Absorbed Dose Determination in External Beam Radiotherapy: An International Code of Practice for Dosimetry Based on Standards of Absorbed Dose to Water. International Atomic Energy Agency (IAEA), Vienna.

[2] IAEA-TECDOC-1543, 2007, On-site Visits to Radiotherapy Centres: Medical Physics Procedures. International Atomic Energy Agency (IAEA), Vienna.

Energy Responses of Radiophotoluminescent Glass Dosimeters to Photons and Electrons Used in Radiotherapy Treatments

G. Medkour Ishak-Boushaki[a]
A-H. Benali[a,b], M. Allab[a]

[a]Laboratory SNIRM-Faculty of Physics, University of Sciences and Technology Houari Boumediène, BP 32 El-Alia Bab Ezzouar, Algiers Algeria. [b] Faculty of Science of Nature and Life, University Echahid Hamma Lakhdar, El-oued Algeria.

Email address of Corresponding Author: gmedkour@yahoo.com, gmedkour@usthb.dz

BACKGROUND

Thermoluminescent dosimeters (TLD) are widely used in different fields and specially in radiotherapy measurements (in vivo dosimetry on patients). The main advantages of these dosimeters are their nearly tissue equivalent density, their availability in small sizes (suitable for point dose measurements), in different forms (powder, pellet…) and their cheapness.

Besides, the radiophotoluminescent glass dosimeters (RPL) are more dedicated to radiation protection purposes. These detectors are known to have appreciable technical characteristics such as good reproducibility of readout value and long-term stability of the fading effect.

In recent previous works [1, 2], we have undertaken a comparative study of the dosimetric characteristics of both- RPL and TLD dosimeters. We have estimated the simulated responses of these dosimeters (specified as discs of 5 mm diameter and 2 mm thickness) in terms of absorbed dose, output factor, angular and energy dependence for X-rays and clinical electron beams.

In this paper, we focus on the study of the energy responses of the commercially available radiophotoluminescent glass dosimeters (RPL model GD-301) to photons and electrons beams usually used in radiotherapy treatments. The obtained RPL energy responses are compared to those of TLD-100 detectors (usually used for monitoring patient's doses in radiotherapy field).

METHODS

The dosimeters energy responses have been calculated using the Monte Carlo NParticle code version 2005 (MCNP5). The applied clinical radiation qualities were photon rays, of nominal potential energies ranging from 50 to 300 kV and from 4 to 25 MV and clinical electron beams at energies varying from 4 to 20 MeV. The ^{60} Co – rays have been taken as reference irradiation beams.

A comparison of our results to many experimental and simulated data given in the literature [3-5] has been performed.

RESULTS

Our results, evaluated by Monte Carlo simulation, are generally in good agreement with literature data. These results show that, for effective X-ray energies varying from 32 to 207 keV, thermoluminescent dosimeters show an increasing in energy response, relative to ^{60}Co – rays, from 1.02 to 1.39 while the RPL energy response varies from 1.2 to 4.5. For clinical MV photons and clinical electrons, the radiophotoluminescent energy responses variations are

within 4% and 2% respectively and TLD detectors responses are within 5% for photons and 4% for electrons.

CONCLUSIONS

The obtained energy responses show that for clinical electron beams or MV photons, used in radiotherapy treatments, RPL glass and TLD dosimeters have very- close responses within a 5% variation range. For low energy X- ray (< 250 keV), RPL dosimeters present a stronger energy dependence than TLD detectors. Complementary studies, concerning the use of RPL dosimeters with an energy compensation filter, are in progress to support the use of these detectors for monitoring patient's doses in radiotherapy treatments.

REFERENCES

[1] BENALI, A.H., MEDKOUR ISHAK-BOUSHAKI, G., NOURREDDINE, A.M., ALLAB, M., PAPADIMITROULAS, P., " A comparative evaluation of luminescence detectors: RPL-GD 301, TLD-100 and OSL-AL2O3:C, using Monte Carlo simulations", *Journal of instrumentation, V* **12, P**07017 (2017). https://doi.org/10.1088/1748-0221/12/07/P07017.

[2] BENALI, A.H., MEDKOUR ISHAK-BOUSHAKI, G., "Energy response of FD-7 RPL glass dosimeter compared with LiF Mg, Ti and Al_20_3:C dosimeters ", Journal of instrumentation, *V13(2018).* https://doi.org/10.1088/17480221/13/11/P11015

[3] ARAKI, F., OHNO, T., "*The response of a radiophotoluminescent glass dosimeter in megavoltage photon and electron beams",* Medical Physics, Vol. 41, No. 12, December 2014(122102-1 to 8).

[4] RAH, J.E., HONG ,J.Y., AND KIM, G.Y., "A comparison of the dosimetric characteristics of a glass rod dosimeter and a thermoluminescent dosimeter for mailed dosimeter"*, Radiation Measurements* **44** (2009) 18.

[5] RAH, J.,E., HWANG, U., J., JEONG, H., LEE, S.,Y., LEE , LEE, D.,H., DONG HO, S., YOON, M., SE BYEONG, L., LEE, R., SUNG YONG, P., "Clinical application of glass dosimeter for in vivo dose measurements of total body irradiation treatment technique", Radiation Measurements **46** (2011) 40.

IAEA Supported National IMRT Dosimetry Audit in Hungary

C. Pesznyak[a]
B. Melles-Bencsik[a], **E. Gershkevits**[b]

[a]National Institute of Oncology, Budapest, Hungary
[b]North Estonia Medical Centre, Tallinn, Estonia

Email address of Corresponding Author: csilla.pesznyak@gmail.com

BACKGROUND

The new IMRT audit methodology was designed by the International Atomic Energy Agency (IAEA). The main focus of the audit is the dosimetric verification of the planning and delivery of IMRT treatments with the CIRS SHANE Phantom (Figure 1.). The independent and voluntary audit has been carried out in 85% of Hungarian Radiotherapy Centres and it is 91% of all institutions performing IMRT in the country.

METHODS

The IMRT audit reviews the dosimetry, treatment planning and radiotherapy delivery processes using the pre-visit and the on-site-visit approach. The audit is implemented at the national level with IAEA assistance. The national counterparts conduct the IMRT audit at Hungarian radiotherapy centres through analysing the pre-visit questionnaires and performing on-site measurements. TPS calculated doses are compared with ion chamber and Gafchromic EBT3 film dosimetry measurements performed in CIRS SHANE head & neck phantom for a simultaneous integrated boost (SIB) IMRT test case. A set of pre-defined agreement criteria is used to analyse the results for IMRT and VMAT treatments.

RESULTS

Eleven radiotherapy centres in Hungary have participated; 9 Varian and 2 Elekta linear accelerators have been audited as well as TPS that are using 6 AAA (Eclipse), 3 Acuros (Eclipse), 1 Monte Carlo (Monaco) and 1 Collapse Cone (Pinnacle) calculation algorithms. The doses measured with the ion chamber were within 4.5% from calculated ones for all centres. The film was analysed using gamma method (3%, 3 mm) with a threshold of 20%. Passing rates were above 95% for all measurements. All results met the agreement criteria, but a few errors in the workflow were detected and corrected.

CONCLUSIONS

The new IMRT audit is complex, well-constructed and helpful to resolve issues related to imaging, dosimetry and treatment planning for IMRT and VMAT techniques.

ACKNOWLEDGEMENTS

The National Institute of Oncology and the authors thank the International Atomic Energy Agency, especially Joanna Izewska, Pavel Kazantsev and Paulina Wesolowska for lending the CIRS SHANE Phantom and for their scientific and technical support.

Thanks for the voluntary contribution to the following radiation therapy centres: National Institute of Oncology, Budapest; Uzsoki Hospital, Budapest; Oncology Clinic, University of Debrecen; Department of Oncotherapy, University of Pécs; Department of Oncotherapy, University of Szeged, Health Centre of the Kaposvár University; Bács-Kiskun County

Hospital, Kecskemét; Kálmán Pándy County Hospital, Gyula; Csolnoky Ferenc Hospital, Veszprém; Aladár Petz County Hospital, Győr; Józsa András County Hospital, Nyíregyháza.

Figure 1: CIRS SHANE Phantom in coronal, 3D and axial planes respectively.

REFERENCES

[1] KAZANTSEV, P., et al., New IAEA end-to-end on-site IMRT audit methodology: Pilot test results, Book of synopses: International Conference on Advances in Radiation Oncology ICARO2 (2017) 218-219.

[2] FOLLOWILL, D.S., et al., The Radiological Physics Center's standard dataset for small field size output factors, Journal of applied clinical medical physics **13** 5 (2012) 3962.

[3] LECHNER, W., et al., A multinational audit of small field output factors calculated by treatment planning systems used in radiotherapy, Physics and Imaging in Radiation Oncology **5** (2018) 58-63.

The IAEA End-to-End On-Site IMRT Audit Methodology: First National Implementation Results

P. Kazantsev[a]
P. Wesolowska[a], E. Gershkevitsh[b], M. do Carmo Lopes[c], T. Santos[c], C. Pesznyak[d], B. Melles-Bencsik[d], J. Venius[e], B. Petrovic[f], J. Izewska[a]

[a]International Atomic Energy Agency, Vienna, Austria
[b]North Estonia Medical Centre, Tallinn, Estonia
[c]Instituto Portugues De Oncologia De Coimbra Francisco Gentil, Coimbra, Portugal
[d]National Institute of Oncology, Budapest, Hungary
[e]National Cancer Institute, Vilnus, Lithuania
[f]Oncology Institute of Vojvodina, Sremska Kamenica, Serbia

Email address of Corresponding Author: p.kazantsev@iaea.org

BACKGROUND

An end-to-end on-site audit methodology to verify the medical physics aspects of intensity modulated radiation therapy (IMRT) in radiotherapy centres has been developed by the IAEA and successfully tested in a multicentre study [1]. Several countries adopted the methodology and implemented the audit at the national level. Overview of results of the first four countries is presented.

METHODS

The audit methodology utilizes a specially developed "Shoulders, Head and Neck, End-to-end" (SHANE, CIRS Inc.) phantom representing a head and neck (H&N) region of an adult human in geometry and material composition. Dose measurements are performed with a small volume ion chamber located at specific positions and with a gafchromic EBT3 film (Ashland, USA) in a coronal plane. During an on-site visit, the SHANE phantom undergoes a typical pathway of a patient in a radiotherapy centre, from computed tomography (CT) imaging through treatment planning to irradiation. The core component of the audit is comparison of the treatment planning system (TPS) calculated doses with those measured by ion chamber in four locations within three planning target volumes (PTVs, 5% tolerance) and organ at risk (OAR, spinal cord, 7% tolerance), and comparison of film measured dose distribution with the corresponding TPS calculated dose map (global gamma analysis with 3%/3mm criteria and 20% threshold, 90% gamma passing rate tolerance limit). Additionally, before the on-site visit takes place, the audited institution has to perform a set of exercises including small field output factors and profiles calculation. The audit package developed consists of the detailed methodology description, instructions and data reporting forms for an auditor and an audited institution staff, a set of CT images and structures of the SHANE phantom.

RESULTS

Up to date, four countries (Hungary, Lithuania, Portugal and Serbia) submitted to the IAEA the audit results of 35 institutions which on average covers about 90% of all institutions performing IMRT in these countries. Of those, 26/8/1 institutions used in the audit Varian/Elekta/Accuray linacs with 6 MV beams (two were flattening filter free), 25/7/1/1/1 performed calculations using Eclipse/Monaco/XiO/Pinnacle/VoLo TPS, 27/6/1/1 used VMAT/Dynamic MLC/Step and shoot/Tomotherapy treatment delivery methods.

Pre-visit activities were in most cases completed smoothly by all participating institutions although calculation results of small field parameters showed high variability. TPSs tend to overestimate MLC defined small field output factors compared to the IROC-Houston reference dataset [2] which supports earlier findings of the IAEA [3]. The calculated cross-plane profile of 2×2 cm^2 field has approx. 5% standard deviation (SD) in size while 20-80% penumbra has 17.7% SD even for a homogeneous set of Varian linac/Eclipse TPS/Millenium 120 MLC equipment which highlights the issue of accurate small field commissioning.

On-site audit results using ion chamber measurements in a SHANE phantom are given in Fig. 1. All but one results fell into the tolerance limits with the averages ± 1 SD of: 1.010±0.018 (IC_PTV_7000), 1.001±0.019 (IC_PTVn1_6000), 1.003±0.019 (IC_PTVn2_5400), 1.005±0.034 (IC_SpinalCord). Film measurements resulted in the average of 97.2%±2.5% gamma pass rate.

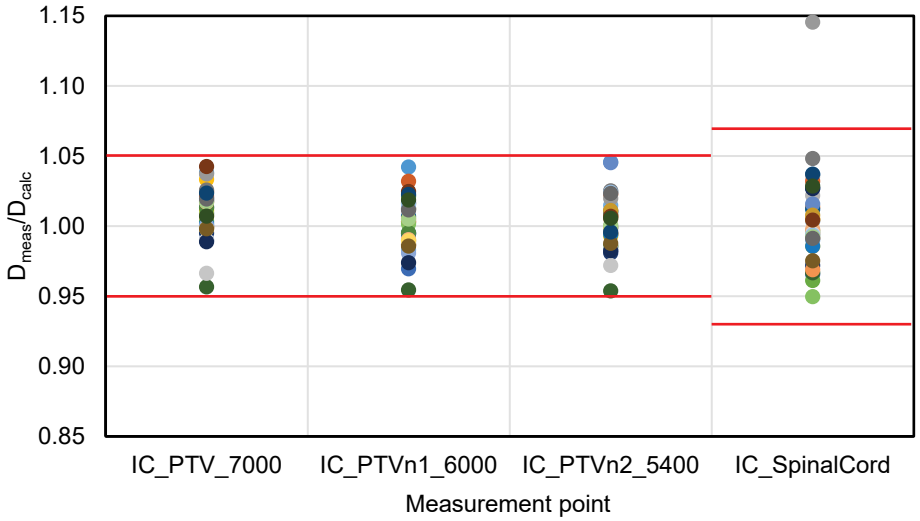

Figure 1. Results of ion chamber measurements in relation to calculations for 4 measurement points in terms of D_{meas}/D_{calc}. Tolerance levels of 5% and 7% are indicated with red line. The result outside tolerance was rectified through the follow-up action.

CONCLUSIONS

Although some suboptimal parameters were identified and corrected across the audit participants, dose measurement results generally fell within the established tolerance limits. Therefore, national implementation of the on-site end-to-end IMRT audit confirmed adequate quality of the medical physics aspects of IMRT treatments for H&N cancer in the participating countries.

REFERENCES

[1] KAZANTSEV, P., et al., New IAEA end-to-end on-site IMRT audit methodology: Pilot test results, Book of synopses: International Conference on Advances in Radiation Oncology ICARO2 (2017) 218-219.

[2] FOLLOWILL, D. S., et al., The Radiological Physics Center's standard dataset for small field size output factors, Journal of applied clinical medical physics / American College of Medical Physics **13** (2012) 3962.

[3] LECHNER, W., et al., A multinational audit of small field output factors calculated by treatment planning systems used in radiotherapy, Physics and Imaging in Radiation Oncology **5** (2018) 58-63.

National Trial Runs of a Remote End-to-End Dosimetry Audit for IMRT and VMAT Treatments

P. Wesolowska[a]
P. Kazantsev[a], T. Bokulic[a], V. Alves[b], L. Suming[c], D. Ekendahl[d], K. Chelminski[e], A. Samper[f], S. Vinatha[g], J. Izewska[a]

[a]International Atomic Energy Agency, Vienna, Austria
[b]Instituto Nacional De Câncer, Rio De Janeiro, Brazil
[c]Chinese Centre for Disease Control and Prevention, Beijing, China
[d]National Radiation Protection Institute, Prague, Czech Republic
[e]Maria Sklodowska-Curie Memorial Cancer Centre and Institute of Oncology, Warsaw, Poland
[f]National Institute of Oncology and Radiobiology, Havana, Cuba
[g]Radiation Standards Section, Radiation Safety Systems Division, Bhabha Atomic Research Centre Trombay, Mumbai, India

Email address of Corresponding Author: p.wesolowska@iaea.org

BACKGROUND

A new methodology for end-to-end remote dosimetric quality audit for intensity modulated radiotherapy (IMRT) and volumetric modulated arc therapy (VMAT) treatments for national dosimetry audit networks (DAN) was developed within the IAEA Co-ordinated Research Project (CRP) [1] and tested at the national level. The aim of this audit was to verify the entire radiotherapy chain including imaging, treatment planning and dose delivery. The results of national trial runs performed in six countries (Brazil, China, Cuba, Czech Republic, India, Poland) are presented here.

METHODS

Each participating hospital received from its national DAN a solid phantom made of polystyrene of 15×15×15 cm^3 containing IMRT QA insert with the solid water structures representing planning target volume (PTV) and organ at risk (OAR). The insert was preloaded with a piece of Gafchromic EBT3 film (Ashland, USA) and four thermoluminescent dosimeters (TLDs, two in PTV and two in OAR). Participants were equipped with a set of instructions and datasheets and asked to scan the phantom, contour the structures, create the treatment plan and irradiate the phantom. The treatment prescription was to deliver 4 Gy to PTV in two fractions and limit the dose to OAR to 2.8 Gy.

Each DAN processed the dosimeters following the IAEA CRP guidelines which allowed for comparison of national results. TLD evaluation results were compared with the treatment planning system (TPS) calculated dose. The gamma index passing rate results were given for films analysed against TPS calculated dose maps (3% dose difference, 3 mm distance-to-agreement (DTA), 20% dose threshold, global gamma). Comparisons of film profiles passing through the PTV and OAR with those derived from the treatment plan were made.

RESULTS

The results obtained in national runs were for 56 hospitals equipped with 17 different accelerator models, 10 multileaf collimator (MLC) models, 8 TPS types with 8 dose calculation algorithms. Table 1 summarises the TLD results obtained for every national trial run. The average of the measured to stated dose ratio (D_{meas}/D_{stated}) in PTV was 0.999 with the standard

deviation of 0.049. In 73% cases the results were within 5% tolerance limits. All measured doses in OAR were below 2.5 Gy which confirmed that the verified plans were acceptable, however a larger scatter of D_{meas}/D_{stated} was observed with the standard deviation of 0.092 due to high dose gradients in OAR. Regarding film measurements, only six hospitals had gamma passing rates below 90% criterion. Two of them failed both the film and TLD criteria. In total 19/56 (approx. 34%) hospitals failed the audit which is similar to findings of IROC-Houston postal end-to-end IMRT audit results analysis study [2].

Table 1. TLD results of national trial runs. The average measured to stated dose ratio ± 1 standard deviation is given.

		TLD location					
Country number	**# of sets**	**PTV_S**	**PTV_I**	**PTV average**	**OAR_S**	**OAR_I**	**OAR average**
1	11	1.007±0.031	1.006±0.029	**1.006±0.029**	0.992±0.043	1.003±0.040	**0.997±0.041**
2	5	0.988±0.012	1.000±0.023	**0.994±0.018**	0.963±0.028	0.979±0.028	**0.971±0.028**
3	2	0.980±0.011	0.971±0.033	**0.976±0.021**	0.993±0.103	1.000±0.092	**0.996±0.092**
4	3	1.007±0.015	1.007±0.032	**1.007±0.023**	1.040±0.046	1.020±0.061	**1.007±0.023**
5	13	0.970±0.040	0.974±0.044	**0.972±0.041**	0.998±0.147	0.968±0.122	**0.983±0.133**
6	22	0.990±0.051	1.039±0.061	**1.014±0.061**	1.017±0.097	1.019±0.095	**1.018±0.095**
Total	56	**0.989±0.042**	**1.010±0.053**	**0.999±0.049**	**1.003±0.096**	**1.000±0.089**	**1.002±0.092**

CONCLUSIONS

The methodology was straightforward for implementation at the national level. It was shown that the audit is capable of detecting suboptimal performance of hospitals in delivering advanced radiotherapy treatments, which should motivate participants to strengthen local quality assurance procedures.

REFERENCES

[1] WESOLOWSKA, P., et al., OC-0357: Pilot study of a remote end-to-end dosimetry audit for IMRT and VMAT treatments, Radiotherapy and Oncology **119** (2016) S164-S165.

[2] CARSON, M. E., et al., Examining credentialing criteria and poor performance indicators for IROC Houston's anthropomorphic head and neck phantom, Medical physics **43** (2016) 6491-6496.

An In-Vivo Dosimetry Audit of Superficial Radiotherapy Treatment Using TLD-100H Dosimeters

O. C. Choi[a]
H. Weatherburn[a]

[a]Cancer Centre London, 49 Parkside, Wimbledon. UK SW19 5NB

Email address of Corresponding Author: oi-ching.choi@cancercentrelondon.co.uk

BACKGROUND

The purpose of this study is to audit the measured results following implementation of in-vivo dosimetry for kV treatment since 2015 with mini TLD-100H dosimeters.

Although few treatment errors related to superficial treatment have been reported, recent concerns have been expressed regarding the accuracy of delivered dose during courses of kilovoltage (kV) radiotherapy treatment (1, 2, 3): 1. Due to a recent incident involving kV treatment in Dublin 2018 (4); 2. That measured data in BJR supplement 25 may differ from the clinical treatment areas (5), eg curved areas with bones or air-cavity underneath (2); 3. Lack of in-vivo treatment verification in kV treatment (2) in the UK; 4. Palmer et al (2016) (1) reported that only 36% of centres in the UK used software for dose calculations, though most of the errors happened during the calculation process for non-planed treatments (3).

METHODS

A batch of mini-TLD 100H (Harshaw) with dimension 3.2 x 3.2 x 0.15mm were used to measure doses of 3-6.5Gy per fraction delivered with 60-160kV X-rays from an Xstrahl superficial X-ray Unit. 2 measurement chips wrapped inside a paper pack were place at the field centre. All chips readings were made after 24 hours. The range of sensitivities of the TLD chips was ±12.0%, when the Element Correction Coefficient (ECC) was individually measured for the chips. The measurement accuracy of the TLDs was ±2.2%. BJR 25 (5) backscatter factors and Percentage Depth Doses were employed. 'Stand-off' or 'stand-in' corrections were made to the field centre when calculating treatment doses. Some of the treatments were undertaken in irregular or elongated fields (e.g. 10cm x 1cm).

RESULTS

45 measurements made in 2018 are reported. Figure 1 shows the results comparing calculated and measured dose. The mean measured dose was 3.6% less than the mean calculated dose, which is similar to the results of Palmer 2017(2). It may suggest data used from BJR supplement 25 (5) are involved in under-estimating the actual dose to the patients.

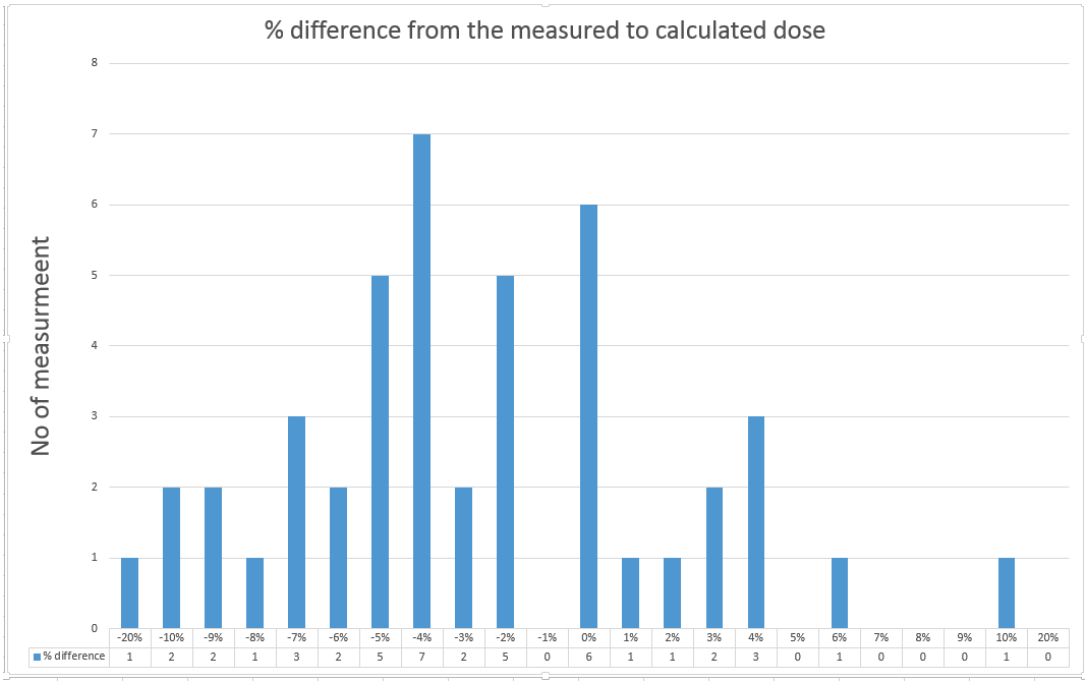

Figure 1. Histogram of TLD measurements results

CONCLUSIONS

Mini Harshaw TLD-100 is stable and accurate enough to evaluate in-vivo dosimetry in kilovoltage treatment. It is good enough to detect significant treatment errors but it takes at least 24 hours to get the result.

The under-estimate dose suggests no increased backscattered dose from bone underneath because 89% (40/45) of the measurements are extremities with bone close to the skin. This contradicts the conclusion of Palmer et al 2017 (2).

However, improvement to the method is required for more complicated dose verification, i.e. in situations with stand offs, irregular or elongated fields, or uneven surface with cavities. This dosimetry audit is on-going and the role of using of standard data from BJR supplement 25 (5) is also being evaluated.

REFERENCES

[1] PALMER, A.L., PEARSON M, WHITTARD, P., MCHUGH, K.E., EATON, D.J., Current status of kilovoltage (kV) radiotherapy in the UK: installed equipment clinical workload, physics quality control and radiation dosimetry. Br J Radiol (2016); 89:20160641

[2] PALMER, A.L., JAFARI, S.M., MONE, I., MUSCAT, S. Evaluation and clinical implementation of in vivo dosimetry for kV radiotherapy using radiochromic film and micro-silica bead thermoluminescent detectors. Physica Medica 42 (2017):47-54

[3] PUBLIC HEALTH ENGLAND. Safer Radiotherapy. The Radiotherapy newsletter of Public Health England. (2017) 23

[4] COLEMAN LEGAL PARTNERS. Unintended overexposure of a patient during kilo-Voltage radiotherapy treatment at St Luke's hospital, Dublin, in March (2018). Available from https://colemanlegalpartners.ie/excessive-radiation-dose/

[5] BRITISH INSTITUTE OF RADIOLOGY. Central axis depth dose data for use in radiotherapy. (1996) British Journal Radiology Supplement 25. London, UK. 1996.

Analysis of Results of National and IAEA/WHO Dosimetry Quality Audit in Radiotherapy Departments of Ukraine: Problems and Prospects for Improvement

L.Stadnyk
O.Shalopa

Grigorev Institute for Medical Radiology, Pushkinskaya str., 82, Kharkiv, 61024, Ukraine

Email address of Corresponding Author: Lstadnyk@ukr.net

BACKGROUND

To ensure the effectiveness of radiotherapy the quality of evaluation of the target tumor volume, treatment planning, clinical dosimetry and the accuracy of the dose delivery to tumor are very important stages of cancer treatment. In accordance with ICRU and IAEA requirements in radiotherapy the overall uncertainty of delivery of an absorbed dose should not exceed 5%. In this work the analysis of results of national and IAEA/WHO dosimetry quality audit in radiotherapy departments are presented. The reasons of possible mistakes of irradiation and the ways to improve the situation with the quality of clinical dosimetry are discussed.

METHODS

In Ukraine the IAEA/WHO postal TLD-audit of dose calibration quality in external radiotherapy started from 1998. A number of 433 radiation beams were checked during 1998-2017 (every radiotherapy unit was checked every 2-3 years). Since 2011, the national TLD-audit was organized on an unofficial basis and 114 external radiation beams were checked. Only since 2018 in accordance with the normative act of State Nuclear Regulatory Inspectorate of Ukraine, the participation in the national TLD-audit is mandatory for all radiotherapy units.

RESULTS

Results of postal TLD-audit of dose calibration quality in radiotherapy are shown in Fig. 1-2.

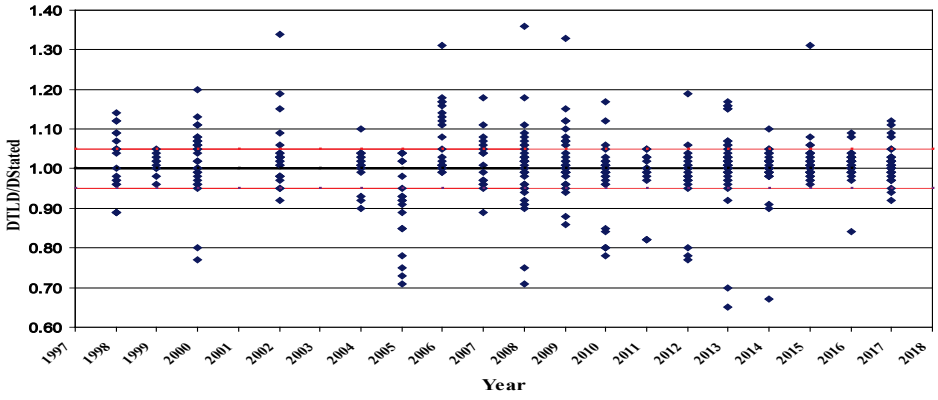

Figure 1. Results of IAEA/WHO TLD postal audits in Ukraine

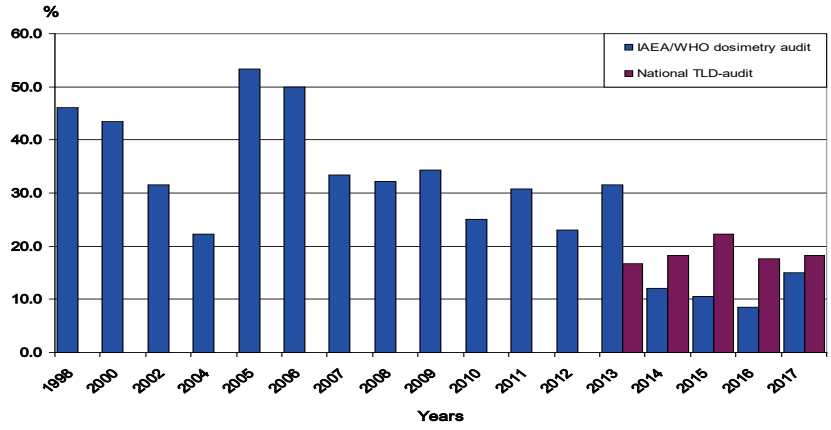

Figure 2. Fraction of results exceeding the 5% acceptance limit

The IAEA/WHO TLD-audit in 1998-2013 showed that at the first stage of dosimetry audit, the results for 25-50 % radiation units were very bad: the errors of dose delivery had been exceeding the 5% acceptance limit. After second stage the bad, non-acceptable results accounted for 3.8-22.2 % of radiation beams.

The analysis of the distribution of errors of TLD-audit with unacceptable results showed: the errors in the range of 5-10 % were observed in 58 % cases, in range of 10-20 % - in 32 % and more than 20 % for 10 % cases.

To establish the sources of errors the results of questionnaire of radiotherapy departments and the data sheets of TLD audit were analyzed. The potential sources of errors during TLD irradiations had been found. The errors of 5-10% range could be associated with: the using of obsolete dosimeters 27012 and VAJ-18 with calibration error near 5-7 %; the differences in values of the constants in calculation absorbed dose algorithms from reference literature; irregular accounting of source decay etc. The errors 10-15% could be related with irradiation technique which was used for irradiation of TLD capsules and calculation of doses (SSD or SAD-technique); the absence of correction factor from Air kerma to the absorbed dose in water if dosimeter was calibrated in Air kerma units. Errors over 20 % could be related with calculation of the irradiation time for depth 5 cm and irradiation of TLDs in holder with depth 10 cm; different random errors of the exposure time calculation.

Since 2014, due to the IAEA technical support in frame of National TC-project, when the 25 Oncology Hospitals received the modern dosimetry equipment (UNIDOS E and water phantoms), 65 medical physicists were trained on TRS 398 "Absorbed dose determination in external beam radiotherapy" the results of dosimetry audit of dose calibration quality have become significantly better than in previous years: 8.6-15 % of radiotherapy units in IAEA dosimetry audit and 17-22 % in national dosimetry audit had errors more than 5 %.

CONCLUSIONS

To eliminate errors in dose calibration, it is necessary to organize national training for medical physicists on permanent base and implement in practice the international dosimetry protocol IAEA TRS № 398: Absorbed Dose Determination in External Beam Radiotherapy.

Diagnostic Radiology Medical Physics

Measurement of Thyroid Radiation Doses by OSLD During Mammography Screening

A. Chougule[a]
G. K. Jain[b], **R. Verma**[a]

[a]Department of Radiological Physics, SMS Medical College & Hospital, Jaipur-302004, India
[b]Department of Radiation Oncology, MG Medical College & Hospital, Jaipur-302022, India

Email address of Corresponding Author: arunchougule11@gmail.com

BACKGROUND

Breast cancer is the most common cancer among women worldwide contributing about 25% of the total number of cases diagnosed. Breast cancer incidence is increasing in India and is a leading cause of cancer related death in women. Mammography screening for early cancer detection is widely practiced. Indian Council of Medical Research (ICMR 2015) stated that the breast cancer incidence varies in India from 5 to 30 per 100,000 female population per year in rural and urban areas respectively. Overall, breast cancer is second most common cancer among women in India contributing 21% incidence. However, breast cancer is more common in urban female as compared to cancer cervix. Mammography is a very crucial examination for early detection of breast cancer as it involves use of low energy X-rays. The lower the energy of X-rays, the higher is the probability of its absorption by the tissue. The thyroid gland is one of the most sensitive organs at risk in the vicinity of the breast. This study was planned to quantify the scatter radiation dose to right and left lobe of the thyroid gland during routine screening mammography examination.

METHODS

The study included 350 women within the age group of 35-60 years and with Body Mass Index (BMI) range of 22-29. A set of common information were recorded from each of the participants during each examination such as patient ID, age, weight, height, compressed breast thickness and machine parameters. All of them were screened on Hitachi Hologic LORAD M-IV^{TM} screen-film mammography system single handedly. In-vivo dosimetry measurements were made using optically stimulated luminescent dosimeter (OSLD) detectors taped appropriately to the skin overlying on right and left lobe of thyroid gland. The OSL system used is a commercial InLight^{TM} microStar reader system, manufactured by Landauer Inc. (Glenwood, Ill). OSL dosimeters were Al_2O_3:C nanoDots^{TM} (10 X 10 X 2 mm). The radiographic parameters used during two dimensional (2D) mammography ranged from 28-30 KV and 16-22 mAs respectively. The standard two view 2D mammography technique of two craniocadual views (CC) and two mediolateral oblique views (MLO) was used during screening examinations.

RESULTS

The average thyroid skin dose per examination was 0.42 ± 0.31 mGy per mammographic examination (range: 0.25 - 0.96 mGy). The MLO view was found to give a 2.1-fold higher skin dose at the thyroid than the CC view. Average compressed breast thickness was observed 4.9±1.0 cm ranging from 3.2 to 7.2 cm.

CONCLUSIONS

The single examination doses to the thyroid were not found to be particularly high, however the expected higher frequency of screening examinations will increase the number of patients receiving such or even higher radiation doses in case of multiple examinations.

Measurement Techniques Comparisons in CT Scan: Paediatric Neck Phantom Study

M. Alssabbagh[a]
J. Wong[b], A. Tajuddin[c], M. AbdulManap[d], R. Zainon[d]

[a]Jordan Energy and Minerals Regulatory Commission, Nuclear & Radiation Sector, Amman, Jordan
[b]Department of Biomedical Imaging, Faculty of Medicine, University of Malaya, Malaysia
[c]School of Physics, Universiti Sains Malaysia, Pinang, Malaysia
[d]Advanced Medical and Dental Institute, Universiti Sains Malaysia, Pinang, Malaysia

Email address of Corresponding Author: sabmomo75@gmail.com

BACKGROUND

More than 11 % of all CT tests are conducted for paediatric patients, and between 30 % and 80 % of these procedures are done on the neck and head, including the thyroid gland [1]. Thyroid cancer is considered to be the third most widespread cancer in children, as it represents 0.5% to 1.5% of the total of paediatric cancer cases [2]. The most appropriate direct method to measure the absorbed doses in CT examinations is the use of physical phantoms. Mathematical methods may also be employed to estimate the effective dose to a specified organ/tissue. The most important dose related parameters displayed on the CT console are the $CTDI_{vol}$ and the DLP [3].

METHODS

The 3D model of thyroid gland designed by Alssabbagh et.al [4] was used in this study to fabricate a solid version of 10 years paediatric thyroid phantom for CT dosimetry purposes. The model has two holes for the accommodation of two sets of TLDs in each lobe (figure 1). A dual-energy Siemens SOMATOM Definition (128 detectors) CT scanner was used. The usual protocol used in the hospital for neck scan (covered a scan length of 12 cm) was followed. Two voltages (80 kVp and 140 kVp) were set and the automatic current modulation feature was used. The exposure from the scout image was also considered in this study. A comparison between the effective dose to the neck-thyroid area obtained from the reported dosimetry quantities in CT console and the TLD results was performed. The location of the TLDs were considered in this comparison.

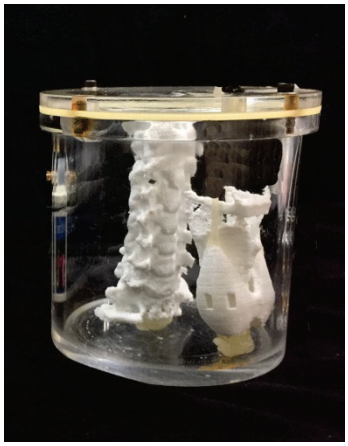

Figure 1. The 3D thyroid-neck phantom loaded with the dosimeters under CT scan.

RESULTS

The diameter of 16 cm PMMA where considered in the console to obtain the CTDIvol. The conversion k-factors of the neck for 10-years old paediatric neck (0.0079 $mSv.mGy^{-1}.cm^{-1}$) were used to calculate the effective dose E from the system-reported DLP. The appropriate tissue-weighting factor (W_T) (0.04) [5] was used to calculate the effective dose to the thyroid from the dosimeters, as shown in table 1.

Table 1. The effective dose from Neck DLP and dosimeters.

Phantom	**$CTDI_{vol}$** (mGy)	**DLP (**mGy.cm)	***E*** (mSv)	**TLD** (mGy)	**E** (mSv)
Thyroid-Neck (10 y)	19.95	223	1.7617	25.73	1.025

CONCLUSIONS

The results showed that the calculated effective dose from reported DLP is higher than the one measured with the TLD dosimeters by a factor of ≈ 2. This may be due to the fact that the TLD dosimetry study provides direct measurements in the middle of the thyroid gland, while the system-provided dosimetric quantities displayed in the CT console only help calculate an estimate of the dose in the neck area, including the radiosensitive gland. However, The $CTDI_{vol}$ helps estimate the dose in the central axis over a scanned volume, which the thyroid phantom fell in this volume in our case. It is important to consider the variation of absorbed dose in CT due to various types of CT scanner, scanning protocols and the different scan lengths that may be selected. Therefore, development of recommendations regarding good practice in CT, especially for paediatric, should be considered, especially regarding the fact that the use of CT is on the rise.

REFERENCES

[1] WARTOFSKY L., VAN NOSTRAND D. 2006. Thyroid Cancer: A Comprehensive Guide to Clinical Management. 2nd ed. Humana Press; 708 pp.

[2] CHIESA F., TRADATI N., CALABRESE L., GIBELLI B., GIUGLIANO G., PAGANELLI G., DE CICCO C., GRANA C., TOSI G., DEFIORI E., CAMMARANO G., CUSATI A, ZURRIDA S. 2004. Thyroid disease in northern Italian children born around the time of the Chernobyl nuclear accident. Ann Oncol. 15*(*12*):* 1842–6 pp.

[3] AAPM 2008. AAPM Report No. 96 - The Measurement, Reporting, and Management of Radiation Dose in CT. American Association of Physicists in Medicine. 1-34 pp.

[4] ALSSABBAGH M., TAJUDDIN A., MANAP M.A., ZAINON R. 2017. Fabrication of a thyroid phantom for image quality in nuclear medicine using the 3D printing technology. ARPN J Eng Appl Sci. 12*(9):* 2798–802 pp.

[5] ICRP 2007. ICRP 103: The 2007 Recommendations of the International Commission on Radiological Protection. Ann ICRP. 37 330.

Audit and Optimization of Patient Skin Radiation Dose During Percutaneous Nephrolithotomy: A Preliminary Experience

S. C. Uniyal
V. Chaturvedi, M. Biswas

Swami Rama Himalayan University, Dehradun, India

Email address of Corresponding Author: dr.suniyal@gmail.com

BACKGROUND

Fluoroscopy is used in many surgical procedures, but the concern for patient radiation dose is largely neglected therein. The International Commission of Radiological Protection (ICRP) has published a document on radiological protection in fluoroscopically guided procedures performed outside the imaging department in which emphasis has given to radiation dose monitoring in such procedures [1]. Percutaneous nephrolithotomy (PCNL) is a fluoroscopy guided technique which is extensively used in operation theatres to treat renal calculi. It is an endoscopic surgical procedure performed in several steps such as percutaneous renal access, track dilation and stone manipulation requiring fluoroscopy guidance [2]. In such procedures, patient's skin is most *vulnerable* for fluoroscopic exposures and high radiation doses during complex fluoroscopy procedures may cause skin injuries of deterministic nature. It may also increase the risk of stochastic health effects to the patient [3]. In the present study, peak skin dose (PSD) was evaluated during a number of PCNL procedures. The fluoroscopy time used during each procedure was carefully recorded to evaluate its effect on patient dose.

METHODS

The study included a total of 50 consecutive PCNL procedures performed in urology operation theatre using Siemens Siremobil Compact L mobile C-arm fluoroscopy unit (Siemens Ltd, Mumbai). The Gafchromic XR-RV3 film used for measurement of PSD was calibrated for X-ray beam energies used during the procedure. At each beam energy, film samples of size 2 cm × 2 cm were exposed with eleven dose values (20, 40, 90, 150, 200, 300, 400, 500, 600, 700 and 800 mGy) by placing each sample on the top of a polymethyl methacrylate (PMMA) phantom of size 20×20×20 cm^3. The scanning of films was performed in an Epson Expression 11000XL flatbed document scanner and the optical densities (ODs) were analyzed with Image-J software. A calibration curve for the film was plotted between OD and corresponding values of radiation dose (D). This curve was used to obtain a second order polynomial fit equation to be used for subsequent determination of PSD from films exposed during PCNL procedures. During PCNL procedures, a full sheet of Gafchromic XR-RV3 was wrapped in a surgical sheet and placed under the renal area of the patient in such a way that the yellow side of the film faced the under-couch X-ray tube. Scanning of the irradiated films and analysis of their images were performed according to the same method as used during calibration of films. PSD was evaluated corresponding to the region of maximum exposure on the film.

RESULTS

As depicted in Figure 1, the values of PSD were found to be in the range of 23.8 to 851.0 mGy with the mean value of 250.3.9 mGy (SD ± 223.64), which are below the deterministic threshold of 2 Gy required for developing skin effects such as transient erythema and skin burn. An average correlation ($R^2 = 0.51$) was found between the recorded values of fluoroscopy time and the corresponding values of PSD measured during PCNL procedures in this study.

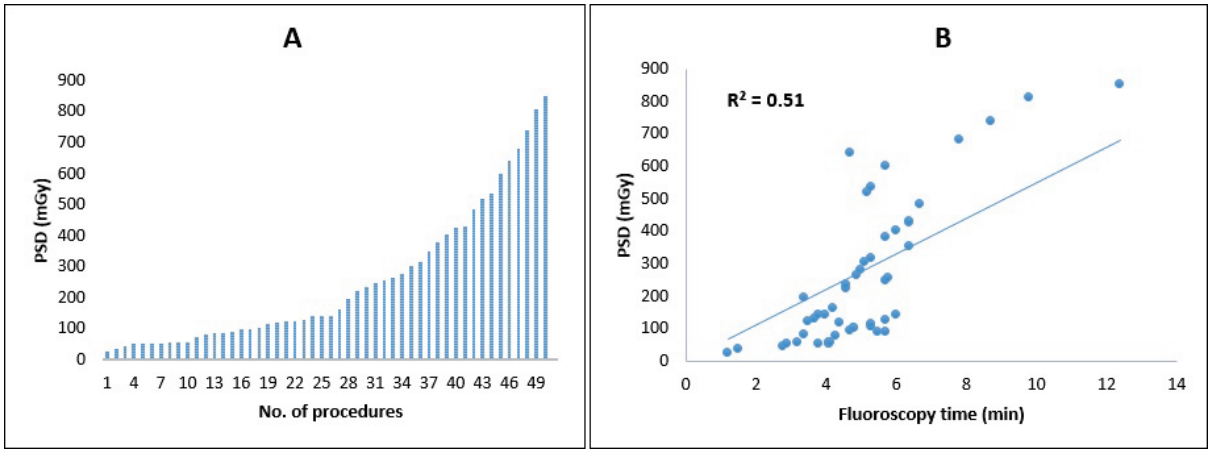

Figure. 1. Peak skin doses (A); and correlation between PSD & fluoroscopy time for PCNL procedures (B)

CONCLUSIONS

The results of this study show that the individual skin exposures during PCNL are generally under the level required to cause any deterministic skin injury. However, likelihood of higher radiation dose may not be denied due to varying complexities in the procedure. So, monitoring patient dose during PCNL procedures is well justified. Surgeons should consider to skip unnecessary exposures and minimize the duration of fluoroscopy for optimization of patient radiation dose.

ACKNOWLEDGMENTS

This work was supported by the Atomic Energy Regulatory Board, Government of India (Grant number: AERB/CSRP/Proj. No. 57/01/2014).

REFERENCES

[1] INTERNATIONAL COMMISSION ON RADIOLOGICAL PROTECTION, Radiological Protection in Fluoroscopically Guided Procedures Performed Outside the Imaging Department, Publication 117 ICRP. Ann. ICRP 40(6) (2010).

[2] KO R., SOUCY F., DENSTEDT J.D., RAZVI H., Percutaneous nephrolithotomy made easier: a practical guide, tips and tricks". BJU Int. 101(5) (2008) 535-9.

[3] BALTER S., MILLER D.L., Patient skin reactions from interventional fluoroscopy procedures. Am. J. Roentgenol. (2014) W335-42.

Optimization of Doses in Paediatric CT: Preliminary Results of an IAEA/CRP Project

P. Costa[a]
D. Nersissian,[a], V. Guerra, E. Gebrim[b]

[a]Institute of Physics, University of São Paulo, São Paulo-SP, 05508-090, Brazil
[b]Institute of Radiology of the School of Medicine of the University of São Paulo, São Paulo-SP, 05403-010, Brazil

Email address of Corresponding Author: pcosta@if.usp.br

BACKGROUND

The estimation of radiation risks requires measurement of organ doses for paediatric patients submitted to procedures involving ionizing radiation. Such measurements have been prioritized by many studies and have been the basis of guidelines, policies and institutional rules around the world [1]. Radiation doses in CT examinations must receive special attention, due to the increase in the frequency of this kind of procedures in children and the fact of these procedures potentially deliver high doses when compared to other imaging options. Moreover, doses should be evaluated for various child body sizes. These facts have raised concerns about the risk to the children´s health caused by radiation exposure to CT procedures, especially considering the higher radiosensitivity of tissues in children.

In this study, a dose optimization process for paediatric protocols was applied according to the IAEA recommendations [1]. This implementation is part of the IAEA/CRP E2.40.20 project and includes the production of a report with a critical analysis of the impact of implementing optimized protocols, including guidelines and the development of educational tools for training clinical staff involved in paediatric CT procedures.

METHODS

The protocol optimization focused on Head and Thorax exams, primarily. The first strategy was comparing the configuration of these protocols with the suggested one by the American Association of Physicists in Medicine (AAPM) in the Alliance for Quality Computed Tomography for routine pediatric Chest CT and Head CT for the specific equipment (Philips – Brilliance 64). The responsible radiologist and the radiographer checked the proposal and suggested some changes. The first comment was that protocols were high-dose and they liked to try some lower mAs values than the suggested by AAPM.

The medical physicist and the responsible radiographer have adapted the protocols for some ages for Head CT (0 - 1 year, 1 - 2 years, 2 - 6 years, 6 - 16 years and 16 - 20 years) in axial mode and one protocol for helical mode, when 3D reconstructions were necessary. For Chest CT, just three age ranges were used (0 - 1 year, 1 - 10 years and 10 - 15 years), all in helical mode.

RESULTS

The quantities CTDI, DLP, charge (mAs) and scan length were evaluated using data from the DICOM header of the examinations. These quantities were evaluated using box plots in order to extract their statistical significance and proceed to a robust comparison between the optimized and pre-optimized protocols [2]. Figure 1 shows an example of one of these box plots for one of the age groups.

Figure 1. Box-plot for brain CT procedures conducted in patients with age group of 5-10 years old. The red plot presents the values before the optimization process and the green box the results after the optimization.

CONCLUSIONS

The first results indicated significant dose reductions without perceptive loss in image quality of these two general exams. Future work will include a similar study on a scanner that is currently used for emergency imaging.

REFERENCES

[1] INTERNATIONAL ATOMIC ENERGY AGENCY, *Dosimetry in Diagnostic Radiology for Paediatric Patients*, *Human Health Series 24*. 2013.

[2] SERNA, A., et al., Optimization of CT protocols using cause-and-effect analysis of outliers. Physica Medica: European Journal of Medical Physics, 2018. 55: p. 1-7.

Patient Doses from Contrast Enhanced Spectral Mammography

S. Avramova-Cholakova[a]
E. Kulama[a], Z. Buchakliev[b], V. Arsov[c]

[a]Imperial College Healthcare NHS Trust, London W6 8RF, UK
[b]Acibadem City Clinic Oncology Hospital, 66A Tsarigradsko shosse, 1784 Sofia, Bulgaria
[c]Oncology Clinic Sofia, 1 Andrey Saharov, 1784 Sofia, Bulgaria

Email address of Corresponding Author: simona.avramova-cholakova1@nhs.net

BACKGROUND

Contrast enhanced spectral mammography (CESM) is an emerging technology proving to be useful in diagnosis problem-solving, disease staging and others [1]. There is very limited data available on patient exposure from this technology. The aim of this study is to estimate patient and phantom doses from two CESM systems.

METHODS

The two CESM systems are Senographe Essential/Senobright, GE Healthcare, situated in Bulgaria (1) and in the UK (2). The methodology described in the European Guidelines [2] and the conversion factors provided for CESM were applied [3].

RESULTS

The results from the phantom study on both systems are presented in Table 1, including the target/filter combination and tube voltage chosen by the system and the mean glandular dose (MGD) per low (LE) and high (HE) energy beams, as well as the total MGD from both LE and HE exposures.

Table 1. PMMA phantom results.

PMMA + spacer (mm)	20+1	30+2	40+5	45+8	50+10	60+15	70+20
(1) T/F kV LE	Mo/Rh 27	Mo/Rh 27	Rh/Rh 29	Rh/Rh 31	Rh/Rh 31	Rh/Rh30	-
(1) T/F kV HE	Mo/Cu 46	Mo/Cu 46	Rh/Cu 45	Rh/Cu 47	Rh/Cu 47	Rh/Cu 49	-
(1) MGD LE (mGy)	1.53	1.17	1.85	2.45	2.27	3.1	-
(1) MGD HE (mGy)	0.24	0.23	0.49	0.68	0.66	0.77	-
(1) MGD total (mGy)	1.77	1.41	2.34	3.14	2.94	3.87	-
(2) T/F kV LE	Mo/Rh 27	Mo/Rh 27	Rh/Rh 29	Rh/Rh 29	Rh/Rh 31	Rh/Rh30	Rh/Rh30
(2) T/F kV HE	Mo/Cu 46	Mo/Cu 46	Rh/Cu 45	Rh/Cu 45	Rh/Cu 47	Rh/Cu 49	Rh/Cu 49
(2) MGD LE (mGy)	1.56	1.19	1.88	1.73	2.36	3.14	2.74
(2) MGD HE (mGy)	0.27	0.26	0.55	0.53	0.70	0.79	0.74
(2) MGD total (mGy)	1.82	1.45	2.44	2.26	3.06	3.93	3.48

Data were analyzed for a total of 49 patients on the first and 44 patients on the second system. The results from the patient study are presented in Table 2, including statistical data (is the standard deviation and Q is the quartile) on compressed breast thickness, MGD per LE and HE exposure and the total MGD (LE plus HE contribution) per projection, either medio-lateral oblique (MLO) or cranio-caudal (CC). The HE contribution to MGD was found to be from 14% up to 32% of the LE MGD. Furthermore, comparison was performed with data from full field digital mammography from the UK breast screening programme. Lower MGD per projection was reported from 1.42 mGy up to 2.52 mGy [4]. CESM at the present moment is mainly used for diagnostic purposes with expected net benefit for the patient.

Table 2. Patient statistics and MGD.

System / projection		1 / MLO	1 / CC	2 / MLO	2 / CC
Total No of projections		98	98	85	87
Compressed breast thickness (mm)	Mean ± σ (min, max)	54.0 ± 12.4 (24, 84)	50.9 ± 12.0 (17, 75)	58.5 ± 18.5 (24, 97)	56.0 ± 15.2 (23, 89)
	Median (1^{st}, 3^{rd} Q)	54 (46, 62)	52 (43, 60)	59 (44, 73)	56 (44, 67)
MGD per exposure LE (mGy)	Mean ± σ (min, max)	2.14 ± 0.59 (1.10, 3.53)	2.08 ± 0.61 (1.12, 3.53)	2.56 ± 0.79 (1.26, 3.77)	2.53 ± 0.79 (1.18, 3.84)
	Median (1^{st}, 3^{rd} Q)	2.00 (1.72, 2.31)	1.87 (1.73, 2.29)	2.53 (1.89, 3.38)	2.46 (1.90, 3.38)
MGD per exposure HE (mGy)	Mean ± σ (min, max)	0.56 ± 0.19 (0.23, 0.84)	0.53 ± 0.19 (0.23, 0.84)	0.62 ± 0.21 (0.26, 0.86)	0.62 ± 0.21 (0.26, 0.86)
	Median (1^{st}, 3^{rd} Q)	0.49 (0.47, 0.68)	0.49 (0.31, 0.68)	0.71 (0.35, 0.82)	0.71 (0.35, 0.82)
MGD per projection (mGy)	Mean ± σ (min, max)	2.69 ± 0.76 (1.33, 4.37)	2.61 ± 0.78 (1.35, 4.37)	3.18 ± 0.99 (1.52, 4.63)	3.15 ± 0.99 (1.44, 4.70)
	Median (1^{st}, 3^{rd} Q)	2.36 (2.12, 2.99)	2.27 (2.12, 2.96)	3.24 (2.38, 4.20)	3.17 (2.38, 4.20)

CONCLUSIONS

A study of patient doses from CESM is performed on two systems of the same type. Doses are somewhat higher in comparison to planar mammography according to some studies.

REFERENCES

[1] PATEL, B.K, LOBBES, M.B.I, LEWIN, J. Contrast enhanced spectral mammography: A Review, Semin Ultrasound CT MR **39(1)** (2018) 70-79.

[2] EUROPEAN UNION. European guidelines for quality assurance in breast cancer screening and diagnosis, 4^{th} ed. Supplements, Luxembourg (2013).

[3] DANCE, D.R., YOUNG, K.C. Estimation of mean glandular dose for contrast enhanced digital mammography: factors for use with the UK, European and IAEA breast dosimetry protocols, Phys.Med.Biol. **59** (2014) 2127-2137.

[4] YOUNG, K.C., ODUKO, J.M. Radiation doses received in the UK breast screening programme in 2010 to 2012, BJR **89** (2016).

Patient Maximum Skin Dose in Interventional Radiology and Cardiology Procedures: Summary of EURADOS Working Group 12 Activities

O. Ciraj-Bjelac[a]
J. Dabin[b], **J. Farah**[c], **Z Knezevic**[d], **F. Malchair**[e], **T. Siiskonen**[f], **on behalf of EURADOS WG12**

[a]Vinca Institute of Nuclear Sciences, University of Belgrade, Vinca, Serbia
[b]Belgian Nuclear Research Centre, Mol, Belgium
[c]Hôpitaux Universitaires Paris-Sud, Pôle Imagerie et Médecine Nucléaire, Le Kremlin-Bicêtre, France
[d]RuđerBoškovićInstitute, Zagreb, Croatia
[e]Centre Hospitalier Universitaire de Liège, ZEPHYRA, Liège, Belgium
[f]Radiation and Nuclear Safety Authority, Helsinki, Finland

Email address of Corresponding Author: ociraj@vinca.rs

BACKGROUND

Fluoroscopically guided interventional procedures in radiology (IR) and cardiology (IC) are techniques that have had wide diffusion in the last decades. Nevertheless, prolonged exposures due, for instance, to complicated interventional procedures or inappropriate equipment may result in high doses to both patients and staff members, in particular, with potentially high radiation doses to the skin of a patient. Evermore, as the number and complexity of interventional procedures have been steadily growing, it becomes crucial to provide patient-specific, skin dose estimate during these procedures. Working group 12 of EURADOS is dealing with various aspects of dosimetry in medical imaging. To tackle this issue, EURADOS Working group 12 has initiated a number of activities to estimate the maximum skin dose in various procedures in radiology and cardiology.

METHODS

This work presents Working group 12 activities in the area of dosimetry for interventional procedures in cardiology and radiology. It includes characterization of different dosimetric methods for skin dose assessment in interventional procedures, the application for skin doses measurement in clinical practice and the establishment of trigger levels. Latter is performed in order to evaluate the feasibility of identifying a common dosimetric indicator that correlates with the maximum skin dose.

RESULTS

Several types of dosimeters have been used to estimate patient's skin dose distribution. Luminescence detectors usually show good energy and dose response in clinical beam qualities. However, the poor spatial resolution of such point-like dosimeters may far outweigh their good dosimetric properties. Gafchromic® films are probably the most convenient and affordable solution for clinical routine. The overall uncertainty associated with the use of XR-RV3 Gafchromic® films to determine skin dose in the interventional environment can realistically be estimated to be around 20% (k=1). This uncertainty can be reduced to within 5% if carefully monitoring scanner, film and fitting-related errors or it can easily increase to over 40% if minimal care is not taken. Ideally, the skin dose alert levels could be set as a function of an online dose indicator to prevent skin injuries and to identify which patients require follow-up. However, variation in procedure’s complexity, level of optimization, user’s

skill level and techniques in performing the procedure result in large dispersion of dose indicators corresponding to a pre-determined skin dose.

CONCLUSIONS

The results of characterization of different dosimetric methods for skin dose assessment in interventional procedures, are presented. Both skin dose measurements using GafChromic® films and TLDs provide reasonably accurate determination of the skin dose alert levels. In the future, software-based dose mapping tools may provide a more user-friendly approach to follow-up patient skin dose in real time during the procedure provided they are well validated and benchmarked against measurements.

REFERENCES

[1] DABIN J, NEGRI A, FARAH J, et al., Characterization of grids of point detectors in maximum skin dose measurement in fluoroscopically-guided interventional procedures, Phys. Med.2015, 31(8): 1112–17.

[2] FARAH J, TRIANNI A, CIRAJ-BJELAC O, et. al., Characterization of XR-RV3 GafChromicTM films in standard laboratory and clinical conditions and means to estimate uncertainties and reduce errors, Med. Phys. 42(7) (2015) 4211-26.

[3] JARVINEN H, FARAH J, SIISKONEN T, et al., Feasibility of setting up generic alert levels for maximum skin dose in fluoroscopically guided procedures, Phys Med. 2018; 46:67-74.

[4] KOPEC R, NOVÁK L, CARINOU E, et.al., Intercomparison of Gafchromic films, TL chips and TL foils for the measurements of skin dose in interventional radiology. Radiat. Meas. 2014, 71: 282–6.

Comparison of Average Glandular Dose and Image Quality of Electronic and Geometric Magnification Mammogram: A Phantom Study

S. Moshiri[a]
R. R. Haghighi[b], M. E. Fazilat Moaddeli[b], S. Sefidbakht[b], F. Zarei[b], P. Pishdad[b], Z. Gholami Bardeji[b], V. C. Vani[c], S. Chatterjee[d]

[a]Department of Nuclear and Reactor Engineering, Islamic Azad University, Arsanjan 73761168, Fars, Iran
[b]Medical Imaging Research Center, Shiraz University of Medical Sciences, Shiraz 7134845794, Iran
[c]Department of Instrumentation and Applied Physics, Indian Institute of Science, Bangalore 560012, India
[d]Ongil, 79 D3, Sivaya Nagar, Reddiyur Alagapuram, Salem 636004, India.

Email address of Corresponding Author: sravanfarr@gmail.com

BACKGROUND

Magnification mammogram is a diagnostic tool to detect micro-calcifications in early stage of breast cancer. There is a controversy in using geometric magnification and electronic one to detect micro-calcifications in diagnostic mammography. It is known that the fibro-glandular tissues are very sensitive to radiation dose. Geometric magnification with reduced distance between x-ray source and breast increases radiation dose and risk of stochastic effect of fibro-glandular tissues. On the other hand, spatial resolution of digital mammogram is dependent on the pixel size of the image detector in addition to the focal spot size. This study tries to evaluate the average glandular dose and image quality in images with geometric magnification and digital zoom with the accessible phantoms [1-4].

METHODS

Two digital mammography systems with the capability of digital and geometric magnification were selected in this study. High contrast (or resolution) part of Digmam phantom was used to assess magnified images produced by geometric and digital zoom. Also, the micro-calcification groups inside the ACR phantom are used to evaluate the ability of geometric and digital magnification images, figure 1(a and b). Automatic exposure control used in both geometric and digital (in contact position) magnification modes to provide images of Digmam and ACR phantoms. Average glandular dose is measured by multifunction meter (Black Piranha). It has to be noted that in digital zoom, phantom is placed on the top of the detector (contact mode) while for geometric magnification after removal of the grid, phantom placed on top of the magnification plate of the mammography system (1.5X and 1.8X magnifications). Two radiologists with more than 10 years experience on mammography reports are evaluated all phantom images.

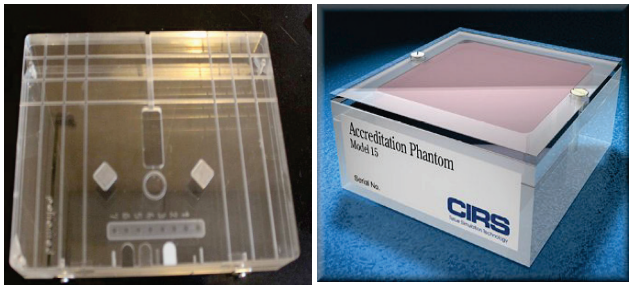

(a) (b)

Figure 1. Phantoms (a) Digmamm and (b)ACR used to evaluate the quality of images.

RESULTS

Image analysis show that in two mammography systems digital zoom (in contact position) reveals 5 to 7 line per millimeter of the high contrast part of the phantom which is comparable to the similar images produced in geometric magnification. ACR images show that at least 3 groups of specks (mimic micro-calcification) can be seen in both methods, geometric and digital magnification. Results of dose measurement shows that average glandular dose in 1.5X and 1.8X geometric magnification positions are about 2 and 3 times higher than that of contact position to produce digital magnification views as can be seen in table 1.

Table 1. Exposure factors and the related average glandular dose measured for contact, 1.5X and 1.8X geometric magnification.

View	kVp	mAs	AVG (mGy)
Contact	28	100	0.885
1.5X	28	100	2.034
1.8X	28	100	2.879

CONCLUSIONS

Finding of this study demonstrates that spatial resolution and the ability of the geometric and digital magnifications are comparable to detect the same number of lines pairs per millimeter and group of specks mimic micro-calcifications. Average glandular dose in digital mammography is considerably less (at least 2 times) than geometric magnification. Therefore, spot compression views with digital zoom mammogram may replace geometric magnification with less average glandular dose and equal spatial resolution and image quality.

REFERENCES

[1] Fisher U,Baum F,Obenauer S,Funke M,Hermann KP,Grabbe E., Digital Full Field mammography Comparison Between Radiographic Direct Magnification and Digital Monitor Zooming,Radiolge (2002) 42:261-264

[2] Sankararaman S., Andrew K., Srinivasan R., Ioannis S.D, Oris, Carl J, Detection of simulated Microcalcification in a Phantom with Digital Mammography: Effect of Pixel Size, Radilogy: Volume244: Number 1-July2007

[3] Min J., Kim Eun-Kyoung et al, Characterization of microcalcification: Can digital monitor zooming replace magnification mammography in full-field digital mammography? Eur Radiol (2009) 19:310-317

[4] Moraux-Wallyun M., Chaveron C., Bachelle F. et al. Comparison between electronic zoom and geometric magnification on digital mammography. J Radiol 2010; 91:879-967

Scattered Dose Measurement for a Mobile C-arm Fluoroscopy System: Patient Thickness Factor

S. I. Saufi[a]
S. Husaini[b]

[a]Nuclear Medicine Department, Hospital Sultanah Aminah, Johor Bahru Jalan Persiaran Abu Bakar Sultan, 80100 Johor Bahru, Johor, Malaysia
[b]Medical Physics Group, Malaysia Nuclear Agency, 43000, Kajang, Malaysia

Email address of Corresponding Author: syarul_iman@moh.gov.my

BACKGROUND

It is well documented that scattered radiation is the main contributor to the occupational exposure of radiation workers. This study aimed to investigate the spatial distribution of scattered radiation doses rate induced by the operation of C-arm machine (Toshiba SXT-1000A) on the (irradiated) water phantom of different thicknesses. The scatter radiation is dependent on a number of factors and the radiation around the patient does not distribute uniformly or symmetrically. Although safety precautions are considered, an increase in the occurrence of radiation-induced eye cataracts has been reported. As a consequence, in 2011 the International Committee for Radiological Protection (ICRP) lowered the eye lens dose limit for staff dramatically from 150 mSv per year to 20 mSv per year.

METHODS

Water phantoms with different sizes 10 cm x 30 cm x 30 cm, 20 cm x 30 cm x 30 cm and 25 cm x 30 cm x 30 cm were used. They were exposed to X-ray radiation from a mobile c-arm fluoroscopy system with automatic brightness control (ABC) mode function. An ion chamber (1,800 cc) model Radcal 20X6-1800) was used to measure scattered radiation at two different levels namely abdomen (100 cm from the floor) and eye level (160 cm from the floor). The ion chamber was placed at nine different positions (Point A to Point I) around the examination table. The scattered radiation distributions around the phantom were determined. Please refer to Figure 1 for the study set-up

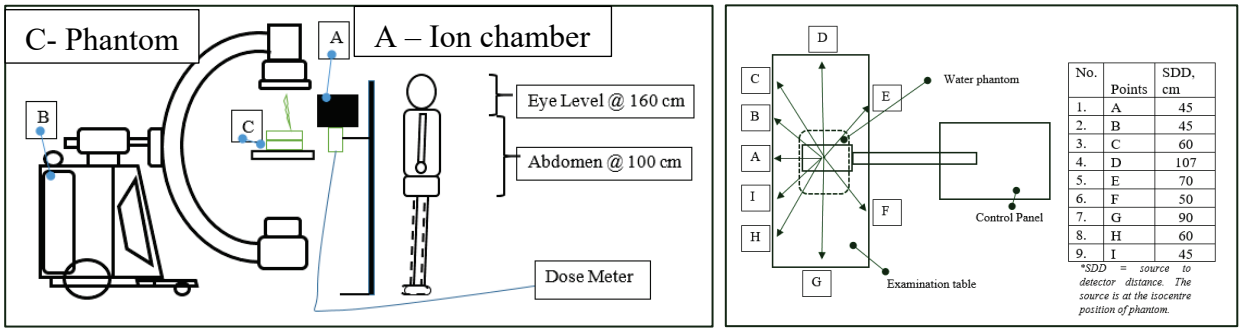

Figure 1. Study set-up.

RESULTS

Based on the results, the dose rate of scattered radiation for the 25 cm thick phantom recorded the highest reading (25.60 ± 0.01 mR/hr - 478.60 ± 0.00 mR/hr), followed by the 20 cm thick phantom (12.66 ± 0.01 mR/hr - 260.90 ± 0.01 mR/hr). It was found that 10 cm thick phantom recorded the lowest reading among three sizes, (2.24 ± 0.02 mR/hr – 58.66± 0.00 mR/hr). The results obtained are presented in Table 1.

The dose rate of over-couch X-ray tube configuration is dominant, especially at the eye level. The result of scattered radiation at Point A showed that it is the riskiest position where the radiation dose reading is the highest among all three phantom thicknesses. This is due to the distance factor between the ion chamber and isocentre of the water phantom. The lowest reading result at Point D also due to the distance factor. It was noted that the scattered radiation increases linearly with the phantom thickness. The higher result of the scattered radiation could probably lead to higher exposures for staff.

Table 1. Result of scattered radiation

Patient Thickness	Minimum (mR/hr)	Maximum (mR/hr)
25 cm	25.60 ± 0.01	478.60 ± 0.00
20 cm	12.66 ± 0.01	260.90 ± 0.01
10 cm	2.24 ± 0.02	58.66 ± 0.00

CONCLUSIONS

The spatial distributions of the scattered radiation induced by the irradiation of water phantoms of varying thickness on a mobile c-arm machine has been established. The scatter pattern has been recognized at every point based on the potential of the location of radiation worker inside the operating theatre (OT) room. From the result, we can conclude that the scattered radiation increases linearly with the phantom thickness. Therefore, the radiation protection principle and the concept of ALARA and optimization should be strengthened especially during the clinical procedure inside the Operating theatre (OT) room.

REFERENCES

[1] 43th Radiological Advisory Committee (RAC) Meeting Annual Report. Ministry of Health April 3, (2018).

[2] D.R. DANCE S. CHRISTOFIDES A.D.A. MAIDMENT I.D. MCLEAN K.H. NG et. al. Diagnostic Radiology Physics A Handbook for Teachers and Students. International Atomic Energy Agency. (2014).

[3] Laws of Malaysia. Atomic Energy Licensing Act 1984. The Commissioner Of Law Revision, Malaysia Under The Authority Of The Revision Of Laws Act 1968 In Collaboration With Percetakan Nasional Malaysia Bhd. (2006).

[4] H. SALLEH, S. B. SAMAT, M. K. MATORI, M. J. M. ISA, Anode-Cathode Position: How It Influences The Radiation Risk To Staff Involved in Fluoroscopy Procedures. Switzerland, Trans Tech Publications, Advanced Materials Research Vol. 1087, (2015), pp 405-409.

Machine Learning as a Novel Tool in X-ray Angiographic Imaging Optimization: Comparison to a Validated Channelized Hotelling Observer Model (CHO)

V. Trojani[a,b]
M. Bertolini[b], A. Nitrosi[b], M. Iori[b]

[a]Scuola di Specializzazione in Fisica Sanitaria, Alma Mater Studiorum - Università di Bologna, Bologna, Italy
[b]Servizio di Fisica Medica, AUSL - IRCCS di Reggio Emilia, Reggio Emilia, Italy

Email address of Corresponding Author: valeria.trojani@studio.unibo.it

BACKGROUND

Optimization of imaging protocols has always been important in radiation protection; through contrast-detail curves of dedicated phantoms it is possible to choose the optimal clinical protocol in order to deliver the minimum dose to the patient while maintaining image quality. Contrast-detail curves are usually obtained using human observers but it is a time-consuming process; thus, the study of observer model software mimicking human behavior in object detection tasks was employed.

One of the most known models is the Channelized Hotelling Observer (CHO), due to its high capability to reproduce human behavior from the correlation of pixels from object-present images and background-only images. Previous studies pointed out that CHO models in x-ray angiography perform well in the 0.5mm–4mm diameters [1], while their efficiency drop at higher diameter dimensions (because of the limited range of frequencies that can be included in channel profiles). In fact, adding channel profiles centered at low frequencies limits the dimension of the sub-ROI image inputs the model can process [2], thus narrowing the range of analyzable detail dimensions. Machine learning models have been used in recent years in pattern recognition tasks and, through the use of delta-radiomic features, they can be a complementary tool to CHO models.

The aim of this preliminary study is to find a possible dosimetric optimization of clinical protocols of an angiography system (GE Discovery IGS 740). A contrast-detail phantom simulation in clinical scatter conditions was used, and efficiencies of a CHO model and a machine learning model are compared in order to inspect the applicability of this framework.

METHODS

A Leeds TO10 phantom was used. The phantom details used were: 6 diameters (size range: 2mm –11.1 mm), each with 9 contrasts (declared range: 0.012–0.930 at 70kVp 1.00 with 1mmCu filtration). For smaller detail dimensions the signal area was not high enough to assure good statistics for feature extraction. TO10 has been imaged between two 10 cm thick homogeneous solid water slabs. Two FOVs (32cm and 20cm) were used. Fluoroscopy images were taken using an abdominal protocol at 2 dose levels (low and normal) at 15fps; cineangiography images were acquired using an abdominal protocol at 15fps at 2 dose levels (low and normal). Radiomic features were extracted from the detail-present and from the background-only image sets, pre-sampled at 64 gray levels, following public guidelines [3]. 44 delta-features (i.e. the relative feature values change between the two sets) were evaluated. Feature selection with 10-fold cross-validation LASSO (Least Absolute Shrinkage and Selection Operator) was carried out to identify a subset of features able to best predict the data

and to remove redundant predictors. Two quadratic-SVMs (Support Vector Machine) were trained on 3 different acquisitions for each FOV with a 25% hold-out validation (positive classifier for images with detail, negative otherwise). This model was compared to a previously validated [4] CHO (40 Gabor channels with eye-internal noise) and human responses. Their respective contrast-detail curves were computed using a threshold visibility of 75%. Wilcoxon signed-rank test was performed on two contrast-detail curves obtained from acquisitions and not used in model training.

RESULTS

The features included in the model after selection were 18. For FOV=32cm the AUC for its SVM was 0.91, while for FOV=20cm AUC was 0.88. Relative differences between human results and SVM predictions were all under 25% for both FOVs, significantly smaller than the CHO, which, for higher diameters, held relative differences up to 35% for FOV=32cm and 60% for FOV=20cm. It is important noting that the SVM does not find fluoroscopy with FOV=20cm normal dose level (17.6 mGy/min) statistically different (p-value=0.6) from the cineangiography FOV=32cm low dose level (42.1 mGy/min), meaning a dose reduction of about 70%.

CONCLUSIONS

The stability of the machine learning model in high detail diameters compared to the CHO makes it a performing tool in dosimetric optimization of imaging protocols. In terms of patient radiation protection, it can be used to detect the best clinical protocol which delivers the lowest dose possible while maintaining comparable visibility of structures of interest, leading to significant dose reductions.

REFERENCES

[1] FAVAZZA, C. et al. Implementation oaf a channelized Hotelling observer model to assess image quality of x-ray angiography systems, Journal of Medical Imaging **2** (2015) 015503-3.

[2] FERRERO, A., FAVAZZA C. et al. Practical implementation of Channelized Hotelling Observers: Effect of ROI size, Proc SPIE Int Soc Opt Eng (2017) 10132

[3] ZWANENBURG, A. Image biomarker standardisation initiative, (2016) arXiv1612.07003

[4] BERTOLINI, M. et al. Implementation of Channelized Hotelling Observer (CHO) to assess image quality of GE Discovery IGS 740 angiography system. (2018) (abstract accepted at European Congress of Radiology 2019).

Diagnostic Reference Levels for Routine Radiography Examinations of Model Adult Human Subjects in Southwest Nigeria

J. Achuka[a]
M. Aweda[b], **M. Usikalu**[a]

[a]Covenant University, Ota, Ogun State, Nigeria
[b]Lagos University Teaching Hospital, Idi-Araba, Lagos, Nigeria

Email address of Corresponding Author: justina.achuka@covenantuniversity.edu.ng

BACKGROUND

Radiation protection of patients in diagnostic X-ray imaging has become an important subject today due to fast technological advancement of imaging equipment. This medical X-ray imaging revolution has caused a rapid increase in number and complexity of procedures that are accompanied by significant patient absorbed dose variations [1,2]. The goal of diagnostic X-ray imaging is to use the optimal technique that will produce acceptable image quality with minimal patient dose [3,4]. However, this feat has been found difficult to achieve in practice due to diversities in X-ray equipment and examination protocols [2]. Patient dose from X-ray diagnosis varies significantly between countries, diagnostic centres, X-ray equipment, procedure type and from one operator to another [5,6]. Dose reference levels serve as the guidance level to curtail superfluous dose and enhance patient safety. There are international, national and, local dose reference levels (DRLs) worldwide. Nigeria has no indigenous DRLs yet, but has adopted the International Atomic Energy Agency (IAEA) standards; hence, the need for national and local DRL development. This study is set out to develop local standard DRLs for diagnostic X-ray examinations in Southwest Nigeria.

METHODS

A total of 600 average (70±5 kg) adult human subjects were investigated in 9 secondary/tertiary healthcare institutions located in southwest Nigeria. The quality control of the X-ray machines was conducted using MagicMax quality control kits (IBA Dosimetry, Germany). Informed consent was obtained from each patient before the commencement of the examination. Institutional consent was obtained from each of the hospitals used and also from the Nigerian Institute of Medical Research (NIMR). Entrance skin dose was determined using thermoluminiscence dosimeters (TLD-100) from RadPro International GmbH, Germany. Irradiation of chips was conducted at the Secondary Standard Dosimetry Laboratory (SSDL) of the National Institute of Radiation Protection and Research (NIRPR), Ibadan. TLD detectors were read using the Harshaw Reader (Model 3500). A total of three coded TLD detectors were used to determine the entrance skin dose (ESD) for each examination. PCXMC software (version 20Rotation) was used to evaluate the effective dose.

RESULTS

The results obtained from this study showed that the diagnostic reference levels for routine radiography examinations in Southwest Nigeria are 1.32 mGy, 1.94 mGy, 2.16 mGy, 4.94 mGy, 7.96 mGy, 1.27 mGy and 1.38 mGy for chest PA, cervical spine (CS) AP, CS LAT, lumbar spine (LS) AP, LS LAT, upper extremity AP/LAT and lower extremity AP/LAT respectively. Table 1 presents the mean kVp, mAs, entrance skin dose (ESD), DRL and the effective doses. LS LAT has the highest DRL value.

Table 1. Number of patients, exposure parameters and DRL for model adult human subject in radiography examinations in southwest Nigeria.

Examination	No of patients	Mean kVp	Mean mAs	Mean ESD (mGy)	DRL (mGy)	Effective dose (mSv)
Chest PA	228	84±17.11	19±12.57	1.00±0.40	1.32	0.55
CS AP	51	76±3.25	20±8.90	1.56±1.04	1.94	0.29
CS LAT	48	79±7.89	35±39.14	1.97±1.49	2.16	0.64
LS AP	49	84±7.86	42±19.46	3.76±2.18	4.94	1.53
LS LAT	49	91±10.29	47±19.84	6.70±4.30	7.96	1.45
Upper Extremities	44	67±13.00	20±30.83	1.16±0.61	1.27	0.005
Lower Extremities	131	63±7.50	11±10.19	1.05±0.55	1.38	0.005

CONCLUSIONS

The DRLs obtained in this study showed the possibility of dose harmonization in Southwest Nigeria. Similar study is recommended in other regions of the country in order to develop national DRL for Nigeria.

REFERENCES

[1] INTERNATIONAL ATOMIC ENERGY AGENCY, Radiological protection for medical exposure to ionizing radiation, Safety standards series No. RS-G-1.5, IAEA, Vienna (2002).

[2] KORIR, G.K., WAMBANI, J.S., OCHIENG, B. O., Optimization of patient protection and image quality in diagnostic radiology, East African Medical Journal **87** (2010) 127-133.

[3] UNITED STATES ENVIRONMENTAL PROTECTION AGENCY, Radiation protection guidance for diagnostic and interventional X-ray procedures, Federal Guidance Report No 14, EPA-402-R-10003, Washington D.C (2014).

[4] MILLER, D.L., SCHAUER, D., The ALARA principle in medical imaging. AAPM Newsletter **40** (2015) 38-40.

[5] HART, D., SHRIMPTON, P. C., Fourth review of the UK national patient dose database. British Journal Radiology **85** (2012) 957–958.

[6] WAMBANI, J.S., ONDITI, E.G., KORIR, G.K, KORIR, I.K., Patient doses in general radiography examinations, The South African Radiographer **53** (2015) 22-26.

CTDI of Wide Beam Collimation Diagnostic CBCT

J. Saaring[a]
D. Šutov[a]

[a]Tartu University Hospital, L. Puusepa 8, Tartu, Estonia, 50406

Email address of Corresponding Author: juhan.saaring@kliinikum.ee

BACKGROUND

CTDI is a useful tool for assessing dose reference levels and for comparisons between different protocols and equipment [1]. In CBCT, beam collimations often exceed the traditional dose profile integrating length of 100 mm and additional equipment is needed. IAEA has proposed a method for CTDI estimation for wide beam collimation CBCT equipment using standard equipment [1]. Wide beam collimation CTDI is calculated as [2]:

$$CTDI_{100,(N\times T)>40} = CTDI_{100,ref} \times \left(\frac{CTDI_{free-in-air,N\times T}}{CTDI_{free-in-air,ref}} \right)$$

Where $CTDI_{100,ref}$ is measured in phantom at a reference beam collimation of $NxT_{ref} < 40$ mm, $CTDI_{free\text{-}in\text{-}air,ref}$ is measured in air at the reference beam collimation and $CTDI_{free\text{-}in\text{-}air,NxT}$ is measured in air at beam collimation NxT > 40 mm.

The aim of this study is to investigate the relationship between $CTDI_{free\text{-}in\text{-}air}$ values at different beam collimations and tube voltages. The hypothesis is that ($CTDI_{free\text{-}in\text{-}air,NxT}$ / $CTDI_{free\text{-}in\text{-}air,ref}$) ≈ 1 and CTDI estimation in wide beam collimation CBCT could be made easier by excluding the free-in-air measurements.

METHODS

The measurements are made on a Siemens Multitom RAX diagnostic radiography system equipped with CBCT option. Beam collimations up to 27 cm in the isocentre can be used with tube voltages ranging 40 – 150 kV.

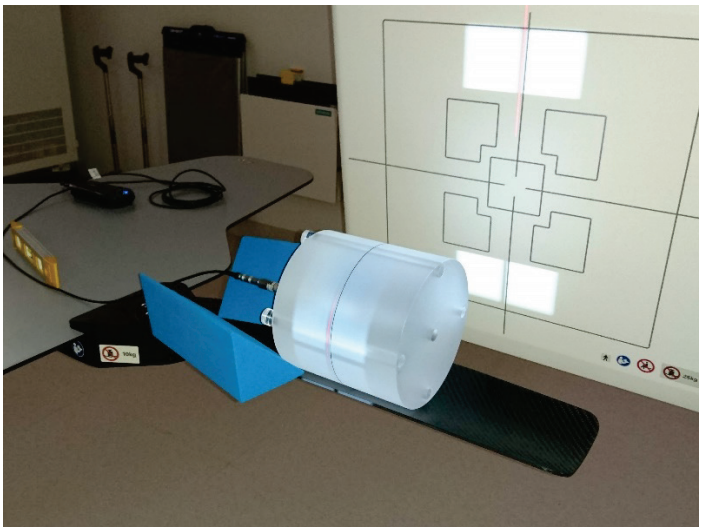

Figure 1. Setup for in-phantom dose profile measurement

Beam profile measurements are made with RTI Electronics CTDI Dose Profiler point dose dosimeter and a standard CTDI phantom.

The point dose dosimeter is stepped through the beam profile at sufficient intervals, resulting data is compiled into dose profiles. Dose profiles are measured at several beam collimations exceeding 40 mm, up to 270 mm. Two reference dose profiles are measured at beam collimations < 40 mm. Several different tube voltages are used to cover the range used in diagnostic radiology.

Data is analyzed and measurement errors are calculated.

RESULTS

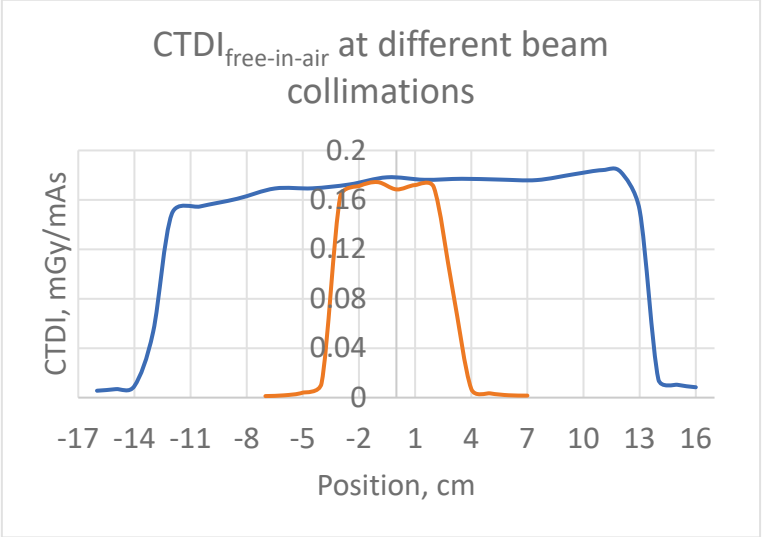

Figure 1. $CTDI_{free\text{-}in\text{-}air}$ for 7 cm (red) and 27 cm (blue) beam collimations at 60 kV

Preliminary results, measurement made at 60 kV, beam collimations 70 mm and 270 mm:

$CTDI_{free\text{-}in\text{-}air,NxT}$ = 0,17 mGy/mAs

$CTDI_{free\text{-}in\text{-}air,ref}$ = 0,16 mGy/mAs

CONCLUSIONS

Preliminary results show that the difference between $CTDI_{free\text{-}in\text{-}air,NxT}$ and $CTDI_{free\text{-}in\text{-}air,ref}$ is negligible. Further measurements are to be made at different beam collimations and tube voltages to confirm this.

REFERENCES

[1] EFOMP-ESTRO-IAEA, Quality control in cone-beam computed tomography (CBCT), Final version (2017)

[2] SYKES, J.R., LINDSAY, R., IBALL, G.,THWAITES, D.I., Dosimetry of CBCT: methods, doses and clinical consequences, Journal of Physics: Conference Series 444 (2013) 012017.

Patient Doses in Common Pediatric CT Examinations in Tunisia: Implementation of National Diagnostic Reference Levels

A. Bouaoun[a]
L. Ben Omrane[b], W. Douira Khomssi[c], M. Mogaadi[d], H. Mahjoubi[a], A. Hammou[e]

[a]University of Tunis El Manar, Higher Institute of Medical Technologies of Tunis (ISTMT), LR13ES07,Laboratory of Biophysics and Medical Technologies, Tunis, Tunisia
[b]National Center of Radiation Protection, Tunis, Tunisia
[c]Children Hospital Tunis, Tunis, Tunisia
[d]University Hospital of Bizerte, Bizerte,Tunisia
[e]Faculty of Medicine, Tunis, Tunisia

Email address of Corresponding Author: bouaounabir@yahoo.fr

BACKGROUND

The usefulness of CT in the medical management of patients is undeniable and its use continues to grow, despite increased associated patient doses. CT radiation doses may be a problem in children because of their higher radiosensitivity and longer life expectancy as compared to adults.

METHODS

This work focuses on the determination, by experimentation and simulation, of the radiation doses for a total sample of 916 children, categorized in four age groups (<1, 1-5, 5-10, 10-15 y). The children underwent the most frequent pediatric CT scans performed in seven different facilities, representing five major geographic regions in Tunisia, an adequate sample for the development of National Diagnostic Reference Levels. Dose evaluations included $CTDI_{vol}$, DLP, Effective Doses and organ doses.

Dose measurements for the determination of CTDI were performed using a CT reference PMMA 16 cm diameter phantom, representing a child placed at the isocentre of the CT scanner. A calibrated pencil-type ionization chamber Model RaySafe Xi with 10 cm sensitive length was used in conjunction with the protocols of the ImPACT group [1] and the IAEA TRS457 [2].

CT organ doses and effective doses were obtained using the ImPACT CT Dosimetry software package ver.1.0.4 (27/05/2011) [3].

The different pediatric CT protocols and practices as well as the image quality were also evaluated.

RESULTS

Results showed large variations in doses different radiology departments. The proposed national DRLs, in terms of 75th percentile, across all age categories, were 26–51 mGy ($CTDI_{vol}$) and 384– 978 mGy.cm (DLP) for Head examinations; 8–16mGy ($CTDI_{vol}$) and 118–579 mGy.cm (DLP) for Chest examinations; and 9–18mGy ($CTDI_{vol}$) and 353–1073 mGy.cm (DLP) for Abdomen examinations (Table 1).

Table 1. Proposed National DRLs for Head, Chest and Abdomen examinations

		Head		Chest		Abdomen	
		Median	**75thPer**	**Median**	**75th Per**	**Median**	**75th Per**
$CTDI_{vol}$	**<1**	22,7	**25,9**	7,8	**7,8**	8,8	**8,8**
	1-5	31,2	**37,6**	7,9	**9,8**	8,2	**12,8**
	5-10	42,4	**50,7**	10,3	**12,2**	16,4	**16,6**
	10-15	46,8	**50,8**	15,0	**16,3**	17,3	**18,5**
DLP	**<1**	344	**384**	118	**118**	353	**353**
	1-5	545	**664**	245	**330**	244	**485**
	5-10	822	**873**	284	**442**	388	**1204**
	10-15	817	**978**	502	**597**	737	**1073**

Median Effective dose estimates for the total sample were 2.2–2.7 mSv, 6.3–8.8 mSv and 6.6–15.8 mSv for head, chest and abdomen examinations, respectively. Organ doses can reach 52 mGy for Eye lens and Brain (Head CT), 62 and 20 mGy for Breast and Thyroid, respectively, (Chest CT) and vary between 3 and 58 mGy for Colon (Abdomen CT).

Our results were in good agreement with some previous studies and higher than others. These variations suggest that pediatric patients are still exposed to a large amount of unnecessary radiation and the optimization is not fulfilled.

CONCLUSIONS

This is the first pediatric CT dose assessment entirely based on a national pilot study. This study shows that optimizing protection for pediatric CT procedures should be a priority especially within the regional hospitals.

The implementation of corrective actions will take place after the initial DRLs. These actions, including recommendations and guidelines to good practice, should be a joint effort of all stakeholders, including health authorities, radiation protection regulators, professional societies and universities using interdisciplinary working groups.

REFERENCES

[1] ImPACT CT Scanner Dose Survey. *Measurement Protocol*. Version 5.0. St. George's Healthcare NHSTrust, London, UK (1997).

[2] International Atomic Energy Agency (IAEA).*Dosimetry in Diagnostic Radiology: An International Code of Practice.* TRS N° 457(2007)

[3] ImPACT CT Dosimetry Calculator, Version 1.0.4. St. George's Healthcare NHS Trust,London, UK, 27 May (2011)

Establishment of Diagnostic Reference Levels (DRLs) for Medical Radiography Examinations in Madagascar

T. Razakarimanana[a]
R. D. Randriantsizafy[a], J. L. R. Zafimanjato[a], H. F. Randriantseheno[a], T. H. Randriamora[a], M. A. L. Ralaivelo[a], B. Vololoniaina[b]

[a]Institut National des Sciences et Techniques Nucléaires (INSTN-Madagascar), POBox 3907, Antananarivo, Madagascar.
[b]Faculté des Sciences, Université d'Antananarivo, PO Box 566, Antananarivo, Madagascar.

Email address of Corresponding Author: langoriat@yahoo.fr

BACKGROUND

Ionizing radiations have an indispensable role in diagnostic radiology and clinical treatments of patients. The delivered doses to the patients should be well optimized to minimize the harmful effect of the X-ray examinations [1].

METHODS

For this work, patient and radiographic data (high voltage, filtration, field size and focus to skin distance examinations…) for many paediatric and adult patients performing these X-rays examination parameters have been collected. These data have been collected for some hospitals in Madagascar using these different technologies of the X-rays machines. Entrance Surface Air Kerma (ESAK) was determined for each patient [2], using the X- rays tube output and calibrated thermoluminescent dosimeters (TLD-100) at the Secondary Standard Dosimetry Laboratory of the "Institut National des Sciences et Techniques Nucléaires –Madagascar". The QC kit for X-ray (model PTW NOMEX Multimeter and 3036 Radcal dosimeters) was used for the purpose of these measurements.

Patient Dosimetry Using TLD

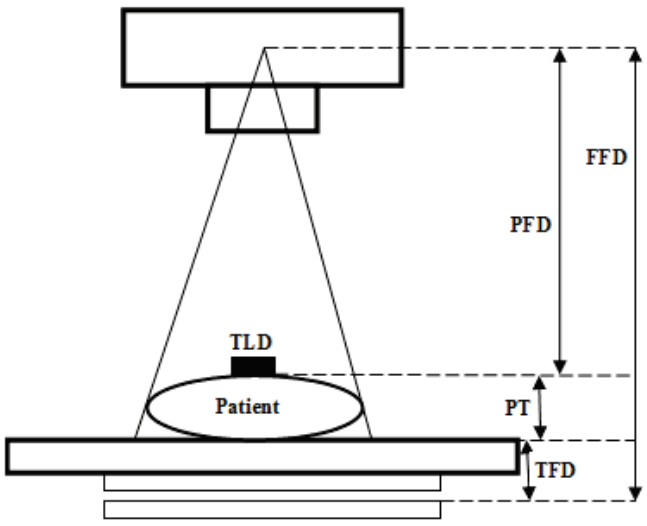

F.F.D: Focal Film Distance

P.T: Patient Thickness

T.F.D: Table Film Distance

P.F.D: Patient focal Distance

Figure 1. Patient ESAK measurement using TLD.

RESULTS

Table 1.Summary of mean, minimum, maximum ESAK values for all age groups

X-Ray examination	Age (Year)	ESAK (mGy)		
		Minimum	Maximum	Mean
Abdomen [AP]	[0 - 1]	0.011	0.180	0.095
	[1 - 5]	0.008	0.628	0.318
	[5 - 10]	0.186	1.251	0.718
	[10 - 15]	0.172	1.612	0.730
Chest [PA/ LAT]	[0 - 1]	0.010	0.730	0.370
	[1 - 5]	0.043	0.536	0.204
	[5 - 10]	0.016	0.761	0.271
	[10 - 15]	0.022	0.144	0.283
Head [PA]	[1 - 5]	0.300	0.393	0.360
	[5 - 10]	0.163	0.774	0.464
	[10 - 15]	0.192	1.454	0.604
Hand region	[1 - 5]	0.072	0.114	0.099
	[5 - 10]		0.072	0.072
Abdomen [AP]	Adult	0.546	3.515	1.795
Chest [PA]		0.125	4.24	0.562
Head [PA]		0.862	1.712	1.199
Hand Region		0.123	0.835	0.700

CONCLUSIONS

The variations of exposition doses versus the age of the peadiatric patient are not significant.

During X-ray examination, adult patients received significant exposure dose compared with children. Measurements and calculations performed throughout the present work represent a good asset to implement a national data base and then, to establish a national Dose Reference Levels [3].

REFERENCES

[1] Office de ProtectionContre les Rayonnements Ionisation et Societe Francaisede Radiologie. Les procedures radiologiques descriteres de qualite et optimisation des doses. Transposition de la Directive 97/43 Euratom. Rapport d'etape du 31 juillet 2000. p. 122.

[2] Hanan Fawaz Akhdar, Master, Assessment of Entrance Skin Dose and Effective Dose of Some Routine X-ray Examinations Using Calculation Technique, King Saud University Collage of Science Department of Physics and Astronomy, 2006/2007 G.

[3] International Atomic Energy Agency. International basic safety standards for protection against ionizing radiations and for safety of radiation sources. IAEA Safety Series No. 115-1. IAEA. Vienna (1994).

A Baseline Survey of Diagnostic Reference Levels for the Three Most Frequent X-ray Procedures in the Bulawayo Metropolitan Province: The Possibility of Dose Reduction

N. Ncube
E. Maguranyanga, G. Azangwe

National University of Science and Technology, Zimbabwe

Email address of Corresponding Author: ellen.maguranyanga@nust.ac.zw

BACKGROUND

An Integrated Regulatory Review Service (IRRS) mission conducted in Zimbabwe by the International Atomic Energy Agency in 2014, noted some gaps in the national regulatory framework for radiation safety for it to align with the IAEA Safety Standards, which are the international benchmark for safety. One of the paramount gaps was the fact that although the regulations allow for establishment of Diagnostic Reference Levels, they have not been implemented for optimisation of medical exposures to radiation. United Nations Scientific Committee on Effects of Atomic Radiation (UNSCEAR) has reported medical exposures as the greatest contributor of man-made exposures to the population worldwide and trends of the medical use of radiation have been shown to escalate over the years (IAEA, 2007). Surveys conducted in different countries for the same type of procedures show doses that differ by orders of magnitude according to IAEA (IAEA, 1995) and Essien et al. (2016), further showing the need for standardisation which may effectively be achieved through the establishment of DRLs. Bulawayo, a cosmopolitan city in Zimbabwe, which caters for patients not only from the Bulawayo Metropolitan province but also surrounding provinces like Matabeleland North, Matabeleland South and Midlands has not only shown an increase in acquisition of diagnostic radiology equipment but has also taken a great technological shift from conventional to digital technology. These factors make it vital that DRLs be established as a matter of urgency because digital radiography comes with the risk of overexposures that can go undetected. The aim of this study was to establish DRLs starting with three most frequent procedures in Bulawayo.

METHODS

An indirect method of measuring ESAK was adopted in the development of DRLs using semiconductor detectors (Nnamdi and Jibiri, 2016., Kowo, 2013). A total number of seven x-ray rooms were used in the study from three major public hospitals and two frequented private centres considering all adult patients who reported to the facilities during the study period for chest PA, pelvis AP and lumbar spine AP procedures. Patient exposure parameters, x-ray tube focus-to-couch and focus-to-patent surface distances were measured and used in the calculation of DRLs. Statistical analysis was used in computing DRLs as the third quartile values of the mean ESAK distribution obtained in the seven x-ray rooms for the three procedures.

RESULTS

Large variations on ESAK values were observed within x-ray rooms as well as among different x-ray rooms and the characteristic of lower doses associated with digital systems (Direct Digital Radiography and Computed Radiography) was not observed from the results obtained, showing the need for dose optimisation in the province. The DRLs established in the study were comparable to some published DRLs although it was noted that there is room for further

optimisation. 3.98 mGy was established for the chest PA procedure, 6.92 mGy for the lumbar spine AP procedure and 9.04 mGy for the pelvis AP procedure.

CONCLUSIONS

The conclusion and recommendations of the study are for the established DRLs to be implemented in Bulawayo as well as countrywide and also for standardisation of procedures in the country.

REFERENCES

[1] ESSIEN, I. E., INYANG, S. O. & EGBE, N., Entrance Surface Air Kerma for Skull, Pelvis and Abdomen X-ray Examinations in Some Diagnostic Radiology Facilities in Akwa Ibom State, Nigeria. Radiation Science and Technology., Volume Vol. 2, pp. 6-12. (2016).

[2] INTERNATIONAL ATOMIC ENERGY AGENCY,. Technical Report Series No. 457 Dosimetry in Diagnostic Radiology: An International Code of Practice, Vienna: IAEA (2007)

[3] INTERNATIONAL ATOMIC ENERGY AGENCY,. *IAEA*-Tecdoc-796 : Radiation Doses in DIagnostic Radiology and Methods for Dose Reduction, Vienna: IAEA. (1995)

[3] NNAMDI N. JIBIRI, C. J. O., Evaluation of dose-area product of common radiographic examinations towards establishing a preliminary diagnostic reference levels (PDRLs) in Southwestern Nigeria. Journal of Applied Clinical Medical Physics, Volume 17. (2016)

[4] KOWO, F., An Establishment of Diagnostic Reference Levels for Adults During Common General Radiography Examinations at Central Hospitals in Harare and Chitungwiza, s.l.: s.n. (2013)

Patient Dose Reduction in Three Lebanese Interventional Cardiology Suites

C. Rizk[a,b]
G. Fares[b], F. Vanhavere[c] and J. Farah[d]

[a]Lebanese Atomic Energy Commission, National Council for Scientific Research, P.O.Box.11-8281, Beirut, Lebanon
[b]Saint-Joseph University, P.O.Box.11-514 Riad El Solh, Beirut 1107 2050, Lebanon
[c]Belgian Nuclear Research Centre (SCK-CEN), Boeretang 200, BE-2400 Mol, Belgium
[d]Paris-Sud University Hospitals, 94270 Le Kremlin-Bicêtre, France

Email address of Corresponding Author: c.rizik@cnrs.edu.lb

BACKGROUND

Radiation risks associated to fluoroscopically-guided interventional procedures [1,2] require keeping patient doses as low as possible while achieving the optimal benefits to health for optimized patient and medical staff radiation protection.

METHODS

The study prospectively collected exposure parameters (e.g. air kerma-area product (P_{KA}), air kerma at patient entrance reference point ($K_{a,r}$), fluoroscopy time (FT) and number of images (NoI)) for interventional cardiology patients treated between April 2016 and December 2017 by 15 interventional cardiologists at 3 private Lebanese hospitals. The study population hence includes 1726 patients who underwent diagnostic coronary angiography (DCA) procedures, 644 patients receiving percutaneous coronary interventions (PCI).

The 3 fluoroscopic units used in this study were GE/Innova 2100 in hospitals A and B and Siemens/Artis Zee in hospital C. All the devices were Single-plane x-ray units equipped with flat panel detectors. The tubes had an inherent filtration of 3.5 mm Al for hospitals A and B and 2.5 mm Al for hospital C at 70 kV. Additional copper filters ranged in thicknesses from 0.2 to 0.3 mm Cu. 15 frames/s were used in both fluoroscopy and cine acquisition modes in all the hospitals.

Two simple optimization measures were implemented in each hospital. These include increasing the additional filtration (from 0.3 to 0.6 mm Cu for hospitals A and B and from 0.2 to 0.6 mm Cu for hospital C in fluoroscopy mode) and decreasing the number of frames (from 15 to 7.5 frames/s in fluoroscopy mode for hospitals A and B and from 15 to 7.5 frames/s in cine acquisition mode for hospital C).

The collection of exposure parameters were performed during the pre-dose reduction period P0 (one year from hospitals A and B and 3 months from hospital C) and the post-dose reduction period P1 (9 months for hospitals A and B and 1 year for hospital C)

RESULTS

Compared with the pre-dose reduction period P0, patients' median P_{KA} (respectively $K_{a,r}$) value in the post-dose reduction period P1 was reduced by 34%, 12% and 55% (37%, 9% and 54%) during DCA in hospitals A, B and C respectively. These were 40%, 16% and 43% (43%, 16% and 40%) during PCI. The Mann-Whitney U test showed that P_{KA} and $K_{a,r}$ were significantly lower ($p < 0.05$) for both DCA and PCI when compared between P0 and P1.

Nonetheless, one should note that median P_{KA} and $K_{a,r}$ values during PCI in hospitals A and B remain higher than the recent European diagnostic reference levels (P_{KA} = 85 Gycm^2 and $K_{a,r}$ =1200 mGy)[3] and need further optimization.

Table 1. The median of exposure parameters per procedure type for the patient population performed in the pre-dose reduction (P0) and post-dose reduction (P1) periods in the participating hospitals

Procedure Type	Hospital	Periods	Number of	FT (min)	P_{KA} (Gycm²)	$K_{a,r}$ (mGy)	NoI
DCA	A	P0	195	2.4	44	569	522
		P1	83	2.5	29	361	270
	B	P0	301	2.2	57	696	509
		P1	281	2.1	50	636	503
	C	P0	148	2.6	22	372	339
		P1	718	2.3	10	170	231
PCI	A	P0	146	11.4	171	2211	1239
		P1	100	12.5	102	1264	1179
	B	P0	113	7.3	155	1778	900
		P1	95	7.5	130	1501	864
	C	P0	37	11.2	42	722	475
		P1	143	8.2	24	431	373

CONCLUSIONS

The present study highlights that simple dose-reduction strategies can yield high exposure reduction (12-55% for P_{KA} and 9-54% for $K_{a,r}$) for DCA and PCI. Further efforts are needed to optimize the medical exposures in hospitals A and B. Radiation protection training of the medical staff and/or optimization of the x-ray unit's settings/protocol could reduce the doses and protect the patient and the medical staff from the harmful effects of radiation.

REFERENCES

[1] NATIONAL COUNCIL ON RADIATION PROTECTION AND MEASUREMENTS, Radiation dose management for fluoroscopically-guided interventional medical procedures, Report No. 168, Bethesda, Maryland (2011).

[2] INTERNATIONAL COMMISSION ON RADIOLOGICAL PROTECTION, Radiological Protection in Cardiology, Publication 120, Pergamon Press, Oxford and New York (2013).

[3] SIISKONEN, T., CIRAJ-BJELAC, O., DABIN, J., Establishing the European diagnostic reference levels for interventional cardiology, Physica Medica **54**(2018) 42-48.

Diagnostic Reference Levels for Diagnostic Radiology Examinations in Northern Iran

F. Niksirat[a]
A. Shabestani Monfared[a], M. R. Deevband[b], M. Paymard[a], R. Bordbar[a], M. Nabahati[a], K. E. Gorji[a]

[a]Babol University of Medical Sciences, Babol, Iran
[b]Shahid Beheshti University of Medical Sciences, Tehran, Iran

Email address of Corresponding Author: monfared1345@gmail.com

BACKGROUND

In the field of medical imaging, the radiation protection of the patients is based on the basic principles of practice justification and dose optimization [1, 2]. The International Commission of Radiation Protection (ICRP) introduced Diagnostic Reference Level (DRL) as a useful tool for limiting variations in dose among diagnostic imaging centers [3, 4]. The aim of this study was to investigate the current levels of patient radiation dose for some common radiography examinations in northern Iran.

METHODS

In this study, 13 public hospitals in the north of Iran were selected for review and required data collected for 10 adult patients with mean weight of 70±10kg in each projection. questionnaire, comprising information on the patient data; the institutional data and X-ray machine data (kVp, mAs, HVL, FSD, output in clinical kVps, production year image receptor type, generator type, grid usage, and exposure setting) were obtained and recorded. In order to measure x-ray output tube, the dosimeter RTI model Barracuda calibrated has been applied for measuring air karma within energy range of 40-150kvp. ESAK and ESD parameters, usually used for monitoring DRL in radiography, were calculated. Also Mean Glandular Dose (MGD) represents the effective dose absorbed by the breast was estimated and calculation done in order to define DRL.

RESULTS

The regional DRL was settled for Skull (PA), Skull (Lat), Cervical spine (AP), Cervical spine (Lat), Chest (PA), Chest (Lat), Abdomen (AP), Lumbar spine (AP), Lumbar spine (Lat), Pelvis (AP), Thoracic spine (AP), and Thoracic spine (Lat) in computed radiography examinations. Table 1 presents the summary of minimum, maximum, average dose and regional diagnostic reference levels (mGy) for each X-ray examinations. DRL for mammographic views (Craniocaudal and mediolateral oblique) are suggested 0.71 and 1.07 respectively.

Table 1. Summary of minimum, maximum, average dose and regional diagnostic reference levels (mGy) for each X-ray examinations

Examination	Mean ± SD	Min	Max	Third quartile (DRL)
Skull (AP/PA)	0.97±0.41	0.32	2.14	1.3
Skull (LAT)	0.86± 0.39	0.3	2.13	1.17
Cervical Spine (AP)	0.52±0.26	0.17	1.38	0.77
Cervical Spine (LAT)	0.66±0.31	0.02	0.15	0.06
Chest (PA)	0.6±0.31	0.13	1.12	0.63
Chest (LAT)	0.85±0.43	0.25	1.98	1.11
Thoracic Spine (AP)	1.44±0.5	0.6	3.23	1.73
Thoracic Spine (LAT)	2±0.77	0.64	4.72	2.35
Lumbar Spine (AP)	2.36±1.29	0.85	7.2	2.69
Lumbar Spine (LAT)	3.62±1.78	0.9	10.2	4.22
Pelvis (AP)	1.43±0.69	0.56	3.58	1.23
Abdomen (AP)	1.65±0.79	0.58	4.04	2

CONCLUSIONS

The results of this study provide valuable information about the patient dose in northern Iran. The wide variations in the patient dose levels, even in the same procedures carried out by different radiographers is mainly due to the choice of different exposure setting, focus to film distance and finally output of the x-ray units. Periodic quality control testing and monitoring the technical performance of radiographers might effectively improve the image quality and reducing dose to patients.

REFERENCES

[1] ROCH P, CÉLIER D, DESSAUD C, ETARD C. Using diagnostic reference levels to evaluate the improvement of patient dose optimisation and the influence of recent technologies in radiography and computed tomography. European journal of radiology. 2018 Jan 1;98:68-74.

[2] ICRP. 1990 Recommendation of the International Commission on Radiological Protection. ICRP Publication 60. Ann ICRP. 1991;21(1–3).

[3] SULEIMAN ME, BRENNAN PC, MCENTEE MF. Diagnostic reference levels in digital mammography: A systematic review. Radiat Prot Dosimetry 2015;167:608-19.

[4] SULIMAN I, MOHAMMEDZEIN T. Estimation of adult patient doses for common diagnostic X-ray examinations in Wad-madani, Sudan: derivation of local diagnostic reference levels. Australasian Physical & Engineering Sciences in Medicine. 2014;37(2):425-9.

Radiotherapy Medical Physics

Novel Technique for Radiation Dose Visualization in Large Space

M. Piksis[a]

[a]Institute Of Biomedicine and Nanotechnology, Riga Technical University, Riga, Latvia

Email address of Corresponding Author: martins.piksis@gmail.com

BACKGROUND

Radiation protection planning is very important aspect of occupational health. Radiation protection planning could be greatly enhanced by providing staff with a simple and easy to use tool to make source simulations and generate 3D visualizations.

This study sought to create the 3D visualization method that any potential user could emulate and adapt for a variety of purposes. Furthermore, this software could be a useful tool for generation of 3D visualizations for augmented reality applications.

METHODS

A field is divided into a set of finite elements with each element containing a series of bounds, an intensity value and a central coordinate. Each element is considered to act as a single representation of an intensity value for a field within the local bounds of that element. These elements are geometrically simple shapes such as cubes or boxes. These individual elements can be thought of as a physical representation of a volumetric pixel (voxel) [4]. Voxels can be used to represent data in a three-dimensional space as they contain both a physical location and a value at that location. Using basic shapes simplifies the arrangement of these elements into a single model where all the elements can be fitted together so their boundaries do not overlap each other. Theoretically an intensity value is not limited to a single type of information (e.g., dose rate); any type of information could be visualized using this method. Example dose visualization is shown in Figure 1.

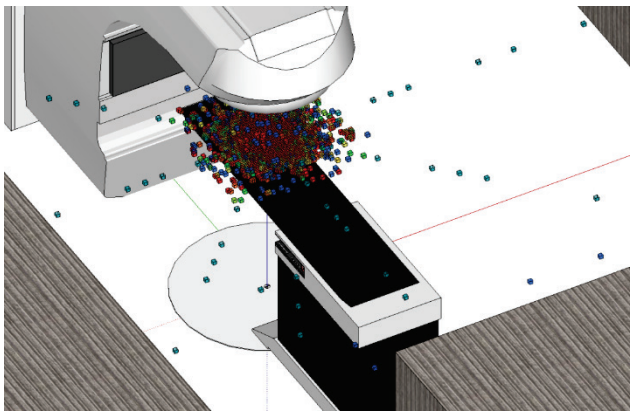

Figure 1. Experimental radiation field visualization for Varian Clinac iX, 6MV, field 40x40cm.

RESULTS

Software accuracy was evaluated in the following stages:

1) assessment of the radiation source Monte Carlo model accuracy relative to the measurements in water phantom,

2) visualized dose model accuracy relative to the $KERMA_{AIR}$ measurements – point dose in software compared with measured dose at specified coordinate in room.

For evaluation purposes a linear accelerator Varian Clinac iX head model was created. Monte Carlo simulations were performed for 6MV beam at the field sizes of 5 cm x 5 cm, 10 cm x 10 cm, 15 cm x 15 cm and 20 cm x 20 cm. Results verified relative to the measurement in IBA Blue Phantom. Established MC linac head model accuracy assessed as appropriate for the continuation of the experiment.

For further evaluation of the program was created for the linac bunker 3D model, with radiation source (linac) inside.

Radiation source data was taken from simulations mentioned above. After completion of the visualization, point doses from model was taken for 46 points and compared with measured dose under the same conditions.

Results obtained vary between 3.54% and 21.09% in relation to the measured dose. In addition, there is a trend that the error increases with increasing distance from isocenter. It could be explained by the fact that the precision of measurement is less at lower dose rate. The numerical values are partly summarized in the Table 1.

Table 1. Calculated error [%] of simulated dose vs. measured dose.

X [cm]	Y [cm]	Z [cm]	Δ%
0	0	100	3.54
50	50	100	8.32
300	300	100	21.09

CONCLUSIONS

In this study, a novel methodology for the display of 3D radiation fields was developed. A new approach was formulated which focused on keeping the field definition process separate from the modeling process to maximize potential definition techniques.

The types of expected issues associated with 3D radiation field visualizations were discussed and analyzed. Overall design requirements for this type of program development were established and eventually shown to have been achieved. The software product obtained in this study, of course, require improvements and adjustments, but generally it has been demonstrated that it is able to operate for its intended purposes.

REFERENCES

[1] Monte Carlo Team, Monte Carlo N-Particle Transport Code, Version 5 Volume 1.
[2] https://www.khronos.org/collada/, Website last accessed on 12.10.2015
[3] https://www.ruby-lang.org/en/, Website last accessed on 12.10.2015
[4] JOSEPH G., CHAPUT A. Generic Methodology For The 3-Dimensional Visualization Of Radiation Fields, University of Ontario Institute of Technology, Oshawa, Canada, 2010

Angular Dependence of Absorbed Dose of a Two Dimensional Detector Matrixx- Comparison to Manufacturer Provided Data

B. Petrovic[a,b]
M. Marjanovic[a,b] , I. Gencel[a], V. Malešević[b]

[a]Institute of oncology Vojvodina, Radiotherapy department, Sremska Kamenica, Serbia
[b]Faculty of sciences, Department of physics, University of Novi Sad, Serbia

Email address of Corresponding Author: nsbim@EUnet.rs

BACKGROUND

Clinical implementation of advanced external beam radiotherapy techniques such as volumetric modulated arc therapy (VMAT) or intensity modulated radiation therapy (IMRT) requires well developed quality assurance (QA) programme but also pre-treatment verification of patient therapy plan and gamma analysis. In VMAT technique, many parameters of the linear accelerator are changing (speed of gantry rotation, speed of multileaves collimator (MLC) as well as dose rate), and must be synchronized in order to deliver the plan from the treatment planning system (TPS). The TPS provides data on gantry angle positions, MLC positions and number of monitor units for defined arc segment through a number of control points in the plan. This information is supplied to the linac, which uses these control points to vary speed and position of gantry and MLC, as well as the dose rate. The verification can be done in different ways, of which mostly used are 2D detector arrays and radiochromic films. The detector that we used clinically was Matrixx Evolution detector (manufacturer IBA Dosimetry, Germany). Matrixx consists of 1020 vented ionization chambers arranged in a field of 24.4 cm x 24.4 cm, with pixel-to-pixel distance of 7.62 mm. The volume of each chamber is 0.08 cm^3 of 4.5 mm diameter and 5 mm height. The effective depth of measurement is ~3.6 mm below the detector surface. In case of rotating gantry and fixed detectors positions, the response of ionisation chambers with gantry angle should be determined, or used one provided by manufacturer.

METHODS

The Matrixx detector was CT scanned in clinical conditions, exported to TPS Monaco (Elekta, UK), contoured and then the treatment plan was generated. The plan consisted of a set of fixed beams 10 cm x 10 cm, gantry angles 0° - 360° step 10°, except in lateral beams where in gantry angle range 80° - 100° step was 2°, and 260° - 280° step was also 2°, which sums up 52 angles. The beam used was 6 MV from a Versa HD (manufacturer Elekta, UK). The prescription point was to the isocenter. Two sets of measurements were done: with gantry angle sensor and without gantry angles sensor. The gantry angle correction factors with gantry angle sensor were compared with the results without gantry angle sensor, and with correction factors supplied by IBA (so called LUT tables). Clinical correction factors were calculated for the selected pixels according to formula: Correction factor for the row i and column j pixel calculated as $CF_{ij}=(TPS_{ij}/M_{ij})/(TPS_{ij}/M_{ij})^0$, where $(TPS_{ij}/M_{ij})^0$ is the value at 0 degree gantry angle: TPS_{ij} is the TPS data at angle 0, and M_{ij} is the measurement at 0 degrees averaged over four central pixels. Since the central axis as projected to the Matrixx surface, is actually surrounded by four pixels, the data are calculated as the mean value of central 4 pixels. The plot was generated in Origin, as dependence of CF on gantry angle.

RESULTS

Measurement sets with and without gantry angle sensor show good agreement (less than ±1% difference), for beam angles 0°-80° and 280°-360°, for all other angles the discrepancy is greater, ~5% except between angles 92°-98° and 264°-268° where it goes up to 13%. This confirms the necessity of using the gantry angle correction. When compared to TPS data, great difference is also observed in these angles, which indicates necessity of use of correction factors dependant on angle and energy. The correction factors were calculated for 6 MV and 10 cm x 10 cm field, for central pixels, and results are given in Graph 1. Black dots are defaults supplied by manufacturer, while red dots represent measured averaged pixel values when gantry angle sensor is used, and blue triangles the results when gantry angle sensor is not used. The under response was measured on angles above the patient table (86-90) and 270-274 deg, while overresponse on angles 92-98 deg and 100-268 deg. The LUT factors provided by manufacturer correspond well to the measured data.

CONCLUSIONS

The results clearly show the influence of gantry angle dependence on result of dosimetric verification of QA patient plan. The correction factors for this particular detector were calculated and compared to IBA provided, and their correlation agree with literature data.

REFERENCES

[1] Y SHIMOHIGASHI, et al, Angular dependence correction of MatriXX and its application to composite dose verification, Journal of applied clinical medical physics 13 (5), 2012

[2] RAMESH BOGGULA, et al, Evaluation of a 2D detector array for patient specific VMAT QA with different setups2011 Phys. Med. Biol. 56 7163

[3] Y. SEKAR, et al, Characterization and clinical evaluation of a novel 2D detector array for conventional and flattening filter free (FFF) IMRT pre-treatment verification, Z Med Phys 28 (2018) 134–141

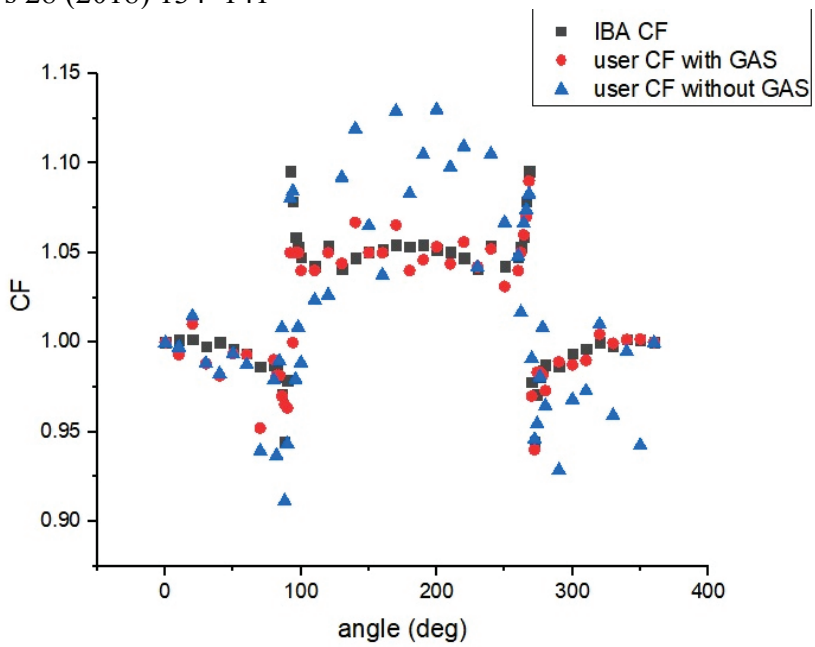

Markus and Pinpoint Ionization Chamber Detectors Behavior with Out-of-Field Dose

A. Abdelaal[a]
E. M. Attalla[b], **W. M. Elshemey**[c]

[a]Radiotherapy Department, Nasser Institute, Cairo, Egypt
[b]National Cancer Institute, Cairo University, Egypt
[c]Biophysics Department, Faculty of Science, Cairo University, EGYPT

Email address of Corresponding Authors: attalla.ehab@gmail.com, welshemey@sci.cu.edu.eg

BACKGROUND

The occurrence of secondary malignancies in patients treated with radiation was found to be maximum in the normal tissue surrounding the target where the highest dose was delivered [1]. An increased risk of cancer incidence after exposure to low doses has been previously reported [2, 3].

In clinical photon beams, the dose outside the geometrical field limits is produced by photons originating from head leakage, scattering at the beam collimators and the flattening filter (head scatter) and scattering from the directly irradiated region of the patient or phantom [4].

An accurate assessment of the secondary cancer risk following a treatment with radiation requires a detailed knowledge of the dose profile outside the tumor [5].

TPSs are modeling the treatment fields to deliver adequate dose to PTVs. Many planning algorithms are developed for accurate dose predication in field dosimetry, while out-of-field dose predictions are poor [6, 7].

METHODS

This work aims to provide a comparison between Markus and Pinpoint ionization chamber detectors that are frequently used in electron and photon dosimetry, respectively in radiotherapy. This is carried out through the application of these detectors in estimation of the out-of-field dose with important dosimetric parameters such as field size (from 5 x5 cm^2 to 30 x30 cm^2) and depth (from 1.5 cm to 30 cm) at energy 6 MV and collimator angle 0° at SSD 100 cm.

RESULTS

Results show that, the Markus and Pinpoint detectors both reported an increase in out-of-field dose with field size, depth. In almost all measurements, Pinpoint detector reported considerably higher out-of-field dose values compared to Markus. For 6 MV and 0° collimator angle, the out-of-field dose at field size of 5 x 5 cm^2 (depth of 1.5 cm) is 1.9% for Pinpoint detector compared to 1.1% for Markus and at field size of 30 x 30 cm^2 (depth of 1.5 cm) is 7.3% for Pinpoint detector compared to 4.4% for Markus. The out-of-field dose for a depth of 1.5 cm (field size of 10 x 10 cm^2) is 3.1% for Pinpoint detector compared to 2.3% for Markus and for a depth of 30 cm (field size of 10 x 10 cm) is 7.9% for Pinpoint detector compared to 5.5% for Markus. Measured out-of-field dose by pinpoint detector underestimated in the calculated at different field sizes (2.6% instead of 3.2% at field size of 10 x 10 cm^2 and 5.2% instead of 7.3% at field size of 30 x 30 cm^2) and different depths (2.7% instead of 3.1% at depth of 1.5 cm and

4.1% instead of 4.2% at depth of 30 cm) in the contrary to the measured out-of-field dose by Markus detector which overestimated in the calculated at different field sizes (2.7% instead of 2.3% at field size of 10 x 10 cm^2 and 5.2% instead of 4.4% at field size of 30 x 30 cm^2) and different depths (2.7% instead of 1.1% at depth of 1.5 cm and 4.1% instead of 3.4% at depth of 30 cm).

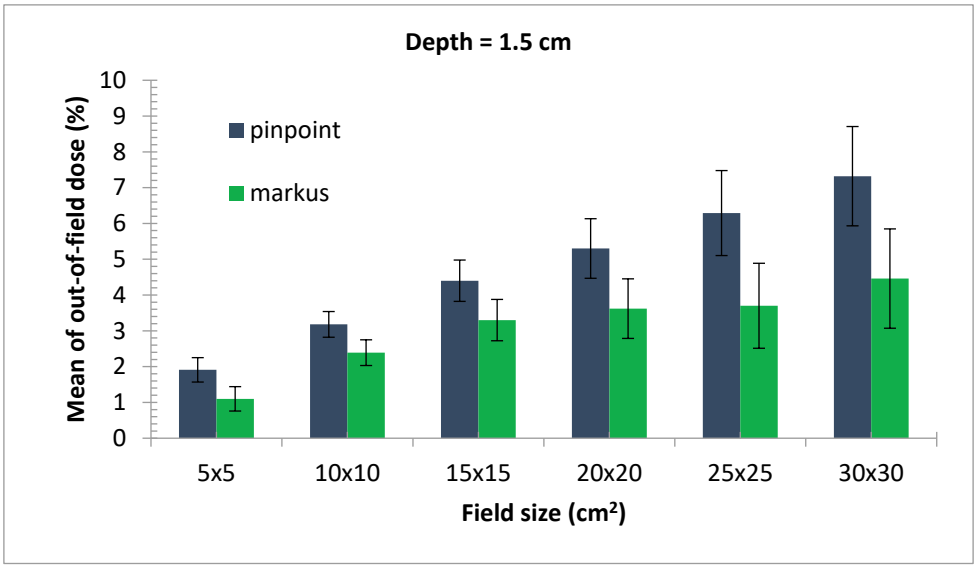

CONCLUSIONS

The considerably higher out-of-field dose values reported by Pinpoint detector compared to Markus can be explained due to the relatively higher sensitivity of Pinpoint detector in the detection of low doses (such as out-of-field doses).

REFERENCES

[1] Dörr, W., & Herrmann, T. (2002). Cancer induction by radiotherapy: dose dependence and spatial relationship to irradiated volume. Journal of radiological protection, 22(3A), A117.

[2] Pierce, D.A. and Preston, D.L. (2000). Radiation-related cancer risks at low doses among atomic bomb survivors. Radiation research, 154(2), pp.178-186.

[3] Preston, D.L., Shimizu, Y., Pierce, D.A., Suyama, A. and Mabuchi, K. (2003). Studies of mortality of atomic bomb survivors. Report 13: Solid cancer and noncancer disease mortality: 1950-1997. Radiation research, 160(4), pp.381-407.

[4] Chofor, N., Harder, D., Willborn, K. C., & Poppe, B. (2012). Internal scatter, the unavoidable major component of the peripheral dose in photon-beam radiotherapy. Physics in medicine and biology, 57(6), 1733.

[5] Xu, X.G., Bednarz, B. and Paganetti, H. (2008). A review of dosimetry studies on external-beam radiation treatment with respect to second cancer induction. Physics in medicine and biology, 53(13), p. R193.

[6] Jang, S. Y., Liu, H. H., & Mohan, R. (2008). Underestimation of low-dose radiation in treatment planning of intensity-modulated radiotherapy. International Journal of Radiation Oncology* Biology* Physics, 71(5), 1537-1546.

[7] Kaderka, R., Schardt, D., Durante, M., Berger, T., Ramm, U., Licher, J. and La Tessa, C. (2012). Out-of-field dose measurements in a water phantom using different radiotherapy modalities. Physics in medicine and biology, 57(16), p.5059.

Neutron Dose Measurements Comparison from Medical LINAC with Different Detectors

S. Savatović[a], S. Peric[a]
M. Severgnini[b,c], G. Giannini[a,b]

[a]Physics department, University of Trieste, Italy
[b]INFN, section of Trieste, Italy
[c]SC di Fisica Sanitaria, Azienda Ospedaliero-Universitaria "Ospedali Riuniti", Trieste, Italy

Email address of Corresponding Author: sara.savatovic@gmail.com

BACKGROUND

A secondary dose to the patient in a high-energy x-ray external beam radiotherapy treatment (≥10 MV) is due to neutron radiation, which is a by-product of the [γ,n] reactions with high-Z materials in the LINACs head. The amount of secondary neutron dose varies with LINAC model and treatment room design, the seek of an adequate, quick and easy way of measuring neutron dose around the treatment couch is essential for providing useful information in treatment planning for patients with highly radiosensitive zones [1].

METHODS

The measurements took place in the Radiotherapy department of the Maggiore Hospital in Trieste providing an Elekta-Synergy 3028 LINAC, where the medical physics staff also kindly supplied also a Berthold LB 6411 neutron probe and a RW3 Slab Phantom.

Two methods for assessing out of field neutron dose at various distances from the isocenter have been inspected: a specially designed *mini-phantom neutron dosimeter* (in polyethylene and boron enriched carbon fiber) based on Bubble Detectors (BTS & BD-PND) and the *Berthold LB 6411* neutron probe.

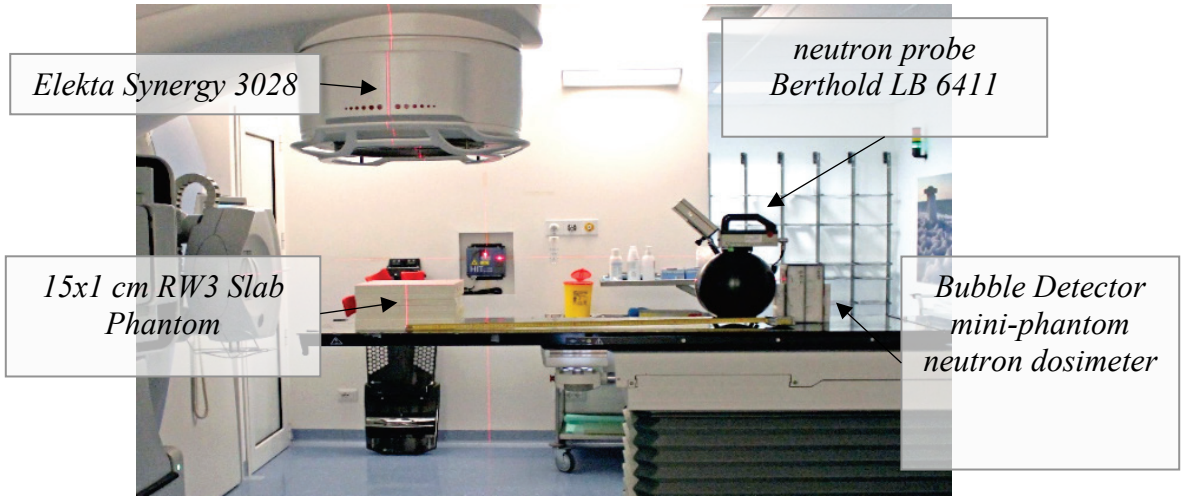

Figure 1. Experimental set-up at Maggiore Hospital, Trieste.

The *mini-phantom neutron dosimeter* had four modules, each with a polyethylene drawer containing a Bubble Dosimeter for thermal neutron energies (BDT) and one for fast neutron energies (BD-PND) separated by a boron enriched carbon fiber plate, apt for neutron attenuation analysis.

RESULTS

Graph 1. shows the out of field relative neutron dose measured at various distances from the isocenter along the treatment couch for a 15 MV photon beam striking a 15x30x30 cm^3 RW3 Slab Phantom with field size 1x1 cm^2 and 10x10 cm^2. The Bubble Dosimeters considered are those in the closest external module, and the red dotted lines show an ideal narrow beam geometry approximation to point-like source at isocenter.

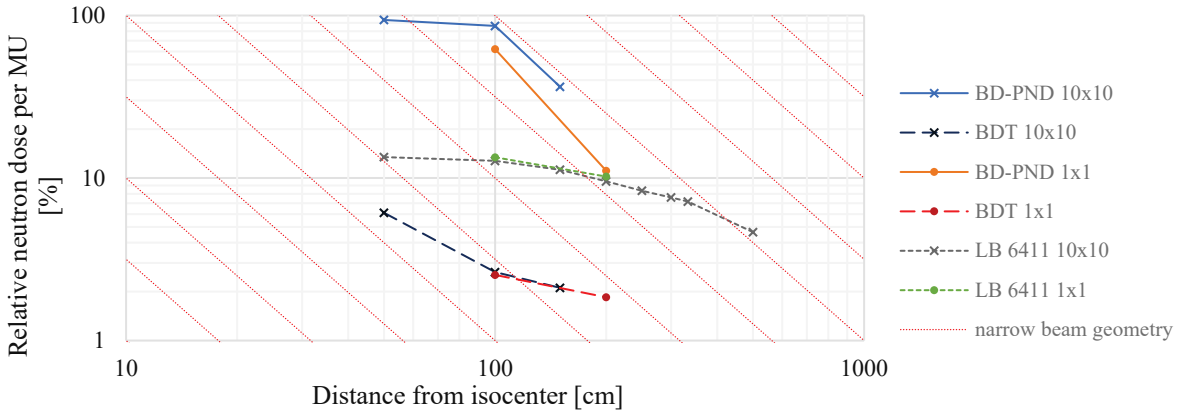

Graph 1. Of out of field measured neutron dose comparison.

Dose attenuation in the *mini-phantom neutron dosimeter* proved the existence of a scattered neutron component from the bunker walls. A dose decrement was observed in the nearest modules while an increment occurred in the farther external module.

CONCLUSIONS

The acquired data shows the neutron probe's underestimation of the present neutron dose due to dead time issues in fields with pulsed time structure [2], which instead does not affect the Bubble Dosimeters readings, where fast neutron dose prevails. BDTs and BD-PNDs are suitable for neutron dose determination in a radiotherapy treatment because of their energy sensibility to the primary components of a LINACs neutron energy spectrum [3], while monitoring with the neutron probe Berthold LB 6411 results not recommendable in these conditions.

REFERENCES

[1] KRY, S.F., et al., AAPM 158: Measurement and calculation of dose outside the treated volume for external-beam radiation therapy, Medical Physics 44 (2017) e391-e429.

[2] CARESANA, M., et al., Intercomparison of radiation protection instrumentation in pulsed neutron field, Nuclear Instruments and Methods in Physics Research Section A: Accelerators, Spectrometers, Detectors and Associated Equipment **737** (2014) 203-213.

[3] HARRISON R.M., et al., Dosimetry for second cancer risk estimation in radiotherapy: measurements in water phantoms, EURADOS Report 2017-01.

Dosimetric Measurements of Stereotactic Cones Using Eight Different Detectors

E. Gershkevitsh[a]
B. Casar[b], **I. Mendez**[b]

[a]North Estonia Medical Centre, J. Sütiste tee 19, Tallinn, Estonia
[b]Institute of Oncology, Zaloska 2, Ljubljana, Slovenia

Email address of Corresponding Author: eduardger@yahoo.co.uk

BACKGROUND

Commissioning of stereotactic cones requires careful selection of appropriate detectors. Recently published the IAEA Code of Practice (TRS-483) provides valuable information and guidance on dosimetry of small static photon fields [1]. The aim of the current work was to review the suitability of several detectors for commissioning of stereotactic cones, to compare detector specific output correction factors (OCF) with those published in the TRS-483 and to supplement it with the data on three new detectors.

METHODS

Eight commercial detectors have been used to measure output factors and profiles for stereotactic cones on Varian TrueBeam linear accelerator using 6 MV with and without flattening filter (WFF and FFF, respectively) and 10 FFF beams. The nominal cone diameters were 4, 5, 7.5, 10, 12.5, 15 and 17.5 mm and jaw size settings 50x50 mm^2 (MLC retracted). The detectors included: IBA Razor diode, IBA Razor chamber, IBA nanoRazor chamber, PTW diode P (60008), PTW diode E (60012), PTW SRS diode (60018), PTW MicroDiamond (60019) and Sun Nuclear Edge diode. The detectors were positioned with their stem parallel to the beam axis, except Edge diode which was positioned horizontally due to its design. PTW MP3-M water tank was used for the measurements and detectors were positioned with their effective point at a depth of 10 cm (SSD=90 cm) and profiles with the step size of 0.2 mm were acquired in X and Y direction. Penumbra and field sizes were calculated for each detector from FWHM. For output factor measurements the detectors were connected to PTW Unidos Webline electrometer and the maximum reading was found for each detector and three smallest cones by moving it in the increments of 0.2 mm along X and Y axis.

For the determination of OCF and cone sizes two reference detectors have been used (Standard Imaging Exradin W1 scintillator and Ashland Gafchromic EBT3 film) with the approach described elsewhere [2].

The equivalent square field sizes were found using the following relation to the measured radius of the cone [1]:

$$S_{clin} = r\sqrt{\pi} = 1.77r$$

RESULTS

Detector specific correction factors for different detectors and three energies are presented in Figure 1.

The largest variation is seen for PTW diode P (60008) and IBA nanoRazor chamber. It should be noted however, that both studied ion chambers, IBA nanoRazor chamber and IBA Razor

chamber were positioned with their stem parallel to the beam. While for IBA Razor chamber such positioning resulted in the smallest correction among the studied detectors for all cones except the smallest 4 mm due to small active area cross-section for the beam and minimized stem effect, the IBA nanoRazor chamber showed larger correction despite being smallest in active volume (0.003 cm^3). The minimal correction for IBA nanoRazor chamber was seen when it was positioned perpendicular to the beam (data not shown). Moreover, the parallel positioning of the IBA nanoRazor chamber leads to overresponse which is typically seen for solid state detectors, but not for ion chambers.

PTW MicroDiamond (60019), IBA Razor diode and IBA Razor chamber had the smallest field size differences with the film, while IBA Razor diode and PTW SRS diode (60018) had the smallest penumbra values.

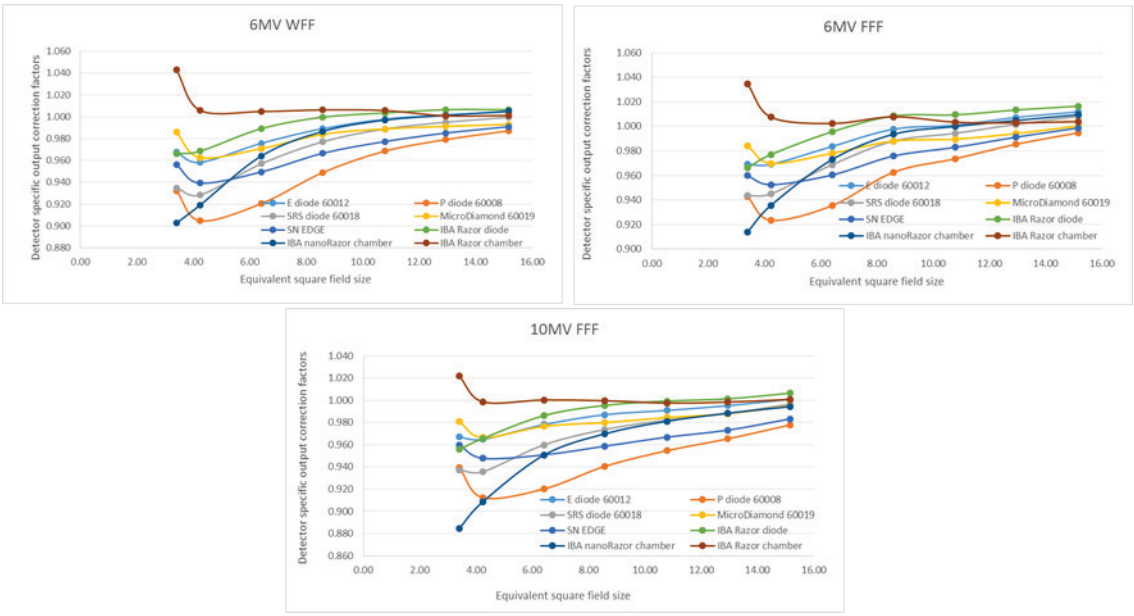

Figure 1. Detector specific output correction factors for three energies and eight detectors.

CONCLUSIONS

The detector specific correction factors were determined for stereotactic cones and eight different detectors and compared with the data published in the TRS-483. The detector specific correction factors for three new detectors are provided and could be a valuable supplement to already published data. The variation of OCF with orientation of the ion chamber stem in relation to the beam axis for smallest cones were found to be significant due to different volume effect and should be accounted for during the measurements.

REFERENCES

[1] PALMANS, H., ANDREO, P., HUQ, S., SEUNTJENS, J. Dosimetry of small static fields used in external beam radiotherapy: An IAEA-AAPM International Code of Practice for reference and relative dose determination. Technical Report Series No. 483. (IAEA TRS-483). 2017

[2] CASAR, B., GERSHKEVITSH, E., MENDEZ, I., JURKOVIĆ, S., HUQ, S. A novel method for the determination of field output factors and output correction factors for small static fields for six diodes and a microdiamond detector in megavoltage photon beams, *Med Phys.* 2018. DOI: 10.1002/mp.13318

Monte Carlo Dosimetric Characterization of a Bebig Co0.A86 Co-60 Brachytherapy Source

D. Z. Ndlovu[a]
G. Azangwe[a]

[a]National University of Science and Technology, Bulawayo, Zimbabwe.

Email address of Corresponding Author: dndlovu25@gmail.com

BACKGROUND

Dose characteristics from miniaturised encapsulated HDR brachytherapy sources such as ^{60}Co or ^{192}Ir are used in treatment planning systems and for dose calculations. These depend on the source design and the radioisotope used. Experimental procedures and measurements are recommended by the AAPM TG-43 to be carried out to verify the dose distribution of brachytherapy sources before use [1]. Mpilo Central Hospital has a Multisource Afterloader unit (Eckert & Ziegler BEBIG GmbH, Germany) that is being used for gynaecological treatment of cancer. It uses a BEBIG ^{60}Co radioisotope of Co0.A86 model. The purpose of this study was to use MCNP 6.1 a Monte Carlo code to independently obtain dosimetric parameters of a brachytherapy ^{60}Co source as per AAPM-TG 43 recommendation.

METHODS

Dosimetric parameters of a Co0.A86 BEBIG Co-60 source model were obtained using the geometric design from the manufacturer Eckert & Ziegler BEBIG GmbH, Germany. The ^{60}Co source spectrum was obtained from (NuDat, 2004) with the gamma portion of the spectrum considered in the source definition.

Air kerma strength, S_k was simulated with air kerma scored using air filled concentric cylindrical rings of 1 cm thick and 1 cm high along the transverse source axis. Simulations were performed *in vacuo* to avoid correction of photon attenuation by air. A spherical water phantom of 50 cm in radius with the source at the center was used to obtain two dose rate distribution functions. The first dose rate distribution function (*along and away*) was obtained using the grid of cylindrical rings of 0.05 cm thick and 0.05 cm high longitudinal to the source axis (*along*), scored at varying distances transverse to the entire source axis (*away*). The second grid system was composed of concentric spherical sections of 0.05 cm thick and an angular width of 1 degree in the polar angle using the AAPM TG-43 coordinate system.

RESULTS

Simulated air-kerma strength had a percentage deviation of 0.33 % to the certified source strength. Obtained dose rate constant value at the TG-43 reference point had a percentage difference of less than 0.2 % to that of the consensus data [2] for the same source model. This was also comparable with that obtained by other researchers [3-6] having a greatest percentage deviation of 0.73 % to that obtained by (Rogers & Thomson, 2016).

Comparisons were made with other researchers for dose rate values $\dot{D}(y,z)$ of along-away 2D Cartesian lookup data at away distances of y = 1 cm, 2 cm, 5 cm and 10 cm and for anisotropy function $F(r,\theta)$ at polar angles ranging from 0 degrees to 179 degrees and at radial distances of 1 cm, 4 cm, 10 cm and 20 cm. The data was found to be in good agreement at these comparison points. However, notable differences were at peripheral polar angles which were the positions

of source tip and the steel cables. Similar agreements in results were also noted for TG-43 radial dose function, *gL(r)* at distances from r = 0.25 cm to r = 20 cm.

CONCLUSIONS

Monte Carlo simulations for a BEBIG Co0.A86 Co-60 source have been performed as per recommendations of the AAPM TG-43 to obtain full dosimetric parameters using MCNP 6.1 code. Air kerma strength results were in good agreement with those in the certificate. AAPM TG-43 parameters that include dose rate constant, 2D along and away dose rate table, anisotropy function and radial dose function were determined. They were found to be in good agreement with values obtained by other researchers. Validation of treatment planning system can also be performed using these dosimetric datasets.

REFERENCES

[1] RIVARD, M. J. et al., 2004. Update of AAPM Task Group No.43 Report: A revised AAPM protocol for brachytherapy dose calculations. American Association of Medical Physicists in Medicine, 31(3), pp. 633-674.

[2] PÉREZ-CALATAYUD, J. et al., 2012. Dose Calculation for photon-emitting brachytherapy sources with average energy higher than 50keV; Full report of the AAPM and ESTRO. Report of the HEBD Working Group. , s.l.: College Group.

[3] ROGERS, D. & THOMSON, R., 2016. E&Z BEBIG GmbH, Multisource Co-60 HDR Co0.A86, Ottawa: Carleton University.

[4] GRANERO, D., PEREZ-CALATAYUD, J. & BALLESTER, F., 2007. Technical note: Dosimetric study of a new Co-60 source used in brachytherapy. The International Journal of Medical Phyiscs Research and Practice, 34(9), pp. 3485-3488.

[5] GUERRERO, R., ALMANSA, J. F., TORRES, J. & LALLENA, A. M., 2014. Dosimetric characterization of the 60Co BEBIG Co0.A86 high dose rate brachytherapy source using PENELOPE. Physica Medica, pp. 960-967.

[6] SELVAM, P. & BHOLA, S., 2010. Technical Note: EGSnrc-based dosimetric study of the BEBIG 60Co HDR Brachytherapy sources. Journal of Medical Physics, 37(3), pp. 1365-70.

[7] NuDat, 2004. National Nuclear Data Center. [Online] Available at: http://www.nndc.bnl.gov/nudat2 [Accessed 28 12 2017].

Comparison of Beam Characteristics in Reference and Non-Reference Conditions and Treatment Plans for Flattening and Flattening Free Photon Beams

A. T. Feye[a]
P. Chiovati[b]

[a]Jimma Univerversity, P.O.Box 378,Jimma,Ethiopia
[b]CRO Aviano 33081 PN,Italy

Email address of Corresponding Author: abe.duguma@gmail.com

BACKGROUND

The objective of this thesis is to evaluate dosimetric difference between flattening filter free (FFF) and flattened (FF) photon beams of Varian True Beam^{TM} linear accelerator and to investigate the difference in treatment plan quality of different treatment techniques for selected brain cancer with flattening filter beam and flattening filter free beam.

METHODS

Non-reference condition dosimetry was performed with IBA water phantom dosimeter system (RFA-Blue Phantom) with Omni-Pro Accept-7 software. AAPM TG-51 and IAEA TRS-398 protocol were used for dosimetry in reference condition for both flattening and flattening filter free photon beams. Comparison was made between the two protocols for the two beams. The procedure for Dosimetric Leaf Gap and MLC transmission factor measurements were carried out according to Varian specified guidelines. The chamber used for beam data collection and measurements were CC13, A14SL, A1SL, PTW30012 and FC56-G.

For treatment plan comparison fourteen patients with brain cancer were studied. A total of twenty-eight treatment plans were generated using flattening filter beams and flattening filter free beams among which 10 SRS, 6 SRT, 6 VMAT and 6 IMRT plans.

Standard clinical constrains were provided by the physician for planning target volume (PTV) and OARs. These were applied to generate the treatment plans. All plans were optimized and calculated using AAA algorithm of Eclipse treatment planning system. All treatment parameters such as iso-center position and beam set up were set to be identical for the flattened and the FFF beam plans. The homogeneity index (HI), gradient index (GI), target coverage (TC) and conformity number (CN) extracted from Dose-volume curves were used to compare the plan quality. The monitor unit number and beam on time were used to evaluate the delivery efficiency of treatment plans.

RESULTS

Compared with FF beams, D_{max} was shallower for FFF beams for all field sizes; the ionization curve shows smaller gradient for FFF beams in build up region. The FFF beams depth-dose curve shows a faster dose falloff compared with FF beams. As compared to FF beams, the output factor for FFF beams shows less variation with field sizes. FFF beams had lower MLC transmission and Dosimetric leaf separation than the FF beams.

In all four techniques the FFF beams provides the same TC as the FF beams. However, the use of 6MV FFF beams offers a clear benefit in delivery time when compared to 6MV FF beams, especially for SRS treatment techniques. It was obtained that compared to 6MV FF beam 6MV FFF spared 54.4%, 12.9%, 24.3% and 32.16 % of Beam On Time (BOT) in SRS, VMAT, SRT and IMRT techniques respectively. With regard to MU no significance difference were observed for VMAT and SRS techniques, but clear difference in MU were obtained in SRT and IMRT techniques: 6MV FFF uses higher MU amount than 6MV FF to achieve the same TC. The highest difference was obtained in IMRT in which 6MV FFF uses MU 1.5 times those of 6MV FF. From DVH analysis of OARs, FFF plans obtained better normal tissue sparing effect than FF plans in all four techniques.

CONCLUSIONS

As expected, removal of flattening filter alters various commissioning associated parameter such as beam quality, MLC Leaves Transmission factor and Dosimetric leaf separation. It was observed that IAEA-TRS398 and AAP-TG51 protocols give comparable results for both flattened and flattening filter free photon beams for dosimetry in reference condition. Negligible difference in beam quality conversion factor was observed using the two protocols for both FFF and FF beams. Similarly negligible difference in ion recombination of available chambers was obtained using the two protocols. However, relatively higher recombination correction factor was observed for FFF beams as compared to FF beams with the same nominal energies for both protocols. The FFF has the benefit of faster treatment delivery with smaller dose to normal tissues. Those features will help to increase patient safety, increase patient comfort and reduce chance of developing secondary cancers after radiotherapy. In this study, we observed that, compared to 6MV FF beams, 6MV FFF beams obtained clear time sparing effect in IMRT and SRS techniques. However, in IMRT relatively higher MUs were used by 6MV FFF as compared to 6MV FF to obtain the same TC. Anyway, in compromise with its highest time sparing effect and insignificant difference in MUs between FFF and FF beams, for SRS techniques we can conclude that 6MV FFF beams is a good choice for brain treatment with SRS techniques.

REFERENCES

[1] AL-AHBABI SS, BRADLEY D, BEYOMI M, et al. A comparison of protocols for external beam radiotherapy beam calibrations. Appl Radiat Isot.2012;70:1331–1336.

[2] ALMOND P R, BIGGS P J, COURSEY B M, HANSON W F, HUQ M S, NATH R AND ROGERS D W 1999 AAPM's TG-51 protocol for clinical reference dosimetry of high-energy photon and electron beams *Med. Phys.* **26** 1847–70

[3] ANDREO P, BURNS D T, HOHLFELD K, HUQ M S, KANAI T, LAITANO F, SMITH V G AND VYNCKIER S 2000 Absorbed dose determination in external beam radiotherapy: an international code of practice for dosimetry based on standards of absorbed dose to water *IAEA Technical Report Series* No 398 International Atomic Energy Agency, Vienna (the updated version 12 issued in 2006)

[4] CASHMORE J, RAMTOHUL M, FORD D. Lowering whole-body radiation doses in pediatric intensity-modulated radiotherapy through the use of unflattened photon beams. Int J Radiat Oncol Biol Phys. 2011;80:1220–7.

[5] FOGLIATA et al. Flattening filter free beams from True beam and Versa HD units: Evaluation of the parameter for quality assurance, Med.phys.43 (1), January 2016.

[6] HALL E J, WU C. Radiation-induced second cancers: The impact of 3D-CRT and IMRT. Int J Radiat Oncol Biol Phys. 2003;56:83–88.

[7] HRBACEK J, LANG S, KLÖCK S. Commissioning of photon beams of a flattening filter-free linear accelerator and the accuracy of beam modeling using an anisotropic analytical algorithm. Int J Radiat Oncol Biol Phys. 2011;80:1228–37

[8] J E LYE et a*l* 2016. Comparison between the TRS-398 code of practice and the TG-51 dosimetry protocol for flattening filter free beams. *Phys. Med. Biol.* 61 N362

[9] KARLSSON M AND ZACKRISSON B. Exploration of new treatment modalities offered by high energy (up to 50 MeV) electrons and photons. Radiother Oncol. 1997;43(3):303–09

[10] KINOSHITA et.al 2017,Comparison of AAPM addendum to TG-51,IAEA TRS-398, and JSMP12: Calibration of photon beams in water, Radiation oncology physics

[11] KOSUNEN A, ROGERS D. Beam quality specification for photon beam dosimetry. Med Phys. 1993;20:1181–1188.

[12] KRY et al 2012.Ion recombination correction factors (P_{ion}) for Varian TrueBeam high-dose-rate therapy beams. Journal of applied clinical medical physics, volume 13, number6

[13] MARTEN AND TOMMY KNOOS, Combining tissue phantom ratios to provide a beam quality specifier for flattening filter free photon beams,Med.phys.41(11),November 2014.

[14] MC EWEN M, DEWERD L, IBBOTT G, et al. Addendum to the AAPM's TG-51 protocol for clinical reference dosimetry of high-energy photon beams. Med Phys. 2014;41:041501–041520

[15] M LE ROY et al. Assessment of small volume ionization chambers as reference dosimeters in high energy photon beams,Phys.Med.Bio.56(2011),5637-5650.

[16] MUIR B, ROGERS D. Monte Carlo calculations of kQ, the beam quality conversion factor. Med Phys. 2010;37:5939–5950.

[17] VASSILIEV ON, TITT U, PONISCH F, KRY SF, MOHAN R, GILLIN MT. Dosimetric properties of photon beams from a flattening filter free clinical accelerator. Phys Med Biol. 2006;51(7):1907–17

[18] WANG L, ROGERS D. The replacement correction factors for cylindrical chambers in high-energy photon beams. Phys Med Biol. 2009;54:1609–1620.

[19] WULFF J, HEVERHAGEN J, ZINK K. Monte-Carlo-based perturbation and beam quality correction factors for thimble ionization chambers in high-energy photon beams. Phys Med Biol. 2008;53:2823–2836.

[20] XIAO et al. Flattening filter free accelerators: a report from the AAPM Therapy Emerging Technology Assessment Work Group. J. Med phys.2015 volume 16,no 3.

[21] YUE YAN et al. Dosimetric differences in flattened and flattening filter-free beam treatment plans,J.Med,phys.2016 Apr –Jun;92-99.

Impact of Use of IAEA TRS483 Correction Factors on Commissioning of Small Field Dose Calculation Algorithm

A. Toutaoui
S. Bencheikh, R. Louelh, H. Mahmoudi, M. Belmessaoud

Hôpital Chahids Mahmoudi, Tizi-Ouzou, Algeria

Email address of Corresponding Author: abdelkader.toutaoui@gmail.com

BACKGROUND

Accurate dose measurement for small photon beams used in radiotherapy is subject to large uncertainties. Solid state detectors (diode, micro-diamond, plastic scintillator, ...) are commonly used due to their small sensitive volumes and their high sensitivity. However, measurements of the response of some of these detectors up to more than 10% have been reported in the measurement of output factors in small fields [1, 2]. These results and the need to improve the accuracy of measurements dosimetric parameters of the small photon beams used in modern radiotherapy techniques (IMRT, VMAT, SRS, ...) motivated the development and publication of a new code of practice, IAEA TRS 483, providing correction factors capable of unifying measurements from a wide range of small field dosimeters [3,4].

In this study, we demonstrate the use and validation of the correction factors of this IAEA code of practice in the commissioning of the BrainLab iPlan treatment planning system in the radiotherapy department at the Hôpital Chahids Mahmoudi (Tizi-Ouzou, Algérie). Small fields are obtained either with a multi-leaf collimator or with circular cones.

METHODS

The small photon beam output factors required for the commissioning of the Brainlab Iplan TPS were measured on a Varian iX23 accelerator for MLC shaped field sizes of 0.5×0.5, 1×1, 2×2, 3×3 and 4×4 cm^2 with multiple back up jaw sizes. The output factors of photon beams collimated by circular cones of 4, 7.5, 10, 12.5, 15, 17.5 and 20 mm in diameter were also measured. Measurements were made with PTW micro-diamond (60019) and diode (60017) detectors in photovoltaic mode. Specific correction factors for detector and field size in Table 26 of the IAEA TRS 483 report were used to correct all readings [3]. Correction factors corresponding to the smallest aperture (MLC or jaws) were used for each measurement. For field sizes for which correction factors are not tabulated in the IAEA report, a linear interpolation between the nearest tabulated values has been performed. Measurements with a dosimeter that did not require correction factors such as Gafchromic EBT3 film were performed and compared to the IAEA corrected readings. The uncorrected raw data and the corrected OF were plotted together and compared.

RESULTS

The corrected output factors measured as a function of field size for MLC shaped beams and as function of cone diameter for circular beams using two solid state detectors are compared to ones measured with EBT3 Gafchromic films. For the entire range of field sizes from 5 to 40 mm, for square MLC shaped fields, the results measured by the two solid-state detectors agree with each other to about 1%, with maximum deviation of 0.8 % for the smallest field size of 5×5 mm^2. For the circular beams, the agreement is within 2%. This deviation is observed for the 4 mm diameter cone.

CONCLUSIONS

Excellent agreement has been shown between the IAEA corrected output factors between multiple detectors for both square MLC shaped small field and cones. The results were further validated by comparison with dosimeters such as EBT Gafchromic film that do not require correction factors. In particular, for the smallest field size measurement required by the BrainLab iPlan TPS (5 mm MLC opening), the well validated output factor result is below the historically utilized output factor region suggested by BrainLab. These results motivate change in practice and further clinical translation of the recommendations in the IAEA TRS 483 report for iPlan users.

REFERENCES

[1] LIU P et al., Radiotherapy and Oncology 112.3 (2014): 442-446
[2] BENMAKHLOUF et al., Med Phys 41 (4) 041711, 2014.
[3] IAEA, TRS. 483. Dosimetry of small static fields used in external beam radiotherapy: an IAEA-AAPM International Code of Practice for reference and relative dose determination (2017).
[4] HUQ MS et al., Med Phys 45 (9) 2018.

Small Field Dosimetry in Clinical Practice: Estimation of Micro Ionization Chamber Correction Factor Using Radiochromic Film

A. Allaith[a]

[a]International Centre of Theoretical Phyisics, Trieste, Italy

Email address of Corresponding Author: allaith1990@hotmail.com

BACKGROUND

Stereotactic radiation treatments require small field delivery. The dosimetry of such fields is challenging, and a specific formalism was introduced in the last decade. The primary aim of this study was to determine the correction factors of 10 MV small square beam ($k_{Q_{s,Q}}^{f_s f_{ref}}$ or k^{fs}) and small modulated beam ($k_{Q_{pcsr,Q}}^{f_{pcsr} f_{ref}}$ or k^{pcsr}) for Pinpoint PTW-31016 ionization chamber, using the Gafchromic EBT3 as reference detector. The secondary objective was to apply $k_{Q_{pcsr,Q}}^{f_{pcsr} f_{ref}}$ on stereotactic radiosurgery treatment (SRS).

METHODS

Two different sets of measurements were performed for the estimation of k^{fs} and k^{pcsr} for the Pinpoint PTW-31016 ionization chamber, delivered on RW3 phantom at 10 cm depth. The reference field for the correction factors estimation was 5x5cm^2. Firstly, for k^{fs} estimation a set of square beams was delivered to the detectors with different field size with 2Gy dose prescription at the isocenter. For k^{pcsr} correction factors four modulated beam with geometry similar to the SRS plan were produced with the Monaco treatment planning system (TPS) and delivered to the detectors at gantry 0° in a sliding window technique. The calculated k^{pcsr} was then plotted as a function of beam segment area in order to find a fitting curve that can be used to correct ionization chamber measurements in pre-treatment verification of SRS plan. The estimation of k^{pcsr}, derived from that fitting, was verified with two clinical patient plans by comparing the corrected chamber measurement with the film measurement and with the calculated dose from the Monaco TPS.

RESULTS

k^{fs} increases as the field dimensions decrease: for 3x3cm^2, 2.5x2.5cm^2 and 2x2cm^2 k^{fs} is close to unity, as expected, while it is 1.027(±2.3%) for the 1.5x1.5cm^2 and 1.067(±2.9%) for the 1x1cm^2. For the 0.5x0.5cm^2 field, k^{fs} is estimated, from the fitting, to be 1.16(±1%). k^{pcsr} increases as the segment area decreases and for the modulated beams considered the range of variation was between 1.003 and 1.089.

k^{fs} estimated in this work are in good agreement with published data of k^{fs} at 10MV: the differences are 0.1% for 2x2 cm^2, 1.5% for the 1x1 cm^2 and 1% for the 0.5x0.5 cm^2 field. The k^{pcsr} fitting curve showed an excellent agreement, with R^2=0.999, and hence the fitting curve can be used to estimate the k^{pcsr} of modulated beams used in SRS treatment. When we apply the k^{pcsr} on the two ion chamber values of the clinical plans, we find a good agreement with the film dosimetry: dose difference between chamber and film are <0.5%. The ion chamber measurement after correction shows a better agreement with the TPS calculation (DVH mean dose to the chamber): dose discrepancy improved from 3.7% to 1.4%.

CONCLUSIONS

The good agreement with the published data of k^{fs} allows us to use them to correct the Pinpoint PTW-31016 chamber measurements. k^{pcsr} estimated from the fitting curve can be used to correct the ion chamber pre-treatment verification of the SRS coplanar beam; further work is required to extend these results for the verification of other kind of SRS treatment, especially when non-coplanar beams are used.

REFERENCES

[1] ASSOCIAZIONE ITALIANA RADIOTERAPIA ONCOLOGIA. Trattamento delle neoplasie primitive e secondarie del sistema nervoso centrale, Gruppo di studio AIRO Sulle neoplasie SNS, 2011.

[2] INTERNATIONAL ATOMIC ENERGY AGENCY. Dosimetry of small static fields used in external photon beam radiotherapy, international Code of Practice for reference and relative dose determination, TECHNICAL REPORTS SERIES No. 483, IAEA, Vienna 2017

[3] INTERNATIONAL ATOMIC ENERGY AGENCY. Absorbed Dose Determination in External Beam Radiotherapy: An International Code of Practice for Dosimetry Based on Standards of Absorbed Dose to Water, Technical Reports Series No.398, IAEA, Vienna 2000

[4] ALFONSO R, ANDREO P, CAPOTE R, et al. A new formalism for reference dosimetry of small and nonstandard fields. Med Phys. 2008; 35:5179–5186

[5] CHUNG E, SOISSON E, SEUNTJENS J. Dose homogeneity specification for reference dosimetry of nonstandard fields. Med Phys. 2012;39(1):407–14.

[6] CHUNG, E., BOUCHARD, H. AND SEUNTJENS, J. Investigation of three radiation detectors for accurate measurement of absorbed dose in nonstandard fields. Med. Phys. 2010; 37: 2404-2413.

Commissioning of Total Body Irradiation for a New Installation

F. Kiragga[a]
R. Vidimari[b]

[a]University of Trieste/International Center for Theoretical Physics, Strada Costiera, 11 – I-34151 Trieste, Italy.
[b]Medical Physics Department, Azienda Sanitaria Universitaria Integrata di Trieste, Italy

Email address of Corresponding Author: jireh4festo@gmail.com

BACKGROUND

Any quality Bone Marrow Transplant (BMT) requires Total Body Irradiation (TBI) as part of the preparatory conditioning regimen. A BMT replaces the patient's diseased bone marrow with stem cells from a healthy donor (allogenic transplant) or from the patient himself (autologous transplant) [1].

The main action of Total Body Irradiation (TBI) is undoubtedly total (by means of supra-lethal doses) or partial (with sub-myeloablative doses) eradication of radiosensitive hematological malignancies [2].

TBI is a special radiotherapeutic technique that delivers to a patient's whole body a dose uniform to within ± 10% of the prescribed dose. It is primarily used for suppressing the immune system before BMT. In vivo dosimetry is of critical relevance before any TBI is carried out because of the complexity in calculation of the dose at different points in the patient and also due to the increased risk of patient movements due to the long duration of treatment.

The task for in vivo dosimetry in the case of TBI is threefold: to determine the dose at the dose specification point, usually taken at mid-pelvis or mid-abdomen, to estimate the homogeneity of the midline dose distribution at different loci in cranio-caudal direction and to monitor the dose at the level of organs at risk (lungs, liver, etc.) [3].

The delivery of an accurate dose to the patient is dependent firstly on the accuracy to which a radiation beam can be calibrated in a uniform water-like medium and secondly, the dose at any point of interest within the patient must be calculated and correlated to this calibration dose. However, there are a number of physical parameters that should be considered and optimized for each institution implementing TBI. The most common parameters relate to: the energy of radiation, treatment distance, choice of antero-posterior (AP) treatments or lateral treatments or a combination of these and dose rate [4].

METHODS

Calibration of detectors, Gafchromic EBT^3 (GAF), MOSFETs and Ionization chambers (CI), was done under reference conditions for use in TBI conditions. Three reference positions: Source Axis Distance (SAD) 5m (2m from the wall), SAD 4.5 m (2.5 m from wall) and SAD 4m (3 m from wall) were chosen with minimal or no backscatter from the wall. A treatment technique: Lateral-Lateral (LL), gantry angle 90^o, collimator angle 0^o and 6MV energy was chosen with respect to the nature of the bunker. Percentage Depth Doses (PDDs) were evaluated, first with a big water phantom and then with RW3 slab phantom (30x30x30 cm^3) at the three positions and then compared. The flatness and symmetry of the profiles were evaluated from the water PDD data. The beam quality was also determined using TPR_{10}^{20} in TBI conditions. Then *in vivo* doses were measured with both GAF and CI using RW3 phantom

by taking three points on the RW3 phantom: 5 cm from entrance (entrance dose), middle slab (midline dose) and 5 cm from the exit (exit dose). These were compared for GAF and CI. Additionally, previsional calculations for Monitor Units (MU) were made to achieve the nominal prescribed dose of 2Gy at the umbilicus, with 1Gy from either side of the patient. Lastly, the absorption of lead and plexiglass as shielding materials was measured and the corresponding absorption curves plotted.

RESULTS

The beam was characterized in different setups. A length of 140 cm (pediatric) was found to be in the flatness region with a dose variation of 3% while 170 cm (adult) had a dose variation of 10%. TPR_{10}^{20} was found to be 0.692 at 2.5 m from the wall. The correction factor (for all influence quantities) changed from 0.994 in isocentric conditions to 0.991 in TBI conditions. GAF, MOSFETs were calibrated and a calibration curve was plotted for GAF while a table of calibration factors was made for the MOSFETs. A dose variation of less than 2% was achieved between Farmer chamber and GAF readings at similar points in the RW3 phantom.

CONCLUSIONS

The beam characteristics were important to understand the behavior of the beam in non-reference conditions (TBI conditions) and were within tolerance range. as dose variations of up ±10% is allowed.

REFERENCES

[1] PODGORSAK, E.B., Radiation Oncology Physics: A Handbook for Teachers and Students. (2005) Published by the IAEA

[2] ISTITUTO SUPERIORE DI SANITÀ (ISTISAN), Guidelines for quality assurance in total body irradiation. English version. Edited by Maria Antonella Tabocchini and Vincenza Viti, vi, 45 p. Rapporti 05/47 (2005)

[3] VAN DAM, J., MARINELLO G, Methods for In vivo Dosimetry in external Radiotherapy. 1st edition. ESTRO and Garant publishers (1994)

[4] VAN DYK, J., Dosimetry for total body Irradiation. Radiother.Oncol.9: 107 – 118 (1987)

An Analytical Formalism for the Assessment of Dosimetric Uncertainties Due to Positioning Uncertainties

W. Lechner[a,b]
D. Georg[a,b], **H.Palmans**[c,d]

[a]Department of Radiation Oncology, Division Medical Physics, Medical University Vienna, 1090 Vienna, Austria
[b]Christian Doppler Laboratory for Medical Radiation Research for Radiation Oncology, Medical University of Vienna, Austria
[c]EBG MedAustron GmbH, Marie-Curie Straße 5, 2700 Wiener Neustadt, Austria
[d]National Physical Laboratory, Teddington TW 11 0LW, United Kingdom

Email address of Corresponding Author: wolfgang.lechner@akhwien.at

BACKGROUND

The assessment of the type-B uncertainty due to detector positioning in small photon fields. This uncertainty can be caused by uncertainties in the determination of the position of the maximum dose, the step width of the scanning phantom and uncertainties in collimator (re-)positioning when changing the field size. While positioning makes up an important contribution to the overall dosimetric uncertainty of small fields, there is limited consensus how to assess this uncertainty and published uncertainty estimates for similar experimental conditions can vary by up to an order of magnitude.

METHODS

Assuming that the beam profile of small photon fields near the maximum dose can be approximated by a second order polynomial (D(x)) and the probability distribution of the relative position of the detector (x) to the position of the maximum dose (x_0) within a maximum displacement (a) can be described by a rectangular function (p(x)), the expectance value (E), its variance (var) and relative type-B standard uncertainty, $u_{B,r}$, can be expressed as:

$$D(x) = p_0 + p_1 x + p_2 x^2 \tag{1}$$

$$p(x) = \frac{1}{2a} \tag{2}$$

$$E = \int_{-a}^{a} D(x + x_0) p(x) dx = p_0 - \frac{{p_1}^2}{4p_2} + \frac{a^2\ p_2}{3} \tag{3}$$

$$var = \sigma^2 = \int_{-a}^{a} (D(x + x_0) - E)^2 p(x) dx = \frac{4a^4\ {p_2}^2}{45} \tag{4}$$

$$u_{B,r} = \frac{\sqrt{\sigma^2}}{E} \tag{5}$$

A beam profile of a 0.5 x 0.5 cm² 6 MV beam produced by a Versa HD (Elekta AB, Stockholm, Sweden) was acquired using a microDiamond (PTW, Freiburg, Germany) with a step width of 0.1 mm. Eq. (1) was fitted to the measured beam profile. The relative standard uncertainty contribution to the absorbed dose, $u_{B,r}$ was calculated according to Eq. (5) and plotted as a function of the maximum deviation (a) between detector and maximum dose in Figure 1.

RESULTS

As expected, the relative standard uncertainty contribution to the absorbed dose due to uncertainties in detector positioning increased with increasing maximum detector displacement relative to the maximum dose. For a maximum displacement of 0.2 mm, 0.5 mm and 1 mm the uncertainty was below 0.1%, 0.5% and 1.9%, respectively.

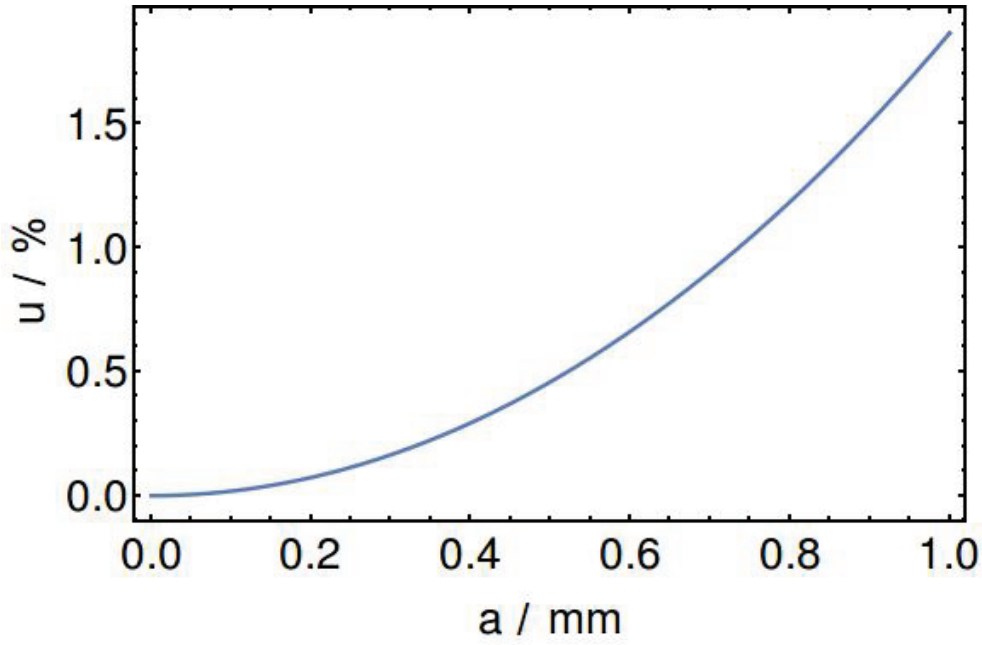

Figure 1. The relative dosimetric uncertainty due to positioning as a function of the maximum displacement.

CONCLUSIONS

The proposed formalism allows an assessment of the relative standard uncertainty contribution to the absorbed dose due to positioning uncertainties based on beam profile measurements and could contribute to harmonization of uncertainty estimation in small field dosimetry. The example given, which is representative for typical small fields of size 0.5 cm, shows that positioning tolerance in dosimetry should be below 0.5 mm for limiting the uncertainty contribution to 0.5%.

Testing the IAEA/AAPM Code of Practice TRS 483 for Small Fields Dosimetry at KFSHRC in Varian True Beam, Cyberknife and Tomotherapy Machines

M. Arib[a]
A. Nobaha, W. Al-Najara, A. Alkafia, F. Alzorkania, M. Shehadeha, U. Mwidua, B. Moftaha, F. Mahyouba

[a]Biomedical Physics Department, King Faisal Specialist Hospital and Research Centre, Riyadh 11211, Kingdom of Saudi Arabia

Email address of Corresponding Author: marib@kfshrc.edu.sa

BACKGROUND

An International code of practice for reference and relative dosimetry of small static used in external beam radiotherapy, TRS 483, was jointly published by the IAEA and AAPM. This dosimetry protocol is intended to fill the gap left by the universally adopted codes of practices such as TRS398 and TG51 when dealing with small field sizes.

At the Department of Biomedical Physics belonging to King Faisal Specialist Hospital and Research Centre, we have undertaken to test the procedures described in TRS 483 for a set of ionization chambers and an Edge detector using a 6 MV flattened photon beam from a Varian True Beam machine, circular beams obtained with a cyberknife and several rectangular fields from a Tomotherapy machine. For the varian machine, measurements were performed in a full circle 3D scanner (San Nuclear Co.) for the Cyberknife and Tomotherapy machines, we have used a solid water phantom.

METHODS

For the measurement of the quality index, the formalism proposed in the TRS 483 (Palmans equation) in order to determine TPR20,10(10) or %dd(10,10)X, starting from TPR20,10(S) or %dd(S)X, was verified at the Varian True beam and Tomotherapy machines for several field sizes using different detectors. The experimental values of the beam quality index were found to be consistent with the calculated ones using the formula of the code of practice (maximum deviation for TPR -0.68% for 2 x 2 cm2) field.

The second part of the work concerns the measurement of the output factors. We have measured this factor for the three machines using a Sun Nuclear Edge detector, a PTW pin-point and semi-flex chambers and an IBA CC01 chamber. The field sizes were ranging from 0.5 cm x 0.5 cm to 10 cm x 10 cm for the Varian accelerator, from 1 cm to 6 cm diameters for the Cyberknife and from 1 cm x 0.625 cm to 5 cm x 40 cm for Tomotherapy machine. The field output factors were calculated using the output correction factors given in TRS 483 COP. The values obtained with the different detectors were compared.

For each center, the standard deviation with respect to the mean value of the field output factors measured with these three different detectors was calculated for each field as a measure for the agreement amongst the determined field output factors.

RESULTS

For field sizes lying between 10 cm x 10 cm and 1 cm x 1 cm, the values of $TPR_{20,10}(10)$ calculated from the measured $TPR_{20,10}(S)$, ranged between 0.665 and 0.669. The values of

%dd(10), calculated from the measured %dd(S) ranged from 65.04% and 66.29%. This gives maximum deviations of 0.2% 1 % respectively at 4 cm x 4 cm. The deviation reaches 0.6% and 3% respectively at 2 cm x 2 cm. Higher deviations were obtained for 0.5 cm x 0.5 cm (-8.7% and 10.6% respectively) stressing that the Palmans expressions are actually valid down to 4 cm x 4 cm but can be utilized until 2 cm x 2 cm with higher uncertainties.

Regarding the output factors, at the Varian True Beam accelerator, it is shown that the consistency between the calculated field output factors obtained with the three detectors was within maximum +/- 0.8 %. Maximum deviations are observed at the 1 cm x 1 cm field size (Fig. 1 and 2).

Similar results were obtained for the Cybernife and the Tomotherapy machines.

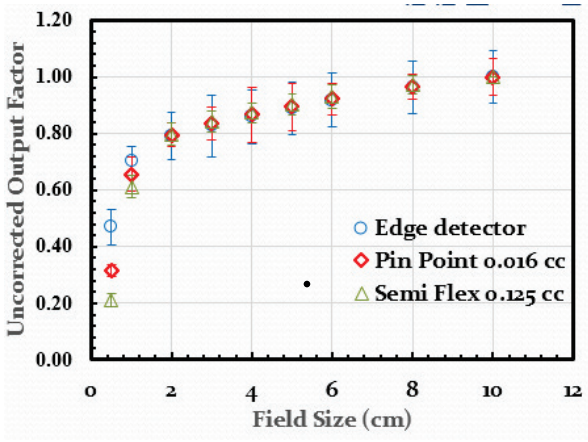

Fig. 1. Uncorrected output factors

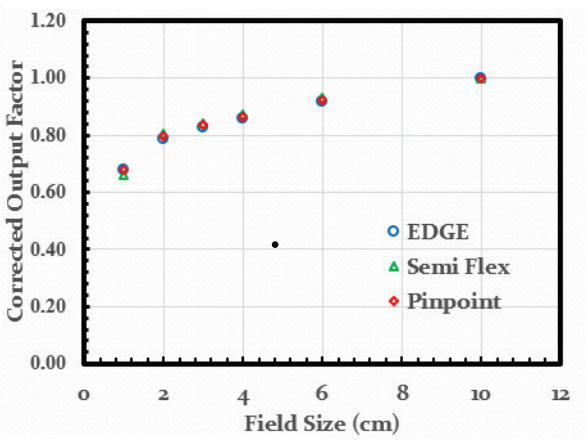

Fig. 2. Corrected output factors

CONCLUSIONS

Using the formalism of the IAEA/AAPM TRS 483 code of practice on small field dosimetry, the quality indexes $TPR_{20,10}$ and %dd for a field size 10 x 10 cm² can be determined with sufficient accuracy using the experimental data of $TPR_{20,10}(S)$ and %dd(S) in machine specific reference fields down to 4 cm x 4 cm. Better compliance between the calculated and experimentally determined beam quality specifiers are observed for $TPR_{20,10}$ and larger discrepancies are observed for field sizes lower than 2 cm x 2 cm which is compliant with the validity of Palmans formalism.

Regarding the field output factors, it is shown that by applying the field output correction factors, the consistency of the Field output factors is considerably improved for all the detectors used in our study for the three investigated machines.

REFERENCES

[1] Palmans H, Andreo P, Huq MS, Seuntjens J, Christaki K. Dosimetry of Small Static Fields used in External Beam Radiotherapy: An IAEA–AAPM International Code of Practice for Reference and Relative Dose Determination. Technical Report Series No. 483. Vienna: International Atomic Energy Agency; 2017

Nuclear Medicine Medical Physics

Dosimetric Study of Pediatric PET/CT Tests

F. Paiva[a]
P. Santana[b], **A. Mourão**[a,c], **F. Santos**[a]

[a] Department of Nuclear Engineering, Federal University of Minas Gerais, Av. Antônio Carlos 6627, CEP: 31270-901, Pampulha, Belo Horizonte, MG, Brazil
[b]Medical School, Federal University of Minas Gerais, Av. Professor Alfredo Balena, 190, CEP: 30123970, Santa Efigênia, Belo Horizonte, MG, Brazil
[c]Biomedical Engineering Center, Federal Center for Technological Education of Minas Gerais, Av. Amazonas, 5253 - Sala 113. CEP: 30421-169, Nova Suíça, Belo Horizonte, MG, Brazil

Email address of Corresponding Author: fgpaiva92@gmail.com

BACKGROUND

Positron Emission Tomography (PET) associated with Computed Tomography (CT) scanning is becoming increasingly important in noninvasive imaging studies and in the monitoring of children with known or suspected malignant diseases [1, 2]. These compound tomographic scanners allow the fusion of functional images obtained from the administration of radionuclides, such as ^{18}F, and anatomical images generated by X-ray beam attenuation from CT [3-5]. Although the immediate benefit to the individual patient may be substantial, relatively high radiation doses associated with PET/CT, compared with conventional exams have raised health care. This is especially concerning for children, who are more sensitive to radiation-induced carcinogenesis and have many remaining years of life for the development of cancer [6].

METHODS

In this study, the absorbed and effective doses generated by the CT scan and incorporated by the administration of the radionuclide ^{18}F-FDG were evaluate in the most radiosensitive organs. To evaluate the CT dose, radiochromic film strips (Gafchromic XR-QA2) [7,8] were placed into two pediatric body phantoms, similar to children of 6 and 8 years, built by PMMA volumes, as shown in Figure 1. The CT protocol performed was the standard pediatric whole-body scanning used in the service where the study was done.

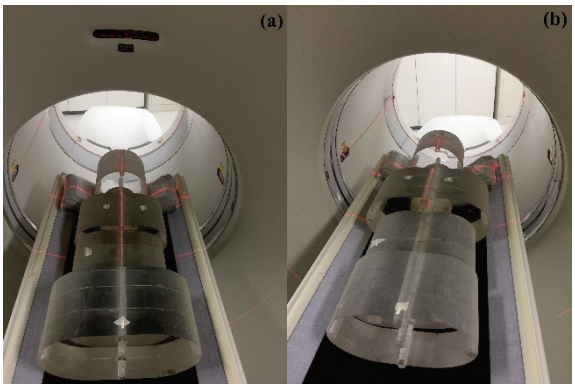

Figure 1. Pediatric PMMA phantoms. 6 years old (a) and 8 years old (b).

The activity of the radiopharmaceutical ^{18}F-FDG to be injected may vary according to the patient mass and the detector sensitivity. The Effective Dose was evaluated using the biokinetic model proposed by the International Commission on Radiological Protection (ICRP) number 106 [9]. The protocol used was 3.33 MBq.kg^{-1} (0.09 mCi.kg^{-1}), this amount is commonly used

in the service were the study was done, and it was multiplied by the mass of each phantom, 24 kg for the 6 years old and 31 kg for the 10 years old.

RESULTS

The absorbed doses from CT scan were approximately 21% higher in the 10-year phantom. This can be explained by the scan distance, which was 62.1 cm for the 6-year phantom and 73.9cm for the 10-year phantom. For the 6-year phantom, the organs that presented the highest absorbed dose from CT scan were bone marrow, thyroid and gonads. In the 10-year phantom, the highest absorbed doses were found in the esophagus, bone marrow, stomach and thyroid. The different values found are due to the variations in the format and size of the phantoms. Analyzing the effective dose from ^{18}F, the bladder had a higher value, explained by the excretion route of the radiopharmaceutical.

CONCLUSIONS

The CT scans were responsible for more than 60% of the effective dose in the PET/CT examination for both phantoms, hence the importance of the tomographic protocol optimization, reducing doses to the minimum necessary. It is important to emphasize the different patient mass value, used to define the amount of ^{18}F-FDG. This amount of radiopharmaceutical reflects directly on the dose estimate of PET test.

REFERENCES

[1] STAUSS, J. et al. Guidelines for 18F-FDG PET and PET-CT imaging in paediatric oncology. European journal of nuclear medicine and molecular imaging, v. 35, n. 8, p. 1581-1588, 2008.

[2] JADVAR, Hossein et al. PET and PET/CT in pediatric oncology. In: Seminars in nuclear medicine. WB Saunders, 2007. p. 316-331.

[3] CZERNIN, Johannes; SCHELBERT, Heinrich. PET/CT imaging: facts, opinions, hopes, and questions. The Journal of Nuclear Medicine, v. 45, p. 1S, 2004.

[4] GERBAUDO, Victor H. (Ed.). A Case-based Approach to PET/CT in Oncology. Cambridge University Press, 2012.

[5] FLUX, Glenn et al. The impact of PET and SPECT on dosimetry for targeted radionuclide therapy. Zeitschrift für medizinische Physik, v. 16, n. 1, p. 47-59, 2006.

[6] GELFAND, Michael J.; LEMEN, Lisa C. PET/CT and SPECT/CT dosimetry in children: the challenge to the pediatric imager. In: Seminars in nuclear medicine. WB Saunders, 2007. p. 391-398.

[7] ALNAWAF, Hani et al. Absorption spectra response of XRQA radiochromic film to x-ray radiation. Radiation measurements, v. 45, n. 1, p. 129-132, 2010.

[8] ISP. (2010). International specialty products. Gafchromic XR catalogue. 8p.15.

[9] ICRP. (2008) Radiation dose to patients from radiopharmaceuticals. Addendum 3 to ICRP Publication 53. ICRP Publication 106. Approved by the Commission in October 2007. Ann ICRP;38(1-2):1–197.

Development of Internal Dosimetry Tool using PYTHON 3.7 for Human Dose Estimation of New radiopharmaceuticals in Indonesia

D. Andini[a]
S. Tri Wahyudi, T. H. A. Wibawa[b], Iswahyudi[b], N. R. Hidayati[c], I. Daruwati[b]

[a]Faculty of Mathematics and Natural Sciences,Bogor Agriculutural University, Jl.Raya Dramaga,Kampus IPB Dramaga,Bogor 16680,Indonesia
[b]Center for Applied Nuclear Science and Technology,Jl.Tamansari No.71,Bandung 40132,Indonesia
[c]Center for Technology of Radiation Safety and Metrology, Jl. Lebak Bulus Raya No. 49, Jakarta 12070, Indonesia

Email address of Corresponding Author: inn98@batan.go.id

BACKGROUND

The development of radiopharmaceutical production in Indonesia has been growing rapidly in last few years. This development requires internal dosimetry study to show the estimated radiation risk which will be received by human body after the radiopharmaceutical has been administered for the first time. Residence time is one of important parameters in internal dosimetry study which need to be investigated to find human doses estimation. Residence time is defined as the ratio between activities that accumulate in the target organ (Ã) and injected activity (A_0). Some studies also referring the residence time as the time integrated activity coefficient (TIAC) [1]. There is well known internal dosimetry tool that can be utilized for calculating the TIAC, namely OLINDA/EXM ver.1 from Vanderbilt University. However, the software is not commercially available at the moment. Furthermore, other freeware tools for estimating the human dose need the TIAC as the input. Hence, for this reason, developing an internal dosimetry tool on freeware basis will be useful not only for researchers, but also students in medical physics studies. The purpose of this study was to develop an internal dosimetry tool by using Phyton 3.7 by applying the biodistribution data of ^{99m}Tc-MDP and ^{99m}Tc-GSH in normal mice to get the TIAC and will be compared to the TIAC produced by using OLINDA/EXM Ver.1.

METHODS

The method used in this study were consisted 3 steps, which was started from the biodistribution test of ^{99m}Tc-MDP and ^{99m}Tc-GSH in Swiss male mice, the TIAC calculations using Python 3.7 and OLINDA / EXM and. The biodistribution test of ^{99m}Tc-MDP and ^{99m}Tc-GSH were done by performing biodistribution test for ^{99m}Tc-MDP and ^{99m}Tc-GSH to 12 normal mice through intravenous injection. At 2, 4, 6 hours, and 24 hours after injection, 3 time mice were sacrificed for each time interval, and counted for the muscle, intestine, liver, stomach, spleen, kidney, heart, lungs, bones, brain and bladder, so that the value of% ID per gram of animal organs is obtained. This value was converted into % ID of human using the equation (1) [2]

$$(\%ID)human = \left[\left(\frac{\%ID}{organ}\right) animal\ x\ (kg_{TB})animal\right] x\ \left(\frac{g\ organ}{kg_{TB}}\right) human \qquad (1)$$

After the %ID in human has been obtained from OLINDA / EXM, by input the data of % ID in human organs and the interval time to Fit Data to Model menu in the OLINDA / EXM. Then the TIAC of each organ were produced as a reference data for the TIAC calculation using Python 3.7. In this method, % ID of human organs and time of counting are divided into 2

variables, x and y, then input data were created as a list data in editor of PyCharm-Python 3.7. After optimizing the curve function by the regression exponential function and use the trapezoid method to obtain the area under the curve[5]. The TIAC was displayed in the PyCharm-Python 3.7 Run menu.

RESULTS

Table 1. The Result of TIAC calculations by OLINDA/EXM and Python.

Residence Time/TIAC (hour)						
	^{99m}Tc-MDP			^{99m}Tc-GSH		
Organ	**OLINDA/ EXM**	**Python**	**STD**	**OLINDA/ EXM**	**Python**	**STD**
Muscle	2.23E-01	2.23E-01	0.00E+00	3.51E-01	3.53E-01	1.27E-03
Bone	5.73E+00	5.73E+00	2.48E-03	1.23E+00	1.24E+00	4.10E-03
LLI	1.68E-02	1.69E-02	7.07E-05	5.74E-02	5.69E-02	3.90E-04
Liver	2.94E-01	2.96E-01	1.58E-03	1.03E-01	1.03E-01	1.60E-04
Spleen	1.57E-02	1.61E-02	2.60E-04	4.75E-03	4.78E-03	2.12E-05
Kidneys	5.90E-02	5.95E-02	3.30E-04	4.74E-01	4.78E-01	2.80E-03
Heart	9.16E-03	9.18E-03	1.41E-05	8.20E-03	8.25E-03	3.54E-05
Lungs	5.13E-02	5.13E-02	2.83E-05	6.76E-02	6.80E-02	2.70E-04
Brain	3.47E-03	3.51E-03	2.47E-05	3.10E-02	3.10E-02	1.77E-05
Stomach	5.62E-03	5.84E-03	1.60E-04	7.25E-03	7.28E-03	2.12E-05
Bladder	1.71E-02	1.71E-02	3.25E-05	3.75E-03	3.76E-03	7.07E-06
	MEAN		**4.50E-04**	**MEAN**		**8.30E-04**

The results show that TIAC of each organ as calculated by Phyton 3.7 have slightly different and low standard deviation (4.5E-04 and 8.3E-04) toward the TIAC produced by OLINDA/EXM Ver.1. However, some works need to be done for verifying the consistency. This work might need use other radiopharmaceuticals in the future, for longer half live radiopharmaceutical other than ^{99m}Tc.

CONCLUSIONS

Python can be utilized as internal dosimetry tool for calculating the TIAC, since it gives slight difference from OLINDA/EXM ver.1, which will support the development of radiopharmaceutical production and nuclear medicine practices in Indonesia.

REFERENCES

[1] Lassmann,M, et al, EANM Dosimetry Committee Guidance Document : Good Practice of Clinical Dosimetry Reporting, Eur J Nucl Med Mol Imaging,Vol.38,(2011), pp.192-200.

[2] Rasaneh S, et al, Synthesis And Biodistribution Studies Of 177Lu-Trastuzumab As A Therapeutic Agent In The Breast Cancer Mice Model, Journal Of Labelled Compounds And Radiopharmaceutical,Vol.53,No.9 , (2010), pp.575-579.

Technetium-99m Nanoradiopharmaceuticals for Decreasing the Patients Internal Dose

A. Nabipour Chakoli[a]
R. Serkan[b], **M. Sadeghi**[c]

[a]Nuclear Science and Technology Research Institute, Tehran, Iran
[b]Science and Research branch, Islamic Azad University, Tehran, Iran
[c]Iran University of Medical Science, Tehran, Iran

Email address of Corresponding Author: anabipour@aeoi.org.ir

BACKGROUND

Radiopharmaceuticals are the key tools of medicine in general and nuclear medicine in particular, both in the context of diagnosis and therapy. The radiopharmaceutical chemistry demonstrates its capability to contribute to the industrial development of new drugs [1-3]. Nanomaterials, due to their unique capabilities and purported minimal side effects in treating variety of sicknesses, nanomaterials have a wide range of biomedical applications. The emergence of nanomaterials science and radiopharmacy, which is creation and utilization of materials at the nanometer scale, has been a great influence on radiopharmaceutical industry. Growth of nuclear medicine has been due mainly to the availability of Technetium-99m (Tc-99m) radiopharmaceuticals; this single isotope is used in over 80% of all diagnostic procedures. Each year, roughly 25 million procedures are carried out with Tc-99m radiopharmaceuticals, and this figure is projected to grow at a rate of about 15% per annum. Now a days, various colloids of nano size Tc-99m are used for diagnosis. In this research, the effect of nanoTc-99m nanoradiomedicine on the internal dose of patients are studied [4-7].

METHODS

Various kinds of industrialized Tc-99m nanocolloides that applied for diagnosis are considered. The internal dose of patients after injection of Tc-99m nanocolloides are compared with custom Tc-99m colloids for each organ. The whole body internal dose is determined for each injection.

RESULTS

Tc-99m radiopharmaceuticals are used in several diagnostic procedures, from the use of pertechnetate for thyroid uptake to the use of Tc-99m-octreotide derivatives for imaging neuroendocrine tumors. Owing to its multiple oxidation states, Tc-99m has a versatile chemistry, making it possible to produce a variety of complexes with specific desired characteristics, which is a major advantage of Tc-99m for radiopharmaceutical development. There are hundreds of Tc-99m complexes useful for diagnostic procedures, of which over thirty are used in clinical studies (Fig. 1).

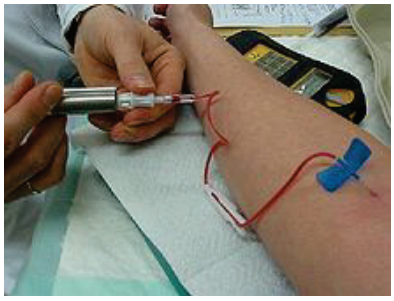

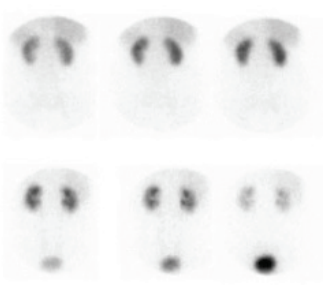

Fig. 1. A Tc-99m injection contained in a shielded syringe and the images obtained with 132MBq of Tc-99m-MAG3 and their corresponding renograms for both whole kidneys [8].

The results show that application of Tc-99m Human Serum Aalbumin nanocolloid decreases the activity and hence decreases the undesirable exposed dose to patient. Also, table 1 presents the effective whole body dose, during application various kits of Tc-99m for diagnosis of diseases.

Table 1. Maximum effective dose of Tc-99m kits exposed to patient (whole body).

Kit	Injected Activity (MBq)	Effective radiation dose whole body (mSv)
Tc-99m Human serum albumin nanocolloid	500	2.3
Tc-99m -MAG3	185	4.86
Tc-99m Human serum albumin	500	3.95
Tc-99m Albumin Macro aggregate	500	6.0
Tc-99m Albumin Miacrosphare	500	5.5

CONCLUSIONS

This research elucidate that the radiation risk can be reduced using nanoradiomedicines, without affecting the quality of the diagnostic information. Comparing the average dose to various organs in patients is necessary for various radio medicines and for calculation of effective dose equivalent and total effective dose, significant for an estimation of potential risk due to the administration of the radioactivity to a patient. Optimization of imaging instruments and using nano radio pharmaceuticals the exposed dose to patient will be decreased gradually.

REFERENCES

[1] Moonen M, Jacobsson L. Effect of administered activity on precision in theassessment of renal function using gamma camera renography. Nucl MedCommun. 1997;18:346 – 351.

[2] Vestergren E, Jacobsson L, Moonen M, Eklund I, Sixt R, Mattsson S.Administered activity ofTc-MAG3 for gamma camera renography inchildren. Nucl Med Commun. 1999;20:799 –806.

[3] Moonen M, Jacobsson L, Granerus G, Friberg P, Volkmann R. Determinationof split renal function from gamma camera renography: a study ofthree methods. Nucl Med Commun. 1994;15:704 –711.

[4] Mattsson S, Jacobsson L, Vestergren E. The basic principles in assessmentand selection of reference doses: considerations in nuclear medicine. RadiatProtDosimetry. 1998;80:23–30.

[5] Taylor A Jr, Eshima D, Fritzberg AR, Christian PE, Kasina S. Comparisonof iodine-131 OIH and technetium-99m MAG3 renal imaging in volunteers.J Nucl Med. 1986;27:795–803.

[6] Jafri RA, Britton KE, Nimmon CC. Technetium-99m MAG3, a comparisonwith iodine-123 and iodine-131 orthoiodohippurate, in patients with renaldisorders. J Nucl Med. 1988;29:147–158.

[7] Itoh K, Tskamoto E, Kakizaki H, et al. Phase II of Tc-99m-MAG3 in patients with nephrourologic diseases. Clin Nucl Med. 1993;18:387–393.

[8] Marlén P. Díaz, Eric E. Aparicio, Oscar D. Rizo, Reinaldo R. Díaz and Carlos H. Rodríguez. Tc-Administered Activity 99m-TcMAG3 optimization in Renography for Adults. 2003;31:216-221.J. Nucl. Med. Technol.

Patient Specific Dosimetry of 99m-Tc-MDP by SPECT/Planar Images and NCAT Phantom Using GATE

A. A. Parach[a]
S. Taghizadeh[a], **S. K. Razavi-Ratki**[b]

[a]Depatment of medical physics,Shahid Sadoughi university of medical sciences,Yazd, Iran
[b]Depatment of radiology,Shahid Sadoughi university of medical sciences,Yazd, Iran

Email address of Corresponding Author: aliparach@gmail.com

BACKGROUND

Bone scan is a nuclear medicine scan examination, which leads to find specific disorders in the bone. Methylene diphosphonate (MDP) is a common radionuclide used to bone scan. This combination absorbed by the bone tissue and excreted by the kidneys and bladder. Usually organ absorbed dose can be used by MIRD method that has some simplification that lead to underestimation or overestimation of organ absorbed dose or some methods used CT data for attenuation map that impose extra more dose to patients. The purpose of this study was to estimate the organ absorbed dose of patients under 99mTc_MDP bone scan by specific dosimetry method using NCAT phantoms and GATE Monte Carlo code and then compared with MIRD derived data.

METHODS

Twenty female patients who were referred to the Nuclear Medicine Department for bone disorders, were examined and two planar images and one SPECT image at 1, 3 and 5 hours after injection were taken, for every patient. The cumulative activity of each organ was obtained using the combination of SPECT/planar method. Then absorbed dose was calculated for each patient (for seven organs) by using the MIRD Method as well as the GATE Monte Carlo simulation code. The NCAT phantom (set to each patient data) was used as attenuation map in the GATE code simulation method.

RESULTS

Bladder, kidneys, ovaries, spleen, bone, liver, muscle, heart walls and lungs had the highest absorption dose, respectively, in both calculations performed by Mirdose Method and GATE code. According to the calculation of P_value, the most adaptation in calculating the absorption dose between the two methods is the spleen organ and the lowest match belongs to the lungs. Summary of patient's organ doses and comparison to other patients can be seen in Figure 1.

CONCLUSIONS

Since the women studied in this study had different diseases, bone disorders and biological characteristics, and some of them were metastases due to the disease, this led to a difference in the mean absorbed dose in their organs. In this study, Monte Carlo method based on NCAT phantom, which was set to each patient data, was used to calculate the absorbed dose of different organs of each patient and we can conclude that this method can be useful for patient specific dosimetry instead of some fixed anatomical data used in MIRD method.

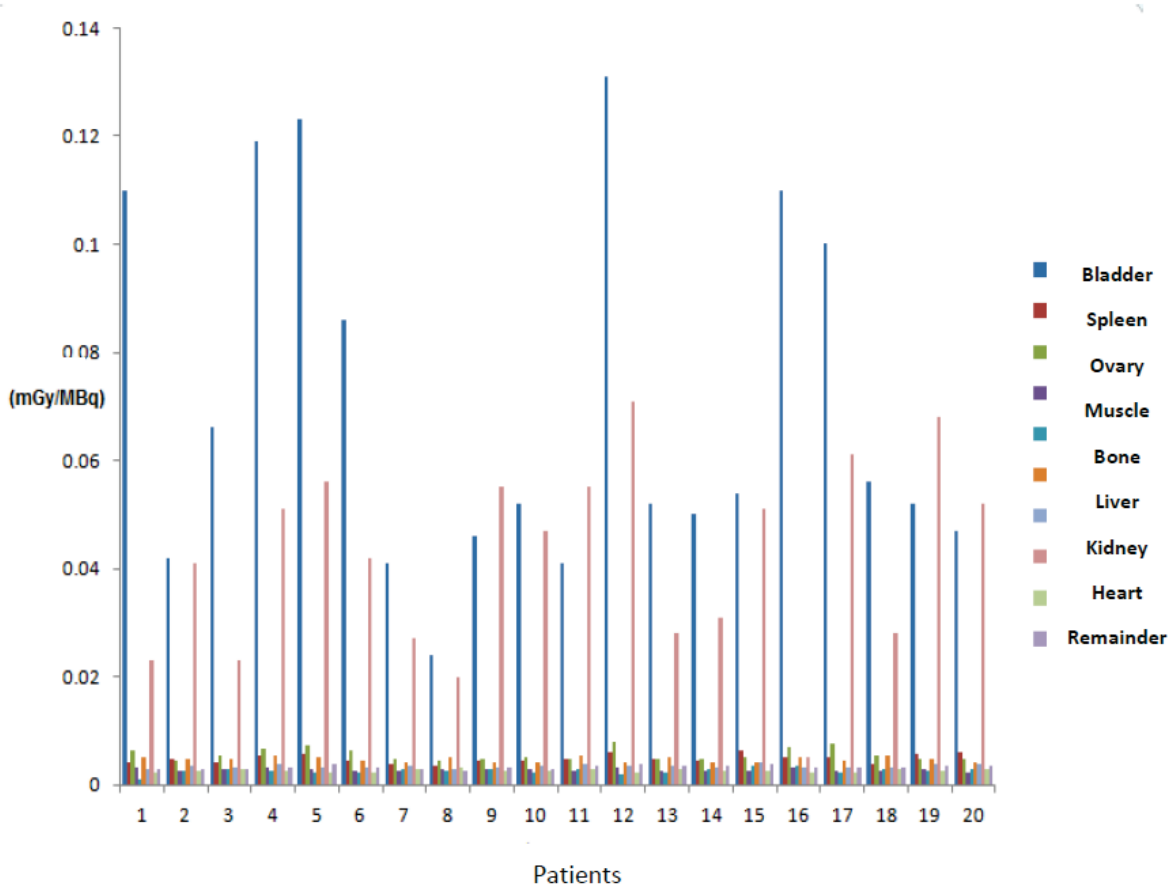

Figure1. difference between various organs of each patient and comparing to other patients.

REFERENCES

[1] ARORA S, DHULL VS, KARUNANITHI S, PARIDA GK, SHARMA A, SHAMIM S. 99m Tc-MDP SPECT/CT as the one-stop imaging modality for the diagnosis of early setting of Kienbock's disease. Revista Española de Medicina Nuclear e Imagen Molecular (English Edition). .7-185:(3)34;2015

[2] ZHAO Z, LI L, LI F, ZHAO L. Single photon emission computed tomography/spiral computed tomography fusion imaging for the diagnosis of bone metastasis in patients with known cancer. Skeletal radiology. 2010;39(2):.147

[3] HELAL N. Patient organs dose calculations in nuclear medicine. Int J Res Rev Appl Sci. 2012;11(1):.61-153

[4] RAVANBOD MR, NEMATI R, JAVADI H, NABIPOUR I, ASSADI M. Diffuse hepatic and spleen uptake of Tc-99m MDP on bone scintigraphy resembling liver-spleen scintigraphy in a patient of plasma cell tumor. Case reports in radiology. 2014;.2014

[5] ŞAHIN E, ELBOĞA U, KALENDER E. An Incidental Finding of Extraosseous Uptake in Technetium 99m Methylene Diphosphonate Bone Scintigraphy: Uterine Leiomyoma. Journal of Medical Imaging and Radiation Sciences. 2014;45(2):.3-141

[6] LU C-C, LIN H-H, CHUANG K-S, DONG S-L, WU J, NI Y-C, et al. Development and validation of a fast voxel-based dose evaluation system in nuclear medicine. Radiation Physics and Chemistry. 2014;104:355-9

Activity Quantification on Planar Imaging for an Animal SPECT Imaging System (HiRe SPECT)

H. Poorbaygi[a]
S. Namdarian [b], **A. Hadadi** [b], **M. Aboudzadeh**[a]

[a]Radiation Application Research School, Nuclear Science and Technology Research Institute, Tehran, Iran
[b]Radiation Application Research, School Science and. Research Branch, Islamic Azad University, Tehran

Email address of Corresponding Author: hpourbeigi@aeoi.org.ir

BACKGROUND

Nuclear medicine images can be used for quantitative tasks such as estimating organ absorbed dose and the quantification of radionuclide distribution has been a goal since the early days of nuclear medicine. The IAEA Human Health reports No.9 describes and analyses the physical effects that degrade image quality and affect the accuracy of quantification [1]. The quantitative of activity in animal gamma cameras leads to the acquisition of valuable information in this field, so it has recently been considered [2]. The high resolution animal SPECT imaging System (HiReSPECT, PNP Co., Incubation center for Medical Equipment and Device, Tehran, Iran) was established at the Nuclear Science and Technology Research Institute (NSTRI) [3]. It could be used on the development and research on production of radiopharmaceuticals. In this study, quantitative of activity is experimentally done on the planar images, which are related to the ^{99m}Tc imaging of small animal (mouse and rats) using HiRe SPECT system.

METHODS

In this research, experimental samples included images of Plexiglas phantom containing ^{99m}Tc in point and volume form. After selecting the planar images, the activity accumulation area (ROI) was determined and then then counting values were recorded. Finally, for the accuracy checking the results of calibration curve, an animal testing was performed on mouse with of ^{99m}Tc radiopharmaceutical. In this method for planar imaging, ROIs were defined for whole source into phantom from anterior and posterior views. Assuming a source located in a uniform medium, the attenuation of the count rate measured in the two projections can be described by the following equation:

$$A = \frac{\sqrt{C_A \cdot C_P}}{K \cdot e^{-\mu T/2} \cdot \dfrac{\sinh(\mu \cdot l/2)}{\mu \cdot l/2}}$$

Where C_A and C_P represent the anterior and posterior counts (cps), K is the sensitivity of air (cps per μCi), l is source thickness, μ is attenuation coefficient and T is the total thickness of the tissue.

RESULTS

Activity estimates were also made for two cylindrical sources included ^{99m}Tc syringes in dimeter of 1.5 cm and 2cm. Result of activity measurement (A2) and comparison with the real activity (A1) shown in figure 1. Animal testing was performed on mouse and Sulphur colloid labeled with ^{99m}Tc with activity of 463± 4% μCi was injected into the mouse by a syringe. The planar imaging was performed for 600 seconds after an hour of the injection, and the anterior and posterior images of the animal (abdominal region and liver) were obtained. In figure 2, the

accumulation of radioactive in the mouse liver shown with the target area (FOV) of 5 *10 cm^2. The thickness of the rat liver area (l) was 1.8 cm and the total thickness was 3.4 cm (T). The activity estimation parameters from the anterior and posterior planar images are listed in Table 1.

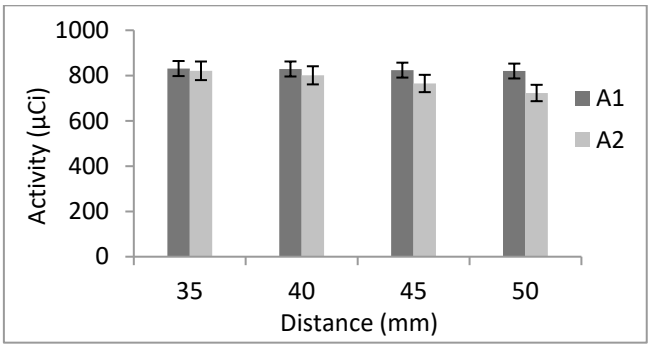

Figure 1. Comparison of activity measurements for a volumetric source with thickness of 2cm and a phantom thickness of 3.6 cm X ray tube.

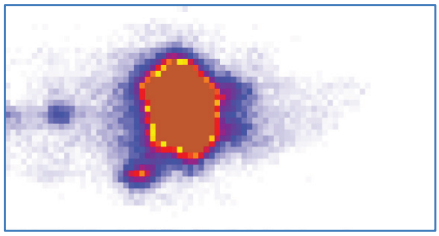

Figure 2. Drawing of ROI on planar image for the 99mTc labeled radiopharmaceutical in the mouse liver

Table 1. Estimation of activity for the rat liver by planar imaging

Collimators distance	T	l	C_A	C_B	K	Estimated activity	Real activity
45mm	3.4cm	1.8 cm	386cps	378cps	0.95	520 µCi	463µCi

CONCLUSIONS

In this research, the sensitivity coefficients and relative percentages of estimated activity were studied in the planar image for small animal (mouse and rat). The results indicated that with respect to spot sources, the "opposite views" method was closely associated with a high degree of precision (relative difference about 1-7%). In case of volumetric source, this difference is about 10-14%.

REFERENCES

[1] INTERNATIONAL ATOMIC ENERGY AGENCY, Quantitative Nuclear Medicine Imaging: Concepts, Requirements and Methods, IAEA Human Health Reports No. 9, Vienna, (2014).

[2] CHAO W., et. al. , Absolute quantitative total-body small-animal SPECT with focusing pinholes Eur. J. Nucl. Med. Mol. Imaging, 37, p.2127–2135,(2010)

[3] S. SAJEDI, S., et al. , Design and development of a high resolution animal SPECT scanner dedicated for rat and mouse imaging, Nucl. Instr. Meth. Phys. Res. A, 741, p.169–176,(2014).

Radiation Protection

Calculation of the Dose Received by Occupationally Exposed Workers in the Radiotherapy Service of the Hospital "V. I. Lenin."

F. Pérez González[a]
R. Velázquez Cruz[b], O. Fornet Rodríguez[c], P. Borjas Hernández[a]

[a]Provincial General Teaching Hospital of Holguín "V. I. Lenin ". Ave. Lenin No 2 Holguín.
[b]Center of Investigations and Environmental Services of Holguín. 18 St. and Maceo. Holguín.
[c]Territorial Delegation CITMA Holguín. Peralta St. No16. Holguín.

Email address of Corresponding Author: franciscopg@infomed.sld.cu

BACKGROUND

The biological effects of exposures to low doses of ionizing radiation are still under study. The probability of a stochastic effect attributable to radiation increases with the dose and probably, at low doses, is proportional to the dose [1]. The acquisition of reliable data on the low dose to which statistically significant amounts of individuals are exposed under controlled conditions is an important element to continue advancing in this area.

Among the practices in which you can make a real assessment of this issue is Radiotherapy with cobalt sources [2], because the dose rates to which the staff is exposed and the time they are exposed are very accurately known and an individual and area monitoring is established as part of good practice and of radiological safety regulations.

METHODS

In the present work is evaluated, for the different functions exercised by the Occupational Exposed Workers of Cobaltotherapy at the "V. I. Lenin " hospital, the result of the whole body individual dosimetry (Hp (10)), for a five years period, with thermoluminescent dosimeters (TLD), provided monthly, by the Secondary Laboratory of Dosimetry of the national Center for Protection and Radiations Hygiene.

This analysis is complemented with the calculations coming from the area dosimetric monitoring carried out with its own equipment, by the Radiological Protection Service of the Hospital, by a specialized external service and by the results of the area monitoring that as part of the regulatory inspections, the Regulatory Authority performs in matters of radiological safety.

RESULTS

As a result of the work it is demonstrated that the individual dosimetry with TLD only allows to know the dose received monthly, when this is higher than the detection threshold of the method and at the level of registration approved in the country (0.1 mSv), and have obtained the values of the doses received by all the Occupational exposed staff of the service, grouped by functions they perform and by years, during the five-year period, mainly, by means of calculations based on the values of the area monitoring, and in those cases in which they exceed the registration level, by the reported readings of the TLD, which allows their absolute assessment, as well as their comparison with the dose restriction and the established dose limit.

CONCLUSIONS

The analysis made, allows us to conclude that it is advisable, under controlled conditions of exposure, in order to obtain quantifiable periodic dose values, that the Secondary Laboratory Service, report the dose received in the dosimeter above the level of registration of received doses and maintain strict dosimetric monitoring of area and control of personnel exposure time, so that reliable dose values could be available to investigate non-conformities in the implementation of work procedures and to act in response to these irregularities, as well as with a view to correlating the doses received in the event of long-term manifestations of health effects of the exposed workers.

REFERENCES

[1] INTERNATIONAL COMMISSION ON RADIOLOGICAL PROTECTION, Publication 105. Radiological Protection in Medicine. Sociedad Argentina de Radioprotección. 2007

[2] INTERNATIONAL ATOMIC ENERGY AGENCY. Evaluation of occupational exposure due to external sources of radiation. Safety Reports Series No. 38 Vienna, 2004.

[3] INTERNATIONAL ATOMIC ENERGY AGENCY Applying Radiation Safety Standards in radiotherapy. Vienna, 2006.

[4] INTERNATIONAL ATOMIC ENERGY AGENCY. PROTECCIÓN RADIOLÓGICA OCUPACIONAL. Colección de Normas de Seguridad No RS-G-1.1. Viena. 2004.

Active Personal Dosemeter Response for Non-Standard 100 kV X-ray Beams

N. Krzanovic
O. Ciraj-Bjelac, M. Zivanovic

Vinca Institute of Nuclear Sciences, University of Belgrade, M. P. Alasa 12-14, Vinca, Serbia

Email address of Corresponding Author: krzanovic@vinca.com

BACKGROUND

The medical sector is one of the major users of ionizing radiation sources that requires special attention in terms of patient and occupational radiation protection. Accurate dosimetry is an essential part of effective radiation protection. Use of active personal dosimeters (APDs) is extremely useful in occupational radiation protection in diagnostic and interventional radiology, owing the fact that scatter radiation from patients is a major source of occupational exposure. APDs allow immediate dose information (in terms of Hp(10)) with an additional audio alarm if a certain dose or dose rate level has been exceeded. In laboratory conditions, these dosimeters are calibrated in the standard radiation quality series (N-series) [1]. As these dosimeters are used in a clinical environment, it is important to test the performance of the APDs in various non-standard radiation fields, typical for clinical conditions.

METHODS

The tested dosemeter is an EPD Mk2.1, Thermo Fisher Scientific, which has already been tested in different standard beam qualities, such as S-Co, S-Cs and N-series [2]. EPD Mk2.1 has shown good performance according to the criteria set by IEC 61526 [2,3]. The reference radiation quality chosen for this research is the N-100. The APD response was calculated as the quotient of the APD indication in various non-standard beam qualities to that in the reference beam quality. An ionization chamber 32002 with electrometer Unidos (PTW, Freiburg, Germany) was used as a reference standard. Radiation beam qualities used are presented in Table 1. The APD and the ionization chamber were placed at 300 cm source to point of test distance, following the standard radiation protection dosemeter calibration procedure [1]. The EPD was mounted on a standard ISO water slab phantom, and was irradiated for 30 s, for each radiation quality.

Table 1. Radiation qualities used for the EPD response testing.

Beam number	Radiation quality	Total filtration [mm]	Half value layer [mm Cu]	International Standard [1,4]
1	N-100	4.0 Al + 5.0 Cu	1.13	IAEA SRS 16
2	/	0.4 Al + 5.0 Cu	1.12	/
3	/	4.0 Al + 2.0 Cu	0.84	/
4	/	4.0 Al + 2.5 Sn	1.29	/
5	RQR8	3.5 Al + 0.4 Al	0.15	IAEA TRS 457
6	/	3.5 Al + 4.0 Al	0.26	/
7	RQT8	3.5 Al + 0.4 Al + 0.2 Cu	0.33	IAEA TRS 457
8	/	3.5 Al + 4.0 Al + 0.2 Cu	0.40	/

RESULTS

In Figure 1, the results of the APD response deviation due to the variation of the total beam filtration for the X-ray tube voltage of 100 kV are presented.

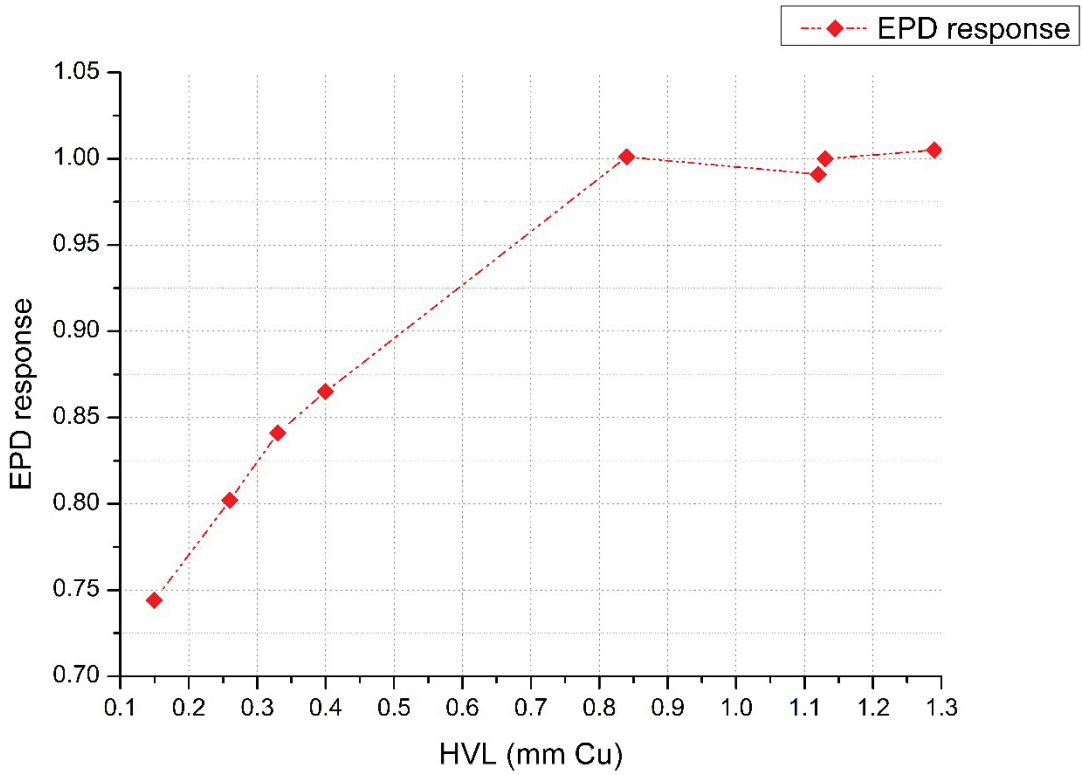

Figure 1. Relative APD response normalized to the response value measured for the N-100, whose HVL = 1.13 mm Cu.

CONCLUSIONS

The APD tested in this paper, displayed an under-response for the X-ray beams whose total filtration had reduced or no copper filtration, with a maximum deviation from the N-100 radiation quality of approximately -25% (the TRS457 RQR8 quality). The APD response deviation greatly increases as the HVL declines, relative to the N-100 response value.

REFERENCES

[1] *Safety Report Series No. 16 Calibration of Radiation Protection Monitoring Instruments,* International Atomic Energy Agency, Vienna, 2000.

[2] Krzanovic, N., Zivanovic, M., Ciraj-Bjelac, O., Lazarevic, Dj., Ceklic, S., Stankovic, S. Performance testing of selected types of electronic personal dosemeters in X- and gamma radiation fields. Health Physics. 113, 252-261 (2017). DOI: 10.1097/HP.0000000000000704.

[3] International Electrotechnical Commission. Radiation protection instrumentation - Measurement of personal dose equivalents Hp(10) and Hp(0,07) for X, gamma, neutron and beta radiations - Direct reading personal dose equivalent meters, IEC 61526; 2010.

[4] *Technical Report Series No. 457 Dosimetry in Diagnostic Radiology: An International Code of Practice,* International Atomic Energy Agency, Vienna, 2007.

Assessment of Internal Radiation Dose Due to Intake of Iodine-131 for Radiation Workers in Nuclear Medicine in Vietnam

Q. H. Nguyen[a]

[a]Vietnam Agency for Radiation and Nuclear Safety – VARANS

Email address of Corresponding Author: nqhuong@most.gov.vn, nqhuong.vr@gmail.com

BACKGROUND

In accordance with Vietnamese Laws, the need for individual assessment of internal radiation dose must be conducted when there is a risk of radioactive substances entering the body or of skin contamination. Individual assessment of internal radiation dose must generally be arranged in at least the following duties involving use of radiation:

- Work in laboratories with unsealed sources;

- Handling of radioactive substances in an easily volatile or dusty form, and in quantities that are significant for radiation exposure;

- Handling of unsealed sources containing iodine isotopes (especially I-131, I-125 and I-123) in quantities that are significant for radiation exposure;

- Work in rooms where radionuclides or radio-pharmaceuticals are manufactured.

To determine the committed effective dose or the equivalent dose to some organ due to internal radiation, the activity of radioactive substances in the body is measured directly from the body, from a part thereof, or from excretions thereof, and the dose is estimated from the measurement result.

The assessment of internal radiation dose caused will help to decide on any further actions warranted by the incident and on optimization of radiation protection measures.

Due to technical difficulties, in Vietnam, the assessment of internal radiation dose has been conducted in small scale, mainly focused on the workers handling iodine radiopharmaceutical. Two methods for determination of internal dose due to intake I-131 during the preparation and handling of iodine radiopharmaceutical products have been compared. The first method was based on the measurement of I-131 in 24-hour urine samples while the second method was based on the measurement in vivo of I-131 in thyroid. This report will present the procedure and result of the assessment of internal radiation dose from iodine-131 for radiation workers in nuclear medicine in Vietnam by the method of analyzing urine samples.

METHODS

Urine Sampling Procedures

- Twenty-four hours after handling I-131 radiopharmaceutical, the workers urinate on a 0.5-liter plastic can;

- Treat urine with formaldehyde solution to prevent urine from decomposing;

- Take 40 ml of urine into a plastic bottle, plastic bottle be designed with cylindrical (40 mm of diameter and 35 ml of volume);

- Determination of activity of urine samples in Low Resolution Gamma Spectra. Measurement time is from 1000 to 10000 seconds.

Method of Calculation of Internal Dose

Biokinetics and energy deposition enables to define an estimate of internal dose due to intake I-131 by the following expression

$$E = e(50)*Intake$$

In which: **E [Sv]** is an estimate of internal dose due to intake I-131; **e(50) [Sv/Bq]** is the dose coefficient per unit intake and it depends on the radionuclide, the chemical form of the radionuclide, the intake pathway, the age at intake; **Intake [Bq]** is retained/excreted activity.

$$Intake = A0/m(t)$$

In which: **m(t) [Bq/Bq of intake]** is model prediction; **A0 [Bq]** is the activity of the sample at the time of sampling.

$$A0 = A*e^{(0.693*t/8.04)}$$

In which: **A [Bq]** is activity of the sample at the time of measuring defined by Low Resolution Gamma Spectra.

m(t) and **e(50)** could be obtained from ICRP Publication 119, 78 and 54

RESULTS

Table 1. The estimation of internal dose due to intake I-131 in 2017 and 2018

No.	ID of Worker	Internal dose due to intake I-131 in 2017 (mSv)	Internal dose due to intake I-131 in 2018 (mSv)
1	IN_DOSE_1	4.351	0.449
2	IN_DOSE _2	1.872	1.112
3	IN_DOSE _3	1.996	0.983
4	IN_DOSE _4	1.618	1.757
5	IN_DOSE _5	4.290	3.455
6	IN_DOSE _6	2.434	2.037
7	IN_DOSE _7	5.611	2.183
8	IN_DOSE _8	4.148	2.274

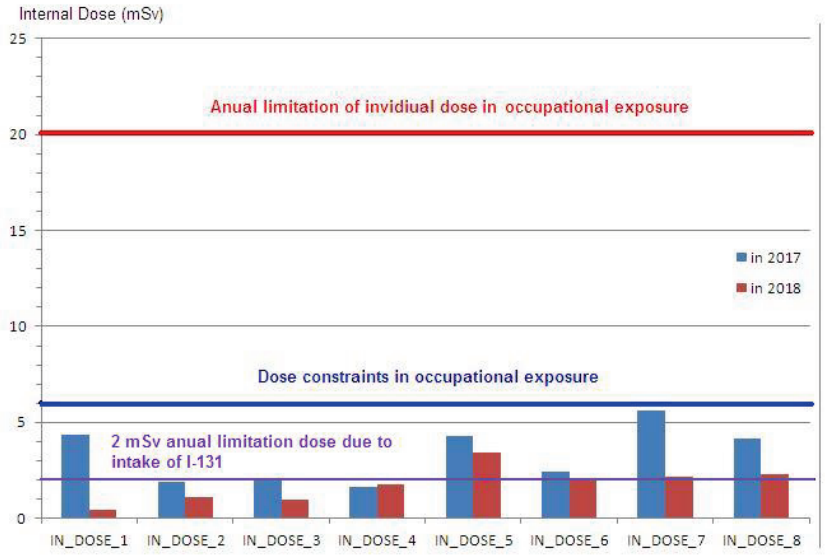

Figure 1. The comparison of internal dose due to intake I-131 in 2017 and 2018 with limitation doses

CONCLUSIONS

- Internal doses for the nuclear medicine workers in Vietnam have been assessed on the basis of urine activity measurement data of I-131;

- The internal radiation dose from iodine-131 for radiation workers was detected in all of nuclear medicine hospitals surveyed in 2017 and 2018;

- The internal dose by inhalation of I-131 contributes significantly to total dose of workers (approximately 30%);

- 5 workers (in 2017) and 4 workers (in 2018) have been expected to exceed 2 mSv resulted from an annual intake of I-131. The internal radiation doses from iodine-131 of 4 workers have almost reached the dose constraints in occupational exposure in 2017;

- Monitoring internal dose by inhalation or ingestion of radionuclides is an urgent requirement in Vietnam today.

REFERENCES

[1] IAEA, General Safety Guide No. GSG-7, Occupational Radiation Protection (2018)
[2] IAEA, Safety Reports Series No. 37, Methods for Assessing Occupational Radiation Doses Due to Intakes of Radionuclides (2004)

Determination of T(3; $^{90}Sr^{90}Y$; 0°) for the Calculation of $H_p(3)$ in Beta Radiation

J. T. Alvarez R[a]
M. R. Cabrera V[a]

[a]SSDL, ININ, carretera Federal Mexico Toluca S/N, La marqueza, Ocoyoacac, Mexico, 52750

Email address of Corresponding Author: trinidad.alvarez@inin.gob.mx

BACKGROUND

It is well known that the dosimetric quantities of effective dose E and the organ equivalent dose H_T of the ICRP/ICRU dose limitation systems are not measurable quantities, [1]. Therefore, the ICRU proposed to develop a system of operational quantities for area and individual monitoring. For the case of beta radiation fields, the operational quantities of personal dose equivalent for the skin $H_p(0.07)$ and $H_p(3)$ for the lens of the eye are realized by the use of a primary extrapolation ion chamber standard and BSS1 or BSS2 radiation sources [2].

In the case of the 3 mm deep lens inside the eye, the appropriate dosimetric quantity is the personal equivalent dose at a depth of 3 mm: $H_p(3)$, defined as: [3]

$$H_P(3) = h_{p,D}(3;\ source;\alpha) \cdot D_{R\beta} \cdot (1 - \tau_{br})$$

Where:

$$h_{p,D}(3;\ source;\alpha) = T(3;\ source;0°) \cdot R(3;\ source;\alpha)$$

Being $T(3;\ source;0°)$ the transmission factor at a 0° angle of the source and d = 3 mm; and $R(3;\ source;\alpha)$ the complement of the transmission factor at depth d = 3 mm and angle α.

METHODS

To determine $T(3;\ source;\ 0°)$, we have:

$$T(3;\ source;\ 0°) = I(3;\ source;\ 0°)\ /\ I(0.07;\ source;\ 0°)$$

The measurement of the ionization currents are made with an extrapolation ion chamber, and they are corrected for air density k_{ab}. $T(3;\ ^{90}Sr^{90}Y;\ 0°)$, corresponding to the 90Sr/90Y 1850 MBq source, is only determined at a distance of 30 cm and 0°, without the use of the homogenizer filter of the BSS1 standard. The main idea is to extend the range of validity of the correction k_{ab} as indicated in the ISO 6980 part 2 [3]. In fact, the SSDL-ININ is located at an altitude of 3000 m above sea level, further the range of thicknesses have to be covered the 3 mm of the lens is considered. To correct for these differences in environmental conditions and attenuation, the correction c_{abs} for the transmission factor is calculated as:

$$c_{abs}\,(d) = \frac{T(d')}{T(d)}$$

$T(d')$ is calculated for the environmental conditions of the SSDL-ININ and $T(d)$ is for the reference environmental conditions for an air density of ρ_0.

The deviation in air density ρ_{air} of the SSDL-ININ from the reference air density ρ_0 is interpreted as the addition (for $\rho_{air}>\rho_0$) or subtraction (for $\rho_{air}<\rho_0$) of a small layer of ICRU tissue in front of the extrapolation chamber. The total thickness considering this small layer d is given by: [4]

$$d = d_{t,abs} + d_{t,entr} + d_{t,air,1} + d_{t,air,2}$$

Where: $d_{t,abs}$ is the thickness of the PMMA sheet which represents the depth of the lens of the eye; $d_{t,entr}$ is the extrapolation chamber window thickness; $d_{t,air,1}$ is the thickness of the layer of air given by the deviation in air density between the beta source and the chamber; and $d_{t,air,2}$ is the thickness of the layer of air at the effective point inside the cavity of the extrapolation chamber.

RESULTS

For the determination of the value of the $T(3; {}^{90}Sr{}^{90}Y; 0°)$ transmission coefficient from the ionization current measurements, the following regression equation $T(d)$ vs d with a polynomial of order 3 was obtained:

$$T(d) = 0.973046 + 0.380402\, d - 0.331645\, d^2 + 0.048344\, d^3$$

CONCLUSIONS

The most probable value for $T\left(3; {}^{90}Sr{}^{90}Y; 0°\right)$ is: **0.5049 ± 0.0243,** with uc(k=1), for a source-detector distance of 30 cm for the SSDL-ININ; which is 5.7% higher than that reported by Behrens: $T\left(3; {}^{90}Sr{}^{90}Y; 0°\right)$ = **0.4759 ± 0.0048** U(k=2) in [2]. However, the range of ININ's value contains the Behrens's value. The variables that affect the value of $T(3; source; 0°)$ are as follows: the energy of the radiation source; SDD distance; environmental conditions; the effective thickness of the absorbers. It is likely that a better characterization of the density and thickness of the absorbers is the main assignable cause of the deviation.

REFERENCES

[1] INTERNATIONAL COMMISSION ON RADIOLOGICAL PROTECTION, Conversion Coefficients for use in Radiological Protection against External Radiation, ICRP Publication 74, Annual ICRP **26**, (1996) 1

[2] BEHRENS R. AND G. BUCHHOLZ. Extensions to the Beta Secondary Standard BSS 2 Consolidated version from www.ptb.de; Version 1.4; 2015-02-122, Physikalisch-Technische Bundesanstalt (PTB), https://www.ptb.de/cms/fileadmin/internet/fachabteilungen/abteilung_6/6.3/f_u_e/bss2cons.pdf, (last access: 12/12/2017)

[3] ISO 6980-2:2004 Nuclear energy -- Reference beta-particle radiation -- Part 2: Calibration fundamentals related to basic quantities characterizing the radiation field, Geneve (2004)

[4] BRUZENDORF AND JENZ, Determination of depth–dose curves in Beta Dosimetry, Radiation Protection Dosimetry, **151**, (2012) 203

Influence of the Protection Screen Positioning on the Eye Lens Dose for Staff Involved in Interventional Procedures: A Monte Carlo Study

P. Bozovic
O. Ciraj-Bjelac, J. S. Petrovic, A. Kojic

Vinca Institute of Nuclear Sciences, University of Belgrade, M.P. Alasa 12-14, Vinca, Serbia

Email address of Corresponding Author: bozovic@vinca.rs

BACKGROUND

The radiation doses to the staff involved in interventional procedures are significantly higher than the exposure of staff performing common diagnostic procedures due to increase in both the number of procedures performed worldwide as well as in complexity and duration of exposure time of a single procedure. This fact requires specific attention in terms of occupational radiation protection in interventional cardiology and interventional radiology. A new dose threshold for tissue reactions also resulted in a reduction in the annual dose limit for eye lens from 150 mSv to 20 mSv [1]. In the context of this new dose limitation, there is evidence that the dose limit may be exceeded for certain groups of health professionals if appropriate personal and collective protective tools are not used, or if the use of these devices is not adequate [2, 3]. Consequently, dosimetry for eye lens has become an important research topic to the radiation protection scientific community.

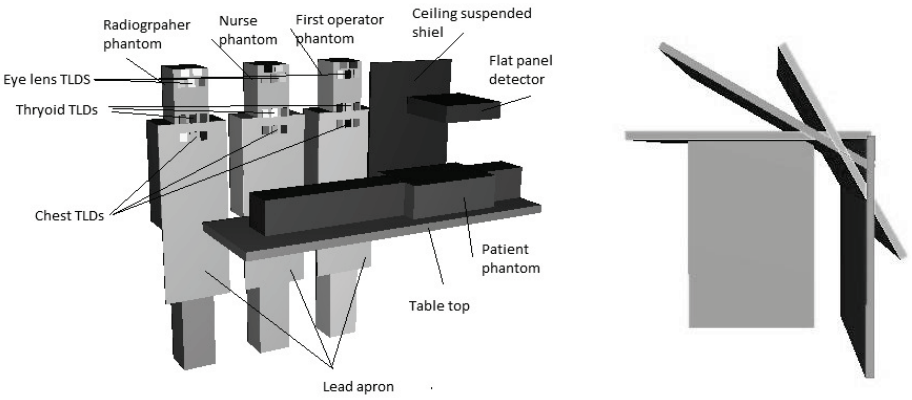

Figure 1. Radiation beam qualities with first and second HVLs.

METHODS

Simulations were performed using Monte Carlo code MCNPX. X-ray tube was modeled as a photon point source directed in cone of beams and photon spectrum was obtained from the Spectrum processor described in IPEM Report 78 for 80 and 110 kV tube voltages. Distance from source position to the flat panel detector positioned above the source was 120 cm with tabletop placed in the middle of that distance. All operators and patient bodies were modeled as a 180 x 40 x 20 cm^3 phantom of muscle tissue which consisted of head, torso and legs sections. Ceiling suspended shield was modeled as a 85 x 60 x 2 cm^3 rectangular plate made from lead glass. Five simulated TLDs, modeled as 5 x 4 x 1 cm^3 block filled with ^{6}LiF, were positioned in front of the eyes (one is placed between eyes, two on the outside and two above the eyes). Influence of the ceiling suspended shield on reduction of eye lens doses was evaluated for four positions (Figure 1 right): parallel with patient body (0° rotation), two

intermediate positions (30° and 60° rotation) and perpendicular to the patient body (90° rotation). Results of the simulations were obtained using F6 tally.

RESULTS

Table 1 present reduction factors for the left and right eye lens dose for positions of the first operator, nurse and radiographer, respectively for different positions of the ceiling suspended shield.

Table 1. Efficiency of radiation protection tools for the left and right eye of staff for different angulation of and tube voltages.

Screen position	Screen angle	Tube voltage	Physician		Nurse		Radiographer	
			Left eye lens	Right eye lens	Left eye lens	Right eye lens	Left eye lens	Right eye lens
1	0°	80	52	1.6	1.0	1.0	1.0	1.0
		110	60	3.8	1.1	1.0	1.1	1.0
2	30°	80	129	87	12	11	3.7	2.8
		110	114	100	21	12	3.7	3.4
3	60°	80	4.3	36	13	12	4.1	3.7
		110	4.0	33	23	13	4.1	4.6
4	90°	80	1.0	4.3	12	12	4.1	3.7
		110	1.0	4.2	22	13	4.1	5.1

CONCLUSIONS

It is important to underline that the ceiling suspended screen is primarily effective for the first operator. Using only one protective screen leaves positions of the nurse and radiographer less protected Employing an additional suspended ceiling shield significantly reduces the dose to the eye lenses of the second and third operator by the factor similar to those for the first operator, as shown in Table 1.

REFERENCES

[1] DIRECTIVE, E.C., Laying down basic safety standards for protection against the dangers arising from exposure to ionizing radiation, Final version of the proposal, based on the Article **31** (2013)

[2] VANO, E., et al., Radiation cataract risk in interventional cardiology personnel, Radiation research **174** 4 (2010) 490-495.

[3] CIRAJ-BJELAC, O., et al., Occupational exposure of the eye lens in interventional procedures: how to assess and manage radiation dose, Journal of the American College of Radiology **13** 11 (2016) 1347-1353.

Occupational Radiation Monitoring at the Clinica Las Condes Hospital: A Seven Years Follow-Up Study

J. Rodriguez

Clinica Las Condes, Estoril 450, Las Condes, Santiago, Chile

Email address of Corresponding Author: fmjlrp@yahoo.com

BACKGROUND

Safety culture, in the field of Radioprotection, is a concept that increasingly is part of the daily work of institutions that use ionizing radiation and a very important element to be taken into account by those responsible for their radiological protection [1], and the Radiological Protection Program is an intrinsic part of this culture.

A Radiological Protection Program includes different aspects that must be taken into account in its implementation: the shielding of sources and facilities, radiological surveillance, the personnel that work in these facilities and training [2]. Monitoring the results of the personal dosimetry of all Occupationally Exposed Workers (OEW) is the main indicator of the effectiveness of radiological protection in a given institution.

In Chile, the Ministry of Health has established, through Supreme Decrees No. 3/85 and No. 133/84, the radiological surveillance of TOE [3, 4]. On the other hand, the Institute of Public Health of Chile, in its ordinary 1893 of the year 2010, regulates that only the doses that reach or exceed 0.1 mSv will be registered, expressing any value below this as “MRL” (Minimum Registration Level) [5].

The objective of this work was to evaluate the behavior of the effective dose values, to the whole body, that workers of Clínica Las Condes received during the last 7 years (2012-2018) and in this way, to verify the impact that the implementation has had of the Radiological Protection Program in Clínica Las Condes.

METHODS

The occupationally exposed workers of the services that use ionizing radiations were taken into account in an important way, the quarterly record was kept for seven years of the doses reported.

To optimize the statistical management of the values to be analyzed, a database was created where the demographic, labor and quarterly dosimetries of each of the workers participating in this study were recorded.

The variables that were followed in this study were: The number of workers occupationally exposed by service, the annual average of equivalent dose or Hp(10) per service, the number of workers whose annual dose did not exceed 0.1 mSv in each service and the totals of the institution for each of the years analyzed.

RESULTS

The DosPerCLC database was elaborated using the Microsoft Access tool (Microsoft Corp.) where all the data of each of the workers under radiological surveillance of the institution were recorded with the possibility of obtaining all the statistical data for immediate and posteriori analyzes.

Around 513 workers per year were in the radiological surveillance program with personal dosimetry between 2012 and 2018 with an average dose of 0.13 mSv per year. Table 1

Table 1. Dosimetric data

	Average	**2012**	**2013**	**2014**	**2015**	**2016**	**2017**	**2018**
Dose (mSv)	**0,13**	0,16	0,13	0,11	0,13	0,14	0,15	0,09
Workers	**513**	411	462	475	523	546	610	566
Nº MRL value annual	**397**	300	359	368	413	431	436	474
% MRL	**77**	73	78	77	79	79	71	84

CONCLUSIONS

Through the results it can be seen that the workers in Clinica Las Condes work in a safe environment, since in general the average dose was 0.1 mSv, that is 10 times less than the allowable dose for the general public (1 mSv) according to ICRP 103 [6]. The implementation of the Radiological Protection Program at Clinica Las Condes has fulfilled its objective, in the sense of keeping the doses of workers as low as possible.

It is possible, from the retrospective analysis of the dose values reported, to monitor the impact of radiological surveillance of a given institution, leaving open the possibility of a more global review in a multicenter study and thus assess the impact to country level of existing policies on Radiological Protection.

REFERENCES

[1] INTERNATIONAL RADIATION PROTECTION ASSOCIATION. Guiding Principles for Establishing a Radiation Protection Culture. International Radiation Protection Association (IRPA). Edition 2014.

[2] INTERNATIONAL ATOMIC ENERGY AGENCY. Radiation protection and safety of radiation sources: international basic safety standards. STI/PUB/1578. Vienna. International Atomic Energy Agency, 2014.

[3] MINISTERIO DE SALUD. REPÚBLICA DE CHILE. “Reglamento de protección radiológica de instalaciones radiactivas” (Regulation of radiological protection of radioactive facilities). Decreto Supremo Nº 3 de 1985.

[4] MINISTERIO DE SALUD. REPÚBLICA DE CHILE. “Reglamento sobre autorizaciones para instalaciones radiactivas o equipos generadores de radiaciones ionizantes, personal que se desempeña en ellas, u opere tales equipos y otras actividades afines” (Regulation on authorizations for radioactive facilities or ionizing radiation generating equipment, personnel who work in them, or operate such equipment and other related activities). Decreto Supremo Nº 133 de 1984.

[5] INSTITUTO DE SALUD PÚBLICA DE CHILE. Ordinario 1893. 23 de Diciembre de 2010.

[6] INTERNATIONAL COMMISSION ON RADIOLOGICAL PROTECTION. The 2007 Recommendations of the International Commission on Radiological Protection. ICRP Publication 103. Ann. ICRP 37 (2-4), 2007.

^{131}Iodine Routine Monitoring Program: Ten Years Evaluation

M. Terán[a]
L. Fernández[a], **J. C. Hermida**[b]

[a]Universidad de la República, Facultad de Química, Área Radioquímica, Av. Gral. Flores 2124 Montevideo Uruguay.
[b]Centro de Medicina Nuclear e Imagenología Molecular. Hospital de Clínicas. Av. Italia s/n.

Email address of Corresponding Author: mterangretter@gmail.commailto:myemail@domain.com

BACKGROUND

The Centre of Nuclear Medicine and Molecular Imaging of the University Hospital (CMNIM) jointly with the Radiochemistry Department of the Faculty of Chemistry settled the Internal Dosimetry Laboratory (IDL) in 2004. This group works both in monitoring potential internal contaminations with 131-Iodine in occupationally exposed personnel (OEP) due to the manipulation of open sources for therapy purposes and performing individualized dosimetry in patients treated with ^{131}I and ^{177}Lu [1]. In the framework of the IAEA Technical Cooperation Project RLA9075 entitled "Strengthening of the national infrastructure for compliance with regulations and requirements regarding radiological protection for end users", the IDL received a donation of a Captus 3000 (Capintec) equipment in 2008. This allowed the group to perform the monitoring according to the ICRP requirements. Taking into account that the CMNIM provides 260 GBq of ^{131}I per year with ^{131}I therapy, the aim of this work is to analyse the evolution of the Effective Committed Dose E (50) of technicians, physicians, radiopharmacists and nursing staff since 2008 to date.

METHODS

The protocol was developed in the framework of the ARCAL RLA/09/049 [2]. The methodology consisted in the following steps:

a) Calibration of the detection system Captus 3000 (Capintec) NaI (Tl) 2x2'' detector.

1. Energy calibration with reference sources of ^{137}Cs and ^{152}Eu

2. Efficiency calibration with ^{133}Ba reference sources provided by IRD (Brazil). The radionuclide was embedded in Whatman 1 paper with the shape of a thyroid supported in a tissue equivalent material simulating a neck.

3. Determination of the minimum detectable activity (AMD) according to the formula:

$$AMD = \frac{4.65\sigma f}{\eta} + \frac{3}{\eta T}$$

Where σf is the error of the background
η is the efficiency of the detector
T is the time measurement

4. Determination of counting accuracy.

b) Measurement of the OEP neck at 25 cm distance from the detector, 300 seconds, fortnightly.

c) Effective committed dose estimation E (50) considering fast inhalation route, an AMD of 5 µm, a Retention Fraction m (t): 7.41×10^{-2} and a Dose Coefficient e (g): 1.1×10^{-8} Sv/Bq [3].
d) Report of the results to the OEP and the Regulatory Authority.

RESULTS

The derivate registration and investigation limits were settled in 1 (yellow) and 5 (red) mSv/year respectively. Figure 1, shows the measurements results of E(50) in the period 2008-2018 in full blue line, the upper and lower control lines (dotted purple lines)were settled in ± 3σ of the average doses (green).

Figure 1: E (50) values 2008-2018

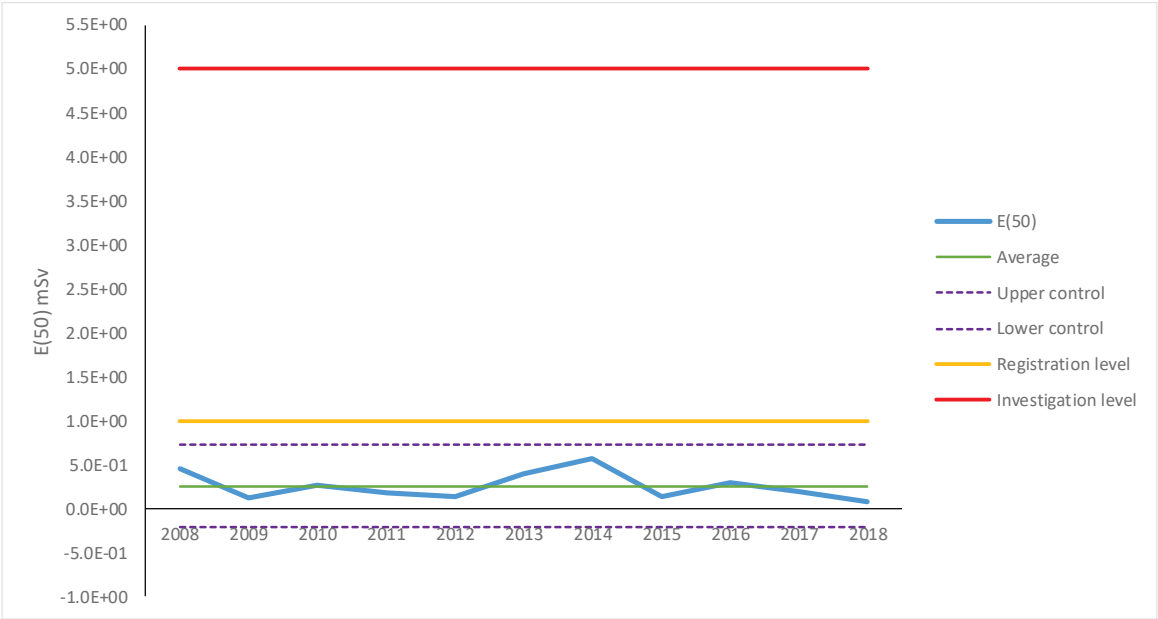

CONCLUSIONS

The implementation of the program reached the 46% of the OEP involved in the manipulation of ^{131}I open sources in the Nuclear Medicine area. The method was robust and easy to implement in routine. The IDL participated in three regional intercomparisons promoted by the IAEA achieving excellent results, which confirms the accuracy of the measuring protocols. The E (50) values were always below the registration levels, nevertheless they are submitted to the Regulatory Authority who keeps a national dose registry. Despite the high amounts of ^{131}I delivered doses, E (50) presents low values. This program is seen as an opportunity of continuous improvement in optimization of the practice and education of the OEP in Nuclear Medicine area.

REFERENCES

[1] INTERNATIONAL ATOMIC ENERGY AGENCY VIENNA General Safety Requirements Part 3 ISBN 978–92 –0–135310–8 ISSN 1020–525X14
[2] ICRP, 1994. Dose Coefficients for Intakes of Radionuclides by Workers. ICRP Publication 68. Ann. ICRP 24 (4).
[3] PR/ARCAL LXXVIII/04 ARCAL RLA/09/049.Procedimiento para determinación *in vivo* de radionucleidos en el cuerpo humano (2005).

Determination of the Effective Dose in a Radiotherapy Bunker

M. Castrillón
E. Hermosilla, J. Rodríguez

Department of Radiotherapy, Clinica Las Condes, Santiago, Chile.

Email address of Corresponding Author: mcastrillon@clinicalascondes.cl

BACKGROUND

The main uses of effective dose are the prospective dose assessment for the optimization of radiological protection and the demonstration of compliance with dose limits for regulatory purposes [1-2]. In recent years, studies have focused on the evaluation of effective dose received by patients during their treatment, including exposure due to diagnostic and setup images before and during treatment respectively [3-4]. To know the value of effective dose within a radiation therapy bunker can be important in the event of an accidental situation involving the permanence of a worker or the patient's companion, or the conscious loss of the personal dosimeter inside the bunker.

METHODS

This study measures effective doses in a radiotherapy bunker using a 6MV photon beam of an Oncor Impression Plus linear accelerator (*Siemens Healthineers*), 10x10cm^2 field, SSD=95cm, 200MU. Different groups of BeOSL dosimeters (*OSL Control Chile*) were irradiated. These were positioned on the treatment table at different distances from the isocenter (50, 100 and 150cm). A RW3 solid phantom centered on the beam axis was used as scatter material (Figure 1). The following dependencies were evaluated: gantry and couch angulation, beam energy (6 and 18MV), monitor units (100 and 200MU), dosimeters orientation (front-back and front-side), and attenuation effect by interposition between dosimeters. The measurements were repeated using Farmer ionization chamber (IC) TN30013 (*PTW Freiburg*) located at the same distances from the isocenter, and using buildup cap.

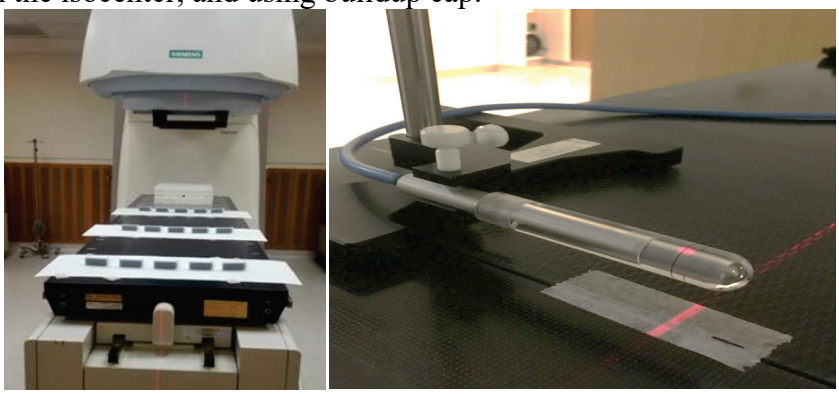

Figure 1. Distribution of dosimeters and ionization chamber in the measurement distances

RESULTS

For monitor unit dependence, the average deviation between the measurements obtained with the dosimeters and with the IC was below 1%. For energy dependence, the difference between the average values measured with dosimeters and with IC for both energies at the distances used was below 3%. The maximum differences obtained when comparing the frontal vs. lateral and frontal vs. posterior position were 5% and 2% respectively, for all distances. Likewise,

attenuation effect by interposition between dosimeters presents differences less than 5%, being greater for the largest distance. In the case of the gantry angulation dependence, the dosimeters show a deviation below 5% for 0° and 90° angles. The attenuation couch is responsible so that the measurements with dosimeters and IC are significantly much lower than those other angulations. Figure 2 shows the average values of the readings with dosimeters and with IC for different gantry and couch angles.

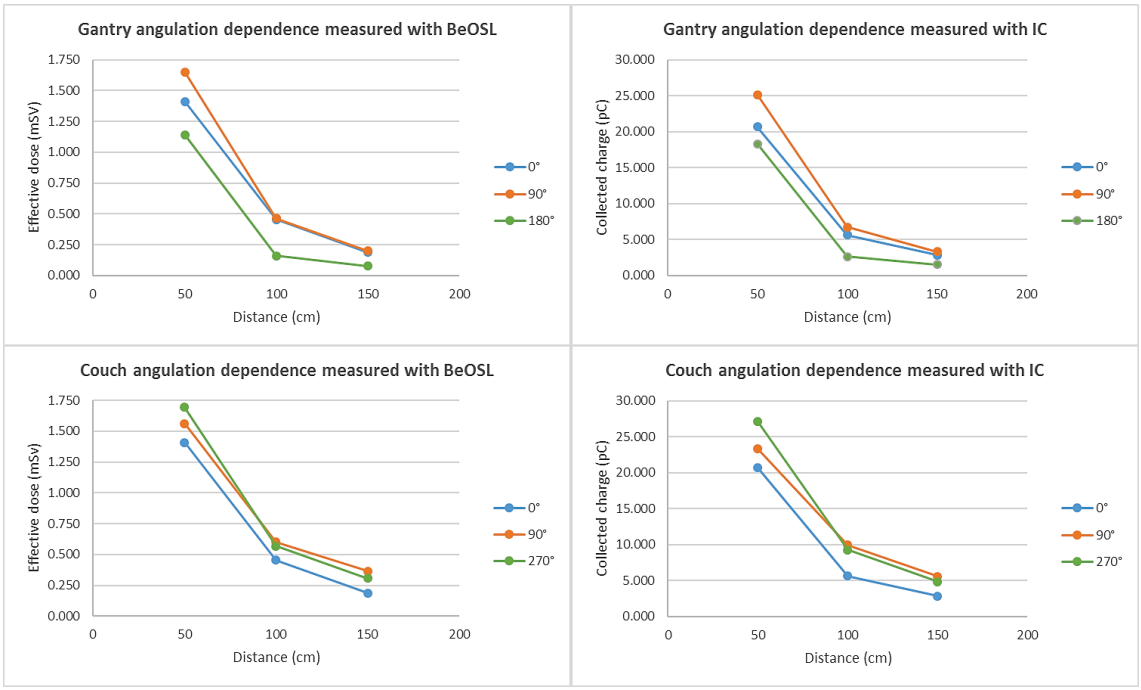

Figure 2. Gantry and couch angulation dependences measured with BeOSL and IC.

CONCLUSIONS

This study establishes the parameters to be taken into account in order to use the BeOSL dosimeters in the determination of effective dose in a radiotherapy bunker and its comparison in the ionization chamber. Percentage differences between the measurement methods are within 10% for all distances and couch angles evaluated, and 5% for the other tests carried out, except for the gantry angulation. The response of both detectors was similar, which highlights the reliability of the results provided by the OSL dosimeters, since the high precision, accuracy and stability of the ionization chamber is known. Acknowledgments to OSL Control Chile for supporting this research and the dosimeters provided.

REFERENCES

[1] INTERNATIONAL COMMISSION ON RADIOLOGICAL PROTECTION, The 2007 recommendations of the International Commission on Radiological Protection, Publication 103, Oxford (2007).

[2] FISHER, D.R., FAHEY, F.H., Appropriate use of effective dose in radiation protection and risk assessment, Health Physics 113(2) (2017) 102-109.

[3] USELMANN, A.J., THOMADSEN, B.R., On effective dose for radiotherapy based on doses to nontarget organs and tissues, Medical Physics 42(2) (2015), 977-982.

[4] HARRISON, R., Out-of-field doses in radiotherapy: Input to epidemiological studies and dose-risk models, Physica Medica 42 (2017), 239-246.

The Neutron Dose Angular Distribution from a Medical Linear Accelerator Equipped with a Compact Neutron Photoconverter

S. Peric[a], S. Savatović[a]
K. Alikaniotis[b], M. Severgnini[c], G. Giannini[b,a]

[a]Physics department, University of Trieste, Italy
[b]INFN, section of Trieste, Italy
[c]SC di Fisica Sanitaria, Azienda Ospedaliero-Universitaria "Ospedali Riuniti", Trieste, Italy

Email address of Corresponding Author: serena.peric@gmail.com

BACKGROUND

Linear accelerators e-Linacs are defective in creation of an undesired neutron dose, which is absorbed by the patient with the photon beam. For a combined photoneutron therapy [1] [2] it is necessary to study the neutron dose angular distribution from a compact neutron photonconverter (Micro PHONES) equipment [1] [2] [3] that can produce and moderate neutrons. These measurements are realized with a 3D support for bubble dosimeters.

METHODS

By gracious permission of the Radiotherapy Department at Maggiore Hospital in Trieste, two measurements were achieved at a linear accelerator Elekta-Synergy 3028 LINAC. The purpose was finding the 3D angular distribution of the neutron dose around a solid angle. A support in alveolar polycarbonate has been suitably designed to seat bubble dosimeters (BDT and PD-BND) [4] at certain angles [6]. The support was also able to move along the examination table in order to analyze the whole solid angle. The measurements were set to evaluate the micro PHONES task and compare the spatial neutron dose emission from the e-Linac with and without the equipment.

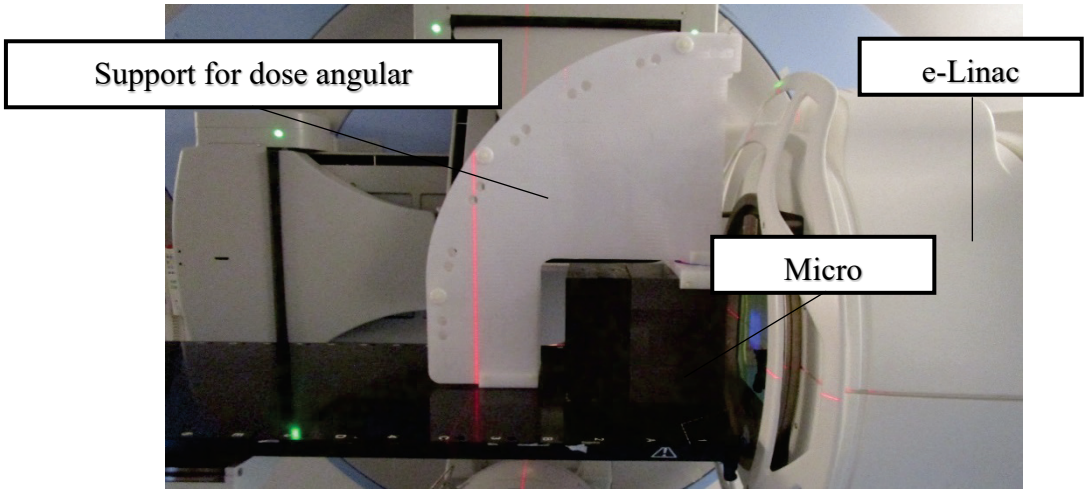

Figure 1. Micro PHONES with support for dose angular distribution

RESULTS

Figure 1 compares the measurement of neutron dose collected with the micro PHONES and without it. The collected fast neutron dose [5] (Gy/mSv) are presented in blue, and the thermal one (also calculated in Gy/mSv) in red. The graph shows an increase in dose in the vertical and horizontal directions, but also a decrease one with the use of micro PHONES.

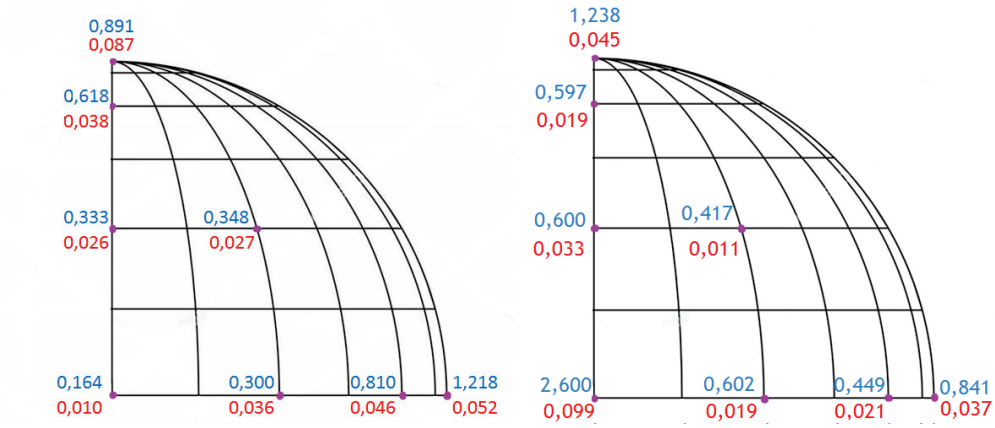

Figure 1. Fast and thermal neutron dose along the solid angle.

CONCLUSIONS

The undesired fast neutron dose absorption by the patient is reduced by 93,5% along the beam axis direction at the (0°,0°) angle. The thermal dose is scattered along the two-axis finding both maximum values at 90° degrees, considering the geometrical structure of the equipment. A collimated beam is mandatory to perform a combined photoneutron therapy [1-2].

REFERENCES

[1] COSTA, M., et al., Intense Thermal Neutron Fields From A Medical-type Linac: The E_libans Project, Radiation protection dosimetry **180** 1-4 (2017) 273-277.

[2] ALIKANIOTIS, K., et al., Radiotherapy dose enhancement using BNCT in conventional LINACs high-energy treatment: Simulation and experiment, Reports of Practical Oncology & Radiotherapy **21** 2 (2016) 117-122.

[3] DURISI, E., et al., Design and simulation of an optimized e-linac based neutron source for BNCT research, Applied Radiation and Isotopes **106** (2015) 63-67.

[4] VANHAVERE, F., LOOS, M., PLOMPEN, A., WATTECAMPS, E., THIERENS, H., A combined use of the BD-PND and BDT bubble detectors in neutron dosimetry, Radiation Measurements **29** 5 (1998) 573-577.

[5] FERREIRA, T., RASBAND, W., Image J User Guide, 2012.

[6] KOSAKO, K., et al., Angular distribution of photoneutrons from copper and tungsten targets bombarded by 18, 28, and 38 MeV electrons, Journal of nuclear science and technology **48** 2 (2011) 227-236.

Correlation of Eye Lens and Whole Body Dose Among Staff Members in Two Finnish Nuclear Medicine Units

C. Lindholm[a]
O. Sipilä[b], A.-L. Manninen[c], M. Lehtinen[a], T. Siiskonen[a]

[a]Radiation and Nuclear Safety Authority (STUK), POB 14, 00811, Helsinki, Finland
[b]HUS Medical Imaging Center, Helsinki University Hospital, POB 440, FIN-00029 HUS, Finland
[c]OYS Department of Nuclear Medicine and Radiology, Oulu University Hospital, POB 50, FIN-90029 Oulu, Finland

Email address of Corresponding Author: carita.lindholm@stuk.fi

BACKGROUND

Epidemiological evidence has shown that the lens of the eye is more radiosensitive than previously considered. The ICRP has recommended that the occupational exposure limit for the lens should be reduced from 150 mSv to 20 mSv per year averaged over periods of 5 years, with no single year exceeding 50 mSv [1]. The new radiation safety legislation follows the ICRP recommendation.

The purpose of the study was:

- to investigate the eye lens doses of technicians in nuclear medicine units of busy university hospitals, and,

- to determine the association between individually measured eye lens dose and whole body dose

METHODS

The measurements of eye lens dose equivalent ($H_p(3)$) were performed at nuclear medicine units of Helsinki and Oulu University Hospitals. The respective measurement periods in each unit were 21 (7 technicians) and 8 (8 technicians). The length of one measurement period varied between 8 to 20 days, and this was synchronized with the periods of the official staff dosimeters for measuring the whole body dose ($H_p(10)$). $H_p(3)$ values were measured using EYE-D dosemeters with inserted thermoluminescence detectors (MCP-N) attached to technicians' glasses or to a head band [2]. The detectors were calibrated and read in the Radiation Metrology Laboratory at STUK for gamma radiation, as it was considered that, with the radionuclides used, the major contribution to the $H_p(3)$ would come from gamma. The work tasks included PET-CT, gamma camera / SPECT-CT and radiopharmacy related tasks including patient preparation and care. For F-18-FDG studies, the radiotracer was provided by a commercial company and an automatic injector was utilized in both nuclear medicine units. After background correction, the collected $H_p(3)$ data were correlated to the $H_p(10)$ data. Also, the maximum and mean annual eye lens doses were estimated from the measurement data assuming similar working conditions and tasks for the technicians during the whole year.

RESULTS

A correlation was found between the measured $H_p(3)$ and $H_p(10)$ values (Pearson's coefficient $r= 0.90$). The mean values of $H_p(3)$ and the corresponding values of $H_p(10)$ measured per period were 77 µSv and 108 µSv, respectively, including all technicians and measuring periods. The

maximum estimated annual dose to the lens of the eye was below 4 mSv and the mean 1,2 mSv.

CONCLUSIONS

In this study, the eye lens doses correlated with the whole body doses. The estimated annual eye lens doses for nuclear medicine technicians in these study settings seemed to stay well below the new eye lens dose limit.

REFERENCES

[1] INTERNATIONAL COMMISSION ON RADIOLOGICAL PROTECTION. Statement on tissue reactions, ICRP **4825** (2011).

[2] BILSKI, P., et al., The new EYE-D™ dosemeter for measurements of Hp (3) for medical staff, Radiation Measurements **46** 11 (2011) 1239-1242.

Radiation Protection Dosimetry of Medical Workers using Their Fingernails

H. Yasuda[a]
C. A. B. Gonzales[b], S. Hirota[a]

[a]Department of Radiation Biophysics, Hiroshima University, 1-2-3 Kasumi, Minami-ku, Hiroshima 734-8553, Japan
[b]Phoenix Leader Education Program for Renaissance from Radiation Disaster, Hiroshima University, 1-2-3 Kasumi, Minami-ku, Hiroshima 734-8553, Japan

Email address of Corresponding Author: hyasuda@hiroshima-u.ac.jp

BACKGROUND

Fingernail in combination with a device of electron spin/paramagnetic resonance (abbreviated to "ESR" here) has a good potential as a dosimetric tool for the assessment of accidental high-dose exposure of hands that could occur in medical facilities performing X-ray diagnosis or radiopharmaceutical manufacturing. While notable developments in the application of fingernail dosimetry are seen in recent studies [1-3], few data on medical applications are available and fundamental investigations are still needed in this field.

With this thought, we have been investigating the possibility of the fingernail dosimetry for protecting the medical workers against unexpected, high-dose exposures. More concretely, we have been checking the stabilities of ESR signals from the fingernails linked with storage conditions and other influential factors, focusing on the variability in the dose responses among the individuals having different physiological properties (age, sex, etc.).

METHODS

Fingernail samples were voluntarily provided from seven healthy adults (3 male and 4 female) of Asian type. Those fingernail pieces, mostly 1-2 mm wide and 4-5 mm long, were cut by themselves with one specific nail cutter. Right after clipping, the samples were pooled and placed in sealed small plastic bags, and then stored in darkness at room temperature (20°C) inside the vacuum desiccator (30% humidity). No additional cuts or no other treatments were given to the samples between harvesting and irradiation.

Three sets of fingernail pieces from each person with 20 mg each were irradiated with doses of 35 Gy and 70 Gy □-rays of ^{137}Cs sources using a commercial irradiator (Gammacell40 Exactor Low Dose Rate Research Irradiator, Best Theratronics Ltd., Canada); the dose rate was 0.85 Gy min^{-1}. Other one set from the same person was kept unirradiated as a control.

The ESR spectra were measured at room temperature by using a X-band ESR spectrometer (JES-FA 100, JEOL Inc., Chiba, Japan) with the microwave frequency of ~9.4 GHz. The fingernail samples were put into a □5 mm quartz tube with a covered black sheet and positioned at the center of the cavity. The acquisition parameters were as follows: (1) microwave power: 1 mW, (2) sweep width: 10 mT, (3) modulation width: 0.25 mT, (4) sweeping time: 60 sec and (5) time constant: 0.03 sec. Each sample was scanned 10 times. During the spectra acquisition, a standard sample of MgO: Mn^{2+} was fixed at the bottom of the ESR cavity. The measured spectra were analyzed by using an exclusive software (A-System Data Processing version 3.9.2.0, JEOL Resonance Inc., Chiba, Japan). In the dose-response analyses, the peak-to-peak amplitude with subtraction of the background signal was considered as the amount of the radiation-induced radicals detected by the ESR spectrometer. Measurements of ESR signals were carried out at 5 mins, 6h, 12h, 24h, 3d, 5d, 7d, 14d, 21d, 28d, and 39d after irradiation.

In the periods between sample collections and all subsequent procedures (i.e., irradiations and ESR measurements), all the samples were kept in darkness inside the vacuum desiccator at room temperature.

RESULTS

The dose responses of the ESR signals taken from 7 donors are shown in Figure 1. The plot indicates an average and the error bar shows the standard deviation of the data of three samples from each donor.

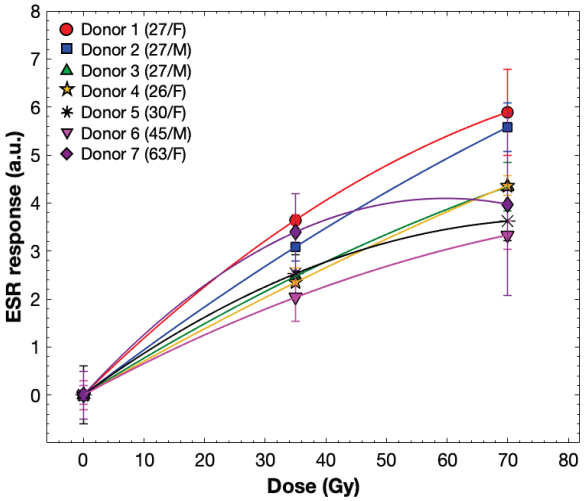

Figure 1. Dose response curves of vacuum-stored samples irradiated to γ-rays from the Cs-137 source. Each data set is fitted with a second-order function of the form $y=ax+bx^2$.

In regard to the responses to 70 Gy exposure, the fingernails of younger donors (D1-D4) were higher than those of older donors (D5-D7). The linearity of the dose response of the oldest donor's fingernails (D7) were notably worse than those of other younger donors. Also, the most rapid fading of the radiation-induced ESR signal was found in the samples of the oldest donor (D7) (not shown).

Thus, we assume that the fingernail that was more damaged in daily life by the various environmental or physiological stressors would lower the capacity of radical formation induced by radiation; probably the age is not the only factor causing such different dose-response characteristics. To verify this assumption, we are continuing the investigations with cooperation of more donors.

CONCLUSIONS

From the findings obtained in the present study, it is expected that human fingernails could be useful for routine examinations of accidental exposures of medical workers. For practical applications of this method, it is critically important to establish a simple method of dose calibration for the individuals who have different ages, lifestyles, health status, etc. that should affect the radical formation/trapping processes in the fingernails.

REFERENCES

[1] TROMPIER, F., KORNAK, L., CALAS, C., et al. Protocol for emergency EPR dosimetry in fingernails. Radiat. Meas. **42** (2007) 1085.

[2] ROMANYUKHA, A., TROMPIER, F., REYES, R.A., et al. Electron paramagnetic resonance radiation dose assessment in fingernails of the victim exposed to high dose as result of an accident. Radiat Environ Biophys **53** (2014) 755.

[3] SHOLOM, S., MCKEEVER, S.W.S. Emergency EPR dosimetry technique using vacuum-stored dry nails, Radiat. Meas. **88** (2016) 41.

Update of the EURADOS Strategic Research Agenda – Challenges for Dosimetry of Ionising Radiation in Medical Applications

F. Vanhavere[a]
W. Rühm[b], J. F. Bottollier Depois[c], H. Schuhmacher[d], E. Fantuzzi[e], J. Alves[f], P. Fattibene[g], M. A. Lopez[h], M. Caresano[i], P. Olko[j], H. Stadtmann[k], I. Clairand[c], P. Gilvin[l], A. Vargas[m], H. Rabus[d], B. Breustedt[n], R. Harrison[o], C. Woda[b], Ž. Knežević[p]

[a]Belgian Nuclear Research Centre (SCK-CEN), Mol, Belgium
[b]Helmholtz Center Munich, Institute of Radiation Protection, Neuherberg, Germany
[c]Institut de Radioprotection et de Sûreté Nucléaire (IRSN), Fontenay-aux-Roses Cedex, France
[d]Physikalisch Technische Bundesanstalt (PTB), Braunschweig, Germany
[e]ENEA, Radiation Protection Institute, Bologna, Italy
[f]Instituto Superior Técnico (IST), CTN, Portugal
[g]Istituto Superiore di Sanità (ISS), Rome Italy
[h]Centro de Investigaciones Energéticas, Medioambientales y Tecnológicas (CIEMAT, Madrid, Spain
[i]Dipartimento di Energia, Politecnico di Milano, Milano, Italy
[j]Instytut Fizyki Jądrowej (IFJ), Krakow, Poland
[k]Seibersdorf Labor GmbH, Seibersdorf, Austria
[l]Public Health England, Chilton, Didcot, United Kingdom
[m]Instituto de Técnicas Energéticas, Universitat Politécnica de Catalunya, Barcelona, Spain
[n]Karlsruhe Institute of Technology, Karlsruhe, Germany
[o]University of Newcastle, Newcastle, UK
[p]Ruđer Bošković Institute (RBI), Zagreb, Croatia

Email address of Corresponding Author: filip.vanhavere@sckcen.be

BACKGROUND

The European Radiation Dosimetry Group (EURADOS) was founded in 1981. It comprises a self-sustainable network of about 70 European institutions, such as research centres, university institutes, reference laboratories, dosimetry services and companies. The aim of the network is to promote European cooperation in research and development in the dosimetry of ionizing radiation and its implementation in routine practice, in order to contribute to compatibility within Europe and conformance with international practices.

METHODS

In 2014 the European Radiation Dosimetry Group (EURADOS) has published its first Strategic Research Agenda (SRA) which was intended to contribute to the identification of future research needs in radiation dosimetry in Europe. This SRA of EURADOS is being used as a guideline for the activities of the EURADOS Working Groups. It is noted that the efforts of EURADOS to develop an SRA for dosimetry, complement efforts of other European platforms such as MELODI, ALLIANCE, NERIS and EURAMED which have developed their own SRA in the fields of low-dose research, radioecology, emergency preparedness, and medical applications, respectively. Taken together, these SRAs will allow identification of research needs in Europe, in the general scientific field of radiation research, with the final goal of improving radiation protection of workers and the public. A detailed version of the present EURADOS SRA can be downloaded as a EURADOS report, from the EURADOS website (www.eurados.org).

Of course an SRA is not a static document and should be regularly updated. The first periodic update is now on-going. An important milestone in the process to update the EURADOS SRA was the organisation of stakeholder workshop in 2016. In total 24 international organisations were represented in a one day meeting. Among them, there were several organisations from the medical field (EANM, EFOMP, ESR, ESTRO, PTCOG), and the IAEA was also represented. A detailed summary of this workshop can be downloaded as a EURADOS report.

RESULTS

A preparation document was drafted that forms the basis of the SRA update. This document includes for each challenge information on which recent research projects have been performed, which new important publications were published, and which evolution took place in the state-of-the-art. The input of the stakholder workshop was also included in this preparation document. In this document, also a new structure of the SRA was proposed. The 5 visions were mainly kept, but the challenges were reorganised. These are the 5 main visions in the new SRA:

Vision 1 – Towards Updated Dose Concepts and Quantities

Vision 2 - Towards Improved Radiation Risk Estimates Deduced from Epidemiological Cohorts

Vision 3 - Towards an Efficient Dose Assessment in Case of Radiological Emergencies

Vision 4 - Towards an Integrated Personalized Patient Dosimetry in Medical Applications

Vision 5 - Towards an Improved Radiation Protection of Workers and the Public

Next to this, there will be chapters on education and training, harmonization and computational methods, which are considered cross-sectional topics.

All the medical dosimetric research topics related to patients are grouped in one vision. This vision is subdivided in three challenges:

- To improve patient and ambient dosimetry in modern external beam therapy
- To improve patient dosimetry in diagnostic and therapeutic nuclear medicine
- To optimize patient dose and risk estimations in interventional radiology and CT

Some examples of recent activities in these three fields of the EURADOS Working Groups are out of field dose measurements in proton therapy, microdosimetry in alpha therapy and skin dose mapping in interventional cardiology. Of course there are also links in the other visions with the medical applications of ionising radiation. All dosimetric aspects of workers in the medical fields are treated in vision 5. Vision 1 is including the link between the physical aspects of the track structure and the biological damage (micro and nano dosimetry). And in Vision 2 retrospective dosimetry for medical epidemiological cohorts is included.

Research on the applications of ionising radiation in medical applications has always been important for EURADOS. Two working groups are working specifically on these applications: WG9 (Radiation Dosimetry in Radiotherapy) and WG12 (Dosimetry in Medical Imaging). In these working groups, there is already a collaboration with several medical societies, like PTCOG, EANM and EFOMP.

The recently founded platform for radiation protection research in medical applications EURAMED has also published a first strategic research agenda. Their SRA is much broader and takes into account also imaging, patient dose repositories, and other aspects. While the EURADOS SRA clearly focusses on dosimetry aspects, there is a nice coherence and complementarity in both SRA's. Future collaboration between both platforms will ensure further refinement and synergy. The collaboration in the working groups with the medical societies and EURAMED will continue in the future.

CONCLUSIONS

The new version of the EURADOS SRA will be finalised at the end of 2019 and will include several dosimetric challenges for the medical applications.

Radiobiology

Microdosimetric Measurements to Characterize with LET Spectra the Target Volumes in Ion-Beam Therapy

G. Magrin[a]
P. Fossati[a], **M.D. Dominietto**[b], **H. Palmans**[a,c]

[a]EBG MedAustron, Marie Curie-Str. 5, 2700 Wiener Neustadt, Austria
[b]Center for Proton-Therapy, Paul Scherrer Institut, 5232 Villigen PSI, Switzerland
[c]Acoustics and Ionising Radiation Division, National Physical Laboratory (NPL), Teddington, Middlesex, UK

Email address of Corresponding Author: giulio.magrin@medaustron.at

BACKGROUND

Today's LET (Linear Energy Transfer) inputs for the models used in the Treatment Planning Systems (TPSs) of carbon ion therapy are not based on experimental measurements. LET is obtained indirectly from computations based on analytical models and Monte Carlo simulations and the data for each volume of interest are provided as simple mean values, the track average LET, L_T, and the dose-averaged LET, L_D. The information carried out from mean quantities is limited since the radiation effectiveness varies widely and non-monotonously at different LET intervals. For instance, it the last millimeters before stopping, the LET values of the carbon-ion radiation range from few keV·µm^{-1} to 1000 keV·µm^{-1}. Correspondingly, the differences of the induced biological effect are significant.

Microdosimetric spectra collected in therapeutic ion beams can be used to provide the needed LET distributions and to benchmark analytical and Monte Carlo computations of LET. Currently, direct microdosimetric measurements are infrequent and not directly implemented to clinical routine. The challenges are developing novel detectors which allow an easy implementation to ion-beam therapy practice and elaborating methodologies to reevaluate the experimental data in terms of detector-independent LET distributions.

METHODS

The microdosimeters that have been specifically developed in recent years for the characterization of therapeutic ion-beams are the most various. Tissue-equivalent proportional counter, gas-electron-multiplier chambers, silicon, and diamond diodes are substantially different in shapes and in composition of the sensitive volume. The process to provide univocal LET spectra, independently from the chosen detector, can be divided in two steps. The first step is the so-called 'method of LET analysis' which evaluates from the generic microdosimetric spectrum the distribution of LET for the same material of the detector [Kellerer 1972]. The second step consists in converting this, to the LET distribution that refers to a 'standard' material, which can be arbitrarily chosen as water. A novel approach to perform this conversion was proposed in a recent study [Magrin 2018].

RESULTS

The LET distributions obtained are used to represent the heterogeneity of the radiation in that position. Within the spectrum, the dose fractions can be separated referring to several LET intervals which are assumed to be responsible of different biological effectiveness. In figure 1, the spectrum is separated, for clearness, in only three areas in particular emphasizing the area between 100 and 200 keV·µm^{-1}, which is generally recognized as a significant interval in terms of increase of biological effectiveness. There is, however, no predefined number and extension of the intervals in which the spectra should be divided.

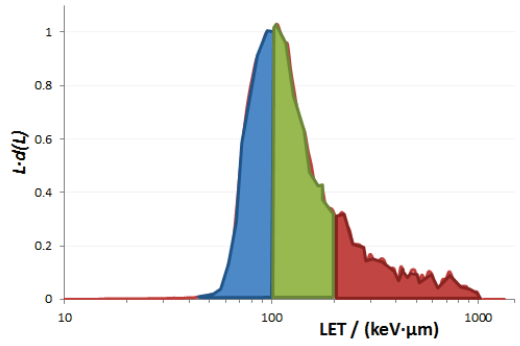

Figure 1. LET distribution of carbon ions in water obtained from a microdosimetric spectrum. The three colored areas correspond to the fraction of dose delivered by the irradiation at the LET intervals: $L_D < 100$; $100 \leq L_D < 200$; $L_D \geq 200$ (expressed in keV·µm^{-1})

The LET spectra are assessed at different depths corresponding to the range at which the microdosimeters are positioned. The information from the LET distributions can be recombined (see figure 2) to obtain depth-dose curves in which the doses are separated according to the different LET intervals.

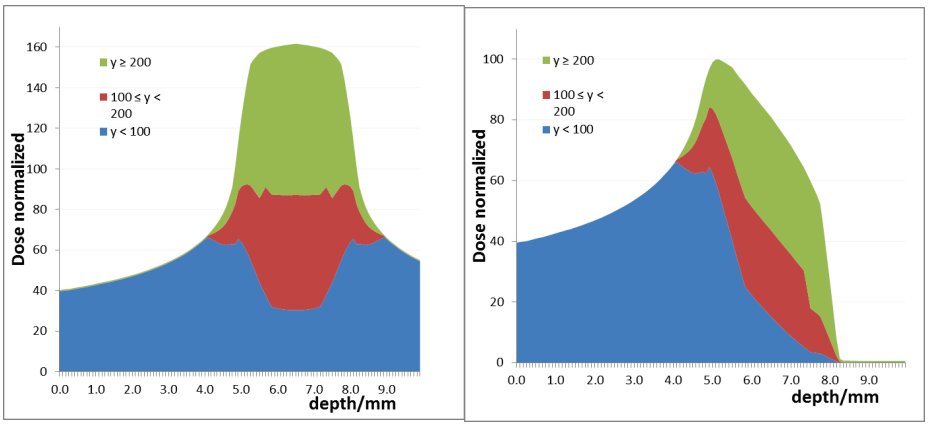

Figure 2. Depth-dose curves for one field (left) and two opposite fields (right) showing the fraction of dose delivered at the three LET intervals described in Figure 1

CONCLUSIONS

Microdosimeters can be used for the experimental characterization of the beams in terms of mean values of LET and, more significantly, in terms of frequency and dose distribution of LET. From those, the fraction of dose delivered at specific LET intervals with sub-millimetric resolution is obtained. Preliminary studies are focusing on assessing the fraction of doses delivered at different LET intervals for two distinct cases of small and large osteosarcomas and to correlate to those the probability of local control [Fossati 2019].

Beam models obtained combining the dosimetry-based and LET-distribution-based features can be generated and used in TPS algorithms.

REFERENCES

[1] Kellerer A, An algorithm for LET-analysis Phys. Med. Biol. 17 (1972) 232–40
[2] Magrin G, A method to convert spectra from slab microdosimeters in therapeutic ion beams to the spectra referring to microdosimeters of different shapes and material, Phys. Med. Biol. 63 (2018) 215021 (15pp)
[3] Fossati P, et al. Presented at this IDOS 2019 Symposium, Vienna (2019)

Effect of Photon Energy on the Structural Properties of Rats RBCs

R. Hammam[a]
F. Ali[b], **A. El-Sersy**[a]

[a]National Institute for Standards (NIS), Tersa st., El-Haram, Giza, Egypt
[b]Biophysics Department, Cairo University, Giza, Egypt

Email address of Corresponding Author: reham.hamdy87@gmail.com

BACKGROUND

The International Commission on Radiological Protection (ICRP) Publication 119 [1] recommended that low energy X-rays have effects similar to those of high energy γ rays.

Michael Bellamy 2013 [2] indicates that Low-energy electron and photon radiations produce greater dense ionization clusters than those of high-energy γ rays. Recent studies have attributed the biological effects of ionizing radiation to the induction of double stranded breaks (DSBs) in DNA. When the relative biological effectiveness (RBE) was compared with the relative DSBs induction, results indicated nearly two-fold increase in the yield of DSBs for low-energy photons [3].

Some studies confirmed that mammography X-rays having a radiobiological effectiveness of 1.3 compared with 250 kVp X-rays, and value of 2 when compared with higher-energy γ rays [4]. The low-energy X-rays used in screening mammography are expected to be more biologically effective than high-energy X- or γ rays [5]. Low-energy X-rays produce an increased risk of approximately a factor of 2 when compared with high energy photons based on in-vitro studies [6].

Therefore, the aim of the present work is to study the resulting biological effect after whole-body exposure of male albino rats to equal doses of X- and γ rays but with different energies and to use these variations of biological effects to estimate Gy-Sv conversion factor.

METHODS

In this work, the effect of photon energy on the mechanical properties of the red blood cells (RBCs) of male albino rats after whole-body exposure to a fixed dose was studied. Eighty male albino rats were equally divided into 8 groups. i.e. A - H. Animals in group A were used as control and were not exposed to any type of radiation, while animals in groups B - H underwent whole-body exposure to the same radiation dose but at different rates and energies. RBCs mechanical properties were tested by measuring osmotic fragility, solubility with non-ionic detergent and examining blood films.

RESULTS

It is possible to state here that, in-vivo irradiation of RBCs with low energy photons (X-ray) led to changes in the packing properties of the phospholipid macromolecules forming the RBCs cell wall leading to decreased cell membrane elasticity. It is well known that the binding forces between these molecules which are van der waals electric forces are one of the main parameters that play the main role of ion transport across the cell membrane to attain the resting potential [7]. The change of ion transport may lead to the loss of the +ve electric charges on the surface of the cell wall which act as repulsive forces between adjacent cells preventing sticking. This phenomenon was obviously noticed from the cell's morphology for X-ray exposed groups.

One more important point worthy to be mentioned here is that cell to cell communication occurs through the flexoelectricity generated during multiple bending of the cell wall [8] which will generate bioelectric impulses. Changes in the packing properties of the macromolecules forming the cell membrane will deteriorate its flexibility properties and hence cell to cell communication. The net result of the phenomena is the deterioration of the metabolic function of the RBCs. Furthermore, the most significant change in the solubilization curves profile was recorded for exposure to low energy photons (X-ray). And again, the severity of the alterations was energy dependent.

CONCLUSIONS

From the present work, it may be concluded that post exposure effects are energy dependent. The resulting hazards were found to be widely varying for the same absorbed dose, where the severity of the hazards was higher at exposure to lower energies as recorded in RBCs films. Energy dependency of the studied parameter was interpreted in the framework of Hp (10) variation with photon energy as that of ISO 4037. Data of Solubilisation energy dependency relative to that of control was used to re-evaluate the numerical value of Gy-Sv conversion factor and to suggest an empirical equation for (h) value. The concerned Gy-Sv conversion factor in the present study is of importance for personal dose calculations and to fulfill the ALARA principle, since it is essential and of great importance to assess risk due to the wide-range use of low energy X-rays for mammography screening and other diagnostic applications.

REFERENCES

[1] INTERNATIONAL COMMISSION ON RADIOLOGICAL PROTECTION, Compendium of dose coefficient based on ICRP Publication 60,Publication 119, (2012).

[2] Michael Bellamy, Keith Eckerman, Oak Ridge., Relative biological effectiveness of low energy electrons and photons. Office of Radiation and Indoor Air, U. S. Environmental Protection Agency (EPA) (2013).

[3] Ying Liang, Qibin Fu, Xudong Wang, Feng Liu, Gen Yang, Chunxiong Luo, Qi Ouyang and Yugang Wang., Relative biological effectiveness for photons: implication of complex DNA double-strand breaks as critical lesions. Physics in Medicine & Biology. 62(2017)6.

[4] Brenner, D. J. and Amols, H. I. , Enhanced risk from low-energy screen-film mammography X-rays. Br. J. Radiol. 62(1989)910.

[5] Brenner, D. J., Sawant, S. G.,Hande,M. P.,Miller,R.C., Elliston, C. D., Fu, Z., Randers-Pehrson, G. and Marino, S. A. , Routine. Screening mammography: how important is the radiation-risk side of the benefit-risk equation? Int. J. Radiat. Biol. 78(2002)1065.

[6] Slonina D., Spekl K., Panteleeva A., Brankovic K., Hoinkis C. and Dorr W., Induction of micronuclei in human fibroblasts and keratinocytes by 25 kV x-rays. Radiat. Environ. Biophys. 42(2003)55.

[7] Kabaso D.,Gongadze E., Perutkova S., Matschegewski C., Karalj-Iglic V., Beck U., Van Rienen U., and Iglic A., mechanics and electrostatics of the interactions between osteoblasts and titanium surface" Computer methods in biomechanics and biomedical engineering., 14 (2011) 469.

[8] Alexander G. Petrov, Flexoelectricity of model and living membranes" Biochimica et Biophysica Acta 1561(2001) 1.

Which Quantities for Physics Driven Optimization of Carbon Ion Radiotherapy Plans?

P. Fossati[a]
V. Patera[b], **A. Schiavi**[b], **G. Magrin**[a]

[a]EBG MedAustron, Marie Curie-Str. 5, 2700 Wiener Neustadt, Austria
[b]Department of Basic and Applied Sciences for Engineering, Università la Sapienza, Roma

Email address of Corresponding Author: piero.fossati@medaustron.at

BACKGROUND

Carbon ion Radiotherapy (CIRT) is employed in clinical practice since 24 years. Treatment are optimized and reported in terms of Relative Biological Effectiveness (RBE) weighted dose. RBE is calculated voxel by voxel and depends on the details of the mixed field of particles. RBE models are based on simplifications and extrapolations, most notably they do not account for the inter- and intra-patients heterogeneity in dose response curves and do not consider modifications that occur during fractionated treatments. In clinical practice there is an emerging request to consider not only the nominal RBE but optimize also some lower level physical parameters. It is not entirely clear which physical parameter is the best candidate to describe efficacy of carbon ions not only in the nominal conditions but also for the biological worst case (non re-oxygenating quiescent cancer stem cell). The two most used RBE models rely on the Linear Energy Transfer or LET mean values (Local Effect Model, LEM) or on the lineal energy dose-mean lineal energy, $\bar{y}_D$ (Microdosimetric Kinetic Model, MKM). Mean values of LET and lineal energy are generally used to specify the 'radiation quality' which characterize the clinical efficacy of a radiation field, however neither of the two is a perfect equivalent of the density of ionization events, that is the biologically most relevant parameter. Clinical data have shown that probability of local control in osteosarcoma treated with exclusive CIRT depends critically on target size [1, 2]. Part of this dependency may be due to the difference in microscopic dose deposition patterns between big and small targets.

METHODS

In the first step CIRT Treatment plans for small (< 500 cc) and large (> 1000 cc) osteosarcomas will be compared. Several physical quantities will be analyzed to identify factors potentially correlated with lower local control probability.

For both models, the quantitative validation is still lacking. Using LET and lineal energy complete distributions instead of simple mean values will give the possibility of separating, for the same irradiation fields, the fraction of doses delivered at specific intervals.

In terms of LEM model, the voxel by voxel LET spectra will be analyzed. The hypothesis is that a higher risk of local recurrence may be due to a large number of voxels not receiving enough high-LET dose. For each voxel inside the clinical target volume, CTV, the percentage of absorbed dose deposited at LET > LETt than a given threshold will be investigated in order to determine, empirically it is expected that, in order to be effective, about 20% of deposited dose should be delivered at LET > 100 $keV \cdot \mu m^{-1}$.

In terms of MKM models, the risk of local recurrence will be analyzed in terms of complete lineal-energy spectra collected in each voxel. Analogously to the LEM model, it is expected

that the effectiveness of the radiation is linked to a percentage of dose delivered at linear energy values exceeding 100 $keV \cdot \mu m^{-1}$.

LET and microdosimetric distributions will be evaluated through both experimental measurements [3] and Monte Carlo simulations.

In the second step, plans will be re-optimized including the physical quantities determined in the first step as objective for the cost function.

CONCLUSIONS

A potential outcome of this analysis is the correlation of tumor local-control probability with the dose delivered at specific intervals of LET or lineal energy values.

REFERENCES

[1] Mohamad O, Imai R, Kamada T, Nitta Y, Araki N; Working Group for Bone and Soft Tissue Sarcoma. Carbon ion radiotherapy for inoperable pediatric osteosarcoma. Oncotarget. 2018 May 1;9(33):22976-22985. doi: 10.18632/oncotarget.25165. eCollection 2018 May 1. PubMed PMID: 29796166; PubMed Central PMCID: PMC5955418.

[2] Matsunobu A, Imai R, Kamada T, Imaizumi T, Tsuji H, Tsujii H, Shioyama Y, Honda H, Tatezaki S; Working Group for Bone and Soft Tissue Sarcomas. Impact of carbon ion radiotherapy for unresectable osteosarcoma of the trunk. Cancer. 2012 Sep 15;118(18):4555-63. doi: 10.1002/cncr.27451. Epub 2012 Feb 22. PubMed PMID: 22359113.

[3] Magrin G., Fossati P., Dominietto M., Palmans H. Microdosimetric Measurements to Characterize with LET Spectra the Target Volumes in Ion-Beam Therapy Presented at this IDOS 2019 Symposium, Vienna (2019)

Other Related Topics

Modern Self-Contained, Dry-Storage Irradiators

G. S. Mickum[a]
Z. J. Hope[a], R. O. Rushton[a]

[a]Hopewell Designs, Inc. 5940 Gateway Dr. Alpharetta GA 30004 USA

Email address of Corresponding Author: Spencer.Mickum@HopewellDesigns.com

BACKGROUND

The early small-animal radiation delivery platforms for high dose rate research relied on the self-contained research irradiator, the Gammacell 220, for dose effects, characterization, and other research activities [1]. This legacy irradiator remains a radiobiology industry mainstay, but is no longer supported by its manufacturer. Modernizing this legacy model would necessitate improvement of the external dose rate to operators and improved uniformity within the irradiation chamber. Improved uniformity would greatly benefit the technical challenge of non-uniform radiation field within the irradiator. The study includes development of several high-fidelity monte-carlo models utilizing the Los Alamos National Laboratory MCNP N-particle code [2] to investigate optimization of this self-contained cobalt-60 research irradiator.

METHODS

Simulation of the concept design was completed with two goals: to ensure the radiation protection of the system meets modern requirements and to validate the dose intensity and uniformity will meet or exceed tolerances set by the benchmark case of the legacy system. The noteworthy point of investigation was the radiation streaming pathway out the top of the irradiator during the transition between irradiation and loading modes of operation. Also the modern irradiator allows for rotation of the sources to facilitate source loading and to improve dose uniformity due to differing specific activity concentrations between pencil sources. The concept design designated as the GR420 is shown in vertical cross section in Figure 1.

All radiation protection and dose results were compared to the benchmark case of the Gammacell 220.

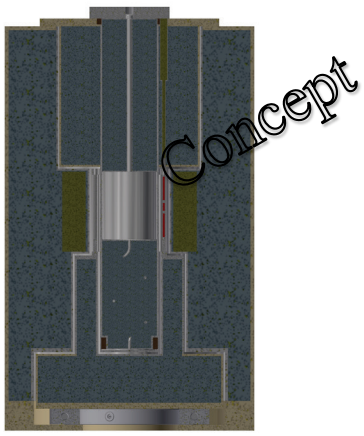

Figure 1. GR420 Vertical Cross Section.

RESULTS

A weight window generator mesh and the density reduction method were used for variance reduction of the monte carlo simulations of the Gammacell 220 and GR420. A source loading of 24kCi Co-60 dispersed between eight pencil sources was simulated to account for the expected range of isotopic non-uniformities with an average difference in specific activities of ±8% and up to ±20%. The shielding requirements for the GR420 were set for an external dose rate of less than 20 uSv/hr – more than an order of magnitude lower than the legacy system.

Several perturbations of the GR420 concept were explored to understand the relationship of the external dose rate and transition distance between loading and irradiation positions. Integrated shielding as an alternative to the clam-shell type collar shield surrounding the sample chamber was found to be an improvement to vertical streaming out the top of the irradiator. The largest contrast in the external radiation profiles between the legacy and modern irradiators was directly above the irradiation during chamber transition.

A discretized mesh of tally points was simulated to investigate the dose uniformity and centerline dose rates of the legacy and modern irradiators with two- and three-dimensional renderings of the chamber irradiation field. Due to the increased chamber size of the GR420, the center dose rate and dose uniformity of the chamber are slightly decreased as the radius from the chamber center to the surrounding ring of sources increases from 7.75 cm for the Gammacell 220 to 9 cm for the GR420. A selection of comparison results are shown in Table 1. However, the source cage design of the Gammacell 220 inherently created an irradiation environment where higher field intensity (hot spots) occurs since the chamber is non-rotational. Such conditions present a technical challenge given each experiment has a unique geometry (e.g. cell culture plates, cell vials, mice (different sizes)). These hot spots are removed through the rotation of the sources around the sample chamber with the GR420, removing the higher field intensity gradients and allowing for much lower standard deviation of dose delivered between samples placed equidistant from the center of the chamber.

Table 1. Modern and Legacy Irradiator Comparison.

Irradiator	**GR420**	**Gammacell 220**
Available Source Slots	24	48
Chamber Size [L]	5.3	3.8
Center Doserate [Gy/min]	200	270
Dose Uniformity Ratio	1.90±31%	1.81±29%
Chamber Transition Dose [Gy]	3.1%	3.8%
External Transition Dose [uSv/hr]	<50 uSv/hr	>1000 uSv/hr
Weight [kg]	6800	4540

CONCLUSIONS

This work is an ongoing effort to characterize the challenges of utilizing the legacy self-contained irradiation system and develop a new design that meets the benchmark needs while introducing appreciable improvements in the irradiation field and the ease of use. Results support the transition to an integrated shielding design irradiation with source rotation. The modern design ensures low external rates and improves the interior radiation field by removal of higher field intensity gradients due to isotopic non-uniformities in the pencils.

REFERENCES

[1] Atomic Energy of Canada Limited, Gamma Cell 220 Irradiation Unit, Specifications, April 1974.

[2] T. Goorley, et al., "Initial MCNP6 Release Overview", Nuclear Technology, 180, pp 298-315 (Dec 2012).

Dosimetric Characterization for Cell Irradiations in Preclinical Studies with a Small Animal Irradiator

I. Silvestre[a]
A. Westhorpe[b], R. Carter[b], A. Subiel[a], R. A. Sharma[b], G. Schettino[a]

[a]National Physical Laboratory (NPL). Hampton Road, Teddington. Middlesex. TW11 0LW. United Kingdom.
[b]UCL Cancer Institute. Paul O'Gorman Building. University College London. 72 Huntley Street. London WC1E 6BT. United Kingdom.

Email address of Corresponding Author: ileana.silvestre.patallo@npl.co.uk

BACKGROUND

The need for standardization and improved dosimetry for pre-clinical studies has become a priority for clinical and translational radiotherapy working groups. At UCL Cancer Institute, a small animal irradiator SARRP (Xstrahl) is used for both: in vivo and in vitro (cells) irradiations. The geometrical conditions for cell irradiations don't allow for the use of Muriplan treatment planning system. Full backscatter conditions required by dosimetry protocols are also not possible. Therefore, an accurate dosimetry of the beam in those delivering conditions is required. The current study presents a dosimetric characterization of the SARRP for cell irradiations.

METHODS

SARRP's beam quality in terms of Half Value Layer (HVL) was determined in the conditions of the cabinet enclosure. Cu filters were placed at the filters' holder, mounted at 23 cm from the source, the chamber was fixed at 59 cm from the source. An adequate distance (exceeding 40 cm) between the chamber and the floor of the cabinet was also achieved.

The formalism from IPEMB code of practice for the determination of absorbed dose for x-rays below 300 kV at 2 cm depth (in WT1 solid water) [1] was followed. Output in reference conditions for the use of SARRP with Muriplan (SSD 33 cm, 3.5 cm of underlying solid water material, plus 1 cm PMMA slab platform) was determined. A secondary standard dosimetry kit, directly traceable to NPL's Air Kerma primary standard free-air ionisation chamber was used (Dose1 electrometer, PTW 30012 ionization chamber).

One of the challenges in the dosimetry for cell irradiators is to evaluate the effect of the lack of a full backscatter condition, when petri dishes are placed directly over the irradiation platforms. A set of ionization chamber measurements were performed in the SARRP, starting from reference conditions, and varying the thickness of the water equivalent material underneath the chamber from 1 to 4 cm, while keeping the SSD constant (at 33 cm).

EBT3 films were calibrated and used for relative measurements of dose, in conditions similar to those used in cell irradiations. Films were processed and analyzed with FilmQA Pro software.

Alanine pellets, calibrated at NPL's keV radiation facility, were employed to measure dose in the SARRP's reference conditions. At UCL, three different sized petri dishes are used to irradiate cell cultures. WT1 phantoms were designed to simulate the petri dishes (with 3.5, 5.5 and 9 cm diameter) with an insert for four pellets (with their centres at depths: 1.25, 3.75, 6.25

and 8.75 mm). Irradiations with same dose would allow to evaluate open field's relative depth doses and the effect of lateral scatter conditions in different size phantoms.

RESULTS

Values of the percentage transmission through the different added thickness of Cu were plotted. The measured HVL was 0.669 mm Cu. The value was compared to the one in the manufacturer commissioning report (measured in the factory conditions) and the difference was 0.15%.

Output in reference conditions for the clinical use of the SARRP was 3.648 Gy/min. Repeated measurements show a repeatability with a coefficient of variation of 0.34%. A difference with the commissioning report provided by the manufacturer was 0.2%.

In the SARRP platform, varying the thickness of the backscatter material from 4 cm to 1 cm, reduces the output by 6.6 %.

The dose profile of the open field measured with the EBT3 film exposed at the distance of the irradiation platform, showed a region of high dose in the longitudinal orientation of the field (Figure 1).

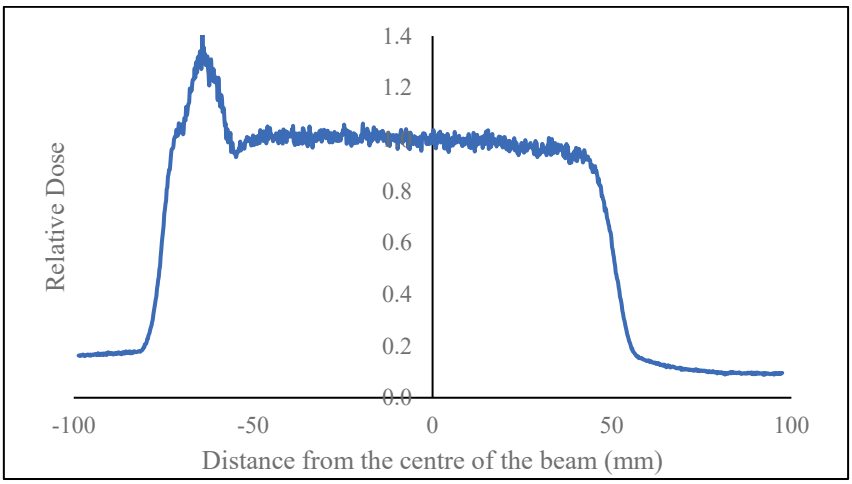

Figure 1. Open field profile in the longitudinal (Y) direction.

Alanine pellet measurements of output in reference conditions agree with the chamber measurements within 2%. Due to the lateral scatter effect, pellets in the 9 cm phantom showed 1.8 % larger dose when compared to the 5.5 cm phantom. For the 9 cm phantom, the dose at depth of 8.75 mm is 92.2% of the dose at the surface.

CONCLUSIONS

The region of high dose in the profile of the open field is caused by a misplacement of the Cu filter slider. SARRP devices used for cell irradiations with the open field should include profile measurements at the surface, as part of the routine quality assurance. Relative measurements in conditions of cells' irradiations, improve the accuracy of the dosimetry.

REFERENCES

[1] KLEVENHAGEN, S.C., et al., The IPEMB code of practice for the determination of absorbed dose for x-rays below 300 kV generating potential (0.035 mm Al–4 mm Cu HVL; 10–300 kV generating potential), Phys Med Biol. **41** (1996) 2605.

International Atomic Energy Agency
IAEA-CN-273
Vienna International Centre
PO Box 100
Wagramer Strasse 5
1400 Vienna, Austria
Tel.: +43 1 2600 (0) plus extension
Fax: +43 1 26007
Email: official.mail@iaea.org

CN-273

18-02070E